Magdolna Hargittai
István Hargittai

Symmetry through the Eyes of a Chemist

3rd Edition

Springer

Symmetry through the Eyes of a Chemist

Magdolna Hargittai · István Hargittai

Symmetry through the Eyes of a Chemist

Third Edition

Springer

Magdolna Hargittai
István Hargittai
Budapest University of Technology and Economics
P. O. Box 91
H-1521 Budapest
Hungary
hargittaim@gmail.com
istvan.hargittai@gmail.com

ISBN: 978-1-4020-5627-7 e-ISBN: 978-1-4020-5628-4

DOI 10.1007/978-1-4020-5628-4

Library of Congress Control Number: 2008926635

© Springer Science+Business Media B.V. 2009
No part of this work may be reproduced, stored in a retrieval system, or transmitted
in any form or by any means, electronic, mechanical, photocopying, microfilming, recording
or otherwise, without written permission from the Publisher, with the exception
of any material supplied specifically for the purpose of being entered
and executed on a computer system, for exclusive use by the purchaser of the work.

Printed on acid-free paper

9 8 7 6 5 4 3 2 1

springer.com

Preface

It is gratifying to launch the third edition of our book. Its coming to life testifies about the task it has fulfilled in the service of the community of chemical research and learning. As we noted in the Prefaces to the first and second editions, our book surveys chemistry from the point of view of symmetry. We present many examples from chemistry as well as from other fields to emphasize the unifying nature of the symmetry concept. Our aim has been to provide aesthetic pleasure in addition to learning experience. In our first Preface we paid tribute to two books in particular from which we learned a great deal; they have influenced significantly our approach to the subject matter of our book. They are Weyl's classic, *Symmetry*, and Shubnikov and Koptsik's *Symmetry in Science and Art*.

The structure of our book has not changed. Following the Introduction (Chapter 1), Chapter 2 presents the simplest symmetries using chemical and non-chemical examples. Molecular geometry is discussed in Chapter 3. The next four chapters present group-theoretical methods (Chapter 4) and, based on them, discussions of molecular vibrations (Chapter 5), electronic structures (Chapter 6), and chemical reactions (Chapter 7). For the last two chapters we return to a qualitative treatment and introduce space-group symmetries (Chapter 8), concluding with crystal structures (Chapter 9).

For the third edition we have further revised and streamlined our text and renewed the illustrative material. We have expanded the sections dealing with biopolymers and quasicrystals in particular. We have added an Epilogue.

We dedicated the first edition to the memory of József Pollák (1901–1973), who was the stepfather of one of us (IH). The third edition we dedicate to our children and grandchildren, and to the memory of our parents.

We note with pleasure our joint interest in both chemistry and symmetry for the past forty years that is behind this book. Our joint writing efforts have been an important facet of our professional as well as married life for these forty years.

Budapest, January 2008

Magdolna Hargittai
István Hargittai

Acknowledgments

We thank our colleagues and our students who have helped the creation of this book over the years, especially at the University of Connecticut (Storrs); Eötvös Loránd University (Budapest); University of Texas (Austin); University of Hawaii (Honolulu); Budapest University of Technology and Economics; University of North Carolina (Wilmington); and elsewhere. We also appreciate the helpful comments and suggestions from the reviewers of our book and from its users and readers from all over the world. We would like to express our gratitude to Professor Emil Molnár for helpful consultations.

In connection with the preparation of the third edition of this book, we owe special thanks to Ms. Mária Kolonits, Ms. Judit Szücs, and Mr. Zoltán Varga for their most careful technical help in many aspects of the work.

For over forty years our research in structural chemistry has been generously funded by the Hungarian Academy of Sciences and lately also by the Hungarian National Scientific Research Funds. We are also grateful for support to Eötvös University and especially to the Budapest University of Technology and Economics.

Contents

1 Introduction . . . 1
References . . . 20

2 Simple and Combined Symmetries . . . 25
2.1. Bilateral Symmetry . . . 25
2.2. Rotational Symmetry . . . 33
2.3. Combined Symmetries . . . 37
2.3.1. A Rotation Axis with Intersecting Symmetry Planes . . . 37
2.3.2. Snowflakes . . . 39
2.4. Inversion . . . 53
2.5. Singular Point and Translational Symmetry . . . 55
2.6. Polarity . . . 57
2.7. Chirality . . . 60
2.7.1. Asymmetry and Dissymmetry . . . 66
2.7.2. Vital Importance . . . 69
2.7.3. *La coupe du roi* . . . 74
2.8. Polyhedra . . . 76
References . . . 91

3 Molecular Shape and Geometry . . . 97
3.1. Isomers . . . 98
3.2. Rotational Isomerism . . . 100
3.3. Symmetry Notations . . . 104
3.4. Establishing the Point Group . . . 105
3.5. Examples . . . 107
3.6. Consequences of Substitution . . . 115
3.7. Polyhedral Molecular Geometries . . . 119

3.7.1. Boron Hydride Cages 123
3.7.2. Polycyclic Hydrocarbons 125
3.7.3. Structures with Central Atom 133
3.7.4. Regularities in Nonbonded Distances 136
3.7.5. The VSEPR Model 139
3.7.6. Consequences of Intramolecular Motion 152
References 161

4 Helpful Mathematical Tools 169
4.1. Groups 169
4.2. Matrices 176
4.3. Representation of Groups 183
4.4. The Character of a Representation 189
4.5. Character Tables and Properties of Irreducible Representations 191
4.6. Antisymmetry 197
4.7. Shortcut to Determine a Representation 204
4.8. Reducing a Representation 206
4.9. Auxiliaries 208
4.9.1. Direct Product 209
4.9.2. Integrals of Product Functions 209
4.9.3. Projection Operator 211
4.10. Dynamic Properties 212
4.11. Where Is Group Theory Applied? 213
References 214

5 Molecular Vibrations 217
5.1. Normal Modes 217
5.1.1. Their Number 218
5.1.2. Their Symmetry 220
5.1.3. Their Types 224
5.2. Symmetry Coordinates 225
5.3. Selection Rules 227
5.4. Examples 229
References 237

6 Electronic Structure of Atoms and Molecules 239
6.1. One-Electron Wave Function 241
6.2. Many-Electron Atoms 249

6.3. Molecules 252
6.3.1. Constructing Molecular Orbitals 252
6.3.2. Electronic States 261
6.3.3. Examples of MO Construction 263
6.4. Quantum Chemical Calculations 287
6.5. Influence of Environmental Symmetry 290
6.6. Jahn–Teller Effect 294
References 308

7 Chemical Reactions 313
7.1. Potential Energy Surface 315
7.1.1. Transition State, Transition Structure 316
7.1.2. Reaction Coordinate 319
7.1.3. Symmetry Rules for the Reaction Coordinate 320
7.2. Electronic Structure 324
7.2.1. Changes During a Chemical Reaction 324
7.2.2. Frontier Orbitals: HOMO and LUMO 325
7.2.3. Conservation of Orbital Symmetry 326
7.2.4. Analysis in Maximum Symmetry 327
7.3. Examples 328
7.3.1. Cycloaddition 328
7.3.2. Intramolecular Cyclization 343
7.3.3. Generalized Woodward–Hoffmann Rules 350
7.4. Hückel–Möbius Concept 350
7.5. Isolobal Analogy 356
References 364

8 Space-Group Symmetries 371
8.1. Expanding to Infinity 371
8.2. One-Sided Bands 375
8.3. Two-Sided Bands 378
8.4. Rods, Spirals, and Similarity Symmetry 381
8.5. Two-Dimensional Space Groups 395
8.5.1. Simple Networks 401
8.5.2. Side-Effects of Decorations 406
8.5.3. Moirés 408
References 410

9 Crystals 413
9.1. Basic Laws 417
9.2. The 32 Crystal Groups 423
9.3. Restrictions 424
9.4. The 230 Space Groups 432
9.4.1. Rock Salt and Diamond 438
9.5. Dense Packing 440
9.5.1. Sphere Packing 442
9.5.2. Icosahedral Packing 446
9.5.3. Connected Polyhedra 449
9.5.4. Atomic Sizes 453
9.6. Molecular Crystals 456
9.6.1. Geometrical Model 457
9.6.2. Densest Molecular Packing 466
9.6.3. Energy Calculations and Structure Predictions 470
9.6.4. Hypersymmetry 474
9.6.5. Crystal Field Effects 476
9.7. Beyond the Perfect System 483
9.8. Quasicrystals 489
9.9. Returning to Shapes 494
References 496

Epilogue 505

Other Titles by the Authors 507

Index 509

Chapter 1

Introduction

> Artists treat facts as stimuli
> for the imagination,
> while scientists use their imagination
> to coordinate facts.
> *Arthur Koestler* [1]

Fundamental phenomena and laws of nature are related to symmetry and, accordingly, symmetry is one of science's basic concepts. Perhaps it is so important in human creations because it is omnipresent in the natural world. Symmetry is beautiful although alone it may not be enough for beauty, and absolute perfection may even be irritating. Function, utility, and aesthetic appeal are the reasons for symmetry in technology and the arts.

Much has been written about symmetry, for example, in Béla Bartók's music [2]. It is not known, however, whether he consciously applied symmetry or was simply led intuitively to the golden ratio so often present in his music. Another unanswerable question is how these symmetries contribute to the appeal of Bartók's music, and how much of this appeal originates from our innate sensitivity to symmetry. Bartók declined to discuss the technicalities of his composing and merely stated that he created after nature.

The world around us abounds in symmetries and they have been studied for centuries. More recently, research has probed into the role of symmetry in human interactions along with representatives of the animal kingdom. Special attention has been given to mate selection. One of the first appearances of this facet of symmetry in the popular press was an article in *The New York Times*, with an intriguing title, "Why Birds and Bees, Too, Like Good Looks" [3].

M. Hargittai, I. Hargittai, *Symmetry through the Eyes of a Chemist*, 3rd ed.,
DOI: 10.1007/978-1-4020-5628-4_1, © Springer Science+Business Media B.V. 2009

The above examples illustrate that we like to consider symmetry in a broader sense than how it just appears in geometry. The symmetry concept provides a good opportunity to widen our horizons and to bring chemistry closer to other fields of human activities. An interesting aspect of the relationship of chemistry with other fields was expressed by Vladimir Prelog in his Nobel lecture [4]:

> Chemistry takes a unique position among the natural sciences for it deals not only with material from natural sources but creates the major parts of its objects by synthesis. In this respect, as stated many years ago by Marcelin Berthelot, chemistry resembles the arts; the potential of creativity is terrifying.

Of course, even the arts are not just for the arts' sake and chemistry is certainly not done just for chemistry's sake. But in addition to creating new medicines, heat-resistant materials, pesticides, and explosives, chemistry is also a playground for the organic chemist to synthesize exotica including propellane and cubane, for the inorganic chemist to prepare compounds with multiple metal–metal bonds, for the stereochemist to model chemical reactions after a French parlor trick (cf. Section 2.7), and for the computational chemist to create undreamed-of molecules and to write detailed scenarios of as yet unknown reactions. Symmetry considerations play no small role in all these activities. The importance of blending fact and fantasy was succinctly expressed by Arthur Koestler in the chapter-opening quotation. Lucretius gave an early illustration of an imaginative use of the concept of shape in the first century BCE: "atoms with smooth surfaces would correspond to pleasant tastes, such as honey; but those with rough surfaces would be unpleasant" [5].

Chemical symmetry has been noted and investigated for centuries in crystallography which is at the border between chemistry and physics. It was more physics when crystal morphology and other properties of the crystal were described. It was more chemistry when the inner structure of the crystal and the interactions between its building units were considered. Later, descriptions of molecular vibrations and the establishment of selection rules and other basic principles happened in all kinds of spectroscopy. This led to another uniquely important place for the symmetry concept in chemistry with practical implications.

The discovery of handedness, or chirality, in crystals and molecules brought the symmetry concept nearer to the chemical laboratory. All this, however, concerned more the stereochemist, the structural chemist, the crystallographer, and the spectroscopist rather than the synthetic chemist. Symmetry used to be considered to lose its significance as soon as the molecules entered the chemical reaction. Orbital theory and the discovery of the conservation of orbital symmetry have encompassed even this area. It was signified by the 1981 Nobel Prize in chemistry awarded to Kenichi Fukui and Roald Hoffmann (Figure 1-1): "for their theories, developed independently, concerning the course of chemical reactions" [6].

During the past half a century, fundamental scientific discoveries have been aided by the symmetry concept. They have played a role in the continuing quest for establishing the system of fundamental particles [7]. It is an area where symmetry breaking has played as important a role as symmetry. The most important biological discovery since Darwin's theory of evolution was the double helical structure of the matter of heredity, DNA, by Francis Crick and James D. Watson (Figure 1-2) [8]. In addition to the translational symmetry of helices (see, Chapter 8), the molecular structure of deoxyribonucleic acid as a whole has C_2 rotational symmetry in accordance with the complementary nature of its two antiparallel strands [9]. The discovery of the double helix was as much a chemical discovery as it was important for biology, and lately, for the biomedical sciences.

In the 1980s, two important discoveries in molecular science and solid-state science were intimately connected with symmetry. One

Figure 1-1. Kenichi Fukui (*left*), 1994, and Roald Hoffmann, 1994 (photographs by the authors).

Figure 1-2. *Left*: James D. Watson, 2003; *Center*: a sculpture of the double helix by Bror Marklund at Uppsala University; and *Right*: Francis Crick (photographs by the authors).

was the C_{60} molecule, buckminsterfullerene [10] and fullerene chemistry. It has greatly contributed to the emergence of nanoscience and nanotechnology. The other discovery was the quasicrystals [11]. Buckminsterfullerene will be mentioned again in Section 3.7. and the quasicrystals in Section 9.8. Here, we present only some general considerations.

The C_{60} molecule was named after Buckminster Fuller (1895–1983), the American designer (Figure 1-3). The U.S. Pavilion at the Montreal Expo 1967 (Figure 1-4) was built according to his design and it inspired the discoverers of buckminsterfullerene in finding the

Figure 1-3. *Left*: Buckminster Fuller, 1973 (photograph by and courtesy of Lloyd Kahn, Bolinas, California); *Right*: Avogadro and his law on an Italian stamp.

Figure 1-4. The U.S. Pavilion at the Montreal Expo 1967 with a pentagon indicated in the close-up (photographs taken in 1995 by the authors).

structure of C_{60}. Fuller was not a bona fide scientist, but geometry was central to his peculiar philosophy. To him Avogadro's law (Figure 1-3) showed that chemists considered volumes as material domains and not merely as abstractions. Fuller recognized the importance of synergy for chemistry [12]:

> Chemists discovered that they had to recognize synergy because they found that every time they tried to isolate one element out of a complex or to separate atoms out, or molecules out, of compounds, the isolated parts and their separate behaviors never explained the associated behaviors at all. It always failed to do so. They had to deal with the wholes in order to be able to discover the group proclivities as well as integral characteristics of parts. The chemists found the Universe already in complex association and working very well. Every time they tried to take it apart or separate it out, the separate parts were physically divested of their associative potentials, so the chemists had to recognize that there were associated behaviors of wholes unpredicted by parts; they found there was an old word for it—synergy.

Curiously, Avogadro has also been proposed to be the godfather of fullerenes for he was the inventor of the concept of monoelemental compounds [13]. The suggestion came from D. E. H. Jones who had

brought up the idea of the hollow-shell graphite molecule almost two decades prior to the discovery of buckminsterfullerene [14]. Jones also referred to a biological analogy of what would be considered today a model of a giant fullerene molecule. A few pentagons are seen interspersed in the generally hexagonal pattern of *Aulonia hexagona* shown in Figure 1-5 [15]. The similarity is striking to Fuller's Geodesic Dome at the 1967 Montreal Expo.

In chemistry, the first suggestion of a C_{60} molecule came from Eiji Osawa (Figure 1-6) who tried to construct closed three-dimentional molecules with aromaticity and hit on the truncated icosahedral shape purely on the basis of symmetry considerations [17]. The next step was the computational work by Gal'pern (Figure 1-6) and Bochvar who determined the truncated icosahedral shape for C_{60} to represent an energy minimum [18]. These early reports originally appeared in Japanese and in Russian, respectively. They had no impact and received recognition only after the work of Harry Kroto, Richard Smalley, Robert Curl (Figure 1-7), and their students had brought great publicity to the new molecule.

The Geodesic Dome played an important role in leading the discoverers of buckminsterfullerene to the right hypothesis about its molecular structure. Both Kroto and Smalley had visited the Dome almost two decades before, and what they could vaguely remember assisted them and their colleagues to arrive at the highly symmetrical truncated icosahedral geometry (Figure 1-8) (see, also, Section 2.8

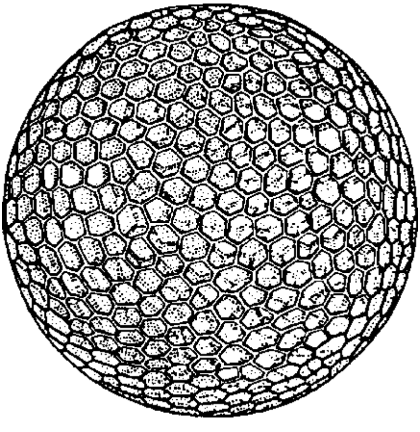

Figure 1-5. Ernst Häckel's *Aulonia hexagona* in D'Arcy W. Thompson, *On Growth and Form* [16].

Figure 1-6. Eiji Osawa (*left*), 1994 (photograph by the authors) and Elena Gal'pern (courtesy of Elena Gal'pern, Moscow).

on Polyhedra) during the exciting days following the crucial experiment [19].

Mathematicians have, of course, known for a long time [21] that one can close a cage of even-number of vertices with any number of hexagons (except one), provided that 12 pentagons are included in the network. The truncated icosahedron has 12 pentagons and 20 hexagons, and it is one of the semi-regular solids of Archimedes (see, Section 2.8). Leonardo da Vinci (1452–1519) drew a hollow framework of this structure to illustrate the book *De Divina Proportione* by Luca Pacioli (Figure 1-8). All such carbon substances

Figure 1-7. The principal discoverers of buckminsterfullerene: *From left to right*, Robert F. Curl, 1998; Harold W. Kroto, 1994; and Richard E. Smalley, 2004 (photographs by the authors).

Figure 1-8. Models of the truncated icosahedron: Leonardo da Vinci's drawing for Luca Pacioli's *De Divina Proportione* (*left*) and decoration at the Topkapi Sarayi in Istanbul (photograph by the authors) [20].

whose cage molecules contain 12 pentagons and various numbers of hexagons, are called fullerenes, of which C_{60} has the special name buckminsterfullerene. Another artful representative of this shape is above an entrance to an exhibition hall at the Topkapi Palace (Topkapi Sarayi, in Turkish) in Istanbul (Figure 1-8).

An early and beautiful example of the fullerene-type structures was found in China [22]. Dragon sculptures are common in China as guards standing in front of important buildings. They appear in pairs. The female has a baby lion under the left paw and the male has a sphere under the right paw. This sphere is said to represent a ball made of strips of silk which was a favorite toy in ancient China. The surface of the ball is usually decorated by a regular hexagonal pattern. We know, however, that it is not possible to cover the surface of the sphere by a regular hexagonal pattern. Usually, there are considerable chunks of the sphere hidden by the dragon's paw and the stand itself on which the dragon and the sphere stand. There is at least one dragon sculpture (Figure 1-9) under whose paw the sphere is decorated by a hexagonal pattern interspersed by pentagonal shapes. This sculpture stands in front of the Gate of Heavenly Purity in the Forbidden City, and dates back to the reign of Qian Long (1736–1796) of the Qing Dynasty. Balls made of strips of silk are popular decorations in Japan. They are called temari and patterns corresponding to the buckminsterfullerene structure occur among them [23].

Figure 1-9. Gold-plated dragon sculpture in front of the Gate of Heavenly Purity (Qianqingmen) in the Forbidden City, Beijing, with close-up (photographs by the authors) [24].

Incidentally, the stormy interest in buckminsterfullerene started subsiding a few years after the initial discovery because the original discoverers only observed but failed to produce the substance, so no chemistry could have been performed on it. Wolfgang Krätschmer and Donald Huffman (Figure 1-10) and their students changed this situation in 1990 when they obtained quantities of C_{60} from graphite in a discharge experiment [25]. Their work made the new substance commonly available. The buckminsterfullerene story had an appeal for a broad readership even beyond chemists [26].

The other important symmetry-related discovery was the quasicrystals. Both the truncated icosahedral structure of buckminsterfullerene and the regular but nonperiodic network of the quasicrystals are related to fivefold symmetry. In spite of this intimate connection between them at an intellectual level, their stories did not cross. The conceptual linkage between them is provided by Fuller's physical geometry and this is also what relates them to the icosahedral structure of viruses (see, Section 9.5.2 on Icosahedral Packing).

The actual experimental discovery of quasicrystals was a serendipity, notwithstanding some pertaining predictions [28]. It used

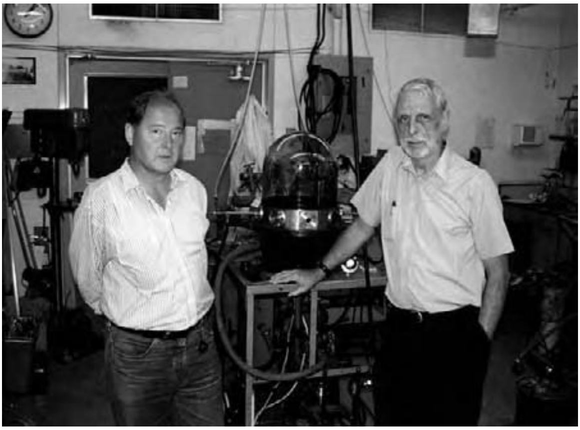

Figure 1-10. Wolfgang Krätschmer and Donald Huffman re-enacting their first production of buckminsterfullerene, in 1999 in Tucson, Arizona (photograph by the authors) [27].

to be a fundamental dogma of crystallography that fivefold symmetry is a noncrystallographic symmetry. We shall return to this question in Section 9.3. There have been many attempts to cover the surface with regular pentagons without gaps and overlaps and some examples [29] are shown in Figure 1-11. Then, Roger Penrose found two elements that, by appropriate matching, could tile the surface with long-range pentagonal symmetry though only in a nonperiodic way

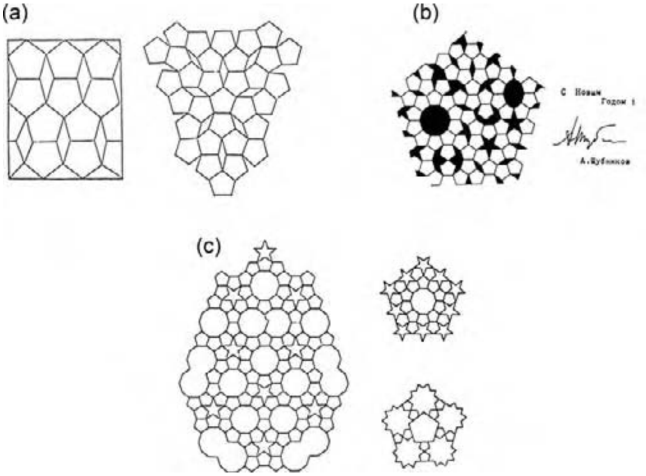

Figure 1-11. Attempts of pentagonal tiling by (**a**) Dürer (after Crowe) [32]; (**b**) Shubnikov (after Mackay); and (**c**) Kepler (after Danzer et al.) [33, 34].

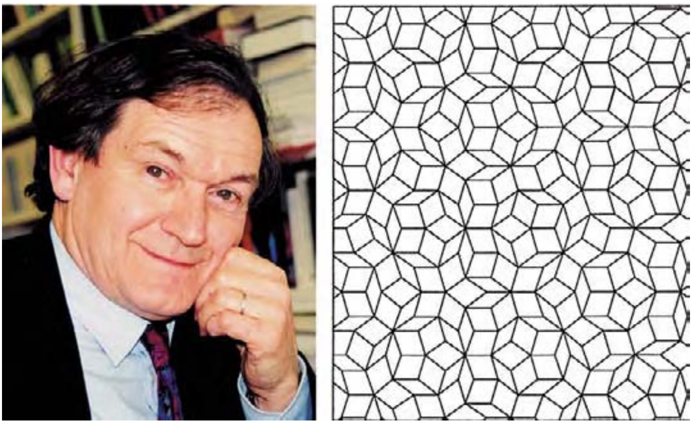

Figure 1-12. Roger Penrose, 2000 (photograph by the authors) and a Penrose tiling.

(Figure 1-12) [30]. This pattern was extended by Alan Mackay into the third dimension and he even produced a simulated diffraction pattern that showed 10-foldedness (Figure 1-13) [31]. It was about the same time that Dan Shechtman was experimenting with metallic phases of various alloys cooled with different speeds and observed 10-foldedness in an actual electron diffraction experiment (Figure 1-14) for the first time. The discovery of quasicrystals has added new perspective to crystallography and the utilization of symmetry considerations.

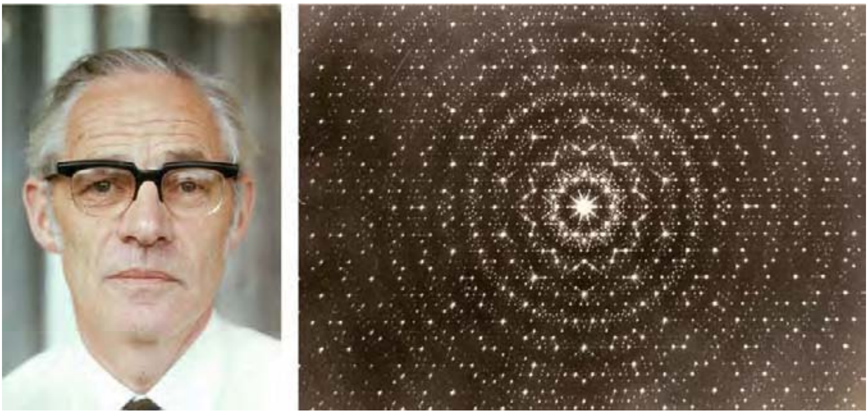

Figure 1-13. Alan L. Mackay, 1982 (photograph by the authors) and his simulated "electron diffraction" pattern of three-dimensional Penrose tiling [31] (photograph courtesy of Alan Mackay, London).

Figure 1-14. Dan Shechtman (photograph by the authors) and his electron diffraction pattern with 10-fold symmetry (photograph courtesy of Dan Shechtman, Haifa).

While considering the symmetries of individual molecules or extended structures, we should not lose sight of the place of symmetry considerations in the large picture of studying nature. In this, we turn to the chemical engineer turned theoretical physicist Eugene P. Wigner (1902–1995). He worked out fundamental relationships of profound importance for the place of symmetry with respect to the laws of nature and observable physical phenomena. In this discussion, the term physics stands for physical sciences that include chemistry. In his Nobel lecture, Wigner stated that the symmetry principles "provide a structure and coherence to the laws of nature just as the laws of nature provide a structure and coherence to a set of events," the physical phenomena [35]. David J. Gross, a recent Nobel laureate physicist summarized Wigner's teachings in a simple diagram [36]:

Symmetry principles → Laws of nature → Physical phenomena

Wigner (Figure 1-15) was well known for his legendary politeness and modesty that was perceived by some as somewhat forced and artificial. However, there was nothing forced or artificial when he showed modesty in formulating the principal task of physics and stressed the limitations in its ambitions:

> Physics does not endeavor to explain nature. In fact, the great success of physics is due to a restriction of its objectives: it only endeavors to explain

Figure 1-15. Eugene P. Wigner with one of the authors in 1969, in front of the (then) Department of Physics at the University of Texas at Austin (photograph by unknown photographer).

> the regularities in the behavior of objects. This renunciation of the broader aim, and the specification of the domain for which an explanation can be sought, now appears to us an obvious necessity. In fact, the specification of the explainable may have been the greatest discovery of physics so far. . . .
>
> The regularities in the phenomena which physical science endeavors to uncover are called the laws of nature. The name is actually very appropriate. Just as legal laws regulate actions and behavior under certain conditions but do not try to regulate all actions and behavior, the laws of physics also determine the behavior of its object of interest only under certain well-defined conditions but leave much freedom otherwise [37].

To emphasize the pioneering character of Wigner's contribution, we quote another Nobel laureate theoretical physicist, Steven Weinberg, according to whom "Wigner realized, earlier than most physicists, the importance of thinking about symmetries as objects of interest in themselves" [38]. Wigner had formulated his views on symmetries in the 1930s when physicists talked about symmetries in the context of specific theories of nuclear force. "Wigner was able," Weinberg continues, "to transcend that and he discussed symmetry in a way, which didn't rely on any particular theory of nuclear force" [39].

Another Nobel laureate physicist, Gerard ‘t Hooft traced back to Wigner the notion that symmetry can break in many different ways and that “Both symmetry and symmetry breaking are examples of patterns that we see in Nature” [40].

Beyond Wigner’s statements of general validity, the question may be asked whether “chemical symmetry” differs from any other kind of symmetry? Furthermore, whether symmetries in the various branches of the physical sciences can be distinguished as to their characteristic features and whether they could be hierarchically related? The symmetries in the great conservation laws of physics [41] are, of course, present in any chemical system. The symmetries of molecules and their reactions are part of the fabric of biological structure. Left-and-right symmetry is so important for living matter that it may be matched only by the importance of “left-and-right” symmetry in the world of fundamental particles, including the violation of parity, as if a circle is closed, but that is, of course, an oversimplification.

When we stress the importance of symmetry, it is not equivalent with declaring that everything must be symmetrical. In particular, when the importance of left-and-right symmetry is stressed, it is their relationship, rather than their equivalence, that has outstanding significance.

It has already been referred to that symmetry considerations have continued their fruitful influence on the progress of contemporary chemistry. This is so for contemporary physics as well. It is almost surprising that fundamental conclusions with respect to symmetry could be made even during recent decades. It was related by C. N. Yang that Paul A. Dirac considered Albert Einstein’s most important contributions to physics “his introduction of the concept that space and time are symmetrical” [42]. The same Dirac also had the prescience to write as early as 1949 that “I do not believe that there is any need for physical laws to be invariant under reflections” [43]. Then, in 1956, Tsung Dao Lee and Chen Ning Yang (Figure 1-16) suggested a set of experiments to show that conservation of parity may be violated in the weak force of nuclear interations [44]. Indeed, three different experiments almost simultaneously confirmed Lee and Yang’s supposition within months [45]. The discovery happened “swiftly” during an “exciting period” [46]. It had long-range effects and since then *broken symmetries* have received increasing attention [47]. The term “relates to situations in which

Figure 1-16. Tsung Dao Lee and Chen Ning Yang at the time of the Nobel ceremonies in December 1957 in Stockholm (courtesy of the Manne Siegbahn Institute through Ingmar Bergström, Stockholm).

symmetries which we expect to hold are valid only approximately or fail completely" [48]. The three basic possibilities are incomplete symmetry, symmetry broken by circumstances, and spontaneously broken symmetry.

"Symmetry is a stunning example of how a rationally derived mathematical argument can be applied to descriptions of nature and lead to insights of the greatest generality" [49]. But what is symmetry? We may not be able to answer this question satisfactorily, at least not in all its possible aspects. According to the crystallographer (and symmetrologist) E. S. Fedorov—as quoted by A. V. Shubnikov—"symmetry is the property of geometrical figures to repeat their parts, or more precisely, their property of coinciding with their original position when in different positions" [50]. To this, the symmetrologist (and crystallographer) A. V. Shubnikov added that while symmetry is a property of geometrical figures, obviously, "material figures" may also have symmetry. He further stated that only parts which are in some sense equal among themselves can be repeated, and noted the two kinds of equality, to wit, congruent equality and mirror equality. These two equalities are the subsets of the metric equality concept of Möbius, according to whom "figures are equal if the distances between any given points on one figure are equal to the distances between the corresponding points on another figure" [51]. According to the geometer H. S. M. (Donald) Coxeter,

"When we say that a figure is 'symmetrical' we mean that there is a congruent transformation which leaves it unchanged as a whole, merely permuting its component elements" [52].

Symmetry also connotes harmony of proportions, which is a rather vague notion, according to Hermann Weyl [53]. This very vagueness, at the same time, often comes in handy when relating symmetry and chemistry, or generally speaking, whenever the symmetry concept is applied to real systems. Mislow and Bickart [54] communicated an epistemological note on chirality in which much of what they have to say about chirality, as this concept is being applied to geometrical figures versus real molecules, solvents, and crystals, is true about the symmetry concept as well. They argue that "it is unreasonable to draw a sharp line between chiral and achiral molecular ensembles: in contrast to the crisp classification of geometric figures, one is dealing here with a fuzzy borderline distinction, and the qualifying 'operationally' should be implicitly or explicitly attached to 'achiral' or 'racemic' whenever one uses these terms with reference to observable properties of a macroscopic sample." Further, they quote Scriven [55]: "when one deals with natural phenomena, one enters 'a stage in logic in which we recognize the utility of imprecision.'" The human ability to geometrize non-geometrical phenomena greatly helps to recognize symmetry even in its "vague" and "fuzzy" variations. In accordance with this, Weyl referred to Dürer who "considered his canon of the human figure more as a standard from which to deviate than as a standard toward which to strive" [56].

Symmetry in its rigorous sense helps us to decide problems quickly and qualitatively. The answers lack detail, however [57]. On the other hand, the vagueness and fuzziness of the broader interpretation of the symmetry concept allow us to talk about degrees of symmetry, to say that something is more symmetrical than something else. An absolutist geometrical approach would allow us to distinguish only between symmetrical and asymmetrical possibly with dissymmetrical thrown in for good measure. So there must be a range of criteria according to which one can decide whether something is symmetrical, and to what degree. These criteria may very well change with time. A case in point is the question as to whether or not molecules preserve their symmetry upon entering a crystal structure or upon the crystal undergoing phase transition. Our notion about structures and symmetries may evolve as more accurate data become available

(though their structures and symmetries are unchanged, of course, by our notions). A whole new approach is developing to analyze symmetry properties in terms of a continuous scale rather than of a discrete “yes/no” [58].

Recognizing structural and other kinds of regularities has always been important in chemistry. Above we quoted Wigner in connection with the tasks of the physical sciences. He stressed the importance of observing regularities. He learned this from his mentor in preparing his doctoral research, Michael Polanyi. Wigner mentioned this in his two-minute speech at the Nobel award banquett in Stockholm in 1963:

> I do wish to mention the inspiration received from Polanyi. He taught me, among other things, that science begins when a body of phenomena is available which shows some coherence and regularities, that science consists in assimilating these regularities and in creating concepts which permit expressing these regularities in a natural way. He also taught me that it is this method of science rather than the concepts themselves (such as energy) which should be applied to other fields of learning [59].

Linus Pauling was a master in noticing regularities among large amounts of data. It has been argued, for example, that at the time of the first edition of *The Nature of the Chemical Bond* [60], Linus Pauling had access to less than 0.01% of the structural information of 50 years later, yet his ideas on structure and bonding have stood the test of time [61].

The history of periodic tables and especially Dmitrii I. Mendeleev’s seminal discovery, also demonstrates chemists’ never-ending quest for beauty and harmony [62]. He was looking for a simple system for presenting the elements as he was writing a general chemistry text for his students. The Soviet stamp block, issued for the centennial of the Periodic Table, depicts its earliest version (Figure 1-17a). Approximately 700 periodic tables were published during the first one hundred years after the original discovery in 1869. E. G. Mazurs [63] collected, systematized, and analyzed them in a unique study. Classification of all the tables reduced their number to 146 different types

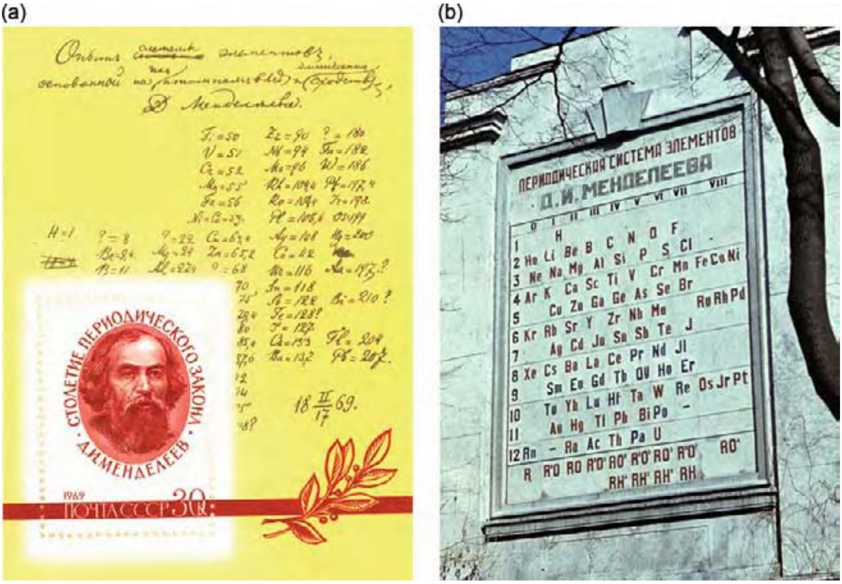

Figure 1-17. (**a**) Soviet stamp block issued to the centenary of Mendeleev's Periodic System; (**b**) The Periodic Table of the Elements as a fresco at what is today the Mendeleev Institute of Metrology in St. Petersburg and was the Board of Weights and Measures in Mendeleev's time (photograph by and courtesy of Alexander Belyakov, St. Petersburg) [65].

and subtypes which are described by such terms as "helices, space lemniscates, space concentric circles, space squares, spirals, series tables, zigzags, parallel lines, step tables, tables symmetrical about a vertical line, mirror image tables, tables of one revolution and of one row, tables of planes, revolutions, cycles, right side as well as left side electronic configuration tables, tables of concentric circles and parallel lines, right side as well as left side shell and subshell tables." Figure 1-17b shows the traditional, rectangular-shaped table in form of a wall-decoration displayed on the facade of the St. Petersburg college building where Mendeleev used to work. The characteristic symmetry of this arrangement is periodicity itself. Figure 1-18 is a spiral representation of the Periodic System (drawn proportionally to the increasing mass of the elements, prior to the understanding of the foundation of the system in the electronic structure of the elements) [64].

The quest for symmetry and harmony has, of course, contributed more than mere aesthetics in establishing the Periodic Table of

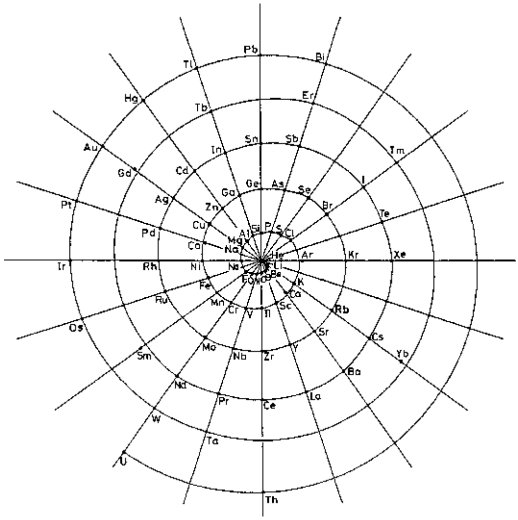

Figure 1-18. Spiral periodic system, after H. Erdmann [66] (computer graphics by Judit Molnár, Budapest).

the elements. Beauty and reason blend in it in a natural fashion. C. A. Coulson, theoretical chemist and professor of mathematics, concluded his Faraday lecture on symmetry with the words:

> Man's sense of shape—his feeling for form—the fact that he exists in three dimensions—these must have conditioned his mind to thinking of structure, and sometimes encouraged him to dream dreams about it. I recall that it was Kekulé himself who said: "Let us learn to dream, gentlemen, and then we shall learn the truth." Yet we must not carry this policy too far. Symmetry is important, but it is not everything. To quote Michael Faraday writing of his childhood: "Do not suppose that I was a very deep thinker and was marked as a precocious person. I was a lively imaginative person, and could believe in the *Arabian Nights* as easily as in the Encyclopedia. But facts were important to me, and saved me." It is when symmetry interprets facts that it serves its purpose: and then it delights us because it links our study of chemistry with another world of the human spirit—the world of

order, pattern, beauty, satisfaction. But facts come first. Symmetry encompasses much—but not quite all! [67]

References

1. A. Koestler, *Insight and Outlook,* Macmillan, London and New York, 1949.
2. E. Lendvai, in *Module, Proportion, Symmetry, Rhythm,* G. Kepes, ed., George Braziller, New York, 1966.
3. N. Angier, "Why Birds and Bees, Too, Like Good Looks." *The New York Times*, February 8, 1994, p. C1. The title of the article can be taken as referring to one of Cole Porter's most popular songs "Let's Do It" ("Let's Fall in Love") that starts with the words, "that's why birds do it, bees do it,. . ."
4. V. Prelog, "Chirality in Chemistry." *Science* 1976, 193, 17–24.
5. Quoted in C. A. Coulson, "Symmetry." *Chem. Britain* 1968, 4, 113–120.
6. *Nobel Foundation Directory*.
7. See, e.g., M. Veltman, *Facts and Mysteries in Elementary Particle Physics.* World Scientific, Singapore, 2003; L. Lederman (with D. Teresi), *The God Particle: If the Universe Is the Answer, What Is the Question?* Mariner Books, 2006; F. Wilczek, *Fantastic Realities: 49 Mind Journeys and a Trip to Stockholm.* World Scientific, Singapore, 2006.
8. J. D. Watson, F. H. C. Crick, "A Structure for Deoxyribose Nucleic Acid." *Nature* 1953, April 25, 737–738.
9. See, e.g., I. Hargittai, *The DNA Doctor: Candid Conversations with James D.Watson*. World Scientific, Singapore, 2007, pp. 10, 169, 173–174.
10. H. W. Kroto, J. R. Heath, S. C. O'Brien, R. F. Curl, R. E. Smalley, "C_{60}: Buckminsterfullerene." *Nature* 1985, 318, 162–163.
11. D. Shechtman, I. Blech, D. Gratias, J. W. Cahn, "Metallic Phase with Long Range Orientational Order and No Translational Symmetry." *Phys. Rev. Lett.* 1984, 53, 1951–1953.
12. R. B. Fuller, *Synergetics: Explorations in the Geometry of Thinking*, Macmillan, New York, 1975, p. 4.
13. D. E. H. Jones, "Dreams in a Charcoal Fire—Predictions about Giant Fullerenes and Graphite Nanotubes." *Phil. Trans. R. Soc. London* 1993, 343, 9–18.
14. D. E. H. Jones, "Ariadne." *New Scientist* 1966, 35, 245.
15. D. W. Thompson, *On Growth and Form*, Cambridge University Press, 1961.
16. Ibid.
17. E. Osawa, "Superaromacity" (in Japanese). *Kagaku* (Kyoto) 1970, 25, 854–863.
18. D. A. Bochvar, E. G. Gal'pern, "Hypothetical Systems: Carbododecahedron, s-Icosahedron, and Carbo-s-Icosahedron." *Dokl. Akad. Nauk S. S. S. R.* 1973, 209, 610–612.

19. See, e.g., H. W. Kroto, "C_{60}^{B} Buckminsterfullerene, Other Fullerenes and the Icospiral Shell." In *Symmetry 2, Unifying Human Understanding*, I. Hargittai, ed., Pergamon Press, Oxford and New York, 1989, pp. 417–423.
20. I. Hargittai, "Buckminsterfullerene in the Sarayi." *Chem. Intell.* 1996, 2(4), 4.
21. P. C. Gasson, *Geometry of Spacial Forms*, Ellis Horwood, Chichester, 1983, pp. ix–x.
22. I. Hargittai, "Fullerene geometry under the lion's paw." *Math. Intell.* 1995, 17(3), 34–36.
23. I. Hargittai, "Japanese symmetries." *Forma* 1994, 8, 327–333.
24. Hargittai, *Math. Intell.* 34–36.
25. W. Krätschmer, L. D. Lamb, K. Fostiropoulos, D. R. Huffman, "Solid C_{60}: a new form of carbon." *Nature* 1990, 347, 354–358.
26. H. Aldersey-Williams, *Perfect Symmetry: The Discovery of the Buckyball*. Wiley, New York, 1995; J. Baggott, *Perfect Symmetry: The Accidental Discovery of Buckminsterfullerene*. Oxford University Press, 1994.
27. B. Hargittai, I. Hargittai, "Rising to New Heights." *Chem. Intell.* 2000, 6(3), 42–43. This article is a pictorial report about the experiment at the Department of Physics at the University of Arizona on August 30, 1999, in which Donald Huffman and Wolfgang Krätschmer re-enacted the first ever production of buckminsterfullerene.
28. A. L. Mackay, "Crystallography and the Penrose Pattern." *Physica* 1982, 114A, 609–613.
29. D. W. Crowe, in *Fivefold Symmetry*, I. Hargittai, ed., World Scientific, Singapore, 1992, p. 465; L. Danzer, B. Grünbaum and G. C. Shephard, "Can All Tiles of a Tiling Have Five-fold Symmetry?" *Am. Math. Monthly* 1982, 89, 568–570 and 583–585; A. L. Mackay, "De Nive Quinquangula: On the Pentagonal Snowflake." *Kristallografiya (Sov. Phys. Crystallogr.)* 1981, 26, 910–919 (517–522).
30. R. Penrose, "Pentaplexity." *Math. Intell.* 1979/80, 2, 32–37.
31. Mackay, *Physica*, 609–613.
32. D. W. Crowe, "Albrecht Dürer and the Regular Pentagon." In *Fivefold Symmetry*, ed. I. Hargittai, World Scientific, Singapore, 1992, pp. 465–487, p. 483.
33. L. Danzer, B. Grünbaum, G. C. Shephard, "Can All Tiles of a Tiling Have Five-fold Symmetry?" *Am. Math. Monthly* 1982, 89, 568–570 and 583–585.
34. Mackay, *Kristallografiya (Sov. Phys. Crystallogr.)* 910–919 (517–522).
35. E. P. Wigner, Nobel lecture. In *Nobel Lectures Including Presentation Speeches and Laureates' Biographies: Physics 1963–1970*. World Scientific, Singapore, 1998, pp. 6–17.
36. D. J. Gross, "Symmetry in Physics: Wigner's Legacy," *Physics Today* December 1995, 46–50.

37. Wigner, *Nobel Lectures Including Presentation Speeches and Laureates' Biographies: Physics 1963–1970*, pp. 6–17, pp. 6–7.
38. Steven Weinberg interview in M. Hargittai, I. Hargittai, *Candid Science IV: Conversations with Famous Physicists*. Imperial College Press, London, 2004, pp. 20–31, pp. 29–30.
39. Ibid.
40. Gerard 't Hooft interview in Hargittai, Hargittai, *Candid Science IV*, pp. 110–141, p. 121.
41. See, e.g., R. Feynman, *The Character of the Physical Law*, The MIT Press, Cambridge, MA, 1967.
42. C. N. Young, "Symmetry and Physics." In *The Oskar Klein Memorial Lectures. Vol. 1: Lectures by C. N. Yang and S. Weinberg with translated reprints by O. Klein*. Ed. Gösta Ekspong, World Scientific, Singapore, 1991, pp. 11–33, p. 23.
43. P. A. M. Dirac, "Forms of Relativistic Dynamics." *Rev. Mod. Phys*. 1949, 21, 392–399. See, also, R. H. Dalitz, R. Peierls, "Paul Adrien Maurice Dirac." *Biogr. Mem. Fellows Roy. Soc*. 1986, 32, 137–185, p. 159.
44. T. D. Lee, C. N. Yang, "Question of Parity Conservation in Weak Interactions." *Phys. Rev.* 1956, 104, 254–258.
45. C. S. Wu, E. Ambler, R. W. Hayward, D. D. Hoppes, R. P. Hudson, "Experimental test of parity conservation in beta decay." *Phys. Rev*. 1957, 105, 1413–1415; R. L. Garwin, L. Lederman, M. Weinrich, "Observations of the Failure of Conservation of Parity and Charge Conjugation in Meson Decays: the Magnetic Moment of the Free Muon." *Phys. Rev*. 1957, 105, 1415–1417; J. I. Friedman, V. L. Telegdi, "Nuclear Emulsion Evidence for Parity Nonconservation in the Decay Chain. $\pi^+ - \mu^+ - e^+$." *Phys. Rev*. 1957, 105, 1681–1682.
46. C.-S. Wu, "The Discovery of Nonconversation of Parity in Beta Decay." In R. Novick, ed., *Thirty Years since Parity Nonconservation: A Symposium for T. D. Lee*. Birkhäser, Boston, 1988, pp. 18–35, p. 19.
47. See, e.g., M. Hargittai, "Fifty years of parity violation—and its long-range effects." *Struct. Chem.* 2006, 17, 455–457.
48. R. Peierls, "Broken symmetries (Dirac Memorial Lecture, Cambridge, 15 June 1992)." *Contemp. Phys*. 1992, 33, 221–226; p. 221.
49. G. M. Edelman, *Bright Air, Brilliant Fire: On the Matter of Mind*. BasicBooks, 1992, p. 199.
50. A. V. Shubnikov, *Simmetriya i antisimmetriya konechnykh figur,* Izd. Akad. Nauk S.S.S.R., Moscow, 1951.
51. H. S. M. Coxeter, *Regular Polytopes,* Third Edition, Dover Publications, New York, 1973.
52. Ibid.
53. H. Weyl, *Symmetry*. Princeton University Press, Princeton, New Jersey, 1952, p. 3.
54. K. Mislow, P. Bickart, "An Epistemological Note on Chirality." *Israel J. Chem.* 1976/77, 15, 1–6.
55. M. Scriven, "The Logic of Criteria." *J. Philos*. 1959, 56, 857–868.

56. Weyl, *Symmetry*, p. 65.
57. R. G. Pearson, *Symmetry Rules for Chemical Reactions, Orbital Topology and Elementary Processes,* Wiley-Interscience, New York, 1976.
58. See, e.g., H. Zabrodsky, D. Avnir, in *Advances in Molecular Structure Research*, M. Hargittai and I. Hargittai, eds., JAI Press, Greenwich, Connecticut, 1994; D. Avnir, O. Katzenelson, S. Keinan, M. Pinsky, Y. Pinto, Y. Salomon, H. Zabrodsky Hel-Or, "The Leasurement of Symmetry and Chirality: Conceptual Aspects." In D. H. Rouvray, ed., *Concepts in Chemistry: A Contemporary Challenge*. Wiley, New York, 1996, pp. 283–324.
59. E. P. Wigner, "City Hall Speech—Stockholm, 1963." In E. P. Wigner, *Symmetries and Reflections: Scientific Essays*. Indiana University Press, Bloomington, Indiana, 1963, pp. 262–263.
60. L. Pauling, *The Nature of the Chemical Bond,* Cornell University Press, Ithaca, NY, 1939 (2 nd edition 1940, 3rd edition 1960).
61. P. Murray-Rust, in *Computer Modelling of Biomolecular Processes*, J. M. Goodfellow and D. S. Moss., eds., Ellis Horwood, New York, 1992.
62. E. R. Scerri, *The Periodic Table: Its Story and Its Significance*. Oxford University Press, 2007.
63. E. G. Mazurs, *Graphic Representations of the Periodic System During One Hundred Years*, The University of Alabama Press, University, Alabama, 1974.
64. H. Erdmann, *Lehrbuch der anorganischen Chemie*, Dritte Auflage, F. Vieweg und Sohn, Braunschweig, 1902.
65. B. Hargittai, I. Hargittai, "Dmitrii I. Mendeleev: A Centennial." *Structural Chemistry* 2007, 18, 253–255.
66. Erdman, *Lehrbuch der anorganischen Chemie*.
67. C. A. Coulson, "Symmetry." *Chem. Britain* 1968, 4, 113–120.

Chapter 2

Simple and Combined Symmetries

Beauty is the first test. . .
Godfrey Harold Hardy [1]

2.1. Bilateral Symmetry

The simplest and most common of all symmetries is bilateral symmetry, yet at first sight, it does not appear as overwhelmingly important in chemistry as in our every-day life. The human body has bilateral symmetry, except for the asymmetric location of some internal organs. A unique description of the symmetry of the human body is given by Thomas Mann in *The Magic Mountain* as Hans Castorp is telling about his love to Clawdia Chauchat* [2]:

> How bewitching the beauty of a human body, composed not of paint or stone, but of living, corruptible matter charged with the secret fevers of life and decay! Consider the wonderful symmetry of this structure: shoulders and hips and nipples swelling on either side of the breast, and ribs arranged in pairs, and the navel centered in the belly's softness, and the dark sex between the thighs. Consider the shoulder blades moving beneath the silky skin of the back, and the back-bone in its descent to the paired richness of the cool buttocks, and the great branching of vessels

*This passage is in French in both the German original and English translation of Mann's *The Magic Mountain* (see, References).

M. Hargittai, I. Hargittai, *Symmetry through the Eyes of a Chemist,* 3rd ed.,
DOI: 10.1007/978-1-4020-5628-4_2, © Springer Science+Business Media B.V. 2009

> and nerves that passes from the torso to the arms by way of the arm pits, and how the structure of the arms corresponds to that of the legs!

Earlier, Mann discusses the symmetry of the human body in more detail, stressing the harmony between its external appearance and internal organization [3]:

> It leaned thus, turning to smile, the gleaming elbows akimbo, in the paired symmetry of its limbs and trunk. The acrid, steaming shadows of the armpits corresponded in a mystic triangle to the pubic darkness, just as the eyes did to the red, epithelial mouth-opening, and the red blossoms of the breast to the navel lying perpendicularly below. . .
>
> For Hans Castorp understood that this living body, in the mysterious symmetry of its blood-nourished structure, penetrated throughout by nerves, veins, arteries, and capillaries; with its inner framework of bones—marrow-filled tubular bones, blade-bones, vertebræ—which with the addition of lime had developed out of the original gelatinous tissue and grown strong enough to support the body weight; with the capsules and well-oiled cavities, ligaments and cartilages of its joints, its more than two hundred muscles, its central organs that served for nutrition and respiration, for registering and transmitting stimuli, its protective membranes, serous cavities, its glands rich in secretions; with the system of vessels and fissures of its highly complicated interior surface, communicating through the body-openings with the outer world—he understood that this ego was a living unit of a very high order, remote indeed from those very simple forms of life which breathed, took in nourishment, even thought, with the entire surface of their bodies.

Figure 2-1. Egyptian sculpture from 2700 BCE (photograph by and courtesy of László Vámhidy, Pécs, Hungary).

The bilateral symmetry of the human body is emphasized by the static character of many Egyptian sculptures (Figure 2-1). Mobility and dynamism, however, do not diminish the impression of bilateralness of the human body (Figure 2-2).

Figure 2-2. Bilateral symmetry of the human body: Sculptures at the top of a building at Piccadilly Circus, London (photograph by the authors).

Already Kepler noted in connection with the shape of the animals that the

> . . .upper and lower depends on their habitat, which is the surface of the earth . . . The second distinction of front and back is conferred on animals to put in practice motions that tend from one place to another in a straight line over the surface of the earth . . . bodily existence entailed the third diameter, of right and left, should be added, whereby an animal becomes so to speak doubled [4].

Bilateral symmetry is very common in the animal kingdom (Figure 2-3). It always appears when *up* and *down* as well as *forward* and *backward* are different, whereas left-bound and right-bound motion have the same probability. As translational motion along a straight line is the most characteristic for the vast majority of animals on Earth, their bilateral symmetry is trivial. This symmetry is characterized by a *reflection plane*, or *mirror plane*, and its usual label is *m*.

Bilateral symmetry is found in some flowers, conspicuously, in orchids (Figure 2-4). Also, leaves often have bilateral symmetry, but it may be only accidental for a tree. Generally, trees and many other

Figure 2-3. Animals of bilateral symmetry (photographs by Zoltán Bagosi, Budapest Zoo, used with permission).

Figure 2-4. Flowers and leaves of bilateral symmetry (photographs by the authors).

plants have radial, cylindrical, or conical symmetries with respect to the trunk and stem. Although these symmetries may occur in a very approximate way, they can be recognized without any ambiguity (Figure 2-5).

Figure 2-5. Conical and radial symmetries of trees (photographs by the authors).

The symmetry plane of the human face is sometimes emphasized by artists (Figure 2-6a–c) while other artists idealize the faces they present (Figure 2-6d–f). Of course, there are minute variations, or even considerable ones as we age, between the left and right sides of the human face (see, e.g., Figure 2-7). Differences between the left and right hemispheres of the brain have been the subject of intensive studies [5].

Bilateral symmetry has outstanding importance in man-made objects due to its functional role. The bilateral symmetry of various vehicles, for example, is determined by their translational motion. On the other hand, the cylindrical symmetry of the Lunar Module is consistent with its function of vertical motion with respect to the

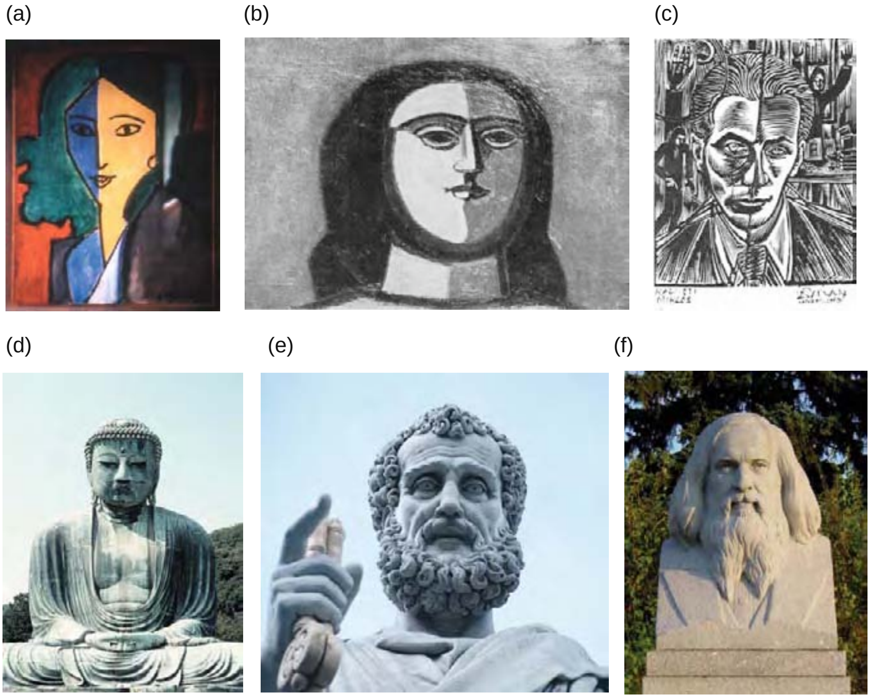

Figure 2-6. Human faces in artistic expression. (**a**) Henri Matisse, *Portrait of Lydia Delektroskaya* (reproduced by permission from the State Hermitage Museum, St. Petersburg); (**b**) Jenő Barcsay, *Woman's head* (used with permission from Ms. Barcsay); (**c**) George Buday, *Miklós Radnóti*, wood-cut, 1969 (used with permission from George Buday, R. E.); (**d**) Buddha sculpture in Japan; (**e**) St. Peter at the St. Peter's Square, Rome; (**f**) Bust of D. I. Mendeleev in front of Moscow State University (**d**; **e**; **f**, photographs by the authors).

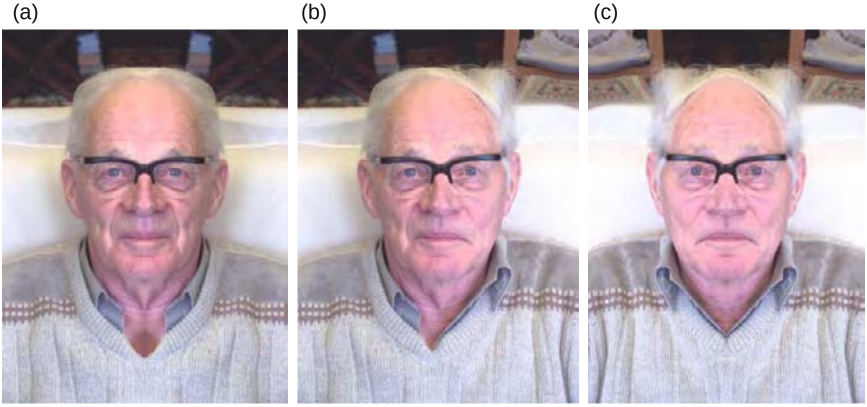

Figure 2-7. Professor Alan L. Mackay's face; (**a**) Right-side composite; (**b**) Original; (**c**) Left-side composite (photographs by the authors, used with permission of Alan L. Mackay, London).

moon's surface. Examples of cylindrical symmetry, related to the preferential importance of the vertical direction are the stalactites and the stalagmites in caves (Figure 2-8), formed of calcium carbonate. The occurrence of radial-type symmetries rather than more restricted ones necessitates a spatial freedom in all relevant directions. Thus, for example, the copper formation in Figure 2-9a has a tendency to form cylindrically symmetric structures. On the other hand, the solidified iron dendrites obtained from iron-copper alloys, after dissolving away the copper, display bilateral symmetry in Figure 2-9b.

Both folk music and music by master composers are rich in symmetries. Figure 2-10 shows two examples with bilateral symmetry. The first example is from Bartók's *Microcosmos* series written specifi-

Figure 2-8. Calcium carbonate stalactites and stalagmites in a cave in southern Germany (photographs by the authors).

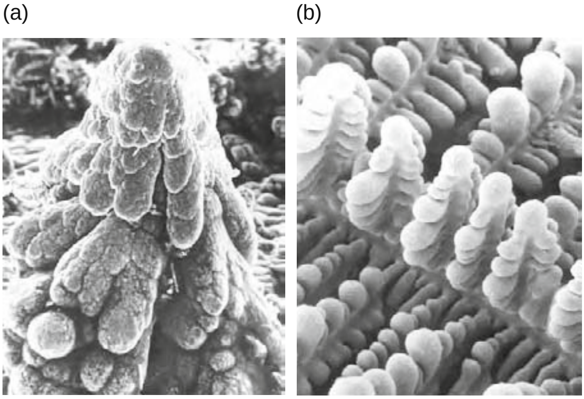

Figure 2-9. (**a**) Electrolytically deposited copper, magnification × 1000. Courtesy of Maria Kazinets, Beer Sheva; (**b**) Directionally solidified iron dendrites from an iron-copper alloy after dissolving away the copper, magnification × 2600. Courtesy of J. Morral, Storrs, Connecticut.

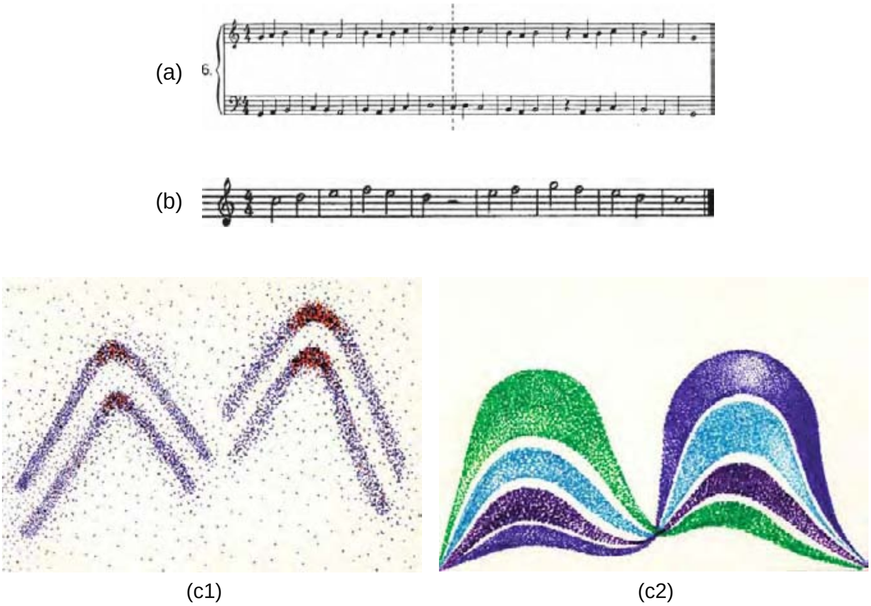

Figure 2-10. (**a**) Bartók: *Microcosmos, Unisono No. 6*. The vertical dasched line indicates the plane of reflection; (**b**) Bartók: *Microcosmos, Unisono No. 1*; (**c**) Drawings inspired by the *Unisono No. 1* by early teenagers, Komló Music School (courtesy of Mária Apagyi, Pécs, Hungary).

Figure 2-11. Double-headed eagles in (*left*) Madrid; (*center*) Prague; and (*right*) Moscow (photographs by the authors).

cally for children. Figure 2-10a of *Unisono No. 6* illustrates a mirror plane which includes a sound. The introductory piece of the *Microcosmos* is depicted in Figure 2-10b. It has only approximate bilateral symmetry though the two halves are markedly present. When some school children in their early teens were asked to express their impressions in drawing while listening to this piece of music for the first time, they invariably produced patterns with bilateral symmetry. Two of the drawings are reproduced in Figure 2-10c.

Weyl calls bilateral symmetry also heraldic symmetry as it is so common in coats of arms [6]. Characteristically, the eagles of the Habsburgs (Figure 2-11a and b) and the Russian Romanovs (Figure 2-11c) were double headed.

2.2. Rotational Symmetry

The contour of the simple and powerful oriental symbol yin yang (Figure 2-12a) has twofold rotational symmetry in that a half rotation about the axis perpendicular to the midpoint of the drawing brings back the original figure. This rotation axis is a symmetry axis. The Taiwanese stamp with two fish (shown in Figure 2-12b) is reminiscent of yin yang.

The *order* of a rotation symmetry axis tells us how many times the original figure reoccurs during a complete rotation. The *elemental angle* is the smallest angle of rotation by which the original

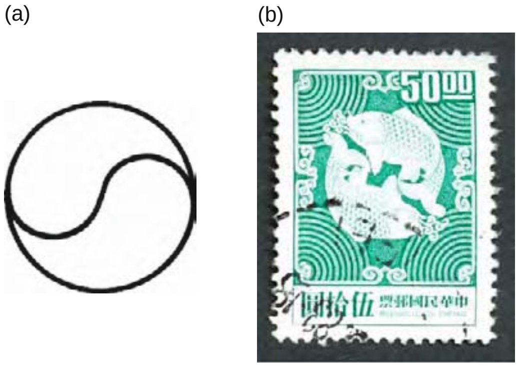

Figure 2-12. Contour of yin yang and two fish on a Taiwanese stamp.

figure is reproduced. Thus, for twofold rotational symmetry, the order of the rotation axis is two and the elemental angle is 180°. The corresponding numbers for threefold, fourfold, etc., rotational symmetries are three and 120°, four and 90°, etc., respectively. The order of rotation axes (n) may be 1, 2, 3, ... up to infinity, ∞, thus it may be any integer. The order 1 means that a complete rotation is needed to bring back the original figure, thus there is a total absence of symmetry which means asymmetry. A one-fold rotation axis is an identity operator. The other extreme is the infinite order; the circle has such symmetry. This means that any, even infinitesimally small rotation leads to congruency.

Figures 2-13–2-15 illustrate rotational symmetries in flowers, rotating parts of machinery, and hubcaps. Seldom does exclusively rotational symmetry have functional importance in flowers. In contrast, the motion of rotating parts in machinery is reinforced by having only rotational symmetry and no symmetry planes. There

Figure 2-13. Hawaiian flowers with only rotational symmetry (photographs by the authors).

Figure 2-14. Rotating parts of machinery (photographs by the authors).

are hubcaps with rotational symmetry only, but just as well can a hubcap with multiple symmetry planes fulfill its function—serving as protection and decoration. It is only our perception that might favor a hubcap with rotational symmetry over a hubcap with higher symmetry. The perception is that rotation favors motion whereas symmetry planes stop motion. This is why we suggest that recycling companies, banks, and transportation companies often choose logos with rotational symmetry only. A small sampler of examples is presented in Figure 2-16. Finally, a curious appearance of rotational only symmetries is found in sculptures of two, three or even more interweaving fish and dolphins (Figure 2-17).

Figure 2-15. Hubcaps with only rotational symmetry (photographs by the authors).

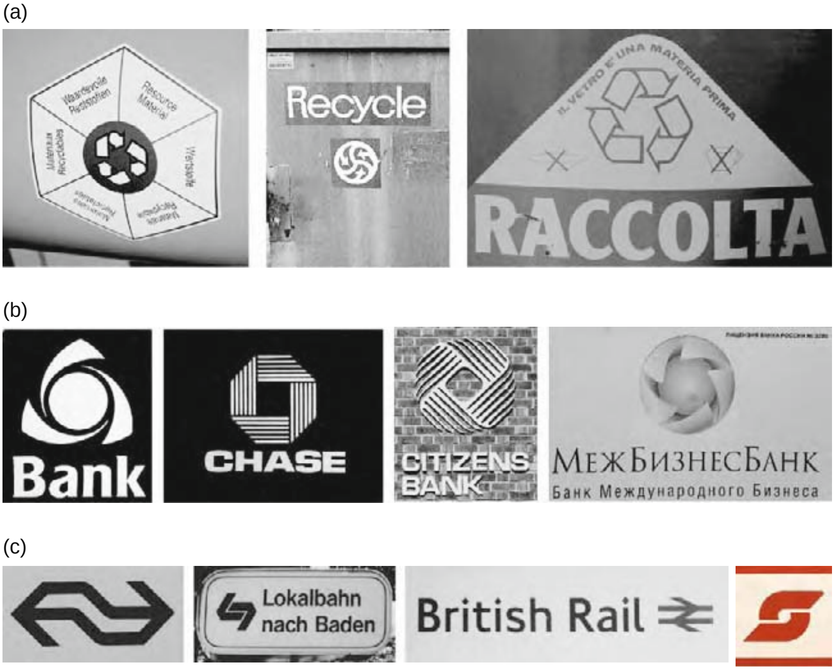

Figure 2-16. Logos: (**a**) Recycling; (**b**) Banking; (**c**) Transportation (photographs by the authors).

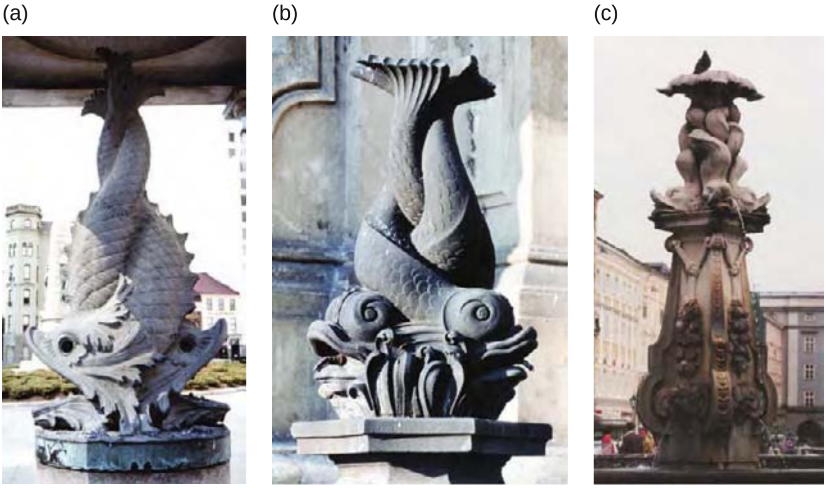

Figure 2-17. Sculptures of interweaving fish and dolphins: (**a**) Twofold in Washington, DC; (**b**) Threefold in Prague; (**c**) Fourfold in Linz, Austria (photographs by the authors).

2.3. Combined Symmetries

The symmetry plane and the rotation axis are symmetry elements. If a figure has a symmetry element, it is symmetrical. If it has no symmetry element, it is asymmetrical. Even an asymmetrical figure has a one-fold rotation axis; or, actually, an infinite number of one-fold rotation axes.

The application of a symmetry element is a *symmetry operation* and the symmetry elements are the *symmetry operator*s. The consequence of a symmetry operation is a *symmetry transformation*. Strict definitions refer to geometrical symmetry, and will serve us as guidelines only. They will be followed qualitatively in our discussion of primarily non-geometric symmetries, according to the ideas of the Introduction.

So far symmetries with *either* a symmetry plane *or* a rotation axis have been discussed. These symmetry elements may also be combined. The simplest case occurs when the symmetry planes include a rotation axis.

2.3.1. A Rotation Axis with Intersecting Symmetry Planes

A dot between *n* and *m* in the label $n{\cdot}m$ indicates that the axis is in the plane. This combination of a rotation axis and a symmetry plane produces further symmetry planes. Their total number will be *n* as a consequence of the application of the *n*-fold rotational symmetry to the symmetry plane. The complete set of symmetry operations of a figure is its symmetry group.

Figure 2-18 shows two flowers. The *Vinca minor*[†] has four-fold rotational symmetry and no symmetry plane. The Norwegian tulip has three-fold rotational symmetry with the axis of rotation in a symmetry plane. The three-fold rotation axis will, of course, rotate not only the flower but any other symmetry element, in this case the symmetry plane, as well. The 120° rotations will generate altogether three symmetry planes, and these planes will make an angle of 60° with each other. There is though an alternative description of the symmetries of the Norwegian tulip. Start with recognizing the

[†]This plant has been used to extract physiologically important alkaloids. One of the derivatives has become an important medicine that dilates blood vessels in the brain. Cavinton® has been a popular drug for improving memory.

Figure 2-18. *Top left*: *Vinca minor*; *Top right*: Norwegian tulip; *Bottom*: stone-carvings along the Via Appia Antica in Rome (photographs by the authors).

three symmetry planes cutting through the petals. The three symmetry planes are at 120° relative to each other. Where they intersect, that line is an axis of threefold rotation. The two flowers we chose for closer examination have been immortalized by a Roman artist: The lower part of Figure 2-18 shows an ancient stone carving along Via Appia Antica in Rome depicting two flowers that may very well represent *Vinca minor* and the Norwegian tulip.

Fivefold symmetry appears frequently among primitive organisms. Examples are shown in Figure 2-19. They have fivefold rotation axes and intersecting (vertical) symmetry planes as well. The symmetry class of the starfish is $5{\cdot}m$. This starfish consists of ten congruent parts, with each pair related by a symmetry plane. The whole starfish is unchanged either by 360°/5 = 72° rotation around the rotation axis, or by mirror reflection through the symmetry planes which intersect at

an angle of 36°. Fivefold rotation with coinciding mirror reflection is quite common among fruits and flowers. This symmetry is also rather common among molecules. On the other hand, this symmetry is used to be considered absent in the world of crystals as will be discussed in more detail in the chapter on crystals.

Examples of *n·m* symmetries are shown in Figure 2-20. It is a much favored symmetry by designers of important buildings.

2.3.2. Snowflakes

In addition to a rotation axis with intersecting symmetry planes (which is equivalent to having multiple intersecting symmetry planes), snowflakes have a perpendicular symmetry plane. This combination of symmetries is labeled *m·n*:*m* and it is characteristic of many other

(a)

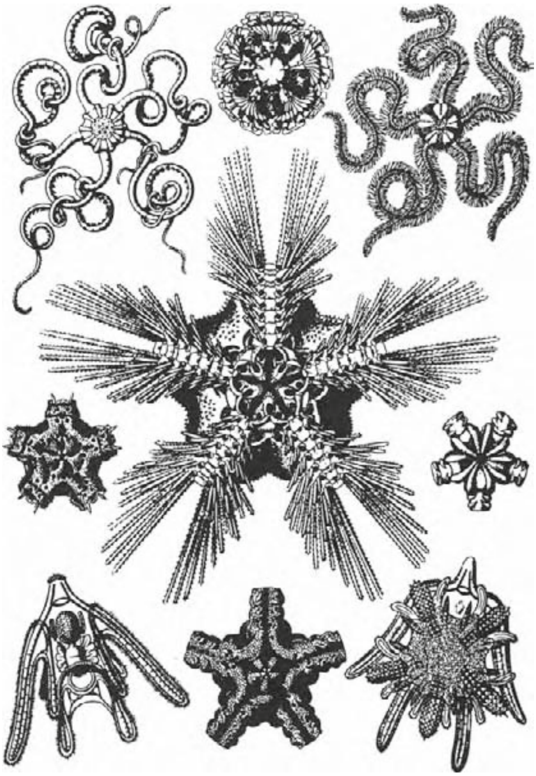

Figure 2-19. (**a**) Starfish after Haeckel [7]; (Continued)

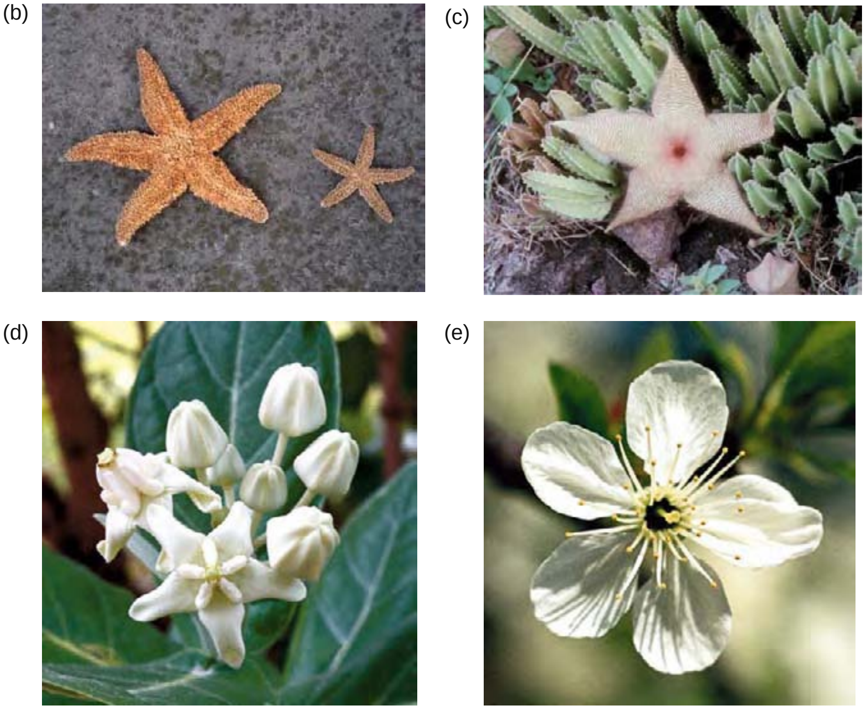

Figure 2-19. (**b**) Starfish; (**c**) Carrion flower (*Stapelia gigantea pallida* in Honolulu, Hawaii) [8]; (**d**) Flower in Hawaii; (**e**) Apple blossom (**b–e**, photographs by the authors).

highly symmetrical objects, such as prisms, bipyramids, bicones, cylinders, and ellipsoids. Due to their high symmetries, these shapes are relatively simple. Some examples are shown in Figure 2-21; they all have $m \cdot n : m$ symmetries: the pentagonal prism, $m \cdot 5 : m$, the trigonal bipyramid, $m \cdot 3 : m$, and the bicone and the cylinder, $m \cdot \infty : m$ symmetry.

One of the most beautiful and most common examples of this symmetry is the $m \cdot 6 : m$ symmetry of snow crystals. The virtually endless variety of their shapes and their natural beauty make them outstanding examples of symmetry. The fascination in the shape and symmetry of snowflakes goes far beyond the scientific interest in their formation, variety, and properties. The morphology of the snowflakes is determined by their internal structures and the external conditions of their formation. The mechanism of snowflake formation has been the subject of considerable research efforts. It is well known that

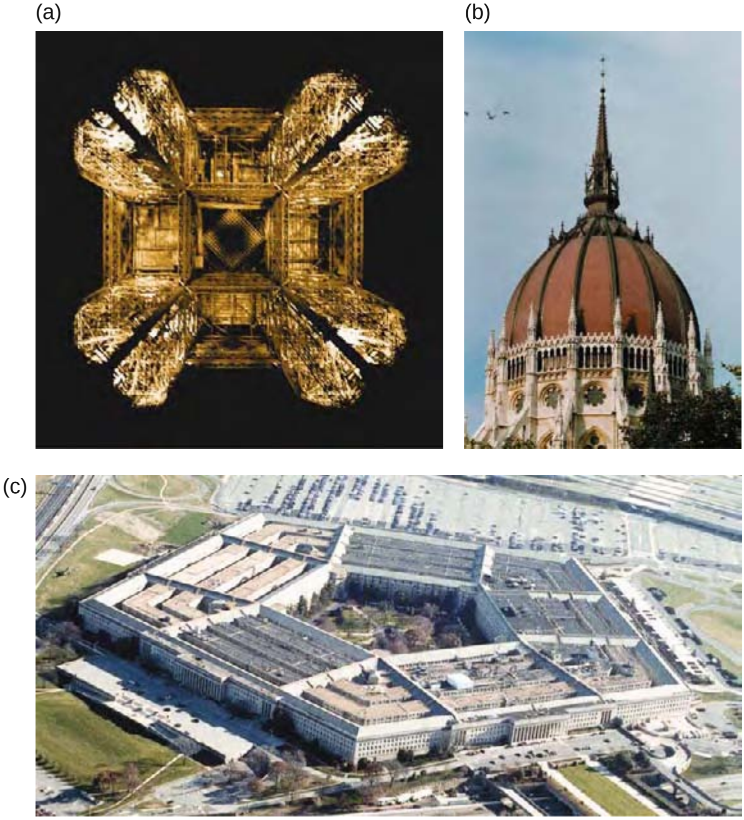

Figure 2-20. Examples in architecture: (**a**) Eiffel Tower, Paris, from below; (**b**) Cupola of the Parliament building in Budapest; (**c**) Pentagon in Washington, DC (photographs by the authors).

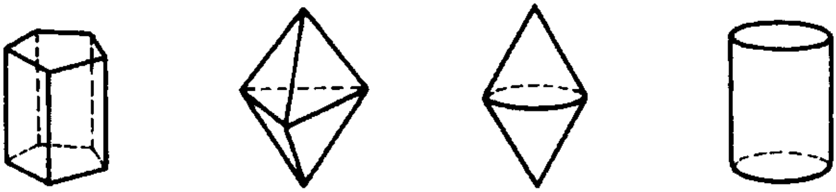

Figure 2-21. Examples of $m{\cdot}n{:}m$ symmetries: from the left, pentagonal prism; trigonal bipyramid; bicone; cylinder.

the internal hexagonal arrangement of the water molecules produced by the hydrogen bonds is responsible for the hexagonal symmetry of snowflakes. This does not explain yet the countless number of different shapes of snowflakes, and why even the smallest variations from the basic underlying shape of a snowflake are repeated in all six directions.

According to L. L. Whyte, the translator of Kepler's *New Year's Gift*, the snowflake is "an important clue to the shaping agencies of nature..." [9]. As the puzzling questions concerning snowflakes are related to their morphology rather than to their internal structures, these questions will be discussed at some length in the present section. The process of solidification of fluids into crystals has been simulated by mathematical models. These simulations showed that crystals with sharp tips grew rapidly and had high stability, while crystals with fat shapes grew slowly and were less stable. However, when these slowly growing shapes were slightly perturbed, they tended to split into sharp, rapidly growing tips. This observation led to the hypothesis of the so-called *points of marginal stability* [10]. According to this model, the snow crystal may start with a relatively stable shape. The crystal may, however, be easily destabilized by a small perturbation. A rapid process of crystallization from the surrounding water vapor ensues. The rapid growth gradually transforms the crystal into another semi-stable shape. A subsequent perturbation may then occur resulting again in a new direction of growth with a different rate. The marginal stability of the snowflake makes the growing crystal very sensitive to even slight changes in its microenvironment.

The uniqueness of snowflakes may be related to the marginal stability. The ice starts crystallizing in a flat six-fold pattern of water crystals so it is growing in six equivalent directions. As the ice is quickly solidifying, latent heat is released which flows between the growing six bulges. The released latent heat retards the growth in the areas between these bulges. This model accounts for the dendritic or tree-like growth. Both the minute differences in the conditions of two growing crystals and their marginal stability make them develop differently. "Something that is almost unstable, will be very susceptible to changes, and will respond in a large way to a small force" [11]. At each step of growth slightly new micro-environmental conditions are encountered, causing new and new variations in the branches. However, it is assumed that each of the six branches will encounter

exactly the same micro-environmental conditions, hence their almost exact likeness.

The marginal stability model is attractive in its explanation of the great variety of snowflake shapes. It is somewhat less convincing in explaining the repetitiveness of the minute variations in all six directions since the micro-environmental changes may occur also across the snowflakes themselves and not only between the spaces assigned to different snowflakes.

In order to explain the morphological symmetry of the dendritic snow crystals, D. McLachlan [12] suggested a mechanism decades ago, which has not yet been seriously challenged. He posed the very question already mentioned above: “How does one branch of the crystal know what the other branches are doing during growth?” McLachlan noted that the kind of regularity encountered among the snowflakes is not uncommon among flowers and blossoms or among sea animals in which hormones and nerves coordinate the development of the *living* organisms.

McLachlan’s explanation for the coordination of the growth among the six branches of a snow crystal is based on the existence of thermal and acoustical standing waves in the crystal. As the snowflake grows by deposition of water molecules upon a small nucleus, it undergoes thermal vibrations at temperatures between 250 and 273 K. The water molecules strike and bounce off the nucleus and those which stay add to the growth. Branching occurs at points with high concentration of water molecules. If the starting ice nucleus has the hexagonal shape shown in Figure 2-22a and the conditions favor dendritic growth, then the six corners would be receiving more molecules and would be releasing more heat of crystallization than the flat portions. The dendritic development evolving from this situation is shown in Figure 2-22b. The next stage in the development of a snowflake is the production of a new set of equally spaced dendritic branches determined by the modes of vibration along the spines of the flake. The long spines of Figure 2-22c are thought to be particular molecular arrays which correspond to the ice structure. The molecules are vibrating and the energy distribution between the modes of vibration is influenced by the boundary conditions. When one of the spines becomes “heavily loaded” at some point, then nodes are induced along this spine. These nodes will eject dendritic branches that are equally spaced as indicated in Figure 2-22d–f. The question of how the standing waves in

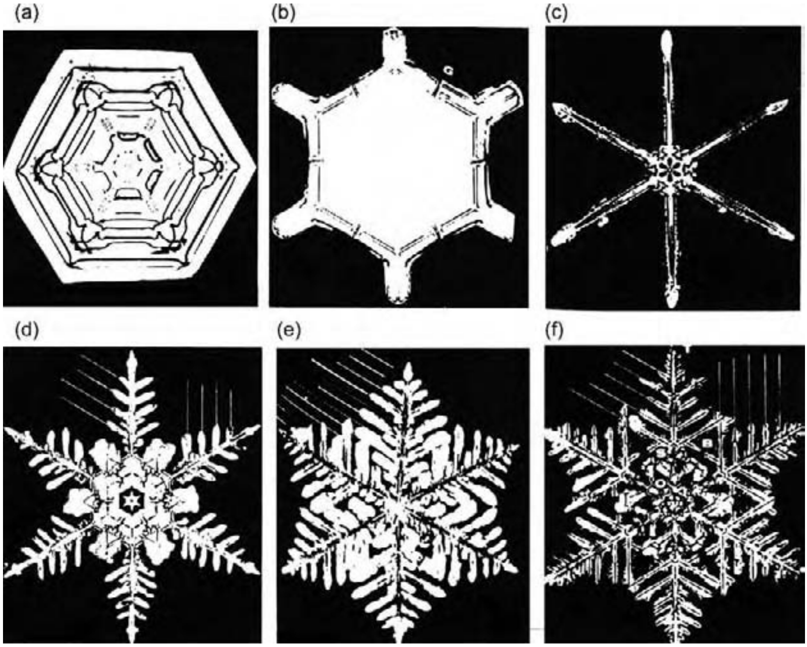

Figure 2-22. McLachlan's selection [13] of Bentley's snowflake images [14] to illustrate the coordinated growth of the six branches of a snowflake based on the standing wave theory.

one of the six branches are coupled with those in the other branches is answered by considering the torque about an axis through the intersection point. This torque transmits the same frequencies and induces the same nodes in all the branches. Thus, McLachlan asserts that the dendritic development is identical in all six branches and is independent of the particular branch in which the change in the conditions occurred.

Intensive research has continued into the mechanism of snowflake formation [15]. This research encompasses the broader question of dendritic crystal growth. New approaches, such as fractal models, and copious use of computer simulation have greatly facilitated these attempts. It is fascinating how dendritic growth penetrates even chemical synthetic work witnessed by the development of *dendrimer chemistry* of ever increasing complexity, which is an example of nano-chemistry par excellence [16]. An illustration is given in Figure 2-23.

Returning to the snowflakes, an eloquent description of their beauty and symmetry is given by Thomas Mann in *The Magic Mountain* [18]:

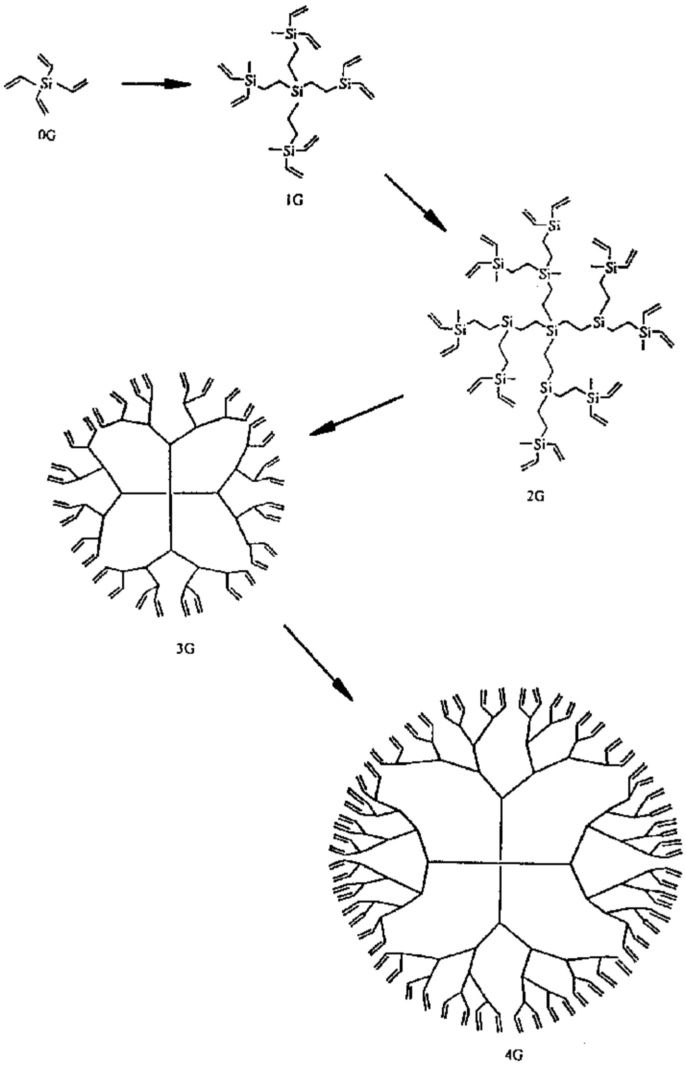

Figure 2-23. Dendrimers in chemistry after Tomalia and Durst [17], reproduced with permission from Springer-Verlag.

> . . . Indeed, the little soundless flakes were coming down more quickly as he stood. Hans Castorp put out his arm and let some of them to rest on his sleeve; he viewed them with the knowing eye of the nature-lover. They looked mere shapeless morsels; but he had more than once had their like

> under his good lens, and was aware of the exquisite precision of form displayed by these little jewels, insignia, orders, agraffes—no jeweller, however skilled, could do finer more minute work. Yes, he thought, there was a difference, after all, between this light, soft, white powder he trod with his skis, that weighed down the trees, and covered the open spaces, a difference between it and the sand on the beaches at home, to which he had likened it. For this powder was not made of tiny grains of stone; but of myriads of tiniest drops of water which in freezing had darted together in symmetrical variation—parts, then, of the same inorganic substance which was the source of protoplasm, of plant life, of the human body. And among these myriads of enchanting little stars, in their hidden splendour that was too small for man's naked eye to see, there was not one like unto another and endless inventiveness governed the development and unthinkable differentiation of one and the same basic scheme, the equilateral, equiangular hexagon. Yet each, in itself—this was the uncanny, the anti-organic, the life-denying character of them all—each of them was absolutely symmetrical, icily regular in form. They were too regular, as substance adapted to life never was to this degree—the living principle shuddered at this perfect precision, found it deathly, the very marrow of death—Hans Castorp felt he understood now the reason why the builders of antiquity purposely and secretly introduced minute variation from absolute symmetry in their columnar structures.

The coldness and lifelessness of too much symmetry is as beautifully expressed by Thomas Mann as the beauty of the hexagonal symmetry of the snow crystal. Michael Polányi remarked that an environment that was perfectly ordered was not a suitable human habitat [19]. Crystallographers Fedorov and Bernal simply stated “Crystallization is death” [20].

Human interest in snowflakes has a long history. The oldest known recorded statement on snowflake forms dates back to the second century BCE and comes from China according to Needham and Lu Gwei-Djen [21]. Six was a symbolic number for water in many classical Chinese writings. The contrast between five-pointed plant structures and six-pointed snowflakes has become a literary commonplace in subsequent centuries. Of several relevant citations collected by Needham and Lu Gwei-Djen, one is reproduced here, from a statement by a physician from 1189 [22],

> . . . the reason why double-kernelled peaches and apricots are harmful to people is that the flowers of these trees are properly speaking five-petalled yet if they develop with sixfold (symmetry), twinning will occur. Plants and trees all have the five-fold pattern; only the yellow-berry and snowflake crystals are hexagonal. This is one of the principles of Yin and Yang. So if double-kernelled peaches and apricots with an (aberrant) sixfold (symmetry) are harmful, it is because these trees have lost their standard rule.

The examination of snowflake shapes and their comparison with other shapes has apparently been a great achievement in East Asia. The involvement of Yin and Yang amply demonstrates how much importance was given to these studies. As a forerunner of the modern investigations of the correlation between snowflake shapes and environmental, i.e., meteorological conditions, the following passage from the thirteenth century is cited [23]: “The Yin embracing the Yang gives hail, the Yang embracing the Yin gives sleet. When snow gets six-pointedness, it becomes snow crystals. When hail gets three-pointedness, it becomes solid. This is the sort of difference that arises from Yin and Yang.”

The first known sketches of snowflakes from Europe in the sixteenth century did not reflect their hexagonal shape. Johannes Kepler was the first in Europe, who recognized the hexagonal symmetry of the snowflakes as he described it in his Latin tractate entitled *The Six-cornered Snowflake* published in 1611 [24]. By this time Kepler had already discovered the first two laws of planetary motion and thus found the true celestial geometry when he turned his

attention to the snowflakes. He considered their perfect form and, for the first time, sought the origin of shape and symmetry in the internal structure. The relationship between crystal habit and the internal structure will be discussed in the chapter on crystals (Chapter 9).

Descartes observed and recorded the shapes of snow crystals. Some of his sketches from 1635 are reproduced in Figure 2-24 after U. Nakaya [25]. As these were the first drawings of hexagonal snowflakes recorded, it was quite an achievement that even rare versions such as those composed of a hexagonal column with plane crystals developed at both ends could be found among them. More of such important contributions in this field occurred in the seventeenth century [26], among them Hooke's observations using his microscope. Branching in snow crystals has also been recorded by several investigators. Among the later works, Scoresby's observations and sketches are especially important [27]. Figure 2-25 reproduces some of them. Scoresby, who later became an arctic scientist made these drawings in his log book in 1806 at the age of 16 while he was on a voyage with his father to the Greenland whale fisheries.

There are two fundamental books—collections of snowflake pictures—available today as a result of photomicrography. W. A. Bentley devoted his lifetime to taking photomicrographs of snow crystals and collected at least 6000 of them, and about half of them appeared in his book co-authored with W. J. Humphreys [30]. This most well-known book on snowflakes is probably unsurpassable. Bentley's photomicrographs have been reproduced innumerable times in various places—sometimes without indicating the source. Some

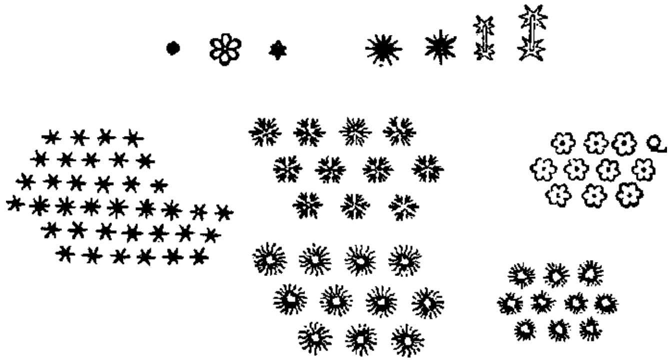

Figure 2-24. Snow crystals by Descartes from 1635 after Nakaya [28].

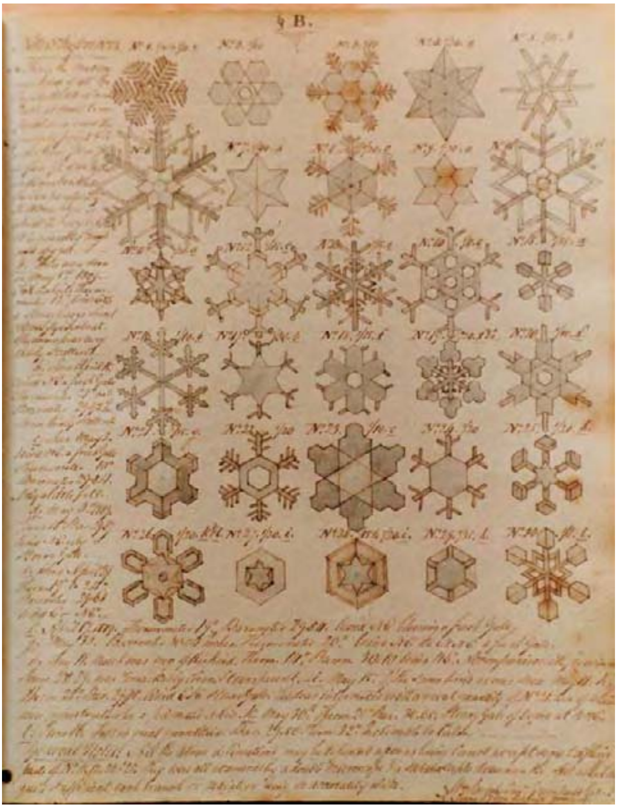

Figure 2-25. Scoresby's sketches of snowflakes from his log book (1806) after Stamp and Stamp [29]. Reproduced by permission.

characteristic examples of snowflakes from this collection are shown in Figure 2-26.

The other outstanding contribution is Nakaya's [32]. He recorded the naturally occurring snow crystals, classified them, and investigated their mass, speed of fall, electrical properties, frequency of occurrence, and so on. In addition, Nakaya and co-workers developed methods of producing snow crystals artificially in their laboratory at Hokkaido University in Sapporo. Nakaya and co-workers succeeded in determining the conditions of formation of all different types of snowflakes. The major part of the general classification of snow crystals by Nakaya is given in Table 2-1 and Figure 2-27. The hexagonal plane crystals are the most common and the best known.

Nakaya made important contributions not only to observing the perfect or near perfect symmetries of the snow crystals but also the

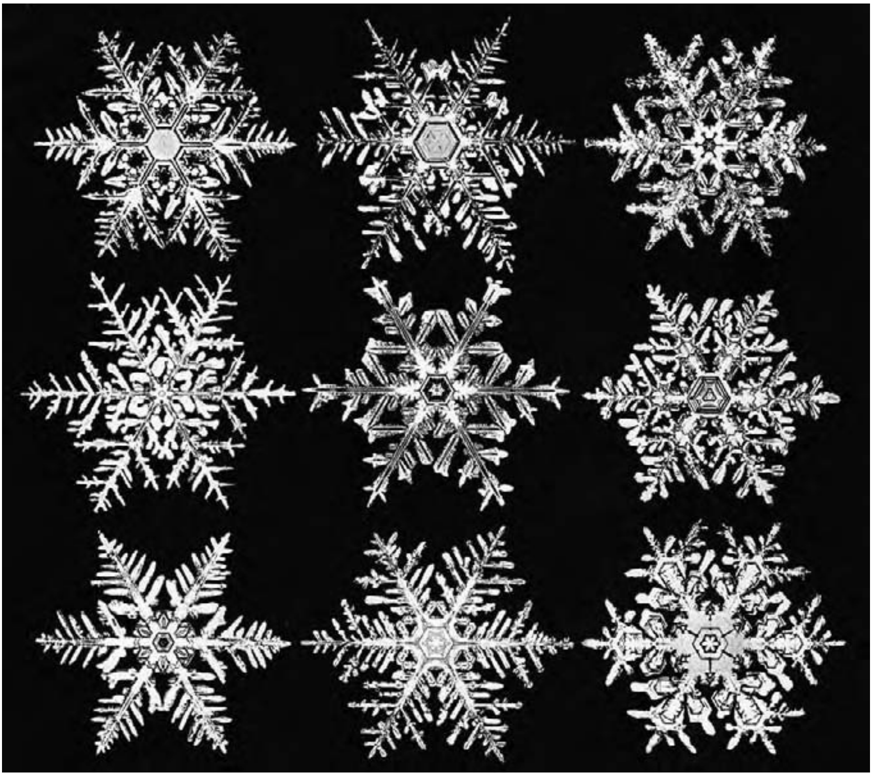

Figure 2-26. Snowflake photomicrographs by Bentley, from Bentley and Humphreys [31].

distortions from hexagonal symmetry. Of course, the atomic arrangement is always hexagonal, but the morphology or crystal habit may be less than perfectly regular hexagonal. Nakaya calls such crystals *malformed* and states that these asymmetric crystals may be more common than the symmetric ones. Of course, the question of symmetry is a matter of degree. Even the snowflakes which are considered to be most symmetrical may reveal slight differences in their branches when examined closely. Currently intensive work is going on in studying snowflakes at the California Institute of Technology [34] and other laboratories. Meteorological research continues to probe into the various weather conditions to investigate the circumstances of snowflake formation. This work involves field work and observations as well as studying century-old records in archives. A recent article in *The New York Times* focused attention to these marvels of nature [35].

Table 2-1. Part of Nakaya's General Classification of Snow Crystals[a]

Main groups	Subgroups	Types
Needle (N)	1. Simple	a. Elementary needle
		b. Bundle of needles
	2. Combination	
Columnar (C)	1. Simple	a. Pyramid
		b. Bullet
		c. Hexagonal
	2. Combination	a. Bullets
		b. Columns
Plane (P)	1. Regular developed in plane	a. Simple plate
		b. Branches in sector form
		c. Plate with simple extensions
		d. Broad branches
		e. Simple stellar form
		f. Ordinary dendritic form
		g. Fernlike
		h. Stellar form with plates at ends
		i. Plate with dendritic extensions
	2. Irregular number of branches	a. Three-branched
		b. Four-branched
		c. Others

Table 2-1. (Continued)

Main groups	Subgroups	Types
	3. Twelve branches	a. Fernlike b. Broad branches
	4. Malformed many varieties	
	5. Spatial assemblage of plane branches	a. Spatial hexagonal b. Radiating
Column/plane combinations (CP)	1. Column with plane at both ends	a. Column with plates b. Column with dendrites
	2. Bullets with plates	a. Bullets with plates b. Bullets with dendrites
	3. Irregular	
Columnar with extended side planes (S)		
Irregular snow particles (I)	1. Ice	
	2. Rimed	
	3. Miscellaneous	

[a] After U. Nakaya, *Snow* (in Japanese), Iwanami-Shoten Publ. Co., Tokyo, 1938 (latest printing, 1987).

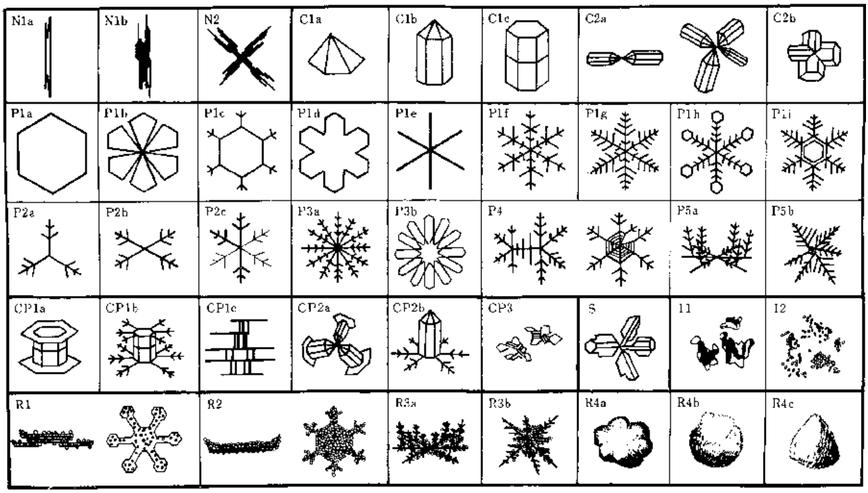

Figure 2-27. From Nakaya's general classification of snow crystals [33].

2.4. Inversion

What is the symmetry of the 1,2-dibromo-1,2-dichloro-ethane molecule as shown in Figure 2-28? There is no symmetry plane and no rotation axis. However, any two atoms of the same kind are related by a line connecting them and going through the midpoint of the central bond. This midpoint is the only symmetry element of this molecule and it is called the symmetry center or *inversion point*. The application of this symmetry element interchanges the atoms, or more generally, any two points located at the same distance from the center along the line going through the center. This interchange is called *inversion*. The notation of inversion symmetry is *i*.

An inversion may also be represented as the consecutive application of two simple symmetry elements, namely a twofold rotation and mirror-reflection, or vice versa. For the molecule in Figure 2-28, this could be described, for example, in the following way: (a) rotate the molecule by 180° about the C–C bond as the rotation axis and (b) apply a symmetry plane perpendicular to and bisecting the C–C bond; or (a) apply a twofold rotation axis perpendicular to the ClCCCl plane and going through the midpoint of the C–C bond and then (b) apply a mirror plane coinciding with the ClCCCl plane. These operations are indicated in Figure 2-28 and in

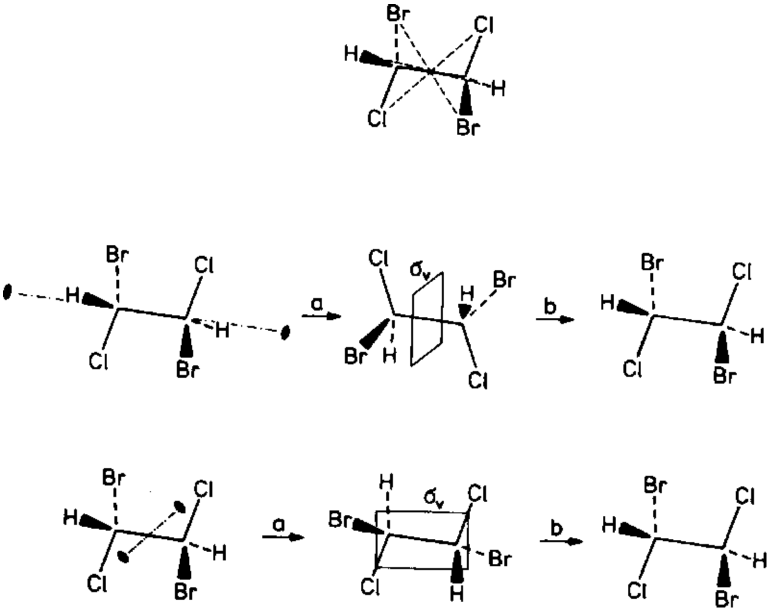

Figure 2-28. The 1,2-dibromo-1,2-dichloroethane molecule. Its center of symmetry is the midpoint of the C–C bond. An inversion is equivalent to the consecutive application of twofold rotation and reflection.

both examples the results are invariant to the order in which the two operations are performed.

The sphere is a highly symmetrical object which possesses a center of symmetry. Conjugate locations on the surface of a sphere are related by an inversion through the center of symmetry. The geographical consequences of such an inversion are emphasized in a newspaper article on New Zealand by the famous journalist, the late James Reston in his *Letter from Wellington. Search for End of the Rainbow* [36]:

> Nothing is quite the same here. Summer is from December to March. It is warmer in the North Island and colder in the South Island. The people drive on the left rather than on the right. Even the sky is different—dark blue velvet with stars of the Southern Cross—and the fish love the hooks.

Madrid, Spain, corresponds approximately to Wellington, New Zealand, by inversion.

The notation of the symmetry center or inversion center is $\bar{1}$ while the corresponding combined application of twofold rotation and mirror-reflection may also be considered to be just one symmetry transformation. The symmetry element is called a mirror-rotation symmetry axis of the second order, or twofold mirror-rotation symmetry axis and it is labeled $\tilde{2}$. Thus, $\bar{1} \equiv \tilde{2}$.

The twofold mirror-rotation axis is the simplest among the mirror-rotation axes. There are also axes of fourfold mirror-rotation, sixfold mirror-rotation, and so on. Generally speaking, a 2*n*-fold mirror-rotation axis consists of the following operations: a rotation by $(360/2n)^\circ$ and a reflection through the plane perpendicular to the rotation axis. The symmetry of the snowflake involves this type of mirror-rotation axis. The snowflake obviously has a center of symmetry. The symmetry class $m{\cdot}6{:}m$ contains a center of symmetry at the intersection of the six-fold rotation axis and the perpendicular symmetry plane. In general, for all $m{\cdot}n{:}m$ symmetry classes with n even, the point of intersection of the n-fold rotation axis and the perpendicular symmetry plane is also a center of symmetry. When n is odd in an $m{\cdot}n{:}m$ symmetry class, however, there is no center of symmetry present.

2.5. Singular Point and Translational Symmetry

The midpoint of a square is unique, there is no other point equivalent to it (Figure 2-29); it is called a singular point. A corner of the same square is not singular, the symmetry transformations of the square reproduce it, and there are altogether four equivalent corner points of the square. The same argument applies if the point happens to be on one of the symmetry axes of the square. An arbitrarily chosen point in a square will have 7 other equivalent points because of the symmetry transformations of the square, so altogether there will be eight equivalent points. In an asymmetric figure each point is singular and the multiplicity of each point is one.

The symmetry classes characterizing figures or objects which have at least one singular point are called point groups. The center of the circular pattern of the pavement in Figure 2-30a is a singular point. Another pattern is displayed by the pavement in Figure 2-30b, consisting of identical arcs. If it is supposed that this pavement

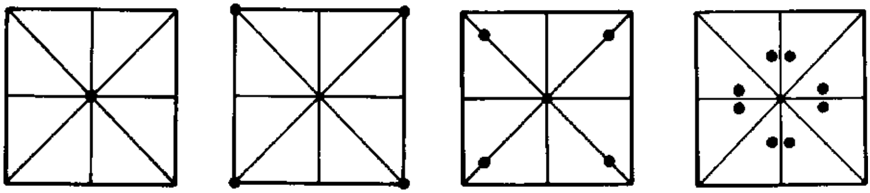

Figure 2-29. Singular point and the equivalence of points in a square.

is a fragment of an infinitely large one, there is no singular point in it. Assuming an infinite extent for this pavement pattern is natural because of its periodicity. The absence of a singular point leads to regularity expressed in infinite repetition which characterizes translational symmetry. This kind of symmetry precludes the presence of singular points though does not preclude the presence of a singular line or plane. The symmetry classes characterizing entities with translational symmetry are called space groups. One-dimensional space groups describe the symmetries involving infinite repetition or periodicity in one direction, two-dimensional space groups those involving periodicity in two directions and three-dimensional space groups describe the symmetry classes when periodicity is present in all three directions. Figure 2-31 and Table 2-2 summarize the possible cases considering dimensionality and periodicity.

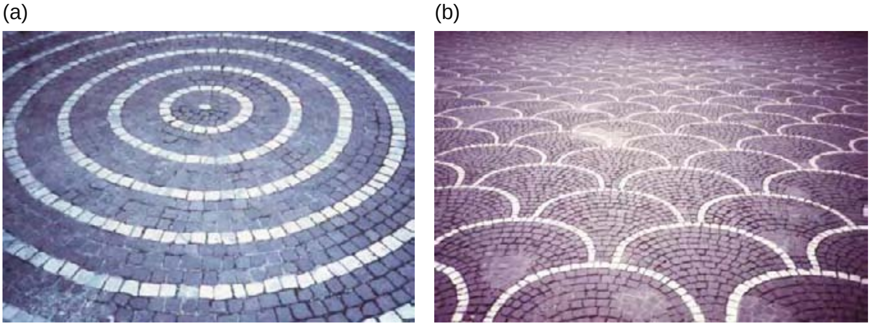

Figure 2-30. Pavements in L'Aquila, Italy (photographs by the authors). The system of concentric circles (**a**) Has point-group symmetry and the pattern of arcs; (**b**) If extended to infinity, has space-group symmetry.

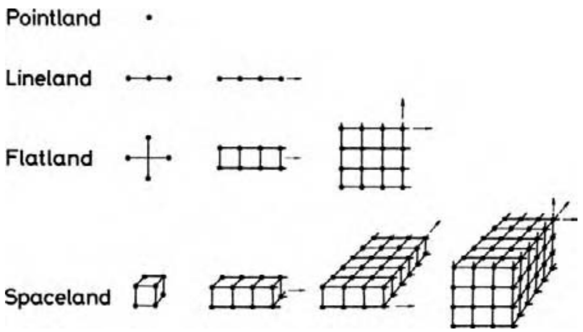

Figure 2-31. Dimensionality and periodicity in point groups and space groups. This figure is consistent with Table 2-2.

2.6. Polarity

A line is polar if its two directions can be distinguished and a plane is polar if its two surfaces are not equivalent. This definition of polarity has, of course, nothing to do with charge separation. A polar line has a "head" and a "tail" and a polar plane has a "front" and a "back." A vertical line on the surface of the Earth is polar with respect to gravity and a sheet of paper with one of its sides painted is polar with respect to its color.

An axis is polar if its two ends are not brought into coincidence by the symmetry transformations of the symmetry group of its figure. An analogous definition applies to the two sides of a polar plane.

If a symmetry group includes a center of symmetry, polarity is excluded because in a centrosymmetric figure a directed line or segment of a face changes direction by the inversion. In the case of the absence of a center of symmetry, there will be at least one directed line or face which is not accompanied by parallel counterparts reversed in direction.

The significance of polar axes can be demonstrated, for example, in crystal morphology. A few examples will be mentioned here following Curtin and Paul's review of the chemical consequences of the polar axis in organic crystal chemistry [37]. Figure 2-32a shows a centrosymmetric acetanilide crystal. The faces occur in parallel pairs and the crystal is non-polar. On the other hand, the p-chloroacetanilide crystal shown in Figure 2-32b is noncentrosymmetric and some of the

Table 2-2. Dimensionality (m) and Periodicity (n) of Symmetry Groups G_n^m after Engelhardt[a]

Periodicity / Dimensionality	$n = 0$ no periodicity	$n = 1$ periodicity in one direction	$n = 2$ periodicity in two directions	$n = 3$ periodicity in three directions
$m = 0$, Dimensionless	G_0^0			
$m = 1$, One-dimensional	G_0^1	G_1^1		
$m = 2$, Two-dimensional	G_0^2	G_1^2	G_2^2	
$m = 3$, Three-dimensional	G_0^3	G_1^3	G_2^3	G_3^3

[a]W. Engelhardt, *Matematischer Unterricht* 1963, 9(2), 49.

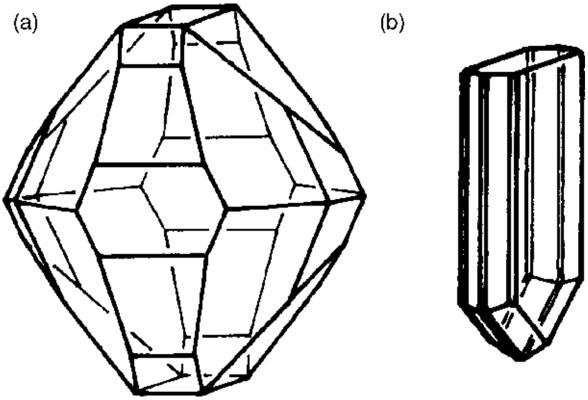

Figure 2-32. Two crystals from Groth's *Chemische Kristallographie* [38]. (**a**) Centrosymmetric rhombic bipyramidal acetanilide; (**b**) Noncentrosymmetric rhombic pyramidal p-chloroacetanilide.

faces occur without parallel ones at the opposite end of the crystal. This crystal has a polar axis parallel to its long direction.

The morphological symmetry differences between the acetanilide and p-chloroacetanilide crystals originate from their internal structures. The acetanilide molecules appear in pairs and the two molecules in each pair are related by an inversion center. On the other hand, the p-chloroacetanilide molecules are all aligned in one direction. The molecular arrangements in the two crystals are shown in Figure 2-33.

Even very simple structures may form polar crystals. For example, in a polar crystal composed of diatomic molecules AB, the molecular axis will be oriented more along the polar direction of the crystal than perpendicular to it. Furthermore, as there is an ABAB... array in the crystal, it is required that the spacing between the atom A and the two adjacent atoms B be unequal in order to have a polar axis present,

A B   A B   A B...

Curtin and Paul characterize this situation from the point of view of a submicroscopic traveler proceeding along this array of atoms. The observer is able to determine the direction of travel thanks to the difference in spacing. The distance is always longer from atom B to atom A and shorter from atom A to the next atom B in one direction whereas the reverse is true in the opposite direction.

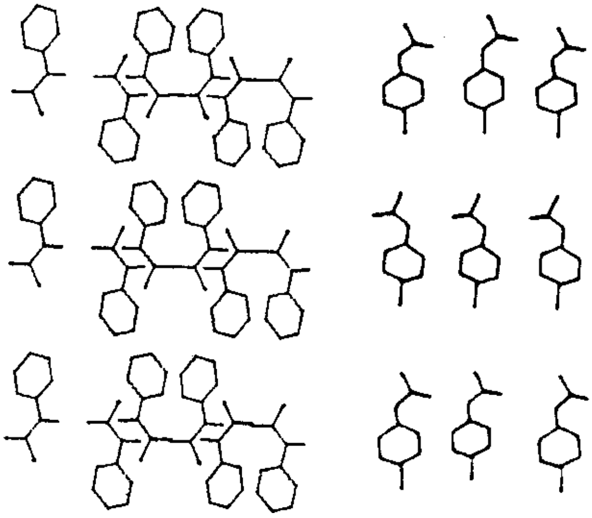

Figure 2-33. *Left*: The centrosymmetric arrangement of acetanilide molecules of the crystal resulting in centrosymmetric crystal habit; *Right*: The p-acetanilide molecules are aligned in a head-tail orientation resulting in the occurrence of a polar axis of the crystal habit [39]. Both are reprinted with permission from © 1981 American Chemical Society and D. Y. Curtin and I. C. Paul.

Crystal polarity may have important consequences in the chemical behavior. In solid/gas reactions, for example, crystal polarity may be a source of considerable anisotropy. There are also important physical properties characterizing polar crystals, such as pyroelectricity and piezoelectricity and others [40]. The primitive cell of a pyroelectric crystal possesses a dipole moment. The separation of the centers of the positive and negative charges changes upon heating. In this process the two charges migrate to the two ends of the polar axis. Piezoelectricity is the separation of the positive and negative charges upon expansion/compression of the crystal. Both pyroelectricity and piezoelectricity have practical uses.

2.7. Chirality

There are many objects, both animate and inanimate, which have no symmetry planes but which occur in pairs related by a symmetry plane and whose mirror images cannot be superposed. W. H. Thompson, Lord Kelvin, wrote: “I call any geometrical figure or group of points

'chiral', and say it has chirality, if its image in a plane mirror, ideally realized, cannot be brought into coincidence with itself" [41]. He called forms of the same sense *homochiral* and forms of the opposite sense *heterochiral*. The most common example of a heterochiral form is hands. Indeed, the word chirality itself comes from the Greek word for hand, *cheir*. Figures 2-34 and 2-35 show heterochiral and homochiral pairs of hands. Illustrations, however, may be found in the most diverse examples and Figure 2-36 presents a sampler. The simplest chiral molecules are those in which a carbon atom is surrounded by four different ligands—atoms or groups of atoms at the vertices of a tetrahedron. All the naturally occurring amino acids are chiral, except glycine.

A chiral object and its mirror image are enantiomorphous, and they are each other's enantiomorphs. Louis Pasteur (Figure 2-37) was the first who suggested that molecules can be chiral. In his famous experiment in 1848, he recrystallized a salt of tartaric acid and obtained two kinds of small crystals which were mirror images of each other as seen by Pasteur's models in Figure 2-38 preserved at *Institut Pasteur* at Paris. Originally Pasteur may have been motivated to make these large-scale models because Jean Baptiste Biot, the discoverer of optical activity had very poor vision by the time of Pasteur's discovery [42]. Pasteur demonstrated chirality to Biot, who was visibly affected

Figure 2-34. Heterochiral pairs of hands. (**a**) Tombstone in the Jewish cemetery in Prague; (**b**) Sculpture Park in Budapest (photographs by the authors).

Figure 2-35. Homochiral pairs of hands. (**a**) Aguste Rodin, *The Cathedral* in the Rodin Museum, Paris (reproduced by permission, photograph by the authors); (**b**) U.S. stamp; (**c**) Logo with SOS distress sign at a Swiss railway station (photograph by the authors).

by what he saw and told Pasteur: “My dear child, I have loved science so much throughout my life that this makes my heart throb” [43]. The two kinds of chiral crystals have the same chemical composition, but differ in their optical activity. One is laevo-active (L) and the other dextro-active (D). According to the Nobel laureate biologist George Wald, “No other chemical characteristic is as distinctive of living organisms as is optical activity” [44].

The true absolute configuration of molecules could not be determined at Pasteur’s time, so the organic chemist Emil Fischer had arbitrarily assigned an absolute configuration to sugars that had a 50% chance of being correct [45]. It was a great achievement of crystallography when Bijvoet and his associates determined the sense of chirality of molecules [46]. Luckily, Fischer’s guess proved to be correct. By now the absolute configuration has been established for relatively simple molecules as well as for large biological molecules.

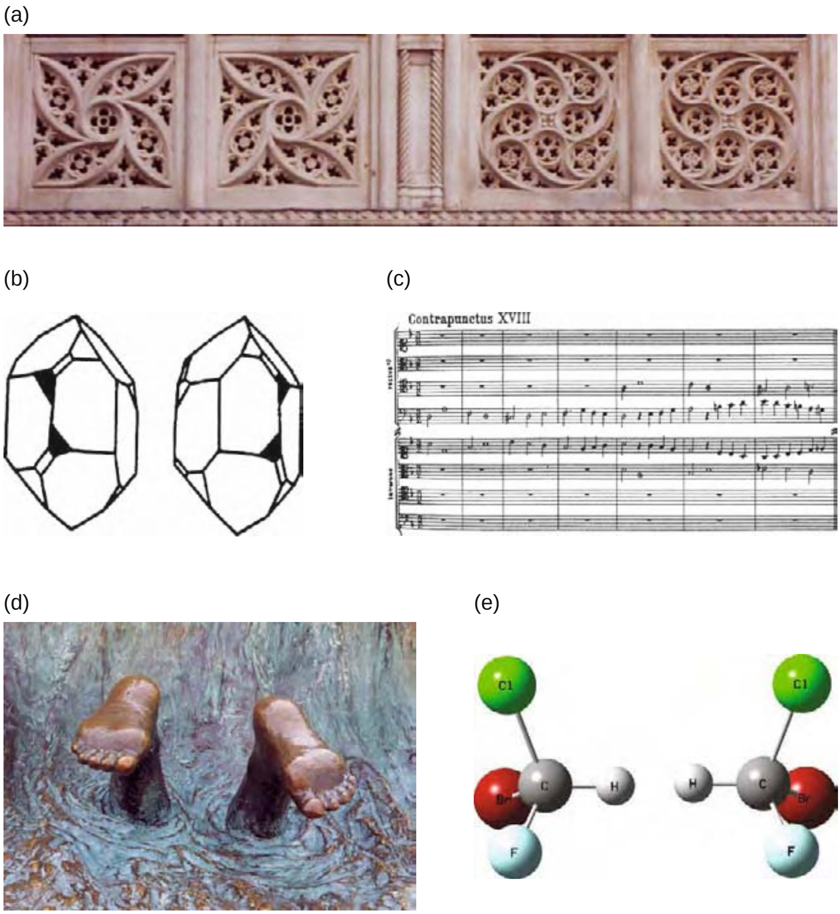

Figure 2-36. Illustrations of chiral pairs. (**a**) Decorations (in Bern, Switzerland, photograph by the authors) whose motifs of fourfold rotational symmetry are each other's mirror images; (**b**) Quartz crystals; (**c**) J. S. Bach, *Die Kunst der Fuge*, *Contrapunctus XVIII*, detail; (**d**) Legs (detail of Kay Worden's sculpture, *Wave*, in Newport, Rhode Island), (photograph by the authors); (**e**) A molecule and its mirror image in which a carbon atom is surrounded by four different atoms, for example, CHFClBr.

If a molecule or a crystal is chiral, it is necessarily optically active. The converse is, however, not true. There are non-enantiomorphous symmetry classes of crystals that may exhibit optical activity.

L. L. Whyte extended the definition of chirality: "Three-dimensional forms (point arrangements, structures, displacements, and other processes) which possess non-superposable mirror images

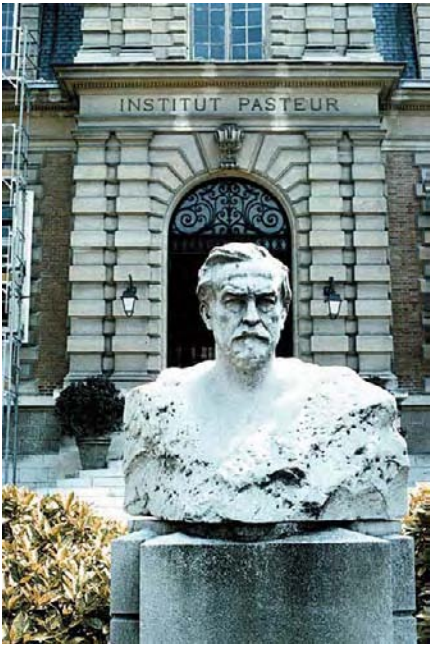

Figure 2-37. Louis Pasteur's bust in front of the *Institut Pasteur*, Paris (photograph by the authors).

are called 'chiral'" [47]. A chiral process consists of successive states all of which are chiral. The two main classes of chiral forms are screws and skews. Screws may be conical or cylindrical and are ordered with respect to a line. Examples for the latter are the left-handed and right-handed helices in Figure 2-39.

Figure 2-38. Pasteur's models at the *Institut Pasteur* (photographs by the authors).

Figure 2-39. *Left*: Left-handed and right-handed helices at the Monastery in Zagorsk, Russia; and *Right*: in an Italian monastery (photographs by the authors).

Vladimir Prelog offered yet another definition of chirality that contains only subtle differences from previous definitions: "An object is chiral if it cannot be brought into congruence with its mirror image by translation and rotation. Such objects are devoid of symmetry elements which include reflexion: mirror planes, inversion centers or improper rotational axes" [48]. Prelog had a beautiful ex libris bookplate by the Swiss graphic artis, Hans Erni (Figure 2-40). Prelog maintained that the drawing represented all three basic paraphernalia necessary for dealing with chirality, viz., human intelligence, a left and a right hand, and two enantiomorphous tetrahedra. These two tetrahedra are not regular because regular tetrahedra could not be chiral due to their symmetry planes.

An interesting overview of the left/right problem in science is given by Martin Gardner [50]. Distinguishing between left and right has also considerable social, political, psychological connotations. For example, left-handedness in children is viewed with varying degrees of tolerance in different parts of the world. Figure 2-41 shows different (homochiral and heterochiral) chairs a quarter of a century ago at the

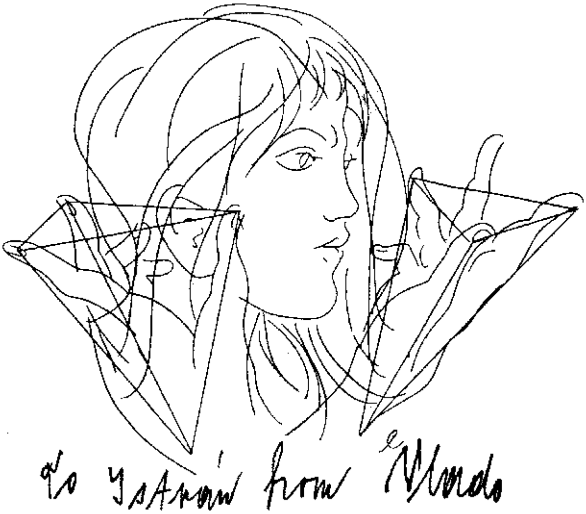

Figure 2-40. Hans Erni's *ex libris* bookplate for Vladimir Prelog with a dedication to one of the authors (courtesy of Vladimir Prelog, Zurich). A peculiar feature of this drawing is that the two hands appear to be inverted and can be imagined as a result of the two arms being crossed [49]. Erni made other versions of this drawing in which the two hands appear to be non-inverted.

University of Connecticut. Older classrooms used to have chairs for the right-handed students only whereas newer chairs were made for both right-handed and left-handed students.

2.7.1. Asymmetry and Dissymmetry

Sometimes the terms asymmetry, dissymmetry, and antisymmetry are confused in the literature although the scientific meaning of these

Figure 2-41. Classrooms with homochiral and heterochiral chairs in the 1980s at the University of Connecticut (photographs by the authors).

terms is in complete conformity with the grammar of these words. Asymmetry means the complete absence of symmetry, dissymmetry means the absence of certain symmetry and antisymmetry means the symmetry of opposites (see Section 4.6). Pasteur used “dissymmetry” for the first time as he designated the absence of a symmetry plane in a figure. Accordingly, dissymmetry did not exclude all elements of symmetry, only the absence of certain symmetries. Chirality is a conspicuous example of dissymmetry.

Pierre Curie suggested a broad application of the term dissymmetry. He called a crystal dissymmetric in case of the absence of those elements of symmetry upon which depends the existence of one or another physical property in that crystal. In Pierre Curie’s original words: “Dissymmetry creates the phenomenon” (“C’est la dissymétrie qui crée le phénomène”) [51]. Namely, a phenomenon exists and is observable due to dissymmetry, i.e., due to the absence of some symmetry elements from the system. Finally, Shubnikov called dissymmetry the *falling out* of one or another element of symmetry from a *given* group [52]. He argued that to speak of the absence of elements of symmetry makes sense only when these symmetry elements are present in some other structures.

Thus, from the point of view of chirality any asymmetric figure is chiral, but asymmetry is not a necessary condition for chirality. All dissymmetric figures are also chiral if dissymmetry means the absence of usually a plane of reflection. In this sense, dissymmetry is synonymous with chirality.

Pasteur was aware of the possible implications of chirality. In his words,

> Is it not necessary and sufficient to admit that at the moment of the elaboration of the primary principles in the vegetable organism, [a dissymmetric] force is present? ... Do these [dissymmetric] actions, possibly placed under cosmic influences, reside in light, electricity, in magnetism, or in heat? Can they be related to the motion of the earth, or to the electric currents by which physicists explain the terrestrial magnetic poles?

Pasteur’s discovery and subsequent work on chirality was a rich starting point for many branches that grew from a common ground.

It is only recently that minute differences have turned up in extremely accurate computational works in the energies of chiral molecules distinguishing them.

An assembly of molecules may be achiral for one of two reasons. Either all the molecules present are achiral, or the two kinds of enantiomorphs are present in equal amounts. Chemical reactions between achiral molecules lead to achiral products. Either all product molecules will be achiral or the two kinds of chiral molecules will be produced in equal amounts. Chiral crystals may sometimes be obtained from achiral solutions. When this happens, the two enantiomorphs will be obtained in (roughly) equal numbers, as was observed by Pasteur. Quartz crystals are an inorganic example of chirality (Figure 2-36b). Roughly equal numbers of left-handed and right-handed crystals are obtained from the achiral silica melt.

Incidentally, Pierre Curie's teachings on symmetry are probably not so widely known as they should be, considering their fundamental and general importance. The fact that his works on symmetry were characterized by extreme brevity may have contributed to this. Marie Curie [53] and Aleksei V. Shubnikov [54] have considerably facilitated the dissemination of Curie's teachings. Our discussion also relies on their works. A critical and fascinating discussion of Pierre Curie's symmetry teachings can be found in the literature [55].

Pierre Curie's above quoted statement concerning the role of dissymmetry in "creating" a phenomenon is part of a broader formulation. It says that in every phenomenon there may be elements of symmetry compatible with, though not required by, its existence. What is necessary is that certain elements of symmetry shall not exist. In other words, it is the absence of certain symmetry elements which is a necessary condition for the phenomenon to exist.

Another important statement of Pierre Curie's is that when several phenomena are superposed in the same system, the dissymmetries are added together. As a result, only those symmetry elements that were common to each phenomenon will be characteristic of the system.

Finally, concerning the symmetry relationships of causes and effects, Marie Curie formulated the following principles from Pierre Curie's teachings (Figure 2-42) [56]. (1) "When certain causes produce certain effects, the elements of symmetry in the causes ought to reappear in the effects produced." (2) "When certain effects reveal a certain dissymmetry, this dissymmetry should be apparent in the

Figure 2-42. Bust of Marie and Pierre Curie in Paris (photograph by the authors).

causes which have given them birth." However, (3) "The converse of these two statements does not hold . . . [and] the effects produced can be more symmetrical than their causes."

2.7.2. Vital Importance

Living organisms contain a large number of chiral constituents, but only *L*-amino acids are present in proteins and only *D*-nucleotides in nucleic acids. This happens in spite of the long-held view that the energy of both enantiomorphs is equal and their formation has equal probability in an achiral environment. However, only one of the two occurs in nature, and the particular enantiomorphs involved in life processes are the same in humans, animals, plants, and microorganisms. The origin of this phenomenon is a great puzzle which, according to Prelog [57], may be regarded as a problem of "molecular theology." Lately, very accurate computational work for relatively small systems has revealed minute differences in energy, which through cooperative effects could have contributed to the dominance of one of the two forms. The last word has not been said about the differences of chiral pairs, and further development may reveal interesting new knowledge.

The problem of preference has long fascinated those interested in the molecular basis of the origin of life [58]. There are, in fact, two questions. One is why do all the amino acids in a protein have the same *L*-configuration or why do all the components of a nucleic acid,

that is, all its nucleotides, have the same *D*-configuration? The other question, the more intriguing one, is why that particular configuration happens to be the *L* for the amino acids and why it happens to be the *D* for nucleotides in all living organisms? This second question seems to be impossible to answer satisfactorily at the present time.

According to Prelog [59], a possible explanation is that the creation of living matter was an extremely improbable event, which occurred only once. We may then suppose that if there are living forms similar to ours on a distant planet, their molecular structures may be the mirror image of the corresponding molecular structures on the earth. We know of no structural reason at the molecular level for living organisms to prefer one type of chirality over another, and the minute energy differences referred to above have not yet found any reasonable interpretation. (There may be reasons at the atomic nuclear level. The violation of parity at the nuclear level has already been referred to in the Introduction). Of course, once the selection is made, the consequences of this selection must be examined in relation to the first question. The fact remains, however, that chirality is intimately associated with life. This means that at least dissymmetry and possibly asymmetry are basic characteristics of living matter. Stephen F. Mason has compiled a meticulous and critical review of this question in the concluding chapter titled "Biomolecular handedness" in his comprehensive treatise, *Chemical Evolution* through the 1980s [60]. Carefully measured optical activities of crystalline materials dissolved in water showed appreciable influence of parity-violating energy differences in the crystallization process in some cases [61].

In 1960, John B. S. Haldane published a note in *Nature* [62] in which he returned to Pasteur's ideas [63] in the wake of the discovery of parity violation. Haldane is quoting Pasteur in French, but what we quote here we communicate in English translation.‡ Haldane begins with mentioning the discovery of parity violation that has led to the notion of the asymmetrical universe. This was first enunciated by Pasteur: "It is inescapable that dissymmetric forces must be operative during the synthesis of the first dissymmetric natural products."

‡We are grateful to Professor Alan L. Mackay (London) for the English translation.

Then Haldane continues quoting Pasteur: “What might these forces be? I, for my part, think that they are cosmological. The universe is dissymmetric and I am persuaded that life, as it is known to us, is a direct result of the dissymmetry of the universe or of its indirect consequences. The universe is dissymmetric.” Although Pasteur believed that there is a sharp gap between vital and nonliving processes, he attributed the dissymmetry of living matter to the dissymmetry of the structure of the universe and not to a vital force.

Concerning the first question, Orgel [64] suggests that we compare the DNA structure to a spiral staircase. The regular DNA right-handed double helix is composed of *D*-nucleotides. On the other hand, if a DNA double helix were synthesized from *L*-nucleotides, it would be left-handed. These two helices can be visualized as right-handed and left-handed spiral staircases, respectively. Both structures can perform useful functions. A DNA double-helix containing both *D*- and *L*-nucleotides, however, could not form a truly helical structure at all since its handedness would be changing. Orgel suggested considering the analogous spiral staircase as depicted in Figure 2-43.

If each component of a complex system is replaced by its mirror image, the mirror image of the original system is obtained. However, if only *some* components of the complex system are replaced by their mirror images, a chaotic system emerges. Chemical systems that are perfect mirror images of each other behave identically, whereas systems in which only some but not all components had been replaced by their mirror images have quite different chemical properties. If, for example, a naturally occurring enzyme made up of *L*-amino acids synthesizes a *D*-nucleotide, then the corresponding artificial enzyme obtained from *D*-amino acids would synthesize the *L*-nucleotide. On the other hand, a corresponding polypeptide containing both *D*- and *L*-amino acids would probably lack the enzymatic activity. A most charming example is given by Lewis Carroll, through his heroine, Alice, when she wonders, “Perhaps Looking-glass milk is not good to drink. . .” [66].

It has been known for some time that the two enantiomers of drugs and pesticides may have vastly different responses in a living organism. Natural products extracted from plants and animals are pure—in that they contain only one of the two possible enantiomers—

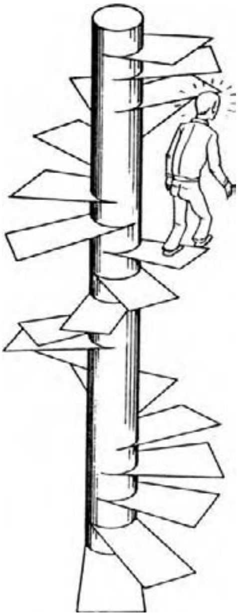

Figure 2-43. Helical staircase with changing handedness from Orgel (reproduced with permission from Leslie L. Orgel, Ja Jolla, California) [65].

while the synthesized ones are obtained in a 1:1 ratio of the two versions. In some cases, the other member of the twin is harmless, in addition to the one exerting the beneficial action. In other cases, however, the drug molecule has an "evil twin."

A tragic example was the thalidomide case. It was known as Contergan in Europe, and it is N-phthaloyl-α-aminoglutarimide (its model is shown in Figure 2-44). It was originally marketed as a sedative in the late-1950s. It was also given to pregnant women suffering from morning sickness. The drug was marketed as a racemate and by the early 1960s, many birth defects in Western Europe were associated with thalidomide. When thalidomide was administered to pregnant women in the first trimester of their pregnancy, it acted as a teratogen, causing stunted or deformed arms and legs in the infants. In the wake of the many tragedies, the drug was withdrawn from the market. The tragedies occurred worldwide except in the Soviet block where it was not available and the United States where the Food

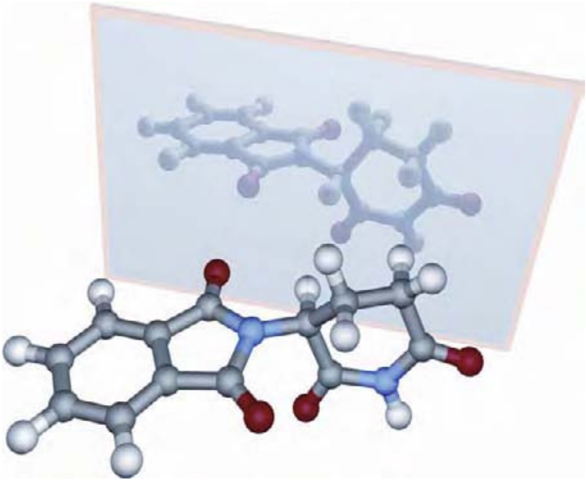

Figure 2-44. Thalidomide images (Computer drawing by Ilya Yanov, Jackson, Mississippi).

and Drug Administration (FDA) had never approved it. The lack of approval originated from the mistaken belief by an FDA agent who suspected incidences of peripheral neuropathy, which, as it turned out, was unconnected with the teratogenic effect of thalidomide.

Research on thalidomide did not stop with its removal from the market. For a while, it was used as an excellent example of one version being beneficial and the other harmful. Accordingly, it was suggested that had the beneficial isomer been resolved and administered selectively, the tragedies could have been avoided. Later studies, however, reported that thalidomide undergoes rapid interconversion between the enantiomers in the human organism, so resolvation could not have eliminated the dangers. Thalidomide research continues due to its potentials for beneficial uses as, for example, in treating inflammatory and autoimmune diseases [67]. The thalidomide tragedies facilitated the introduction of stringent regulations about the approval of chiral drugs especially in the European Union and the United States.

There are a few examples on the next page in which twin-enantiomers have different properties.

Right-hand version		*Left-hand version*
	Ethambutol	
Treats tuberculosis		Causes blindness
	Penicillamine	
Treats joints		Very toxic
	Naproxen	
Reduces pain, fever, inflammation (however, carries the risk of heart disease)		Toxic for the liver
	Propoxyphene*	
Pain reliever		Cough medicine
	Norgestrel	
Negligible contraceptive activity, but no harmful effect		Contraceptive
	Asparagin	
Bitter		Sweet
	Carvon	
Caraway smell		Spearmint smell
	Limonene	
Lemon smell		Orange smell

In the light of the above set of examples, it is obvious why it is so important to produce chirally “pure” substances [68]. Three scientists from among those who worked out reliable and efficient techniques for this purpose were awarded the Nobel Prize for Chemistry in 2001, K. Barry Sharpless, William S. Knowles, and Ryoji Noyori. The Swedish academician who introduced the three scientists at the award ceremony stressed that they “have developed chiral catalysts in order to produce only one of the [chiral] forms” [69]. Chiral production and separation continue to be among the most practical problems in the application of chemical advances [70].

2.7.3. *La coupe du roi*

Among the many chemical processes in which chirality/achirality relationships may be important is the fragmentation of some molecules and the reverse process of the association of molecular fragments. Such fragmentation and association can be considered generally and not just for molecules. The usual cases are those in which an achiral object is bisected into achiral or heterochiral halves. On the

* Note that the names of the respective medications are each other’s mirror images, Darvon® versus Novrad®.

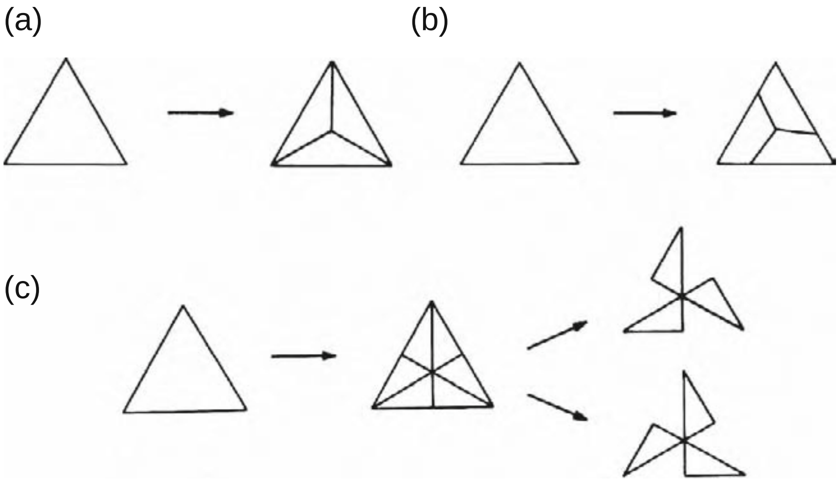

Figure 2-45. Dissection of an equilateral triangle into (**a**) Achiral; (**b**) Homochiral; and (**c**) Heterochiral segments after Shubnikov and Koptsik [72]. Used with permission from Nauka Publishers, Moscow.

other hand, if an achiral object can be bisected into two homochiral halves, it cannot be bisected into two heterochiral ones. A relatively simple case is the tessellation of planar achiral figures into achiral, heterochiral, and homochiral segments. Such tessellations are illustrated for the equilateral triangle in Figure 2-45 [71].

Anet et al. [73] have cited a French parlor trick called *la coupe du roi*—the *royal section*—in which an apple is bisected into two homochiral halves, as shown in Figure 2-46. An apple can be easily bisected into two achiral halves. On the other hand, it is impossible to bisect an apple into two heterochiral halves. Two heterochiral halves, however, can be obtained from two apples, both cut into two homochiral halves in the opposite sense. According to *la coupe du roi* two vertical half cuts are made through the apple. One cut goes from the top to the equator, and another, perpendicularly, from the bottom to the equator. In addition, two nonadjacent quarter cuts are made along the equator. If all this is properly done, the apple should separate into two homochiral halves.

The first chemical analog of *la coup du roi* was demonstrated by Cinquini et al. [74] by bisecting the achiral molecule of cis-3,7-dimethyl-1,5-cyclooctanedione into homochiral halves, viz. 2-methyl-1,4-butandiol. The reaction sequence is depicted in

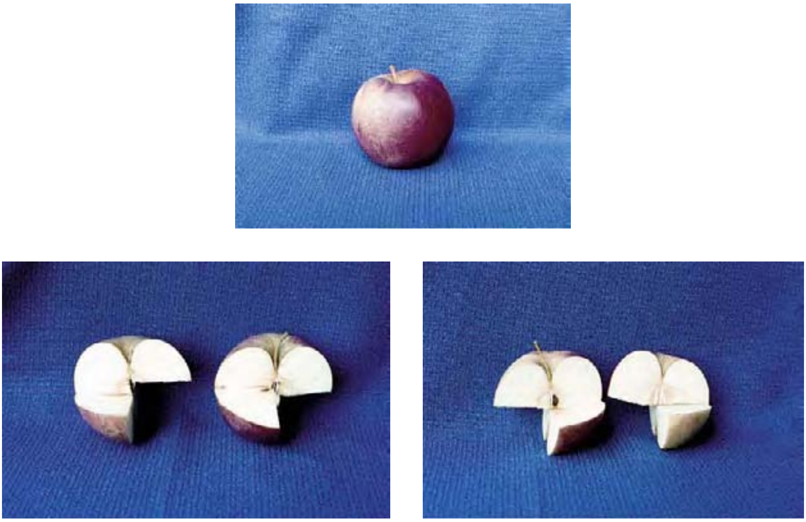

Figure 2-46. The French parlor trick *la coupe du roi*: An apple can be cut into two homochiral halves in two ways which are enantiomorphous to each other. (An apple cannot be cut into two heterochiral halves. Two heterochiral halves originating from two different apples cannot be combined into one apple).

Figure 2-47 after Cinquini et al. [75] who painstakingly documented the analogy with the pomaceous model. Only examples of the *reverse coupe du roi* had been known prior to their work. Thus Anet et al. [76] reported the synthesis of chiral 4-(bromomethyl)-6-(mercaptomethyl)[2.2]metacyclophane. They then showed that two homochiral molecules can be combined to form an achiral dimer as shown in and illustrated by Figure 2-48.

2.8. Polyhedra

"A convex polyhedron is said to be *regular* if its faces are regular and equal, while its vertices are all surrounded alike" [79]. A polyhedron is convex if every dihedral angle is smaller than 180°. The dihedral angle is the angle formed by two polygons joined along a common edge.

There are only five regular convex polyhedra, a very small number indeed. The regular convex polyhedra are called *Platonic solids* because they constituted an important part of Plato's natural philosophy. They are: the tetrahedron, cube (hexahedron), octahedron,

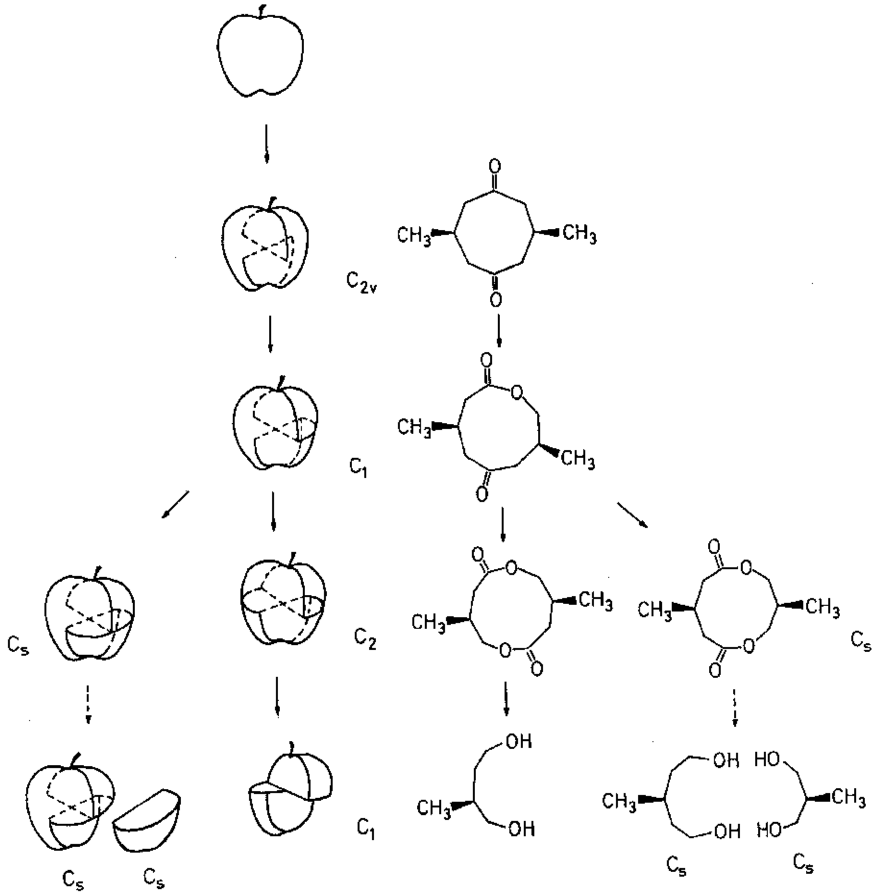

Figure 2-47. *La coupe du roi* and the reaction sequence transforming *cis*-3,7-dimethyl-1,5-cyclooctanedione into 2-methyl-1,4-butanediol. After Cinquini et al. [77].

dodecahedron, and the icosahedron. The faces are regular polygons; regular triangles, regular pentagons, or squares.

A *regular polygon* has equal interior angles and equal sides. Figure 2-49 presents a regular triangle, a regular quadrangle, i.e., square, a regular pentagon, and a few more. As the number of sides approaches infinity, the circle is the limit. The regular polygons have an *n*-fold rotational symmetry axis perpendicular to their plane and going through their midpoint. Here *n* is 1, 2, 3, . . . up to infinity for the circle.

The five regular polyhedra and some of their characteristic symmetry elements are shown in Figure 2-50 with their parameters

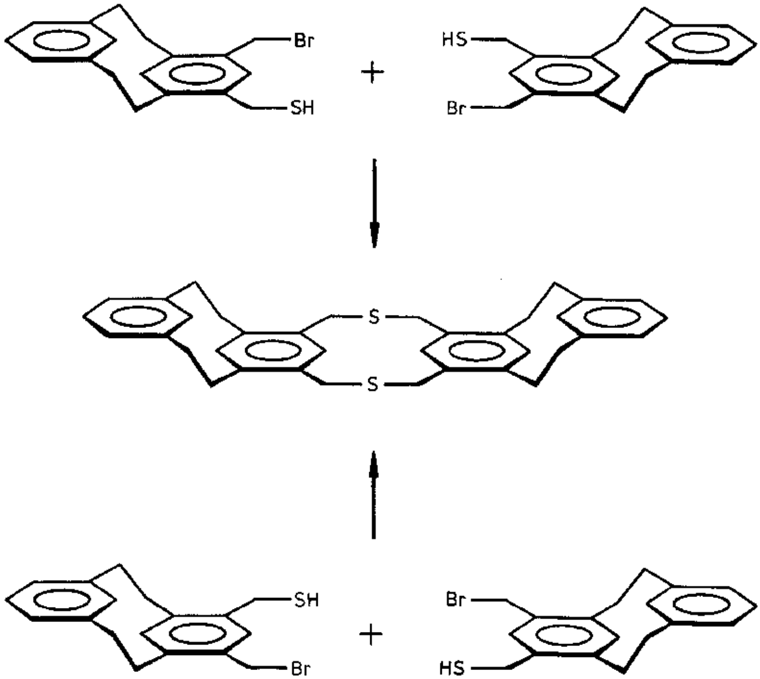

Figure 2-48. *Reverse la coup du roi* and the formation of dimer from two homochiral 4-(bromomethyl)-6-(mercaptomethyl) [2.2]metacyclophane molecules. After Anet et al. [78]. Reprinted with permission from © 1983 American Chemical Society and Kurt Mislow.

compiled in Table 2-3. A commemorative stamp honoring Leonhard Euler and his equation, $V - E + F = 2$, where V, E, and F are the number of vertices, edges, and faces, are reproduced in Figure 2-51. The equation is valid for polyhedra having any kind of polygonal

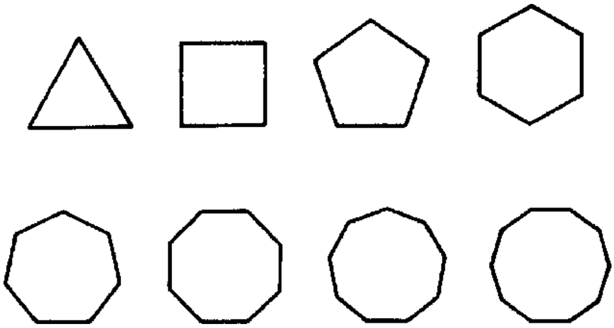

Figure 2-49. Regular polygons.

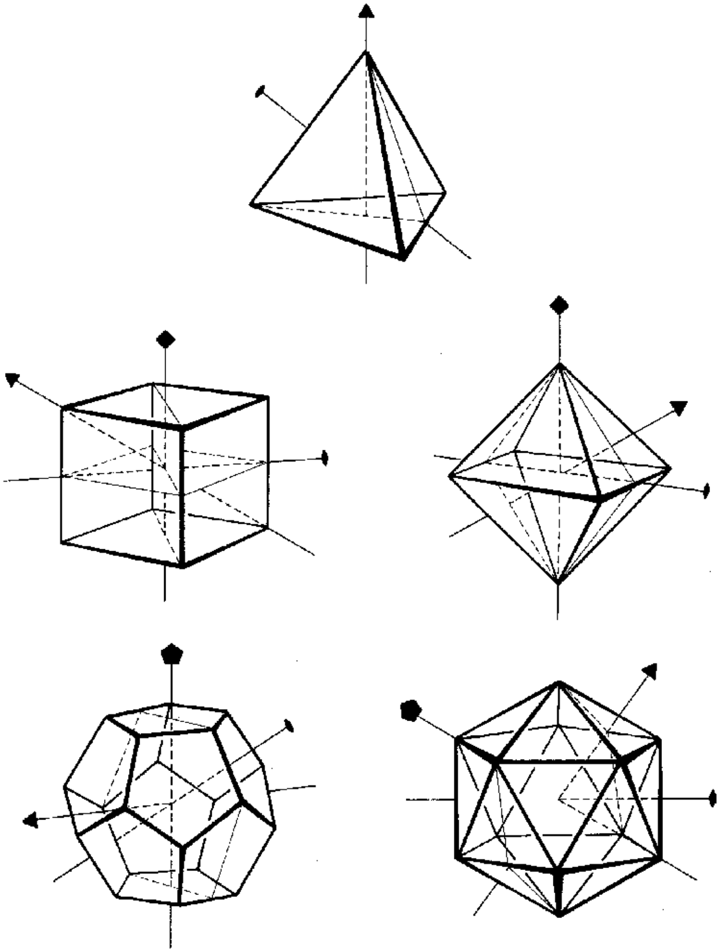

Figure 2-50. The five Platonic solids with some of their characteristic symmetry elements.

faces. According to Weyl [80], the existence of the tetrahedron, cube, and octahedron is a fairly trivial geometric fact, but the discovery of the regular dodecahedron and the regular icosahedron was "one of the most beautiful and singular discoveries made in the whole history of mathematics." However, according to Coxeter [81], to ask the question who first constructed the regular polyhedra is like asking the question who first used fire.

Many primitive organisms have the shape of the pentagonal dodecahedron. As will be seen later, pentagonal symmetry used to be considered forbidden in the world of crystal structures. Belov [82] suggested that the pentagonal symmetry of primitive organisms represents their

Table 2-3. Characteristics of the Regular Polyhedra

Name	Polygon	Number of faces	Vertex figure	Number of vertices	Number of edges
Tetrahedron	3	4	3	4	6
Cube	4	6	3	8	12
Octahedron	3	8	4	6	12
Dodecahedron	5	12	3	20	30
Icosahedron	3	20	5	12	30

defense against crystallization. Polyhedral-shaped radiolarians from Ernst Haeckel's book [83] have been reproduced frequently in treatises on symmetry; in Figure 2-52, we show a few of them. Two artistic representations of the regular pentagonal dodecahedron are shown in Figure 2-53.

Figure 2-54 shows Kepler and his planetary model based on the regular solids [84]. According to this model the greatest distance of one planet from the sun stands in a fixed ratio to the least distance of the next outer planet from the sun. There are five ratios describing the distances of the six planets which were known to Kepler. A regular solid can be interposed between two adjacent planets so that the inner planet, when at its greatest distance from the sun, lays on the inscribed sphere of the solid, while the outer planet, when at its least distance, lays on the circumscribed sphere.

Arthur Koestler in *The Sleepwalkers* called this planetary model [86] "... a false inspiration, a supreme hoax of the Socratic *daimon*, ..." However, the planetary model which is also a densest packing model probably symbolizes Kepler's best attempt at attaining a unified

Figure 2-51. Euler and his equation, $e - k + f = 2$, corresponding to $V - E + F = 2$, where the German *e* (*E*cke), *k* (*K*ante), and *f* (*F*läche) correspond to *v*ertex (*V*), *e*dge (*E*), and *f*ace (*F*) in English, respectively (East German postal stamp).

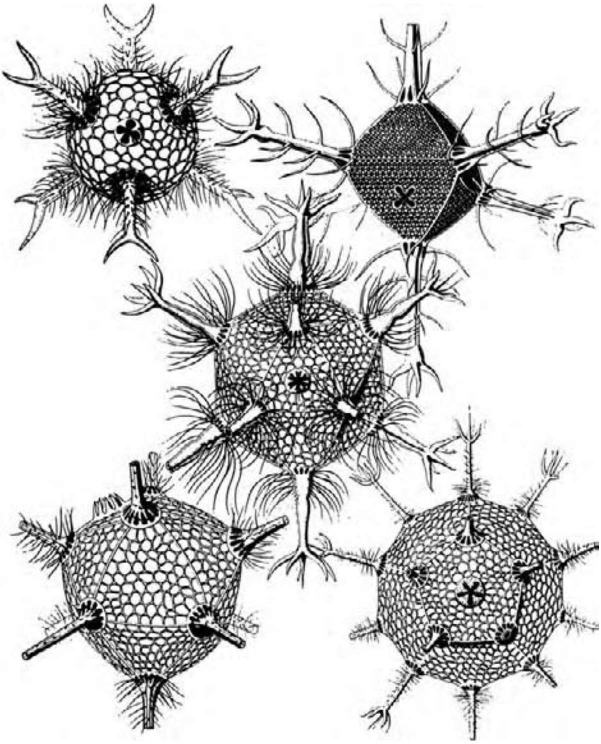

Figure 2-52. Radiolarians from Haeckel's book [85].

view of his work both in astronomy and in what we call today crystallography.

Inorganic chemistry is especially rich in systems that can be described by two or more polyhedra, nested into each another. An interesting case is the $W_6S_8(PEt_3)_6$ crystal [88] in which there is a central octahedron formed by the tungsten atoms, surrounded by a sulfur cube that is enveloped by an octahedron formed by the phosphine ligands (Figure 2-55). Structures in which several polyhedra are nested in each other are sometimes called *keplerates*, referring to Kepler's beautiful structure of the nested five Platonic solids [90].

There are excellent monographs on regular figures, of which we single out those by Coxeter and by László Fejes Tóth as especially noteworthy [91]. The Platonic solids have very high symmetries and one especially important common characteristic. None of the rotational symmetry axes of the regular polyhedra is unique, but each axis

(a) (b)

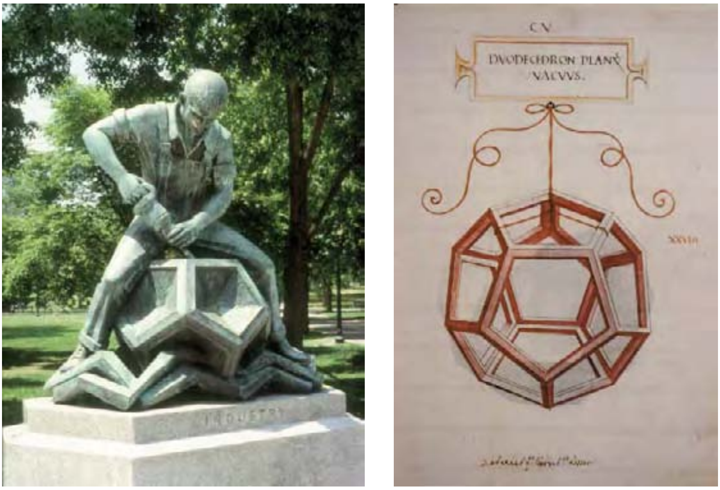

Figure 2-53. Two artistic representations of the regular pentagonal dodecahedron. (**a**) Pentagonal dodecahedron as part of the sculpture symbolizing “Industry” at the Commons in Boston (photograph by the authors); (**b**) Leonardo da Vinci’s dodecahedron in a book of Luca Pacioli, *De Divina Proportione*, published in 1509.

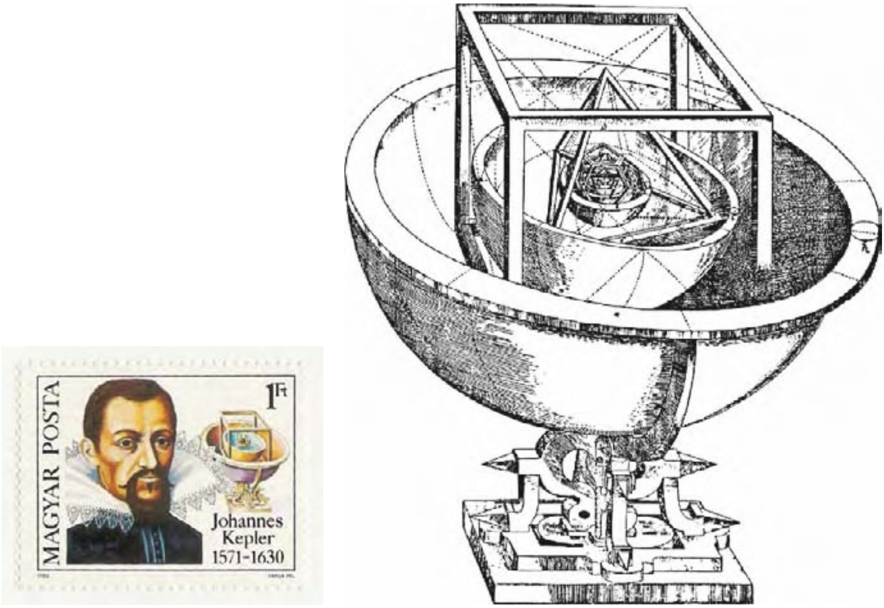

Figure 2-54. Johannes Kepler on Hungarian memorial stamp and his Planetary Model based on the regular solids [87].

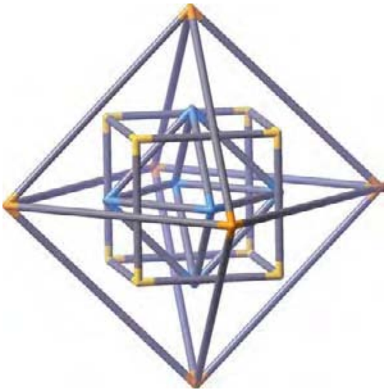

Figure 2-55. Nesting of different regular polyhedra in the structure of $W_6S_8(PEt_3)_6$, after Saito et al. [89].

is associated with several equivalent axes to itself. The five regular solids can be classified into three symmetry classes:

Tetrahedron	$3/2 \cdot m = 3/\tilde{4}$
Cube and Octahedron	$3/4 \cdot m = \tilde{6}/4$
Dodecahedron and Icosahedron	$3/5 \cdot m = 3/\widetilde{10}$

It is equivalent to describe the symmetry class of the tetrahedron as $3/2 \cdot m$ or $3/\tilde{4}$. The skew line relating two axes means that they are not orthogonal. The symbol $3/2 \cdot m$ denotes a threefold axis, and a twofold axis which are not perpendicular and a symmetry plane which includes these axes. These three symmetry elements are indicated in Figure 2-50. The symmetry class $3/2 \cdot m$ is equivalent to a combination of a threefold axis and a fourfold mirror-rotation axis. In both cases the threefold axes connect one of the vertices of the tetrahedron with the midpoint of the opposite face. The fourfold mirror-rotation axes coincide with the twofold axes. The presence of the fourfold mirror-rotation axis is easily seen if the tetrahedron is rotated by a quarter of rotation about a twofold axis and is then reflected by a symmetry plane perpendicular to this axis. The symmetry operations chosen as basic will then generate the remaining symmetry elements. Thus, the two descriptions are equivalent.

Characteristic symmetry elements of the cube are shown in Figure 2-50. Three different symmetry planes go through the center of the cube parallel to its faces. Furthermore, six symmetry planes connect the opposite edges and also diagonally bisect the faces.

The fourfold rotation axes connect the midpoints of opposite faces. The sixfold mirror-rotation axes coincide with threefold rotation axes. They connect opposite vertices and are located along the body diagonals. The symbol $\tilde{6}/4$ does not directly indicate the symmetry planes connecting the midpoints of opposite edges, the twofold rotation axes, or the center of symmetry. These latter elements are generated by the others. The presence of a center of symmetry is well seen by the fact that each face and edge of the cube has its parallel counterpart. The tetrahedron, on the other hand, has no center of symmetry.

The octahedron is in the same symmetry class as the cube. The antiparallel character of the octahedron faces is especially conspicuous. As seen in Figure 2-50, its fourfold symmetry axes go through the vertices, the threefold axes go through the face midpoints, and the twofold axes go through the edge midpoints.

The pentagonal dodecahedron and the icosahedron are in the same symmetry class. The fivefold, threefold and twofold rotation axes intersect the midpoints of faces, the vertices and the midpoints of edges of the dodecahedron, respectively (Figure 2-50). On the other hand, the corresponding axes intersect the vertices and the midpoints of faces and edges of the icosahedron (Figure 2-50).

Consequently, the five regular polyhedra exhibit a dual relationship as regards their faces and vertex figures. The tetrahedron is self-dual (Table 2-3).

It is an intriguing question as to why there are only five regular polyhedra? Keeping in mind the definition that a regular polyhedron has equal and regular polygons as its faces and all of its vertices are alike, the explanation is rather simple. Take first the simplest regular polygon, the equilateral triangle, as the face for a polyhedron. At least three of them need to join at a vertex to make a solid. This is the basis for the tetrahedron. When there are four and five of them, the octahedron and icosahedron are obtained, respectively. However, when we try to have six equilateral triangles to join at a common vertex, they will lie flat, yielding a regular hexagon. Obviously, larger numbers are out, too. Take now the next regular polygon, the square. Three of them at a vertex will yield the cube. Four squares, however, will lie in a plane; thus, with the square, there is only one kind of regular polyhedron. The next regular polygon is the regular pentagon. Joining three of them will eventually lead to the regular dodecahedron. Four of them cannot fit. It is impossible to build a

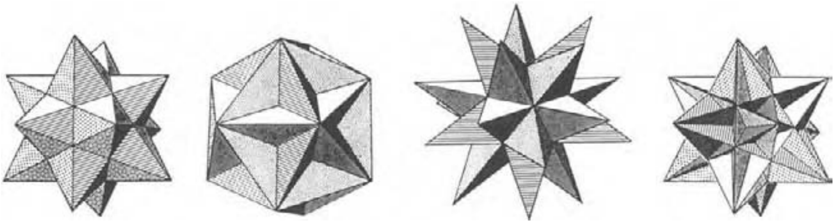

Figure 2-56. The four regular star polyhedra [93]. *From the left*, the small stellated dodecahedron; great dodecahedron; great stellated dodecahedron; and the great icosahedron. Used by permission from Oxford University Press.

polyhedron with three regular hexagons in the vertex since they will lie flat. Here, we reached the limit.

If the definition of regular polyhedra is not restricted to convex figures, their number rises from five to nine [92]. The additional four are depicted in Figure 2-56; they are called by the common name of regular star polyhedra. One of them, viz., the great stellated dodecahedron, is illustrated by the decoration at the top of the Sacristy of St. Peter's Basilica in Vatican City in Figure 2-57.

The *sphere* deserves special mention. It is one of the simplest possible figures and, accordingly, one with high and complicated

Figure 2-57. Great stellated dodecahedron as decoration at the top of the Sacristy of St. Peter's Basilica, Vatican City (photograph by the authors).

symmetry. It has an infinite number of rotation axes of infinite order. All of them coincide with body diagonals going through the midpoint of the sphere. The midpoint, which is also a singular point, is the center of symmetry of the sphere. The following symmetry elements may be chosen as basic ones: two infinite-order rotation axes which are not perpendicular plus one symmetry plane. Therefore, the symmetry class of the sphere is $\infty/\infty \cdot m$. Concerning the symmetry of the sphere George Kepes quotes Copernicus [94]:

> . . . the spherical is the form of all forms most perfect, having need of no articulation; and the spherical is the form of greatest volumetric capacity, best able to contain and circumscribe all else; and all the separated parts of the world—I mean the sun, the moon, and the stars—are observed to have spherical form; and all things tend to limit themselves under this form—as appears in drops of water and other liquids whenever of themselves they tend to limit themselves. So no one may doubt that the spherical is the form of the world, the divine body.

An artistic representation of a sphere is shown in Figure 2-58.

Figure 2-58. Artistic representation of a sphere in front of the World Trade Center in New York City, which was also destroyed in the terror attack on September 11, 2001 (photograph by the authors).

Table 2-4. The Thirteen Semiregular Polyhedra

		Number of			Number of rotation axes			
No.	Name	Faces	Vertices	Edges	2-fold	3-fold	4-fold	5-fold
1	Truncated tetrahedron[a]	8	12	18	3	4	0	0
2	Truncated cube[a]	14	24	36	6	4	3	0
3	Truncated octahedron[a]	14	24	36	6	4	3	0
4	Cuboctahedron[b]	14	12	24	6	4	3	0
5	Truncated cuboctahedron	26	48	72	6	4	3	0
6	Rhombicuboctahedron	26	24	48	6	4	3	0
7	Snub cube	38	24	60	6	4	3	0
8	Truncated dodecahedron[a]	32	60	90	15	10	0	6
9	Icosidodecahedron[b]	32	30	60	15	10	0	6
10	Truncated icosahedron[a]	32	60	90	15	10	0	6
11	Truncated icosidodecahedron	62	120	180	15	10	0	6
12	Rhombicosidodecahedron	62	60	120	15	10	0	6
13	Snub dodecahedron	92	60	150	15	10	0	6

[a]Truncated regular polyhedron.
[b]Quasiregular polyhedron.

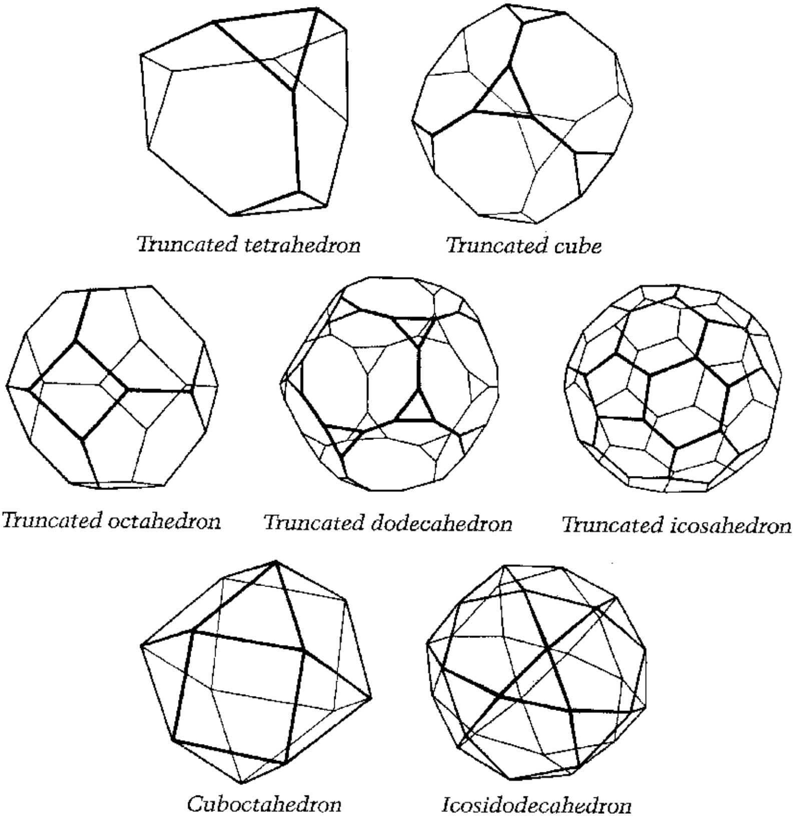

Figure 2-59. The 7 special semi-regular polyhedra. *First two rows*: the so-called truncated regular polyhedra; *Third row*: the quasi-regular polyhedra.

In addition to the regular polyhedra, there are various families of polyhedra with diminishing degrees of regularity. The so-called *semi-regular* or *Archimedean* polyhedra are similar to the Platonic polyhedra in that all their faces are regular and all their vertices are congruent. However, the polygons of their faces are not all of the same kind. The 13 semi-regular polyhedra are listed in Table 2-4 and some of them are depicted in Figure 2-59. Table 2-4 also enumerates their rotation axes.

The simplest semi-regular polyhedra are obtained by symmetrically shaving off the corners of the regular solids. They are the truncated regular polyhedra and are marked with the superscript “a” in Table 2-4. One of them is the truncated icosahedron, the shape of

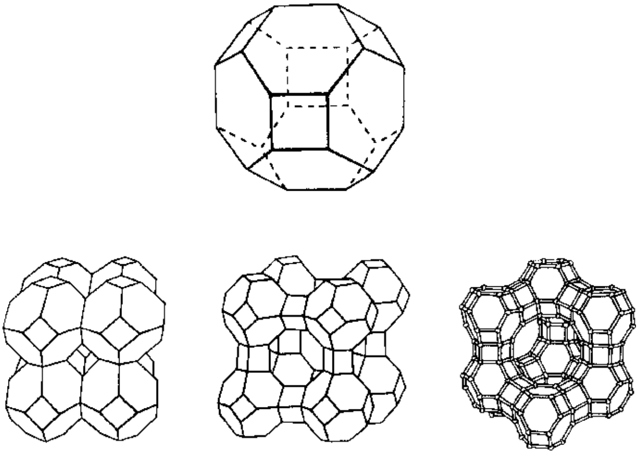

Figure 2-60. Shapes and various modes of linkage of truncated octahedral-shaped sodalite units [97]. Used by permission from Plenum Press and Brian Beagley.

the C_{60} buckminsterfullerene molecule. Two of the semi-regular polyhedra are classified as so-called quasi-regular polyhedra. They have two kinds of faces, and each face of one kind is entirely surrounded by faces of the other kind. They are marked with the superscript "b" in Table 2-4. All these special 7 semi-regular polyhedra are shown in Figure 2-59. The remaining six semi-regular polyhedra may be derived from the other semi-regular polyhedra.

The structures of *zeolites*, aluminosilicates, are rich in polyhedral shapes, including the channels and cavities they form [95]. One of the most common zeolites is sodalite, $Na_6[Al_6Si_6O_{24}]\cdot 2\,NaCl$, whose name refers to its sodium content. The sodalite unit has the shape of a truncated octahedron. The three models of Figure 2-60 represent different modes of linkages between the sodalite units. It is especially interesting to see the different cavities formed by different modes of linkage [96]. Two artistic representations of semi-regular polyhedra are shown in Figure 2-61.

The prisms and antiprisms are also important polyhedron families. A prism has two congruent and parallel faces and they are joined by a set of parallelograms. An antiprism also has two congruent and parallel faces but they are joined by a set of triangles. An infinite number of prisms and antiprisms exist and a few are shown in Figure 2-62. A prism or an antiprism is semiregular if all its faces are

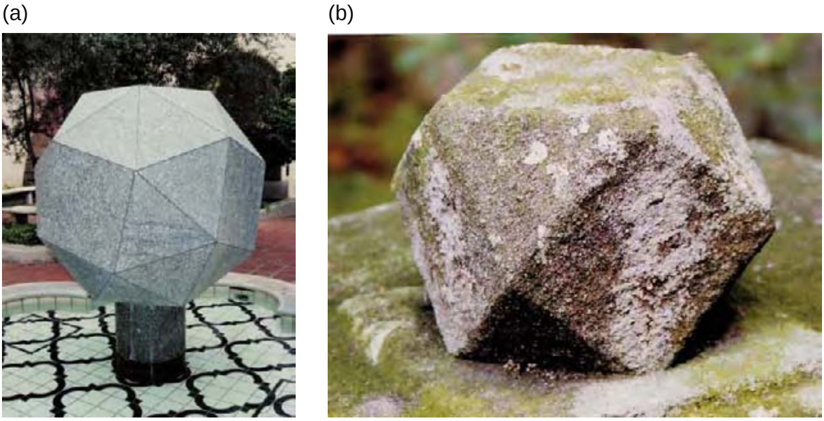

Figure 2-61. Two artistic representations of semi-regular polyhedra (photographs by the authors). (**a**) Snub cube fountain in Pasadena, California [98]; (**b**) Cuboctahedron on top of a garden lantern in the Shugakuin Imperial Villa in Kyoto [99].

regular polygons. A cube can be considered a square prism, and an octahedron a triangular antiprism.

There are many additional polyhedra that are important in discussing molecular geometries and crystal structures. Santiago Alvarez compiled an extensive discussion of polyhedra of varying regularity, their relationships, and many examples from inorganic chemistry [100]. We will return to this topic in the next Chapter.

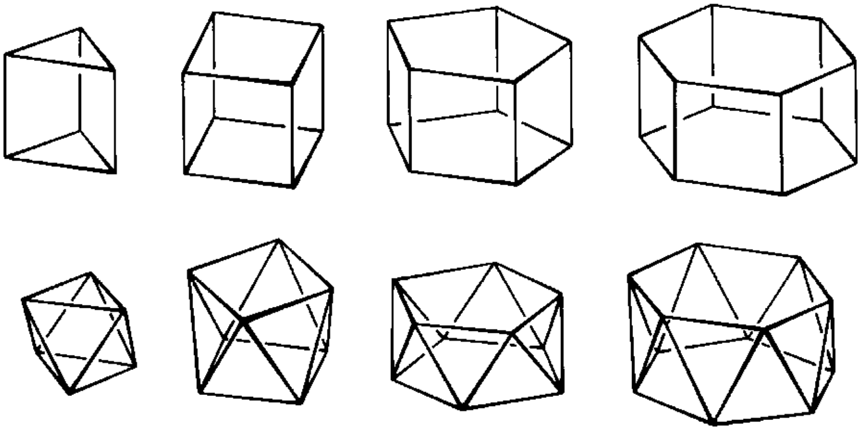

Figure 2-62. Prisms and antiprisms.

References

1. G. H. Hardy, *A Mathematician's Apology,* Cambridge University Press, Cambridge, 1941.
2. T. Mann, *The Magic Mountain*. The cited passage is in French both in the original German (see, e.g., T. Mann, *Der Zauberberg*. S. Fischer Verlag, Frankfurt am Main, 1960; 1974, p. 477; the book was originally published by S. Fischer Verlag, Berlin, 1924) and its English translation (see, e.g., T. Mann, *The Magic Mountain*. Translated from the German by H. T. Lowe-Porter. Alfred A. Knopf, New York, 1946, pp. 342–343). The English translation cited in our text was kindly provided by Dr. Jack M. Davis, Professor of English, University of Connecticut, Storrs, 1984.
3. Mann, *The Magic Mountain*, pp. 276–277 (German edition, pp. 386–387).
4. J. Kepler, *Strena, seu De Nive Sexangula,* 1611. English translation by L. L. Whyte, *The Six-cornered Snowflake,* Clarendon Press, Oxford, 1966.
5. S. P. Springer, G. Deutsch, *Left Brain, Right Brain,* Freeman & Co., San Francisco, 1981; J. B. Hellige, *Hemispheric Asymmetry. What's Right and What's Left*, Harvard University Press, Cambridge, MA, 1993.
6. H. Weyl, *Symmetry,* Princeton University Press, Princeton, New Jersey, 1952, p. 9.
7. E. Häckel (Haeckel), *Kunstformen der Natur*. Vols. 1-10, Verlag des Bibliographischen Instituts, Leipzig, 1899–1904.
8. M. Hargittai, "Hawaiian flowers with fivefold summetry" in I. Hargittai, ed., *Fivefold Symmetry*. World Scientific, Singapore, 1992 pp. 529–541.
9. L. L. Whyte, "Foreword." In J. Kepler (ed.), *The Six-Cornered Snowflake*, pp. v–vii, p. vi.
10. G. Taubes, "The Snowflake Enigma." *Discover* 1984, 5(1), 74–78, p. 75.
11. Ibid.
12. D. McLachlan, "The Symmetry of Dendritic Snow Crystals." *Proc. Natl. Acad. Sci. U.S.A.* 1957, 43, 143–151.
13. Ibid.
14. W. A. Bentley, W. J. Humphreys, *Snow Crystals*. McGraw-Hill, New York and London, 1931.
15. J. Nittmann, H. E. Stanley, "Tip Splitting without Interfacial-Tension and Dendritic Growth-Patterns Arising from Molecular Anisotropy" *Nature* 1986, 321, 663–668; S. Kai, ed., *Pattern Formation in Complex Dissipative Systems,* World Scientific, Singapore, 1992; Y. Furukawa, W. Shimada, "3-Dimensional Pattern-Formation During Growth of Ice Dendrites – Its Relation to Universal Law of Dendritic Growth." *J. Crystal. Growth* 1993, 128, 234–239; R. Kobayashi, "Modeling and Numerical Simulations of Dendritic Crystal-Growth." *Physica D* 1993, 63, 410–423.
16. D. A. Tomalia, "Birth of a New Macromolecular Architecture: Dendrimers as Quantized Building Blocks for Nanoscale Synthetic Organic Chemistry." *Aldrichimica Acta* 2004, 37(2), 39–57.

17. D. A. Tomalia, H. D. Durst, “Genealogically Directed Synthesis – Starburst Cascade Dendrimers and Hyperbranched Structures.” *Top. Curr. Chem*. 1993, 165, 193–313.
18. Mann, *The Magic Mountain*, p. 480.
19. Attributed to M. Polányi. Private communication from Professor W. Jim Neidhardt, New Jersey Institute of Technology, Newark, New Jersey, 1984.
20. A. L. Mackay, ”Generalised Crystallography.” *Izvj. Jugosl. Cent. Kristallogr.* 1975, 10, 15–36; A. L. Mackay, personal communication, 1982.
21. J. Needham, Lu Gwei-Djen, “The Earliest Snow Crystal Observations.” *Weather* 1961, 16, 319–327.
22. Ibid.
23. Ibid.
24. J. Kepler, *The Six-cornered Snowflake.*
25. U. Nakaya, *Snow* (in Japanese), Iwanami-Shoten Publ. Co., Tokyo, 1938 (latest printing, 1987).
26. G. Hellmann, *Schneekrystalle: Beobachtungen und Studien*, Mückenberger, Berlin, 1893.
27. T. Stamp, C. Stamp, *William Scoresby; Arctic Scientist*, Caedmon of Whitby Press, Whitby, North Yorkshire, 1976.
28. Nakaya, *Snow*
29. Stamp, Stamp, *William Scoresby*
30. Bentley, Humphreys, *Snow Crystals*.
31. Ibid.
32. Nakaya, *Snow*.
33. Ibid.
34. K. G. Libbrecht, *The Snowflake*. Voyageur Press, Stillwater, Minnesota, 2003.
35. W. J. Broad, “Snowflakes as Big as Frisbees? Could Be.” *The New York Times* 2007, March 20, pp. F1; F4.
36. J. Reston, *International Herald Tribune*, Thursday, May 7, p. 4, 1981.
37. D. Y. Curtin, I. C. Paul, “Chemical Consequences of the Polar Axis in Organic Solid-State Chemistry.” *Chem. Rev*. 1981, 81, 525–541.
38. P. Groth, *Chemische Kristallographie*. 5 Volumes. Verlag von Wilhelm Engelmann, Leipzig, 1906-1919.
39. Curtin, Paul, *Chem. Rev*. 525–541.
40. G. N. Desiraju, *Crystal Engineering: The Design of Organic Solids*, Elsevier, Amsterdam, 1989.
41. L. Kelvin, *Baltimore Lectures*, C. J. Clay and Sons, London, 1904.
42. J. Applequist, “Optical Activity: Biot’s Bequest.” *Am. Sci*. 1987, 75, 59–68.
43. L. Pasteur, *Researches on the Molecular Asymmetry of Natural Organic Products*. Alembic Club Reprints No. 14. W. F. Clay, Edinburgh, 1897, p. 21.
44. G. Wald, ”The Origin of Optical Activity.“ *Ann. NY Acad. Sci*. 1957, 69, 352–368.
45. E. Fischer, “Einfluss der Configuration auf die Wirkung der Enzyme.“ *Ber. Deutschen Chem. Ges.* 1894, 27, 2985–2993.

46. J. M. Bijvoet, A. F. Peerdeman, A. J. van Bommel, ”Determination of the Absolute Configuration of Optically Active Compounds by Means of X-Rays.” *Nature* 1951, 168, 271–272.
47. L. L. Whyte, ”Chirality.“ *Leonardo* 1975, 8, 245–248; “Chirality.” *Nature* 1958, 182, 198.
48. V. Prelog, “Chirality in Chemistry” (Nobel lecture). *Science* 1976, 193, 17–24.
49. I. Hargittai, B. Hargittai, “Prelog Centennial: Vladimir Prelog (1906–1998).” *Struct. Chem.* 2006, 17, 1–2.
50. M. Gardner, *The New Ambidextrous Universe. Symmetry and Asymmetry from Mirror Reflections to Superstrings*, Third Revised Edition, W. H. Freeman and Co., New York, 1990.
51. P. Curie, “Sur la symétrie dans les phénomenes physiques, symétrie d’un champ eléctrique et d’un champ magnétique.” *J. Phys. (Paris)* 1894, 3, 393–415
52. A. V. Shubnikov, *Simmetriya i antisimmetriya konechnikh figure* (in Russian, *Symmetry and Antisymmetry of Finite Figures*). Izd. Akad. Nauk S.S.S.R., Moscow, 1951.
53. M. Curie, *Pierre Curie, With the Autobiographical Notes of Marie Curie*. Dover Publications, New York, 1963.
54. A. V. Shubnikov, “On the Works of Pierre Curie on Symmetry.” In I. Hargittai, B. K. Vainshtein, eds., *Crystal Symmetries. Shubnikov Centennial Papers*, Pergamon Press, Oxford, 1988, p. 357–364. This is the English translation of the Russian original, A. V. Shubnikov, *Usp. Fiz. Nauk* 1956, 59, 591–602.
55. I. Stewart, M. Golubitsky, *Fearful Symmetry. Is God a Geometer?*, Blackwell, Oxford, 1992.
56. M. Curie, *Pierre Curie.*
57. Prelog, *Science*, 17–24.
58. See, e.g., L. E. Orgel, *The Origins of Life: Molecules and Natural Selection*, John Wiley & Sons, New York, London, Sydney, Toronto, 1973; J. D. Bernal, *The Origin of Life*, The World Publ. Co., Cleveland and New York, 1967.
59. Prelog, *Science*, 17–24.
60. S. F. Mason, *Chemical Evolution: Origins of the Elements, Molecules and Living Systems*, Oxford University Press, England, 1991.
61. A. Szabó-Nagy, L. Keszthelyi, “Demonstration of the Parity-Violating Energy Difference Between Enantiomers.” *Proc. Natl. Acad. Sci. U.S.A.* 1999, 96, 4252–4255.
62. J. B. S. Haldane, “Pasteur and Cosmic Asymmetry.” *Nature* 1960, 185, 87.
63. L. Pasteur, *C. R. Acad. Sci. Paris*, June 1, 1874.
64. Orgel, *The Origins of Life*.
65. Ibid.
66. L. Carroll, *Through the Looking Glass and what Alice found there*; See, e.g., in *The Complete Illustrated Works of Lewis Carroll*. Chancellor Press, London, 1982, p. 127.
67. See, e.g., G. W. Muller, “Thalidomide: From Tragedy to New Drug Discovery.” *Chemtech* 1997, 27(1), 21–25.

68. See, e. g., E. L. Eliel, “Louis Pasteur and Modern Industrial Stereochemistry.” *Croatica Chemica Acta* 1996, 69, 519–533.
69. P. Ahlberg, “The Nobel Prize in Chemistry.” In *Les Prix Nobel—The Nobel Prizes 2001,* Almquist & Wiksell International, Stockholm, 2002, p. 20.
70. See, e.g., S. C. Stinson, “Chiral Drugs.” *Chem. Eng. News* 2000, October 23, 55–78; S. C. Stinson, “Chiral Pharmaceuticals.” Ibid. 2001, October 1, 79–97; A. M. Rouhi, “Chiral Business.” Ibid. 2003, May 5, 45–55; A. M. Rouhi, “Chirality at Work.” Ibid. 2003, May 5, 56–61; R. Winder, “Pure enzymes.” *Chemistry & Industry*. 2006, June 5, 18–19; C. O’Driscoll, “Reflective Work.” Ibid. 2007, May 7, 22–25.
71. A. V. Shubnikov, V. A. Koptsik, *Symmetry in Science and Art*, Plenum Press, New York and London, 1974. Russian original: *Simmetriya v nauke i isskustve*, Nauka, Moscow, 1972.
72. Ibid.
73. F. A. L. Anet, S. S. Miura, J. Siegel, K. Mislow, “La-Coupe-Du-Roi and Its Relevance to Stereochemistry – Combination of 2 Homochiral Molecules to Give an Achiral Product.” *J. Am. Chem. Soc*. 1983, 105, 1419–1426.
74. M. Cinquini, F. Cozzi, F. Sannicoló, A. Sironi, “Bisection of an Achiral Molecule into Homochiral Halves – The 1st Chemical Analog of La Coupe du Roi.” *J. Am. Chem. Soc*. 1988, 110, 4363–4364.
75. Ibid.
76. Anet et al., *J. Am. Chem. Soc*. 1419–1426.
77. Cinquini et al., *J. Am. Chem. Soc*. 4363–4364.
78. Anet et al., *J. Am. Chem. Soc*. 1419–1426.
79. H. S. M. Coxeter, *Regular Polytopes*, Third Edition, Dover Publications, New York, 1973.
80. Weyl, *Symmetry*, p. 74.
81. Coxeter, *Regular Polytopes*.
82. N. V. Belov, *Ocherki po strukturnoi mineralogii (*in Russian, *Notes on structural mineralogy),* Nedra, Moscow, 1976.
83. Häckel, *Kunstformen der Natur*.
84. J. Kepler, *Mysterium cosmographicum,* 1595.
85. Häckel, *Kunstformen der Natur*.
86. A. Koestler, *The Sleepwalkers,* The Universal Library, Grosset and Dunlap, New York, 1963, p. 252.
87. Kepler, *Mysterium Cosmographicum.*
88. T. Saito, A. Yoshikawa, T. Yamagata, H. Imoto, K. Unoura, “Synthesis, Structure, and Electronic Properties of Octakis(μ_3-sulfido)hexakis (triethylphophine) hexatungsten as a Tungsten Analogue of the Molecular Model for Superconducting Chevrel Phases” *Inorg. Chem*. 1989, 28, 3588–3592.
89. Ibid.
90. A. Müller, P. Kögerler, A. W. M. Dress, “Giant Metal-Oxide-Based Spheres and Their Topology: from Pentagonal Building Blocks to Keplerates and Unusual Spin Systems.” *Coord. Chem. Rev*. 2001, 222, 193–218.

91. Coxeter, *Regular Polytopes*; L. Fejes Tóth, *Regular Figures*, Pergamon Press, New York, 1964.
92. Ibid. and H. M. Cundy, A. P. Rollett, *Mathematical Models*, Clarendon Press, Oxford, 1961; M. J. Wenninger, *Polyhedron Models*, Cambridge University Press, New York, 1971; P. Pearce, S. Pearce, *Polyhedra Primer*, Van Nostrand Reinhold Co., New York, 1978.
93. Cundy, Rollett, *Mathematical Models*.
94. N. Copernicus, *De Revolutionibus Orbium Caelestium*, 1543, as cited in G. Kepes, *The New Landscape in Art and Science*, Theobald & Co., Chicago, 1956.
95. W. M. Meier, D. H. Olson, *Atlas of Zeolite Structure Types*, Third Revised Edition, Butterworth-Heinemann, London, 1992.
96. B. Beagley, J. O. Titiloye, "Modeling the Similarities and Differences between the Sodalite Cages (Beta-Cages) in the Generic Materials - Sodalite, Zeolites of Type-A, and Zeolites with Faujasite Frameworks" *Struct.Chem.* 1992, 3, 429–448.
97. Ibid.
98. W. P. Schaefer, "The Snub Cube in the Glanville Courtyard of the Beckman Institute at the California Institute of Technology." *Chemical Intelligencer* 1996, 2(4), 48–50.
99. I. Hargittai, "Imperial Cuboctahedron." *Math. Intell.* 1993, 15(1), 58–59.
100. S. Alvarez, "Polyhedra in (Inorganic) Chemistry." *Dalton Trans.* 2005, 2209–2233.

Chapter 3

Molecular Shape and Geometry

Form is a diagram of forces.
D'Arcy W. Thompson [1]

A molecule is a collection of atoms kept together by interactions among those atoms. For some purposes it is better to consider the molecule as consisting of the nuclei of its constituent atoms and its electron density distribution. Generally, it is the geometry and symmetry of the arrangement of the atomic nuclei that is considered to be the geometry and symmetry of the molecule itself. At a certain point in science history, spatial considerations entered the description of molecules. While we take this for granted today, the first steps in this direction were not without hurdles. The year 1874 was the birth of stereochemistry although the term itself was only introduced as late as 1890, by Victor Meyer to describe the three-dimensional positions of the atoms in a molecule. The basic concepts were proposed by J. H. van 't Hoff and J. A. Le Bel, and van 't Hoff published a booklet called *La Chimie dans l'Espace* (Chemistry in Space) [2]. When the two scientists suggested the idea of the tetrahedral geometrical arrangement of the bonds radiating from the carbon atom, it was revolutionary, and some found it too radical. The most vocal critic of the new views was an outstanding organic chemist, Hermann Kolbe, who ridiculed van 't Hoff in the most blatant way [3]. The true breakthrough came with X-ray crystallography, which yielded a large amount of direct structural information. In time, other powerful techniques joined in and modern structural chemistry commenced. Theories and models appeared in parallel with the growing amount of experimental data, and the observation of trends and regularities greatly facilitated the development of this new field of chemistry [4].

M. Hargittai, I. Hargittai, *Symmetry through the Eyes of a Chemist,* 3rd ed.,
DOI: 10.1007/978-1-4020-5628-4_3, © Springer Science+Business Media B.V. 2009

Molecules are finite figures with at least one singular point in their symmetry description. Thus, point groups are applicable to them. There is no inherent limitation on the available symmetries for molecules. Molecules in the gas phase are considered to be *free*. They are so far apart that they are unperturbed by interactions from other molecules and thus can be considered isolated from each other. On the other hand, intermolecular interactions may occur between the molecules in condensed phases, i.e., in liquids, melts, amorphous solids, or crystals. In the present discussion all molecules will be assumed unperturbed by their environment, regardless of the phase or state of matter in which they exist.

Molecules are never motionless. They are performing vibrations all the time. In addition, the gaseous molecules, and also the molecules in liquids, are performing rotational and translational motion as well. Molecular vibrations constitute relative displacements of the atomic nuclei with respect to their equilibrium positions and occur in all phases, including the crystalline state, and even at the lowest possible temperatures. The magnitude of molecular vibrations is relatively large, amounting to several percent of the internuclear distances. Typically, there are about 10^{12}–10^{14} vibrations per second.

Symmetry considerations are fundamental in any description of molecular vibrations, as will be seen later in detail (Chapter 5). First, however, the molecular symmetries will be discussed, ignoring entirely the motion of the molecules. Various molecular symmetries will be illustrated by examples. A simple model will also be discussed to gain some insight into the origins of the various shapes and symmetries in the world of molecules. Our considerations will be restricted, however, to relatively simple, thus rather symmetrical systems. The importance and consequences of intramolecular motion involving relatively large amplitudes, will be commented upon in the final section of this chapter.

3.1. Isomers

The empirical formula, or sum formula, of a chemical compound expresses its composition. For example $C_2H_4O_2$ indicates that the molecule consists of two carbon, four hydrogen and two oxygen atoms. This formulation, however, provides no information on the

order in which these atoms are linked. This particular empirical formula may correspond to methyl formate (3-1), acetic acid (3-2), and glycol aldehyde (3-3). Only the structural formulae for these compounds, shown below, distinguish among them. This is called structural isomerism.

$HCOOCH_3$ CH_3COOH $HCOCH_2OH$

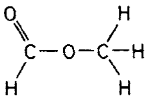

3-1

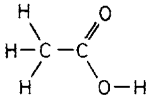

3-2

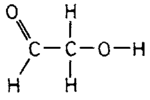

3-3

Although these molecules, as a whole, are not symmetric, some of their component parts may be symmetrical. They possess what is called local symmetry. Similar atomic groups in different molecules often have similar geometries, and thus similar local symmetries. The structural formulae reveal considerable information about these local symmetries, or at least their similarities and differences in various molecules. The above simplified structural formulae are especially useful in this respect. This approach is widely applicable in organic chemistry, where relatively few kinds of atoms build an enormous number of different molecules. A far greater diversity of structural peculiarities is characteristic for inorganic compounds.

The symbol for the carbon atom occurs twice in all three simplifed structural formulae above, a fact that indicates differences in the structural positions of these carbon atoms. The same applies to the oxygen atoms. On the other hand, three hydrogens are equivalent in both methyl formate and acetic acid, with the fourth being different in the two molecules. There are three different types of hydrogen positions in glycol aldehyde.

Molecules are structural isomers if they have the same empirical formula but the distances between corresponding atoms are not the same (Figure 3-1). Structural isomers are of two types. If their atomic connectivities are the same, they are diastereomers, and if their atomic connectivities are different, they are constitutional isomers. Some diastereomers become superimposable by rotation about a bond, and they are called rotational isomers. Depending on the magnitude of the

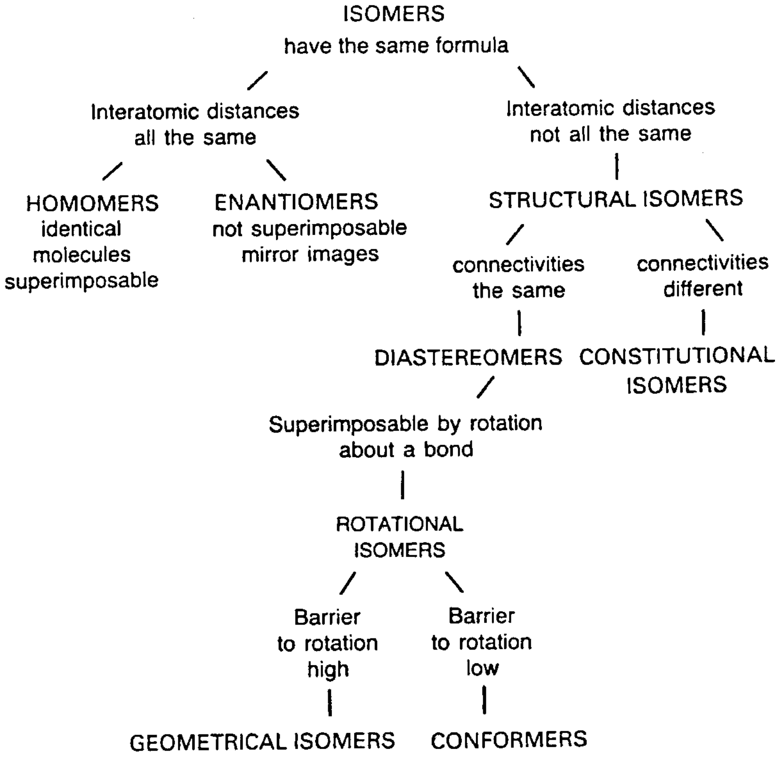

Figure 3-1. The hierarchy of isomers.

barrier to rotation, geometrical isomers (high barrier) and conformers (low barrier) are distinguished.

Identical molecules have the same formula, the same atomic connectivity, and the same distances between corresponding atoms. In addition, they are superimposable (homomers). Enantiomers have the same formula, the same atomic connectivity, and the same distances between corresponding atoms, but they are not superimposable, instead, they are mirror images of each other (cf. Section 2.7 on chirality).

3.2. Rotational Isomerism

The four-atomic chain is the simplest system for which rotational isomers are possible, as shown in Figure 3-2. Rotational isomers, or *conformers*, are various forms of the same molecule related by

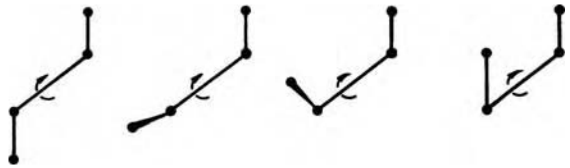

Figure 3-2. Rotational isomerism of a four-atomic chain.

rotation around a bond as axis. The rotational isomers of a molecule are described by the same empirical formula and by the same structural formula. Only the relative positions of the two bonds (or groups of atoms) at the two ends of the rotation axis are changed. The molecular point groups for different rotational isomers may be entirely different.

Rotational isomers can be conveniently represented by so-called projection formulae in which the two bonds (or groups of atoms) at the two ends are projected onto a plane which is perpendicular to the central bond. This plane is denoted by a circle whose center coincides with the projection of the rotation axis. The bonds in front of this plane are drawn as originating from the center, while the bonds behind this plane, i.e., the bonds from the other end of the rotation axis, are drawn as originating from the perimeter of the circle.

The drawings by Degas *End of the Arabesque* and *Seated Dancer Adjusting Her Shoes* may be looked at as illustrations of the staggered and eclipsed conformations of the molecule $A_2B–BC_2$ [5]. The dancers and their projection-like representations are depicted in Figure 3-3 along with the projectional representations of two conformers of the molecule $A_2B–BC_2$. The projections in Figure 3-3 represent views along the B–B bond, i.e., the dancer's body. The plane bisecting the B–B bond is shown by the circle and it corresponds to the dancer's skirt. The dancer's arms and legs refer to the bonds B–A and B–C, respectively. Incidentally, the bouquet in the right hand of the dancer in the staggered conformation might be viewed as a different substituent.

Two important cases in rotational isomerism are distinguished by considering the nature of the central bond. When it is a double bond, rotation of one form into another is hindered by a high potential

barrier. This barrier may be so high that the two rotational isomers will be stable enough to make their physical separation possible. An example is 1,2-dichloroethylene.

The symmetry of the *cis* isomer is characterized by two mutually perpendicular mirror planes generating also a two-fold rotational axis. This symmetry class is labeled *mm*. An equivalent notation is C_{2v} as

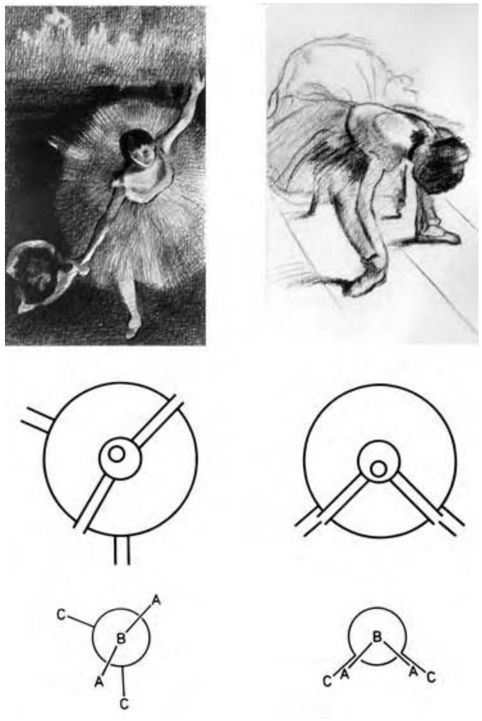

Figure 3-3. Projectional representation of rotational isomers [6]; *Top*, *left*: drawing after Degas' *End of the Arabesque* by Ferenc Lantos; *Right*: drawing after Degas' *Seated Dancer Adjusting Her Shoes* by Ferenc Lantos; *Middle*: contour drawings of the dancers; *Bottom*: staggered and eclipsed rotational isomers of the A_2BBC_2 molecule by projections representing view along the B–B bond.

will be seen in the next section. The *trans* isomer has one twofold rotation axis with a perpendicular symmetry plane, its symmetry class is $2/m$ (C_{2h}).

Rotational isomerism relative to a single bond is illustrated by ethane and 1,2-dichloroethane, both depicted in Figure 3-4. First, take the ethane molecule, $H_3C–CH_3$. During a complete rotation of one methyl group around the C–C bond relative to the other methyl group,

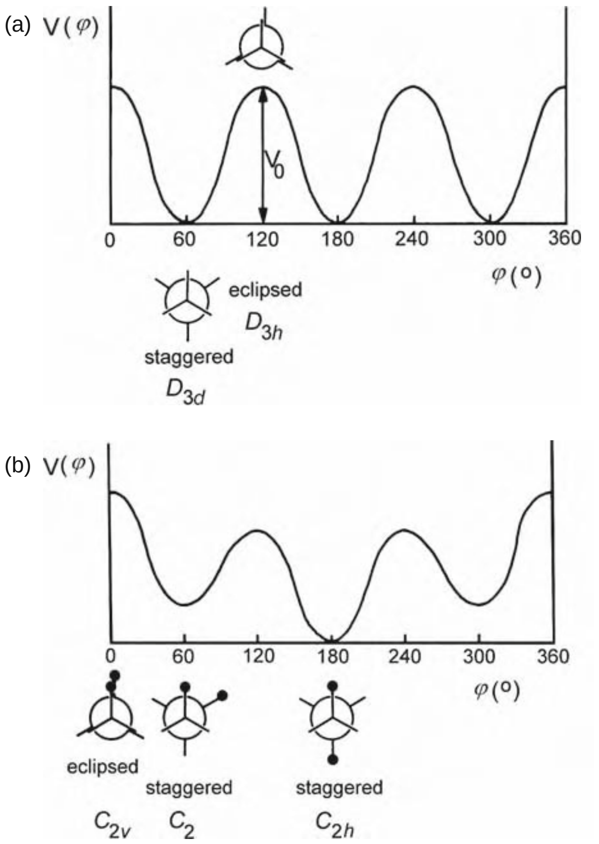

Figure 3-4. Potential energy functions for rotation about a single bond, φ is the angle of rotation. (**a**) Ethane, $H_3C–CH_3$. There are two different symmetrical forms. Both the staggered form with D_{3d} symmetry and the eclipsed form with D_{3h} symmetry occur three times in a complete rotational circuit; (**b**) 1,2-dichloroethane, $ClH_2C–CH_2Cl$. There is no other symmetrical form in the region between the two symmetrical staggered forms shown. The eclipsed form with C_{2v} symmetry and the staggered form with C_{2h} symmetry occur once, while the staggered form with C_2 symmetry occurs twice in a complete rotational circuit.

the ethane molecule appears three times in the stable staggered form and three times in the unstable eclipsed form. As all the hydrogen atoms of one methyl group are equivalent, the three energy minima are equivalent, and so are the three energy maxima, as seen in Figure 3-4a. The situation becomes more complicated when the three ligands bonded to the carbon atoms are not the same. This is seen for 1,2-dichloroethane in Figure 3-4b. There are three highly symmetrical forms. Of these two are staggered with C_{2h} and C_2 symmetries, respectively. The third is an eclipsed form with C_{2v} symmetry. This form has Cl/Cl and H/H eclipsing.

Figure 3-4 shows only the symmetrical conformers by projection formulae. The symmetrical forms always belong to extreme energies, either minima or maxima. The barriers to internal rotation in the potential energy functions depicted in Figure 3-4 are about 10 kJ/mol. Typical barriers for systems where the double bonds would be considered to be the “rotational axis” may be as much as 30 times greater than those for systems with single bonds.

3.3. Symmetry Notations

So far, the so-called International or Hermann-Mauguin symmetry notations have been used in the descriptions in this text. Another, older system by Schoenflies is generally used, however, to describe the molecular point-group symmetries. This notation has been given in parenthesis in the preceding section. The Schoenflies notation has the advantage of succinct expression for even complicated symmetry classes combining various symmetry elements. The two systems are compiled in Table 3-1 [7] for a selected set of symmetry classes. The set includes all point-group symmetries in the world of crystals which are restricted to 32 classes. The reasons and significance of these restrictions will be discussed later in the chapter on crystals (Section 9.3). There are no restrictions on the point-group symmetries for individual molecules, and a few further, so-called *limiting*, classes are also listed in Table 3-1.

The Schoenflies notation for rotation axes is C_n, and for mirror-rotation axes the notation is S_{2n}, where n is the order of the rotation. The symbol i refers to the center of symmetry (cf. Section 2.4). Symmetry planes are labeled σ; σ_v is a vertical plane, which always coincides with the rotation axis with an order of two or higher, and

Table 3-1. Symmetry Notations of the Crystallographic and a Few Limiting Groups

Hermann-Mauguin	Schoenflies	Hermann-Mauguin	Schoenflies
Crystallographic groups			
1	C_1	$\bar{3}m$	D_{3d}
$\bar{1}$	C_i	$\bar{6}$	C_{3h}
m	C_s	6	C_6
2	C_2	$6/m$	C_{6h}
$2/m$	C_{2h}	$\bar{6}m2$	D_{3h}
mm	C_{2v}	$6mm$	C_{6v}
222	D_2	622	D_6
mmm	D_{2h}	$6/mmm$	D_{6h}
4	C_4	23	T
$\bar{4}$	S_4	$m\bar{3}$	T_h
$4/m$	C_{4h}	$\bar{4}3m$	T_d
$4mm$	C_{4v}	432	O
$\bar{4}2m$	D_{2d}	$m3m$	O_h
422	D_4	Limiting groups	
$4/mmm$	D_{4h}	∞	C_∞
3	C_3	$\infty 2$	D_∞
$\bar{3}$	S_6	∞/m	$C_{\infty h}$
$3m$	C_{3v}	∞mm	$C_{\infty v}$
32	D_3	∞/mm	$D_{\infty h}$

σ_h is a horizontal plane, which is always perpendicular to the rotation axis when it has an order of two or higher.

Point-group symmetries not listed in Table 3-1 may easily be assigned the appropriate Schoenflies notation by analogy. Thus, e.g., C_{5v}, C_{5h}, C_7, C_8, etc. can be established. Such symmetries may well occur among real molecules.

These systems of notation have been well established and widely used. Nonetheless, other systems might be and have been suggested though none has gone into practice. We mention here one such suggestion by outstanding mathematicians whose system has merits, but only time will tell whether it might gain acceptance [8].

3.4. Establishing the Point Group

Figure 3-5 shows a possible scheme for establishing the molecular point group that has been widely used to reliably establish molecular symmetries [9].

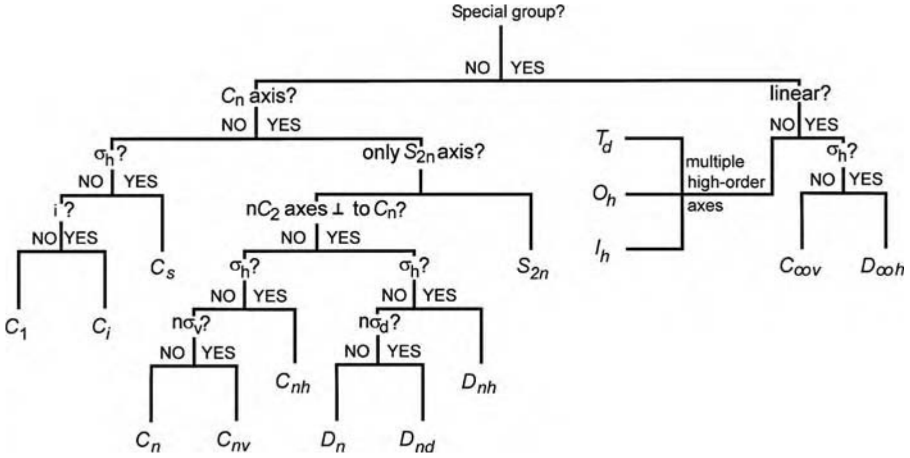

Figure 3-5. Scheme for establishing the molecular point groups [10].

First, an examination is carried out whether the molecule belongs to some "special" group. If the molecule is linear, it may have a perpendicular symmetry plane ($D_{\infty h}$) or it may not have one ($C_{\infty v}$). Very high symmetries are easy to recognize. Each of the groups T, T_h, T_d, O, and O_h, has four threefold rotation axes. Both icosahedral I and I_h groups require ten threefold rotation axes and six fivefold rotation axes. The molecules belonging to these groups have a central tetrahedron, octahedron, cube, or icosahedron.

If the molecule does not belong to one of these "special" groups, a systematic approach is followed. Firstly, the possible presence of rotation axes in the molecule is checked. If there is no rotation axis, then it is determined whether there is a symmetry plane (C_s). In the absence of rotational axes and mirror planes, there may only be a center of symmetry (C_i), or there may be no symmetry element at all (C_1). If the molecule has rotation axes, it may have a mirror-rotation axis with even-number order (S_{2n}) coinciding with the rotation axis. For S_4 there will be a coinciding C_2, for S_6 a coinciding C_3, and for S_8, both C_2 and C_4.

In any case the search is for the highest order C_n axis. Then it is ascertained whether there are n C_2 axes present perpendicular to the C_n axis. If such C_2 axes are present, then there is D symmetry. If in addition to D symmetry there is a σ_n plane, the point group is D_{nh}, while if there are n symmetry planes (σ_d) bisecting the twofold axes,

the point group is D_{nd}. If there are no symmetry planes in a molecule with D symmetry, the point group is D_n.

Finally, if no C_2 axes perpendicular to C_n are present, then the lowest symmetry will be C_n, when a perpendicular symmetry plane is present, it will be C_{nh}, and when there are n coinciding symmetry planes, the point group will be C_{nv}.

3.5. Examples

In this section, actual molecular structures are shown for the various point groups. The Schoenflies notation is used and the characteristic symmetry elements are enumerated.

C_1: There are no symmetry elements except the one-fold rotation axis, or identity, of course. C_1 symmetry is *asymmetry.* Examples are:

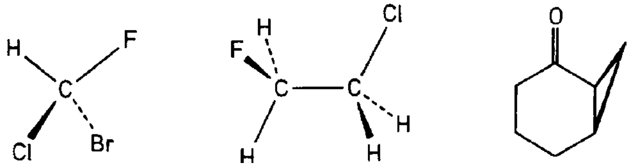

$C_2, C_3, C_4, C_5, C_6, \ldots, C_n$: One twofold, threefold, fourfold, fivefold, sixfold rotation axis, respectively, and it can be continued by analogy. C_n has one n-fold rotation axis. Examples: Figure 3-6a. The most famous molecule that has C_2 symmetry is deoxyribonucleic acid (DNA) whose double helical structure will be discussed in more detail in Chapter 8. Here, suffice it to note that the C_2 symmetry "would make a model of DNA suitable for use as a staircase in a space ship" because "these elements are twofold rotation axes passing through each of the base pairs at right angles to the helical axis; each of them brings one of the chains into congruence with its partner of opposite polarity by a rotation of 180°" [11]. The C_2 symmetry played an important role in the discovery of the double helix and is intimately related to the genetic function of the molecule [12]. Another important biological system that also has C_2 symmetry, even though in an approximate way only, is the photosynthetic reaction center (Figure 3-6b). Whereas the C_2 symmetry of DNA has well-defined functional implications, no such meaning of this symmetry for the process of photosynthesis has been uncovered (yet?) [13]. This is how

chemistry Nobel laureate Johann Deisenhofer who first noticed this symmetry described the moment as he was locating the chlorophyll molecules in the structure [14]:

> It was extremely exciting to localize these features and build models for them. When I stepped back to see the arrangement, the unexpected observation about it was symmetric. There was a symmetry in the arrangement of the chlorophyll that nobody had anticipated. Nobody, to this day, completely

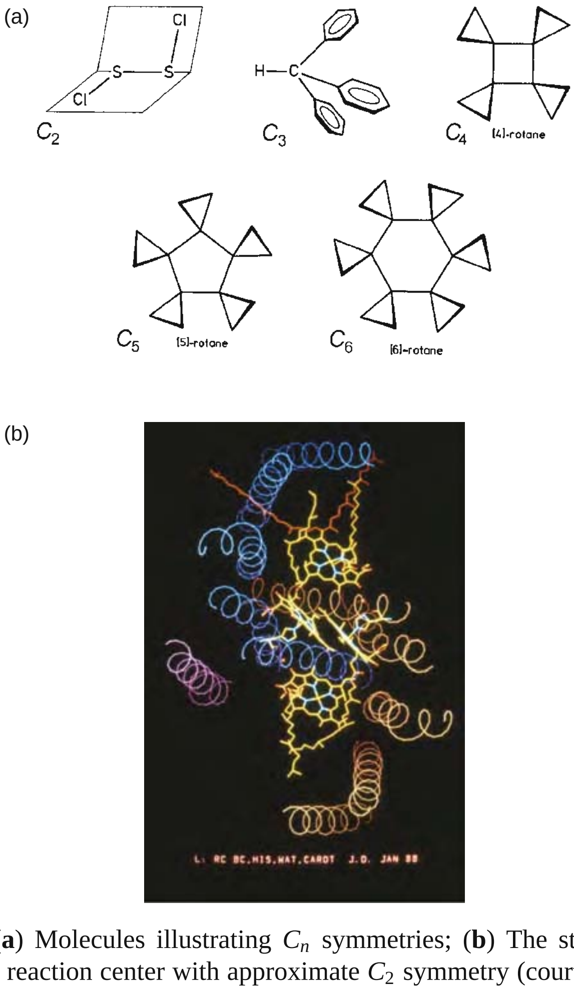

Figure 3-6. (**a**) Molecules illustrating C_n symmetries; (**b**) The structure of the photosynthetic reaction center with approximate C_2 symmetry (courtesy of Johann Deisenhofer, Dallas, Texas) [15].

> understands the purpose of this symmetry. I think it can be understood only on the basis of evolution. I think that the photosynthetic reaction started out as a totally symmetric molecule. Then it turned out to be preferable to disturb its symmetry, sticking to an approximate symmetry but changing subtly the two halves of the molecule. Because of the difference in properties of the two halves, the conclusion had been, before the structure came out, that there cannot be symmetry; that it has to be an asymmetric molecule. Now when people looked at the structure, it looked totally symmetric to the naked eye. That realization was the high point I will never forget.

Deisenhofer's description is a beautiful illustration for some of the ideas about the importance of symmetries occurring in an approximate way as discussed in the Introduction (Chapter 1). The near-C_2 symmetry of the photosynthetic reaction center [16] and its elucidation [17] have been discussed in the literature.

C_i: Center of symmetry. Examples:

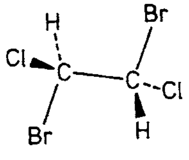
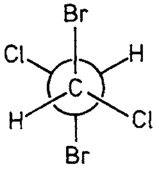

C_s: One symmetry plane. Examples:

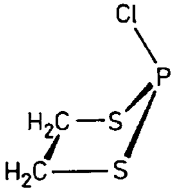
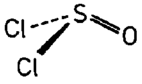
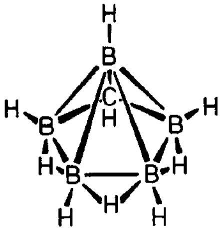

S_4: One fourfold mirror-rotation axis.

S_6: One sixfold mirror-rotation axis, which is, of course, equivalent to one threefold rotation axis plus center of symmetry. Example:

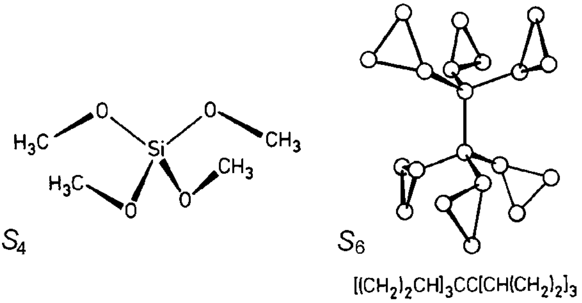

C_{2h}, C_{3h}, ..., C_{nh}: One twofold, threefold, ..., n-fold rotation axis with a perpendicular to it symmetry plane. Examples: Figure 3-7.

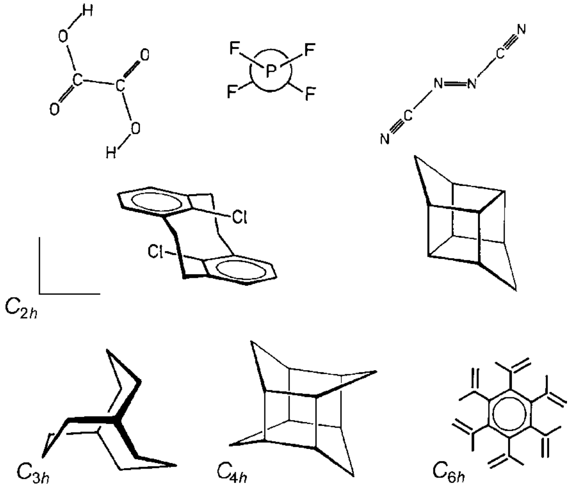

Figure 3-7. Examples with rotational axis and perpendicular symmetry plane, C_{nh}.

C_{2v}, C_{3v}, C_{4v}, C_{5v}, C_{6v}, ..., C_{nv}: C_{2v}, Two perpendicular symmetry planes whose crossing line is a twofold rotation axis; C_{3v}, One three-fold rotation axis with three symmetry planes which include the rotation axis. The angle is 60° between two symmetry planes; C_{4v}, One fourfold rotation axis with four symmetry planes which include the rotation axis. The four planes are grouped in two nonequivalent pairs. One pair is rotated relative to the other pair by 45°. The angle between

the two planes within each pair is 90°. This series can be continued by analogy. When n is even, there are two sets of symmetry planes. One set is rotated relative to the other set by $(180/n)°$. The angle between the planes within each set is $(360/n)°$. When n is odd, the angle between the symmetry planes is $(180/n)°$. Examples: Figure 3-8.

$C_{\infty v}$: One infinite-fold rotation axis with infinite number of symmetry planes which include the rotation axis. Example: Figure 3-8.

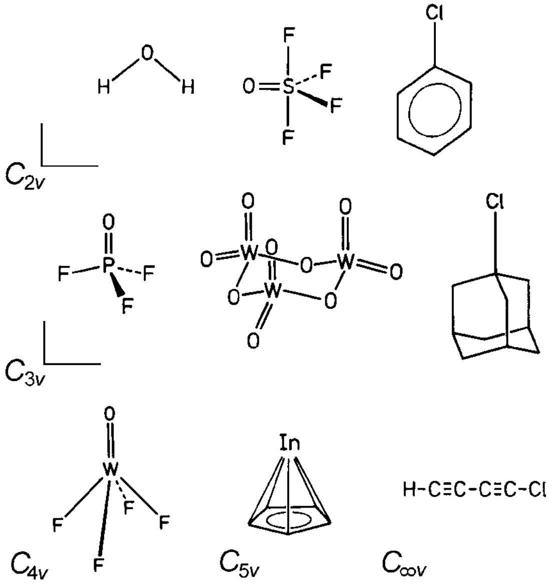

Figure 3-8. Examples with rotation axis and symmetry planes containing the rotation axis, C_{nv}.

D_2: Three mutually perpendicular twofold rotation axes.

D_3: One threefold rotation axis and three twofold rotation axes perpendicular to the threefold axis. The twofold axes are at 120°, so the minimum angle between two such axes is 60° Examples:

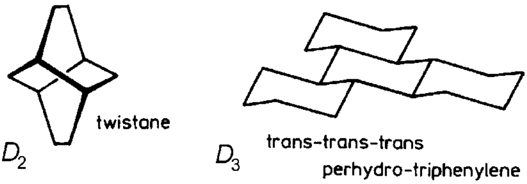

D_4: One fourfold rotation axis and four twofold rotation axes which are perpendicular to the fourfold axis. The four axes are grouped in two nonequivalent pairs. One pair is rotated relative to the other pair by 45°. The angle between the two axes within each pair is 90°.

D_5, D_6, D_7, ..., D_n: This series can be continued by analogy. It is characterized by one n-fold rotation axis and n twofold rotation axes perpendicular to the n-fold axis.

D_{2d}: Three mutually perpendicular twofold rotation axes and two symmetry planes. The planes include one of the three rotation axes and bisect the angle between the other two. Example: Figure 3-9.

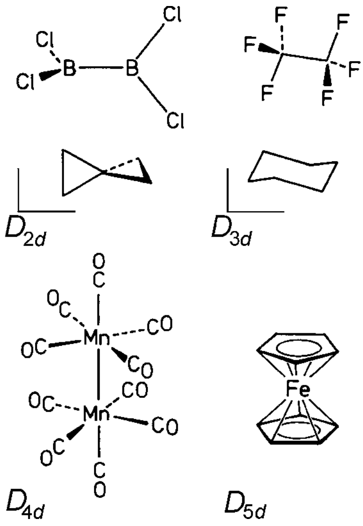

Figure 3-9. D_{nd} symmetries.

D_{3d}: One threefold rotation axis with three twofold rotation axes perpendicular to it, and three symmetry planes. The angle between the twofold axes is 60°. The symmetry planes include the threefold axis and bisect the angles between the twofold axes. Examples: Figure 3-9.

D_{4d}, D_{5d}, D_{6d}, D_{7d}, . . ., D_{nd}: D_{4d} One fourfold rotation axis with four twofold rotation axes perpendicular to it, and four symmetry planes. The angle between the twofold axes is 45°. The symmetry planes include the fourfold axis and bisect the angles between the twofold axes. The series can be continued by analogy. Examples: Figure 3-9.

D_{2h}: Three mutually perpendicular symmetry planes. Their three crossing lines are three twofold rotation axes, and their crossing point is a center of symmetry. Examples: Figure 3-10.

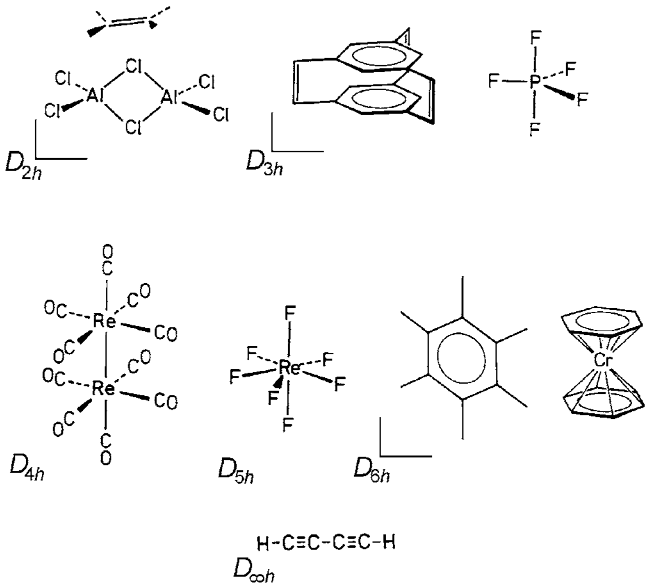

Figure 3-10. D_{nh} symmetries.

D_{3h}: One threefold rotation axis, three symmetry planes (at 60°) which contain the threefold axis, and another symmetry plane perpendicular to the threefold axis. Examples: Figure 3-10.

D_{4h}: One fourfold axis, one symmetry plane perpendicular to it, and four symmetry planes which include the fourfold axis. The four planes make two pairs. One pair is rotated relative to the other pair by 45°. The two planes in each pair are perpendicular to each other. Example: Figure 3-10.

D_{5h}: One fivefold rotation axis, one symmetry plane perpendicular to it, and five symmetry planes which include the fivefold rotation axis. The angle between the adjacent five planes is 36°. Example: Figure 3-10.

D_{6h}: One sixfold rotation axis, one symmetry plane perpendicular to it, and six symmetry planes which include the sixfold axis. The six planes are grouped in two sets. One set is rotated relative to the other

set by 30°. The angle between the planes within each set is 60°. Examples: Figure 3-10.

D_{nh}: The series can be continued by analogy. There will be one n-fold rotation axis, one symmetry plane perpendicular to it, and n symmetry planes which include the n-fold axis. When n is even, there are two sets of symmetry planes. One set is rotated relative to the other set by $(180/n)°$. The angle between the planes within each set is $(360/n)°$. When n is odd, the angle between the symmetry planes is $(180/n)°$.

$D_{\infty h}$: One ∞-fold axis and a symmetry plane perpendicular to it. Of course, there are also ∞ number of symmetry planes which include the ∞-fold rotation axis. Example: Figure 3-10.

T: Three mutually perpendicular twofold rotation axes and four threefold rotation axes. The threefold axes all go through a vertex of a tetrahedron and the midpoint of the opposite face center. The twofold axes connect the midpoints of opposite edges of this tetrahedron. Example: Figure 3-11.

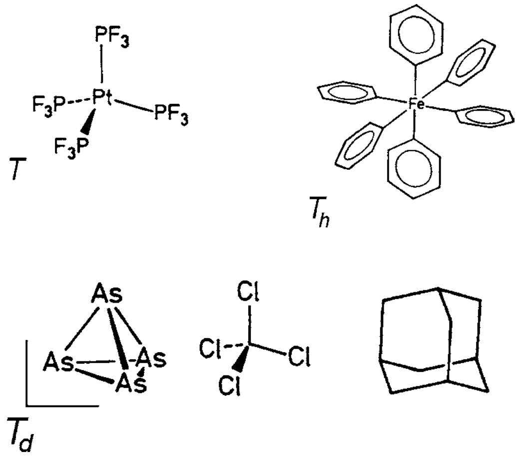

Figure 3-11. *T* symmetries.

T_d: In addition to the symmetry elements of symmetry T, there are six symmetry planes, each two of them being mutually perpendicular. All of these symmetry planes contain two threefold axes. Examples: Figure 3-11.

T_h: In addition to the symmetry elements of symmetry T, there is a center of symmetry, which introduces also three symmetry planes perpendicular to the twofold axes. Example: Figure 3-11.

O_h: Three mutually perpendicular fourfold rotation axes and four threefold rotation axes which are tilted with respect to the fourfold axes in a uniform manner, and a center of symmetry. Examples:

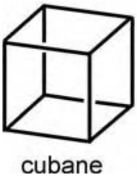

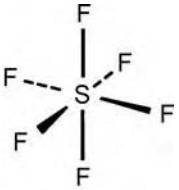

I_h: The most characteristic feature of this point group is the presence of six fivefold rotation axes. Examples:

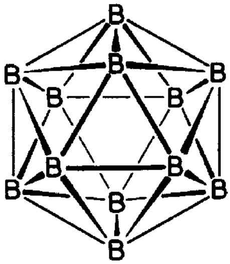

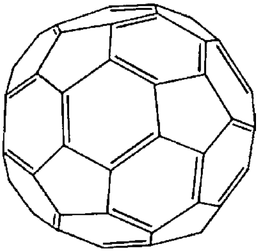

3.6. Consequences of Substitution

A tetrahedral AX_4 molecule, for example, methane, CH_4, has the point group of the regular tetrahedron, T_d. Gradual substitution of the X ligands by B ligands leads to less symmetrical tetrahedral configurations (Figure 3-12 top), until complete substitution is accomplished, where T_d symmetry is re-established. If each consecutive substitution introduces a new kind of ligand, then the symmetry will continue to decrease. This is shown for the tetrahedral case in the bottom of Figure 3-12.

Let us consider now an octahedral AX_6 molecule, e.g., sulfur hexafluoride, SF_6, which has the symmetry of the regular octahedron O_h. Substitution of an X ligand by a B ligand results in an AX_5B

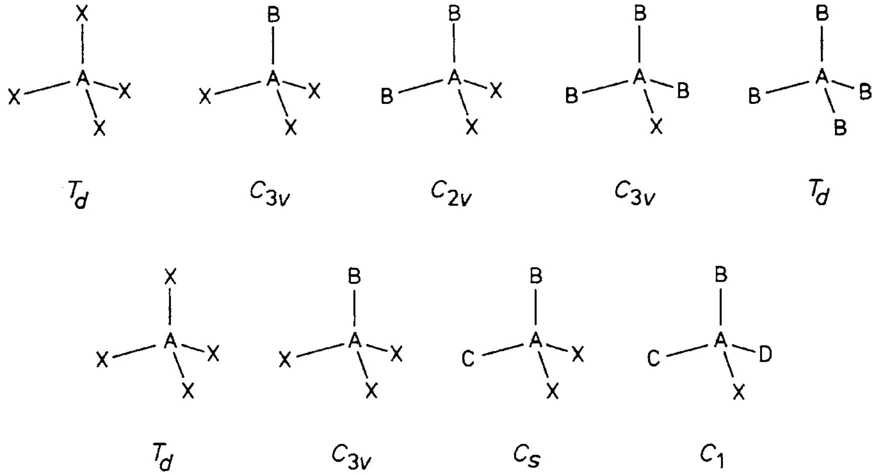

Figure 3-12. Substitution in a tetrahedral AX_4 molecule. *Top*: Gradual substitution of the ligands X by ligands B; *Bottom*: Substitution of the ligands X by different ligands.

molecule whose symmetry is C_{4v}. The substitution of a second X ligand by another ligand B may lead to alternative structures as the sites of the five X ligands after the first substitution are no longer equivalent. The symmetry variations in this substitution process are illustrated in Figure 3-13. A yet larger variety is obtained if each consecutive substitution introduces a new kind of ligand.

Another example among fundamental structures is the benzene geometry, D_{6h}. Gradual substitution of an increasing number of hydrogens by ligands X results in the symmetry variations illustrated in Figure 3-14. As regards the molecular point group, the monosubstituted and the pentasubstituted derivatives are equivalent. All derivatives can be grouped in such pairs with each of the trisubstituted benzenes constituting a pair by itself. Again, only the simplest case is considered here, with one kind of ligand used in all substituted positions. The symmetry decrease in the molecular point group for the substituted derivatives occurs because of the presence of the substituent ligands. It does not presuppose a change in the hexagonal symmetry of the benzene ring itself. Modern structure analyses have determined, however, that an appreciable deformation of the ring may also take place depending on the nature of the substituents. The largest deformation usually occurs at the so-called *ipso* angle adjacent to the substituent. According to the general

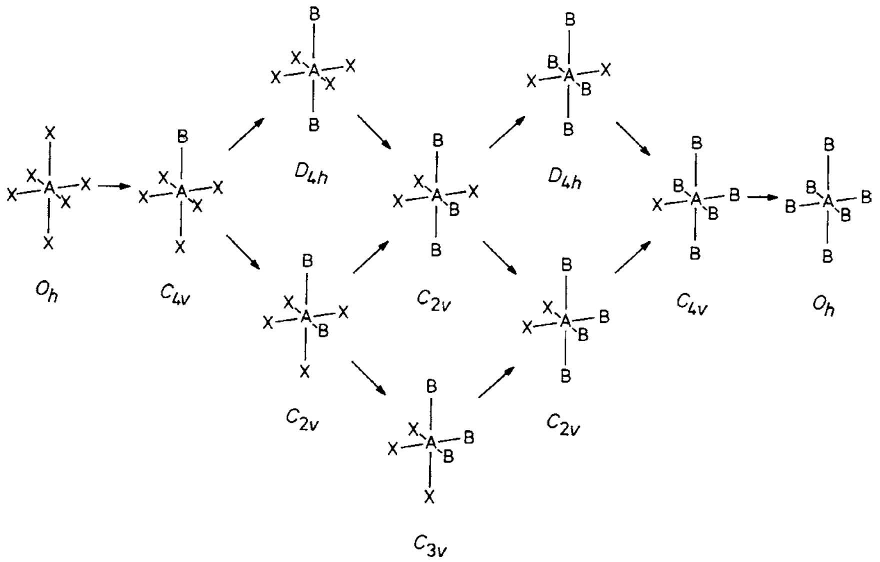

Figure 3-13. Gradual substitution of the ligands X in an octahedral AX_6 molecule by ligands B.

observation, electronegative substituents tend to compress the ring while electropositive substituents elongate it [18].

Complex formation usually implies the association of molecules or other species which may also exist separately in chemically non-extreme conditions. Complex formation often has important consequences on the shapes and symmetries of the constituent molecules, determined also by the energy requirements of the geometrical changes [19]. The $H_3N{\cdot}AlCl_3$ donor–acceptor complex, for example, has a triangular antiprismatic shape with C_{3v} symmetry (Figure 3-15). The symmetry of the donor part (NH_3) remains unchanged in the complex and the geometrical changes are relatively small. On the other hand, there are more drastic geometrical changes in the acceptor part ($AlCl_3$) due to loss of coplanarity of the four atoms and this results in a reduction in the point group. However, the structural changes in the acceptor part may also be viewed as if the complex formation completes the tetrahedral configuration around the central atoms in the component molecules. The nitrogen configuration may be considered to be tetrahedral already in ammonia with the lone pair of electrons being the fourth ligand. For aluminum, it is indeed the complexation that makes the tetrahedral configuration complete.

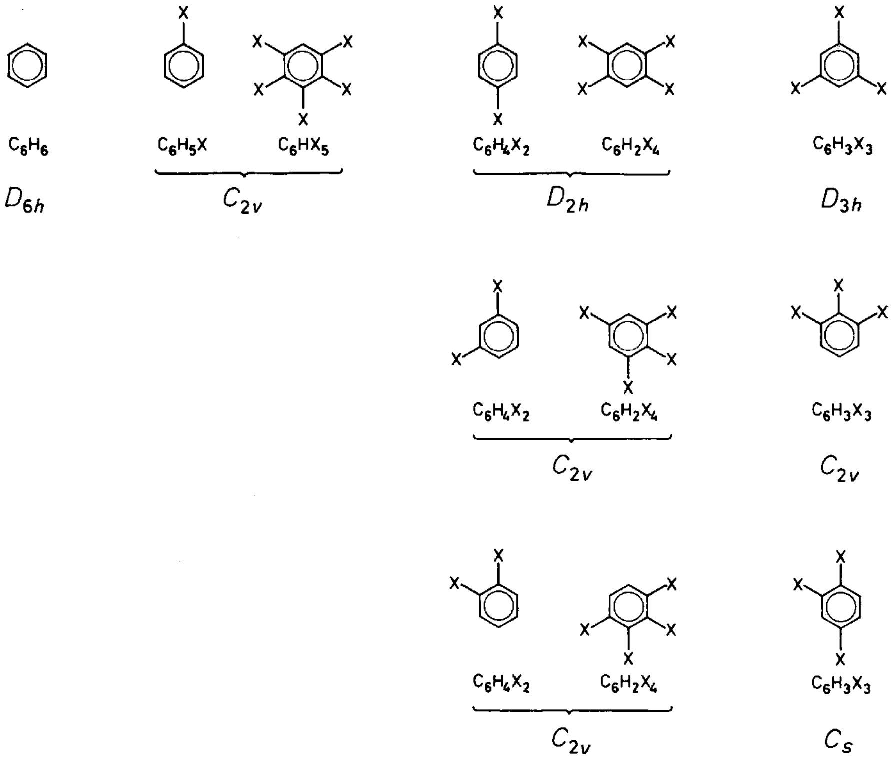

Figure 3-14. The symmetries of benzene and its $C_6H_nX_{6-n}$ derivatives.

Coordination molecules often demonstrate the utility of polyhedra in describing molecular shapes, symmetries, and geometries. Of course, such description may be useful in many other classes of compounds as well.

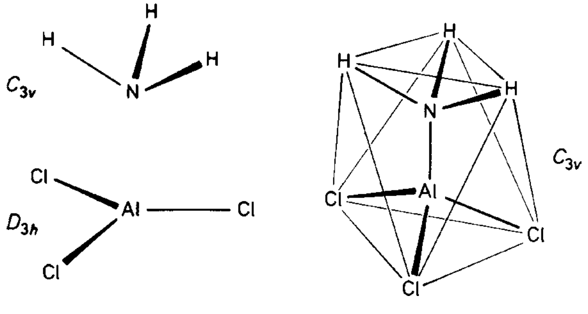

Figure 3-15. The uncomplexed ammonia and aluminium trichloride molecules and the triangular antiprismatic shape of the $H_3N{\cdot}AlCl_3$ donor–acceptor complex.

3.7. Polyhedral Molecular Geometries

In the Preface to the Third Edition of his *Regular Polytopes* [20], the great geometer H. S. M. Coxeter calls attention to the icosahedral structure of a boron compound in which twelve boron atoms are arranged like the vertices of an icosahedron. It had been widely believed that there would be no inanimate occurrence of an icosahedron, or of a regular dodecahedron either.

In 1982, the synthesis and properties of a new polycyclic $C_{20}H_{20}$ hydrocarbon, dodecahedrane, was reported [21]. The twenty carbon atoms of this molecule are arranged like the vertices of a regular dodecahedron. When, in the early 1960s, H. P. Schultz discussed the topology of the polyhedrane and prismane molecules (*vide infra*) [22], at that time it was in terms of a geometrical diversion rather than true-life chemistry. Since then it has become real chemistry.

It should be reemphasized that the above high-symmetry examples refer to isolated molecules and not to crystal structures. Crystallography has, of course, been one of the main domains where the importance of polyhedra has been long recognized, but they are not less important in the world of molecules.

In the First Edition of *Regular Polytopes*, Coxeter stated, "... the chief reason for studying regular polyhedra is still the same as in the times of the Pythagoreans, namely, that their symmetrical shapes appeal to one's artistic sense" [23]. The success of modern molecular chemistry does not diminish the validity of this statement. On the contrary. There is no doubt that aesthetic appeal has much contributed to the rapid development of what could be termed polyhedral chemistry. One of the pioneers in the area of polyhedral borane chemistry, Earl Muetterties, movingly described his attraction to the chemistry of boron hydrides, comparing it to M. C. Escher's devotion to periodic drawings [24]. Muetterties' words are quoted here [25]:

> When I retrace my early attraction to boron hydride chemistry, Escher's poetic introspections strike a familiar note. As a student intrigued by early descriptions of the extraordinary hydrides, I had not the prescience to see the future synthesis developments nor did I have then a scientific

> appreciation of symmetry, symmetry operations, and group theory. Nevertheless, some inner force also seemed to drive me but in the direction of boron hydride chemistry. In my initial synthesis efforts, I was not the master of these molecules; they seemed to have destinies unperturbed by my then amateurish tactics. Later as the developments in polyhedral borane chemistry were evident on the horizon, I found my general outlook changed in a characteristic fashion. For example, my doodling, an inevitable activity of mine during meetings, changed from characters of nondescript form to polyhedra, fused polyhedra and graphs.
>
> I (and others, my own discoveries were not unique nor were they the first) was profoundly impressed by the ubiquitous character of the three-center relationship in bonding (e.g., the boranes) and nonbonding situations. I found a singular uniformity in geometric relationships throughout organic, inorganic, and organometallic chemistry: The favored geometry in coordination compounds, boron hydrides, and metal clusters is the polyhedron that has all faces equilateral or near equilateral triangles...*

The polyhedral description of molecular geometries is, of course, generally applicable as these geometries are spatial constructions. To emphasize that even planar or linear molecules are also included, the term polytopal could be used rather than polyhedral. The real utility of the polyhedral description is for molecules possessing a certain amount of symmetry. Because of this and also because of the introductory character of our discussion, only molecules with relatively high symmetries will be mentioned, but involving quite diverse examples.

Both the tetraarsene, As_4, and the methane, CH_4, molecules have tetrahedral shapes (Figure 3-16) and T_d symmetry. However, there is an important difference in their structures. In the As_4 molecule, all

*Reproduced by permission from Academic Press.

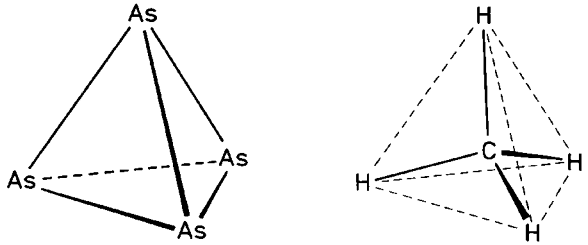

Figure 3-16. The molecular shapes of As_4 and CH_4.

the four constituting nuclei are located at the vertices of a regular tetrahedron, and all the edges of this tetrahedron are chemical bonds between the As atoms. In the methane molecule, there is a central carbon atom, and four chemical bonds are directed from it to the four vertices of a regular tetrahedron where the four protons are located. The edges are not chemical bonds.

The As_4 and CH_4 molecules are clear-cut examples of the two distinctly different arrangements. However, these distinctions are not always so unambiguous. Two independent studies reported the structure of zirconium borohydride, $Zr(BH_4)_4$. Both described its geometry by the same polyhedral configuration, while they differed in the assignment of the chemical bonds (Figure 3-17). The most important

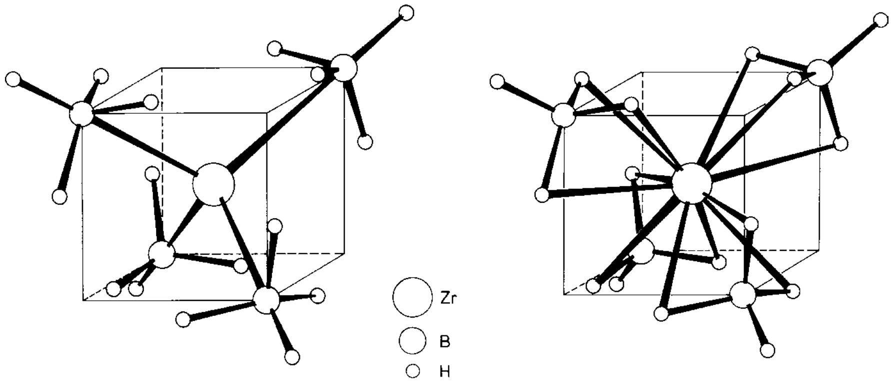

Figure 3-17. The molecular configuration of zirconium borohydride, $Zr(BH_4)_4$, in two interpretations but described by the same polyhedral shape. *Left*: the zirconium atom is directly bonded to the four tetrahedrally arranged boron atoms [28]; *Right*: the zirconium and the tetrahedrally arranged boron atoms are not bonded directly; their linkage is established by four times three hydrogen bridges [29].

difference in the two interpretations concerned the linkage between the central zirconium atom and the four boron atoms situated in the four vertices of a regular tetrahedron. According to one interpretation [20], there are four Zr–B bonds in the tetrahedral arrangement, while according to the other [27], there is no direct Zr–B bond, but each boron atom is linked to the zirconium atom by three hydrogen bridges.

The discovery of buckminsterfullerene (see, also, in Chapter 1) with its intriguing shape, focused attention to polyhedral molecular geometries even by many outside of chemistry. The event is often considered to be the birth of nanoscience and nanotechnology although they existed before even though under less fancy names. Buckminsterfullerene, C_{60}, discovered in 1985 [30], was the first runner-up for the title, "Molecule of the Year" in 1990 [31], and received the title in 1991 [32]. On this occasion, the Editorial of *Science* stated, among others, that

> Part of the exhilaration of the fullerenes is the shock that an old reliable friend, the carbon atom, has for all these years been hiding a secret life-style. We were all familiar with the charming versatility of carbon, the backbone of organic chemistry, and its infinite variation in aromatic and aliphatic chemistry, but when you got it naked, we believed it existed in two well-known forms, diamond and graphite. The finding that it could exist in a shockingly new structure unleashes tantalizing new experimental and theoretical ideas [33].

Then it added something that certainly carried a flavor of the broadest possible implications: "Perhaps the least surprising might be that improving life through science is a path that would see all the citizens of the world holding hands like carbon atoms in C_{60} and like them, welcoming any newcomer, no matter how different his or her skills or challenges." Figure 3-18 shows a series of fullerenes, the C_{20} molecule of the shape of dodecahedron being the smallest. Due to its extreme curvature and supposed reactivity, its existence had been in doubt until 2000, when it was produced from dodecahedrane, $C_{20}H_{20}$ [34].

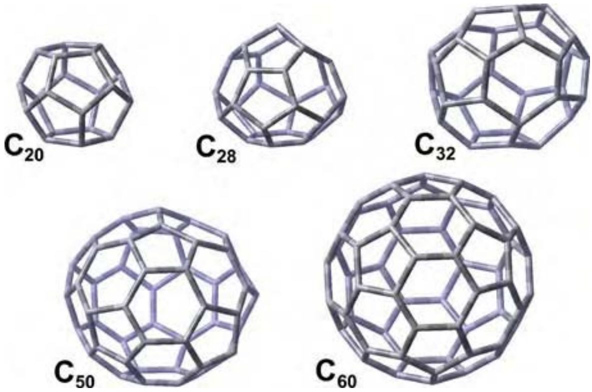

Figure 3-18. A few members of the fullerene family. Buckminsterfullerene, C_{60}, is "the roundest, most symmetrical large molecule found so far" [35].

3.7.1. Boron Hydride Cages

The boron hydrides are one of most beautiful classes of polyhedral compounds whose representatives range from simple to rather complicated systems. Our description here is purely phenomenological. Only in passing is reference made to the relationship of the characteristic polyhedral cage arrangements of the boron hydrides and the peculiarities of multicenter bonding that has special importance for their structures.

All faces of the boron hydride polyhedra are equilateral or nearly equilateral triangles. Those boron hydrides that have a complete polyhedral shape are called *closo* boranes (the Greek *closo* meaning closed). One of the most symmetrical, and, accordingly, most stable polyhedral boranes is the $B_{12}H_{12}^{2-}$ ion. Its regular icosahedral configuration is shown in Figure 3-19. The structural systematics of $B_nH_n^{2-}$ *closo* boranes and related $C_2B_{n\text{-}2}H_n$ *closo* carboranes, are presented in Table 3-2 after Muetterties [36]. In carboranes some of the boron sites are taken by carbon atoms. In the icosahedral ion $[Pt@Pb_{12}]^{2-}$, the platinum atom is inclosed in a regular icosahedral lead cluster [37], analogous to $B_{12}H_{12}^{2-}$.

Another structural class of the boron hydrides is the so-called quasi-*closo* boranes. They are related to the *closo* boranes by removing a framework atom from the latter and adding in its stead a pair of electrons. Thus one of the polyhedron framework sites is taken by an electron pair.

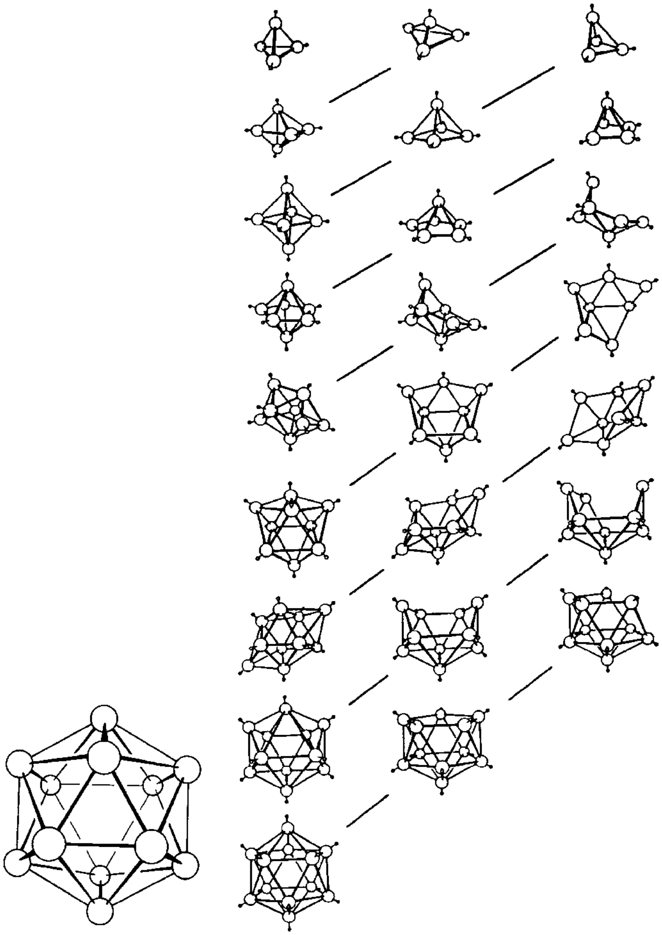

Figure 3-19. Boron skeletons of boron hydrides. *Left*: Regular icosahedral boron skeleton of $B_{12}H_{12}^{2-}$; *Right*: *Closo, nido,* and *arachno* boranes after Williams [38] and Rudolph [39]. The genetic relationships are indicated by *diagonal lines*. Used with permission, copyright (1976) American Chemical Society.

There are boron hydrides in which one or more of the polyhedral sites are truly removed. Figure 3-19 shows the systematics of borane polyhedral fragments as obtained from *closo* boranes, after R. E. Williams [40] and R. W. Rudolph [41]. All the faces of the polyhedral skeletons are triangular, and thus the polyhedra may be termed deltahedra and the derived fragments deltahedral. The starting deltahedra are the tetrahedron, the trigonal bipyramid, the octahedron, the pentagonal bipyramid, the bisdisphenoid, the symmetrically tricapped

Table 3-2. Structural Systematics of $B_nH_n^{2-}$ *closo* Boranes and $C_2B_{n-2}H_n$ *closo* Carboranes[a]

Polyhedron, point group	Borane	Dicarbaborane
Tetrahedron, T_d	(B_4Cl_4)[b]	–
Trigonal bipyramid, D_{3h}	–	$C_2B_3H_5$
Octahedron, O_h	$B_6H_6^{2-}$	$C_2B_4H_6$
Pentagonal bipyramid, D_{5h}	$B_7H_7^{2-}$	$C_2B_5H_7$
Dodecahedron (triangulated), D_{2d}	$B_8H_8^{2-}$	$C_2B_6H_8$
Tricapped trigonal prism, D_{3h}	$B_9H_9^{2-}$	$C_2B_7H_9$
Bicapped square antiprism, D_{4d}	$B_{10}H_{10}^{2-}$	$C_2B_8H_{10}$
Octadecahedron, C_{2v}	$B_{11}H_{11}^{2-}$	$C_2B_9H_{11}$
Icosahedron, I_h	$B_{12}H_{12}^{2-}$	$C_2B_{10}H_{12}$

[a]After E. L. Muetterties, ed., *Boron Hydride Chemistry*. Academic Press, New York, 1975.
[b]B_4H_4 not known.

trigonal prism, the bicapped square antiprism, the octadecahedron, and the icosahedron [42].

A *nido* (nest-like) boron hydride is derived from a *closo* borane by the removal of one skeleton atom. If the starting *closo* borane is not a regular polyhedron, then the atom removed is the one at a vertex with the highest connectivity. An *arachno* (web-like) boron hydride is derived from a *closo* borane by the removal of two adjacent skeleton atoms. If the starting *closo* borane is not a regular polyhedron, then again, one of the two atoms removed is at a vertex with the highest connectivity. Complete *nido* and *arachno* structures are shown in Figure 3-20 together with the starting boranes [43]. The fragmented structures are completed by a number of bridging and terminal hydrogens. The above examples are from among the simplest boranes and their derivatives.

3.7.2. Polycyclic Hydrocarbons

Some fundamental polyhedral shapes are realized among polycyclic hydrocarbons. The bond arrangements around the carbon atoms in such configurations may be far from the energetically most advantageous, causing *strain* in these structures. The strain may be so large as to render particular arrangements too unstable to exist under any reasonable conditions. On the other hand, the fundamental character of these shapes, their high symmetry, and aesthetic appeal make them

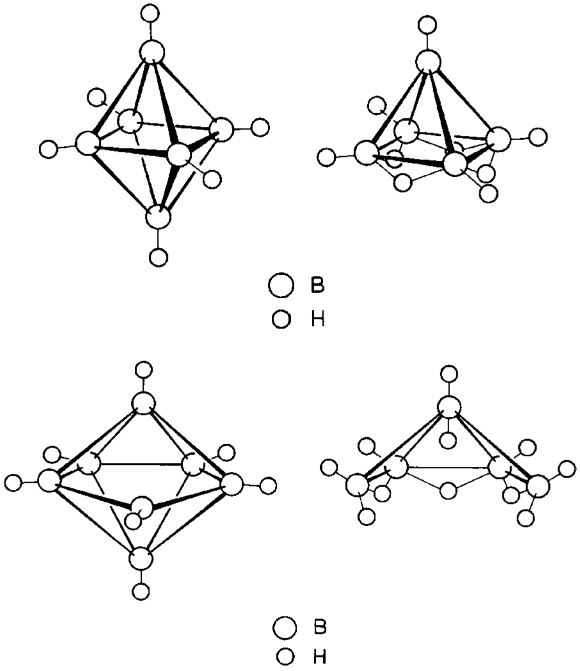

Figure 3-20. Examples of *closo/nido* and *closo/arachno* structural relationships after Muetterties [44]. *Top*: *Closo*-$B_6H_6^{2-}$ and *nido*-B_5H_9; *Bottom*: *Closo*-$B_7H_7^{2-}$ and *arachno*-B_5H_{11}.

an attractive and challenging "playground" to the organic chemist [45]. Incidentally, these substances are often building blocks for such important natural products as steroids, alkaloids, vitamins, carbohydrides, antibiotics, etc.

Tetrahedrane, $(CH)_4$, would be the simplest regular polyhedral polycyclic hydrocarbon (Figure 3-21a). However, since it has such a high strain energy, it has not (yet?) been prepared in spite of considerable efforts [46]. By now, over 10 different derivatives of tetrahedrane have been prepared, for example, tetra-*tert*-butyltetrahedrane (Figure 3-21b) [47]. It is amazingly stable, perhaps because the substituents help "clasp" the molecule together.

The next Platonic solid is the cube, and the corresponding polycyclic hydrocarbon, cubane, $(CH)_8$ (Figure 3-21c), has been known for some time [49]. The strain energy of the CC bonds in cubane is among the highest known. It is unstable thermodynamically but stable kinetically, "like a rock" [50]. Referring to its instability, Marchand

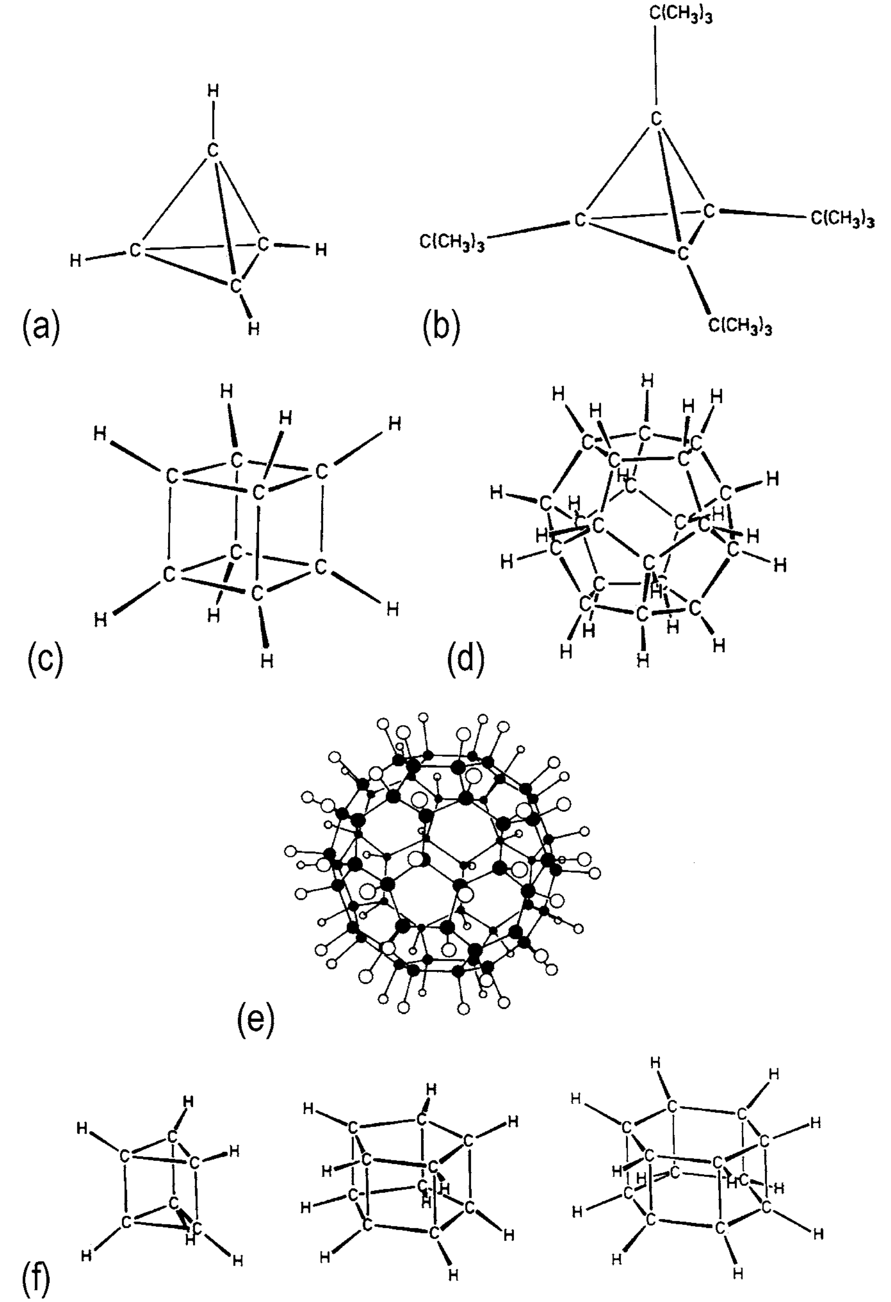

Figure 3-21. Polyhedral molecular models. (**a**) Tetrahedrane, $(CH)_4$; (**b**) Tetra-*tert*-butyltetrahedrane, $\{C[C(CH_3)_3]\}_4$ [48]; (**c**) Cubane, $(CH)_8$; (**d**) Dodecahedrane, $(CH)_{20}$; (**e**) $C_{60}H_{60}$; (**f**) Triprismane, C_6H_6; pentaprismane, $C_{10}H_{10}$; and hexaprismane, $C_{12}H_{12}$.

considered cubane as a physical organic chemist's "subject/patient" by analogy with the clinical psychologists studying deviants to learn more about normal behavior [51]. He also demonstrated the riches of the chemistry developed from the cubane base.

The preparation of dodecahedrane, $(CH)_{20}$, (Figure 3-21d) by Paquette et al. [52] followed Schultz's prediction almost two decades before, concerning possible hydrocarbon polyhedranes [53]:

> Dodecahedrane is the one substance of the series with almost ideal geometry, physically the molecule is practically a miniature ball bearing! One would expect the substance to have a low viscosity, a high melting point, but low boiling point, high thermal stability, a very simple infrared spectrum and perhaps an aromatic-like p.m.r. spectrum. Chemically one might expect a relatively easy (for an aliphatic hydrocarbon) removal of a tertiary proton from the molecule, for the negative charge thus deposited on the molecule could be accommodated on any one of the twenty completely equivalent carbon atoms, the carbanion being stabilized by a 'rolling charge' effect that delocalizes the extra electron.

In the $(CH)_n$ convex polyhedral hydrocarbon series each carbon atom is bonded to three other carbon atoms. The fourth bond is directed externally to a hydrogen atom. Around the all-carbon polyhedron, there is thus a similar polyhedron whose vertices are protons. The edges of the all-carbon polyhedron are carbon–carbon chemical bonds, while the edges of the larger all-proton polyhedron do not correspond to any chemical bonds. This kind of arrangement of the polycyclic hydrocarbons is not possible for the remaining two Platonic solids. There are four bonds meeting at the vertices of the octahedron and five at the vertices of the icosahedron. For similar reasons, only seven of the 13 Archimedian polyhedra can be considered in the $(CH)_n$ polyhedral series. One of them is the so-called "fuzzyball," or $C_{60}H_{60}$, a predicted form of fully hydrogenated buckminsterfullerene (Figure 3-21e) [54]. Table 3-3 presents some characteristics of the polyhedranes.

Table 3-3. Characterization of Polyhedrane Molecules[a]

Name	Formula	Geometry and number of faces (all regular)	Face angles
Tetrahedrane	$(CH)_4$	Triangle, 4	60°
Cubane	$(CH)_8$	Square, 6	90°
Dodecahedrane	$(CH)_{20}$	Pentagon, 12	108°
Truncated tetrahedrane	$(CH)_{12}$	Triangle, 4; Hexagon, 4	60°
Truncated octahedrane	$(CH)_{24}$	Square, 6; Hexagon, 8	90°; 120°
Truncated cubane	$(CH)_{24}$	Triangle, 8; Octagon, 6	60°; 135°
Truncated cuboctahedrane	$(CH)_{48}$	Square, 12; Hexagon, 8; Octagon, 6	90°; 120°; 135°
Truncated icosahedrane	$(CH)_{60}$	Pentagon, 12; Hexagon, 20	108°; 120°
Truncated dodecahedrane	$(CH)_{60}$	Triangle, 20; Decagon, 12	60°; 144°
Truncated icosidodecahedrane	$(CH)_{120}$	Square, 30; Hexagon, 20; Decagon, 12	90°; 120°; 144°

[a] After H. P. Schultz, "Topological Organic Chemistry: Polyhedranes and Prismanes." *J. Org. Chem*. 1965, 30, 1361–1364.

The cubane molecule may also be considered and called tetraprismane (*vide infra*). It may be described as composed of eight identical methine units arranged at the corners of a regular tetragonal prism with O_h symmetry and bound into two parallel four-membered rings conjoined by four four-membered rings. Triprismane, $(CH)_6$ [55], has D_{3h} symmetry and pentaprismane, $(CH)_{10}$ [56], has D_{5h} symmetry. Triprismane, pentaprismane, and hexaprismane, $C_{12}H_{12}$ (not yet prepared), are shown in Figure 3-21f. The quest for a synthesis of pentaprismane is a long story with a happy ending [57]. Hexaprismane, $(CH)_{12}$, which is the face-to-face dimer of benzene has not yet been prepared. A recent study showed that this dimerization would not only be symmetry-forbidden (see, Chapter 7), but would also be hindered by a high energy barrier [58]. Table 3-4 presents some characteristic geometric information on the hydrocarbon prismane molecules. The description of the general *n*-prismane is that it is composed of 2*n* identical methine units arranged at the corners of a regular prism with D_{nh} symmetry and bound into two parallel *n*-membered rings conjoined by *n* four-membered rings.

Incidentally, the *regular* prisms and the *regular* antiprisms are also semiregular, i.e., Archimedian, solids. Moreover, the second prism, in its most symmetrical configuration, is a regular solid, the cube; and the first antiprism, in its most symmetrical configuration, is also a regular solid, the octahedron.

Only a few highly symmetrical structures have been mentioned above. The varieties become virtually endless if one reaches beyond

Table 3-4. Characterization of Prismane Molecules[a]

Name	Formula	Geometry and number of faces (all regular)	Face angles
Triprismane	C_6H_6	Triangle, 2; Square, 3	60°; 90°
Tetraprismane (cubane)	C_8H_8	Square, 6	90°
Pentaprismane	$C_{10}H_{10}$	Pentagon, 2; Square, 5	108°; 90°
Hexaprismane	$C_{12}H_{12}$	Hexagon, 2; Square, 6	120°; 90°
Heptaprismane	$C_{14}H_{14}$	Heptagon, 2; Square, 7	128°34′; 90°
n-Prismane	$C_{2n}H_{2n}$	*n*-gon, 2; Square, *n*	–[b]; 90°

[a]After H. P. Schultz, "Topological Organic Chemistry: Polyhedranes and Prismanes." *J. Org. Chem.* 1965, 30, 1361–1364.
[b]Approaches 180° as *n* increases.

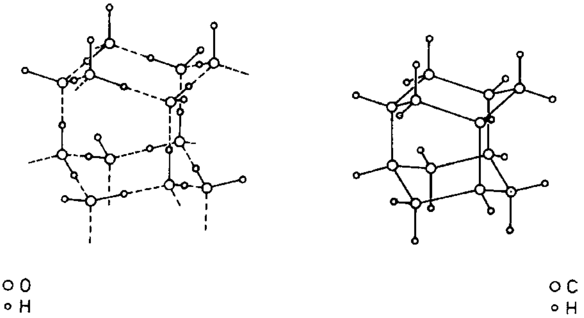

Figure 3-22. *Left*: Ice crystal structure; *Right*: the iceane hydrocarbon molecule.

the most symmetrical convex polyhedral shapes. For example, the number of possible isomers is 5,291 for the tetracyclic structures of the $C_{12}H_{18}$ hydrocarbons with 12 skeletal carbon atoms [59]. Of all these geometric possibilities, however, only a few are stable [60]. One is *iceane* shown in Figure 3-22. The molecule may be visualized as two chair cyclohexanes connected to each other by three axial bonds. Alternatively, the molecule may be viewed as consisting of three fused boat cyclohexanes. The trivial name iceane had been proposed for this molecule by Fieser [61] almost a decade before its preparation [62]. As Fieser was considering the arrangement of the water molecules in the ice crystal (Figure 3-22), he noticed three *vertical* hexagons with boat conformations. The emerging *horizontal* $(H_2O)_6$ units possess three equatorial hydrogen atoms and three equatorial hydrogen bonds available for horizontal building. Fieser further noted that this structure "suggests the possible existence of a hydrocarbon of analogous conformation of the formula $C_{12}H_{18}$, which might be named 'iceane.' The model indicates a stable strain-free structure analogous to adamantane and twistane. 'Iceane' thus presents a challenging target for synthesis" [63]. Within a decade the challenge was met.

There is a close relationship between the adamantane, $C_{10}H_{16}$, molecule and the diamond crystal. The Greek word *adamant* means diamond and diamond has been termed the "infinite adamantylogue to adamantane" [64]. While iceane has D_{3h} symmetry, adamantane has T_d. This high symmetry can be clearly seen when the configuration of adamantane is described by four imaginary cubes packed one inside the other, two of which are shown in Figure 3-23. Similar structures

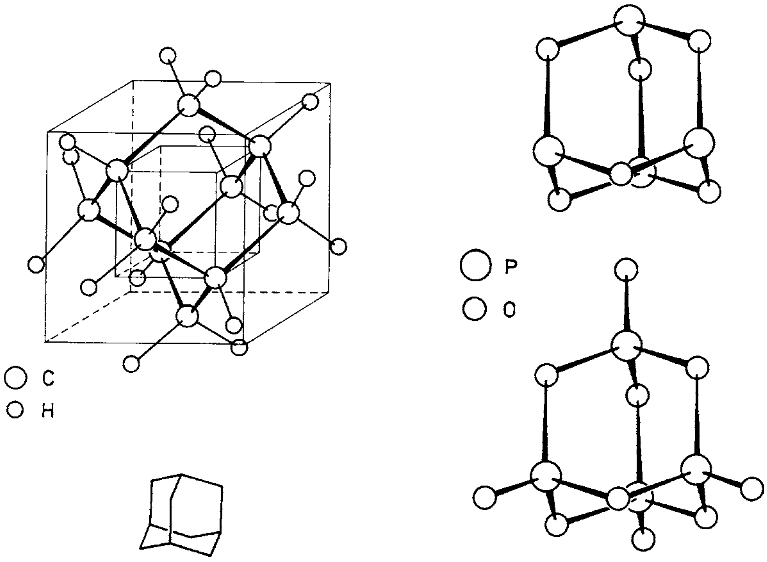

Figure 3-23. Adamantane and its analogs. *Left*: Adamantane, $C_{10}H_{16}$ or $(CH)_4(CH_2)_6$; in two representations; *Right*: P_4O_6 (*top*) and $(PO)_4O_6$ (*bottom*).

are found among inorganic compounds where, by analogy to adamantane, $(CH)_4(CH_2)_6$, the general formula is A_4B_6. Here A may be, e.g., P, As, Sb, or PO, as illustrated in Figure 3-23.

Adamantane molecules may be imagined to join at vertices, edges, or even at faces. Examples are shown in Figure 3-24; most of them, however, have not yet been synthesized [65].

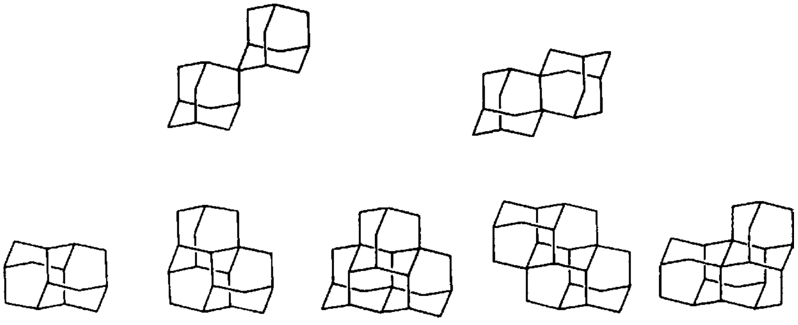

Figure 3-24. Joined adamantanes. *Top, left*: joined at vertices, [1]diadamantane [66]; *Top, right*: joined at edges, [2]diadamantane [67]; *Bottom*: joined at faces, diamantane (congressane) [68], triamantane [69], and three isomers of tetramantane: "iso" C_{3v}; "anti", C_{2h}; and "skew", C_2 [70].

3.7.3. Structures with Central Atom

Adamantane is sometimes regarded as the cage analog of methane while diamantane and triamantane as the analogs of ethane and propane. Methane has, of course, a tetrahedral structure with the point group of the regular tetrahedron, T_d. Important structures may be derived by joining two tetrahedra, or, for example, two octahedra, at a common vertex, edge, or face as shown in Figure 3-25. Ethane, H_3C–CH_3, ethylene, H_2C=CH_2, and acetylene, HC≡CH, may be derived formally from joined tetrahedra in such a way. The analogy with the joining tetrahedra is even more obvious in some metal halide structures with halogen bridges [71]. Thus, e.g., the $Al_2Cl_7^-$ ion may be considered as two aluminum tetrachloride tetrahedra joined at a common vertex, or the Al_2Cl_6 molecule may be looked at as two such tetrahedra joined at a common edge. These examples are shown in Figure 3-26.

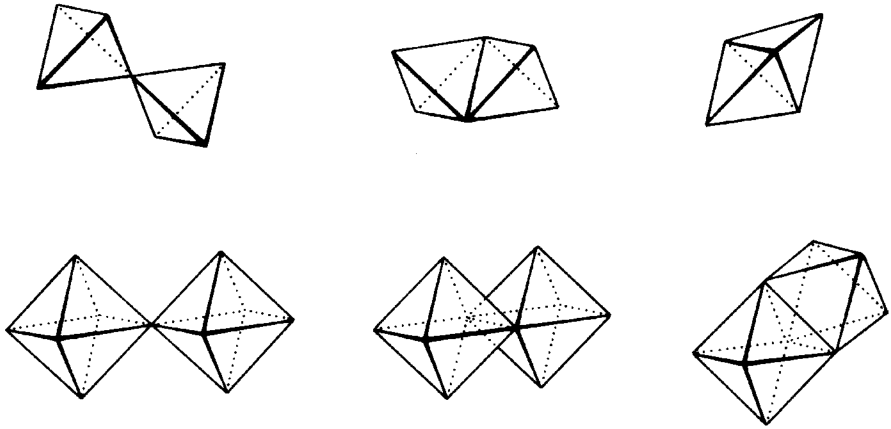

Figure 3-25. Joined tetrahedra and octahedra.

In mixed-halogen complexes, such as potassium tetrafluoroaluminate, $KAlF_4$ [72], there is also a tetrahedral metal coordination. In fact, the regular or nearly regular tetrahedral tetrafluoroaluminate part of the molecule is an especially well defined structural unit. It is relatively rigid, whereas the position of the potassium atom around the AlF_4 tetrahedron is rather loose. The most plausible model for this molecule is also shown in Figure 3-26. The $KAlF_4$ molecule is merely a representative from a large class of compounds with

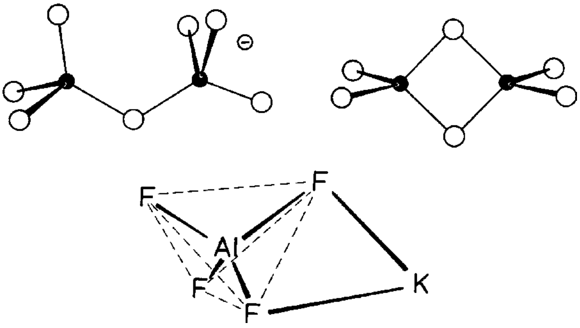

Figure 3-26. The configurations of the $Al_2Cl_7^-$ ion and Al_2Cl_6 and $KAlF_4$ molecules.

great practical importance: the mixed halides have greatly enhanced volatility compared with the individual metal halides.

For tetralithiotetrahedrane, $(CLi)_4$, the structure with the lithium atoms above the faces of the carbon tetrahedron was found in the calculations to be more stable than with the lithium atoms above the vertices (Figure 3-27) [73].

The prismatic cyclopentadienyl and benzene complexes of transition metals are reminiscent of the polycyclic hydrocarbon prismanes. Figure 3-28 shows ferrocene, $(C_5H_5)_2Fe$, for which both the barrier to rotation and the free energy difference between the prismatic (eclipsed) and antiprismatic (staggered) conformations are very small [75]. Figure 3-28 also presents a prismatic model with D_{6h} symmetry for dibenzene chromium, $(C_6H_6)_2Cr$.

Molecules with multiple bonds between metal atoms often have structures with beautiful and highly symmetrical polyhedral shapes. The square prismatic $[Re_2Cl_8]^{2-}$ ion, shown in Figure 3-29, played an important role in the history of the discovery of metal–metal

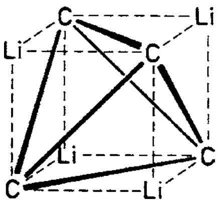

Figure 3-27. Model of the $(CLi)_4$ molecule [74].

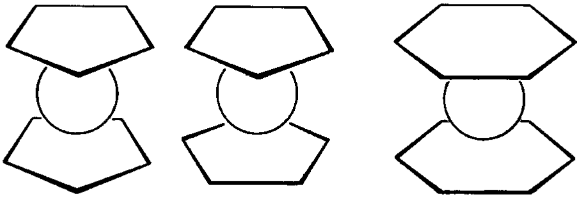

Figure 3-28. Prismatic molecular models. Ferrocene: prismatic (D_{5h}) and antiprismatic (D_{5d}); dibenzene chromium: prismatic (D_{6h}).

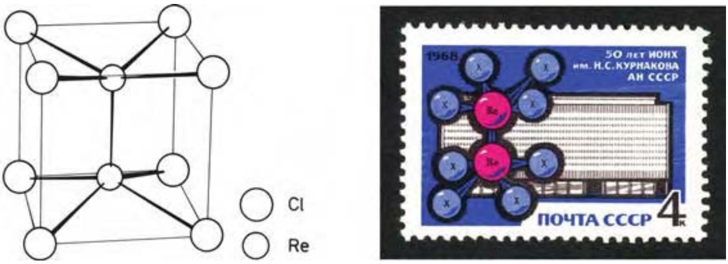

Figure 3-29. The square prismatic structure of the $[Re_2Cl_8]^{2-}$ ion which played a historic role in the discovery of metal–metal multiple bonds (see, text) and a Soviet stamp with the same structure. The building in the background is the research institute in Moscow where the first such structure was prepared.

multiple bonds [76]. The first report of the very short Re–Re bond appeared in 1958, in Russian, from the Inorganic Chemistry Institute of the Soviet Academy of Sciences in Moscow [77]. The authors, Ada Kotel'nikova and V. G. Tronev, recognized the presence of direct metal–metal bonding, but failed to suspect that it might be multiple bonding. The bond was so short that it was suspect. A few years later F. Albert Cotton reinvestigated the structure, confirmed the findings of the Moscow scientists, and introduced the notion of Re–Re quadruple bonding [78]. The original study by Kotel'nikova and Tronev was commemorated on a postage stamp issued for the fiftieth anniversary of their Institute (Figure 3-29).

Figure 3-30 shows another molecule with metal–metal multiple bond. Its shape is similar to the paddles that propel riverboats. There is then a whole class of hydrocarbons called paddlanes [79] and one of their representatives is also shown in Figure 3-30.

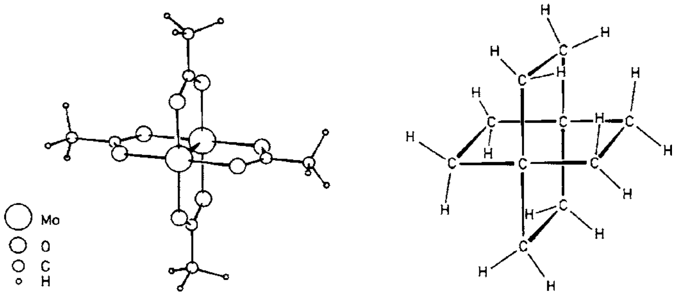

Figure 3-30. *Left*: Dimolybdenum tetraacetate, $Mo_2(O_2CCH_3)_4$ [80]; *Right*: [2.2.2.2]Paddlane.

3.7.4. Regularities in Nonbonded Distances

The structure of the ONF_3 molecule is depicted in Figure 3-31 with the bond lengths, bond angles, and nonbonded distances. The shape of the molecule well approximates a regular tetrahedron formed by three fluorines and one oxygen. The nonbonded F···F and F···O distances representing the lengths of the edges of a tetrahedron are equal within the experimental errors of their determination [81]. The molecule has C_{3v} symmetry, and the central nitrogen atom is obviously not in the center of the tetrahedron of the four ligands.

In some molecular geometries, the so-called intramolecular 1,3 separations are remarkably constant. The "1,3" label refers to the interactions between two atoms in the molecule which are separated by a third atom. The near equality of the nonbonded distances in the ONF_3 molecule is a special case. What is more commonly observed is the constancy of a certain 1,3 nonbonded distance throughout a series of related molecules. Significantly, this constancy of 1,3-distances may be accompanied by considerable changes in the bond lengths

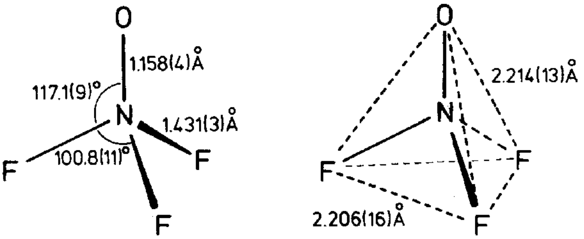

Figure 3-31. The molecular geometry of ONF_3 with: *Left*: bond lengths and bond angles; and *Right*: nonbonded distances [82].

and bond angles within the three-atom group. The intramolecular 1,3 interactions have also been called intramolecular van der Waals interactions, and L. S. Bartell postulated a set of intramolecular nonbonded 1,3 radii [83]. These 1,3 nonbonded radii are intermediate in value between the corresponding covalent radii and "traditional" van der Waals radii, all compiled for some elements in Table 3-5.

Figure 3-32 shows some structural peculiarities which originally prompted Bartell to recognize the importance of the intramolecular nonbonded interactions [84]. It was an interesting observation that the three outer carbon atoms in $H_2C{=}C(CH_3)_2$ were arranged as if they were at the corners of an approximately equilateral triangle, as shown in Figure 3-32. The central carbon atom in this arrangement is obviously not in the center of the triangle, consequently, the bond angle between the bulky methyl groups is smaller than the ideal 120°. In the

Table 3-5. Covalent, 1,3 Intramolecular Nonbonded and van der Waals Radii of Some Elements

Element	Covalent radius[a] (Å)	1,3 Intramolecular nonbonded radius[b] (Å)	Van der Waals radius[a] (Å)
B	0.817	1.33	
C	0.772	1.25	
N	0.70	1.14	1.50
O	0.66	1.13	1.40
F	0.64	1.08	1.35
Al	1.202	1.66	
Si	1.17	1.55	
P	1.10	1.45	1.90
S	1.04	1.45	1.85
Cl	0.99	1.44	1.80
Ga	1.26	1.72	
Ge	1.22	1.58	
As	1.21	1.61	2.00
Se	1.17	1.58	2.00
Br	1.14	1.59	1.95

[a]After L. Pauling, *The Nature of the Chemical Bond*, 3rd ed. Cornell University Press, Ithaca, New York, 1960.

[b]After L. S. Bartell, "Molecular Geometry: Bonded Versus Nonbonded Interactions." *J. Chem. Educ.* 1968, 45, 754–767; C. Glidewell, "Intramolecular Nonbonded Atomic Radii – Application to Heavier *p* Elements." *Inorg. Chim. Acta* 1976, 20, 113–118.

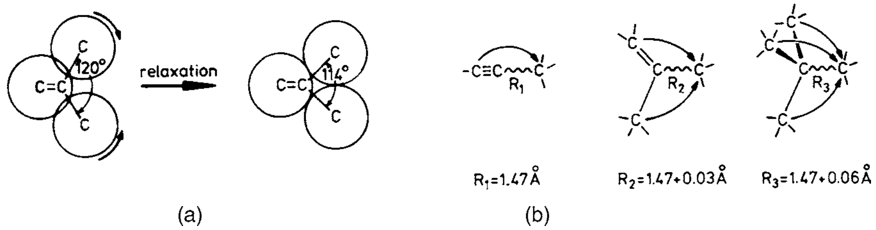

Figure 3-32. Geometrical consequences of nonbonded interactions after L. S. Bartell [85]. (**a**) The three outer carbon atoms of $H_2C{=}C(CH_3)_2$ are in the corners of an approximately equilateral triangle, leading to a relaxation of the bond angle between the ethyl groups; (**b**) Considerations of nonbonded interactions in the interpretation of the C–C single bond length changes in a series of molecules.

other example, in Figure 3-32, the C–C bond lengthening is related to the increasing number of nonbonded interactions. Of course, the 1,3-intramolecular nonbonded radii (Table 3-5) are purely empirical, but so are the other kinds of radii. Thus, the 1,3-nonbonded radii may be updated from time to time.

Of the observations of constancy of nonbonded distances, here we single out one [86]. The O···O nonbonded distances in XSO_2Y sulfones have been found to be remarkably constant at 248 pm in a relatively large series of compounds. At the same time the S=O bond lengths vary up to 5 pm and the O=S=O bond angles up to 5° depending on the nature of the X and Y ligands. The geometrical variations in the sulfone series could be visualized (Figure 3-33) as if the two oxygen ligands were firmly attached to two of the four vertices of the ligand tetrahedron around the sulfur atom, and this central atom were moving along the bisector of the OSO angle depending on the X and Y ligands. The sulfuric acid, H_2SO_4, or $(HO)SO_2(OH)$, molecule has its four oxygens around the sulfur at the vertices of a nearly regular

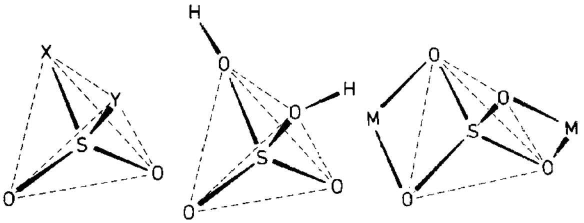

Figure 3-33. Tetrahedral sulfur configurations; *from the left:* sulfones; sulfuric acid; alkali sulfates.

tetrahedron. Compared with the differences in the various OSO angles (up to 20°) and in the two kinds of SO bonds (up to 15 pm), the largest difference among the six O···O nonbonded distances is only 7 pm [87].

The alkali sulfate molecules used to appear in old textbooks with the following structural formula:

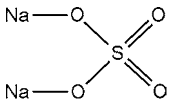

However, the SO_4 groups have nearly regular tetrahedral configuration in such molecules. The metal atoms are located on axes perpendicular to the edges of the SO_4 tetrahedron. Thus, this structure is bicyclic as shown in Figure 3-33.

3.7.5. The VSEPR Model

Numerous examples of molecular structures have been introduced in the preceding sections. They are all confirmed by modern experiments and/or calculations. We would like to know, however, not only the structure of a molecule and its symmetry, but also, *why* a certain structure with a certain symmetry is realized.

It has been a long-standing goal in chemistry to determine the shape and measure the size of molecules, and also to calculate these properties. Today, quantum chemistry is capable of determining the structure of molecules of ever growing complexity, starting from the mere knowledge of the atomic composition, and without using any empirical information. Such calculations are called *ab initio*. The primary results from these calculations are, however, wave functions and energies which may also be considered "raw measurements," similar to some experimental data. At the same time there is a desire to understand molecular structures in simple terms—such as, for example, the localized chemical bond—that have proved so useful to chemists' thinking. There is a need for a bridge between the measurements and calculations on one hand, and simple qualitative ideas, on the other hand. There are several qualitative models for molecular structure that serve this purpose well. These models can explain, for example, why the methane molecule is regular tetrahedral, T_d, why ammonia is pyramidal, C_{3v}, why water is bent, C_{2v}, and why the xenon

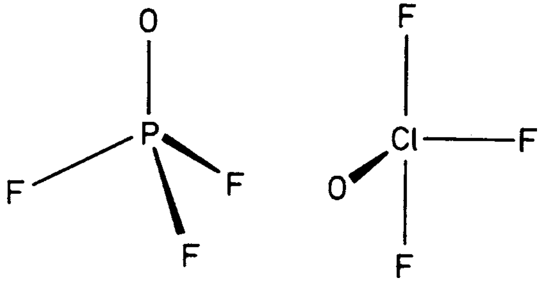

Figure 3-34. Molecular configuration of OPF_3 (C_{3v}) and $OClF_3$ (C_s).

tetrafluoride molecule is square planar, D_{4h}. It is also important to understand why seemingly analogous molecules like OPF_3 and $OClF_3$ have so different symmetries, the former C_{3v}, and the latter C_s, as seen in Figure 3-34.

The structure of a series of the simplest AX_n type molecules will be examined in terms of one of these useful and successful qualitative models. A is the central atom, the Xs are the ligands, and not necessarily all n ligands are the same.

Qualitative models simplify. They usually consider only a few, if not just one, of the many effects that are present and are interacting in a most complex way. The measure of the success of a qualitative model is in its ability to create consistent patterns for interpreting individual structures and structural variations in a series of molecules and, above all, in its ability to correctly predict the structures of molecules, not yet studied or not even yet prepared.

One of the simplest models [88] is based on the following postulate: *The geometry of the molecule is determined* by *the repulsions among the electron pairs in the valence shell of its central atom*. The valence shell of an atom may have bonding pairs and other electron pairs that do not participate in bonding and belong to this atom alone. The latter are called unshared or lone pairs of electrons. The above postulate emphasizes the importance of *both* bonding pairs and lone pairs in establishing the molecular geometry. The model is appropriately called the Valence Shell Electron Pair Repulsion or VSEPR model. The bond configuration around atom A in the molecule AX_n is such that the electron pairs of the valence shell are at maximum distances from each other. Thus, the situation may be visualized in such a way that the electron pairs occupy well-defined domains of the

Table 3-6. Arrangements of Two to Six Electron Pairs That Maximize Their Distances Apart

Number of electron pairs in the valence shell	Arrangement
2	Linear
3	Equilateral triangle
4	Tetrahedron
5	Trigonal bipyramid
6	Octahedron

space around the central atom corresponding to the concept of localized molecular orbitals.

If it is assumed that the valence shell of the central atom retains its spherical symmetry in the molecule, then the electron pairs will be at equal distances from the nucleus of the central atom. In this case the arrangements at which the distances among the electron pairs are at maximum, will be those listed in Table 3-6. If the electron pairs are represented by points on the surface of a sphere, then the shapes shown in Figure 3-35 are obtained by connecting these points. Of the three polyhedra appearing in Figure 3-35, only two are regular, viz., the tetrahedron and the octahedron. The trigonal bipyramid is not a regular polyhedron; although its six faces are equivalent, its edges and vertices are not. Incidentally, the trigonal bipyramid is not a unique solution to the five-point problem. Another, and only slightly less advantageous arrangement, is the square pyramidal configuration.

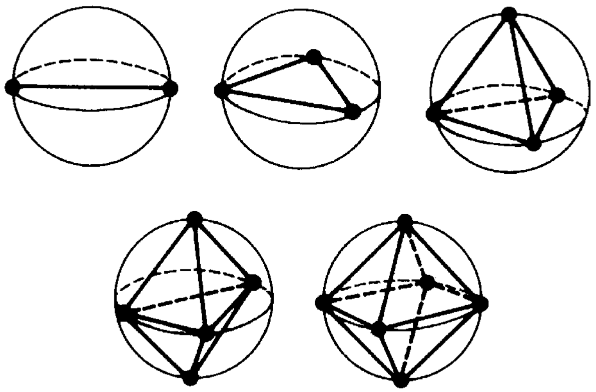

Figure 3-35. Molecular shapes from a points-on-the-sphere model.

The repulsions considered in the VSEPR model may be expressed by the potential energy terms

$$V_{ij} = k/r_{ij}^n$$

where k is a constant, r_{ij} is the distance between the points i and j; and the exponent n is large for strong, or "hard," repulsion interactions and small for weak, or "soft," repulsion interactions. This exponent n is generally much larger than it would be for simple electrostatic Coulomb interactions. Indeed, when n is larger than 3, the results become rather insensitive to the value of n. That is very fortunate because n is not really known. This insensitivity to the choice of n is what provides the wide applicability of the VSEPR model.

3.7.5.1. Analogies

It is easy to illustrate the three-dimensional consequences of the VSEPR model with examples from our macroscopic world. We need only to blow up a few balloons that children play with. If groups of two, three, four, five, and six balloons, respectively, are connected at the ends near their openings, the resulting arrangements are shown in Figure 3-36. Obviously, the space requirements of the various groups of balloons acting as mutual repulsions, determine the shapes and symmetries of these assemblies. The balloons here play the role of the electron pairs of the valence shell.

Another beautiful analogy with the VSEPR model, and one found directly in nature, is demonstrated in Figure 3-37. These are hard-shell fruits growing together. The small clusters of walnuts, e.g., have exactly the same arrangements for two, three, four, and five walnuts in assemblies as predicted by the VSEPR model or as those shown by the balloons. The walnuts—when they grow close to each other—are

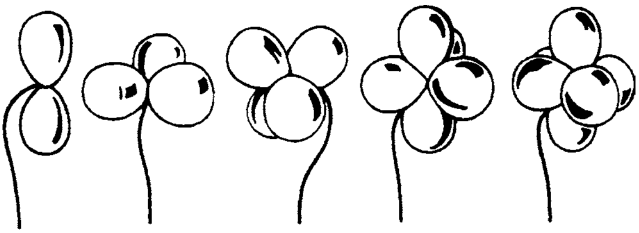

Figure 3-36. Shapes of groups of balloons.

Figure 3-37. Walnut clusters (photographs by the authors).

required to accommodate themselves to each other's company and find the arrangements that are most advantageous considering the space requirements of all. Incidentally, the balloons and the walnuts may take us one step further in analogies as they may be considered as "soft" and "hard" objects, with weak and strong interactions, respectively.

3.7.5.2. Molecular Shapes

Using the VSEPR model, it is simple to predict the shape and symmetry of a molecule from the *total* number of bonding pairs, n, and lone pairs, m, of electrons in the valence shell of its central atom. The molecule may then be written as AX_nE_m where E denotes a lone pair of electrons. Only a few examples will be described here for illustration. For a comprehensive coverage see, e.g., the monograph [89].

First, we consider the methane molecule, shown in the second row of Figure 3-38, together with ammonia and water. Originally, there were four electrons in the carbon valence shell, and these formed four C–H bonds, with the four hydrogens contributing the other four electrons. Thus, methane is represented as AX_4 and its symmetry is, accordingly, regular tetrahedral. In ammonia, originally there were

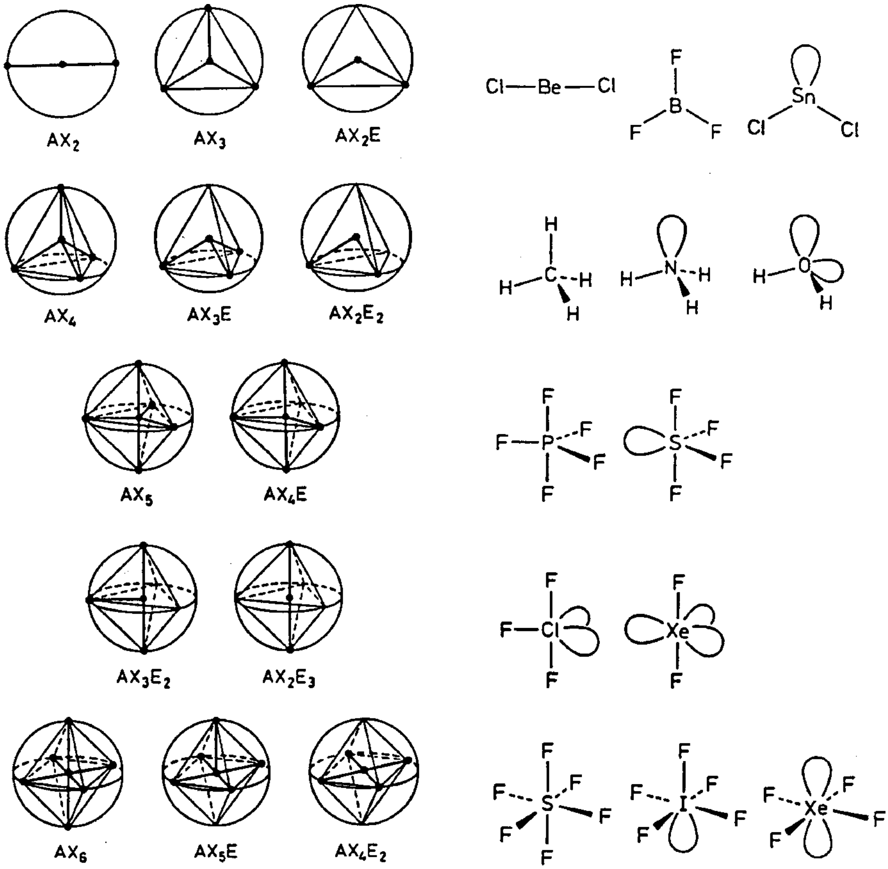

Figure 3-38. Bond configurations with 2, 3, 4, 5, and 6 electron pairs in the valence shell of the central atom [90].

five electrons in the nitrogen valence shell, and the formation of the three N–H bonds added three more. With the three bonding pairs and one lone pair in the nitrogen valence shell, ammonia may be written as AX_3E, and, accordingly, the arrangement of the molecule is related to a tetrahedron. However, only in three of its four directions do we find bonds, and consequently ligands, while in the fourth there is a lone pair of electrons. Hence a pyramidal geometry is found for the ammonia molecule. The bent configuration of the water molecule can be similarly deduced.

In order to establish the total number of electron pairs in the valence shell, the number of electrons originally present and the number of

bonds formed need to be considered. A summary of molecular shapes based on the arrangements of two to six valence shell electron pairs is shown in Figure 3-38.

The molecular shape to a large extent determines the bond angles. Thus, the bond angle X–A–X is 180° in the linear AX_2 molecule, it is 120° in the trigonal planar AX_3 molecule, and 109°28' in the tetrahedral AX_4 molecule. The arrangements shown in Figure 3-38 correspond to the assumption that the strengths of the repulsions from all electron pairs are equal. In reality, however, the space requirements and, accordingly, the strengths of the repulsions from various electron pairs may be different depending on various circumstances as described in the following three subrules [91]:

1. A lone pair, E, in the valence shell of the central atom has a greater space requirement in the vicinity of the central atom than does a bonding pair. Thus, a lone pair exercises a stronger repulsion towards the neighboring electron pairs than does a bonding pair, b. The repulsion strengths weaken in the following order:

$$E/E > E/b > b/b$$

This order is well illustrated by the various angles in sulfur difluoride in Figure 3-39 as determined by ab initio molecular orbital calculations [92]. This is also why, for example, the bond angles H–N–H of ammonia, 106.7°, are smaller than the ideal tetrahedral value, 109.5°. Unless stated otherwise, the parameters in the present discussion are taken from the *Landolt Börnstein* Tables [93].

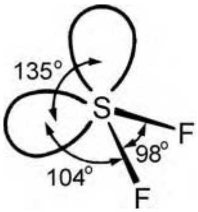

Figure 3-39. The angles of sulfur difluoride as determined by ab initio molecular orbital calculations [94].

2. Multiple bonds, b_m, have greater space requirements than do single bonds and thus exercise stronger repulsions toward the

neighboring electron pairs than do single bonds. The repulsion strengths weaken in the following order:

$$b_m/b_m > b_m/b > b/b$$

A consequence of this is that the bond angles will be larger between multiple bonds than between single bonds. The structure of dimethyl sulfate in Figure 3-40 provides a good example in that it has three different types of OSO bond angles, and they decrease in the following order [95]:

$$S{=}O/S{=}O > S{=}O/S{-}O > S{-}O/S{-}O$$

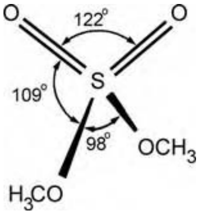

Figure 3-40. The three different kinds of oxygen–sulfur–oxygen bond angles in the dimethyl sulfate molecule as determined by electron diffraction [96].

3. A more electronegative ligand decreases the electron density in the vicinity of the central atom as compared with a less electronegative ligand. Accordingly, the bond to a less electronegative ligand, b_X, has a greater space requirement than the bond to a more electronegative ligand, b_Y. The repulsion strengths then weaken in the following order:

$$b_X/b_X > b_X/b_Y > b_Y/b_Y$$

Consequently, the bond angles are smaller for more electronegative ligands than for less electronegative ligands. An example of this effect can be seen in a comparison of sulfur difluoride (98°) and sulfur dichloride (103°).

It is interesting to compare the implications expressed by these subrules with the depiction of some localized molecular orbitals in Figure 3-41 [97]. The lone pair of electrons occupies more space than do the bonding pairs in the vicinity of the central atom. Also, a bond to a more electronegative ligand such as fluorine occupies less space in

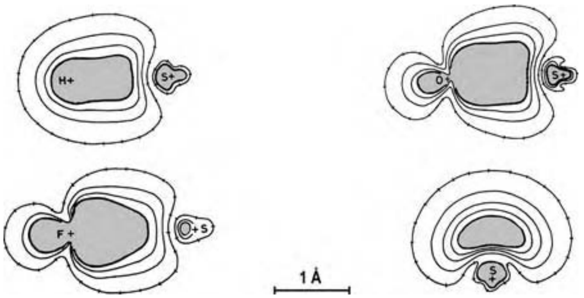

Figure 3-41. Localized molecular orbitals represented by contour lines denoting electron densities of 0.02, 0.04, 0.06, etc. electron/bohr^3 from theoretical calculations for the S–H, S–F, and S=O bonds and the lone pair on sulfur [98].

the vicinity of the central atom than does a bond to a less electronegative ligand such as hydrogen. Finally, a double bond occupies more space than a single bond. The angular ranges of the corresponding contours in the electron density plots are all in good qualitative agreement with the postulates of the VSEPR model.

The VSEPR model has a fourth subrule that concerns the relative availability of space in the valence shell:

4. There is less space available in a completely filled valence shell than in a partially filled valence shell. Accordingly, the repulsions are stronger and the possibility for angular changes are smaller in the filled valence shell than in the partially filled one. Thus, for example, the bond angles of ammonia (107°) are closer to the ideal tetrahedral value than are those of phosphine (94°).

Thus, the differences in the electron pair repulsions may account for the bond angle variations in various series of molecules. The question now arises as to whether these differences have any effect on the *symmetry choice* of the molecules. In the four-electron-pair systems the differences in the electron pair repulsions have a decisive role in the sense that the AX_4, EBX_3, E_2CX_2 molecules have T_d, C_{3v}, and C_{2v} symmetries, respectively. Within each series, however, the symmetry is preserved regardless of the changes in the ligand electronegativities. For example, only the bond angles change in the molecules EBX_3, and EBY_3; the symmetry remains the same.

Ligand electronegativity changes may have decisive effects, however, on the symmetry choices of various bipyramidal systems, of which the trigonal bipyramidal configuration is the simplest.

When five electron pairs are present in the valence shell of the central atom, the trigonal bipyramidal configuration is usually found, although a tetragonal pyramidal arrangement cannot be excluded in some cases. Even intermediate arrangements between these two may appear to be the most stable in some special structures. The trigonal bipyramidal configuration with an equilateral triangle in the equatorial plane has D_{3h} symmetry while the square pyramidal has C_{4v} symmetry. The intermediate arrangements have C_{2v} symmetry or nearly so. Indeed, rearrangements often occur in trigonal bipyramidal structures performing low-frequency large-amplitude motion. Such rearrangements will be illustrated later.

The positions in the D_{3h} trigonal bipyramid are generally not equivalent, and the axial ligand position is further away from the central atom than the equatorial one. This has no effect on the symmetry of the AX_5 structures, and this is comforting from the point of view of the applicability of the VSEPR model in establishing the point-group symmetries of such molecules. On the other hand, when there is inequality among the electron pairs, the differences in the axial and equatorial positions do have importance for symmetry considerations. The PF_5 molecule, as an AX_5 system, shows unambiguously D_{3h} symmetry in its trigonal bipyramidal configuration. However, the prediction of the symmetry of the SF_4 molecule, which may be written as AX_4E, is less obvious. For SF_4 the problem is where will the lone pair of electrons occur?

An axial position in the trigonal bipyramidal arrangement has three nearest neighbors at 90° away and one more neighbor at 180°. For an equatorial position there are two nearest neighbors at 90° and two further ones at 120°. As the closest electron pairs exercise by far the strongest repulsion, the axial positions are affected more than the equatorial ones. In agreement with this reasoning, the axial bonds are usually found to be longer than the equatorial ones. If there is a lone pair of electrons with a relatively large space requirement, it should be found in the more advantageous equatorial position. Accordingly, the SF_4 structure has C_{2v} symmetry, as does the ClF_3 molecule, which is of the AX_3E_2 type. Finally, the XeF_2 molecule is AX_2E_3 with all

three lone pairs in the equatorial plane, hence its symmetry is $D_{\infty h}$. All these structures are depicted in Figure 3-38.

By similar reasoning, the VSEPR model predicts that a double bond will also occupy an equatorial position. Thus, the point group may easily be established for the molecules O=SF_4 (C_{2v}), O=ClF_3 (C_s), XeO_3F_2 (D_{3h}), and XeO_2F_2 (C_{2v}). We note the C_s symmetry for the $OClF_3$ molecule (Figure 3-34) as a consequence of the bipyramidal geometry with both the Cl=O double bond and the lone pair in the equatorial plane. The molecule OPF_3 (Figure 3-34) is only seemingly analogous. There is no lone pair in the phosphorus valence shell in this structure, and thus the molecule has a distorted tetrahedral bond configuration. The P=O double bond is along the three-fold axis, and the point group is C_{3v}, like that for ammonia.

Lone pairs and/or double bonds replaced single bonds in the above examples. Similar considerations are applicable when only ligand electronegativity changes take place. A typical example is demonstrated by a comparison of the structures of PF_2Cl_3 and PF_3Cl_2. The chlorine atoms are less electronegative ligands than the fluorines, and they will be in equatorial positions in *both* structures as seen in Figure 3-42. The point groups are C_{2v} for PF_3Cl_2 and D_{3h} for PF_2Cl_3 [99]. Were the chlorines in the axial positions in PF_3Cl_2, this molecule would also have the much higher symmetry D_{3h}. This is an interesting example also from the point of view that the highest symmetries do not necessarily occur in any given structure. This is not, however, in contradiction with the "Principle of Maximum Symmetry" as stated by I. David Brown, "A compound will adopt the structure with the highest symmetry that is consistent with the constraints acting on it" [100]. In the example above, the constraint is a chemical one, viz., the electronegativity difference between the ligands chlorine and fluorine that leads to a spatial constraint with respect to their bonding electron domains.

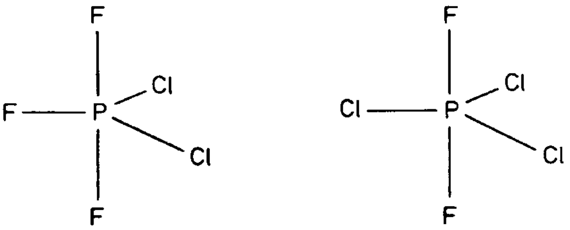

Figure 3-42. The molecular structures of PF_3Cl_2 and PF_2Cl_3 are not analogous: the chlorine ligands occupy equatorial positions in both cases.

All six electron pairs are equivalent in the AX_6 molecule and so the symmetry is unambiguously O_h. An example is SF_6. The IF_5 molecule, however, corresponds to AX_5E and its square pyramidal configuration has C_{4v} symmetry. There is no question here as to the preferred position for the lone pair, as any of the six equivalent sites may be selected. When, however, a second lone pair is introduced, then the favored arrangement is that in which the two lone pairs find themselves at the maximum distance apart. Thus for XeF_4, i.e., AX_4E_2, the bond configuration is square planar, point group D_{4h}. These structures are depicted in Figure 3-38.

The difficulties encountered in the discussion of the five-electron-pair valence shells are intensified in the case of the seven-electron-pair case. Here again the ligand arrangements are less favorable than for the nearest coordination neighbors, i.e., six and eight. It is not possible to arrange seven equivalent points in a regular polyhedron, while the number of nonisomorphic polyhedra with seven vertices is large, viz., 34 [101]. A few of them are shown in Figure 3-43. No single one of them is distinguished, however, from the others on the basis of relative stability. There may be quite rapid rearrangements among the various configurations. One of the early successes of the VSEPR model was that it correctly predicted a non-regular structure for XeF_6 by considering it as a seven-coordination case, AX_6E.

Numerous examples, a wealth of structural data and detailed considerations on the potentials and limitations of the applicability of the VSEPR model are given in a monograph [102].

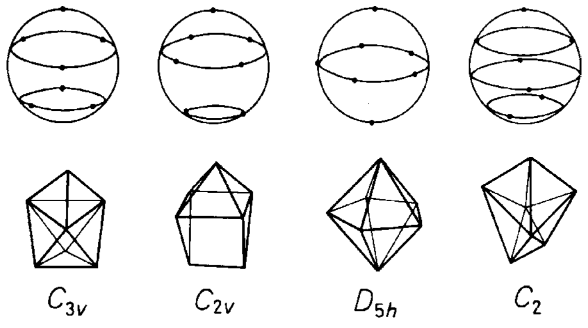

Figure 3-43. A sample of configurations for seven electron pairs in the valence shell.

3.7.5.3. Historical Remarks

The simplicity of the VSEPR model is one of its primary strengths. In addition, the model provides a continuity in the development of the qualitative ideas about the nature of the chemical bond and its correlation with molecular structure. Abegg's octet rule [103] and Lewis' theory of the shared electron pair [104] may be considered as direct forerunners of the model. Lewis' model of the cubical atom deserves special mention. It was instrumental in shaping the concept of the shared electron pair. It also permitted a resolution of the apparent contradiction between the two distinctly different bonding types, viz., the shared electron pair and the ionic electron-transfer bond. In terms of Lewis' theory, the two bonding types could be looked at as mere limiting cases. Lewis' cubical atoms are illustrated in Figure 3-44. They are also noteworthy as an example of a certainly useful though not necessarily correct application of a polyhedral model.

Sidgwick and Powell were first to correlate the number of electron pairs in the valence shell of a central atom and its bond configuration [106]. Then Gillespie and Nyholm introduced allowances for the difference between the effects of bonding pairs and lone pairs, and applied the model to large classes of inorganic compounds [107].

There have been attempts to provide quantum-mechanical foundations for the VSEPR model. These attempts have developed along two lines. One is concerned with assigning a rigorous theoretical basis to the model, primarily involving the Pauli exclusion principle. The other line was the numerous quantum chemical calculations, which have already produced a large amount of structural data consistent with the VSEPR model, demonstrating its ability to capture important effects determining the structure of molecules. It has also been shown that while the total electron density distribution of a molecule does not provide any evidence for the localized electron pairs, the charge concentrations obtained by deriving the second derivative of this distribution parallel the features of these localized pairs [108]. This may be considered as supporting evidence, or even physical basis, for the VSEPR model. We would stress, however, that the VSEPR model is a qualitative tool, and as such, it over-emphasizes some effects and ignores many others. Its simplicity, wide applicability, and predictive power have been repeatedly demonstrated, making it useful both in research and education.

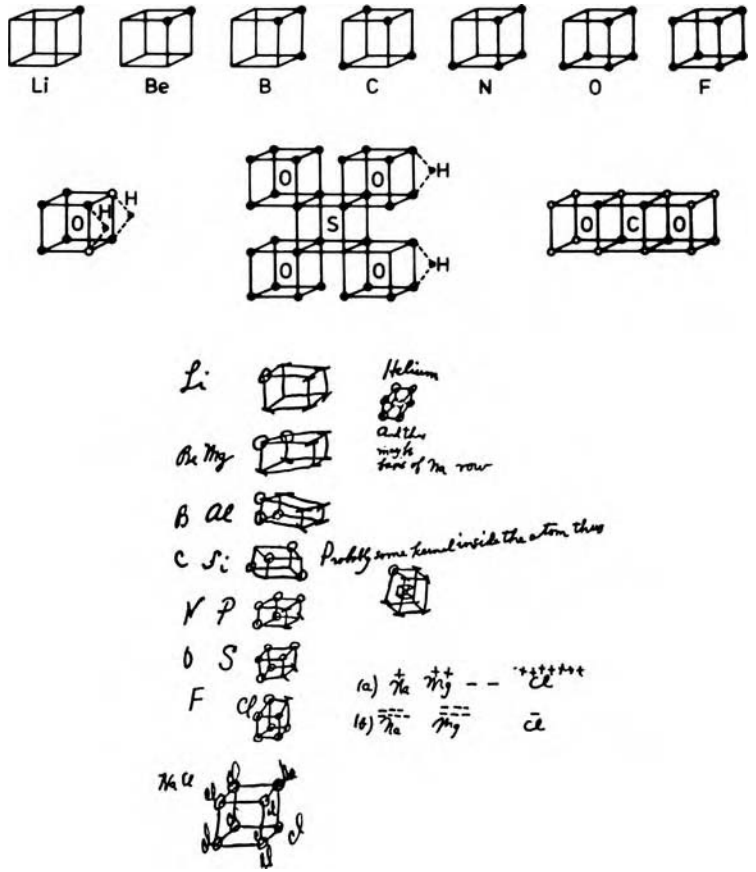

Figure 3-44. G. N. Lewis' cubical atoms and some molecules built from such atoms (*top*) and his original sketches (*bottom*) [105].

3.7.6. Consequences of Intramolecular Motion

Imagine the merry-go-round (Figure 3-45) revolving, and one of the wooden horses getting lifted and, upon its returning to the ground level, the next horse is getting lifted, and so on. In addition to the real revolution of the whole circle, the vertical motion is transmitted from horse to horse which can be considered pseudorotation. If we take a snapshot of the merry-go-round in operation and the exposure is long enough, there will be a blurred image of all the horses up in the elevated position in addition to the ground circle. With a very short exposure, however, we can get an image in which the moment is captured with a single horse being lifted. Another fitting analogy

may be the *Dance* by Henri Matisse (Figure 3-45). Let us imagine the following coreography for this dance: one of the dancers jumps and is thus out of the plane of the other four. As soon as this dancer returns into the plane of the others, it is now the role of the next to jump, and so on. The exchange of roles from one dancer to another throughout the five-member group is so quick that if we take a normal snapshot, we will have a blurred picture of the five dancers. However, if we can use a very short exposure, it will be possible to capture a well-defined configuration of the dancers.

The above descriptions well simulate the *pseudorotation* of the cyclopentane, $(CH_2)_5$, molecule (Figure 3-46), although on a different time scale. This molecule has a special degree of freedom when the out-of-plane carbon atom exchanges roles with one of its two neigh-

Figure 3-45. Merry-go-round in Bologna, Italy (photograph by the authors) and Henri Matisse's *Dance* (The Hermitage, St. Petersburg, reproduced by permission).

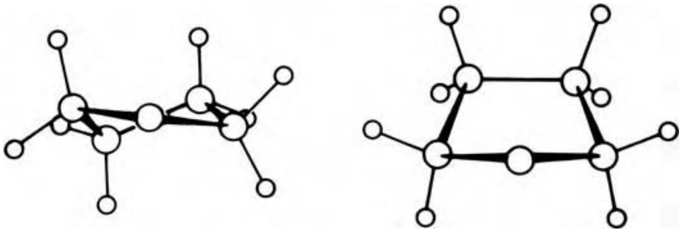

Figure 3-46. Two models of the cyclopentane molecule from its pseudorotation.

boring carbon atoms (and their hydrogen ligands). This is equivalent to a rotation of this motion by $2\pi/5$ about the axis perpendicular to the plane of the in-plane carbons [109]. All three examples emphasize the importance of the *relationship* between the time-scale of motion and the time-scale of measurement. This relationship must be taken into account when making a conclusion about the symmetry of a structure in motion.

In discussing molecular structure, an extreme approach is to disregard intramolecular motion and to consider the molecule to be motionless. A frozen, completely rigid molecule is a hypothetical state corresponding to the minimum position of the potential energy function for the molecule. Such a motionless structure has an important and well-defined physical meaning and is called the *equilibrium structure.* It is this equilibrium structure that emerges from quantum chemical calculations. On the other hand, real molecules are never motionless, not even at the temperatures approaching 0 K. Furthermore, the various physical measurement techniques determine the structures of real molecules. As our discussion of the merry-go-round and Matisse's *Dance* illustrated, the relationship between the lifetime of the configuration under investigation and the time-scale of the investigating technique is of crucial importance.

Large-amplitude, low-frequency intramolecular vibrations may lower the molecular symmetry of the average structure from the higher symmetry of the equilibrium structure. Some examples from metal halide molecules are shown in Figure 3-47.

If we determine the average interatomic distances of symmetric triatomic molecules, for example, the emerging geometry will always be bent, regardless whether the equilibrium structure is linear or bent because of the consequences of bending vibrations (Figure 3-48). In order to distinguish between them, the potential energy func-

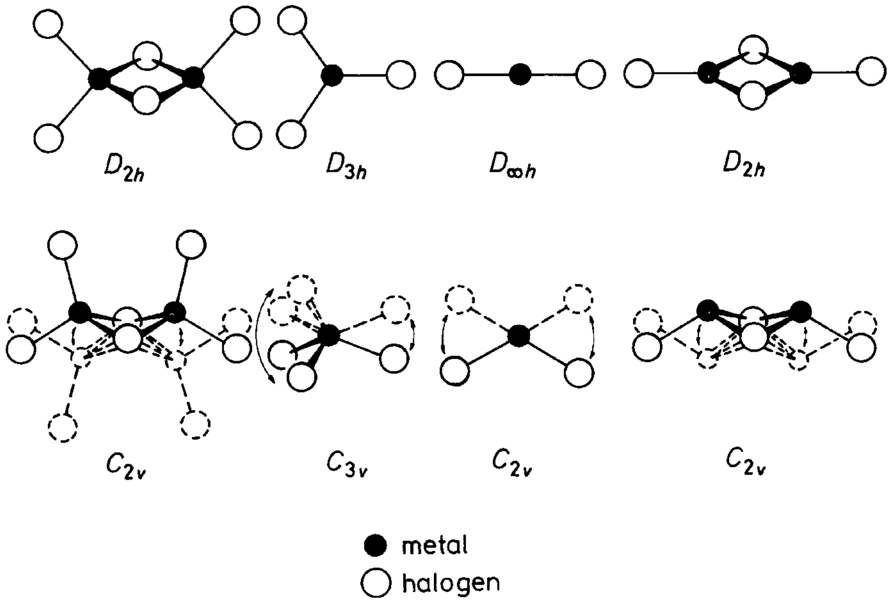

Figure 3-47. Equilibrium versus average structures of simple metal halide molecules with low-frequency, large-amplitude deformation vibrations.

tion describing the bending motion must be scrutinized [110]. The bending potential energy functions of $ZnCl_2$ and $SrBr_2$ are shown in Figure 3-48; the bending angle $\rho_e = 0°$ corresponds to the linear configuration. The minimum of the potential energy appears at $\rho_e = 0°$ for both molecules. It is also seen though that the minimum is much more shallow for $SrBr_2$ than for $ZnCl_2$. Figure 3-48 shows two more bending potential energy functions, those of $SiBr_2$ and, again, of $SrBr_2$, but at very diffent scales as compared with the previous example. The relatively high barrier at $\rho_e = 0°$ for $SiBr_2$ indicates an unambiguously bent configuration. Further enlarging the scale reveals a small barrier at $\rho_e = 0°$ for $SrBr_2$, so small that it lies below the level of the ground vibrational state. Such structures are called quasilinear.

Rapid interconversion of the nuclei takes place in the bullvalene molecule under very mild conditions in fluid media. This process involves making and breaking bonds, but this is accompanied by only very small shifts in the nuclear positions. The molecular formula is $(CH)_{10}$ and the carbon skeleton is shown at the top of Figure 3-49. There are only four different kinds of carbon positions (and hydrogen

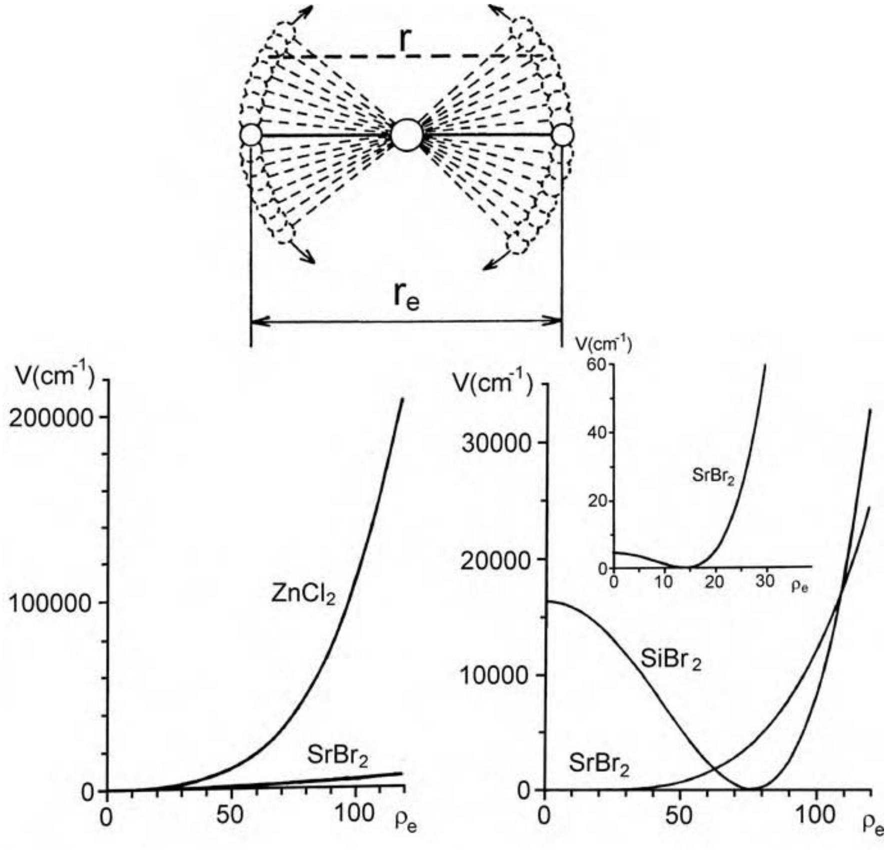

Figure 3-48. Bending motion and a sampler of potential energy functions. *Top*: bending vibration of a linear triatomic molecule, where r is the instantaneous distance between the end atoms and r_e is the equilibrium distance of the linear configuration ($r<r_e$); *Bottom*: Comparison of bending potential functions for linear and bent models of symmetric triatomic molecules [111].

positions, accordingly) and all four positions are being interconverted simultaneously [112].

Hypostrophene is another $(CH)_{10}$ hydrocarbon whose trivial name was chosen to reflect its behavior, the Greek *hypostrophe* meaning turning about [115]. The molecule is ceaselessly undergoing the intramolecular rearrangements indicated at the bottom of Figure 3-49. The atoms have a complete time-averaged equivalence yet hypostrophene could not be converted into pentaprismane.

Permutational isomerism among inorganic substances was discovered by R. S. Berry for trigonal bipyramidal structures [116].

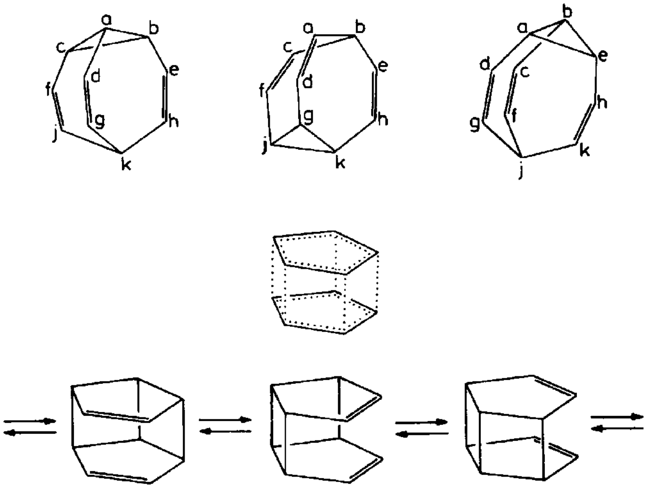

Figure 3-49. The interconversion of bullvalene [113] (*top*) and hypostrophene [114].

Although the trigonal bipyramid and the square pyramid have different symmetries, D_{3h} versus C_{4v}, they easily interconvert by means of bending vibrations as is illustrated in Figure 3-50. The change in the potential energy during this structural reorganization is also shown. The permutational isomerism of an AX_5 molecule, e.g., PF_5, is easy to visualize as the two axial ligands replace two of the three equatorial ones, while the third equatorial ligand becomes the axial ligand in the transitional square pyramidal structure. The rearrangements quickly follow one another without any position being constant for any significant time period. The C_{4v} form originates from a D_{3h} structure and yields then again to another D_{3h} form. A somewhat similar pathway was established for the $(CH_3)_2NPF_4$ molecule in which the dimethylamine group is permanently locked in an equatorial position whereas the fluorines exchange in pairs all the time [117].

The structure of the $(CH_3)_2NPF_4$ molecule and its investigation by NMR spectroscopy is also a good example to demonstrate the importance of the relationship between the lifetime of a configuration and the time-scale of the investigating technique. The ^{31}P NMR spectra of $(CH_3)_2NPF_4$ at *low temperatures* provide evidence of two different kinds of P–F bond in this molecule, viz., axial and equatorial. At low temperatures the interconversion is slow and the lifetimes of the fluorines in the axial and equatorial positions are much greater than the

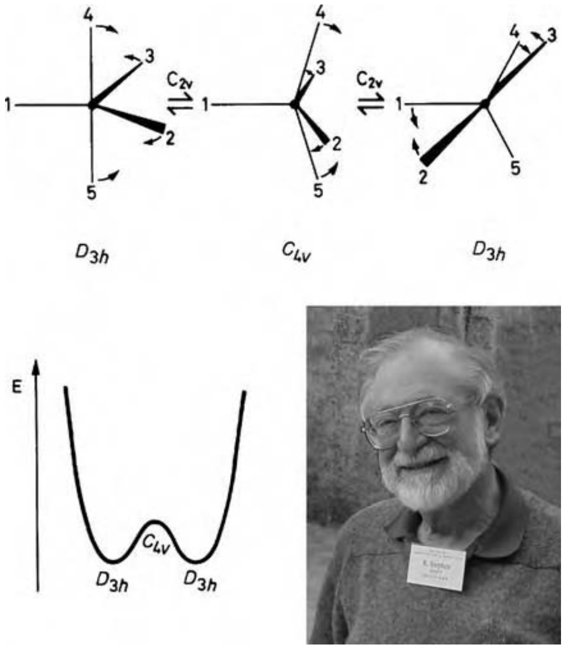

Figure 3-50. Berry-pseudorotation of PF_5-type molecules with a potential energy function and R. Stephen Berry (photograph by the authors).

interaction time for producing the spectrum. So the two kinds of P–F bond give separate resonances in the spectrum. At *higher temperatures* the intramolecular exchange of the fluorine positions accelerates and the lifetimes of the fluorines in the axial and equatorial positions decrease. As the interaction time needed to produce the spectrum remains the same, the spectrum becomes simpler and the nonequivalent fluorines are no longer distinguished. Since the time-scale of NMR spectroscopy is commensurable with the lifetimes of separate configurations in intramolecular motion, different molecular shapes may be observed at different temperatures. Other techniques utilize interactions at different time-scales. Thus, for example, the time-scale of electron diffraction is several orders of magnitude smaller and, accordingly, the two different fluorine positions will always be distinguished in an electron diffraction analysis.

Iodine heptafluoride, IF_7, has a pentagonal bipyramidal structure of at least approximately D_{5h} symmetry [118]. Its dynamic behavior has been desribed by pseudorotation. The rearrangement that characterizes the PF_5 molecule also describes well the permutation of

the atomic nuclei in five-atom polyhedral boron skeletons in borane molecules [119].

W. N. Lipscomb elaborated a general concept for the rearrangements of polyhedral boranes according to which two common triangulated faces are stretched to a square face in the borane polyhedra [120]. There is an intermediate polyhedral structure with square faces. In the final step of the rearrangement, the intermediate configuration may revert to the original polyhedron with no net change, but it may as well turn into a different arrangement. The arrangement has rectangular faces with an orthogonal linkage with respect to the bonding situation in the original polyhedron (Figure 3-51). Of the many possible examples, the rearrangements of dicarba-closo-dodecaboranes are illustrated in Figure 3-52. There are three isomers of this beautiful carborane molecule:

1,2-dicarba-*closo*-dodecaborane, or o-$C_2B_{10}H_{12}$,
1,7-dicarba-*closo*-dodecaborane, or m-$C_2B_{10}H_{12}$, and
1,12-dicarba-*closo*-dodecaborane, or p-$C_2B_{10}H_{12}$.

Whereas the ortho isomer easily transforms into the meta isomer in agreement with the above mentioned model, the para isomer is obtained only under more drastic conditions and only in a small amount [121].

A similar model has been proposed for the so-called carbonyl scrambling mechanism in molecules like $Co_4(CO)_{12}$, $Rh_4(CO)_{12}$,

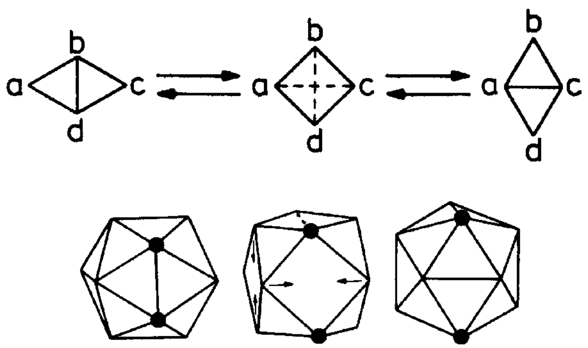

Figure 3-51. Lipscomb model of the rearrangement in polyhedral boranes (*top*) with the polyhedral rearrangement of icosahedron/cuboctahedron/icosahedron [122].

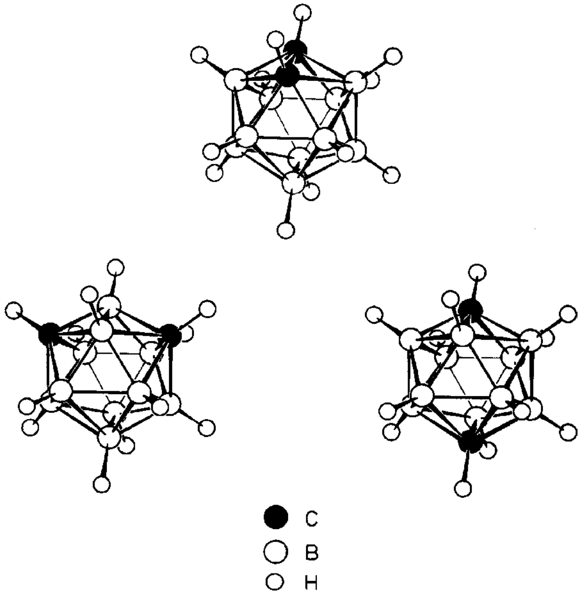

Figure 3-52. Structures of ortho-, meta-, and para-dicarba-*closo*-dodecaborane [123].

and $Ir_4(CO)_{12}$ [124]. The carbonyl ligands can have several modes of coordination, viz., terminal and a variety of bridging possibilities. Rapid interconversion between the different coordination modes is possible, even in the solid state [125]. These metal-carbonyl molecules belong to a large class of compounds whose general formula is $M_m(CO)_n$, where M is a transition metal. The usually small

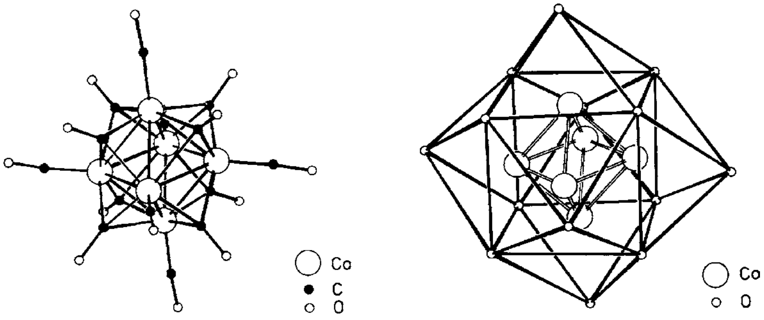

Figure 3-53. The structure of $[Co_6(CO)_{14}]^{4-}$ in two representations after [127]: *Left*: the octahedron of the cobalt cluster possesses six terminal and eight triply bridging carbonyl groups; *Right*: an omnicapped cube of the carbonyl oxygen envelopes the cobalt octahedron.

m-atomic metal clustser polyhedron is enveloped by another polyhedron whose vertices are occupied by the carbonyl oxygens [126]. An attractive example is the structure of $[Co_6(CO)_{14}]^{4-}$ in which the octahedral metal cluster has six terminal and eight triply bridging carbonyl groups, as shown in Figure 3-53. This structure may also be represented by an omnicapped cube enveloping an octahedron, which is also depicted in Figure 3-53. These models are reminiscent of another model in which, also, polyhedra were enveloping other polyhedra. That model was Kepler's planetary system in his *Mysterium cosmographicum* published in 1595 and mentioned in the previous Chapter.

References

1. D. W. Thompson, *On Growth and Form,* Cambridge University Press, 1917.
2. A comprehensive account of the origins and early history of stereochemistry is given in O. B. Ramsay, *Stereochemistry*. Heyden, London, 1981.
3. Kolbe in Ramsay, *Stereochemistry,* p. 93.
4. L. Pauling, *The Nature of the Chemical Bond and the Structure of Molecules and Crystals: An Introduction to Modern Structural Chemistry,* Third Edition, Cornell University Press, Ithaca, New York, 1960.
5. I. Hargittai, "Degas Dancers – An Illustration for Rotational Isomers." *J. Chem. Educ*. 1983, 60, 94. Full color reproductions of the original are available in editions of Degas' work. The original of the drawing with the outstretched hands of ther dancer is in the Louvre, Musée de l'Impressionisme in Paris, and of the other in The Hermitage in St. Petersburg.
6. Hargittai, *J. Chem. Educ*. 94.
7. N. F. M. Henry, K. Lonsdale, eds., *International Tables for X-ray Crystallography,* Vol. I., *Symmetry Groups,* Kynoch Press, Birmingham, 1969.
8. J. H. Conway, D. H. Huson, "The Orbifold Notation for Two-Dimensional Groups." *Struct. Chem.* 2002, 13, 247–257.
9. F. A. Cotton, *Chemical Applications of Group Theory*, Third Edition, Wiley-Interscience, New York, 1990; M. Orchin, H. H. Jaffe, "Symmetry. Point Groups, and Character Tables; I, Symmetry Operations and Their Importance for Chemical Problems." *J. Chem. Educ*. 1970, 47, 372–377.
10. Ibid.
11. M. F. Perutz, *Proteins and Nucleic Acids: Structure and Function*. Elsevier, Amsterdam, 1962, pp. 64 and 66.
12. See, e.g., I. Hargittai, *The DNA Doctor: Candid Conversations with James D. Watson*. World Scientific, Singapore, 2007, p. 10.
13. I. Hargittai, *Candid Science III: More Conversations with Famous Chemists*. Ed. M. Hargittai. Imperial College Press, London, 2003, "Johann Deisenhofer", pp. 342–353.

14. Hargittai, *Candid Science III*, pp. 349–350.
15. Hargittai, *Candid Science III*, p. 345.
16. See, e.g., J. Deisenhofer, H. Michel, "The Photosynthetic Reaction Center from the Purple Bacterium Rhodopseudomonas-Viridis." *Science* 1989, 245, 1463–1473; M. E. Michel-Beyerle, M. Plato, J. Deisenhofer, H. Michel, M. Bixton, J. Jortner, "Unidirectionality of Charge Separation in Reaction Centers of Photosynthetic Bacteria." *Biochim. Biophys. Acta* 1988, 932, 52–70.
17. S. Keinan, M. Pinsky, M. Plato, J. Edelstein, D. Avnir, "Quantitative Evaluation of the Near-C_2 Symmetry of the Bacterial Photosynthetic Reaction Center." *Chem. Phys. Lett*. 1998, 298, 43–50.
18. A. Domenicano, "Structural Substituent Effects in Benzene Derivatives." In *Accurate Molecular Structures*, A. Domenicano and I. Hargittai, eds., Oxford University Press, Oxford, 1992, pp. 437–468; See, also, A. R. Campanelli, A. Domenicano, F. Ramondo, I. Hargittai, "Group Electronegativities from Benzene Ring Deformations: A Quantum Chemical Study." *J. Phys. Chem. A*, 2004, 108, 4940–4948.
19. M. Hargittai, I. Hargittai, *The Molecular Geometries of Coordination Compounds in the Vapour Phase*, Akadémiai Kiadó, Budapest and Elsevier, Amsterdam and New York, 1977; V. Horváth, A. Kovács, I. Hargittai, "Structural Aspects of Donor–Acceptor Interactions." *J. Phys. Chem. A*, 2003, 107, 1197–1202; V. Horváth, I. Hargittai, "Geometrical Changes and Their Energies in the Formation of Donor-Acceptor Complexes." *Struct. Chem.* 2004, 15, 233–236.
20. H. S. M. Coxeter, *Regular Polytopes*, Third Edition, Dover Publications, New York, 1973.
21. R. J. Ternansky, D. W. Balogh, L. A. Paquette, "Dodecahedrane." *J. Am. Chem. Soc*. 1982, 104, 4503–4504.
22. H. P. Schultz, "Topological Organic Chemistry: Polyhedranes and Prismanes." *J. Org. Chem*. 1965, 30, 1361–1364.
23. H. S. M. Coxeter, *Regular Polytopes*. First Edition, Methuen & Co., London, 1948.
24. C. H. MacGillavry, *Symmetry Aspects of M. C. Escher's Periodic Drawings*, Bohn, Scheltema and Holkema, Utrecht, 1976.
25. E. L. Muetterties, in *Boron Hydride Chemistry*, E. L. Muetterties, ed., Academic Press, New York, San Francisco, London, 1975.
26. V. P. Spiridonov, G. I. Mamaeva, "Study of the Zirconium Borohydride Molecule by Electron Diffraction by Gases." *Zh. Strukt. Khim*. 1969, 10, 132–135.
27. V. Plato, K. Hedberg, "An Electron-Diffraction Investigation of Zirconium Tetraborohydride, $Zr(BH_4)_4$." *Inorg. Chem*. 1971, 10, 590–594.
28. Spiridonov, Mamaeva, *Zh. Strukt. Khim*. 132–135.
29. Plato, Hedberg, *Inorg. Chem*. 590–594.
30. H. W. Kroto, J. R. Heath, S. O'Brien, R. F. Curl, R. E. Smalley, "C_{60}: Buckminsterfullerene." *Nature* 1985, 318, 162–163.

31. *Science* 1990, December 12, 250.
32. *Science* 1991, December 20, 254.
33. D. E. Koshland, *Science* 1991, 251, 1162. D. E. Koshland, “Molecule of the Year.” *Science* 1991, 254, 1705.
34. H. Prinzbach, A. Weiler, P. Landenberger, F. Wahl, J. Wörth, L. T. Scott, M. Gelmont, D. Olevano, B. V. Issendorff, “Gas-Phase Production and Photoelectron Spectroscopy of the Smallest Fullerene, C_{20}.” *Nature* 2000, 407, 60–63.
35. *Science* 1991, December 20, 254.
36. Muetterties, *Boron Hydride Chemistry.*
37. E. Esenturk, J. Fettinger, Y.-F. Lam, B. Eichhorn, “$[Pt@Pb_{12}]^{2-}$” *Angew. Chem. Int. Ed. Engl*. 2004, 43, 2132–2134.
38. R. E. Williams, “Carboranes and Boranes; Polyhedra and Polyhedral Fragments.” *Inorg. Chem*. 1971, 10, 210–214.
39. R. W. Rudolph, “Boranes and Heteroboranes – Paradigm for Electron Requirements of Clusters.” *Acc. Chem. Res*. 1976, 9, 446–452.
40. Williams, *Inorg. Chem*. 210–214.
41. Rudolph, *Acc. Chem. Res*. 446–452.
42. S. O. Kang, L. G. Sneddon, in *Electron Deficient Boron and Carbon Clusters*, G. A. Olah, K. Wade, R. E. Williams, eds., Wiley, New York, 1991.
43. Muetterties, *Boron Hydride Chemistry*.
44. Ibid.
45. L. N. Ferguson, “Alicyclic Chemistry: The Playground for Organic Chemists.” *J. Chem. Educ*. 1969, 46, 404–412.
46. See, e.g., A. Nemirowski, H. P. Reisenauer, P. R. Schreiner, “Tetrahedrane—Dossier of an Unknown.” *Chem. Eur. J.* 2006, 12, 7411–7420.
47. G. Maier, S. Pfriem, U. Schafer, R. Matush, “Small Rings. 25. Tetra-tert-butyltetrahedrane.” *Angew. Chem. Int. Ed. Engl.* 1978, 17, 520–521.
48. Ibid.
49. P. E. Eaton, T. J. Cole, “Cubane.” *J. Am. Chem. Soc*. 1964, 86, 3157–3158. See, also, P. E. Eaton, “Cubanes – Starting Materials for the Chemistry of the 1990s and the New Century.” *Angew. Chem. Int. Ed. Engl.* 1992, 31, 1421–1436; A. P. Marchand, “Plato’s Solid, Eaton’s Cage: The Cubane Saga.” *Chem. Intell.* 1995, 1(4), 8–17.
50. Marchand, *Chem. Intell.* p. 10 (Marchand quoting Eaton’s words).
51. Ibid., p. 11.
52. Ternansky et al., *J. Am. Chem. Soc*. 4503–4504.
53. Schultz, *J. Org. Chem*. 1361–1364.
54. R. F. Curl, R. E. Smalley, “Fullerenes.” *Sci. Amer*. October 1991, p. 32.
55. T. J. Katz, N. Acton, “Synthesis of Prismane.” *J. Am. Chem. Soc*. 1973, 95, 2738–2739; V. Ramamurthy, T. J. Katz, “Energy-Storage and Release – Direct and Sensitized Photoreactions of Dewar Benzene and Prismane.” *Nouv. J. Chim*. 1977, 1, 363–365.
56. P. E. Eaton, Y. S. Or, S. J. Branca, “Pentaprismane.” *J. Am. Chem. Soc*. 1981, 103, 2134–2136.

57. D. Farcasiu, E. Wiskott, E. Osawa, W. Thielecke, E. M. Engler, J. Slutsky, P. v. R. Schleyer, “Ethanoadamantane. The Most Stable $C_{12}H_{18}$ Isomer.” *J. Am. Chem. Soc*. 1974, 96, 4669–4671.
58. M. Alonso, J. Poater, M. Solà, “Aromaticity Changes Along the Reaction Coordinate Connecting the Cyclobutadiene Dimmer to Cubane and the Benzene Dimmer to Hexaprismane.” *Struct. Chem.* 2007, 18, 773–783.
59. Williams, *Inorg. Chem*. 210–214.
60. Farcasiu et al., *J. Am. Chem. Soc*. 4669–4671.
61. L. F. Fieser, “Extensions in the Use of Plastic Tetrahedral Models.” *J. Chem. Educ*. 1965, 42, 408–412.
62. C. A. Cupas, L. Hodakowski, “Iceane.” *J. Am. Chem. Soc*. 1974, 96, 4668–4669.
63. Fieser, *J. Chem. Educ*. 408–412.
64. C. Cupas, P. v. R. Schleyer, D. J. Trecker, “Congressane.” *J. Am. Chem. Soc*. 1965, 87, 917–918; T. M. Gund, E. Osawa, V. Z. Williams, P. v. R. Schleyer, “Diamantane. I. Preparation of Diamantane. Physical and Spectral Properties.” *J. Org. Chem*. 1974, 39, 2979–2987.
65. A. Greenberg, J. F. Liebman, *Strained Organic Molecules,* Academic Press, New York, 1978.
66. E. Boelema, J. Strating, H. Wynberg, “Spiro[adamantane-2,2’-adamantane].” *Tetrahedron Lett*. 1972, 1175–1177; W. D. Graham, P. v. R. Schleyer, “Diamond Lattice Hydrocarbons: Spiro[adamantane-2,2’-adamantane].” *Tetrahedron Lett*. 1972, 1179–1180.
67. W. D. Graham, P. v. R. Schleyer, E. W. Hagaman, E. Wenkert, “[2]Diadamantane, the First Member of a New Class of Diamondoid Hydrocarbons.” *J. Am. Chem. Soc*. 1973, 95, 5785–5786.
68. Cupas, Schleyer, Trecker, *J. Am. Chem. Soc*. 917–918; Gund, Osawa, Williams, Schleyer, *J. Org. Chem*. 2979–2987.
69. W. Z. Williams, P. v. R. Schleyer, G. J. Gleicher, L. B. Rodewald, “Triamantane.” *J. Am. Chem. Soc*. 1966, 88, 3862–3863.
70. W. Burns, T. R. B. Mitchell, M. A. McKervey, J. J. Rooney, G. Ferguson, P. Roberts, “Gas-Phase Reactions on Platinum. Synthesis and Crystal Structure of Anti-Tetramantane, a Large Diamondoid Fragment.” *J. Chem. Soc. Chem. Commun*. 1976, 893–895.
71. M. Hargittai, “The Molecular Geometry of Metal Halides.” *Coord. Chem. Rev*. 1988, 91, 35–88.
72. Ibid.
73. G. Rauscher, T. Clark, D. Poppinger, P. v. R. Schleyer, “C_4Li_4, Tetralithiotetrahedrane.” *Angew. Chem. Int. Ed. Engl*. 1978, 17, 276–278.
74. Ibid.
75. A. Haaland, J. E. Nilsson, “Determination of Barriers to Internal Rotation by Electron Diffraction. Ferrocene and Ruthenocene.” *Acta Chem. Scand*. 1968, 22, 2653–2670.
76. I. Hargittai, “The Beginnings of Multiple Metal–Metal Bonds.” I. Hargittai, *Candid Science: Conversations with Famous Chemists*. Ed. M. Hargittai. Imperial College Press, London, 2000, pp. 246–249.

77. A. S. Kotel'nikova, V. G. Tronev, "Complex Compounds of Bivalent Rhenium." *Zh. Neorg. Khim*. 1958, 3, 1008–1027.
78. F. A. Cotton, N. F. Curtis, C. B. Harris, B. F. G. Johnson, S. J. Lippard, J. T. Mague, W. R. Robinson, J. S. Wood, "Mononuclear and Polynuclear Chemistry of Rhenium (III): Its Pronounced Homophilicity." *Science* 1964, 145, 1305–1307.
79. E. H. Hahn, H. Bohm, D. Ginsburg, "The Synthesis of Paddlanes: Compounds in which Quaternary Bridgehead Carbons are Joined by Four Chains." *Tetrahedron Lett.* 1973, 14, 507–510.
80. M. H. Kelley, M. Fink, "The Molecular Structure of Dimolybdenum Tetraacetate." *J. Chem. Phys*. 1982, 76, 1407–1416.
81. V. Plato, W. D. Hartford, K. Hedberg, "Electron-Diffraction Investigation of the Molecular Structure of Trifluoramine Oxide, F_3NO." *J. Chem. Phys*. 1970, 53, 3488–3494.
82. Ibid.
83. L. S. Bartell, "On the Effects of Intramolecular van der Waals Forces." *J. Chem. Phys*. 1960, 32, 827–831.
84. L. S. Bartell, "Molecular Geometry: Bonded Versus Nonbonded Interactions." *J. Chem. Educ*. 1968, 45, 754–767.
85. Ibid.
86. I. Hargittai, *The Structure of Volatile Sulphur Compounds*, Reidel Publ. Co., Dordrecht, Boston, Lancaster, 1985.
87. Ibid.
88. R. J. Gillespie, I. Hargittai, *The VSEPR Model of Molecular Geometry,* Allyn and Bacon, Boston, 1991.
89. Ibid.
90. Ibid.
91. Ibid.
92. A. Schmiedekamp, D. W. J. Cruickshank, S. Skaarup, P. Pulay, I. Hargittai, J. E. Boggs, "Investigation of the Basis of the Valence Shell Electron Pair Repulsion Model by ab Initio Calculation of Geometry Variations in a Series of Tetrahedral and Related Molecules." *J. Am. Chem. Soc*. 1979, 101, 2002–2010.
93. *Landolt-Börnstein, Numerical Data and Functional Relationships in Science and Technology (New Series).* Vols. II/7, II/15, II/21: *Structure Data of Free Polyatomic Molecules,* Springer Verlag Berlin, Heidelberg, New York, 1976, 1987, 1992.
94. Schmiedekamp et al., *J. Am. Chem. Soc*. 2002–2010.
95. J. Brunvoll, O. Exner, I. Hargittai, "Geometry and Conformation of Dimethyl Sulfate as Investigated by Electron-Diffraction and Dipolometry." *J. Mol. Struct*. 1981, 73, 99–104.
96. Ibid.
97. Schmiedekamp et al., *J. Am. Chem. Soc*. 2002–2010.
98. Ibid.

99. C. Macho, R. Minkwitz, J. Rohmann, B. Steger, V. Wölfel, H. Oberhammer, “The Chlorofluorophosphoranes PCl_nF_{5-n} (n = 1–4). Gas-Phase Structures and Vibrational Analyses.” *Inorg. Chem*. 1986, 25, 2828–2835.
100. I. D. Brown, “Topology and Chemistry.” *Struct. Chem.* 2002, 13, 339–355.
101. R. Hoffmann, B. F. Beier, E. L. Muetterties, A. Rossi, “7-Coordination – Molecular-Orbital Exploration of Structure, Stereochemistry, and Reaction Dynamics.” *Inorg. Chem*. 1977, 16, 511–522.
102. Gillespie, Hargittai, *The VSEPR Model of Molecular Geometry*.
103. See, e.g., W. B. Jensen, “Abegg, Lewis, Langmuir, and the Octet Rule.” *J. Chem. Educ*. 1984, 61, 191–200.
104. G. N. Lewis, “The Atom and the Molecule.” *J. Am. Chem. Soc*. 1916, 38, 762–785; G. N. Lewis, *Valence and the Structure of Atoms and Molecules*, Chemical Catalog Co., New York, 1923.
105. Ibid.
106. N. V. Sidgwick, H. M. Powell, “Bakerian Lecture. Stereochemical Types and Valency Groups.” *Proc. R. Soc. London, Ser A* 1940, 176, 153–180.
107. R. J. Gillespie, R. S. Nyholm, “Inorganic Stereochemistry.” *Quart. Rev. Chem. Soc*. 1957, 11, 339–380.
108. R. F. W. Bader, P. J. MacDougall, C. D. H. Lau, “Bonded and Nonbonded Charge Concentrations and Their Relation to Molecular-Geometry and Reactivity.” *J. Am. Chem. Soc*. 1984, 106, 1594–1605; R. F. W. Bader, *Atoms and Molecules: A Quantum Theory*, Oxford University Press, Oxford, U. K., 1990.
109. See, e.g., R. S. Berry, in *Quantum Dynamics of Molecules. The New Experimental Challenge to Theorists,* R. G. Wooley, ed., Plenum Press, New York and London, 1980.
110. See, e.g., M. Hargittai, I. Hargittai, “Linear, bent, and quasilinear molecules.” In *Structures and Conformations of Non-rigid Molecules*, J. Laane, M. Dakkouri, B. van der Veken, and H. Oberhammer, eds., NATO ASI Series C.: Mathematical and Physical Sciences, Vol. 410, pp. 465–489, Kluwer Academic Publishers, Dordrecht, Boston, London, 1993.
111. Ibid.
112. W. v. E. Doering, W. R. Roth, “A Rapidly Reversible Degenerate Cope Rearrangement. Bicyclo[5.1.0]octa-2,5-diene. A rapidly reversible degenerate Cope rearrangement.” Tetrahedron 1963, 19, 715–737 *Tetrahedron* 1963, 19, 715–737; G. Schroeder, “Preparation and Properties of Tricyclo[3,3,2,04,6]deca-2,7,9-triene (Bullvalene).” *Angew. Chem. Int. Ed. Engl*. 1963, 2, 481–482; M. Saunders, “Measurement of the Rate of Rearrangement of Bullvalene.” *Tetrahedron Lett*. 1963, 4, 1699–1702.
113. Ibid.
114. J. S. McKennis, L. Brener, J. S. Ward, R. Pettit, “The Degenerate Cope Rearrangements in Hypostrophene, A Novel $C_{10}H_{10}$ Hydrocarbon.” *J. Am. Chem. Soc*. 1971, 93, 4957–4958.
115. Ibid.
116. R. S. Berry, “Correlation of Rates of Intramolecular Tunneling Processes, with Application to Some Group V Compounds.” *J. Chem. Phys*. 1960, 32, 933–938.

117. G. M. Whitesides, H. L. Mitchell, “Pseudorotation in $(CH_3)_2NPF_4$.” *J. Am. Chem. Soc*. 1969, 91, 5384–5386.
118. L. S. Bartell, M. J. Rothman, A. Gavezzotti, “Pseudopotential SCF-MO Studies of Hypervalent Compounds .4. Structure, Vibrational Assignments, and Intramolecular Forces in IF_7.” *J. Chem. Phys*. 1982, 76, 4136–4143 and references therein; K. O. Christe, E. C. Curtis, D. A. Dixon, “On the Problem of Heptacoordination – Vibrational-Spectra, Structure, and Fluxionality of Iodine Heptafluoride.” *J. Am. Chem. Soc*. 1993, 115, 1520–1526.
119. E. L. Muetterties, W. H. Knoth, *Polyhedral Boranes*, Marcel Dekker, New York, 1968.
120. W. N. Lipscomb, “Framework Rearrangement in Boranes and Carboranes.” *Science* 1966, 153, 373–378.
121. Ibid., and see also, D. M. P. Mingos, D. J. Wales, in *Electron Deficient Boron and Carbon Clusters*, G. A. Olah, K. Wade, R. E. Williams, eds., Wiley, New York, 1991; D. J. Wales, “Rearrangement Mechanisms of $B_{12}H_{12}^{2-}$ and $C_2B_{10}H_{12}$.” *J. Am. Chem. Soc*. 1993, 115, 1557–1567.
122. Lipscomb, *Science*, 373–378.
123. R. K. Bohn, M. D. Bohn, “Molecular Structures of 1,2-, 1,7-, and 1,12-Dicarba-closo-dodecaborane(12), $B_{10}C_2H_{12}$.” *Inorg. Chem*. 1971, 10, 350–355.
124. B. F. G. Johnson, R. E. Benfield, “Structures of Binary Carbonyls and Related Compounds. 1. New Approach to Fluxional Behavior.” *J. Chem. Soc. Dalton Trans*. 1978, 1554–1568.
125. B. E. Hanson, M. J. Sullivan, R. J. Davis, “Direct Evidence for Bridge Terminal Carbonyl Exchange in Solid Dicobalt Octacarbonyl by Variable-Temperature Magic Angle Spinning C-13 NMR-Spectroscopy.” *J. Am. Chem. Soc*. 1984, 106, 251–253.
126. R. E. Benfield, B. F. G. Johnson, “The Structures and Fluxional Behaviour of the Binary Carbonyls – A New Approach. 2. Cluster Carbonyls $M_m(CO)_n$ (n = 12,13,14,15, or 16).” *J. Chem. Soc. Dalton Trans*. 1980, 1743–1767.
127. Johnson, Benfield, *J. Chem. Soc. Dalton Trans*. 1554–1568.

Chapter 4

Helpful Mathematical Tools

> What we have to learn to do we learn by doing.
> *Aristotle* [1]

4.1. Groups

So far our discussion has been non-mathematical. Ignoring mathematics, however, does not make things necessarily easier. Group theory is the mathematical apparatus for describing symmetry operations. It facilitates the understanding and the use of symmetries. It may not even be possible to successfully attack some complex problems without the use of group theory. Besides, groups are fascinating. In his book series, the mathematician, James Newman, characterized group theory in the following way: "The Theory of Groups is a branch of mathematics in which one does something to something and then compares the result with the result obtained from doing the same thing to something else, or something else to the same thing" [2].

This introductory chapter gives the reader the tools necessary to understand the next three chapters in which molecular vibrations, electronic structure, and chemical reactions are discussed. Further reading is recommended for broader knowledge of the subject [3–11].

A mathematical group is a very general idea. It is a collection (set) of symbols or objects together with a rule telling us how to combine them. A simple example is a set of two numbers and addition for the rule. The theory of groups has a wide range of applications far beyond pure mathematics; especially in physics and chemistry. Symmetry and group theory are inherently related to each other. When the symmetries of molecules are characterized by Schoenflies

M. Hargittai, I. Hargittai, *Symmetry through the Eyes of a Chemist,* 3rd ed.,
DOI: 10.1007/978-1-4020-5628-4_4, © Springer Science+Business Media B.V. 2009

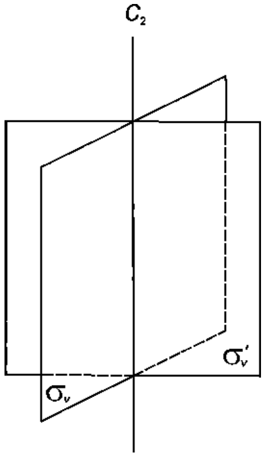

Figure 4-1. Symmetry operations in the C_{2v} point group.

symbols, for example, C_{2v}, C_{3v} or C_{2h}, these symbols represent well-defined groups of symmetry operations. Let us consider first the C_{2v} point group. It consists of a twofold rotation, C_2, and two reflections through mutually perpendicular symmetry planes, σ_v and σ_v', whose intersection coincides with the rotation axis. All the corresponding elements are shown in Figure 4-1. One more operation can be added to these, called the identity operation, E. Its application leaves the molecule unchanged. The set of the operations C_2, σ_v, σ_v', and E together make a mathematical group.

A mathematical group is a set of elements related by certain rules. They will be illustrated on the symmetry operations.

1. *The product of any two elements of a group is also an element of the group.* The product here means consecutive application of the elements rather than common multiplication. Thus, for example, the product $\sigma_v \cdot C_2$ means that first a twofold rotation is applied to an operand* and then reflection is applied to the new operand. Let us perform these operations on the atomic positions of a sulfuryl chloride molecule as is shown in Figure 4-2a. The same final result is obtained by simply applying the symmetry plane σ_v', as is also shown in Figure 4-2b. Thus

* Shortly, we shall use a wide range of operands related to molecular structure.

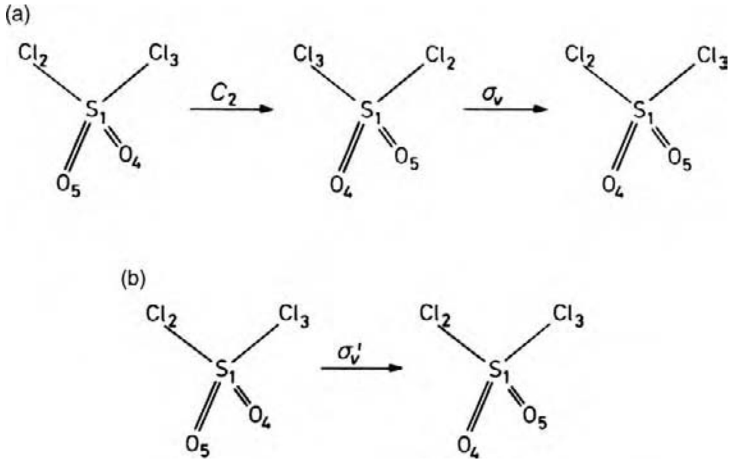

Figure 4-2 (**a**) Consecutive application of two symmetry operations, C_2 and σ_v to the nuclear positions of the SO_2Cl_2 molecule. (**b**) Application of σ_v' to SO_2Cl_2.

$$\sigma_v \cdot C_2 = \sigma_v'$$

The products of the elements in a group are generally not commutative. That means that the result of the consecutive application of the symmetry operations depends on the order in which they are applied. This is why it is so important to read the multiplication sign as "preceded by." Figure 4-3 gives an example for the ammonia molecule, which belongs to the C_{3v} point group. Depending on whether the C_3 operation is applied first and then the σ_v'' or vice versa, the effect is different. There are some groups for which multiplication is commutative, they are called *Abelian groups*. The C_{2v} point group is an example. Thus, in Figure 4-2a we could get the same result first applying the σ_v reflection and then the twofold rotation.

2. *One element in the group must commute with all other elements in the group and leave them unchanged.* This is the *identity element, E*. Thus,

$$E \cdot X = X \cdot E = X$$

3. *The products of the elements in a group are always associative.* That means that if there is a consecutive application of several

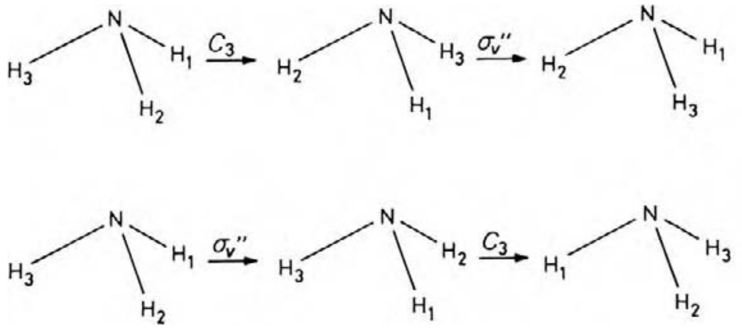

Figure 4-3. Illustration for the non-commutative character of the symmetry operations.

symmetry operations, their application may be grouped in any way without changing the final result as long as the order of the application remains the same. Thus, for example,

$$C_2 \cdot \sigma_v \cdot \sigma_v' = C_2 \cdot (\sigma_v \cdot \sigma_v') = (C_2 \cdot \sigma_v) \cdot \sigma_v'$$

4. *For each element in a group, there is an inverse or reciprocal operation which is also an element of the group* and satisfies the following condition:

$$X \cdot X^{-1} = X^{-1} \cdot X = E$$

For example,

$$C_2 \cdot C_2^{-1} = C_2^{-1} \cdot C_2 = E$$

or

$$\sigma_v \cdot \sigma_v^{-1} = \sigma_v^{-1} \cdot \sigma_v = E$$

The symmetry operation corresponding to an inverse operation can be found in group multiplication tables. These tables contain the products of the elements of a group. An example is shown in Table 4-1, for the C_{2v} point group. Here each element of the group, that is, each

Table 4-1. Group Multiplication Table for the C_{2v} Point Group

C_{2v}	E	C_2	σ_v	σ'_v
E	E	C_2	σ_v	σ'_v
C_2	C_2	E	σ'_v	σ_v
σ_v	σ_v	σ'_v	E	C_2
σ'_v	σ'_v	σ_v	C_2	E

symmetry operation, is listed only once in the initial row at the top and in the initial column at the far left. In forming the product of any two elements, one belonging to the row and the other to the column, the order of the application of the elements is strictly defined. First, the element in the top row is applied, followed by the application of the element in the far left column. The result is found at the intersection of the corresponding column and row. Any one of the results is also a symmetry operation belonging to the C_{2v} point group. In fact, each row and each column in the field of the results is a rearranged list of the initial operations, but no two rows or two columns may be identical. From the C_{2v} multiplication table, it is seen that the inverse operation of C_2 is C_2, since their intersection is E; similarly, the inverse operation of σ_v is σ_v in this group.

The multiplication table of the C_{3v} point group is compiled in Table 4-2. Here,

$$C_3 \cdot C_3 = C_3^2$$

means two successive applications of the threefold rotation. Applying it once yields a 120° rotation, while C_3^2 corresponds to a 240° rotation

Table 4-2. Group Multiplication Table for the C_{3v} Point Group

C_{3v}	E	C_3	C_3^2	σ_v	σ'_v	σ''_v
E	E	C_3	C_3^2	σ_v	σ'_v	σ''_v
C_3	C_3	C_3^2	E	σ''_v	σ_v	σ'_v
C_3^2	C_3^2	E	C_3	σ'_v	σ''_v	σ_v
σ_v	σ_v	σ'_v	σ''_v	E	C_3	C_3^2
σ'_v	σ'_v	σ''_v	σ_v	C_3^2	E	C_3
σ''_v	σ''_v	σ_v	σ'_v	C_3	C_3^2	E

altogether. Accordingly, for example, the meaning of C_5^2 is a rotation by $2 \cdot (360°/5) = 144°$.

The number of elements in a group is called *the order of the group*. Its conventional symbol is h. The group multiplication tables show that $h = 4$ for the C_{2v} point group and $h = 6$ for C_{3v}.

A group may be divided into two kinds of subunit: subgroups and classes. A *subgroup* is a smaller group within a group that still possesses the four fundamental properties of a group. The identity operation, E, is always a subgroup by itself, and it is also a member of all other possible subgroups.

A *class* is a complete set of elements, in our case symmetry operations, of the group that are conjugate to one another (in mathematics they are usually called *conjugacy class*). Elements A and B of a group are *conjugates*, if there is some group element, Z, for which

$$B = Z^{-1} \cdot A \cdot Z$$

Designating a conjugate B to a symmetry operation A is also called a *similarity transformation*. B is a similarity transform of A by Z, or, in other words, A and B are conjugates. Elements belong to one class if they are conjugate to one another. The inverse operation can be applied with the aid of the multiplication table and rule 4 given above,

$$Z^{-1} \cdot Z = Z \cdot Z^{-1} = E$$

To find out what operations belong to the same class within a group, all possible similarity transformations in the group have to be performed. Let us work this out for the C_{3v} point group and begin with the identity operation. Since E commutes with any other elements Z (see under rule 2 above), we have

$$Z^{-1} \cdot E \cdot Z = Z^{-1} \cdot Z \cdot E = E \cdot E = E$$

for all elements in the class. Consequently, E is not conjugate with any other element, and it always forms a class by itself. This is true for all other point groups as well.

Consider now σ_v:

$$E^{-1} \cdot (\sigma_v \cdot E) = E^{-1} \cdot \sigma_v = \sigma_v$$
$$C_3^{-1} \cdot (\sigma_v \cdot C_3) = C_3^{-1} \cdot \sigma_v' = C_3^2 \cdot \sigma_v' = \sigma_v''$$
$$(C_3^2)^{-1} \cdot (\sigma_v \cdot C_3^2) = (C_3^2)^{-1} \cdot \sigma_v'' = C_3 \cdot \sigma_v'' = \sigma_v'$$
$$\sigma_v^{-1} \cdot (\sigma_v \cdot \sigma_v) = \sigma_v^{-1} \cdot E = \sigma_v \cdot E = \sigma_v$$
$$\sigma_v'^{-1} \cdot (\sigma_v \cdot \sigma_v') = \sigma_v'^{-1} \cdot C_3 = \sigma_v' \cdot C_3 = \sigma_v''$$
$$\sigma_v''^{-1} \cdot (\sigma_v \cdot \sigma_v'') = \sigma_v''^{-1} \cdot C_3^2 = \sigma_v'' \cdot C_3^2 = \sigma_v'$$

We have performed all possible similarity transformations for the operation σ_v. As a result, it is seen that the three operations expressing vertical mirror symmetry belong to the same class. We could reach the same conclusion by similarity transformations on either of the other two σ_v operations.

Next let us examine C_3:

$$E^{-1} \cdot (C_3 \cdot E) = E^{-1} \cdot C_3 = E \cdot C_3 = C_3$$
$$C_3^{-1} \cdot (C_3 \cdot C_3) = C_3^{-1} \cdot C_3^2 = C_3^2 \cdot C_3^2 = C_3$$
$$(C_3^2)^{-1} \cdot (C_3 \cdot C_3^2) = (C_3^2)^{-1} \cdot E = C_3 \cdot E = C_3$$
$$\sigma_v^{-1} \cdot (C_3 \cdot \sigma_v) = \sigma_v^{-1} \cdot \sigma_v'' = \sigma_v \cdot \sigma_v'' = C_3^2$$
$$\sigma_v'^{-1} \cdot (C_3 \cdot \sigma_v') = \sigma_v'^{-1} \cdot \sigma_v = \sigma_v' \cdot \sigma_v = C_3^2$$
$$\sigma_v''^{-1} \cdot (C_3 \cdot \sigma_v'') = \sigma_v''^{-1} \cdot \sigma_v' = \sigma_v'' \cdot \sigma_v' = C_3^2$$

According to these transformations, C_3 and C_3^2 are conjugates and thus belong to the same class.

The *order of a class* is defined as the number of elements in the class. For example, the order of the class of the reflection operations in C_{3v} is 3, and the order of the class of the rotation operations is 2. The order of a class, or a subgroup, is an integral divisor of the order of the group.

The mathematical handling of the symmetry operations is done by means of matrices.

4.2. Matrices

A matrix is a rectangular array of numbers, or symbols for numbers. These elements are put between square brackets. A numerical example of a matrix is shown here:

$$\begin{bmatrix} 3 & 1 & 0 & 2 \\ 5 & 7 & 0 & -3 \\ 0 & 0 & -2 & 1 \end{bmatrix}$$

Generally a matrix has *m* rows and *n* columns:

$$\begin{bmatrix} a_{11} & a_{12} & \cdots & a_{1n} \\ a_{21} & a_{22} & \cdots & a_{2n} \\ \cdot & & & \cdot \\ \cdot & & & \cdot \\ \cdot & & & \cdot \\ a_{m1} & a_{m2} & \cdots & a_{mn} \end{bmatrix}$$

The above matrix may be represented by a capital letter *A*. Another notation is $[a_{ij}]$. The symbol a_{ij} represents the matrix element standing in the *i*th row and the *j*th column. The number of rows is *m*, and the number of columns is *n*, and $1 \le i \le m$ and $1 \le j \le n$.

There are some special matrices important for our discussion. A *square matrix* has equal numbers of rows and columns. According to the general notation, a matrix $[a_{ij}]$ is a square matrix if $m = n$. The *dimension* of a square matrix is the number of its rows or columns.

A special square matrix is the *unit matrix*, in which all elements along the top-left-to-bottom-right diagonal are 1 and all the other elements are zero. The short notation for a unit matrix is *E*. Some unit matrices are presented here:

$$\begin{bmatrix} 1 & 0 \\ 0 & 1 \end{bmatrix} \quad \begin{bmatrix} 1 & 0 & 0 \\ 0 & 1 & 0 \\ 0 & 0 & 1 \end{bmatrix} \quad \begin{bmatrix} 1 & 0 & 0 & 0 & 0 \\ 0 & 1 & 0 & 0 & 0 \\ 0 & 0 & 1 & 0 & 0 \\ 0 & 0 & 0 & 1 & 0 \\ 0 & 0 & 0 & 0 & 1 \end{bmatrix}$$

A *column matrix* consists of only one column. Column matrices are used to represent vectors. A *vector* is characterized by its length and direction. A vector in three-dimensional space is shown in Figure 4-4. If one end of the vector is at the origin of the Cartesian coordinate system, then the three coordinates of its other end fully describe the vector. These three Cartesian coordinates can be written as a column matrix:

$$\begin{bmatrix} x_1 \\ y_1 \\ z_1 \end{bmatrix}$$

Thus, this column matrix represents the vector.

While column matrices are used to represent vectors, square matrices are used to *represent symmetry operations.* Performing a symmetry operation on a vector is actually a geometrical transformation. How can these geometrical transformations be translated into matrix "language"? Consider a specific example and see how the symmetry operations of the C_s symmetry group can be applied to the vector of Figure 4-4. For a matrix representation, we first write (or usually just imagine) the coordinates of the original vector in the top

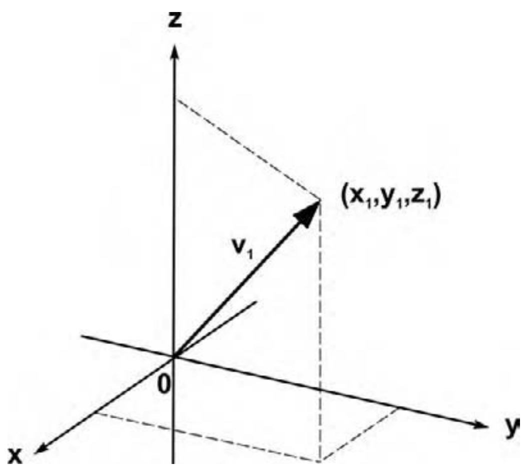

Figure 4-4. Representation of a vector in three-dimensional space.

row and the coordinates of the vector resulting from the symmetry operation in the left-hand column:

$$\begin{array}{rr} & \begin{matrix} x_1 & y_1 & z_1 \end{matrix} \quad \leftarrow \text{original vector} \\ \text{resultant vector} \quad \begin{matrix} x_1' \\ y_1' \\ z_1' \end{matrix} & \begin{bmatrix} & & \\ & & \\ & & \end{bmatrix} \end{array}$$

Then we examine the effect of the symmetry operation in detail. If a coordinate is transformed into itself, 1 is placed into the intersection position, and if it is transformed into its negative self, –1 is put into the intersection. Both these positions will be *along* the diagonal of the matrix. If a coordinate is transformed into another coordinate or into the negative of this other coordinate, 1 or –1 is placed into the intersection position, respectively. These intersection positions will be *off* the matrix diagonal.

There are two symmetry operations in the C_s point group, E and σ_h. The identity operation, E, does not change the position of the vector so it can be represented by a unit matrix.

$$\begin{bmatrix} 1 & 0 & 0 \\ 0 & 1 & 0 \\ 0 & 0 & 1 \end{bmatrix} \cdot \begin{bmatrix} x_1 \\ y_1 \\ z_1 \end{bmatrix} = \begin{bmatrix} x_1 \\ y_1 \\ z_1 \end{bmatrix}$$

Accordingly,

$$E \cdot \mathbf{v}_1 = \mathbf{v}_1$$

If the matrix elements are a_{ij} and the vector components are b_j, then the components of the product vector c_i are given by

$$c_i = \sum_j a_{ij} \cdot b_j .$$

To get the first member of the resulting matrix, all the elements of the first row of the square matrix are multiplied by the consecutive members of the column matrix and then added together. To get the

second member, the same procedure is followed with the second row of the square matrix, and so on, as shown below:

$$\begin{bmatrix} 1 & 0 & 0 \\ 0 & 1 & 0 \\ 0 & 0 & 1 \end{bmatrix} \cdot \begin{bmatrix} x_1 \\ y_1 \\ z_1 \end{bmatrix} = \begin{bmatrix} 1 \cdot x_1 + 0 \cdot y_1 + 0 \cdot z_1 \\ 0 \cdot x_1 + 1 \cdot y_1 + 0 \cdot z_1 \\ 0 \cdot x_1 + 0 \cdot y_1 + 1 \cdot z_1 \end{bmatrix} = \begin{bmatrix} x_1 \\ y_1 \\ z_1 \end{bmatrix}$$

The other symmetry operation of the C_s point group is the horizontal reflection (see Figure 4-5). In matrix language this operation can be written as follows:

$$\begin{array}{c} \\ x_1' \\ y_1' \\ z_1' \end{array} \begin{array}{c} \begin{array}{ccc} x_1 & y_1 & z_1 \end{array} \\ \begin{bmatrix} 1 & 0 & 0 \\ 0 & 1 & 0 \\ 0 & 0 & -1 \end{bmatrix} \end{array} \cdot \begin{bmatrix} x_1 \\ y_1 \\ z_1 \end{bmatrix} = \begin{bmatrix} 1 \cdot x_1 + 0 \cdot y_1 + 0 \cdot z_1 \\ 0 \cdot x_1 + 1 \cdot y_1 + 0 \cdot z_1 \\ 0 \cdot x_1 + 0 \cdot y_1 + (-1) \cdot z_1 \end{bmatrix} = \begin{bmatrix} x_1 \\ y_1 \\ -z_1 \end{bmatrix}$$

$$E \cdot \mathbf{v}_1 = \mathbf{v}_2$$

It often happens that the coordinates are not transformed simply into each other by a symmetry operation. Trigonometric relations must be used to express, for instance, the consequences of three-fold rotation.

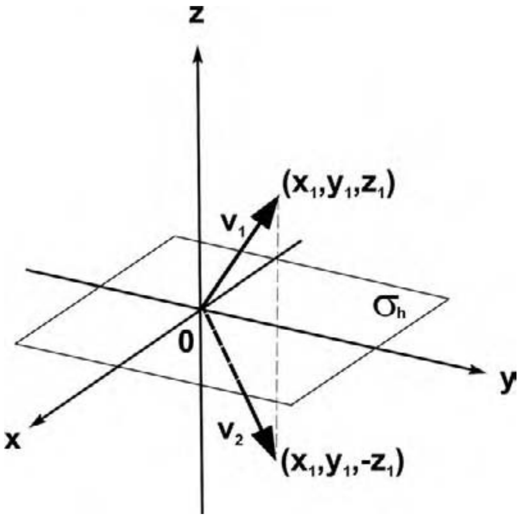

Figure 4-5. Reflection of a vector by a horizontal mirror plane.

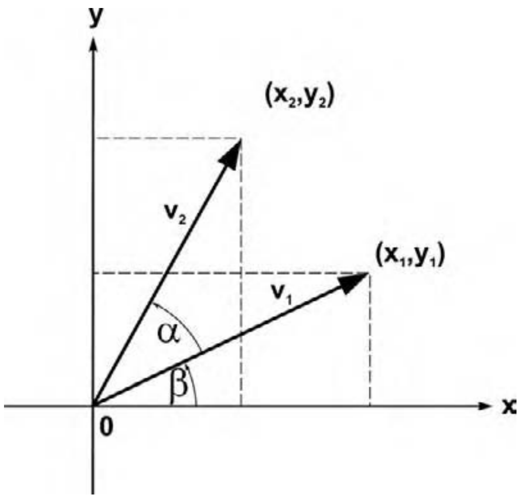

Figure 4-6. Rotation of a vector by an angle α in the *xy* plane.

Figure 4-6 illustrates a vector rotated by an angle α in the *xy* plane. The coordinates of the rotated vector are related to the coordinates of the original vector in the following way (r is the length of the vector, β is an auxiliary angle shown in Figure 4-6, and the rotation is anticlockwise):

$$x_1 = r \cdot \cos\beta \qquad \text{and} \quad y_1 = r \cdot \sin\beta \tag{4-1}$$

$$x_2 = r \cdot \cos(\alpha + \beta) \quad \text{and} \qquad y_2 = r \cdot \sin(\alpha + \beta) \tag{4-2}$$

Utilizing the trigonometric expressions:

$$\cos(\alpha + \beta) = \cos\alpha \cdot \cos\beta - \sin\alpha \cdot \sin\beta \tag{4-3a}$$

$$\sin(\alpha + \beta) = \sin\alpha \cdot \cos\beta + \cos\alpha \cdot \sin\beta \tag{4-3b}$$

and substituting Eqs. (4-3) and (4-1) into Eq. (4-2), we get:

$$x_2 = r \cdot \cos\alpha \cdot \cos\beta - r \cdot \sin\alpha \cdot \sin\beta = x_1 \cdot \cos\alpha - y_1 \cdot \sin\alpha \tag{4-4a}$$

$$y_2 = r \cdot \sin\alpha \cdot \cos\beta + r \cdot \cos\alpha \cdot \sin\beta = x_1 \cdot \sin\alpha + y_1 \cdot \cos\alpha \tag{4-4b}$$

The same equations in matrix formulation:

$$\begin{bmatrix} \cos\alpha & -\sin\alpha \\ \sin\alpha & \cos\alpha \end{bmatrix} \cdot \begin{bmatrix} x_1 \\ y_1 \end{bmatrix} = \begin{bmatrix} x_2 \\ y_2 \end{bmatrix}$$

The square matrix above is the matrix representation of a rotation through an angle α.

Since matrices can be used to represent symmetry operations, the set of matrices representing all symmetry operations of a point group will be a representation of that group. Moreover, if a set of matrices forms a representation of a symmetry group, it will obey all the rules of a mathematical group. It will also obey the group multiplication table. Let the SO_2Cl_2 molecule serve as an example again. This molecule belongs to the C_{2v} point group and some of its symmetry operations have already been illustrated in Figure 4-2.

There are four operations in the C_{2v} point group. The identity operation, E, leaves the molecule unchanged, so we can imagine that the corresponding matrix will be a 5×5 unit matrix.

The twofold rotation (C_2) changes the positions of the two chlorine atoms and also the positions of the two oxygen atoms. The sulfur atom remains in place. To construct the corresponding matrices the same procedure can be applied as used before with a vector. The original nuclear positions of the molecule can be written (or just imagined) at the top row and the nuclear positions resulting from the symmetry operation at the far left column. Thus the C_2 operation will lead to the following result:

$$\begin{bmatrix} 1 & 0 & 0 & 0 & 0 \\ 0 & 0 & 1 & 0 & 0 \\ 0 & 1 & 0 & 0 & 0 \\ 0 & 0 & 0 & 0 & 1 \\ 0 & 0 & 0 & 1 & 0 \end{bmatrix} \cdot \begin{bmatrix} S_1 \\ Cl_2 \\ Cl_3 \\ O_4 \\ O_5 \end{bmatrix} = \begin{bmatrix} S_1 \\ Cl_3 \\ Cl_2 \\ O_5 \\ O_4 \end{bmatrix}$$

σ_v changes the positions of the two chlorines and leaves the other three atoms in place:

$$\begin{bmatrix} 1 & 0 & 0 & 0 & 0 \\ 0 & 0 & 1 & 0 & 0 \\ 0 & 1 & 0 & 0 & 0 \\ 0 & 0 & 0 & 1 & 0 \\ 0 & 0 & 0 & 0 & 1 \end{bmatrix} \cdot \begin{bmatrix} S_1 \\ Cl_2 \\ Cl_3 \\ O_4 \\ O_5 \end{bmatrix} = \begin{bmatrix} S_1 \\ Cl_3 \\ Cl_2 \\ O_4 \\ O_5 \end{bmatrix}$$

Finally, σ_v' changes the positions of the two oxygen atoms, and leaves the sulfur and the two chlorines in their original positions:

$$\begin{bmatrix} 1 & 0 & 0 & 0 & 0 \\ 0 & 1 & 0 & 0 & 0 \\ 0 & 0 & 1 & 0 & 0 \\ 0 & 0 & 0 & 0 & 1 \\ 0 & 0 & 0 & 1 & 0 \end{bmatrix} \cdot \begin{bmatrix} S_1 \\ Cl_2 \\ Cl_3 \\ O_4 \\ O_5 \end{bmatrix} = \begin{bmatrix} S_1 \\ Cl_2 \\ Cl_3 \\ O_5 \\ O_4 \end{bmatrix}$$

Since each of these four 5×5 matrices represent one of the symmetry operations of the C_{2v} point group, the set of these four 5×5 matrices will be a representation of this group. They will also obey the C_{2v} multiplication table. As was shown in Figure 4-2,

$$\sigma_v \cdot C_2 = \sigma_v'$$

The corresponding matrix representations are the following:

$$\underset{\sigma_v}{\begin{bmatrix} 1 & 0 & 0 & 0 & 0 \\ 0 & 0 & 1 & 0 & 0 \\ 0 & 1 & 0 & 0 & 0 \\ 0 & 0 & 0 & 1 & 0 \\ 0 & 0 & 0 & 0 & 1 \end{bmatrix}} \cdot \underset{C_2}{\begin{bmatrix} 1 & 0 & 0 & 0 & 0 \\ 0 & 0 & 1 & 0 & 0 \\ 0 & 1 & 0 & 0 & 0 \\ 0 & 0 & 0 & 0 & 1 \\ 0 & 0 & 0 & 1 & 0 \end{bmatrix}} =$$

$$\begin{bmatrix} 1\cdot1+0\cdot0+0\cdot0+0\cdot0+0\cdot0 & 1\cdot0+0\cdot0+0\cdot1+0\cdot0+0\cdot0\ldots \\ 0\cdot1+0\cdot0+1\cdot0+0\cdot0+0\cdot0 & 0\cdot0+0\cdot0+1\cdot1+0\cdot0+0\cdot0\ldots \\ 0\cdot1+1\cdot0+0\cdot0+0\cdot0+0\cdot0 & 0\cdot0+1\cdot0+0\cdot1+0\cdot0+0\cdot0\ldots \\ 0\cdot1+0\cdot0+0\cdot0+1\cdot0+0\cdot0 & 0\cdot0+0\cdot0+0\cdot1+1\cdot0+0\cdot0\ldots \\ 0\cdot1+0\cdot0+0\cdot0+0\cdot0+1\cdot0 & 0\cdot0+0\cdot0+0\cdot1+0\cdot0+1\cdot0\ldots \end{bmatrix} =$$

$$\underset{\sigma_v'}{\begin{bmatrix} 1 & 0 & 0 & 0 & 0 \\ 0 & 1 & 0 & 0 & 0 \\ 0 & 0 & 1 & 0 & 0 \\ 0 & 0 & 0 & 0 & 1 \\ 0 & 0 & 0 & 1 & 0 \end{bmatrix}}$$

The multiplication is shown here in detail only for the first two columns of the resulting matrix. The elements of the product matrix are given by:

$$c_{ik} = \sum_j a_{ij} \cdot b_{jk}$$

To get the first member of the first row, all elements of the first row of the first matrix are multiplied by the corresponding elements of the first column of the second matrix and the results are added. To get the second member of the first row, all elements of the first row of the first matrix are multiplied by the corresponding members of the second column of the second matrix and the results are added, and so on. To get the second-row members, the same procedure is repeated with the second-row members of the first matrix, and so on. It is also possible to visualize the second matrix as a series of column matrices and then consider the multiplication of each of these column matrices, one by one, by the first matrix.

4.3. Representation of Groups

Any collection of quantities (or symbols) which obey the multiplication table of a group is a *representation* of that group. These quantities are the matrices in our examples showing how certain characteristics of a molecule behave under the symmetry operations of the group. The symmetry operations may be applied to various characteristics or descriptions of the molecule. The particular description to which the symmetry operations are applied forms the *basis* for a representation of the group. Generally speaking, any set of algebraic functions or vectors may be the basis for a representation of a group. Our choice of a suitable basis depends on the particular problem we are studying. After choosing the basis set, the task is to construct the matrices which transform the basis or its components according to each symmetry operation. The most common basis sets in chemical applications are summarized in Section 4.11. Some of them will be used in the following discussion.

Let us now work out the representation of a point group for a very simple basis. We will choose just the *changes*, Δr_1 and Δr_2, of the two N–H bond lengths of the diimide molecule, N_2H_2 (**4-1**).

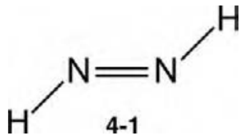

4-1

These two vectors may be used in the description of the stretching vibrations of the molecule. The molecular symmetry is C_{2h}. Figure 4-7 helps to visualize the effects of the symmetry operations of this group on the selected basis. There are four symmetry operations in the C_{2h} point group, E, C_2, i, and σ_h. E leaves the basis unchanged, so the corresponding matrix representation is a unit matrix:

$$E \cdot \begin{bmatrix} \Delta r_1 \\ \Delta r_2 \end{bmatrix} = \begin{bmatrix} 1 & 0 \\ 0 & 1 \end{bmatrix} \cdot \begin{bmatrix} \Delta r_1 \\ \Delta r_2 \end{bmatrix} = \begin{bmatrix} \Delta r_1 \\ \Delta r_2 \end{bmatrix}$$

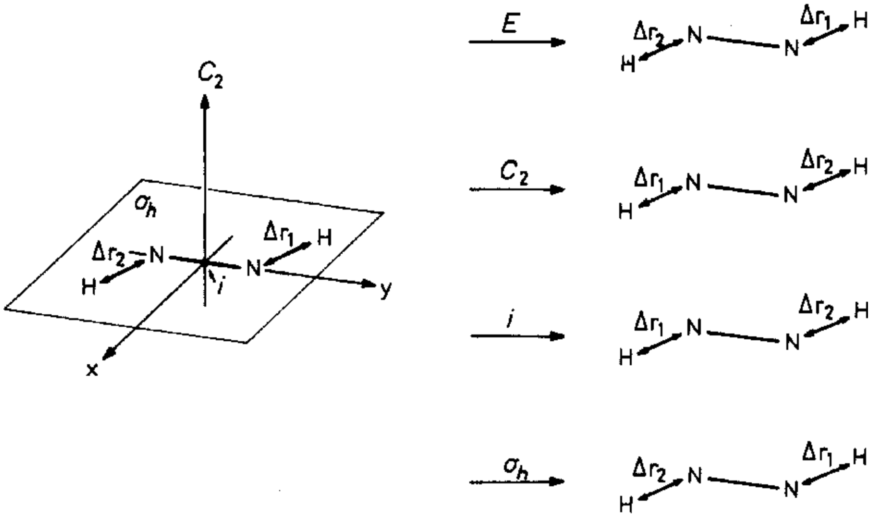

Figure 4-7. The four symmetry operations of the C_{2h} point group applied to the two N–H bond length changes of the HNNH molecule.

Both C_2 and i interchange the two vectors, Δr_1 "goes into" Δr_2 and vice versa;

$$C_2 \cdot \begin{bmatrix} \Delta r_1 \\ \Delta r_2 \end{bmatrix} = \begin{bmatrix} 0 & 1 \\ 1 & 0 \end{bmatrix} \cdot \begin{bmatrix} \Delta r_1 \\ \Delta r_2 \end{bmatrix} = \begin{bmatrix} \Delta r_2 \\ \Delta r_1 \end{bmatrix}$$

$$i \cdot \begin{bmatrix} \Delta r_1 \\ \Delta r_2 \end{bmatrix} = \begin{bmatrix} 0 & 1 \\ 1 & 0 \end{bmatrix} \cdot \begin{bmatrix} \Delta r_1 \\ \Delta r_2 \end{bmatrix} = \begin{bmatrix} \Delta r_2 \\ \Delta r_1 \end{bmatrix}$$

finally, σ_h leaves the molecule unchanged:

$$\sigma_h \cdot \begin{bmatrix} \Delta r_1 \\ \Delta r_2 \end{bmatrix} = \begin{bmatrix} 1 & 0 \\ 0 & 1 \end{bmatrix} \cdot \begin{bmatrix} \Delta r_1 \\ \Delta r_2 \end{bmatrix} = \begin{bmatrix} \Delta r_1 \\ \Delta r_2 \end{bmatrix}$$

With this basis the representation consists of four 2×2 matrices.

Let us take now a more complicated basis, and consider all the nuclear coordinates of HNNH shown in Figure 4-8a. These are the so-called Cartesian displacement vectors and will be discussed in Chapter 5 on molecular vibrations. Let us find the matrix representation of the σ_h operation (see Figure 4-8b). The horizontal mirror plane leaves all x and y coordinates unchanged while all z coordinates will "go" into their negative selves. In matrix notation this is expressed in the following way:

$$\sigma_h \cdot \begin{bmatrix} x_1 \\ y_1 \\ z_1 \\ x_2 \\ y_2 \\ z_2 \\ x_3 \\ y_3 \\ z_3 \\ x_4 \\ y_4 \\ z_4 \end{bmatrix} = \begin{bmatrix} 1 & 0 & 0 & 0 & 0 & 0 & 0 & 0 & 0 & 0 & 0 & 0 \\ 0 & 1 & 0 & 0 & 0 & 0 & 0 & 0 & 0 & 0 & 0 & 0 \\ 0 & 0 & -1 & 0 & 0 & 0 & 0 & 0 & 0 & 0 & 0 & 0 \\ 0 & 0 & 0 & 1 & 0 & 0 & 0 & 0 & 0 & 0 & 0 & 0 \\ 0 & 0 & 0 & 0 & 1 & 0 & 0 & 0 & 0 & 0 & 0 & 0 \\ 0 & 0 & 0 & 0 & 0 & -1 & 0 & 0 & 0 & 0 & 0 & 0 \\ 0 & 0 & 0 & 0 & 0 & 0 & 1 & 0 & 0 & 0 & 0 & 0 \\ 0 & 0 & 0 & 0 & 0 & 0 & 0 & 1 & 0 & 0 & 0 & 0 \\ 0 & 0 & 0 & 0 & 0 & 0 & 0 & 0 & -1 & 0 & 0 & 0 \\ 0 & 0 & 0 & 0 & 0 & 0 & 0 & 0 & 0 & 1 & 0 & 0 \\ 0 & 0 & 0 & 0 & 0 & 0 & 0 & 0 & 0 & 0 & 1 & 0 \\ 0 & 0 & 0 & 0 & 0 & 0 & 0 & 0 & 0 & 0 & 0 & -1 \end{bmatrix} \cdot \begin{bmatrix} x_1 \\ y_1 \\ z_1 \\ x_2 \\ y_2 \\ z_2 \\ x_3 \\ y_3 \\ z_3 \\ x_4 \\ y_4 \\ z_4 \end{bmatrix} = \begin{bmatrix} x_1 \\ y_1 \\ -z_1 \\ x_2 \\ y_2 \\ -z_2 \\ x_3 \\ y_3 \\ -z_3 \\ x_4 \\ y_4 \\ -z_4 \end{bmatrix}$$

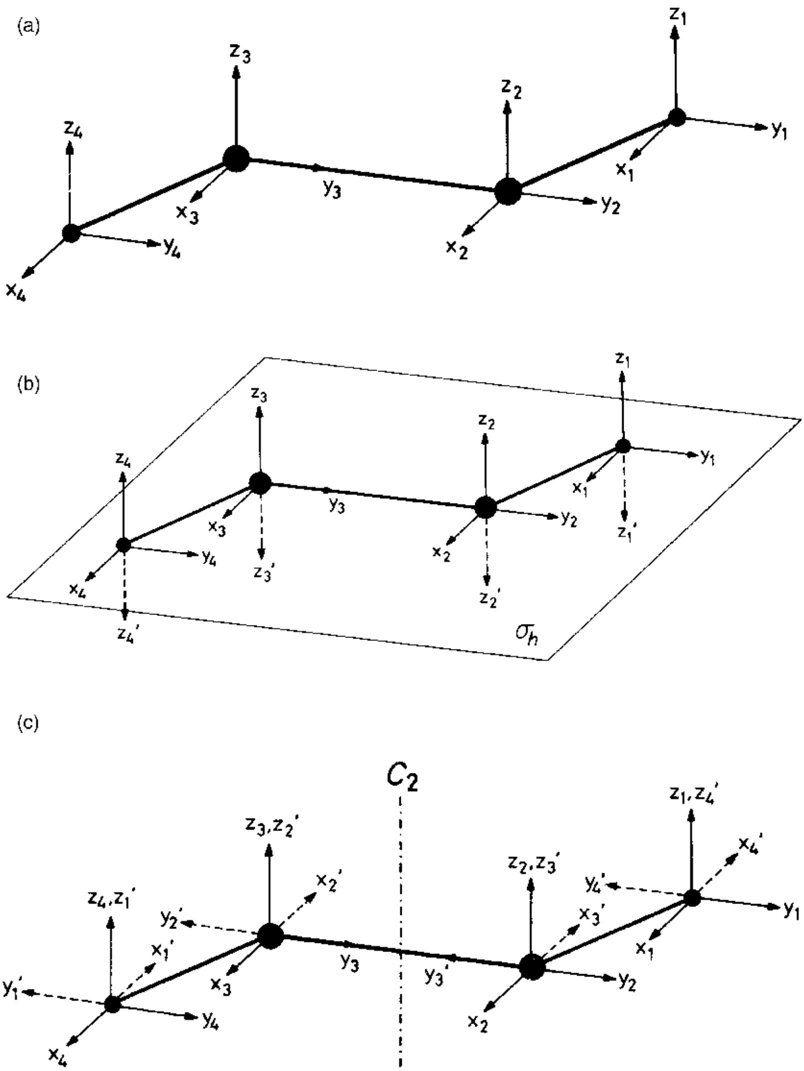

Figure 4-8. (**a**) Cartesian coordinates as basis for a representation; (**b**) Effect of σ_h; (**c**) Effect of C_2.

Take one more operation, the C_2 rotation (Figure 4-8c). This operation introduces the following changes:

$$x_1, y_1, \text{ and } z_1 \text{ to } -x_4, -y_4, \text{ and } z_4,$$
$$x_2, y_2, \text{ and } z_2 \text{ to } -x_3, -y_3, \text{ and } z_3,$$
$$x_3, y_3, \text{ and } z_3 \text{ to } -x_2, -y_2, \text{ and } z_2,$$
$$x_4, y_4, \text{ and } z_4 \text{ to } -x_1, -y_1, \text{ and } z_1.$$

In matrix notation:

$$
C_2 \cdot \begin{bmatrix} x_1 \\ y_1 \\ z_1 \\ x_2 \\ y_2 \\ z_2 \\ x_3 \\ y_3 \\ z_3 \\ x_4 \\ y_4 \\ z_4 \end{bmatrix} = \begin{bmatrix} 0 & 0 & 0 & 0 & 0 & 0 & 0 & 0 & 0 & -1 & 0 & 0 \\ 0 & 0 & 0 & 0 & 0 & 0 & 0 & 0 & 0 & 0 & -1 & 0 \\ 0 & 0 & 0 & 0 & 0 & 0 & 0 & 0 & 0 & 0 & 0 & 1 \\ 0 & 0 & 0 & 0 & 0 & 0 & -1 & 0 & 0 & 0 & 0 & 0 \\ 0 & 0 & 0 & 0 & 0 & 0 & 0 & -1 & 0 & 0 & 0 & 0 \\ 0 & 0 & 0 & 0 & 0 & 0 & 0 & 0 & 1 & 0 & 0 & 0 \\ 0 & 0 & 0 & -1 & 0 & 0 & 1 & 0 & 0 & 0 & 0 & 0 \\ 0 & 0 & 0 & 0 & -1 & 0 & 0 & 1 & 0 & 0 & 0 & 0 \\ 0 & 0 & 0 & 0 & 0 & 1 & 0 & 0 & 0 & 0 & 0 & 0 \\ -1 & 0 & 0 & 0 & 0 & 0 & 0 & 0 & 0 & 0 & 0 & 0 \\ 0 & -1 & 0 & 0 & 0 & 0 & 0 & 0 & 0 & 0 & 0 & 0 \\ 0 & 0 & 1 & 0 & 0 & 0 & 0 & 0 & 0 & 0 & 0 & 0 \end{bmatrix} \cdot \begin{bmatrix} x_1 \\ y_1 \\ z_1 \\ x_2 \\ y_2 \\ z_2 \\ x_3 \\ y_3 \\ z_3 \\ x_4 \\ y_4 \\ z_4 \end{bmatrix} = \begin{bmatrix} -x_4 \\ -y_4 \\ z_4 \\ -x_3 \\ -y_3 \\ z_3 \\ -x_2 \\ -y_2 \\ z_2 \\ -x_1 \\ -y_1 \\ z_1 \end{bmatrix}
$$

Considering all four symmetry operations of the C_{2h} point group, the complete representation of the displacement coordinates of HNNH as basis consists of four 12×12 matrices. Working with such big matrices is awkward and time-consuming. Fortunately, they can be simplifed. We shall not go into the details of how this is done since only the easiest and quickest methods utilizing matrix representations will be used in the next chapters. We shall merely outline the procedure leading from the big unpleasant representations of symmetry operations to simpler tools [12]. With the help of suitable similarity transformations, matrices can be turned into so-called *block-diagonal matrices*. A block-diagonal matrix has nonzero values only in square blocks along the diagonal from the top left to the bottom right. The merits of block-diagonal matrices are best illustrated in their multiplication. Suppose, for example, that two 5×5 matrices are to be multiplied, as follows:

$$
\begin{bmatrix} 2 & 3 & 0 & 0 & 0 \\ 1 & 2 & 0 & 0 & 0 \\ 0 & 0 & 1 & 1 & 0 \\ 0 & 0 & 1 & 1 & 0 \\ 0 & 0 & 0 & 0 & 2 \end{bmatrix} \cdot \begin{bmatrix} 1 & 2 & 0 & 0 & 0 \\ 2 & 1 & 0 & 0 & 0 \\ 0 & 0 & 2 & 2 & 0 \\ 0 & 0 & 1 & 2 & 0 \\ 0 & 0 & 0 & 0 & 1 \end{bmatrix} = \begin{bmatrix} 8 & 7 & 0 & 0 & 0 \\ 5 & 4 & 0 & 0 & 0 \\ 0 & 0 & 3 & 4 & 0 \\ 0 & 0 & 3 & 4 & 0 \\ 0 & 0 & 0 & 0 & 2 \end{bmatrix}
$$

The determination of the first row is already quite complicated:

$$\begin{aligned}
2 \cdot 1 + 3 \cdot 2 + 0 \cdot 0 + 0 \cdot 0 + 0 \cdot 0 &= 8 \\
2 \cdot 2 + 3 \cdot 1 + 0 \cdot 0 + 0 \cdot 0 + 0 \cdot 0 &= 7 \\
2 \cdot 0 + 3 \cdot 0 + 0 \cdot 2 + 0 \cdot 1 + 0 \cdot 0 &= 0 \\
2 \cdot 0 + 3 \cdot 0 + 0 \cdot 2 + 0 \cdot 2 + 0 \cdot 0 &= 0 \\
2 \cdot 0 + 3 \cdot 0 + 0 \cdot 0 + 0 \cdot 0 + 0 \cdot 1 &= 0
\end{aligned}$$

Notice that the product of two equally block-diagonalized matrices—such as those two above—is another similarly block-diagonalized matrix. It is especially important that this resulting matrix can be obtained simply by multiplying the corresponding individual blocks of the original matrices. Check this on the above example:

$$\begin{bmatrix} 2 & 3 \\ 1 & 2 \end{bmatrix} \cdot \begin{bmatrix} 1 & 2 \\ 2 & 1 \end{bmatrix} = \begin{bmatrix} 2 \cdot 1 + 3 \cdot 2 & 2 \cdot 2 + 3 \cdot 1 \\ 1 \cdot 1 + 2 \cdot 2 & 1 \cdot 2 + 2 \cdot 1 \end{bmatrix} = \begin{bmatrix} 8 & 7 \\ 5 & 1 \end{bmatrix}$$

$$\begin{bmatrix} 1 & 1 \\ 1 & 1 \end{bmatrix} \cdot \begin{bmatrix} 2 & 2 \\ 1 & 2 \end{bmatrix} = \begin{bmatrix} 1 \cdot 2 + 1 \cdot 1 & 1 \cdot 2 + 1 \cdot 2 \\ 1 \cdot 2 + 1 \cdot 1 & 1 \cdot 2 + 1 \cdot 2 \end{bmatrix} = \begin{bmatrix} 3 & 4 \\ 3 & 4 \end{bmatrix}$$

$$[2] \cdot [1] = [2]$$

Generally, if two matrices A and B can be transformed by similarity transformation into identically shaped block-diagonalized matrices, their product matrix C will also have the same block-diagonal form:

$$\left[\begin{array}{c:c:c} A_1 & & \\ \hdashline & A_2 & \\ \hdashline & & A_3 \end{array}\right] \cdot \left[\begin{array}{c:c:c} B_1 & & \\ \hdashline & B_2 & \\ \hdashline & & B_3 \end{array}\right] = \left[\begin{array}{c:c:c} C_1 & & \\ \hdashline & C_2 & \\ \hdashline & & C_3 \end{array}\right]$$

The multiplication will also be valid for the individual blocks:

$$\begin{aligned}
A_1 \cdot B_1 &= C_1 \\
A_2 \cdot B_2 &= C_2 \\
A_3 \cdot B_3 &= C_3
\end{aligned}$$

Since the blocks themselves will obey the same multiplication table that the big matrices do, each block will be a new representation for an

operation of the group. Thus, if the above A and B matrices are representations for the respective symmetry operations σ_v and σ'_v in the C_{2v} point group, so will be the matrices A_1, A_2, and A_3 and B_1, B_2, and B_3, respectively. The C_{2v} multiplication table (Table 4-1) shows that

$$\sigma_v \cdot \sigma'_v = C_2$$

and, accordingly, not only the big C matrix but also the small matrices C_1, C_2, and C_3, will be representations of the C_2 operation. This way the big matrices *reduce* into smaller ones which are more convenient to handle. Let us suppose that the above big matrices A, B, and C together with the E matrix constitute a representation for the C_{2v} point group. This is called then a *reducible representation* of the group, indicating that it is possible to find a similarity transformation that reduces all its matrices into new ones with smaller dimension. If this is repeated until it is no longer possible to find a similarity transformation to reduce simultaneously all the matrices of a representation into smaller ones, we call this representation *irreducible*. Suppose now that in the example above the small matrices along the diagonals of the big ones cannot be reduced further by a similarity transformation. In this case each set of the small matrices will be an irreducible representation of the C_{2v} point group. The set of A_1, B_1, C_1, and E_1 will be an irreducible representation, so will be the set of A_2, B_2, C_2, and E_2, and yet another irreducible representation will be the set of A_3, B_3, C_3, and E_3. Thus, the reducible representation was reduced to three irreducible representations. Since the symmetry operations can be applied to all kinds of bases for a molecule, there may be countless numbers of reducible representations. The important thing is that all these representations reduce into a *small and finite number* of irreducible representations for practically all point groups. These irreducible representations, often called *symmetry species*, are then used in many areas of chemistry to describe symmetry properties.

4.4. The Character of a Representation

Considering the sizes of the initial matrices, using irreducible representations is a great improvement. Fortunately, even further simplification is possible. Instead of working with irreducible representations

we can use simply their *characters*. The utility of this approach will be amply demonstrated later. The *character*[*] *of a matrix* is the sum of its diagonal elements. For the following matrix

$$\begin{bmatrix} 1 & 2 & 0 & 3 \\ 0 & 7 & 1 & 1 \\ 1 & 2 & 0 & 0 \\ 1 & -2 & 3 & -4 \end{bmatrix}$$

the character is:

$$1 + 7 + 0 + (-4) = 4$$

Since a representation—reducible or irreducible—is a set of matrices corresponding to all symmetry operations of a group, the representation can be described by the set of characters of all these matrices. For the simple basis of Δr_1 and Δr_2 used before for the HNNH molecule in the C_{2h} point group, the representation consisted of four 2×2 matrices:

characters

$$E = \begin{bmatrix} 1 & 0 \\ 0 & 1 \end{bmatrix} \qquad 1 + 1 = 2$$

$$C_2 = \begin{bmatrix} 0 & 1 \\ 1 & 0 \end{bmatrix} \qquad 0 + 0 = 0$$

$$i = \begin{bmatrix} 0 & 1 \\ 1 & 0 \end{bmatrix} \qquad 0 + 0 = 0$$

$$\sigma_h = \begin{bmatrix} 1 & 0 \\ 0 & 1 \end{bmatrix} \qquad 1 + 1 = 2$$

Thus, the characters of this representation are

$$2 \qquad 0 \qquad 0 \qquad 2$$

[*] In linear algebra this is usually called *trace*.

We do not know yet, however, whether this representation is reducible or irreducible. To answer this question, first we have to know the characters of the irreducible representations of the C_{2h} point group.

4.5. Character Tables and Properties of Irreducible Representations

The characters of irreducible representations are collected in so-called *character tables*. We shall not discuss here how to find the characters of a given irreducible representation. The character tables are always available in textbooks and handbooks, or on the Internet, and some of them are also given in the subsequent chapters of this book. Table 4-3 shows the character table for the C_{2h} point group. The top row contains the complete set of symmetry operations of this group. The left column shows, for the time being, some temporary names. Γ is the generally used label for the representations. The main body of the character table contains the characters themselves. Thus, each row constitutes the characters of an irreducible representation, and the number of rows gives us the number of irreducible representations of the particular point group. The irreducible representations have some important and useful properties:

1. *The sum of the squares of the dimensions of all irreducible representations in a group is equal to the order of the group.* The dimension of an irreducible representation is simply the dimension of any of its matrices, which is the number of rows or columns of the matrix. Since the identity operation always leaves the molecules unchanged, its representation is a unit matrix. The character of a unit matrix is equal to the number of rows or columns of that matrix, as is demonstrated on the next page:

Table 4-3. A Preliminary Character Table for the C_{2h} Point Group

C_{2h}	E	C_2	i	σ_h
Γ_1	1	1	1	1
Γ_2	1	−1	1	−1
Γ_3	1	1	−1	−1
Γ_4	1	−1	−1	1

$$E = \begin{bmatrix} 1 & 0 & 0 \\ 0 & 1 & 0 \\ 0 & 0 & 1 \end{bmatrix} \quad \text{character} = 1 + 1 + 1 = 3$$

$$E = \begin{bmatrix} 1 & 0 \\ 0 & 1 \end{bmatrix} \quad \text{character} = 1 + 1 = 2$$

$$E = [1] \quad \text{character} = 1$$

From this it follows that the *character under E is always the dimension of the given irreducible representation.* The one-dimensional representations are nondegenerate and the two- or higher-dimensional representations are degenerate. The meaning of degeneracy will be discussed in Chapter 6.

2. *The sum of the squares of the absolute values of characters of any irreducible representation in a group is equal to the order of the group.*
3. *The sum of the products of the corresponding characters (or one character with the conjugate of another in case of imaginary characters) of any two different irreducible representations of the same group is zero.*
4. *The characters of all matrices belonging to operations in the same class are identical in a given irreducible representation.*
5. *The number of irreducible representations of a group is equal to the number of classes of that group.*

Let us check these rules on the C_{2h} character table given above. All four irreducible representations have 1 as their character under E, so all of them are one-dimensional. Applying rule 1,

$$1^2 + 1^2 + 1^2 + 1^2 = 4$$

This is, indeed, the order of the group since there are four symmetry operations in C_{2h}. Let us check rule 2 with the Γ_2 representation:

$$1^2 + (-1)^2 + 1^2 + (-1)^2 = 4$$

This is, again, the order of the group. Let us form the sum of the products of Γ_3 and Γ_4 according to rule 3:

$$1 \cdot 1 + 1 \cdot (-1) + (-1) \cdot (-1) + (-1) \cdot 1 = 0$$

Since all four symmetry elements in C_{2h} stand by themselves, rule 4 cannot be checked with this point group. Finally, the number of irreducible representations is four just as the number of classes, according to rule 5.

Table 4-4 shows a preliminary character table for the C_{3v} point group. The complete set of symmetry operations is listed in the upper row. Clearly, some of them must belong to the same class since the number of irreducible representations is 3 and the number of symmetry operations is 6. A closer look at this table reveals that the characters of all irreducible representations are equal in C_3 and C_3^2 and also in σ_v, σ_v', and σ_v'', respectively. Thus, according to rule 4 C_3 and C_3^2 form one class, and σ_v, σ_v', and σ_v'' together form another class.

A complete character table is given in Table 4-5 for the C_{3v} point group. The classes of symmetry operations are listed in the upper row, together with the number of operations in each class. Thus, it is clear from looking at this character table that there are two operations in the class of threefold rotations and three in the class of vertical reflections. The identity operation, E, always forms a class by itself, and the same is true for the inversion operation, i (which is, however, not present in the C_{3v} point group). The number of classes in C_{3v} is 3; this is also the number of irreducible representations, satisfying rule 5 as well.

Consider now the symbols used for the names of the irreducible representations. These are the so-called Mulliken symbols, and their meaning is described below, along with other Mulliken symbols collected in Table 4-6.

Letters A and B are used for one-dimensional irreducible representations, depending on whether they are symmetric or antisymmetric

Table 4-4. A Preliminary Character Table for the C_{3v} Point Group

C_{3v}	E	C_3	C_3^2	σ_v	σ_v'	σ_v''
Γ_1	1	1	1	1	1	1
Γ_2	1	1	1	−1	−1	−1
Γ_3	2	−1	−1	0	0	0

Table 4-5. Complete Character Table for the C_{3v} Point Group

C_{3v}	E	$2C_3$	$3\sigma_v$		
A_1	1	1	1	z	$x^2 + y^2, z^2$
A_2	1	1	−1	R_z	
E	2	−1	0	(x, y) (R_x, R_y)	$(x^2 - y^2, xy)$ (xz, yz)

with respect to rotation around the principal axis of the point group. Antisymmetric behavior here means changing sign or direction.* The character for a symmetric representation is +1, and this is designated by the letter *A*. An antisymmetric behavior is represented by the letter *B* and has −1 character. *E* is the symbol§ for two-dimensional, and *T* (sometimes *F*) the symbol for three-dimensional representations. The subscripts *g* and *u* indicate whether the representation is symmetric or antisymmetric with respect to inversion. The German *gerade* means even and *ungerade* means odd. The superscripts ′ and ″ are used for irreducible representations which are symmetric and antisymmetric with respect to a horizontal mirror plane, respectively. The subscripts 1 and 2 with *A* and *B* refer to symmetric (1) and antisymmetric (2) behavior with respect to either a C_2 axis perpendicular to the principal

Table 4-6. Symbols for Irreducible Representations of Finite Groups

Dimension of Representation	Character under					Symbol(s)			
	E	C_n	i	σ_h	C_2^a or σ_v				
1	1	1				A			
	1	−1				B			
2	2					E			
3	3					T			
			1			A_g	B_g	E_g	T_g
			–1			A_u	B_u	E_u	T_u
				1		A'	B'		
				−1		A''	B''		
					1	A_1	B_1		
					–1	A_2	B_2		

[a] C_2 axis perpendicular to the principal axis

* Antisymmetry will be discussed in the next Section.

§ Not to be confused with the symbol of the identity operation, which is also *E*.

axis or, in its absence, to a vertical mirror plane. The meaning of subscripts 1 and 2 with E and T is more complicated, and will not be discussed here. The character tables of the infinite groups, $C_{\infty v}$ and $D_{\infty h}$, use Greek rather than Latin letters: Σ stands for one-dimensional representations and Π, Δ, Φ etc., for two-dimensional representations.

It is always possible to find a behavior that remains unchanged under any of the symmetry operations of the given point group. Thus, there is always an irreducible representation which has only +1 characters. This is the *totally symmetric irreducible representation,* and it is always the first one in any character table.

The character tables usually consist of four main areas (sometimes three if the last two are merged), as is seen in Table 4-5 for the C_{3v} and in Table 4-7 for the C_{2h} point group. The first area contains the symbol of the group (in the upper left corner) and the Mulliken symbols referring to the dimensionality of the representations and their relationship to various symmetry operations. The second area contains the classes of symmetry operations (in the upper row) and the characters of the irreducible representations of the group.

The third and fourth areas of the character table contain some chemically important basis functions for the group. The third area contains six symbols: x, y, z, R_x, R_y, and R_z. The first three are the Cartesian coordinates that we have already used before as bases for a representation of the C_{2h} point group (see, p. 186). The symbols R_x, R_y, and R_z stand for rotations around the x, y, and z axes, respectively. A popular toy, the spinning top, is helpful in visualizing the consequences of symmetry operations on rotation. Let us work out the characters for rotation around the z axis in the C_{3v} point group (Figure 4-9a). Obviously, the identity operation leaves the rotating spinning top unchanged (character 1). So does the rotation around the same axis since the rotational symmetry axis is indistinguishable from the axis of rotation of the toy. The corresponding character is again 1.

Table 4-7. The C_{2h} Character Table

C_{2h}	E	C_2	i	σ_h		
A_g	1	1	1	1	R_z	x^2, y^2, x^2, xy
B_g	1	−1	1	−1	R_x, R_y	xz, yz
A_u	1	1	−1	−1	z	
B_u	1	−1	−1	1	x, y	

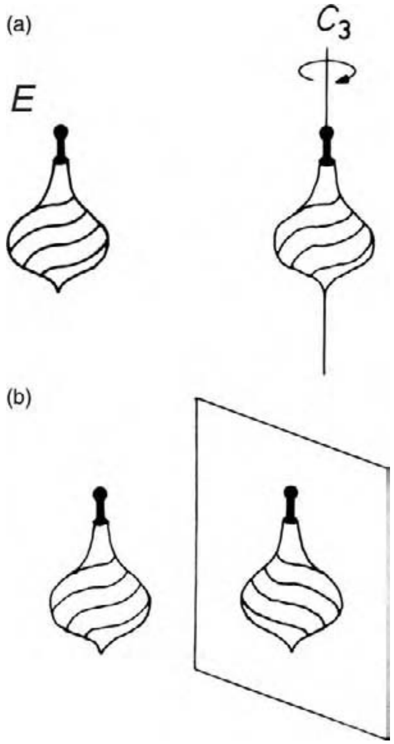

Figure 4-9. (**a**) Applying the identity and the C_3 operation to a rotating spinning top; (**b**) Illustration of the effect of mirror planes on the rotating spinning top.

Now place a mirror next to the rotating toy (Figure 4-9b). Irrespective of the position of the mirror, the rotation of the mirror image will always have the opposite direction with respect to the real rotation. Accordingly, the character will be –1.

Thus, the characters of the rotation around the *z* axis in the C_{3v} point group will be:

$$1 \qquad 1 \qquad -1$$

Indeed, R_z belongs to the irreducible representation A_2 in the C_{3v} character table. In other words, R_z *transforms* as A_2, or, it *forms* a *basis* for A_2.

The fourth area of the character table contains all the squares and binary products of the coordinates according to their behavior under the symmetry operations. All the coordinates and their products listed in the third and fourth areas of the character table are important basis

functions. They have the same symmetry properties as the atomic orbitals under the same names; z corresponds to p_z, $x^2 - y^2$ to $d_{x^2-y^2}$, and so on. We shall meet them again in the discussion of the properties of atomic orbitals.

The term antisymmetry has occurred several times above, and it is a whole new idea in our discussion. It is again a point where chemistry and other fields meet in a uniquely important symmetry concept.

4.6. Antisymmetry

Antisymmetry is the symmetry of opposites [13]. "Operations of antisymmetry transform objects possessing two possible values of a given property from one value to the other" [14]. The simplest demonstration of an antisymmetry operation is by color change. Figure 4-10 shows an identity operation and an antiidentity operation. Nothing changes, of course, in the former whereas merely the black-and-white coloring reverses in the latter. Antimirror symmetry along with mirror symmetry can be found in Figure 4-11.

Not only a symmetry plane but also other symmetry elements may serve as antisymmetry elements. We have already seen the contour of the oriental symbol Yin/Yang representing twofold rotational

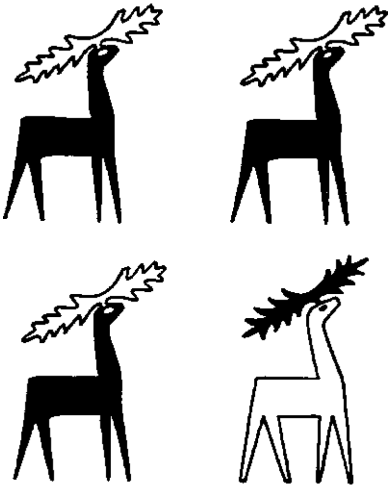

Figure 4-10. Identity operation (*top*) and antiidentity operation (*bottom*).

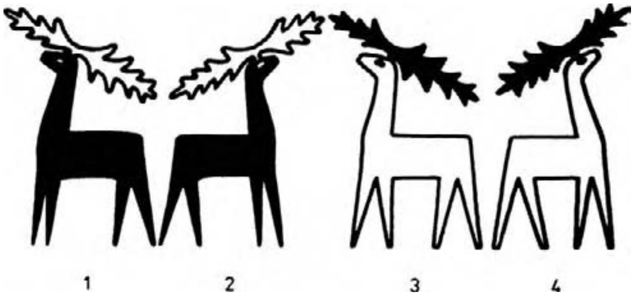

Figure 4-11. Mirror symmetries and antimirror symmetries: 1–2 and 3–4 mirror symmetries; 1–4 and 2–3 antimirror symmetries.

symmetry in Figure 2-12a. The complete sign also has a black/white color change and thus shows twofold antirotational symmetry:

Beside color change this symbol represents a whole array of opposites, such as night/day, hot/cold, male/female, young/old, etc.

Figure 4-12 illustrates different combinations of symmetry elements, for example, twofold, fourfold, and sixfold antirotation axes together with other symmetry elements after Shubnikov [15]. The fourfold antirotation axis includes a twofold rotation axis, and the sixfold antirotation axis includes a threefold rotation axis. The antisymmetry elements have the same notation as the ordinary ones except that they are underlined. Antimirror rotation axes characterize the rosettes in the second row of Figure 4-12. The antirotation axes appear in combination with one or more symmetry planes perpendicular to the plane of the drawing in the third row of Figure 4-12. Finally, the ordinary rotation axes are combined with one or more antisymmetry planes in the two bottom rows of Figure 4-12. In fact, symmetry $1 \cdot \underline{m}$ here is the symmetry illustrated in Figure 4-11. The black-and-white variation is the simplest case of color symmetry.

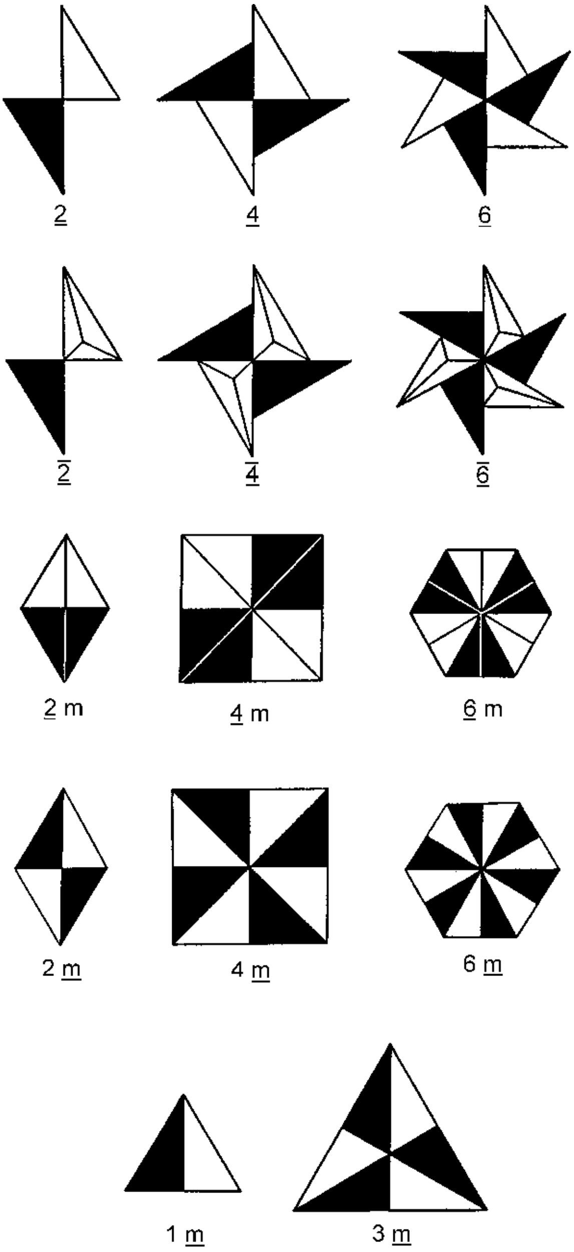

Figure 4-12. Antisymmetry operations. *First row*: antirotation axes $\underline{2}$, $\underline{4}$, $\underline{6}$; *Second row*: antimirror rotation axes $\underline{\bar{2}}$, $\underline{\bar{4}}$, $\underline{\bar{6}}$; *Third row*: antirotation axes combined with ordinary mirror planes $\underline{2}\cdot m$, $\underline{4}\cdot m$, $\underline{6}\cdot m$; *Fourth row*: ordinary rotation axes combined with antimirror planes $2\cdot\underline{m}$, $4\cdot\underline{m}$, $6\cdot\underline{m}$; *Fifth row*: $1\cdot\underline{m}$, $3\cdot\underline{m}$, after Shubnikov [16]. Reproduced with permission from Nauka Publishing Co., Moscow.

Figure 4-13. Ornament on a building in Spain with $4 \cdot \underline{m}$ symmetry. Photograph by the authors.

These considerations become more and more complicated with increasing the number of colors [16–19]. Figure 4-13 shows an example of $4 \cdot \underline{m}$ symmetry. The detail of the tower of a gatehouse at Park Güell (see Figure 4-14), the famous park in Barcelona built by Antoni Gaudi also reveals $4 \cdot \underline{m}$ symmetry, that is, fourfold rotational symmetry combined with antireflection.

All the above examples applied to point groups. Antisymmetry and color symmetry, of course, may be introduced in space-group symmetries as well as examples illustrate in Figures 8-32, 8-37, and 9-46 (in the discussion of space groups). If we look only at the close-up of the tower in Figure 4-14b, it also has tranlational antisymmetry, specifically anti-glide-reflection symmetry together with similarity symmetry (these symmetries will be discussed in Chapter 8).

Color change is perhaps the simplest version of antisymmetry. The general definition of antisymmetry, at the beginning of this section, however, calls for a much broader interpretation and application. The relationship between matter and antimatter is a conspicuous example of antisymmetry. There is no limit to down-to-earth examples, as well as to abstract ones, especially if, again, symmetry is considered rather loosely.

Figure 4-15 is another example of antimirror symmetry involving color change. However, there is more than geometrical correspondence in this Soviet poster from 1987. The text says “This is perestroika to some,” implying dissatisfaction with the way reforms were

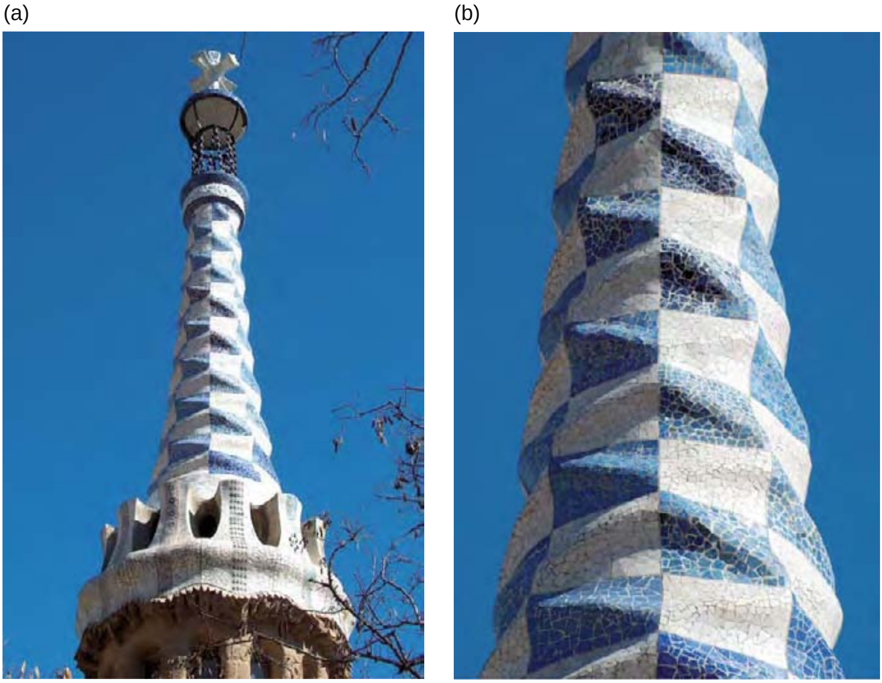

Figure 4-14. (**a**) The top of the tower of a gatehouse in Park Güell by Antoni Gaudi in Barcelona, Spain, with $4\cdot\underline{m}$ symmetry; (**b**) Close-up of the tower, revealing translational antisymmetry together with similarity symmetry. Photograph by the authors.

Figure 4-15. Soviet (1987) poster on *perestroika*. Photograph by the authors.

being carried out, amounting to mere color changes rather than substantial ones.*

Figure 4-16a shows the logo of a sporting goods store in Boston, Massachusetts. Geometrical correspondence is gone, yet we have no difficulty in recognizing the antimirror symmetry relationship. The antireflection plane relates a half-snowflake and a half-sun, symbolizing winter and summer, respectively. There are two coke machines in the picture of Figure 4-16b. There is no geometrical correspondence, but there is color reversal, and reversal of yet another, more important, property, the sugar content. This makes the two machines an example of antisymmetry with some abstraction.

Two old buildings with modern skyscrapers in the background and the houses of a medieval Italian town with a radar locator in the background express the antisymmetric relationship of old and new (Figure 4-17), while the façade of the Notre Dame cathedral showing an angel and the devil expresses the antisymmetry between good and evil (Figure 4-18).

The above examples of antisymmetry may have implied at least as much abstraction as any chemical application. The symmetric and

Figure 4-16. (**a**) Logo of a sporting goods store in Boston, Massachusetts; (**b**) Two coke machines where color change and, even more important, reversal of sugar-content, make the antisymmetric relationship. Photographs by the authors.

---

* The Russian word “perestroika” means restructuring.

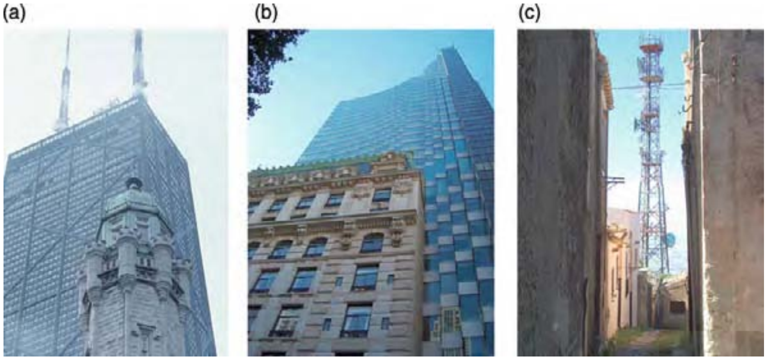

Figure 4-17. Buildings in (**a**) Boston; (**b**) New York City; (**c**) Old buildings in Erice, Sicily, with a radar locator in the background. They all illustrate the antisymmetry between new and old. Photographs by the authors.

antisymmetric behavior of orbitals describing electronic structure, and vectors describing molecular vibrations may be perceived with greater ease after the preceding diversion. Before that, however, some more of group theory will be covered.

Figure 4-18. Façade of the Notre Dame cathedral in Paris illustrating the antisymmetry between good and evil. Photograph by the authors.

4.7. Shortcut to Determine a Representation

It was quite easy to find the irreducible representation of R_z before, as the representation we worked out appeared to be an irreducible representation itself. In most cases, however, a reducible representation is found when the symmetry operations are applied to a certain basis. Now a simpler way will be shown (1) to describe the representation on a given basis without generating the matrices themselves and (2) to reduce them, if reducible, to irreducible representations.

The diimide molecule (**4-1**) is our example again, and the basis is the two N–H bond length changes (see Figure 4-7). It is easy to generate the matrices corresponding to each operation using such a simple basis; however, even this may not be necessary. As mentioned before, instead of the representations themselves, we can work with their characters. For this particular case the characters of the representation have already been determined:

Γ_1	2	0	0	2

But how can we know the character of a matrix without writing down the whole matrix?

Looking back at the effect of the different symmetry operations on HNNH (Figure 4-7) it is recalled, for example, that C_2 interchanges Δr_1 and Δr_2, so the diagonal elements of the matrix will all be 0. Consequently, these vectors do not contribute to the character.

This observation can be generalized: those basis elements that are associated with an atom changing its position during the symmetry operation will have zero contribution to the character. The basis element that is unchanged by a given operation contributes +1 to the character. Finally, the basis element that is transformed into its negative contributes -1. The only complication arises with the rotational operations when the atom does not move during the symmetry operation but the basis element associated with it is rotated by a certain angle. Here the matrix of the rotation has to be constructed as shown in Section 4.2.

Returning to the diimide N–H bond length changes, let us see how the above simple rules work. The identity operation, E, leaves

the molecule unchanged, so the two vectors, Δr_1 and Δr_2, will each contribute +1 to the character:

$$1 + 1 = 2$$

The effect of C_2 has already been looked at. Its character is 0. The effect of the inversion operation is the same as that of C_2, so the character will be

$$0 + 0 = 0$$

Finally, operation σ_h leaves the two bonds unchanged, so both of them contribute +1 to the character:

$$1 + 1 = 2$$

The result is the same as before:

Γ_1	2	0	0	2

Now, check the rules with a larger basis set, the Cartesian displacement coordinates of the atoms of HNNH (see Figure 4-8). Operation E leaves all the 12 vectors unchanged, so its character will be 12. C_2 brings each atom into a different position so their vectors will also be shifted. This means that all vectors will have zero contribution to the character. The same applies to the inversion operation. Finally, as already worked out before, the horizontal reflection leaves all the x and y vectors unchanged and brings the four z vectors into their negative selves. The result is

$$8 + (-4) = 4$$

The whole representation of the displacement vectors is:

Γ_2	12	0	0	4

Both representations we constructed here are reducible since there are no 2- and 12-dimensional representations in the C_{2h} character table (Table 4-7). The next question is how to reduce these representations.

4.8. Reducing a Representation

It was discussed before that the irreducible representations can be produced from the reducible representations by suitable similarity transformations. Another important point is that the character of a matrix is not changed by any similarity transformation. From this it follows that the sum of the characters of the irreducible representations is equal to the character of the original reducible representation from which they are obtained. We have seen that for each symmetry operation the matrices of the irreducible representations stand along the diagonal of the matrix of the reducible representation, and the character is just the sum of the diagonal elements. When reducing a representation, the simplest way is to look for the combination of the irreducible representations of that group—that is, the sum of their characters in each class of the character table—that will produce the characters of the reducible representation.

First, reduce the representation of the two N–H bond length changes of HNNH:

$$\Gamma_1 \quad 2 \quad 0 \quad 0 \quad 2$$

The C_{2h} character table shows that Γ_1 can be reduced to $A_g + B_u$:

C_{2h}	E	C_2	i	σ_h
A_g	1	1	1	1
B_g	1	–1	1	–1
A_u	1	1	–1	–1
B_u	1	–1	–1	1
$A_g + B_u$	2	0	0	2

It may be asked, of course, whether this is the only way of decomposing the Γ_1 representation. The answer is reassuring: *The decomposition of any reducible representation is unique*. If we find a solution just by inspection of the character table, it will be the only one. Often this is the fastest and simplest way to decompose a reducible representation.

A more general and more complicated way is to use a *reduction formula:*

$$a_i = (1/h) \sum_R \chi(R) \cdot \chi_i(R)$$

where a_i is the number of times the ith irreducible representation appears in the reducible representation, h is the order of the group, R is an operation of the group, $\chi(R)$ is the character of R in the reducible representation* and $\chi_i(R)$ is the character of R in the ith irreducible representation. The summation extends over all operations of the group.

The reduction formula can be simplified by grouping the equivalent operations into classes,

$$a_i = (1/h) \sum_Q N \cdot \chi(R)_Q \cdot \chi_i(R)_Q$$

where a_i is the number of times the ith irreducible representation appears in the reducible representation, h is the order of the group, Q is a class of the group, N is the number of operations in class Q, R is an operation of the group, $\chi(R)_Q$ is the character of an operation of class Q in the reducible representation, and $\chi_i(R)_Q$ is the character of an operation of class Q in the ith irreducible representation. The summation extends over all classes of the group.

The reduction formula can only be applied to finite point groups. For the infinite point groups, $D_{\infty h}$ and $C_{\infty h}$, the usual practice is to reduce the representations by inspection of the character table.

For illustration, let us find the irreducible representations of the two examples used before. First, on the basis of the two N–H distance changes of diimide (i.e., Γ_1):

C_{2h}	E	C_2	i	σ_h
A_g	1	1	1	1
B_g	1	–1	1	–1
A_u	1	1	–1	–1
B_u	1	–1	–1	1
Γ_1	2	0	0	2

*Here and hereafter the short expression "character of R" stands for the character of the matrix corresponding to operation R, in accordance with our previous discussion.

The order of the group is 4. The number of times the irreducible representation A_g appears in the reducible representation is

$$\begin{aligned} a_{A_g} &= (1/4)[1 \cdot 2 \cdot 1 + 1 \cdot 0 \cdot 1 + 1 \cdot 0 \cdot 1 + 1 \cdot 2 \cdot 1] \\ &= (1/4)(2 + 0 + 0 + 2) = 4/4 = 1 \end{aligned}$$

In the same way we can deduce the number of times the other irreducible representations appear in Γ_1:

$$\begin{aligned} a_{B_g} &= (1/4)[1 \cdot 2 \cdot 1 + 1 \cdot 0 \cdot (-1) + 1 \cdot 0 \cdot 1 + 1 \cdot 2 \cdot (-1)] = 0 \\ a_{A_u} &= (1/4)[1 \cdot 2 \cdot 1 + 1 \cdot 0 \cdot 1 + 1 \cdot 0 \cdot (-1) + 1 \cdot 2 \cdot (-1)] = 0 \\ a_{B_u} &= (1/4)[1 \cdot 2 \cdot 1 + 1 \cdot 0 \cdot (-1) + 1 \cdot 0 \cdot (-1) + 1 \cdot 2 \cdot 1] = 1 \end{aligned}$$

That is, $\Gamma_1 = A_g + B_u$, and the result is the same as before.

With the 12-dimensional reducible representation of the Cartesian displacement vectors of HNNH, the inspection method probably does not work. However, the reduction formula can be used. The reducible representation is:

Γ_2	12	0	0	4

and with applying the reduction formula, we obtain:

$$\begin{aligned} a_{A_g} &= (1/4)[1 \cdot 12 \cdot 1 + 1 \cdot 0 \cdot 1 + 1 \cdot 0 \cdot 1 + 1 \cdot 4 \cdot 1] = 4 \\ a_{B_g} &= (1/4)[1 \cdot 12 \cdot 1 + 1 \cdot 0 \cdot (-1) + 1 \cdot 0 \cdot 1 + 1 \cdot 4 \cdot (-1)] = 2 \\ a_{A_u} &= (1/4)[1 \cdot 12 \cdot 1 + 1 \cdot 0 \cdot 1 + 1 \cdot 0 \cdot (-1) + 1 \cdot 4 \cdot (-1)] = 2 \\ a_{B_u} &= (1/4)[1 \cdot 12 \cdot 1 + 1 \cdot 0 \cdot (-1) + 1 \cdot 0 \cdot (-1) + 1 \cdot 4 \cdot 1] = 4 \end{aligned}$$

Thus,

$$\Gamma_2 = 4A_g + 2B_g + 2A_u + 4B_u$$

4.9. Auxiliaries

A few additional things need to be mentioned before embarking on chemical applications of group theoretical methods. For detailed descriptions and proofs we refer to References [21–23].

4.9.1. Direct Product

Wave functions form bases for representations of the point group of the molecule [24]. Suppose that f_i and f_j are such functions; then the new set of functions, $f_i f_j$, called the *direct product* of f_i and f_j, is also basis for a representation of the group. The characters of the direct product can be determined by the following rule: *The characters of the representation of a direct product are equal to the products of the characters of the representations of the original functions.* The direct product of two irreducible representations will be a new representation which is either an irreducible representation itself or can be reduced into irreducible representations. Tables 4-8 and 4-9 show some examples for direct products with the C_{2v} and C_{3v} point groups, respectively.

Table 4-8. Character Table and Some Direct Products for the C_{2v} Point Group

C_{2v}	E	C_2	σ_v	σ_v'	
A_1	1	1	1	1	
A_2	1	1	−1	−1	
B_1	1	−1	1	−1	
B_2	1	−1	−1	1	
$A_1 \cdot A_2$	1	1	−1	−1	$= A_2$
$A_2 \cdot B_1$	1	−1	−1	1	$= B_2$
$B_1 \cdot B_2$	1	1	−1	−1	$= A_2$

Table 4-9. Character Table and Direct Products for the C_{3v} Point Group

C_{3v}	E	$2C_3$	$3\sigma_v$	
A_1	1	1	1	
A_2	1	1	−1	
E	2	−1	0	
$A_2 \cdot A_2$	1	1	1	$= A_1$
$A_2 \cdot E$	2	−1	0	$= E$
$E \cdot E$	4	1	0	$= A_1 + A_2 + E$

4.9.2. Integrals of Product Functions

Integrals of product functions often occur in the quantum mechanical description of molecular properties and it is helpful to know their symmetry behavior. Why? The reason is that an integral whose

integrand is the product of two or more functions will vanish unless the integrand is invariant under all symmetry operations of the point group. There is only one irreducible representation whose characters are 1 for each symmetry operation of the point group, and this is the totally symmetric irreducible representation. Therefore, an *integral will be nonzero only if the integrand belongs to the totally symmetric irreducible representation of the molecular point group.*

The representation of a product function can be determined by forming the direct product of the original functions. The representation of a direct product will contain the totally symmetric representation only if the original functions whose product is formed belong to the *same* irreducible representation of the molecular point group. This follows directly from rules 2 and 3 in Section 4.5.

These rules can be extended to integrals of products of more than two functions. For a triple product the integral will be nonzero only if the representation of the product of any two functions is the same as, or contains, the representation of the third function. If the integral is

$$\int f_i \cdot f_j \cdot f_k \, d\tau$$

then the above condition is expressed by

$$\Gamma_{f_i} \cdot \Gamma_{f_k} \subset \Gamma_{f_j}$$

where Γ stands for the representation and $\subset$ means "is or contains." Very often, f_j is a quantum-chemical operator, and then the expressions are:

$$\int f_i \widehat{\text{op}}.\, f_k d\tau$$

or with other notation,

$$\langle f_i | \widehat{\text{op}}. | f_k \rangle$$

and

$$\Gamma_{f_i} \cdot \Gamma_{f_k} \subset \Gamma_{\widehat{\text{op}}.}$$

This kind of condition appears in energy integrals and spectral selection rules, and in the discussion of chemical reactions.

4.9.3. Projection Operator

The *projection operator* is one of the most useful concepts in the application of group theory to chemical problems [25, 26]. It is an operator which takes the non-symmetry-adapted basis of a representation and projects it along new directions in such a way that it belongs to a specific irreducible representation of the group. The projection operator is represented by $\hat{P}^i$ in the following form:

$$\hat{P}^i = (1/h) \sum_R \chi_i(R) \cdot \hat{R}$$

where h is the order of the group, i is an irreducible representation of the group, R is an operation of the group, $\chi_i(R)$ is the character of R in the ith irreducible representation, and $\hat{R}$ means the application of the symmetry operation R to our basis component. The summation extends over all operations of the group.

Consider now the construction of the A_1 symmetry group orbital of the hydrogen s atomic orbitals in ammonia as an example of the application of the projection operator. (The various kinds of orbitals will be discussed in detail in Chapter 6.) The projection operator for the A_1 irreducible representation in the C_{3v} point group is

$$\hat{P}^{A_1} = (1/6) \sum_R \chi_{A_1}(R) \cdot \hat{R}$$

Applying this operator to the s orbital of one of the hydrogens (H1) of ammonia, we obtain

$$\begin{aligned} \hat{P}^{A_1} s_1 \approx\ & 1 \cdot E \cdot s_1 + 1 \cdot C_3 \cdot s_1 + 1 \cdot C_3^2 \cdot s_1 + 1 \cdot \sigma \cdot s_1 \\ & + 1 \cdot \sigma' \cdot s_1 + 1 \cdot \sigma'' \cdot s_1 \\ =\ & s_1 + s_2 + s_3 + s_1 + s_2 + s_3 \approx s_1 + s_2 + s_3 \end{aligned}$$

This expression is an approximation since the numerical factor of 1/6 was omitted. The coefficient (the normalization factor) in the symmetry-adapted linear combinations can be determined at a later stage by normalization. In an actual calculation this is necessary, whereas here we are interested only in the symmetry aspects, which are well represented by the relative values. In fact, the normalization factors will be ignored throughout our discussions.

Application of the projection operator will also be demonstrated pictorially in forthcoming chapters. These representations will emphasize the results of summation of symmetry-sensitive properties while the absolute magnitudes will not be treated rigorously. Thus, for example, the directions of vectors will be summed in describing vibrations, and the signs of the angular components of the electronic wave functions will be summed in describing the electronic structure.

4.10. Dynamic Properties

Molecular properties can be of either static or dynamic nature. A static property remains unchanged by every symmetry operation carried out on the molecule. The geometry of the nuclear arrangement in the molecule is such a property: a symmetry operation transforms the nuclear arrangement into another which will be indistinguishable from the initial.[*] The mass and the energy of a molecule are also static properties.

Dynamic properties, on the other hand, may change under symmetry operations. Molecular motion itself is a most common dynamic property. In our previous discussions of molecular structure, the molecules were mostly assumed to be motionless, and only the symmetry of their nuclear arrangement was considered. However, real molecules are never motionless, and their chemical behavior is influenced by their motion to a great extent.

In order to appreciate the effects of symmetry operations on motion, an example from our macroscopic world is invoked here, following an idea of Orchin and Jaffe [27]. Suppose there exists a long wall of mirror and one walks alongside this mirror (Figure 4-19 left). Our mirror image will be walking with us with the same speed and in the same direction (its velocity will be the same as ours). If we walk now from a distance towards the mirror perpendicularly to it, our mirror image will have a different velocity from ours: the speed will be the same again but the direction will be just the opposite. Both we and our mirror image will be walking towards the plane of the mirror, and if we do not stop in time, we shall collide in that plane (Figure 4-19 right).

[*] Unless, of course, identical atoms are distinguished by labels as, e.g., in Figs. 4-2 and 4-3.

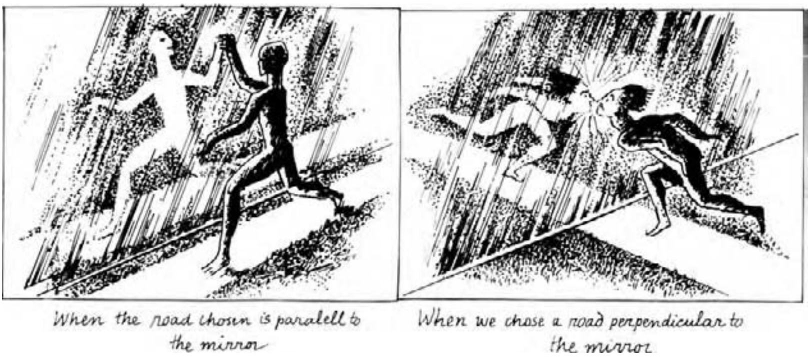

Figure 4-19. Symmetric (*left*) and antisymmetric (*right*) consequencies of the "mirror operation" for two movements. Drawing courtesy of the late György Doczi.

The consequences of the mirror operation were different for the two movements. One was symmetric, and the other was antisymmetric.

There are analogous phenomena for all kinds of molecular motion which may be symmetric and antisymmetric with respect to the various symmetry operations of the molecular point group. The two main kinds of motion in a molecule are nuclear and electronic. The nuclear motion may be translational, rotational and vibrational (Chapter 5). The electronic motion is basically the changes in the electron density distribution (Chapter 6).

4.11. Where Is Group Theory Applied?

It is primarily the description of the dynamic properties that is facilitated by group-theoretical methods. This is, in fact, an understatement. The dynamic properties cannot be fully discussed without group theory. On the other hand, this theory need not be used to determine the point group symmetry of the nuclear arrangement of a molecule, as has been shown before (cf. Figure 3-5).

The first step in the symmetry determination of the dynamic properties is the selection of the appropriate basis. Appropriate here means the correct representation of the changes in the properties examined. In the investigation of molecular vibrations (Chapter 5), either Cartesian displacement vectors or internal coordinate vectors are used. In the description of the molecular electronic structure (Chapter 6), the angular components of the atomic orbitals are frequently used

bases. Since the angular wave function changes its "sign" under certain symmetry operations, its behavior will be characteristic of the spatial symmetry of a particular orbital. Molecular orbitals can also be used as basis of representation. The simple scheme below shows some important areas in chemistry where group theory is indispensable, and the most convenient basis functions are also indicated:

Area	**Basis functions**
Construction of molecular orbitals	Atomic orbitals
Construction of hybrid orbitals	Position vectors pointing toward the ligands
Predicting the decrease of degeneracies of *d* orbitals under a ligand field	*d* Atomic orbitals
Predicting the allowedness of chemical reactions	Molecular orbitals
Determining the number and symmetries of molecular vibrations	Cartesian displacement vectors
Normal coordinate analysis (symmetry coordinates)	Internal coordinate displacements

Group theory is also used prior to calculations to determine whether a quantum-mechanical integral of the type $\int \psi_i\ \hat{\text{o}}\text{p.}\ \psi_j\ d\tau$ is different from zero or not. This is important in such areas as selection rules for electronic transitions, chemical reactions, infrared and Raman spectroscopy, and other spectroscopies.

References

1. A. L. Mackay, *A Dictionary of Scientific Quotations*, Adam Hilger, Bristol, 1991, p. 12/123.
2. J. R. Newman (ed.) *The World of Mathematics*, Dover Publications, Inc., New York, 2003.
3. F. A. Cotton, *Chemical Applications of Group Theory*, Third Edition, Wiley-Interscience, New York, 1990.
4. A. Nussbaum, *Applied Group Theory for Chemists, Physicists and Engineers*, Prentice-Hall, Inc., Englewood Cliffs, New Jersey, 1971.

5. L. H. Hall, *Group Theory and Symmetry in Chemistry*, McGraw-Hill Book Co., New York, 1969.
6. G. Burns, *Introduction to Group Theory with Applications*, Material Science Series, A. M. Alper, A. S. Nowich, eds., Academic Press, New York, 1977.
7. A. Vincent, *Molecular Symmetry and Group Theory: A Programmed Introduction to Chemical Applications*, Second Edition, Wiley-Interscience, New York, 2001.
8. S. F. A. Kettle, *Symmetry and Structure: Readable Group Theory for Chemists*, John Wiley & Sons, Chichester, 2008.
9. H. H. Jaffe, M. Orchin, *Symmetry in Chemistry*, Dover Publications, Inc., New York, 2002.
10. P. R. Bunker, P. Jensen, *Fundamentals of Molecular Symmetry*, Taylor & Francis, London, 2004.
11. B. E. Douglas and C.A. Hollingsworth, *Symmetry in Bonding and Spectra: An Introduction*, Academic Press, Orlando, Florida, 1985.
12. Cotton, *Chemical Applications of Group Theory.*
13. I. Hargittai, M. Hargittai, “Symmetry of Opposites—Antisymmetry.” *Math. Intell.* 1994, 16, 60–66.
14. A. L. Mackay, “Extensions of Space-Group Theory.” *Acta Cryst.* 1957, 10, 543–548.
15. A. V. Shubnikov, *Simmetriya i antisimmetriya konechnikh figur,* Izd. Akad. Nauk S. S. S. R., Moscow, 1951.
16. Ibid.
17. Ibid.
18. A. Loeb, *Color and Symmetry.* Wiley-Interscience, New York, 1971.
19. A. Loeb, in *Patterns of Symmetry,* M. Senechal and G. Fleck, eds., University of Massachusetts Press, Amherst, Massachusetts, 1977.
20. M. Senechal, *Acta Cryst.* 1983, A39, 505.
21. Cotton, *Chemical Applications of Group Theory.*
22. Nussbaum, *Applied Group Theory for Chemists, Physicists and Engineers.*
23. Hall, *Group Theory and Symmetry in Chemistry.*
24. Cotton, *Chemical Applications of Group Theory.*
25. Ibid.
26. Nussbaum, *Applied Group Theory for Chemists, Physicists and Engineers.*
27. M. Orchin, H. H. Jaffe, *Symmetry, Orbitals, and Spectra (S.O.S.),* Wiley-Interscience, New York, 1971.

Chapter 5

Molecular Vibrations

...the atoms march in tune.
Ralph W. Emerson [1]

Vibration is a special kind of motion: the atoms of every molecule are permanently changing their relative positions at every temperature (even at absolute zero) without changing the position of the molecular center of mass. In terms of the molecular geometry these vibrations amount to continuously changing bond lengths and bond angles. Symmetry considerations will be applied to the molecular vibrations in this chapter following primarily References [2–4]. Our brief discussion is only an indication of yet another important application of symmetry considerations. The mentioned references and two other fundamental monographs [5, 6] on vibrational spectroscopy are suggested for further reading. Our primary concern will be to examine in simple terms the following question: What kind of information can be deduced about the internal motion of the molecule from the mere knowledge of its point-group symmetry?

5.1. Normal Modes

The seemingly random motion of molecular vibrations can always be decomposed into the sum of relatively simple components, called *normal modes of vibration*. Each of the normal modes is associated with a certain frequency. Thus, for a normal mode every atom of the molecule moves with the same frequency and in phase. Three characteristics of normal vibrations will be examined: their number, their symmetry, and their type.

M. Hargittai, I. Hargittai, *Symmetry through the Eyes of a Chemist,* 3rd ed.,
DOI: 10.1007/978-1-4020-5628-4_5, © Springer Science+Business Media B.V. 2009

5.1.1. Their Number

Since vibration is only one of the possible forms of motion, it has to be separated from the others, translation and rotation. Consider first a single atom. Its motion can be characterized by the three Cartesian coordinates of its instantaneous position as shown in Figure 5-1. In other words, the atom has three *degrees of motional freedom*. Consider next a diatomic molecule. It will have $2\times 3 = 6$ degrees of freedom. We might think again that the three Cartesian coordinates of each atom describe the motion of the molecule in space. However, this is not quite so. Since the two atoms are not independent from each other, they must move together in space. This means that three degrees of freedom will account altogether for the *translation* of a diatomic molecule (see Figure 5-2) — or of any polyatomic molecule, for that matter. Two other degrees of freedom describe the *rotation* of the diatomic molecule around the center of mass (see Figure 5-3a). The rotation around the z axis (Figure 5-3b) need not be considered as it is the axis of the molecule, and the rotation around it does not change the position of the molecule.

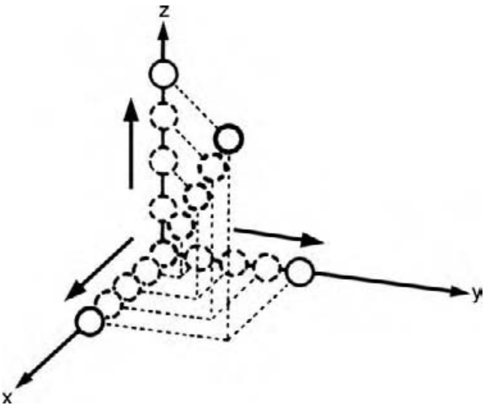

Figure 5-1. Three motional degrees of freedom of an atom.

Thus of the six degrees of freedom, five have been accounted for. The sixth will describe the movement of the two atoms relative to each other without changing the center of the mass. This is the *vibration* of the molecule:

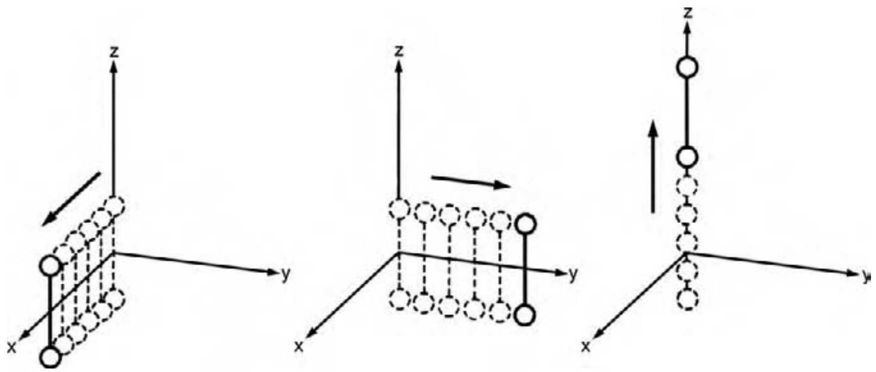

Figure 5-2. The three translational degrees of freedom of a diatomic molecule.

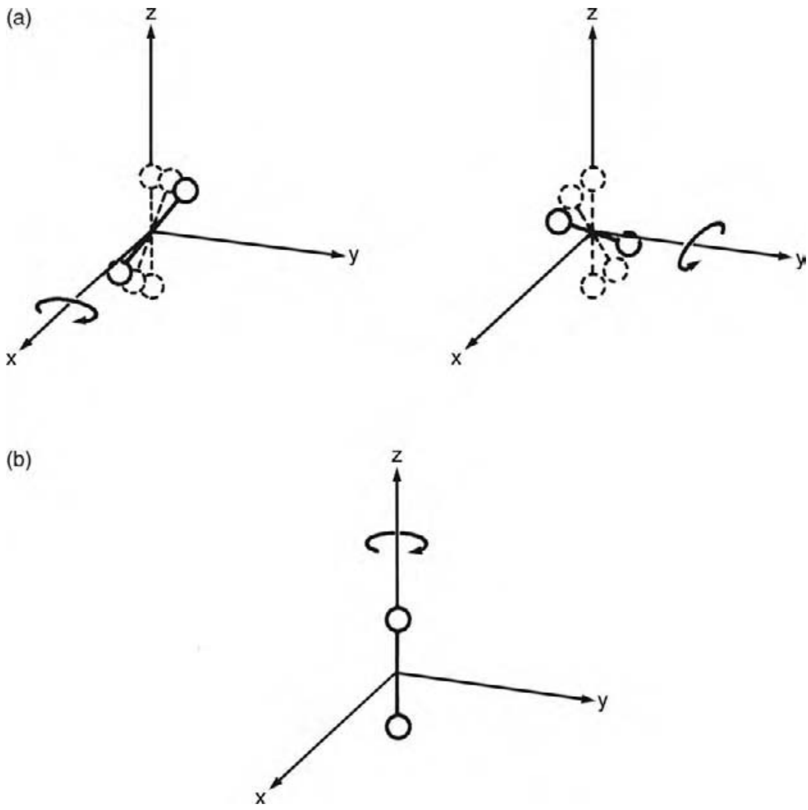

Figure 5-3. Rotation of a diatomic molecule; (**a**) Two rotational degrees of freedom describe the rotation of the molecule around the center of mass; (**b**) Rotation around the molecular axis does not change the position of the molecule.

The complete nuclear motion of an N-atomic molecule can be described with $3N$ parameters; that is an N-atomic molecule has $3N$ degrees of freedom. The translation of a molecule can always be described by three parameters. The rotation of a diatomic or any linear molecule will be described by two parameters and the rotation of a nonlinear molecule by three parameters. This means that there are always 3 translational and 3 (for linear molecules 2) rotational degrees of freedom. The remaining $3N - 6$ (for the linear case $3N - 5$) degrees of freedom account for the vibrational motion of the molecule. They give the number of normal vibrations.

The translational and rotational degrees of freedom, which do not change the relative positions of the atoms in the molecule, are often called *nongenuine modes*. The remaining $3N - 6$ (or $3N - 5$) degrees of freedom are called genuine vibrations or *genuine modes*.

5.1.2. Their Symmetry

The close relationship between symmetry and vibration is expressed by the following rule: *Each normal mode of vibration forms a basis for an irreducible representation of the point group of the molecule*.

Let us use the water molecule to illustrate the above statement. The normal modes of this molecule are shown in Figure 5-4. The point group is C_{2v}, and the character table is given in Table 5-1. It is seen that all operations bring v_1 and v_2 into themselves so their characters will be:

$$\begin{array}{ccccc} \Gamma_{v_1} & 1 & 1 & 1 & 1 \\ \Gamma_{v_2} & 1 & 1 & 1 & 1 \end{array}$$

The behavior of the third normal mode, v_3, is different. While E and σ_v' leave it unchanged, both C_2 and σ_v bring it into its negative self:

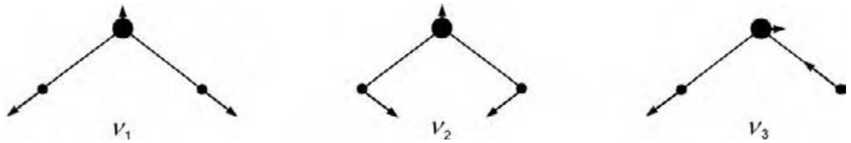

Figure 5-4. Normal modes of vibration for the water molecule. The lengths of the arrows indicate the relative displacements of the atoms.

Table 5-1. The C_{2v} Character Table

C_{2v}	E	C_2	$\sigma_v(xz)$	$\sigma'_v(yz)$		
A_1	1	1	1	1	z	x^2, y^2, z^2
A_2	1	1	–1	–1	R_z	xy
B_1	1	–1	1	–1	x, R_y	xz
B_2	1	–1	–1	1	y, R_x	yz

each atom moves in the opposite direction after the operation. This means that v_3 is antisymmetric to these operations. The characters are:

$$\Gamma_{v_3} \quad 1 \quad -1 \quad -1 \quad 1$$

Looking at the C_{2v} character table, we can say that v_1 and v_2 belong to the totally symmetric irreducible representation A_1, and v_3 belongs to B_2.

It was easy to determine the symmetry of the normal modes of the water molecule because we already knew their forms. Can the symmetry of the normal modes of a molecule be determined without any previous knowledge of the actual forms of the normal modes? The answer is fortunately yes. From the symmetry group of the molecule the symmetry species of the normal modes can be determined without any additional information.

First, an appropriate basis set has to be found. Considering that a molecule has $3N$ degrees of motional freedom, a system of $3N$ so-called *Cartesian displacement vectors* is a convenient choice. A set of such vectors is shown in Figure 5-5 for the water molecule. A separate Cartesian coordinate system is attached to each atom of the molecule, with the atoms at the origin. The orientation of the axes is the same in each system. Any displacement of the atoms can be expressed by a vector, and in turn this vector can be expressed as the vector sum of the Cartesian displacement vectors.

Next, the set of Cartesian displacement vectors is used as a basis for the representation of the point group. As discussed in Chapter 4, the vectors connected with atoms that change their position during an operation will not contribute to the character and thus they can be ignored.

Continuing with the water molecule as an example, the basis of the Cartesian displacement vectors will consist of nine vectors

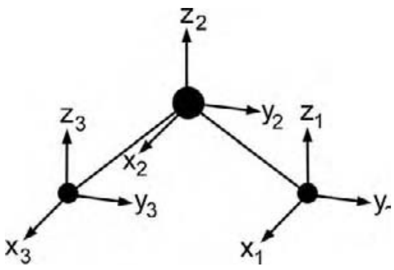

Figure 5-5. Cartesian displacement vectors as basis for representation of the water molecule.

(see Figure 5-5). Operation E brings all of them into themselves, and the character is 9. Operation C_2 changes the position of the two hydrogen atoms, so only the three coordinates of the oxygen atom have to be considered. The corresponding block of the matrix representation is:

$$C_2 = \begin{matrix} x_2' \\ y_2' \\ z_2' \end{matrix} \overset{\begin{matrix} x_2 & y_2 & z_2 \end{matrix}}{\begin{bmatrix} -1 & 0 & 0 \\ 0 & -1 & 0 \\ 0 & 0 & 1 \end{bmatrix}}$$

The character is (– l) + (– 1) + 1 = – 1.

The next operation is σ_v. Again, only the oxygen coordinates have to be considered. Reflection through the xz plane leaves x_2 and z_2 unchanged and brings y_2 into $-y_2$. The character is 1 + 1 + (– 1) = 1.

Finally, operation σ_v' leaves all three atoms in their place, so all the nine coordinates have to be taken into account. Reflection through the yz plane leaves all y and z coordinates unchanged and takes all x coordinates into their negative selves. The character will be: (– 1) + 1 + 1 + (– 1) + 1 + 1 + (–1) + 1 + 1 = 3. The representation is:

$$\Gamma_{tot} \quad 9 \quad -1 \quad 1 \quad 3$$

This is, of course, a reducible representation. Reduce it now with the reduction formula (see Chapter 4):

$$\begin{aligned}
a_{A_1} &= (1/4)[1 \cdot 9 \cdot 1 + 1 \cdot (-1) \cdot 1 + 1 \cdot 1 \cdot 1 + 1 \cdot 3 \cdot 1] \\
&= (1/4)(9 - 1 + 1 + 3) = 3 \\
a_{A_2} &= (1/4)[1 \cdot 9 \cdot 1 + 1 \cdot (-1) \cdot 1 + 1 \cdot 1 \cdot (-1) + 1 \cdot 3 \cdot (-1)] \\
&= (1/4)(9 - 1 - 1 - 3) = 1 \\
a_{B_1} &= (1/4)[1 \cdot 9 \cdot 1 + 1 \cdot (-1) \cdot (-1) + 1 \cdot 1 \cdot 1 + 1 \cdot 3 \cdot (-1)] \\
&= (1/4)(9 + 1 + 1 - 3) = 2 \\
a_{B_2} &= (1/4)[1 \cdot 9 \cdot 1 + 1 \cdot (-1) \cdot (-1) + 1 \cdot 1 \cdot (-1) + 1 \cdot 3 \cdot 1] \\
&= (1/4)(9 + 1 - 1 + 3) = 3
\end{aligned}$$

The representation reduces to:

$$\Gamma_{\text{tot}} = 3A_1 + A_2 + 2B_1 + 3B_2.$$

These nine irreducible representations correspond to the nine motional degrees of freedom of the triatomic water molecule. To obtain the symmetry of the genuine vibrations, the irreducible representations of the translational and rotational motion have to be separated. This can be done using some considerations described in Chapter 4. The translational motion always belongs to those irreducible representations where the three coordinates, x, y, and z, belong. Rotations belong to the irreducible representations of the point group indicated by R_x, R_y, and R_z in the third area of the character tables. In the C_{2v} point group,

$$\Gamma_{\text{tran}} = A_1 + B_1 + B_2$$

and

$$\Gamma_{\text{rot}} = A_2 + B_1 + B_2$$

Subtracting these from the representation of the total motion, we get

$$\begin{array}{rlllll}
\Gamma_{\text{tot}} & = 3A_1 & + A_2 & + 2B_1 & + 3B_2 & \\
-(\Gamma_{\text{tran}} & = A_1 & & + B_1 & + B_2) & \\
-(\Gamma_{\text{rot}} & = & A_2 & + B_1 & + B_2) & \\
\hline
\Gamma_{\text{vib}} & = 2A_1 & & & + B_2 &
\end{array}$$

Thus, of the three normal modes of water, two will have A_1 and one B_2 symmetry. Let us stress again: this information could be derived purely from the molecular point-group symmetry.

5.1.3. Their Types

The normal modes can usually—though not always—be associated with a certain kind of motion. Those connected mainly with changes in bond lengths are the *stretching modes*. The ones connected mainly with changes of bond angles are the *deformation modes*. These may be mainly either in-plane or out-of-plane deformation modes. The simplest deformation mode is the *bending mode*.

Examine now the symmetries of these different types of vibration. For this purpose a new type of basis set is used. Since we are interested in the changes of the geometrical parameters, these changes are an obvious choice for basis set. The geometrical parameters are also called *internal coordinates*, and the basis is the displacement of these internal coordinates.

Let us continue with the water molecule and determine the symmetry of its stretching modes. The molecule has two O–H bonds, so the basis will be the *changes* of these O–H bonds. The representation of this basis set is

$$\Gamma_{str} \quad 2 \quad 0 \quad 0 \quad 2$$

and with inspection of the C_{2v} character table we see that it reduces to $A_1 + B_2$. This means that the stretching of the O–H bonds contributes to the normal modes of A_1 and B_2 symmetry. (We shall later see that these are the symmetric and antisymmetric stretches, respectively.)

The third internal coordinate which can be considered in the water molecule is the bond angle, H–O–H. Its change will be the bending mode. All symmetry operations leave this basis unchanged, so the representation is:

$$\Gamma_{bend} \quad 1 \quad 1 \quad 1 \quad 1$$

and it belongs to the totally symmetric representation, A_1. What can we conclude? B_2 appears only in the stretching mode, so the B_2 normal mode will be a pure stretching mode. The A_1 symmetry mode, however, appears in both the stretching and the bending mode. At

this point we cannot say whether one of the A_1 normal modes will be purely stretch and the other purely bend or they will be a mixture. This depends on the energy of these vibrations. If they are energetically close, they can mix extensively. If they are separated by a large energy difference, they will not mix. In the case of H_2O, for example, the two A_1 symmetry modes are quite well separated, while in Cl_2O they are completely mixed.

Modes of different symmetry never mix, even if they are close in energy. (This is a general rule which will have its analogous version for the transitions among electronic states as will be seen later in Chapters 6 and 7.)

The above analysis of the types of normal modes brings us to the limit where simple symmetry considerations can take us. Nothing yet has been said about the pictorial manifestation of the various normal modes. Above we deduced, for example, that the B_2 normal mode of the water molecule is a pure stretch. The question may also be asked, how does it look? This question can be answered with the help *of symmetry coordinates.*

5.2. Symmetry Coordinates

The symmetry coordinates are symmetry-adapted linear combinations of the internal coordinates. They always transform as one or another irreducible representation of the molecular point group.

Symmetry coordinates can be generated from the internal coordinates by the use of the projection operator introduced in Chapter 4. Both the symmetry coordinates and the normal modes of vibration belong to an irreducible representation of the point group of the molecule. A symmetry coordinate is always associated with one or another type of internal coordinate—that is pure stretch, pure bend, etc.—whereas a normal mode can be a mixture of different internal coordinate changes of the same symmetry. In some cases, as in H_2O, the symmetry coordinates are good representations of the normal vibrations. In other cases they are not. An example for the latter is Au_2Cl_6 where the pure symmetry coordinate vibrations would be close in energy, so the real normal vibrations are mixtures of the different vibrations of the same symmetry type [7]. The relationship between the symmetry coordinates and the normal vibrations can be

established only by calculations called normal coordinate analysis [8, 9]. These calculations necessitate further data in addition to the knowledge of molecular symmetry and are not pursued here.

Return now to the symmetry coordinates of the water molecule. They can be generated using the projection operator. As has been mentioned before, here we are interested only in the symmetry aspects of the symmetry coordinates. Thus, the numerical factors are omitted, and normalization is not considered. First, let us work out the symmetry coordinate involving the stretching vibrations:

$$\begin{aligned}\hat{P}^{A_1}\Delta r_1 &\approx 1\cdot E\cdot\Delta r_1 + 1\cdot C_2\cdot\Delta r_1 + 1\cdot\sigma\cdot\Delta r_1 + 1\cdot\sigma'\cdot\Delta r_1\\ &= \Delta r_1 + \Delta r_2 + \Delta r_2 + \Delta r_1 \approx \Delta r_1 + \Delta r_2\\ \hat{P}^{B_2}\Delta r_1 &\approx 1\cdot E\cdot\Delta r_1 + (-1)\cdot C_2\cdot\Delta r_1 + (-1)\cdot\sigma\cdot\Delta r_1\\ &\quad + 1\cdot\sigma'\cdot\Delta r_1 =\\ &= \Delta r_1 - \Delta r_2 - \Delta r_2 + \Delta r_1 \approx \Delta r_1 - \Delta r_2.\end{aligned}$$

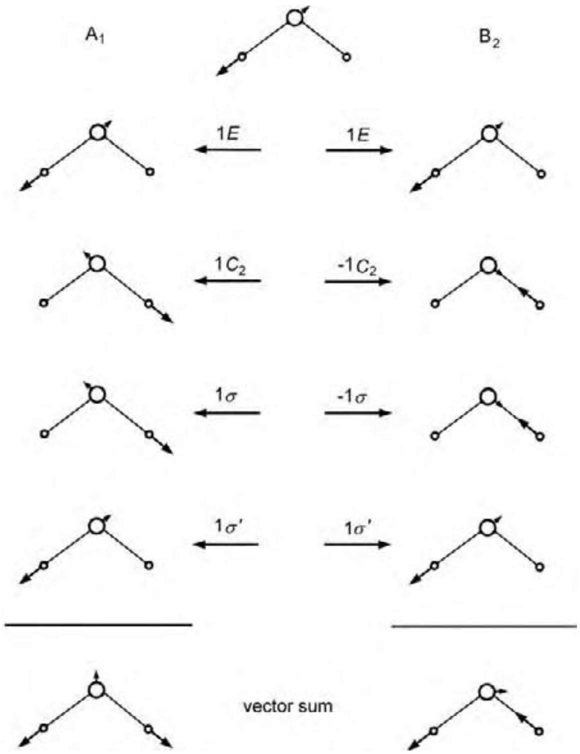

Figure 5-6. Generation of the symmetry coordinates representing bond stretching for H_2O.

The same procedure is presented pictorially in Figure 5-6. The bending mode of the water molecule stands alone (see the v_2 mode in Figure 5-4), so it will be a symmetry coordinate by itself.

Since the symmetry coordinates of water are good approximations of the normal vibrations, the pictorial representations are applicable to them as well. Indeed, the three normal modes of Figure 5-4 are the same as the symmetry coordinates we just derived. The A_1 symmetry stretching mode is called the symmetric stretch while the B_2 mode is the antisymmetric stretch.

5.3. Selection Rules

The vibrational wave function, as any wave function, must form a basis for an irreducible representation of the molecular point group [3].

The total vibrational wave function, Ψ_v, can be written as the product of the wave functions $\Psi_i(n_i)$, where Ψ_i is the wave function of the ith normal vibration (i = 1 through m) in the nth state.

$$\Psi_v = \Psi_1(n_1) \cdot \Psi_2(n_2) \cdot \Psi_3(n_3) \ldots\ldots \Psi_m(n_m)$$

In general, at any time, each of the normal modes may be in any state. There is, however, a situation when all the normal modes are in their ground states and only one of them gets excited into the first excited state. Such a transition is called a *fundamental transition.* The intensity of the fundamental transitions is much higher than the intensity of the other kinds of transitions.* Therefore, these are of particular interest.

The vibrational wave function of the ground state belongs to the totally symmetric irreducible representation of the point group of the molecule. The wave function of the first excited state will belong to the irreducible representation to which the normal mode undergoing the particular transition belongs.

---

*Were the vibrations strictly harmonic, only fundamental transitions would be observable.

A fundamental transition will occur only if one of the following integrals has nonzero value:

$$\langle \Psi_v^{\circ} \; |x| \; \Psi_v^{i} \rangle$$
$$\langle \Psi_v^{\circ} \; |y| \; \Psi_v^{i} \rangle$$
$$\langle \Psi_v^{\circ} \; |z| \; \Psi_v^{i} \rangle$$

Here Ψ_v° is the total vibrational wave function for the ground state, Ψ_v^{i} is the total vibrational wave function for the first excited state referring to the *i*th normal mode and *x*, *y* and *z* are Cartesian coordinates.

The condition for an integral of product functions to have a nonzero value was given in Chapter 4. For the vibrational transitions this condition can be expressed in the following way:

$$\Gamma_{\Psi_v^{\circ}} \cdot \Gamma_{\Psi_v^{i}} \subset \Gamma_x \qquad \text{or} \qquad \Gamma_{\Psi_v^{\circ}} \cdot \Gamma_{\Psi_v^{i}} \subset \Gamma_y \qquad \text{or} \qquad \Gamma_{\Psi_v^{\circ}} \cdot \Gamma_{\Psi_v^{i}} \subset \Gamma_z$$

The considerations on the symmetries of the ground and excited states and the above conditions lead to the selection rule for infrared spectroscopy: *A fundamental vibration will be infrared active if the corresponding normal mode belongs to the same irreducible representation as one or more of the Cartesian coordinates.*

The selection rule for Raman spectroscopy can also be derived by similar reasoning. It says: *A fundamental vibration will be Raman active if the normal mode undergoing the vibration belongs to the same irreducible representation as one or more of the components of the polarizability tensor of the molecule.* These components are the quadratic functions of the Cartesian coordinates given in the fourth area of the character tables. The Cartesian coordinates themselves are given in the third area. Thus, the symmetry of the normal modes of a molecule is sufficient information to tell what transitions will be infrared and what transitions will be Raman active. The normal modes of the water molecule belong to the A_1 and B_2 irreducible representation of the C_{2v} point group. By using merely the C_{2v} character table, it can be deduced that all three vibrational modes will be active in both the infrared and Raman spectra.

Since a particular normal mode may belong to different symmetry species in different point groups, its behavior depends strongly on the molecular symmetry. Just to mention one example, the ν_1 symmetric

stretching mode of an AX_3 molecule is not infrared active if the molecule is planar (D_{3h}). It is infrared active, however, if the molecule is pyramidal (C_{3v}). Vibrational spectroscopy is obviously one of the best experimental tools to determine the symmetry of molecules.

5.4. Examples

The utilization of symmetry rules in the description of molecular vibrations will be further illustrated by a few examples.

Diimide, HNNH. This molecule belongs to the C_{2h} point group (see Figure 4-7). The number of atoms is 4, so the number of normal vibrations is $3 \times 4 - 6 = 6$.

Our first task is to generate the representation of the Cartesian displacement vectors of the four atoms of the molecule (see Figure 4-8a–c). As was shown in Chapter 4 (Section 4.7), the representation is

$$\Gamma_{\text{tot}} \quad 12 \quad 0 \quad 0 \quad 4$$

The reduction of this representation is also given in Chapter 4 (see p. 208). The result is

$$\Gamma_{\text{tot}} = 4A_g + 2B_g + 2A_u + 4B_u$$

These 12 irreducible representations account for the 12 degrees of motional freedom of HNNH. Subtracting the irreducible representations corresponding to the translation and rotation of the molecule (see C_{2h} character table, Table 5-2) leaves us the symmetry species of the normal modes of vibration:

$$\begin{array}{rlllll}
\Gamma_{\text{tot}} & = 4A_g & + 2B_g & + 2A_u & + 4B_u & \\
-\,(\Gamma_{\text{tran}} & = & & + \;\; A_u & + 2B_u &) \\
-\,(\Gamma_{\text{rot}} & = \;\; A_g & + 2B_g & & &) \\
\hline
\Gamma_{\text{vib}} & = 3A_g & & + \;\; A_u & + 2B_u &
\end{array}$$

Next we will see what kind of internal coordinate changes can account for each of these normal modes. There will have to be two N–H stretching modes and one N–N stretching mode. For deformation

Table 5-2. The C_{2h} Character Table and the Representations of the Internal Coordinates of Diimide

C_{2h}	E	C_2	i	σ_h		
A_g	1	1	1	1	R_z	x^2, y^2, z^2, xy
B_g	1	–1	1	–1	R_x, R_y	xz, yz
A_u	1	1	–1	–1	z	
B_u	1	–1	–1	1	x, y	
Γ_{NH}	2	0	0	2	$=A_g + B_u$	
Γ_{NN}	1	1	1	1	$=A_g$	
Γ_{NNH}	2	0	0	2	$=A_g + B_u$	
Γ_{HNNH} [a]	1	1	–1	–1	$=A_u$	

[a] Out-of plane deformation mode.

modes the two N–N–H angle bending modes are obvious choices, and they will be in-plane deformation modes. These constitute five normal vibrations so one is left to be accounted for. In deciding the nature of this normal mode, inspection of the character table may help. Of the above three different kinds of irreducible representations, A_g and B_u are symmetric with respect to σ_h so they must be vibrations within the molecular plane. The five vibrational modes suggested above then account for $3A_g + 2B_u$. The remaining A_u normal mode, however, is antisymmetric with respect to σ_h, so it must involve out-of-plane motion. Consequently, this normal mode will be an out-of-plane deformation mode.

We will work out next the representations of the internal coordinates. The representation of the two N–H distance changes has been given in Chapter 4 (Section 4.3). This and the other representations are all shown in Table 5-2, together with the C_{2h} character table. The Γ_{NH} representation has been reduced to $A_g + B_u$ in Chapter 4 (Section 4.8). The reduction of the Γ_{NNH} representation is the same. Both the N–N stretching and the out-of-plane deformation are already irreducible representations by themselves. Since A_g occurs three times, we cannot tell without calculation whether there will be three pure A_g modes, one N–H stretch, one N–N stretch, and one N–N–H bend, or each of the three A_g modes will be a mixture of these three vibrations. Similarly, there are two B_u symmetry normal vibrations, and they will be either pure N–H antisymmetric stretching and N–N–H bending modes or their mixtures. The only unambiguous assignment is that

the A_u symmetry normal mode will be the out-of-plane deformation mode.

Generate now the symmetry coordinates of HNNH by means of the projection operator (α is the N–N–H angle):

$$
\begin{aligned}
\hat{P}^{A_g}\Delta r_1 &\approx 1\cdot E\cdot\Delta r_1 + 1\cdot C_2\cdot\Delta r_1 + 1\cdot i\cdot\Delta r_1 + 1\cdot\sigma_h\cdot\Delta r_1\\
&= \Delta r_1 + \Delta r_2 + \Delta r_2 + \Delta r_1 \approx \Delta r_1 + \Delta r_2\\
\hat{P}^{B_u}\Delta r_1 &\approx 1\cdot E\cdot\Delta r_1 + (-1)\cdot C_2\cdot\Delta r_1 + (-1)\cdot i\cdot\Delta r_1\\
&\quad + 1\cdot\sigma_h\cdot\Delta r_1 =\\
&= \Delta r_1 - \Delta r_2 - \Delta r_2 + \Delta r_1 \approx \Delta r_1 - \Delta r_2\\
\hat{P}^{A_g}\Delta\alpha_1 &\approx 1\cdot E\cdot\Delta\alpha_1 + 1\cdot C_2\cdot\Delta\alpha_1 + 1\cdot i\cdot\Delta\alpha_1 + 1\cdot\sigma_h\cdot\Delta\alpha_1\\
&= \Delta\alpha_1 + \Delta\alpha_2 + \Delta\alpha_2 + \Delta\alpha_1 \approx \Delta\alpha_1 + \Delta\alpha_2\\
\hat{P}^{B_u}\Delta\alpha_1 &\approx 1\cdot E\cdot\Delta\alpha_1 + (-1)\cdot C_2\cdot\Delta\alpha_1 + (-1)\cdot i\cdot\Delta\alpha_1\\
&\quad + 1\cdot\sigma_h\cdot\Delta\alpha_1 =\\
&= \Delta\alpha_1 - \Delta\alpha_2 - \Delta\alpha_2 + \Delta\alpha_1 \approx \Delta\alpha_1 - \Delta\alpha_2.
\end{aligned}
$$

The same procedure is depicted in Figure 5-7. The forms of the symmetry coordinates of HNNH are shown in Figure 5-8. They might approximate well the normal modes of the molecule, and again, they might not.

Finally, let us decide which normal modes will be infrared active and which ones will be Raman active. The Cartesian coordinates belong to the A_u and B_u irreducible representation of the C_{2h} point group, while their binary products belong to A_g and B_g. Consequently, the selection rules are:

Infrared active: A_u, B_u
Raman active: A_g.

This means that the A_g symmetry stretching modes and the A_g symmetry bending mode will be Raman active, while the B_u symmetry stretching and bending modes will be infrared active. Similarly, the A_u symmetry out-of-plane deformation mode will be infrared active.

Carbon dioxide, CO_2. The molecule is linear and belongs to the $D_{\infty h}$ point group. The number of atoms is 3, so the number of normal vibrations is: $3 \times 3 - 5 = 4$.

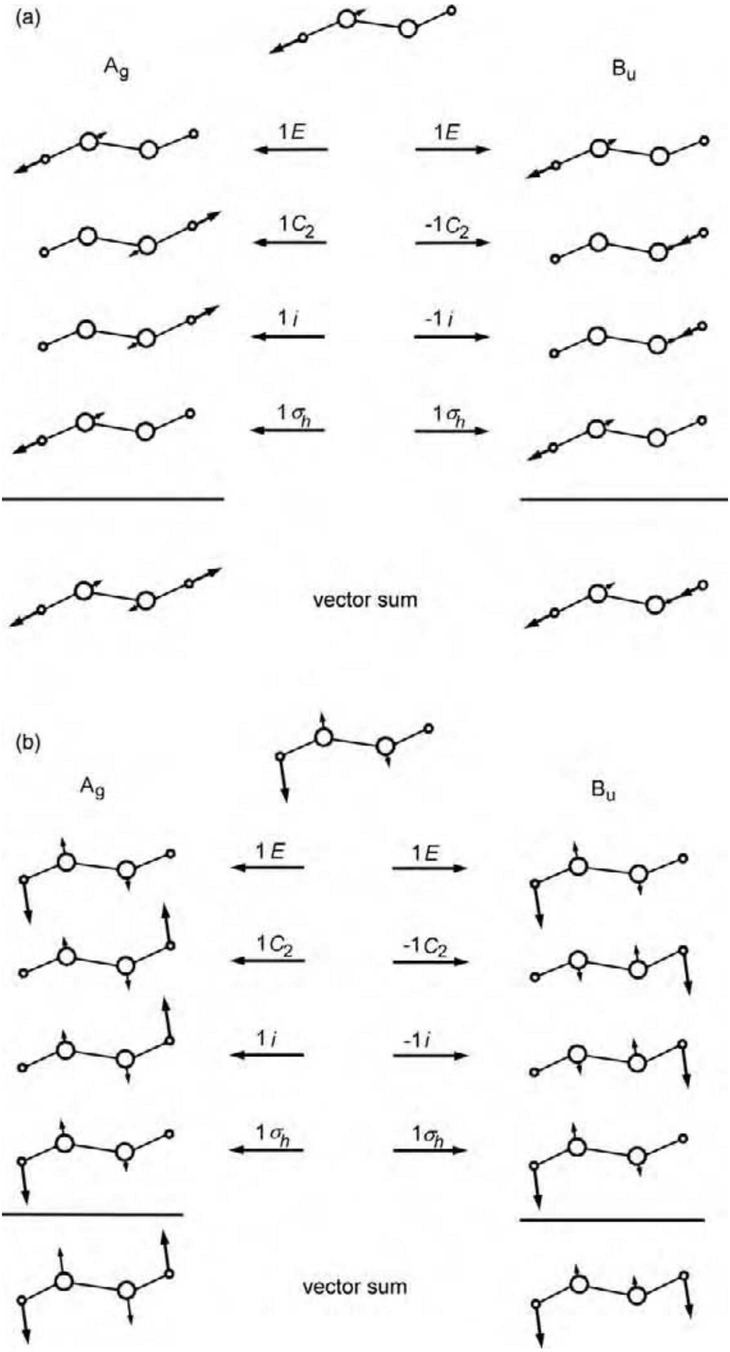

Figure 5-7. Generation of some symmetry coordinates of HNNH; (**a**) Symmetry coordinates corresponding to N–H bond stretches; (**b**) Symmetry coordinates representing in-plane deformation.

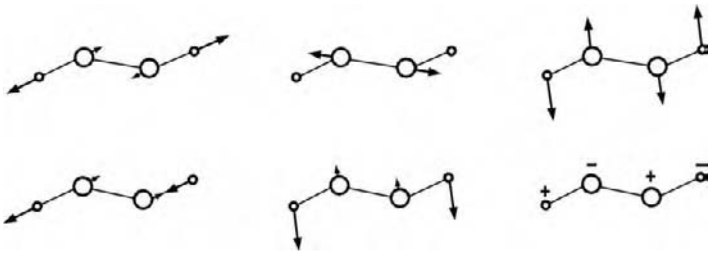

Figure 5-8. Symmetry coordinates for the HNNH molecule.

The set of Cartesian displacement vectors as basis for a representation is shown in Figure 5-9. The symmetry operations of the point group are also shown. The $D_{\infty h}$ character table is given in Table 5-3. Recall (Chapter 4) that the matrix of rotation by an angle Φ is

$$C^{\Phi} = \begin{bmatrix} \cos\Phi & -\sin\Phi \\ \sin\Phi & \cos\Phi \end{bmatrix}$$

The rotation by an arbitrary angle Φ will leave the three z coordinates unchanged and the x and y coordinates mixed according to the above expression. The following matrix represents the C^{Φ} rotation:†

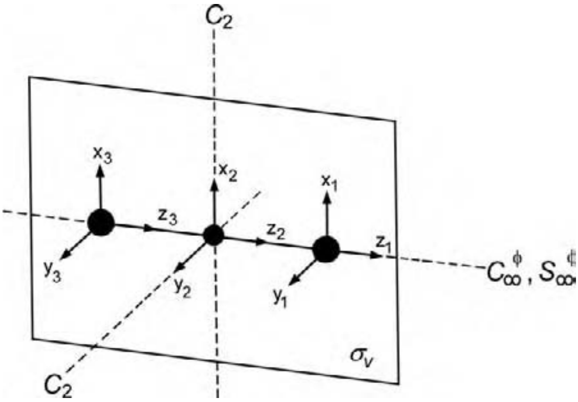

Figure 5-9. Cartesian displacement vectors of CO_2.

†cos is abbreviated by c and sin by s in the matrix.

Table 5-3. The $D_{\infty h}$ Character Table[a]

$D_{\infty h}$	E	$2C_\infty^\Phi$	...	$\infty\sigma_v$	i	$2S_\infty^\Phi$	...	∞C_2		
Σ_g^+	1	1	...	1	1	1	...	1		x^2, y^2, z^2
Σ_g^-	1	1	...	–1	1	1	...	–1	R_z	
Π_g	2	2cΦ	...	0	2	–2cΦ	...	0	(R_x, R_y)	(xz, yz)
Δ_g	2	2c2Φ	...	0	2	2c2Φ	...	0		$(x^2\text{-}y^2, xy)$
...	..	...	...	..	..	...	...	..		
Σ_u^+	1	1	...	1	–1	–1	...	–1	z	
Σ_u^-	1	1	...	–1	–1	–1	...	1		
Π_u	2	2cΦ	...	0	–2	2cΦ	...	0	(x, y)	
Δ_u	2	2c2Φ	...	0	–2	–2c2Φ	...	0		
...	..	...	...	..	..	...	...	..		

[a] c stands for cos.

$$
\begin{array}{c} \\ x_1' \\ y_1' \\ z_1' \\ x_2' \\ y_2' \\ z_2' \\ x_3' \\ y_3' \\ z_3' \end{array}
\begin{array}{c}
\begin{array}{ccccccccc} x_1 & y_1 & z_1 & x_2 & y_2 & z_2 & x_3 & y_3 & z_3 \end{array} \\
\begin{bmatrix}
c\Phi & -s\Phi & 0 & 0 & 0 & 0 & 0 & 0 & 0 \\
s\Phi & c\Phi & 0 & 0 & 0 & 0 & 0 & 0 & 0 \\
0 & 0 & 1 & 0 & 0 & 0 & 0 & 0 & 0 \\
0 & 0 & 0 & c\Phi & -s\Phi & 0 & 0 & 0 & 0 \\
0 & 0 & 0 & s\Phi & c\Phi & 0 & 0 & 0 & 0 \\
0 & 0 & 0 & 0 & 0 & 1 & 0 & 0 & 0 \\
0 & 0 & 0 & 0 & 0 & 0 & c\Phi & -s\Phi & 0 \\
0 & 0 & 0 & 0 & 0 & 0 & s\Phi & c\Phi & 0 \\
0 & 0 & 0 & 0 & 0 & 0 & 0 & 0 & 1
\end{bmatrix}
\end{array}
$$

The character will be: 3 + 6 cosΦ. The other relatively complicated operation is the mirror-rotation by an arbitrary angle, S^Φ. This operation means a rotation around the z axis by angle Φ, followed by reflection through the xy plane. This reflection interchanges the positions of the two oxygen atoms so they need not be considered. The block matrix of the S^Φ operation will be:

$$\begin{array}{c} \\ x_2' \\ y_2' \\ z_2' \end{array} \begin{array}{c} \begin{array}{ccc} x_2 & y_2 & z_2 \end{array} \\ \begin{bmatrix} \cos\Phi & -\sin\Phi & 0 \\ \sin\Phi & \cos\Phi & 0 \\ 0 & 0 & -1 \end{bmatrix} \end{array}$$

The character is: –1 + 2 cos Φ.

Omitting the details of the determination of the remaining characters, the representation of the Cartesian displacement vectors is:

$$\Gamma_{\text{tot}} \quad 9 \quad 3+6\cos\Phi \quad 3 \quad -3 \quad -1+2\cos\Phi \quad -1$$

Subtract the characters of the translational and rotational representations. Remember that CO_2 is linear and the rotation around the molecular axis need not be taken into account.

$$\begin{array}{rcllllll} \Gamma_{\text{tot}} & = & 9 & 3+6\cos\Phi & 3 & -3 & -1+2\cos\Phi & -1 \\ -(\Gamma_{\text{tran}} & = & 3 & 1+2\cos\Phi & 1 & -3 & -1+2\cos\Phi & -1) \\ -(\Gamma_{\text{rot}} & = & 2 & 2\cos\Phi & 0 & 2 & -2\cos\Phi & 0) \\ \hline \Gamma_{\text{vib}} & = & 4 & 2+2\cos\Phi & 2 & -2 & 2\cos\Phi & 0 \end{array}$$

The reduction formula cannot be applied to the infinite point groups (Chapter 4). Here inspection of the character table may help. Since 2 cosΦ at S_∞^Φ appears with the Π_u irreducible representation, it is worth a try to subtract this one from Γ_{vib}:

$$\begin{array}{rcllllll} \Gamma_{\text{vib}} & = & 4 & 2+2\cos\Phi & 2 & -2 & 2\cos\Phi & 0 \\ -(\Gamma_{\Pi_u} & = & 2 & 2\cos\Phi & 0 & -2 & 2\cos\Phi & 0) \\ \hline & & 2 & 2 & 2 & 0 & 0 & 0 \end{array}$$

This representation can be resolved as the sum of Σ_g and Σ_u:

$$\begin{array}{lcrrrrrr} \Sigma_g & = & 1 & 1 & 1 & 1 & 1 & 1 \\ \Sigma_u & = & 1 & 1 & 1 & -1 & -1 & -1 \\ \hline \Sigma_g + \Sigma_u & = & 2 & 2 & 2 & 0 & 0 & 0 \end{array}$$

Thus, the normal modes of the CO_2 molecule will be

$$\Gamma_{\text{vib}} = \Sigma_g + \Sigma_u + \Pi_u$$

Since Π_u is a degenerate vibration, it counts as two, and so we indeed have the four necessary normal vibrations.

The obvious choice for the three internal coordinate changes is the stretching of the two C=O bonds and the bending of the O=C=O angle. Using these as bases for representations we can build up the symmetry coordinates.

Γ_{str}	2	2	2	0	0	0

We have already seen before that this representation reduces as $\Sigma_g + \Sigma_u$. The Π_u normal mode will correspond to the bending vibration.

Since each of the three symmetry species, Σ_g, Σ_u, and Π_u appears only once, the symmetry coordinates will be good representations of the normal modes. There is no possibility for mixing. Figure 5-10 shows the forms of the normal vibrations of the CO_2 molecule. The two bending modes are degenerate; they are of equal energy.

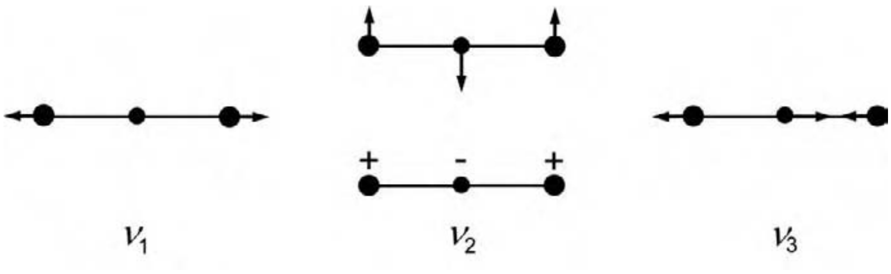

Figure 5-10. Normal modes of vibration of the CO_2 molecule.

Finally, apply the vibrational selection rules to CO_2:

Infrared active: Σ_u, Π_u
Raman active: Σ_g

Accordingly, the symmetric stretching C=O normal mode should appear in the Raman spectrum, while the antisymmetric stretching and the degenerate bending modes are expected to appear in the infrared spectrum.

References

1. A. L. Mackay, *A Dictionary of Scientific Quotations*, Adam Hilger, Bristol, 1991. p. 84/55.
2. D. C. Harris, M. D. Bertolucci, *Symmetry and Spectroscopy: An Introduction to Vibrational and Electronic Spectroscopy*, Oxford University Press, New York, 1978.
3. F. A. Cotton, *Chemical Application of Group Theory*, Third Edition, Wiley-Interscience, New York, 1990.
4. M. Orchin, H. H. Jaffe, *Symmetry, Orbitals, and Spectra (S.O.S)*, Wiley-Interscience, New York, 1971.
5. G. Herzberg, *Infrared and Raman Spectra*, Van Nostrand Company, Princeton, NJ, 1959.
6. E. B. Wilson, Jr., J. C. Decius, P. C. Cross, *Molecular Vibrations*, McGraw-Hill Book Co., New York, 1955.
7. Harris, Bertolucci, *Symmetry and Spectroscopy*, pp. 171–173.
8. Wilson, Decius, Cross, *Molecular Vibrations*.
9. K. Nakamoto, *Infrared Spectra of Inorganic and Coordination Compounds*, Second Edition, John Wiley and Sons, New York, 1970.

Chapter 6

Electronic Structure of Atoms and Molecules

An atom must be at least as complex as a grand piano.
William K. Clifford [1]

Everything that counts in chemistry is related to the electronic structure of atoms and molecules. The formation of molecules from atoms, their behavior and reactivity all depend on the electronic structure. What is the role of symmetry in all this? In various aspects of the electronic structure, symmetry can tell us a good deal; why certain bonds can form and others cannot, why certain electronic transitions are allowed and others are not, and why certain chemical reactions occur and others do not. Our discussion of these points is based primarily on some monographs listed in References [2–8].

To describe the electronic structure, the electronic wave function $\Psi(x, y, z, t)$ is used, which depends, in general, on both space and time. Here, however, only its spatial dependence will be considered, $\Psi(x, y, z)$. For detailed discussions of the nature of the electronic wave function, we refer to texts on the principles of quantum mechanics [9–12]. For a one-electron system the physical meaning of the electronic wave function is expressed by the product of Ψ with its complex conjugate Ψ^*. The product $\Psi^* \cdot \Psi \, d\tau$ gives the probability of finding an electron in the volume $d\tau = dx\, dy\, dz$ about the point (x, y, z).

A many-electron system is described by a similar but multivariable wave function

$$\Psi(x_1, y_1, z_1, \ldots, x_i, y_i, z_i, \ldots, x_n, y_n, z_n).$$

M. Hargittai, I. Hargittai, *Symmetry through the Eyes of a Chemist,* 3rd ed.,
DOI: 10.1007/978-1-4020-5628-4_6, © Springer Science+Business Media B.V. 2009

The product $\Psi^*\cdot\Psi\, d\tau$ gives the probability of finding the first electron in $d\tau_1$, about the point (x_1, y_1, z_1), and the ith electron in $d\tau_i$ about the point (x_i, y_i, z_i), all at the same time.

The symmetry properties of the electronic wave function and the energy of the system are two determining factors in chemical behavior. The relationship between the wave function characterizing the behavior of the electrons and the energy of the system—atoms and molecules—is expressed by the Schrödinger equation. In its general and time-independent form, it is usually written as follows,

$$\hat{H}\Psi = E\Psi \tag{6-1}$$

where $\hat{H}$ is the Hamiltonian operator and E is the energy of the system.

The Hamiltonian operator is an energy operator, which includes both kinetic and potential energy terms for all particles of the system. In our discussion, only its symmetry behavior will be considered. With respect to the interchange of like particles (either nuclei or electrons) the *Hamiltonian must be unchanged* under a symmetry operation. A symmetry operation carries the system into an equivalent configuration, which is indistinguishable from the original. However, if nothing changes with the system, its energy must be the same before and after the symmetry operation. Thus, the Hamiltonian of a molecule is *invariant* to any symmetry operation of the point group of the molecule. This means that it belongs to the totally symmetric representation of the molecular point group.

A fundamental property of the wave function is that it can be used as basis for irreducible representations of the point group of a molecule [13]. This property establishes the connection between the symmetry of a molecule and its wave function. The preceding statement follows from Wigner's theorem, which says that all eigenfunctions of a molecular system belong to one of the symmetry species of the group [14].

In the expression of the energy of a system the following type of integral appears:

$$\int \Psi_i \hat{H} \Psi_j d\tau$$

Depending on the problem, Ψ_i and Ψ_j may be atomic orbitals used to construct molecular orbitals, or they may represent two different

electronic states of the same atom or molecule, etc. The energy, then, expresses the extent of interaction between the two wave functions Ψ_i and Ψ_j. As was shown in Chapter 4, an integral will have a nonzero value only if the integrand is invariant to the symmetry operations of the point group, i.e., it belongs to the totally symmetric irreducible representation.

The above energy integral contains the $\hat{H}$ operator, which always belongs to the totally symmetric irreducible representation. Therefore, the symmetry of the whole integrand depends on the direct product of Ψ_i and Ψ_j. As also was shown in Chapter 4, the direct product of the representations of Ψ_i and Ψ_j belongs to, or contains, the totally symmetric irreducible representation only if Ψ_i and Ψ_j belong to the same irreducible representation. Consequently, *the energy integral will be nonzero only if* Ψ_i and Ψ_j *belong to the same irreducible representation of the molecular point group.*

6.1. One-Electron Wave Function

Before discussing many-electron systems, the hydrogen atom (a one-electron system) will be described. This is essentially the only atomic system for which an exact solution of the wave function is available. The spherical symmetry of the hydrogen atom makes it convenient to express the wave function in a polar coordinate system. Such a system is shown in Figure 6-1 with the proton in the origin. Ignoring the translational motion of the hydrogen atom, the Schrödinger equation can be simplifed as follows [15]:

$$\hat{H}_e\Psi = E\Psi_e \qquad (6\text{-}2)$$

where $\hat{H}_e$ depends only on the coordinates of the electron.

The electronic wave function can be represented as a product of a radial and an angular component:

$$\Psi_e = R(r) \cdot A(\Theta, \Phi) \qquad (6\text{-}3)$$

The radial wave function $R(r)$ depends on two quantum numbers, n and l. The *principal quantum number, n,* determines the electron *shell*. The numbers n = 1, 2, 3, 4, ... correspond to the shells K, L, M, N, respectively. For the hydrogen atom, n completely deter-

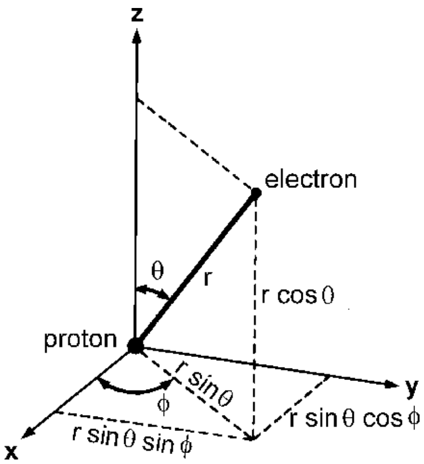

Figure 6-1. The relationship between Cartesian coordinates and spherical polar coordinates, illustrated for the hydrogen atom with the proton at the origin.

mines the energy of the shell, which is inversely proportional to n^2. Since this energy is negative, *E* is smallest for the first (*K*) shell, and increases with increasing *n*. The *azimuthal quantum number, l,* is associated with the total angular momentum of the electron and determines the shape of the *orbitals.* It may have integral values from 0 to *n* – 1. The *s, p, d, f, ...* orbitals correspond to the azimuthal quantum numbers, *l* = 0, l, 2, 3, ..., respectively.

The angular wave function *A*(Θ, Φ) depends also on two quantum numbers, *l* and m_l. The *magnetic quantum number,* m_l, is associated with the component of angular momentum along a specific axis in the atom. Since the hydrogen atom is spherically symmetrical, it is not possible to define a specific axis until the atom is placed in an external electric or magnetic field. This also means that the quantum number m_l has no effect on the energy and shape of the wave function of the hydrogen atom in the absence of such an external field. Generally, m_l may have values –*l*, –*l*+1, ..., 0, ..., *l*–1, *l,* altogether 2*l*+1 of them, and the orbitals are subdivided accordingly.

Usually we refer to the energy of orbitals while what is really meant is the energy of an electron in that orbital. It was mentioned earlier that only the principal quantum number *n* influences the orbital energy in the hydrogen atom. This means that while 1*s* and 2*s* orbitals have different energies, the 2*s* and all three 2*p* orbitals have the same

energy, i.e., these four n = 2 orbitals are degenerate in the hydrogen atom.

In many-electron atoms the value of l also influences the energy of the orbitals; thus, the 2*s* and 2*p* orbitals, the 3*s*, 3*p*, and 3*d* orbitals, or the 4*s*, 4*p*, 4*d*, and 4*f* orbitals will no longer be degenerate. However, there are always three *p* orbitals, five *d* orbitals, and seven *f* orbitals in a shell, and they differ only in the quantum number m_l and will be degenerate. As there are $2l + 1$ values of m_l for an orbital with quantum number l, the *p* orbitals (l = 1) will always be threefold degenerate, the *d* orbitals (l = 2) will always be fivefold degenerate, while the *f* orbitals (l = 3) will always be sevenfold degenerate.

Harris and Bertolucci [16] illustrated the relationship between symmetry and degeneracy of energy levels with a simple and attractive example. There are three parrallelepipeds in Figure 6-2. Each of them has six stable resting positions. The potential energy of these positions depends on the height of the center of the mass above the

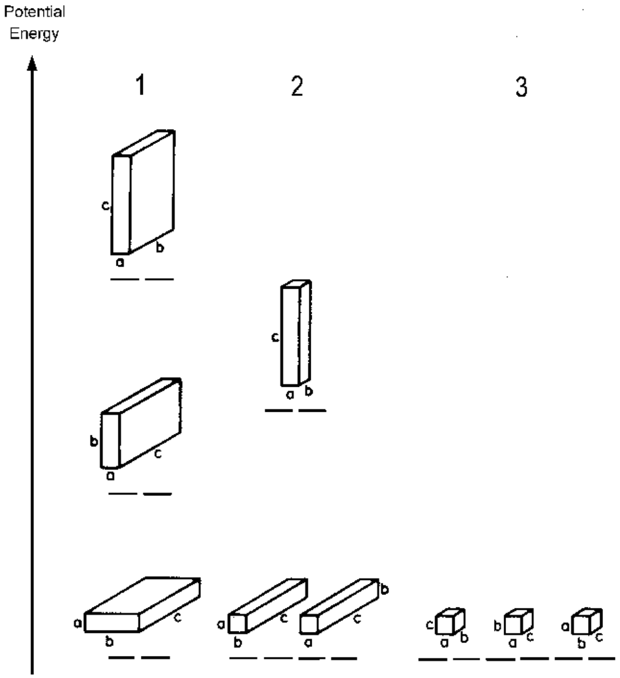

Figure 6-2. Illustration of the interrelation of symmetry and degeneracy after Harris and Bertolucci [17]. Used with permission. See text for details.

supporting surface. This height, in turn, is determined by the choice of face on which the body rests. Three different positions are possible for the first parallelepiped (1) according to its three different kinds of faces. The potential energy of 1 will be largest when it stands on an *ab* face, since its center of mass is at the highest possible position. There are only two energetically different positions for 2 since its center of mass is at the same height when it rests on face *bc* or on face *ac*. Parallelepiped 3 is indeed a cube, and all possible positions will be energetically equivalent. Looking at the degeneracy of the most stable (lowest energy) position, it is twofold degenerate for 1, four-fold degenerate for 2, and six-fold degenerate for the cube. Thus, with increasing symmetry, the degree of degeneracy increases. The connection between symmetry and degeneracy is strikingly obvious. *The greater the degree of symmetry the smaller will be the number of different energy levels and the greater will be the degeneracy of these levels.*

This correlation between symmetry and degeneracy of energy levels is fundamental to understanding the electronic structure of atoms and molecules. This relationship is valid not only when increasing symmetry renders the energy levels degenerate but also when energy levels are split as molecular symmetry decreases.

Let us now return to the wave function description of electronic structure. The separation of the wave function into two parts is convenient since these two parts relate to different properties. The radial part determines the energy of the system and is invariant to symmetry operations. The square of the radial function is related to probability. If we fix the angular variables, Θ and Φ, they define a direction from the nucleus. Then the square of the radial function is proportional to the probability of finding the electron in a volume element along this direction. In order to determine the probability of finding the electron anywhere in a spherical shell surrounding the nucleus at a distance r from the nucleus, integration over both angular variables must be performed. The result is the radial distribution function.

Consider now the angular part of the one-electron wave function. It says nothing about the energy of the system but it can be altered by symmetry operations. Therefore, we shall be dealing with this function in greater detail. The function $A(\Theta, \Phi)$ may have different signs (+ and –) in different spatial regions. A change in sign indicates a drastic change in the wave function. These signs might be thought

of as signs of the amplitudes of the wave function; they certainly have nothing to do with electric charges. The places where the wave function changes sign are called *nodes*. The number of nodes is n–1, where n is the principal quantum number. Again, the squared function has physical significance; it is positive everywhere. The probability of finding an electron at a node is zero. However, as one proceeds in either direction from the nodes, the squared wave function has equal values relating to equal probabilities; to wit, the probability of finding the electron on the "positive" or "negative" side of the wave function is equal.

It usually helps to visualize and understand a problem in a pictorial way. However, since the wave function depends upon three variables, it can be represented only in four dimensions. To overcome this problem, symbolic representations are used to emphasize various properties of the wave function.

The angular wave function, $A(\Theta, \Phi)$, is shown for the H 1*s* and $2p_z$ orbitals in Figure 6-3a. The H 1*s* orbital is positive everywhere, but the $2p_z$ orbital has one node, through which it changes sign. The $A^2(\Theta, \Phi)$ function is shown for the same orbitals in Figure 6-3b. For both orbitals, the shape of this function is similar to the shape of the $A(\Theta, \Phi)$ function, but this function is positive everywhere. It represents the region in space where the electron can be found with a large probability (usually 90 % or more). The boundary surface of this space is determined by the square of the angular function. The squared angular function does not say anything, however, about the variation of the probability density within this surface. That information is contained in the radial distribution function. A way to illustrate the latter is shown for the 1*s* and $2p_z$ orbitals in Figure 6-3c, where a cross section of the electron density

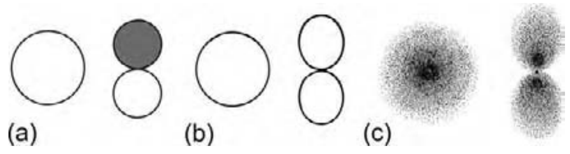

Figure 6-3. Representations of the hydrogen 1*s* and $2p_z$ orbitals; **(a)** Plot of the angular wave function, $A(\Theta, \Phi)$; **(b)** Plot of the squared function, $A^2(\Theta, \Phi)$; **(c)** Cross section of the squared total wave function, Ψ^2, representing the electron density. Reprinted by permission of Thomas H. Lowry [18].

distribution is depicted. The varying amount of shading reflects the square of the radial function. Thus, this picture represents the squared total wave function, Ψ^2. Rotating this picture around any axis for the 1*s* orbital and around the *z* axis for the $2p_z$ orbital would give the three-dimensional representation of the total wave function.

Whereas the square of the angular function has outstanding physical significance, the angular function itself contains valuable information regarding the symmetry properties of the wave function. These properties are lost in the squared angular function.

The well-known shapes of the one-electron orbitals are presented in Figure 6-4; these are, in fact, representations of the angular wave functions. The *f* orbitals will not be discussed further, since their participation in chemical bonding is limited. The representations depicted in Figure 6-4 are used commonly for illustrations because they describe accurately the symmetry properties of the wave function. In order to give the total wave function, however, they must be multiplied by an appropriate radial function. Another representation, shown in Figure 6-5, is a three-dimensional computer drawing of the total function including *both* the radial and the angular functions. These are still *not* real "pictures" of the orbitals, since they represent a cross section of the wave function in one plane only. The vertical scale gives the value of Ψ for each point in the *xy* plane. These diagrams show how the sign and magnitude of Ψ vary in the *xy* plane, and they also help us visualize the electronic wave function as a wave. On the other hand, they do not illustrate its symmetry properties so well as do the simple diagrams in Figure 6-4.

As mentioned before, the symmetry properties of the one-electron wave function are shown by the simple plot of the angular wave function. But, what are the symmetry properties of an orbital and how can they be described? We can examine the behavior of an orbital under the different symmetry operations of a point group. This will be illustrated below via the inversion operation.

The *s* and *d* orbitals are transformed into themselves as the inversion operation is applied to them (Figure 6-6). Both the magnitude and the "sign" of the wave function will remain the same under the inversion operation. These orbitals are said to be *symmetric* with respect to inversion. The effect of the inversion operation on the *p* orbitals is demonstrated in Figure 6-7. Whereas their magnitude does

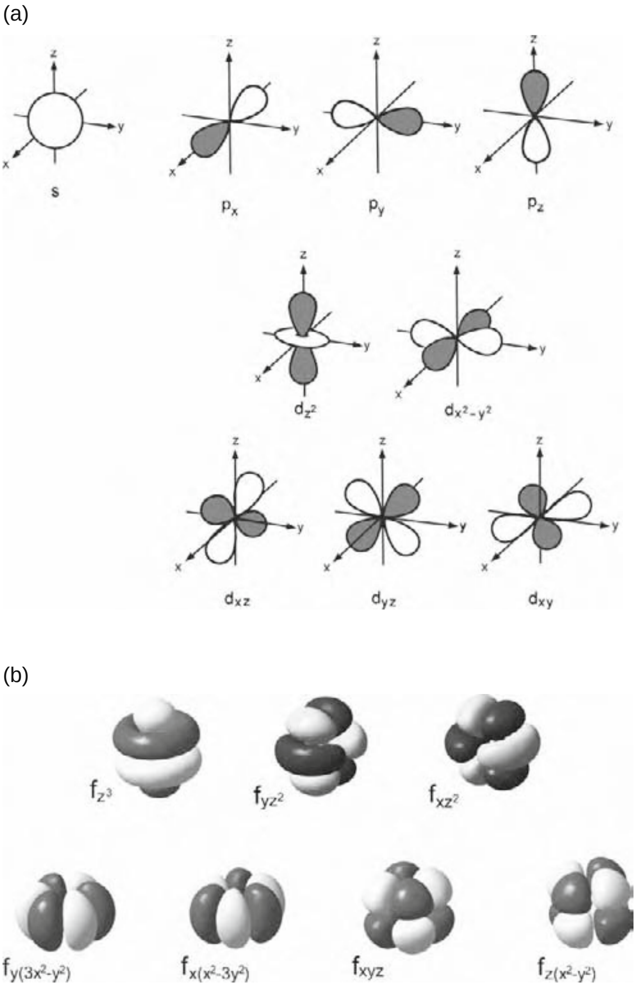

Figure 6-4. Shapes of one-electron orbitals. They are representations of the angular wave function, $A(\Theta, \Phi)$: **(a)** *s*, *p*, and *d* orbitals; **(b)** *f* orbitals.

not change, their "sign" changes upon inversion. These orbitals are said to be *antisymmetric* with respect to inversion. In the character tables, this is indicated by +1 for symmetric and –1 for antisymmetric behavior under each symmetry operation. As mentioned in Chapter 4, the atomic orbitals always belong to the same irreducible representations of the given point group as do their subscripts (x, y, z, xy, $x^2 - y^2$, etc.).

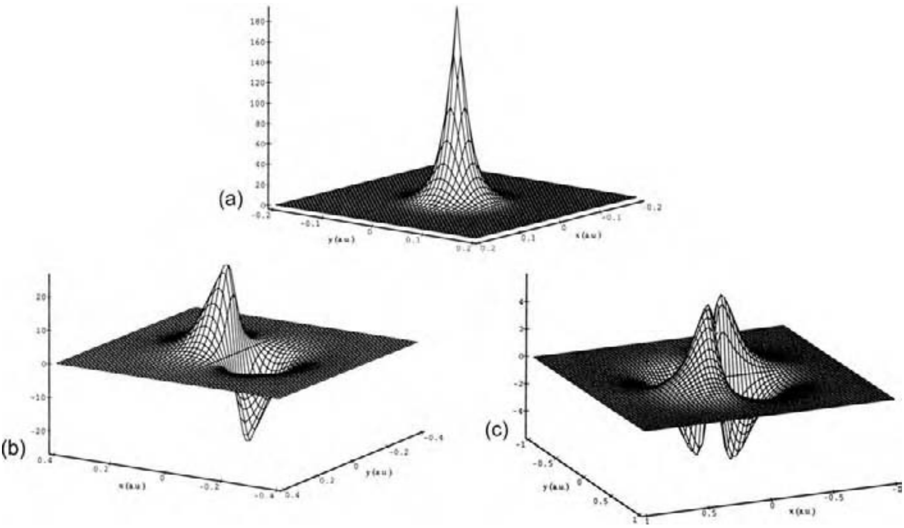

Figure 6-5. Three-dimensional computer drawings of the total wave function, Ψ, of the iodine atom, calculated with a 3-21G basis set [19]. They show the values of Ψ in a cross section. Courtesy of István Kolossváry. **(a)** 1*s* orbital; **(b)** $2p_x$ orbital; **(c)** $3d_{xy}$ orbital.

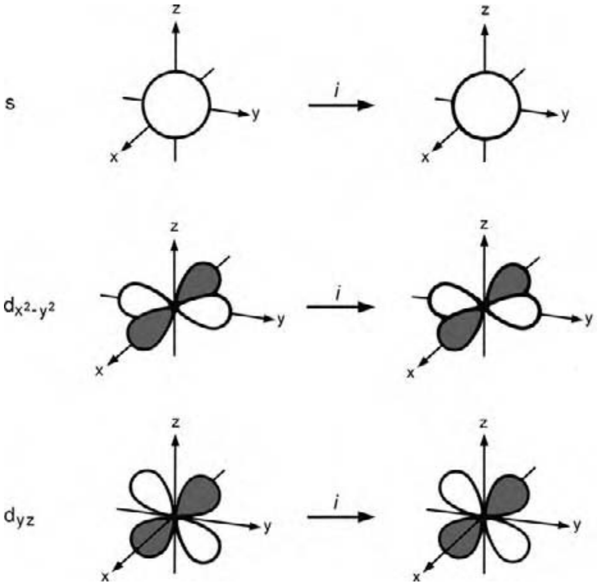

Figure 6-6. The effect of inversion on the *s* and *d* orbitals. They are symmetric to this operation.

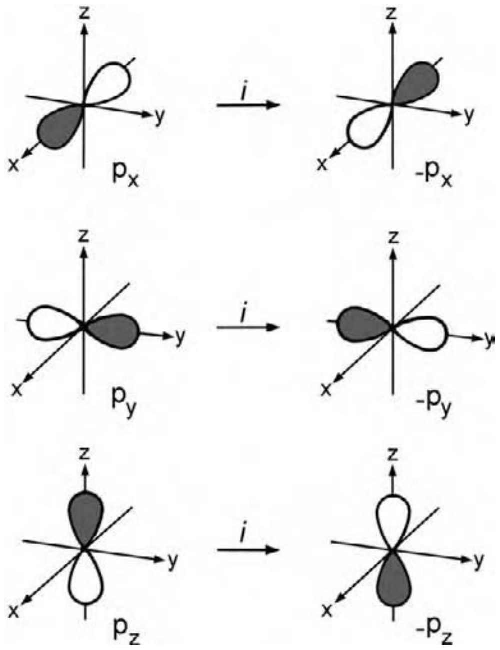

Figure 6-7. The effect of inversion on the *p* orbitals. They are antisymmetric to inversion, as the inversion operation changes their sign.

6.2. Many-Electron Atoms

There is interaction among all the electrons in a many-electron atom. Thus, the wave function for even one electron in a many-electron system will, in principle, be different from the wave function for the one electron in the hydrogen atom. Since the electrons are mutually indistinguishable, it is not possible to describe rigorously the properties of a single electron in such a system. There is no exact solution to this problem, and approximate methods must be adopted.

In the most commonly utilized approximation, the many-electron wave functions are written in terms of products of one-electron wave functions similar to the solutions obtained for the hydrogen atom. These one-electron functions used to construct the many-electron wave function are called *atomic orbitals.* They are also called "hydrogen-like" orbitals since they are one-electron orbitals and also because their shape is similar to that of the hydrogen atom orbitals.

Coulson referred to the atomic orbitals as "personal wave functions" to emphasize that each electron is allocated to an individual orbital in this model [20].

At this point we can, again, appreciate the possibility of separating the total wave function into a radial and an angular wave function. The angular wave function does not depend on *n* and *r*, so it will be the same for every atom. This is why the "shapes"of atomic orbitals are always the same. Hence, symmetry operations can be applied to the orbitals of all atoms in the same way. The differences occur in the radial part of the wave function; the radial contribution depends on both *n* and *r* and it determines the energy of the orbital, which is, of course, different for different atoms.

While the energy of a one-electron orbital depends only on *n*, in a many-electron atom the energy of the orbital is determined by both *n* and *l*. Thus, an electron in a 2*p* orbital has higher energy than an electron in a 2*s* orbital. The order of orbital energies in many-electron atoms is generally as follows:

$$1s < 2s < 2p < 3s < 3p < 4\,s \approx 3d < 4p < 5s < 4d < \ldots$$

There are some cases, however, when the order is changed somewhat. For example, the 3*d* orbital sometimes lies below the 4*s* orbital. A diagram which illustrates the order of orbital energies is shown in Figure 6-8.

In addition to the three quantum numbers used to describe the one-electron wave function, the electron has also a fourth, the *spin quantum number,* m_s. It is related to the intrinsic angular momentum of the electron, called *spin.* This quantum number may assume the values of +½ or –½. Usually the sign of m_s is represented by arrows, (↑ and ↓), or by the Greek letters α and β. Thus, the wave function of an orbital is expressed as

$$\Psi_e = R(r) \cdot A(\Theta, \Phi) \cdot S(s) \tag{6-4}$$

rather than as in Eq. (6-3). However, the introduction of spin does not alter any of the properties discussed previously that relate to the shape and symmetry of the orbitals. The reason is that the spin function is independent of the spatial coordinates.

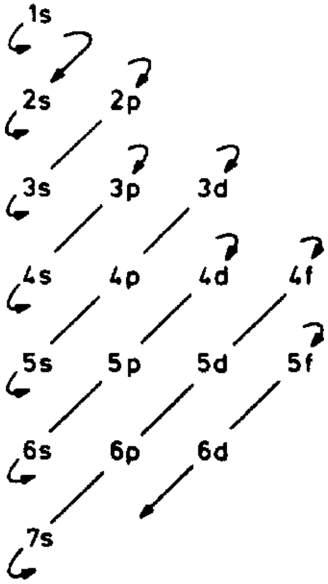

Figure 6-8. The sequence of orbital energies.

An important postulate in connection with the spin of the electron is called the *Pauli principle.* It states that if a system consists of identical particles with half-integral spins, then all acceptable wave functions must be antisymmetric with respect to the exchange of the coordinates of any two particles. In our case, the particles are electrons, and the Pauli principle is formulated accordingly: *No two electrons in an atom can have the same set of values for all four quantum numbers.*

The electronic configuration of an atom tells us how many electrons the atom has in its subshells. A *subshell* is a complete set of orbitals that have the same n and l. The building up of electronic configurations is governed by the Pauli principle and by *Hund's first rule,* according to which, for a given electronic configuration, *the state with the greatest number of unpaired spins has the lowest energy*.

There is a marked periodicity in the electronic configuration of the elements and this is the underlying idea of the periodic table (see Chapter 1). As the chemical properties of the atoms are determined by their electron configuration, the atoms with similar electron configurations will have similar chemical properties.

6.3. Molecules

6.3.1. Constructing Molecular Orbitals

In the discussion of the electronic structure of atoms, the Schrödinger equation could be reduced to one involving only the electrons. This was achieved by separating the electronic energy of the atom from the nuclear kinetic energy, which is essentially determined by the translational motion of the atom.

Such a separation is exact for atoms. For molecules, only the translational motion of the whole system can be rigorously separated, while their kinetic energy includes all kinds of motion, vibration and rotation as well as translation. First, as in the case of atoms, the translational motion of the molecule is isolated. Then a two-step approximation can be introduced. The first is the separation of the rotation of the molecule as a whole, and thus the remaining equation describes only the internal motion of the system. The second step is the application of the Born–Oppenheimer approximation, in order to separate the electronic and the nuclear motion. Since the relatively heavy nuclei move much more slowly than the electrons, the latter can be assumed to move about a fixed nuclear arrangement. Accordingly, not only the translation and rotation of the whole molecular system but also the internal motion of the nuclei is ignored. The molecular wave function is written as a product of the nuclear and electronic wave functions. The electronic wave function depends on the positions of both nuclei and electrons but it is solved for the motion of the electrons only.

As was emphasized before (cf. Chapter 3), a molecule is not simply a collection of its constituting atoms. Rather, it is a system of atomic nuclei and a common electron distribution. Nevertheless, in describing the electronic structure of a molecule, the most convenient way is to approximate the molecular electron distribution by the sum of atomic electron distributions. This approach is called the *linear combination of atomic orbitals* (LCAO) method. The orbitals produced by the LCAO procedure are called *molecular orbitals* (MOs). An important common property of the atomic and molecular orbitals is that both are one-electron wave functions. Combining a certain number of one-electron atomic orbitals yields the same number of one-electron molecular orbitals. Finally, the total molecular wave function is the

sum of products of the one-electron molecular orbitals. Thus, the final scheme is as follows:

One-electron atomic orbitals (AOs)

↓ LCAO

One-electron molecular orbitals (MOs)

↓ multiplication (and summation)

Total molecular wave function

Although both atomic orbitals and molecular orbitals are one-electron wave functions, the shape and symmetry of the molecular orbitals are different from those of the atomic orbitals of the isolated atom. The molecular orbitals extend over the entire molecule, and their spatial symmetry must conform to that of the molecular framework. Of course, the electron distribution is not uniform throughout the molecular orbital. In depicting these orbitals, usually only the portions with substantial electron density are emphasized.

When constructing molecular orbitals from atomic orbitals, there may be a large number of possible linear combinations of the atomic orbitals. Many of these linear combinations, however, are unnecessary. Symmetry is instrumental as a criterion in choosing among them. The following statement is attributed to Michelangelo: “The sculpture is already there in the raw stone; the task of a good sculptor is merely to eliminate the unnecessary parts of the stone.” In the LCAO procedure, the knowledge of symmetry eliminates the unnecessary linear combinations. All those linear combinations must be eliminated that do not belong to any irreducible representation of the molecular point group. The reverse of this statement constitutes the fundamental principle of forming molecular orbitals: *Each possible molecular orbital must belong to an irreducible representation of the molecular point group*. Another equally important rule for the construction of molecular orbitals is that *only those atomic orbitals can form a molecular orbital that belong to the same irreducible representation of the molecular point group.* This rule follows from the general theorem (see p. 210) about the value of an energy integral. This theorem can

be restated for the special case of MO construction as follows: *An energy integral will be nonzero only if the atomic orbitals used for the construction of molecular orbitals belong to the same irreducible representation of the molecular point group.*

The atomic orbitals in an isolated atom possess spherical symmetry. When they are used for MO construction, however, their symmetry must be considered in the symmetry group of the particular molecule. When two atomic orbitals of the same symmetry form a molecular orbital, the symmetry of the molecular orbital will be the same as that of the component atomic orbitals.

In addition to complying with the symmetry rules, successful MO construction requires certain energy conditions. In order for two orbitals to interact appreciably, their energies cannot be too different.

The so-called overlap integral S_{ij} is a useful guide in constructing molecular orbitals. It is symbolized as

$$S_{ij} = \int \psi_i \psi_j \, d\tau \tag{6-5}$$

where ψ_i and ψ_j are the two participating atomic orbitals. The physical meaning of S_{ij} is related to the measure of volume in which there is electron density contributed by both atoms i and j. The knowledge of the sign and magnitude of S_{ij} is especially instructive; they can be arrived at via the following considerations.

Positive overlap results from the combination of adjacent lobes that have the same "sign." The electron density originating from both atoms will increase and concentrate in the region between the two nuclei. The resulting MO is a *bonding orbital.* Some typical bonding atomic orbital combinations are presented in Figure 6-9. Two kinds of molecular orbitals are shown in this figure. A σ orbital is concentrated primarily along the internuclear axis. On the other hand, a π orbital has a nodal plane going through this axis, and its electron density is highest on either side of this nodal plane. The σ orbitals are nondegenerate, while the π orbitals are always doubly degenerate.

Negative overlap results from the combination of adjacent lobes that have opposite "sign." In such an instance, there will be no common electron density in the region between the two nuclei; instead, electron density will concentrate in the outside regions. Such an MO is an *antibonding orbital* and is illustrated in Figure 6-10.

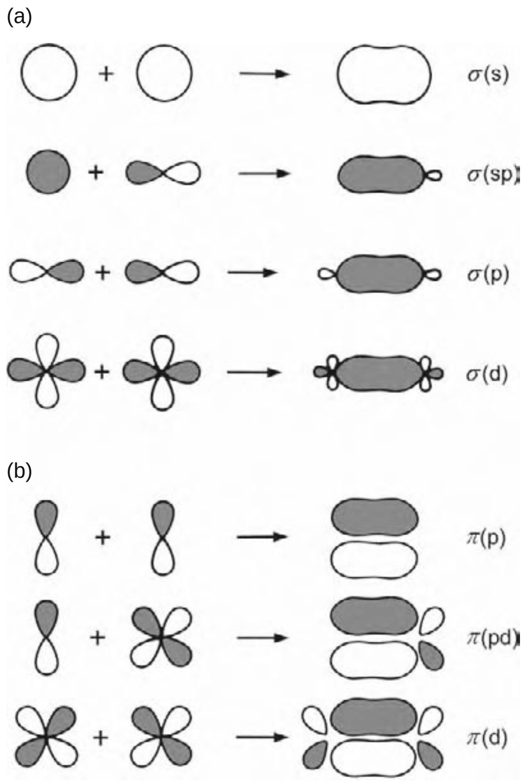

Figure 6-9. Illustration of positive overlap between atomic orbitals. The result is a bonding orbital: **(a)** σ orbitals; **(b)** π orbitals.

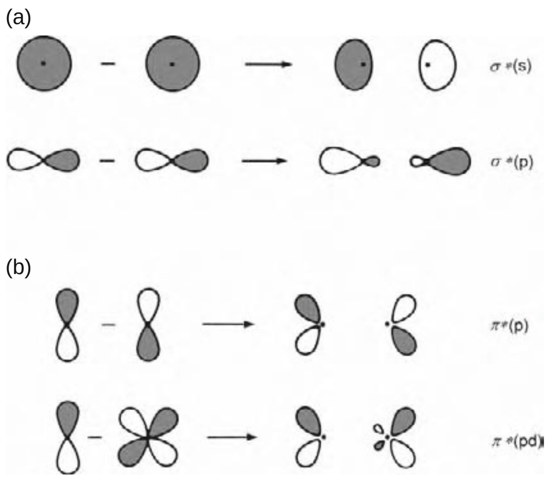

Figure 6-10. Formation of antibonding orbitals by the combination of different lobes of atomic orbitals: **(a)** σ antibonding orbitals; **(b)** π antibonding orbitals.

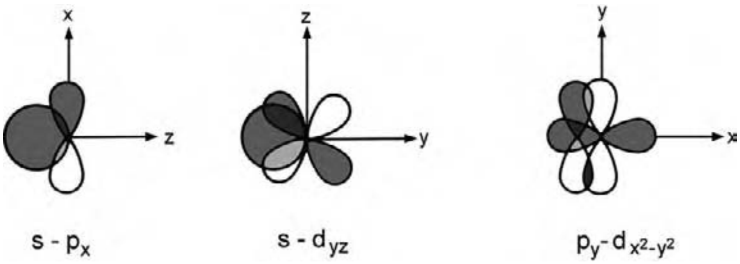

Figure 6-11. Zero overlap between atomic orbitals. There is no net interaction.

Zero overlap means that there is no net interaction between the two atomic orbitals. They have both positive and negative overlaps that cancel each other. Some examples are shown in Figure 6-11.

The energy changes in the formation of homonuclear and heteronuclear diatomic molecules are illustrated in Figure 6-12. The energy of the bonding MO is smaller (larger negative value) than is the energy of the interacting atomic orbitals. On the other hand, the energy of the antibonding MO is larger than is the energy of the interacting atomic orbitals. The largest energy changes occur when the two participating atomic orbitals have equal energies. As the energy difference between the participating atomic orbitals increases, the stabilization of the

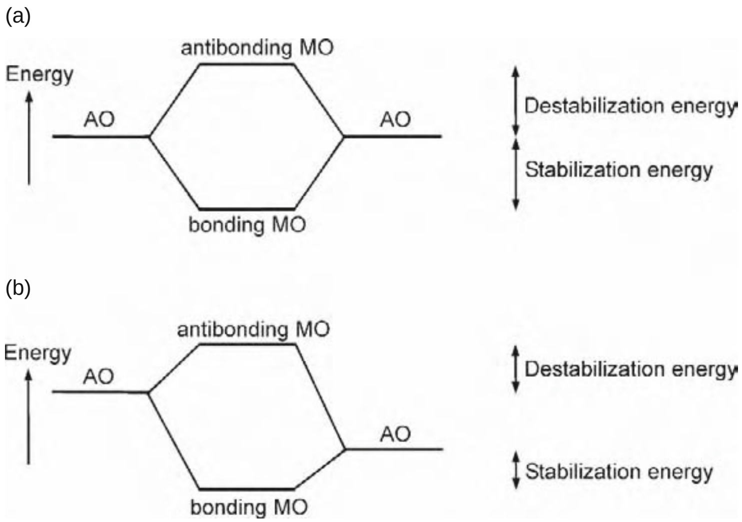

Figure 6-12. Energy changes during MO formation: **(a)** Homonuclear molecules; **(b)** Heteronuclear molecules.

bonding MO decreases. Molecular orbitals are not formed when the participating atomic orbitals possess very different energies.

Thus, both symmetry and energy requirements must be fulfilled in order to form molecular orbitals. Energetically, the 2*s* and 2*p* atomic orbitals are suffìciently similar to form molecular orbitals with each other. For symmetry reasons, however, the p_x and p_y orbitals of one atom of a homonuclear diatomic molecule cannot combine with the 2*s* orbital of the other atom because they belong to different irreducible representations (see Figure 6-13a). On the other hand, for example, the radial extension of the 4*f* orbitals of the lanthanide elements is very small and they are well separated from the valence region, therefore they cannot form molecular orbitals with many ligand orbitals for energetic reasons despite their matching symmetries (see Figure 6-13b) [21].

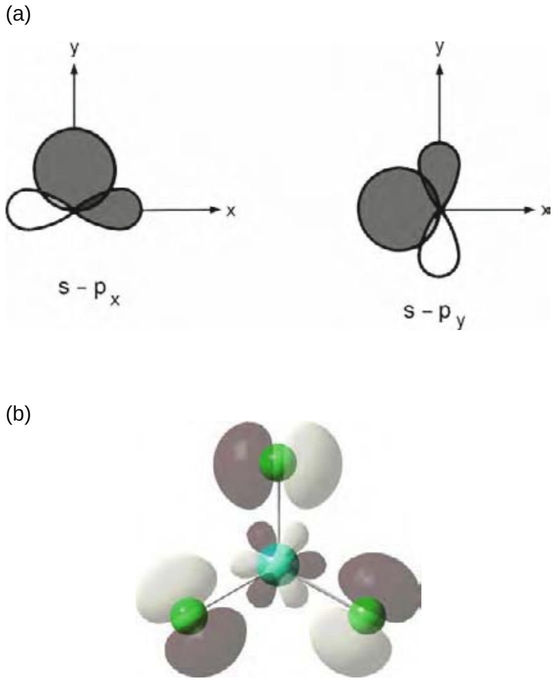

Figure 6-13. **(a)** Combination of the 2*s* and 2p_x (or 2p_y) atomic orbitals does not result in a molecular orbital because their symmetries do not match; **(b)** Combination of the 4*f* orbital of dysprosium and the 2*p* orbitals of chlorine does not result in a molecular orbital because their energies (radial extention) are too different [22].

Knowledge of the symmetry of the MOs is important for practical reasons. The energy of the orbitals can be calculated by costly quantum chemical calculations. The symmetry of the molecular orbitals, on the other hand, can be deduced from the molecular point group and with the use of character tables, a process that requires merely paper and pencil. Then, when all possible solutions that are not allowed by symmetry have been excluded, only the energies of the remaining orbitals need to be calculated.

We are, of course, concerned with the symmetry aspects of the MOs and their construction. As was discussed before, the degeneracy of atomic orbitals is determined by m_l. Thus, all *p* orbitals are threefold degenerate, and all *d* orbitals are fivefold degenerate. The spherical symmetry of the atomic subshells, however, necessarily changes when the atoms enter the molecule, since the symmetry of molecules is nonspherical. The degeneracy of atomic orbitals will, accordingly, decrease; the extent of decrease will depend upon molecular symmetry.

Various methods (described in Chapter 4) can be used to determine the symmetry of atomic orbitals in the point group of a molecule, i.e., to determine the irreducible representation of the molecular point group to which the atomic orbitals belong. There are two possibilities depending on the position of the atoms in the molecule. For a central atom (like O in H_2O or N in NH_3), the coordinate system can always be chosen in such a way that the central atom lies at the intersection of all symmetry elements of the group. Consequently, each atomic orbital of this central atom will transform as one or another irreducible representation of the symmetry group. These atomic orbitals will have the same symmetry properties as those basis functions in the third and fourth areas of the character table which are indicated in their subscripts. For all other atoms, so-called “group orbitals” or “symmetry-adapted linear combinations” (SALCs) must be formed from like orbitals. Several examples below will illustrate how this is done.

First, however, consider the symmetry properties of the central atom orbitals. Take the C_{4v} point group as an example. Its character table is presented in Table 6-1. The p_z and d_{z^2} atomic orbitals of the central atom belong to the totally symmetric irreducible representation A_1, the $d_{x^2-y^2}$ orbital belongs to B_1 and d_{xy} to B_2. The symmetry properties of the (p_x, p_y) and (d_{xz}, d_{yz}) orbitals present a good opportunity

Table 6-1. The C_{4v} Character Table

C_{4v}	E	$2C_4$	C_2	$2\sigma_v$	$2\sigma_d$		
A_1	1	1	1	1	1	z	x^2+y^2, z^2
A_2	1	1	1	−1	−1	R_z	
B_1	1	−1	1	1	−1		x^2-y^2
B_2	1	−1	1	−1	1		xy
E	2	0	−2	0	0	(x, y) (R_x, R_y)	(xz, yz)

for illustrating two-dimensional representations. Taking the three p orbitals as basis functions, the symmetry operations of the C_{4v} point group are applied to them. This is shown in Figure 6-14. The matrix representations are given here:

$$E = \begin{bmatrix} 1 & 0 & 0 \\ 0 & 1 & 0 \\ 0 & 0 & 1 \end{bmatrix}$$

$$C_4 = \begin{bmatrix} 0 & 1 & 0 \\ -1 & 0 & 0 \\ 0 & 0 & 1 \end{bmatrix} \quad C_4^3 = \begin{bmatrix} 0 & -1 & 0 \\ 1 & 0 & 0 \\ 0 & 0 & 1 \end{bmatrix} \quad C_2 = \begin{bmatrix} -1 & 0 & 0 \\ 0 & -1 & 0 \\ 0 & 0 & 1 \end{bmatrix}$$

$$\sigma_v(xz) = \begin{bmatrix} 1 & 0 & 0 \\ 0 & -1 & 0 \\ 0 & 0 & 1 \end{bmatrix} \quad \sigma_v(yz) = \begin{bmatrix} -1 & 0 & 0 \\ 0 & 1 & 0 \\ 0 & 0 & 1 \end{bmatrix}$$

$$\sigma_d = \begin{bmatrix} 0 & 1 & 0 \\ 1 & 0 & 0 \\ 0 & 0 & 1 \end{bmatrix} \qquad \sigma_d' = \begin{bmatrix} 0 & -1 & 0 \\ -1 & 0 & 0 \\ 0 & 0 & 1 \end{bmatrix}$$

All these matrices can be simultaneously block-diagonalized into a 2×2 and a 1×1 matrix. The set of the 1×1 matrices corresponds to p_z and the set of the 2×2 matrices corresponds to p_x and p_y. The representations are:

	E	$2C_4$	C_2	$2\sigma_v$	$2\sigma_d$	
p_z	1	1	1	1	1	A_1
(p_x, p_y)	2	0	−2	0	0	E

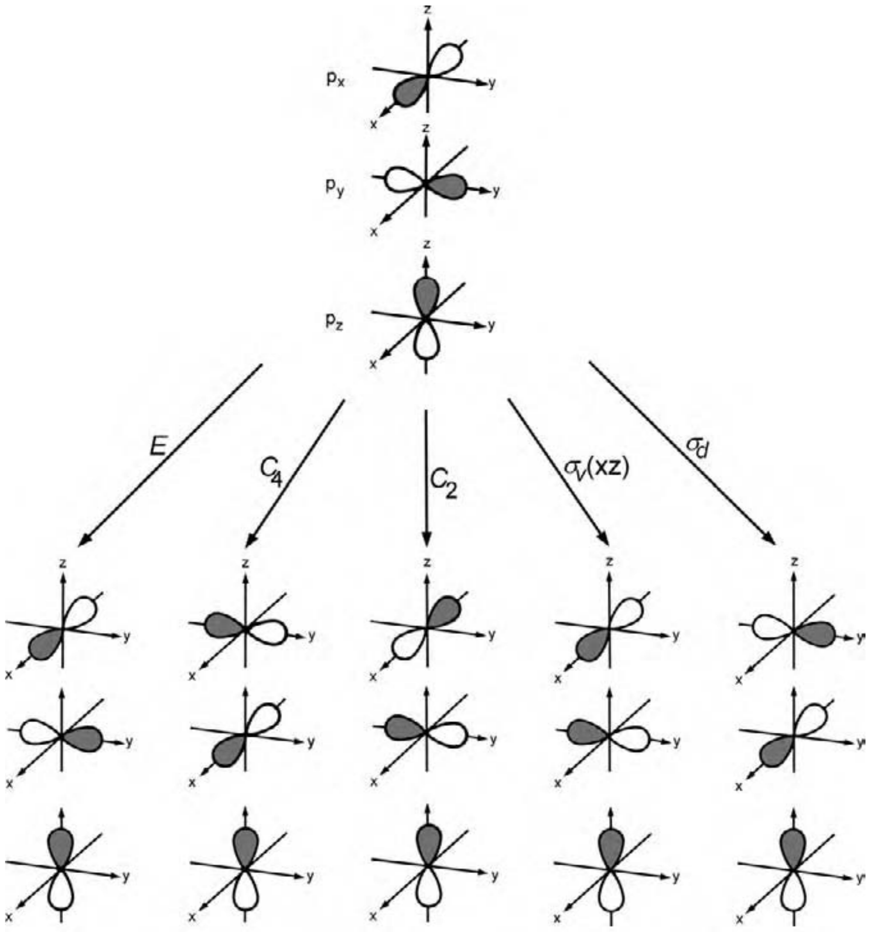

Figure 6-14. The symmetry operations of the C_{4v} point group applied to the 2*p* orbitals.

Notice that the operations C_4 and σ_d transform p_x into p_y and vice versa. They cannot be separated from one another so they *together* belong to the two-dimensional representation *E*.

If two or more atomic orbitals are interrelated under a symmetry operation of the point group and, accordingly, they *together* belong to an irreducible representation, their energies will also be the same. In other words, these orbitals are *degenerate*. Such atomic orbitals are parenthesized in the character tables.

The direct connection between symmetry and degeneracy of the atomic orbitals is demonstrated here once again. The higher the

symmetry of the molecule, the greater will be the interrelation of the orbitals upon symmetry operations. Consequently, their energies become less and less distinguishable. The following example shows how the degeneracy of *p* orbitals decreases with diminishing symmetry:

Free atom	Spherical symmetry	(p_x, p_y, p_z)	Threefold degenerate
O_h point group	T_{1u}	(p_x, p_y, p_z)	Threefold degenerate
C_{4v} point group	A_1	p_z	Nondegenerate
	E	(p_x, p_y)	Twofold degenerate
C_{2v} point group	A_1	p_z	Nondegenerate
	B_1	p_x	Nondegenerate
	B_2	p_y	Nondegenerate

The degree of degeneracy of atomic orbitals always corresponds to the dimension of the irreducible representation to which these atomic orbitals belong. The same is true for molecular orbitals. Thus, knowing the symmetry of a molecule and looking at the character table, one can determine at once the maximum possible degeneracy of its molecular orbitals. The irreducible representation having the highest dimension will show this.

6.3.2. Electronic States

The orbitals and electronic configurations are useful descriptions. However, they are only models, and they employ approximations. The energy of an orbital has rigorous physical significance for systems that contain only a single electron. In many-electron systems, the energy of the orbitals loses its physical meaning, and only the energies of the (ground and excited) states are real. It is these states that are described by the total electronic wave functions. Electronic transitions, in fact, represent changes in the state of an atom or a molecule and not necessarily in the electronic configurations.

We shall not be concerned with the atomic states. The systematic way of determining them is given, for example, in References [4] and [7]. Molecular states and the determination of their symmetries, however, will be briefly introduced [23].

First, let us consider the customary notations. Assume that a hypothetical ground state molecule of the C_{2v} point group has four electrons, two in an A_1 symmetry and two in a B_1 symmetry orbital. In short notation this can be written as $a_1^2b_1^2$. An electron occupying an A_1 symmetry orbital is represented by a_1, the lower-case letter indicating that this is the symmetry of an *orbital* and not of an electronic state. If two electrons occupy an orbital, the notation is a_1^2. The symmetry of a state is represented by capital letters, just as are the irreducible representations.

The symmetry of the electronic states can be determined from the symmetry of the occupied orbitals. There are two different cases:

1. *States with fully occupied orbitals.* An electronic configuration in which all orbitals are completely filled possesses only one electronic state, and it will be totally symmetric. This can be seen for the case of nondegenerate orbitals. The wave function describing the electronic state can be written as the product of the one-electron orbitals. The symmetry of the product is given by the characters of the direct product representation. However, the product of any orbital with itself will always give the totally symmetric representation, no matter what characters it has, both $1 \cdot 1$ and $(-1)\cdot(-1)$ equal 1, i.e., in each class of the point group the characters of the product will be 1. The same is true for degenerate orbitals, although the procedure in this case is not as simple.
2. *States with partially occupied orbitals.* First of all, the completely filled orbitals are ignored for the reasons described above. The symmetry of the state will be given by the direct product of the partially filled orbitals.

Let us consider some examples for the above hypothetical molecule. The supposed ground state and the configurations of two different singly excited states are represented in Figure 6-15.

The ground state $a_1^2b_1^2$ has only fully occupied orbitals, so its symmetry is A_1. The first excited state, $a_1^2b_1a_2$, has one fully occupied orbital, a_1^2, so this is not considered. The symmetry of this state will be given by the direct product $B_1 \cdot A_2$. Table 6-2 lists the direct products under the C_{2v} character table. The symmetry of the state is B_2. The other excited state in our example has the configuration $a_1^2b_1b_2$. The direct product is given in Table 6-2; the state symmetry is A_2.

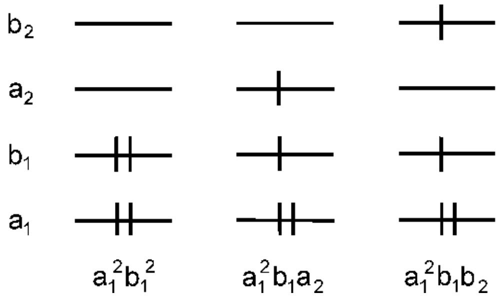

Figure 6-15. Different states of a molecule with C_{2v} symmetry.

Table 6-2. C_{2v} Character Table and Some Direct Product Representations

C_{2v}	E	C_2	$\sigma_v(xz)$	$\sigma_v'(yz)$		
A_1	1	1	1	1	z	x^2, y^2, z^2
A_2	1	1	−1	−1	R_z	xy
B_1	1	−1	1	−1	x, R_y	xz
B_2	1	−1	−1	1	y, R_x	yz
$B_1 \cdot A_2$	1	−1	−1	1	B_2	
$B_1 \cdot B_2$	1	1	−1	−1	A_2	

Since we are concerned only with the spatial symmetry properties, the electron spin and its role in determining the electronic states have been neglected in the above description.

6.3.3. Examples of MO Construction

6.3.3.1. Homonuclear Diatomics

a) Hydrogen, H_2. There are two 1*s* hydrogen atomic orbitals available for bonding. The molecular point group is $D_{\infty h}$. This molecule does not have a central atom, so the symmetry operations of the point group are applied to both 1*s* orbitals, since they *together* form the basis for a representation of this point group. The 1*s* orbital of one hydrogen atom alone does not belong to any irreducible representation of the $D_{\infty h}$ point group. Several symmetry operations of this group transform one of the two 1*s* orbitals into the other rather than into itself (see

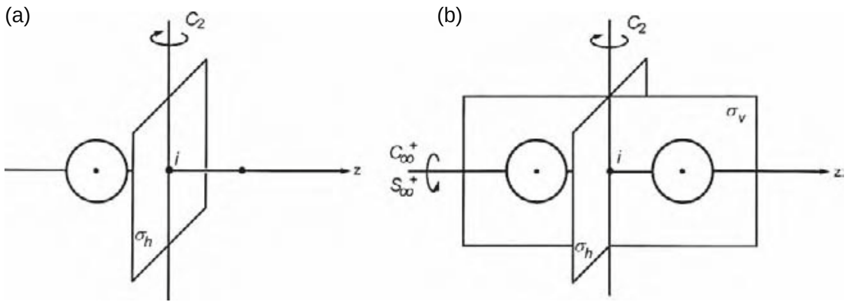

Figure 6-16. Some symmetry operations of the $D_{\infty h}$ point group applied to: (**a**) One 1*s* orbital in the hydrogen molecule; (**b**) The two 1*s* orbitals of the hydrogen molecule together.

Figure 6-16a). Thus, they must be treated together; in this way they form a basis for a representation. All symmetry operations are indicated in Figure 6-16b. The $D_{\infty h}$ character table is given in Table 5-3. The characters of this representation will be

$D_{\infty h}$	E	$2C_\infty^\Phi$	$\infty\sigma_v$	i	$2S_\infty^\Phi$	∞C_2
2 H(1*s*)	2	2	2	0	0	0

This is a reducible representation of the $D_{\infty h}$ point group which reduces to $\sigma_g + \sigma_u$. Two molecular orbitals must be generated, one with σ_g and the other with σ_u symmetry. The two possible combinations are the bonding and antibonding orbitals which can be formed from the two 1*s* atomic orbitals.

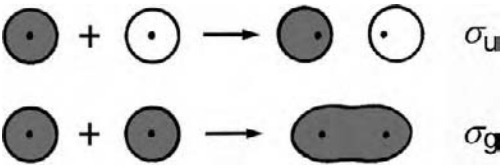

The two electrons in the hydrogen molecule will occupy the lower energy bonding orbital, and none will go into the antibonding orbital.

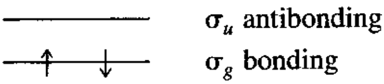

Hence, the molecule is stable.

b) Other Homonuclear Diatomic Molecules. The principle utilized to construct molecular orbitals is the same as that for the hydrogen molecule. For helium, the MO picture is the same as for hydrogen except that here the additional two electrons occupy the antibonding σ_u orbital, and, therefore, the molecule is unstable.

In the series from lithium through neon, similar symmetry considerations apply, except that in these examples the second electron shell must be considered. The two 2*s* orbitals, as was found to be the case for the two 1*s* orbitals, form MOs that possess σ_g and σ_u symmetry. As regards the 2*p* orbitals, the two $2p_z$ orbitals lie along the molecular axis and belong to the same irreducible representation as the 2*s* orbitals. They also combine to give MOs that possess σ_g and σ_u symmetry:

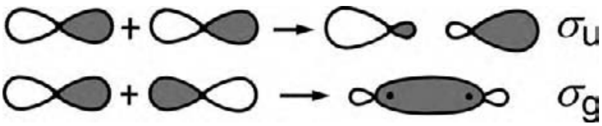

The 2*s* and $2p_z$ orbitals of the same atom belong to the same irreducible representation of the $D_{\infty h}$ point group. Their energies are also similar so they cannot be separated completely. Another way of making linear combinations is to first combine the 2*s* and $2p_z$ orbitals of the same atom

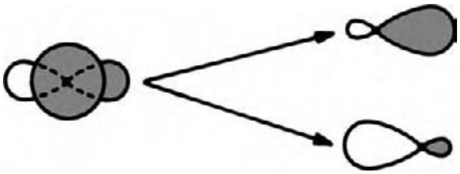

and then combine the resulting orbitals into MOs.

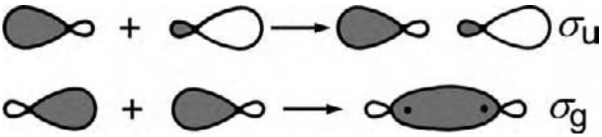

The result is essentially the same as before.

The $2p_x$ and $2p_y$ orbitals of the two atoms together form a representation that reduces to π_g and π_u. These correspond to two doubly degenerate π orbitals, one of which lies in the *yz* plane

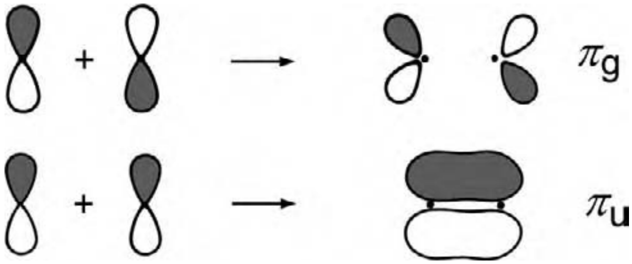

and the other in the *xz* plane. The relative energies of these orbitals are known from energy calculations. In most cases the order is as follows:

$$1\sigma_g < 1\sigma_u < 2\sigma_g < 2\sigma_u < 3\sigma_g < 1\pi_u < 1\pi_g < 3\sigma_u$$

while in some cases $1\pi_u < 3\sigma_g$.

6.3.3.2. Polyatomic Molecules

Before working out actual examples, let us recall what was said about the symmetry properties of atomic orbitals. If there is a central atom in the molecule, its atomic orbitals belong to some irreducible representation of the molecular point group. For the other atoms of these molecules, SALCs are formed from like orbitals. These new orbitals are then coupled with the central atom AOs to form MOs.

If the molecule does not have a central atom (e.g., C_6H_6), we begin with the second step, first forming different group orbitals and then combining them, if possible, into MOs. Examples will be given for both cases.

a) Water, H_2O. The molecular symmetry is C_{2v}. There are six atomic orbitals available for MO construction: two H 1*s*, one oxygen 2*s* and three oxygen 2*p*. They can combine to produce six MOs. As the molecule has a central atom, its AOs will belong to some of the irreducible representations of the C_{2v} point group by themselves. Group orbitals must be formed from the H 1*s* orbitals. The symmetry operations applied to them are shown in Figure 6-17. The C_{2v} character table was given in Table 6-2. The reducible representation is:

C_{2v}	E	C_2	$\sigma_v(xz)$	$\sigma_v'(yz)$
2 H(1*s*)	2	0	0	2

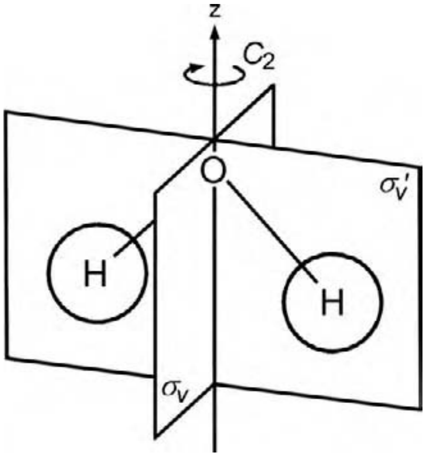

Figure 6-17. The C_{2v} symmetry operations applied to the two hydrogen 1*s* orbitals of water as basis functions.

This representation reduces to $A_1 + B_2$. The projection operator (see Chapter 4) is used to form these SALCs. Since we are interested only in symmetry aspects, numerical factors and normalization are omitted.

$$\begin{aligned}\hat{P}^{A_1}s_1 &\approx 1 \cdot E \cdot s_1 + 1 \cdot C_2 \cdot s_1 + 1 \cdot \sigma \cdot s_1 + 1 \cdot \sigma' \cdot s_1 \\ &= s_1 + s_2 + s_2 + s_1 = 2s_1 + 2s_2 \approx s_1 + s_2 \\ \hat{P}^{B_2}s_1 &\approx 1 \cdot E \cdot s_1 + (-1) \cdot C_2 \cdot s_1 + (-1) \cdot \sigma \cdot s_1 + 1 \cdot \sigma' \cdot s_1 \\ &= s_1 - s_2 - s_2 + s_1 = 2s_1 - 2s_2 \approx s_1 - s_2\end{aligned}$$

Thus, the two hydrogen group orbitals (φ_1 and φ_2) will have the forms:

$\varphi_2 = s_1 - s_2$:

$\varphi_1 = s_1 + s_2$:

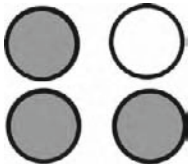

The available AOs are summarized according to their symmetry properties in Table 6-3. Since only orbitals of the same symmetry can overlap, two combinations are possible: one has A_1 symmetry and the

Table 6-3. The Atomic Orbitals of Water Grouped According to their Symmetry Properties

	O orbitals	H group orbitals
A_1	$2s$, $2p_z$	φ_1
A_2		
B_1	$2p_x$	
B_2	$2p_y$	φ_2

other has B_2 symmetry. The remaining two orbitals of oxygen (one with A_1 and the other with B_1 symmetry) will be nonbonding in the water molecule.

If we choose the oxygen $2s$ orbital for bonding and leave the $2p_z$ orbital nonbonding (from the symmetry point of view the opposite choice or a mixed orbital would do just as well; actually if the two arbitals are close in energy, they mix), the MOs of the water molecule can be constructed as shown in Figure 6-18. These MOs are compared with the calculated contour diagrams of the water molecular orbitals in Figure 6-19.

The construction of the molecular orbitals of the water molecule can also be represented by a qualitative MO diagram (see Figure 6-20). The relative energies of the orbitals are also indicated in Figure 6-20. What information can be deduced from such a diagram? First, there are two bonding orbitals occupied by four electrons; these correspond to the two O–H bonds of water. There are two nonbonding orbitals also occupied; these are the two lone pairs of oxygen. Finally, there are two antibonding orbitals that are empty, so there is a net energy gain in the formation of H_2O and the molecule is stable.

b) Ammonia, NH_3. This example is given primarily to illustrate the construction of degenerate molecular orbitals. The symmetry of the molecule is C_{3v}. There are seven atomic orbitals available for bonding: three H $1s$, one N $2s$, and three N $2p$ AOs; hence, seven MOs must be formed. Since the nitrogen atom is a central atom, the coordinate axes can be chosen so that its AOs lie on all symmetry elements of the C_{3v} point group. The pertinent character table is given in Table 6-4. The N $2s$ and $2p_z$ orbitals will have A_1 symmetry and the $2p_x$ and

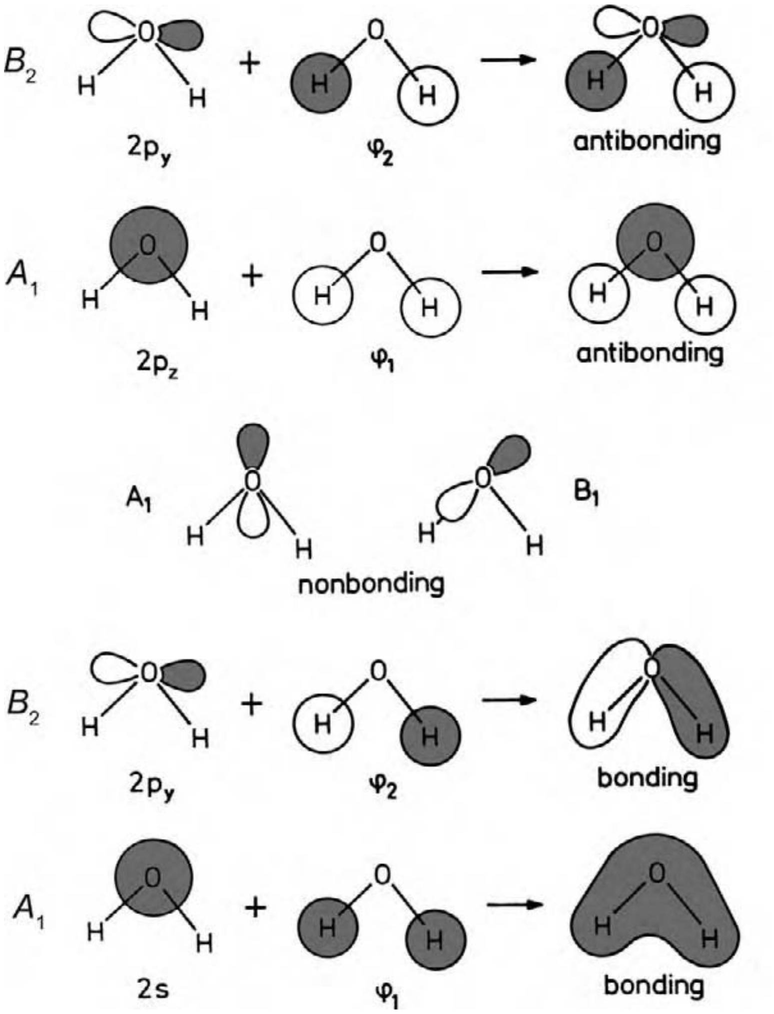

Figure 6-18. Construction of the molecular orbitals of water.

$2p_y$ orbitals together belong to the *E* irreducible representation. Group orbitals must be formed from the three H 1*s* orbitals. The symmetry elements of the C_{3v} point group applied to these orbitals are shown in Figure 6-21; their representation is given in Table 6-4.

This representation can now be reduced by using the reduction formula introduced in Chapter 4:

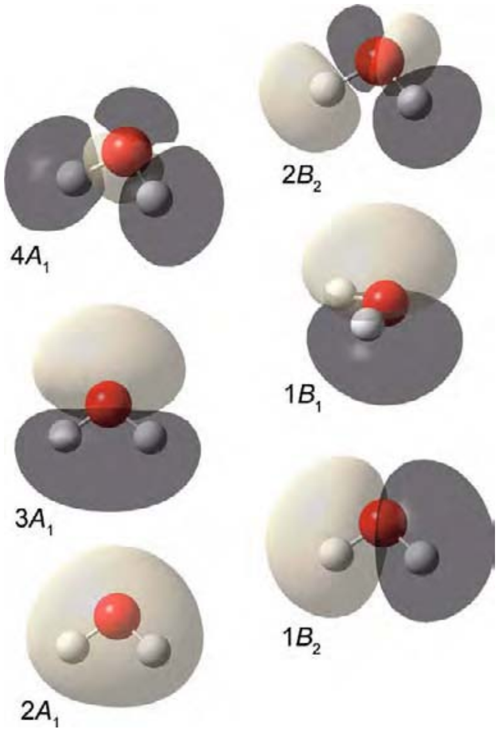

Figure 6-19. Contour diagrams of the molecular orbitals of water. Computer drawing by Zoltán Varga with Gaussview [24].

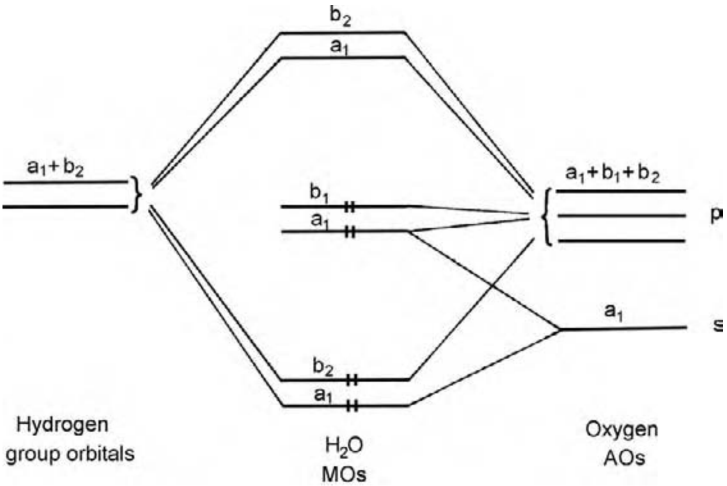

Figure 6-20. Qualitative MO diagram for water.

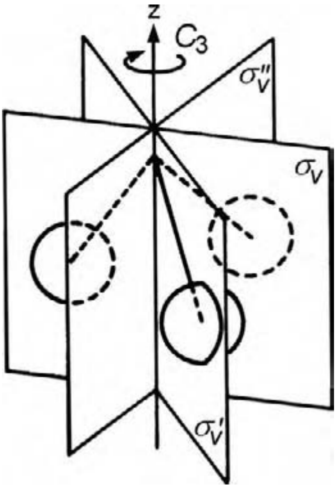

Figure 6-21. The C_{3v} symmetry operations applied to the three hydrogen atom 1*s* orbitals of ammonia as basis function.

Table 6-4. The C_{3v} Character Table and the Reducible Representation of the Hydrogen Group Orbitals of Ammonia

C_{3v}	E	$2C_3$	$3\sigma_v$		
A_1	1	1	1	z	x^2+y^2, z^2
A_2	1	1	−1	R_z	
E	2	−1	0	$(x, y)\ (R_x, R_y)$	$(x^2–y^2, xy)\ (xz, yz)$
3 H(1*s*)	3	0	1		

$$a_{A_1} = (1/6)(1 \cdot 3 \cdot 1 + 2 \cdot 0 \cdot 1 + 3 \cdot 1 \cdot 1) = 1$$
$$a_{A_2} = (1/6)(1 \cdot 3 \cdot 1 + 2 \cdot 0 \cdot 1 + 3 \cdot 1 \cdot (-1)) = 0$$
$$a_E = (1/6)(1 \cdot 3 \cdot 2 + 2 \cdot 0 \cdot (-1) + 3 \cdot 1 \cdot 0) = 1$$

Thus, the representation reduces to $A_1 + E$. Next, let us use the projection operator to generate the form of these SALCs:

$$\hat{P}^{A_1} s_1 \approx 1 \cdot E \cdot s_1 + 1 \cdot C_3 \cdot s_1 + 1 \cdot C_3^2 \cdot s_1 + 1 \cdot \sigma \cdot s_1 + 1 \cdot \sigma' \cdot s_1 + 1 \cdot \sigma'' \cdot s_1$$
$$= s_1 + s_2 + s_3 + s_1 + s_2 + s_3 = 2(s_1 + s_2 + s_3) \approx s_1 + s_2 + s_3$$

The same procedure is illustrated pictorially in Figure 6-22, after Reference [25].

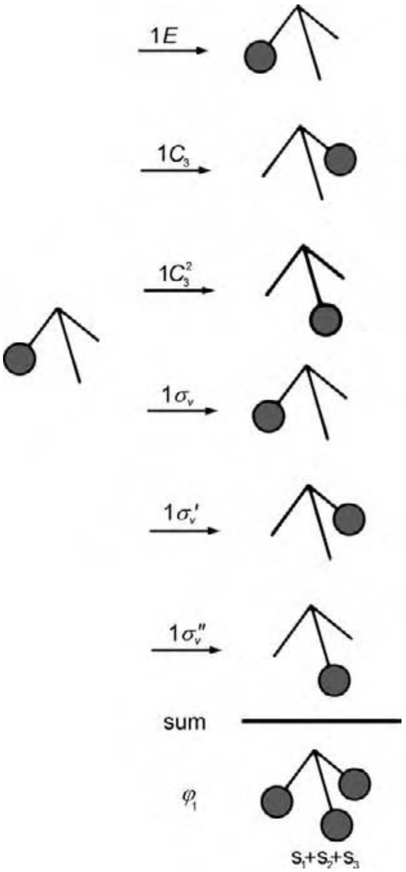

Figure 6-22. Generation of the A_1 symmetry orbital of the 3H group orbitals of ammonia.

For the construction of the E symmetry group orbitals, a time-saving simplification will be introduced [26]. First of all, it utilizes the fact that the rotational subgroup C_n in itself contains all the information needed to construct the SALCs in a molecule that possesses a principal axis C_n. The rotational subgroup of C_{3v} is C_3, and its character table is given in Table 6-5. If we perform the three symmetry operations of the C_3 point group and check the generation of the A_1 symmetry SALC of NH_3 (Figure 6-22), we see that the application of these three operations suffices to define the form of this orbital.

The difficulty in applying the projection operator for this symmetry group arises from the fact that the C_3 character table contains

Table 6-5. The C_3 Character Table

C_{3v}	E	C_3	C_3^2		$\varepsilon = \exp(2\pi i/3)$
A_1	1	1	1	z, R_z	x^2+y^2, z^2
E	$\left\{\begin{matrix} 1 \\ 1 \end{matrix}\right.$	$\begin{matrix} \varepsilon \\ \varepsilon^* \end{matrix}$	$\left.\begin{matrix} \varepsilon^* \\ \varepsilon \end{matrix}\right\}$	$(x, y)\ (R_x, R_y)$	$(x^2-y^2, xy)\ (yz, xz)$

imaginary characters for the E representation. They can be eliminated by following the procedure used in Reference [27]. The character ε corresponds to exp $(2\pi i/n)$, where n is the order of the rotation axis; in our case, 3. Using Euler's formula, $\exp(i\alpha) = \cos\alpha + i \sin\alpha$ (and the complex conjugate of ε will be: $\varepsilon^* = \cos\alpha - i \sin\alpha$), the characters for the E representation will be:

$$\left\{\begin{matrix} 1 & -\frac{1}{2} + i\sqrt{3}/2 & -\frac{1}{2} - i\sqrt{3}/2 \\ 1 & -\frac{1}{2} - i\sqrt{3}/2 & -\frac{1}{2} + i\sqrt{3}/2 \end{matrix}\right\} \begin{matrix} \text{(a)} \\ \text{(b)} \end{matrix}$$

Using two different ways to obtain linear combinations of these characters will make it possible to eliminate the imaginary characters. One way may be summing Eqs. (a) and (b), resulting in

$$2 \quad -1 \quad -1$$

The other linear combination may be obtained by subtraction of Eq. (b) from Eq. (a) and dividing the result by $i\sqrt{3}$. This linear combination results in the "characters"

$$0 \quad 1 \quad -1$$

not satisfying all the relationships of irreducible representations, but it serves our purpose of showing the shape of the SALCs. Our "quasi character table" for the C_3 point group is now:

$$\begin{matrix} A & & 1 & 1 & 1 \\ E & & \left\{\begin{matrix} 2 & -1 & -1 \\ 0 & 1 & -1 \end{matrix}\right\} \end{matrix}$$

When the projection operator is applied to one of the l*s* orbitals of the hydrogen group orbitals with the two *E* representations, the two *E* symmetry doubly degenerate SALCs result:

$$\hat{P}^{E^1} s_1 \approx 2 \cdot E \cdot s_1 + (-1) \cdot C_3 \cdot s_1 + (-1) \cdot C_3^2 \cdot s_1 = 2s_1 - s_2 - s_3$$
$$\hat{P}^{E^2} s_1 \approx 0 \cdot E \cdot s_1 + 1 \cdot C_3 \cdot s_1 + (-1) \cdot C_3^2 \cdot s_1 = s_2 - s_3$$

Figure 6-23 illustrates the same procedure pictorially.

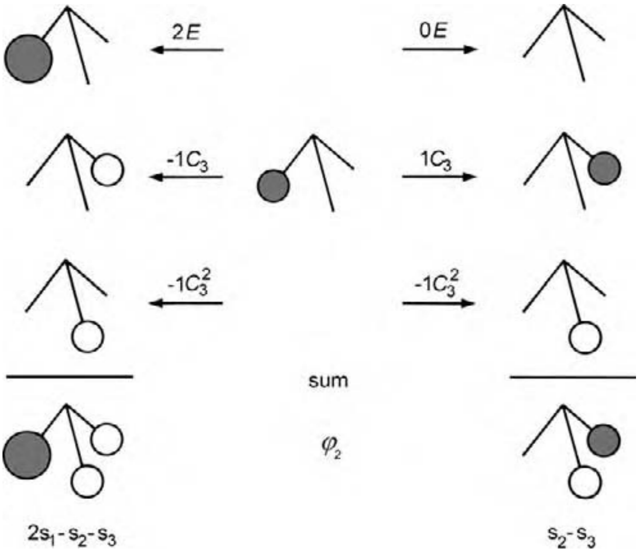

Figure 6-23. Projection of the two *E* symmetry group orbitals of the three H 1*s* orbitals in ammonia.

The next step is the MO construction. The orbitals used for this purpose are summarized in Table 6-6. An A_1 and a doubly degenerate *E* symmetry combination is possible here, and there will be a nonbonding orbital with A_1 symmetry left on nitrogen. Figure 6-24 illustrates the building of MOs. Again, they can be compared with

Table 6-6. The Atomic Orbitals of Ammonia Sorted According to their Symmetry Properties

	N orbitals	H group orbitals
A_1	s, p_z	φ_1
E	(p_x, p_y)	φ_2

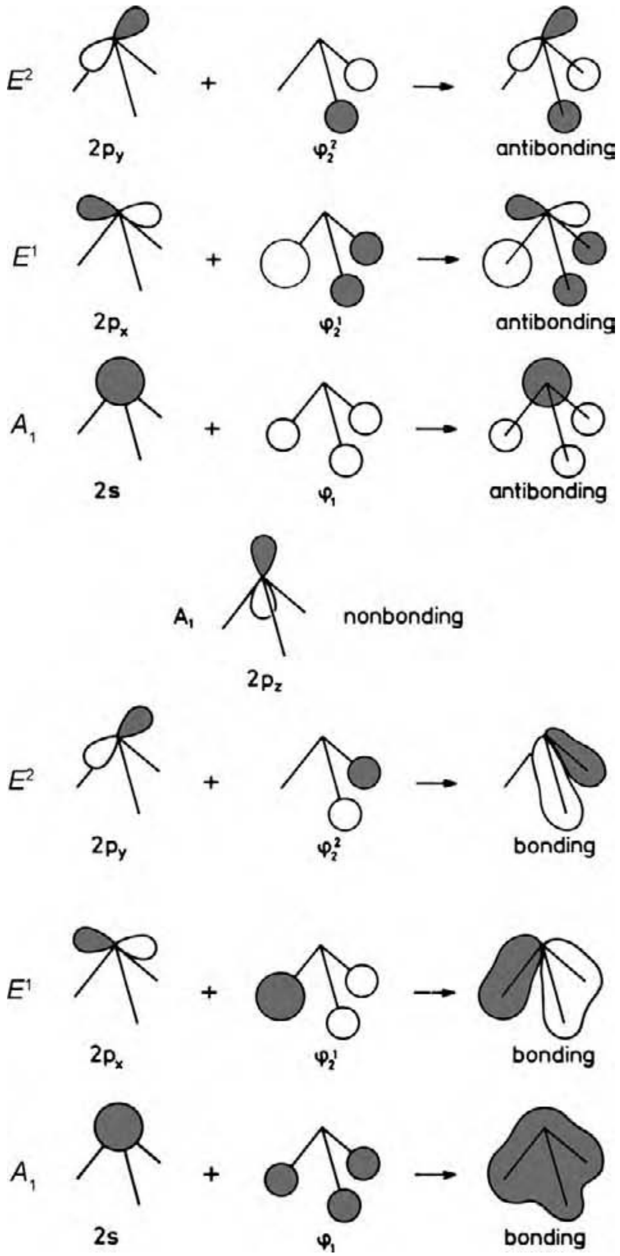

Figure 6-24. Construction of molecular orbitals for ammonia.

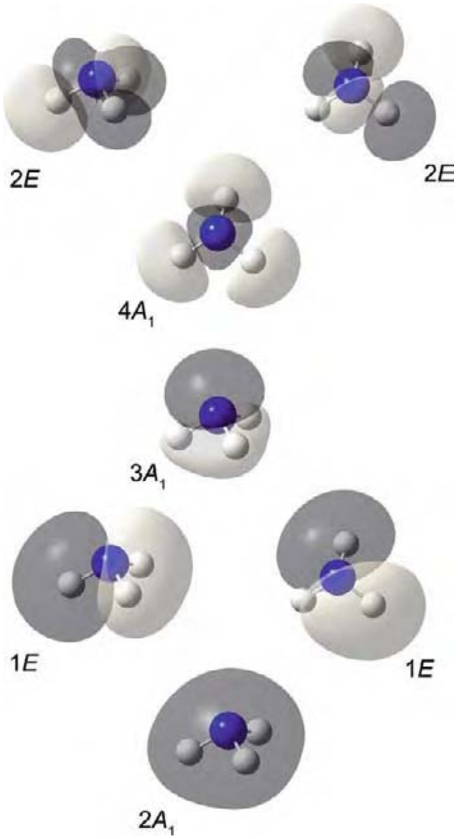

Figure 6-25. Contour diagrams of the molecular orbitals of ammonia. Computer drawing by Zoltán Varga with Gaussview [28].

the calculated contour diagrams of the ammonia molecular orbitals in Figure 6-25. The qualitative MO diagram is given in Figure 6-26. The following conclusions can be drawn: (l) There are three bonding orbitals occupied by electrons; these correspond to the three N–H bonds; (2) there is a nonbonding orbital also occupied by electrons; this corresponds to the lone electron pair; and (3) the three antibonding orbitals are unoccupied, so the MO construction is energetically favorable, and the molecule is stable.

c) Benzene, C_6H_6. The molecular symmetry is D_{6h}. There are 30 AOs that can be used for MO construction; six H 1*s*, six C 2*s*, and 18 C 2*p* orbitals. Since this molecule does not contain a central atom, each AO

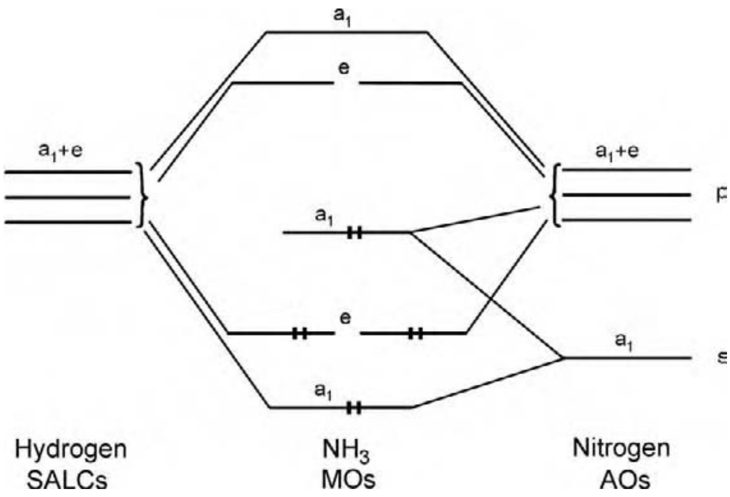

Figure 6-26. Qualitative MO diagram for ammonia.

must be grouped into SALCs in such a way that they can transform according to the symmetry operations of the D_{6h} point group. It is straightforward to combine like orbitals, for example, the hydrogen 1*s* orbitals, the carbon 2*s* orbitals, and so on. The following combinations will be used here:

$$\Phi_1(6\text{ H }1s), \Phi_2(6\text{ C }2s), \Phi_3(6\text{ C }2p_x, 2p_y), \text{ and } \Phi_4(6\text{ C }2p_z).$$

The next step is to determine how these group orbitals transform in the D_{6h} point group. The D_{6h} character table is given in Table 6-7. Since most of the AOs in the suggested group orbitals are transformed into another AO by most of the symmetry operations, the representations will be quite simple, though still reducible:

Γ_{Φ_1}	6	0	0	0	2	0	0	0	0	6	0	2
Γ_{Φ_2}	6	0	0	0	2	0	0	0	0	6	0	2
Γ_{Φ_3}	12	0	0	0	0	0	0	0	0	12	0	0
Γ_{Φ_4}	6	0	0	0	−2	0	0	0	0	−6	0	2

These representations can be reduced by applying the reduction formula.

Table 6-7. The D_{6h} Character Table

D_{6h}	E	$2C_6$	$2C_3$	C_2	$3C_2'$	$3C_2''$	i	$2S_3$	$2S_6$	σ_h	$3\sigma_d$	$3\sigma_v$		
A_{1g}	1	1	1	1	1	1	1	1	1	1	1	1		x^2+y^2, z^2
A_{2g}	1	1	1	1	–1	–1	1	1	1	1	–1	–1	R_z	
B_{1g}	1	–1	1	–1	1	–1	1	–1	1	–1	1	–1		
B_{2g}	1	–1	1	–1	–1	1	1	–1	1	–1	–1	1		
E_{1g}	2	1	–1	–2	0	0	2	1	–1	–2	0	0	(R_x, R_y)	(xz, yz)
E_{2g}	2	–1	–1	2	0	0	2	–1	–1	2	0	0		$(x^2–y^2, xy)$
A_{1u}	1	1	1	1	1	1	–1	–1	–1	–1	–1	–1		
A_{2u}	1	1	1	1	–1	–1	–1	–1	–1	–1	1	1	z	
B_{1u}	1	–1	1	–1	1	–1	–1	1	–1	1	–1	1		
B_{2u}	1	–1	1	–1	–1	1	–1	1	–1	1	1	–1		
E_{1u}	2	1	–1	–2	0	0	–2	–1	1	2	0	0	(x, y)	
E_{2u}	2	–1	–1	2	0	0	–2	1	1	–2	0	0		

First Φ_1:

$$\begin{aligned}
a_{A_{1g}} &= (1/24)(1\cdot 6\cdot 1 + 2\cdot 0\cdot 1 + 2\cdot 0\cdot 1 + 1\cdot 0\cdot 1 + 3\cdot 2\cdot 1 \\
&\quad + 3\cdot 0\cdot 1 + 1\cdot 0\cdot 1 + 2\cdot 0\cdot 1 + 2\cdot 0\cdot 1 + 1\cdot 6\cdot 1 + 3\cdot 0\cdot 1 + 3\cdot 2\cdot 1) \\
&= (1/24)(6+6+6+6) = 24/24 = 1 \\
a_{A_{2g}} &= (1/24)(6-6+6-6) = 0 \\
a_{B_{1g}} &= (1/24)(6+6-6-6) = 0 \\
a_{B_{2g}} &= (1/24)(6-6-6+6) = 0 \\
a_{E_{1g}} &= (1/24)(12-12) = 0 \\
a_{E_{2g}} &= (1/24)(12+12) = 1 \\
a_{A_{1u}} &= (1/24)(6+6-6-6) = 0 \\
a_{A_{2u}} &= (1/24)(6-6-6+6) = 0 \\
a_{B_{1u}} &= (1/24)(6+6+6+6) = 1 \\
a_{B_{2u}} &= (1/24)(6-6+6-6) = 0 \\
a_{E_{1u}} &= (1/24)(12+12) = 1 \\
a_{E_{2u}} &= (1/24)(12-12) = 0
\end{aligned}$$

Thus, the first representation reduces to the following irreducible representations:

$$\Gamma_{\Phi_1} = A_{1g} + E_{2g} + B_{1u} + E_{1u}$$

Without giving details of the other three reductions, the results are:

$$\begin{aligned}
\Gamma_{\Phi_2} &= A_{1g} + E_{2g} + B_{1u} + E_{1u} \\
\Gamma_{\Phi_3} &= A_{1g} + A_{2g} + 2E_{2g} + B_{1u} + B_{2u} + 2E_{1u} \\
\Gamma_{\Phi_4} &= B_{2g} + E_{1g} + A_{2u} + E_{2u}
\end{aligned}$$

Similarly to the case of ammonia, the rotational subgroup of D_{6h}, that is C_6, contains enough information to generate the SALCs of benzene. The C_6 character table is given in Table 6-8, and, again, contains imaginary characters. These can be handled in the same way as was done for ammonia, keeping in mind that the solution is right for the determination of the shape of the SALCs but the derived "quasi-characters" are not real characters.

These "quasi-characters" for the two E representations are:

$$E_1 \quad \begin{Bmatrix} 2 & 1 & -1 & -2 & -1 & 1 \\ 0 & 1 & 1 & 0 & -1 & -1 \end{Bmatrix}$$

Table 6-8. The C_6 Character Table

C_6	E	C_6	C_3	C_2	C_3^2	C_6^5		$\varepsilon = \exp(2\pi i/6)$
A	1	1	1	1	1	1	z, R_z	x^2+y^2, z^2
B	1	–1	1	–1	1	–1		
E_1	$\begin{cases}1\\1\end{cases}$	$\begin{matrix}\varepsilon\\\varepsilon^*\end{matrix}$	$\begin{matrix}-\varepsilon^*\\-\varepsilon\end{matrix}$	$\begin{matrix}-1\\-1\end{matrix}$	$\begin{matrix}-\varepsilon\\-\varepsilon^*\end{matrix}$	$\begin{rcases}\varepsilon^*\\\varepsilon\end{rcases}$	$(x, y)(R_x, R_y)$	(xz, yz)
E_2	$\begin{cases}1\\1\end{cases}$	$\begin{matrix}-\varepsilon^*\\-\varepsilon\end{matrix}$	$\begin{matrix}-\varepsilon\\-\varepsilon^*\end{matrix}$	$\begin{matrix}1\\1\end{matrix}$	$\begin{matrix}-\varepsilon^*\\-\varepsilon\end{matrix}$	$\begin{rcases}-\varepsilon\\-\varepsilon^*\end{rcases}$		(x^2-y^2, xy)

$$E_2 \quad \begin{Bmatrix} 2 & -1 & -1 & 2 & -1 & -1 \\ 0 & 1 & -1 & 0 & 1 & -1 \end{Bmatrix}$$

Benzene consists of 30 MOs; only a few of these will be constructed and shown here. It may be a good exercise for the reader to construct the remaining MOs of benzene by following the procedure demonstrated here. The SALCs are sorted according to their symmetry properties in Table 6-9. Inspection of this table reveals that the first three group orbitals have common irreducible representations, so they can be mixed with each other. They consist of 24 AOs; thus, 24 MOs will be formed. Since each bonding MO has its antibonding counterpart, there will be 12 bonding and 12 antibonding molecular orbitals. The former will be the bonding orbitals of

Table 6-9. The Symmetry of the Different Group Orbitals of Benzene

	Φ_1 H group orbital	Φ_2 C 2*s* group orbital	Φ_3 C $2p_x$, $2p_y$ group orbital	Φ_4 C $2p_z$ group orbital
A_{1g}	+	+	+	
A_{2g}			+	
B_{1g}				
B_{2g}				+
E_{1g}				+
E_{2g}	+	+	++	
A_{1u}				
A_{2u}				+
B_{1u}	+	+	+	
B_{2u}			+	
E_{1u}	+	+	++	
E_{2u}				+

benzene, since there are six C–C and six C–H bonds. The fourth group orbital does not belong to any irreducible representation common to the other three, so it will not be mixed with them. This representation corresponds to the π orbitals of benzene by itself.

Let us now construct the A_{1g} and B_{1u} symmetry σ orbitals of benzene. The totally symmetric representation, A_{1g}, appears three times, once in each of Φ_1, Φ_2, and Φ_3. Two A_{1g} representations can be combined into an MO, and the third one can represent an MO by itself. These three SALCs can be generated by using the projection operator pictorially as shown in Figure 6-27. The forms of these group orbitals are such that $\Phi_2(A_{1g})$ can be taken as an MO by itself (C–C σ bond; cf. also the corresponding orbital, $2A_{1g}$, in the contour diagram in Figure 6-28a), and the other two group orbitals can be combined into molecular orbitals as shown in Figure 6-29. The contour diagram of the bonding MO is depicted by the $3A_{1g}$ orbital in Figure 6-28a.

The next MO will be of B_{1u} symmetry. This irreducible representation also appears in Φ_1, Φ_2, and Φ_3. Take this time the corresponding Φ_1 and Φ_2 group orbitals and combine them into molecular orbitals:

$$\hat{P}^{B_{1u}} s_1 \approx 1 \cdot E \cdot s_1 + (-1) \cdot C_6 \cdot s_1 + 1 \cdot C_3 \cdot s_1 + (-1) \cdot C_2 \cdot s_1 + 1 \cdot C_3^2 \cdot s_1 + (-1) \cdot C_6^5 \cdot s_1 = s_1 - s_2 + s_3 - s_4 + s_5 - s_6,$$

or pictorally:

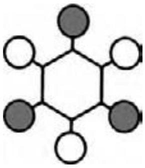

The B_{1u} symmetry SALC of Φ_2, i.e., the group orbital of the six C 2s AOs, will have a similar form:

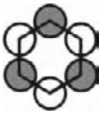

The combination of these Φ_1 and Φ_2 SALCs affords the bonding and antibonding combinations shown in Figure 6-30. The contour diagram corresponding to the bonding MO is the $2B_{1u}$ orbital in Figure 6-28a.

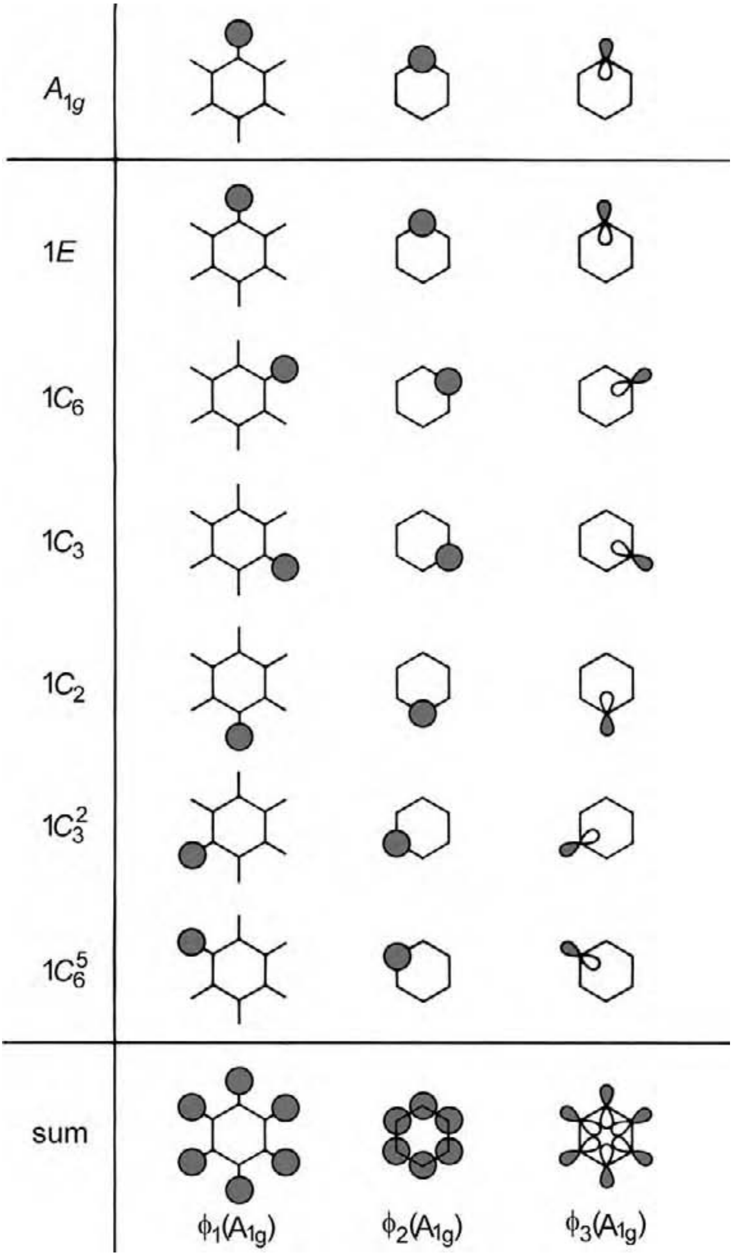

Figure 6-27. Generation of the A_{1g} symmetry group orbitals of benzene.

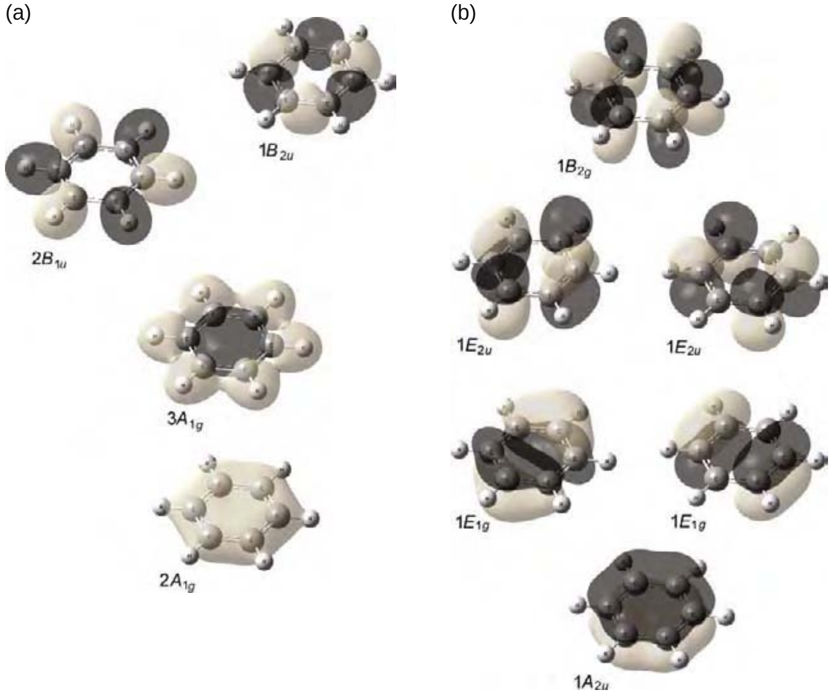

Figure 6-28. Contour diagrams of some molecular orbitals of benzene. Computer drawing by Zoltán Varga with Gaussview [29]: (**a**) σ orbitals; (**b**) π orbitals.

Since there is only one B_{2u} symmetry orbital among the SALCs, the one in Φ_3, it will be a MO by itself. Let us generate this MO:

$$\begin{aligned}\hat{P}^{B_{2u}} p_y(C_1) &\approx 1 \cdot E \cdot p_{y_1} + (-1) \cdot C_6 \cdot p_{y_1} + 1 \cdot C_3 \cdot p_{y_1} \\ &\quad + (-1) \cdot C_2 \cdot p_{y_1} + 1 \cdot C_3^2 \cdot p_{y_1} + (-1) \cdot C_6^5 \cdot p_{y_1} \\ &= p_{y_1} - p_{y_2} + p_{y_3} - p_{y_4} + p_{y_5} - p_{y_6}\end{aligned}$$

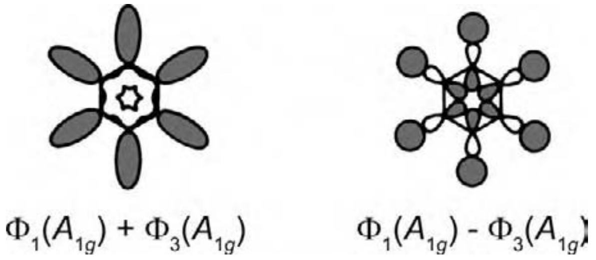

Figure 6-29. Bonding and antibonding combination of A_{1g} symmetry group orbitals of benzene.

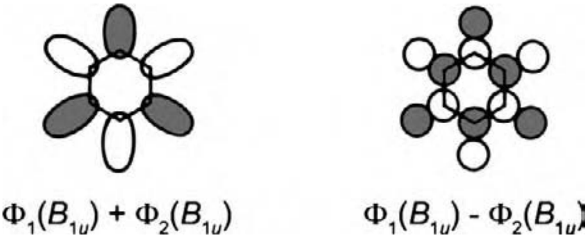

Figure 6-30. Bonding and antibonding combination of B_{1u} symmetry group orbitals of benzene.

This group orbital has the following shape:

Compare the above orbital with $1B_{2u}$ (Figure 6-28a).

The π orbitals of benzene will be the two doubly degenerate and the two non-degenerate combinations of the Φ_4 group orbital itself. All of these are shown below.

A_{2u} symmetry orbital: this corresponds to the totally symmetric representation in the rotational subgroup C_6; so, even without using the projection operator, its form can be given by:

$$\Phi_4(A_{2u}) = p_{z_1} + p_{z_2} + p_{z_3} + p_{z_4} + p_{z_5} + p_{z_6}$$

The corresponding orbital in Figure 6-28b will be the $1A_{2u}$ orbital.

B_{2g} symmetry orbital: using the projection operator, we obtain:

$$\begin{aligned} \hat{P}^{B_{2g}} p_z(C_1) &\approx 1 \cdot E \cdot p_{z_1} + (-1) \cdot C_6 \cdot p_{z_1} + 1 \cdot C_3 \cdot p_{z_1} \\ &\quad + (-1) \cdot C_2 \cdot p_{z_1} + 1 \cdot C_3^2 \cdot p_{z_1} + (-1) \cdot C_6^5 \cdot p_{z_1} \\ &= p_{z_1} - p_{z_2} + p_{z_3} - p_{z_4} + p_{z_5} - p_{z_6} \end{aligned}$$

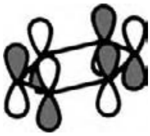

This is the $1B_{2g}$ orbital of Figure 6-28b.

The two E_{1g} symmetry SALCs are constructed in Figure 6-31. Compare them to the contour diagram of the $1E_{1g}$ orbitals in Figure 6-28b.

Finally, the two E_{2u} symmetry orbitals are expressed as follows:

$$\begin{aligned}\hat{P}^{E^1_{2u}} p_z(C_1) \approx\ & 2 \cdot E \cdot p_{z_1} + (-1) \cdot C_6 \cdot p_{z_1} + (-1) \cdot C_3 \cdot p_{z_1} \\ & + 2 \cdot C_2 \cdot p_{z_1} + (-1) \cdot C_3^2 \cdot p_{z_1} + (-1) \cdot C_6^5 \cdot p_{z_1} \\ =\ & 2p_{z_1} - p_{z_2} - p_{z_3} + 2p_{z_4} - p_{z_5} - p_{z_6}\end{aligned}$$

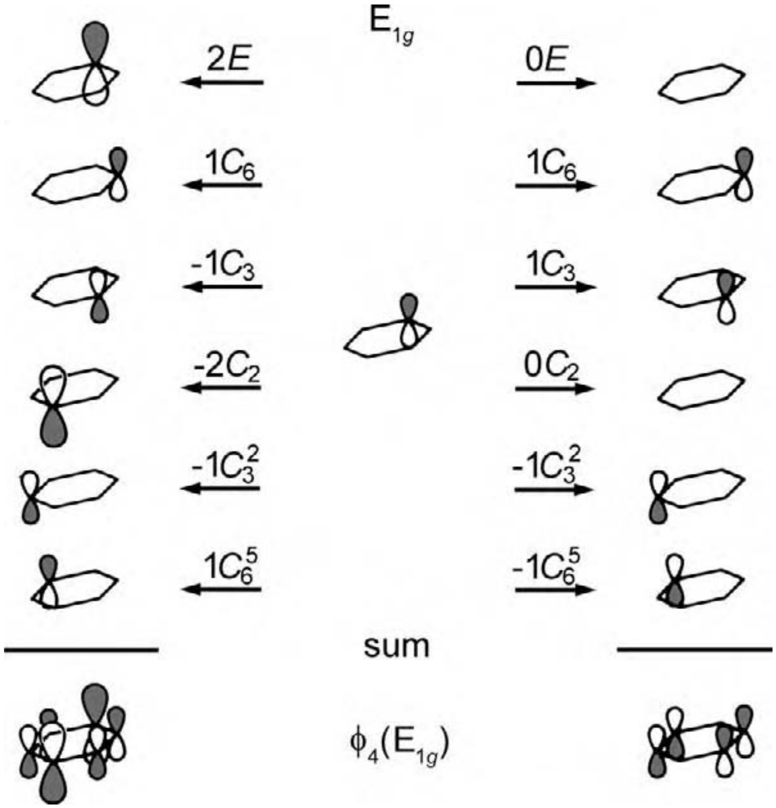

Figure 6-31. The two E_{1g} symmetry group orbitals formed from the carbon $2p_z$ orbitals in benzene.

$$\hat{P}^{E_{2u}^{2}} p_z(C_1) \approx 0 \cdot E \cdot p_{z_1} + 1 \cdot C_6 \cdot p_{z_1} + (-1) \cdot C_3 \cdot p_{z_1} + 0 \cdot C_2 \cdot p_{z_1} + 1 \cdot C_3^2 \cdot p_{z_1} + (-1) \cdot C_6^5 \cdot p_{z_1} = p_{z_2} - p_{z_3} + p_{z_5} - p_{z_6}.$$

Their forms are:

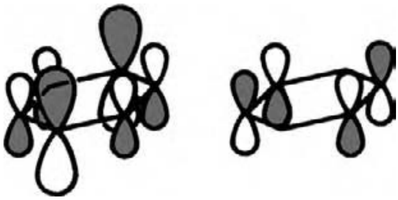

These SALCs correspond to the contour diagram of the $1E_{2u}$ orbital (Figure 6-28b). Figure 6-32 shows the relative energies of the benzene π orbitals.

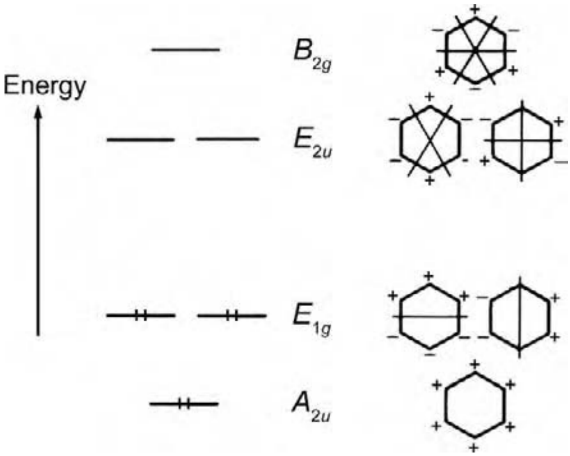

Figure 6-32. Relative energies of the benzene π orbitals.

6.3.3.3. Short Summary of MO Construction

The steps of MO construction can now be summarized as follows:

1. Identify the symmetry of the molecule.
2. List all atomic orbitals that are intended to be used for MO construction.
3. See whether or not the molecule has a central atom. If it does, then look up in the character table the irreducible representations

to which its atomic orbitals belong. If there is no central atom in the molecule, proceed to the next step.

4. Construct group orbitals (SALCs) from the atomic orbitals of like atoms.
5. Use these orbitals as bases for representations of the point group.
6. Reduce these representations to their irreducible components.
7. Apply the projection operator to the AOs for each of these irreducible representations to obtain the forms of the SALCs.
8. These SALCs will either be MOs by themselves, or they can be combined with other SALCs or central atom orbitals of the same symmetry. Each of these combinations will give one bonding and one antibonding MO of the same symmetry.
9. Normalization has been ignored throughout our discussion. However the SALCs must be properly normalized in all calculations [30]. This may be done at the end of the SALC construction, i.e., after step 7 in our list.

6.4. Quantum Chemical Calculations

Gay-Lussac (1778–1850) wrote in 1809: “We are perhaps not far removed from the time when we shall be able to submit the bulk of chemical phenomena to calculaton” [31]. One hundred and ten years later, in 1998, John Pople shared the Nobel Prize in Chemistry “for his development of computational methods in chemistry,” with Walter Kohn (in his case, “for his development of the density-functional theory”), Figure 6-33. So even if Gay-Lussac was, perhaps, somewhat too optimistic, eventually his dreams came true—the development of computational chemistry has been amazing. Quantum chemistry is not a topic of this book, we are only mentioning it briefly because of its inherent relationship to the symmetry concept. For discussion of the topic we refer the reader to a few of the available monographs [32–36].

The results of quantum chemical calculations usually yield the wave functions and the energies of a system. Numerous integrals must be evaluated even for the simplest molecules. Their number can be conveniently reduced, however, by applying the theorem according to which an energy integral, $\int \Psi_i \hat{H} \Psi_j \, d\tau$, is nonzero only if Ψ_i and Ψ_j

Figure 6-33. Walter Kohn (*left*) and John Pople, the 1998 Nobel laureates in Chemistry. Photograph by the authors.

belong to the *same* irreducible representation of the molecular point group.

Most chemical and physical properties of the molecule can be calculated, including the geometry, conformational properties, barrier to internal rotation, relative stabilities of various isomers as well as of different electronic states. Spectroscopic constants, such as dipole moments, quadrupole moments, and vibrational frequencies can be calculated and thermodynamic quantities determined. In the second edition of this book, we wrote: "State-of-the-art calculations of molecular geometry involving relatively light atoms are as reliable as the results of the best experiments"[37]. Since then, there has been a tremendous progress, and today it is possible to calculate much larger systems with good accuracy. The quantum chemical codes as well as the applied basis sets are continuously improving. While years ago, calculation of molecules involving heavy metals, such as the lanthanides or actinides, was a formidable task, today the available effective core potentials make these calculations affordable and more and more reliable. Computational studies of large biological macromolecules have also become an important tool in molecular biology and biological chemistry [38].

Here we focus mostly on one property, molecular geometry. With the ever increasing accuracy of computations, it is important to realize that while calculations provide information on the equilibrium

geometry, the various experiments yield some effective geometries for the molecule, averaged over molecular vibrations. Depending on the magnitude of these vibrations and their structural influence, the equilibrium and average structures may differ to various extents. Examples of rather extreme effects were mentioned in Section 3.7.6. This is why the following caveat has been issued: “For truly accurate comparison, experimental bond lengths [or, generally, geometries] should be compared with computed ones only following necessary corrections, bringing all information involved in the comparison to a common denominator” [39].

The application of computational chemistry is especially advantageous when structural differences rather than absolute values of the structural parameters are sought. Important systematic errors cancel to a large extent in the determination of structural differences in calculations as well as in experiments. The importance of small structural differences in understanding various effects in series of substances has been recognized [40].

Small structural changes are especially important in molecular recognition. It has been noted, e.g., that “... subtle changes of molecular structure may result in severe changes of inclusion behavior of a potential host molecule due to the complicated interplay of weak intermolecular forces that govern host-guest complex formation” [41].

Quantum chemical calculations have also proved to be important tools in aiding the experimental determination of molecular geometry in that they can provide reliable constraints in the experimental analysis (see, e.g., the structure analysis of 2-nitrophenol [42] and of metal halides that have a complex vapor composition [43, 44] or constitute very floppy systems [45]).

The difference is not merely practical, it is conceptual as well. R.D. Levine [46] distinguished between physical and chemical shapes. According to him, the physical shape corresponds to a hard space-filling model, whereas the chemical shape describes how molecular reactivity depends on the direction of approach and distance of the other reagent. In terms of geometry representations, the chemical shape can be related to the average structures determined from the experiments and the physical shape to the hypothetical equilibrium structure.

Quantum chemical calculations, of course, are the exclusive source of information for systems that are not amenable to experimental

study. Such systems include transition states, highly reactive and unstable or even unknown species. Computations are used in drug design, materials science, surface science, just to mention a few new areas. Quantum chemical calculations have proved to be not only complementary to experiments or be their alternatives, but have opened up new research areas as well. Schafer has predicted that chemical research will migrate each year from experiment to computation for the forseeable future [47] and would level off at about 50% each [48].

6.5. Influence of Environmental Symmetry

Symmetry has a major role in two widely used and successful approaches of chemistry, viz., the crystal field and ligand field theories of coordination compounds. This topic has been thoroughly covered in textbooks and monographs on coordination chemistry. Therefore, it is mentioned here only in passing.

Hans Bethe showed that the degenerate electronic state of a cation is split by a crystal field into nonequivalent states [49]. The change is determined entirely by the symmetry of the crystal lattice. Bethe's original work was concerned with ionic crystals, but his concept has more general applications. When an atom or an ion enters a ligand environment, the symmetry of the ligand arrangement will influence the electron density distribution of that atom or ion. The original spherical symmetry of the atomic orbitals will be lost, and the symmetry of the ligand environment will be adopted. As a consequence of the usual decrease of symmetry, the degree of degeneracy of the orbitals decreases.

The *s* electrons are already nondegenerate in the free atom, so their degeneracy does not change. They will always belong to the totally symmetric irreducible representation of the symmetry group. The *p* orbitals, however, are threefold degenerate, and the *d* orbitals are fivefold degenerate. To determine their splitting in a certain point group, we must use them, in principle, as bases for a representation of the group. In practice, we can find in the character table of the point group the irreducible representations to which the orbitals belong. An orbital always belongs to the same irreducible representation as do

Table 6-10. Splitting of Atomic Orbitals in Different Symmetry Environments

	s	p	d
O_h	a_{1g}	t_{1u}	$e_g + t_{2g}$
T_d	a_1	t_2	$e + t_2$
$D_{\infty h}$	σ_g	$\sigma_u + \pi_u$	$\sigma_g + \pi_g + \Delta_g$
D_{4d}	a_1	$b_2 + e_1$	$a_1 + e_2 + e_3$
D_{4h}	a_{1g}	$a_{2u} + e_u$	$a_{1g} + b_{1g} + b_{2g} + e_g$
C_{4v}	a_1	$a_1 + e$	$a_1 + b_1 + b_2 + e$
C_{2v}	a_1	$a_1 + b_1 + b_2$	$2a_1 + a_2 + b_1 + b_2$

its subscripts. Some orbital splittings that accompany the decrease in environmental symmetry are shown in Table 6-10.

As environmental symmetry decreases, the orbitals will become split to an increasing extent. In the C_{2v} point group, for example, all atomic orbitals will be split into nondegenerate levels. This is not surprising since the C_{2v} character table contains only one-dimensional irreducible representations. This result shows at once that there are no degenerate energy levels in this point group. This has been stressed in Chapter 4 in the discussion of irreducible representations.

The symmetry of the ligand environment gives an important but limited amount of information about orbital splitting. Both the octahedral and cubic ligand arrangements, for example, belong to the O_h point group, and we can tell that the d orbitals of the central atom will split into a doubly degenerate and a triply degenerate pair. But nothing is revealed about the relative energies of these two sets of degenerate orbitals.

The problem of relative energies is dealt with by crystal field theory. This theory examines the repulsive interaction between the ligands and the central atom orbitals. Consider first an octahedral molecule (Figure 6-34), and compare the positions of one e_g (e.g., $d_{x^2-y^2}$) and one t_{2g} (e.g., d_{yz}) orbital. The others need not be considered, as they are degenerate with, and thus have the same energy as, one of the e_g or t_{2g} orbitals. The lobes of the $d_{x^2-y^2}$ orbital point towards the ligands. The resulting electrostatic repulsion will destabilize this orbital, and its energies will increase accordingly. The d_{yz} orbital, on the other hand, points in directions between the ligands. This is an energetically more favorable position; hence, the energy of these orbitals will decrease.

Examine now the cubic arrangement in Figure 6-35. It can be seen that the d_{yz} orbital is in a more unfavorable situation relative to

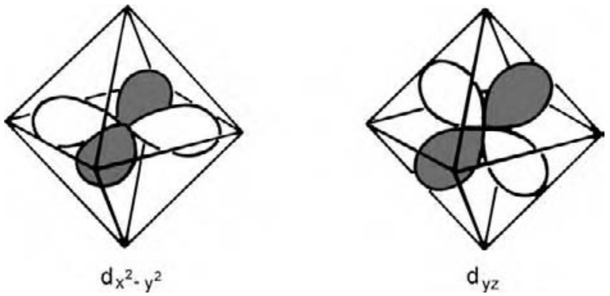

Figure 6-34. The orientation of the different symmetry *d* orbitals in an octahedral environment.

the ligands than is the $d_{x^2-y^2}$ orbital, so their relative energies will be reversed (see Figure 6-36). Some other typical orbital splittings and the corresponding changes in the relative energies are shown in Figure 6-37.

Prediction of Structural Changes. Crystal field theory is frequently applied to account for and even predict structural and chemical changes. A well-known example is the variation of first row transition metal ionic radii in an octahedral environment as illustrated in Figure 6-38 [50]. The dashed line connects the points for Ca, Mn, and Zn, i.e., atoms with spherically symmetrical distribution of *d* electrons. Since the shielding of one *d* electron by another is imperfect, a contraction in the ionic radius is expected along this series. This in itself would account only for a steady decrease in the radii, whereas the ionic radii of all the other atoms are smaller than interpolation from the Ca–Mn–Zn curve would suggest. As is well known, the

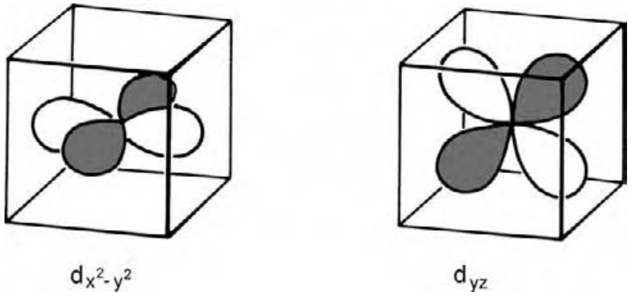

Figure 6-35. The orientation of the different symmetry *d* orbitals in a cubic environment.

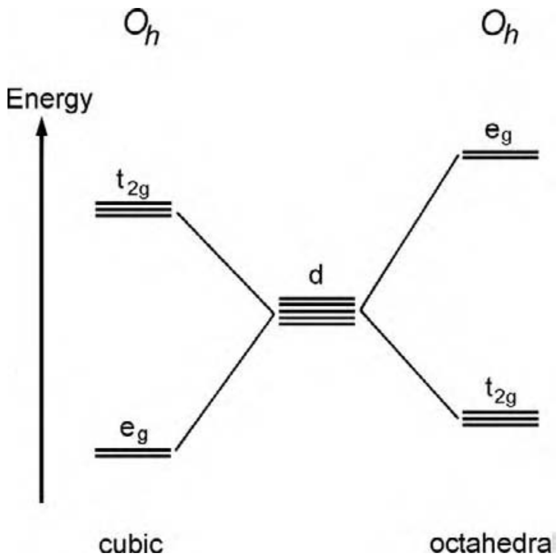

Figure 6-36. Relative energies of the *d* orbitals in octahedral and cubic ligand environment.

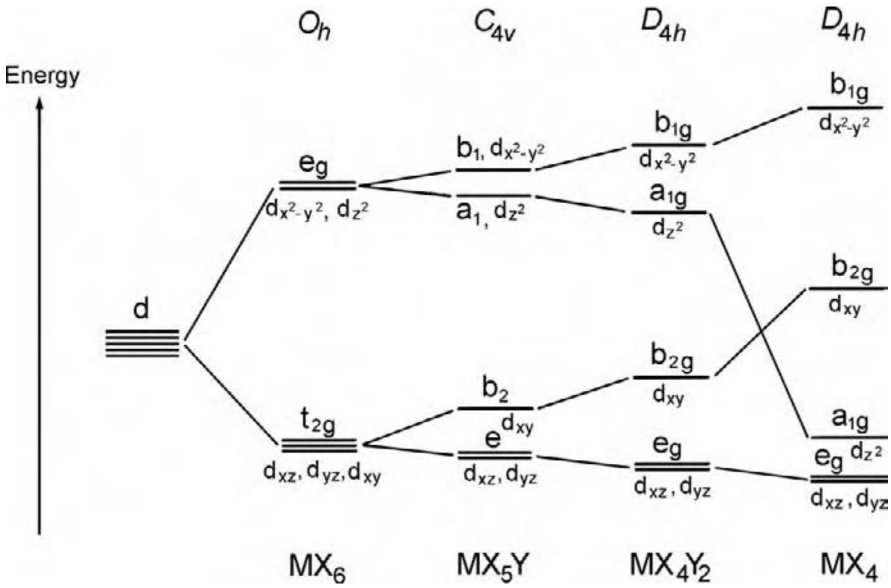

Figure 6-37. The *d* orbital splittings in different ligand environments.

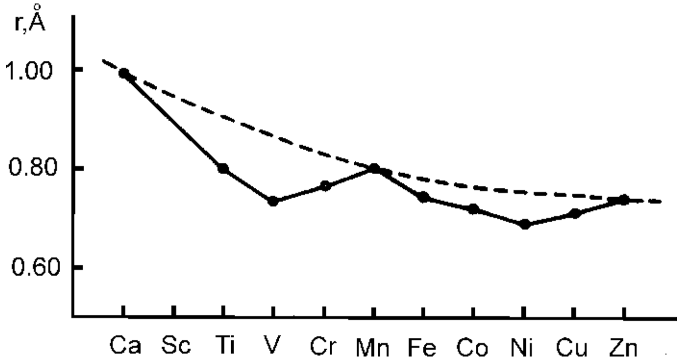

Figure 6-38. The variation of octahedral M^{2+} ionic radii [51].

non-uniform distribution of *d* electrons around the nuclei is the origin of this phenomenon. In the octahedral environment the *d* orbitals split into orbitals with t_{2g} and e_g symmetry. The electrons, added gradually, occupy t_{2g} orbitals in Sc^{2+}, Ti^{2+}, and V^{2+} as well as in Fe^{2+}, Co^{2+}, and Ni^{2+}, if only high-spin configurations are considered. Since these orbitals are not oriented towards the ligands, the degree of shielding between the ligands and the positively charged atomic cores decreases along with the ionic radius. The fourth electron in Cr^{2+} as well as the ninth electron in Cu^{2+} occupy e_g symmetry orbitals. The degree of shielding thus somewhat increases and, accordingly, there is a smaller relative decrease in the ionic radii.

6.6. Jahn–Teller Effect

"Somewhat paradoxically, symmetry is seen to play an important role in the understanding of the Jahn–Teller effect, the very nature of which is symmetry destruction" [52]. In a recent review the original paper published by Jahn and Teller [53] was called "one of the most seminal papers in chemical physics" [54]. Only a brief discussion of this effect will be given here; for more detail we refer the reader to References [55–59]. Bersuker says that all structural instabilities and distortions of high-symmetry configurations of polyatomic systems are of Jahn–Teller origin (here he also refers to other related effects, such as the Renner–Teller effect and the pseudo-Jahn–Teller effect—they will be mentioned later). Bersuker likes to call this the

"Jahn–Teller approach" and he considers the usual formulation of the effect somewhat obsolete [60]. Here, we will mostly discuss the Jahn–Teller effect according to its conventional meaning, but will also discuss briefly Bersuker's approach. According to the original formulation of the Jahn–Teller effect, [61] a non-linear symmetrical nuclear configuration in a degenerate electronic state is unstable and gets distorted, thereby removing the electronic degeneracy until a non-degenerate ground state is achieved. This formulation indicates the strong relevance of this effect to orbital splitting and generally to the relationship of symmetry and electronic structure discussed in previous sections. Owing to the coupling of the electronic and vibrational motions of the molecule, the ground-state orbital degeneracy is removed by distorting the highly symmetrical molecular structure to a lower-symmetry structure. An important aspect of the Jahn–Teller effect is that it represents an exception to the Born-Oppenheimer approximation (see in Section 6.3.1) since it involves the coupling of the electronic and nuclear motions in the molecule. Due to this mixing, a Jahn–Teller distorted molecule is expected to be inherently dynamic.

Jahn–Teller distortion can only be expected if the energy integral

$$\left\langle \Psi_0 \left| \frac{\partial E}{\partial q} \right| \Psi_0 \right\rangle \tag{6-6}$$

has nonzero value (Ψ_0 is the ground-state electronic wave function of the high-symmetry nuclear configuration, and q is a normal mode of vibration). According to what has already been said about the value of an energy integral (Section 4.9.2), this can only happen if the direct product of Ψ_0 with itself is, or contains, the irreducible representation of the q normal mode of vibration:

$$\Gamma_{\Psi_0} \cdot \Gamma_{\Psi_0} \subset \Gamma_q \tag{6-7}$$

Since Ψ_0 is degenerate, its direct product with itself will always contain the totally symmetric irreducible representation and, at least, one other irreducible representation. For the integral to be nonzero, q must belong either to the totally symmetric irreducible representation or to one of the other irreducible representations contained in the direct product of Ψ_0 with itself. A vibration belonging to the totally symmetric representation, however, does not decrease the symmetry

of the molecule. Accordingly, in order to have a Jahn–Teller type distortion, q must belong to one of the other irreducible representations.

Let us see an example, the H_3 molecule, which has the shape of an equilateral triangle. Its symmetry is D_{3h}, the electronic configuration is $a_1'^2e'$, and the symmetry of the ground electronic state is E'. Thus, the electronic state of the molecule is degenerate and is subject to Jahn–Teller distortion.

The symmetry of the normal mode of vibration that can take the molecule out of the degenerate electronic state will have to be such as to satisfy Eq. (6-7). The direct product of E' with itself (see Table 6-11) reduces to $A_1' + A_2' + E'$. The molecule has three normal modes of vibration [(3 × 3) – 6 = 3], and their symmetry species are $A_1' + E'$. A totally symmetric normal mode, A_1', does not reduce the molecular symmetry (this is the symmetric stretching mode), and thus the only possibility is a vibration of E' symmetry. This matches one of the irreducible representations of the direct product $E' \cdot E'$; therefore, this normal mode of vibration is capable of reducing the D_{3h} symmetry of the H_3 molecule. These types of vibrations are called Jahn–Teller active vibrations.

The two E' symmetry vibrations of the H_3 molecule are the angle bending and the asymmetric stretching modes (see Figure 6-39). They lead to the dissociation of the molecule into H_2 and H. Indeed, H_3 is so unstable that it cannot be observed as it would immediately dissociate into H_2 and H. This is one of the reasons why it has been so difficult to find experimental evidence of the Jahn–Teller effect for quite some time. The structures that are predicted to be unstable are often not found, and the observed structures are so different from them that the

Table 6-11. The D_{3h} Character Table and the Reducible Representation $E' \cdot E'$

D_{3h}	E	$2C_3$	$3C_2$	σ_h	$2S_3$	$3\sigma_v$		
A_1'	1	1	1	1	1	1		x^2+y^2, z^2
A_2'	1	1	–1	1	1	–1	R_z	
E'	2	–1	0	2	–1	0	(x, y)	$(x^2–y^2, xy)$
A_1''	1	1	1	–1	–1	–1		
A_2''	1	1	–1	–1	–1	1	z	
E''	2	–1	0	–2	1	0	(R_x, R_y)	(xz, yz)
$E' \cdot E'$	4	1	0	4	1	0	$= A_1' + A_2' + E'$	

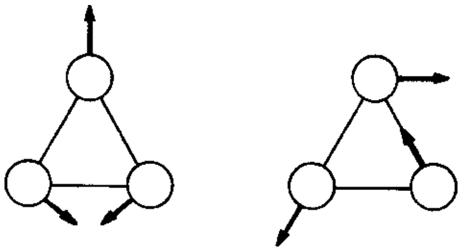

Figure 6-39. The two E' symmetry normal modes of vibration of the H_3 molecule leading to dissotiation.

connection is not obvious (other reasons of the difficulty encountered in observing the Jahn–Teller effect will be given later).

Obviously, only molecules with partially filled orbitals display Jahn–Teller distortion. As was shown in Section 6.3.2, the electronic ground state of molecules with completely filled orbitals is always totally symmetric, and thus cannot be degenerate. In comparison with the above-mentioned unstable H_3 molecule, H_3^+ has only two electrons in an a_1' symmetry orbital; therefore, its electronic ground state is totally symmetric, and the D_{3h}-symmetry triangular structure of this ion is stable (see, e.g., Reference [62]). On the other hand, take the benzene molecule, e.g., whose ground electronic state is of A_{1g} symmetry and the molecule is stable and its structure is well understood. At the same time, in its cation, $C_6H_6^+$, it loses one electron from an e_{1g}-symmetry doubly-degenerate orbital, so that orbital is left with only one electron. The electronic state of the cation has E_{1g} symmetry and thus, it is subject to Jahn–Teller effect. Indeed, its vibrational spectrum is extremely complicated and can only be satisfactory explained if the Jahn–Teller distortion is taken into consideration (see, e.g., Reference [63]).

Transition metals have partially filled d orbitals, and therefore their compounds are obvious candidates for Jahn–Teller systems. Let us consider an example from among the much studied cupric compounds [64]. Suppose that the Cu^{2+} ion with its d^9 electronic configuration is surrounded by six ligands in an octahedral arrangement. We have already seen (Table 6-10 and Figure 6-36) that the d orbitals split into a triply (t_{2g}) and a doubly (e_g) degenerate level in an octahedral environment. For Cu^{2+} the only possible electronic configuration is $t_{2g}^6 e_g^3$.

Suppose now that of the two e_g orbitals, d_{z^2} is doubly while $d_{x^2-y^2}$ is only singly occupied. Thus, the two ligands along the z axis are better screened from the electrostatic attraction of the central ion, and will move farther away from it, than the four ligands in the xy plane. The opposite happens if the unpaired electron occupies the d_{z^2} orbital. In both cases the octahedral arrangement undergoes tetragonal distortion along the z axis, in the former by elongation, while in the latter by compression. The original O_h symmetry reduces to D_{4h}. The symmetry-reducing vibrational mode here is of e_g symmetry and has the form shown in Figure 6-40. The splitting of d orbitals in both environments is given in Table 6-10 and is also shown here:

O_h	$\rightarrow$		D_{4h}	
e_g $(d_{x^2-y^2}, d_{z^2})$	$\rightarrow$	a_{1g} (d_{z^2})	$+$	b_{1g} $(d_{x^2-y^2})$
t_{2g} (d_{xz}, d_{yz}, d_{xy})	$\rightarrow$	e_g (d_{xz}, d_{yz})	$+$	b_{2g} (d_{xy})

Figure 6-41 illustrates the tetragonal elongation and compression of an octahedron. For the Cu^{2+} ion the relative energies of the d_{z^2} and $d_{x^2-y^2}$ orbitals depend on the location of the unpaired electron.

Consider now a qualitative picture of the splitting of the t_{2g} orbitals. If the ligands are somewhat further away along the z axis, their interaction with the d_{xz} and d_{yz} orbitals will decrease, and so will their energy compared with that of the d_{xy} orbital. This is illustrated by the left-hand side of Figure 6-41. Tetragonal

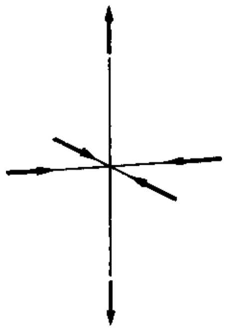

Figure 6-40. The symmetry-reducing vibrational mode of e_g symmetry for an octahedron.

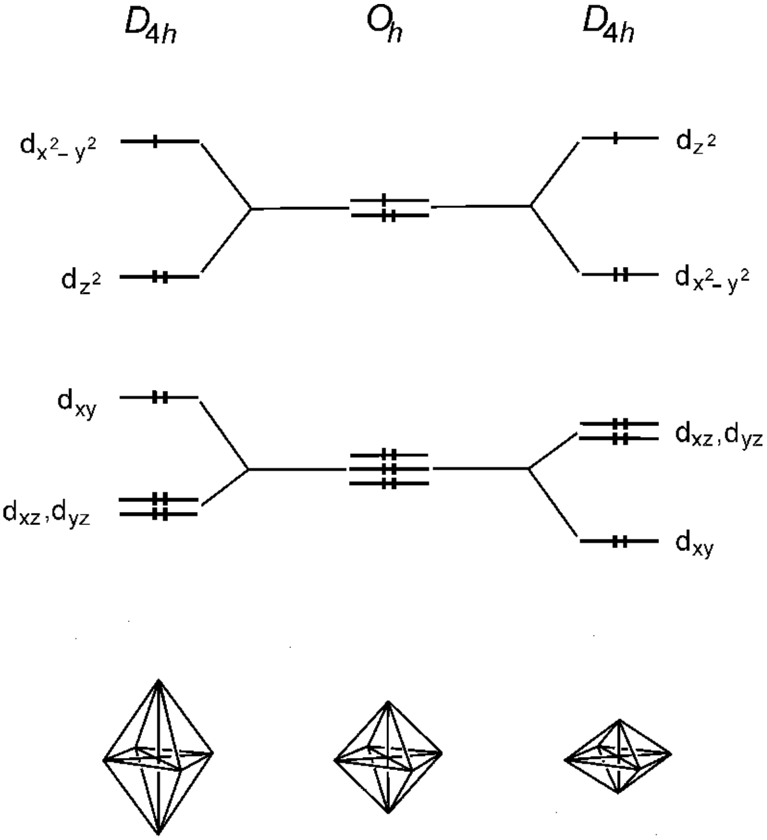

Figure 6-41. Tetragonal distortion of the regular octahedral arrangement around a d^9 ion.

compression can be accounted for by similar reasoning (cf. right-hand side of Figure 6-41).

The splitting of the *d* orbitals in Figure 6-41 shows the validity of the "center of gravity rule." One of the e_g orbitals goes up in energy as much as the other goes down. From among the t_{2g} orbitals, the doubly degenerate pair goes up (or down) in energy half as much as the non-degenerate orbital goes down (or up). Thus, for the Cu(II) compounds the splitting of the fully occupied t_{2g} orbitals does not bring about a net energy change. The same is true for all other symmetrically occupied degenerate orbitals, such as t_{2g}^3, e_g^4, or e_g^2. On the other hand, the occupancy of the e_g orbitals of Cu^{2+} is unsymmetrical, since two electrons go down and only one goes up in energy, and here there is a net energy

gain in the tetragonal distortion. This energy gain is the *Jahn–Teller stabilization energy*.

The above example referred to an octahedral configuration. Other highly symmetrical systems, for example, tetrahedral arrangements, can also display this effect. For general discussion, see, e.g. References [65–67].

The Jahn–Teller effect enhances the structural diversity of Cu(II) compounds [68]. Most of the octahedral complexes of Cu^{2+}, for example, show elongated tetragonally distorted geometry. Crystalline cupric fluoride and cupric chloride both have four shorter and two longer copper–halogen interatomic distances, 1.93 *vs.* 2.27 Å and 2.30 *vs.* 2.95 Å, respectively [69].

The square planar arrangement can be regarded as a limiting case of the elongated octahedral configuration. The four oxygen atoms are at 1.96 Å from the copper atom in a square configuration in crystalline cupric oxide, whereas the next nearest neighbors, two other oxygen atoms, are at 2.78 Å. The ratio of the two distances is much larger than in the usual distorted octahedral configuration [70].

Tetragonal compression around the central Cu^{2+} ion is much rarer; K_2CuF_4 is an example with two shorter and four longer Cu–F distances, viz., 1.95 *vs.* 2.08 Å [71].

There are also numerous cases when experimental investigation failes to provide evidence for Jahn–Teller distortion. For example, several chelate compounds of Cu(II), as well as some compounds containing the $[Cu(NO_2)_6]^{4-}$ ion, show no detectable distortion from the regular octahedral structure (see Reference [72] and references therein).

Bersuker [73–75] has shown the need for a more sophisticated approach to account for such phenomena. We attempt to convey at least the flavor of his ideas here. Jahn–Teller distortions are of a *dynamic* nature in systems under no external influence. This means that there may be many minimum-energy distorted structures in such systems. Whether an experiment will or will not detect such a dynamic Jahn–Teller effect, depends on the relationship between the time scale of the physical measurement used for the investigation, and the mean lifetime of the distorted configurations. If the time period of the measurement is longer than the mean lifetime of the distorted configurations, only an average structure, corresponding to the undistorted

high-symmetry configuration will be detected. Since different physical techniques have different time scales, one technique may detect a distortion which appears to be undetected by another.

The *static* Jahn–Teller effect can be observed only in the presence of an external influence. Bersuker [76, 77] stresses this point as the opposite statement is found often in the literature. According to the statement criticized, the effect is not to be expected in systems where low-symmetry perturbations remove electronic degeneracy. However, it is exactly the low-symmetry perturbations that make the Jahn–Teller distortions static and thus observable. Such a low-symmetry perturbation can be the substitution of one ligand by another. In this case one of the previously equivalent minimum-energy structures, or a new one, will become energetically more favored than the others.

The so-called *cooperative* Jahn–Teller effect is another occurance of the static distortions. Here, interaction, that is, cooperation between different crystal centers, make the phenomenon observable. Without interaction, the nuclear motion around each center would be independent and of a dynamic character.

Lattice vibrations tend to destroy the correlation among Jahn–Teller centers. Thus, with increasing temperature, these centers may become independent of each other at a certain point, and their static Jahn–Teller effects convert to dynamic ones. At this point the crystal as a whole becomes more symmetric. This temperature-dependent static $\Leftrightarrow$ dynamic transition is called a *Jahn–Teller phase transition.* Below the temperature of the phase transition, the cooperative Jahn–Teller effect governs the situation providing static distortion; the overall structure of the crystal is of a lower symmetry. Above this temperature, the cooperation breaks down, the Jahn–Teller distortion becomes dynamic and the crystal itself becomes more symmetric.

The temperature of the Jahn–Teller phase transition is very high for CuF_2, $CuCl_2$, and K_2CuF_4 among the examples mentioned above [78]. Therefore, at room temperature their crystal structures display distortions. Other compounds have symmetric crystal structures at room temperature as their Jahn–Teller phase transition occurs at lower temperatures. Cupric chelate compounds and $[Cu(NO_2)_6]^{4-}$ compounds, such as $K_2PbCu(NO_2)_6$ and $Tl_2PbCu(NO_2)_6$, can be mentioned as examples [79]. Further cooling, however, may make even these structures distorted.

Our last examples of Jahn–Teller distortion are from among gas-phase metal halides, manganese trifluoride and the gold trihalides. Both manganese and gold have partially filled *d* orbitals in their trihalides; manganese has four and gold eight *d* electrons. Manganese trifluoride is one of the typical Jahn–Teller cases in its crystal with a strongly elongated octahedral arrangement of the fluorine atoms around manganese. Without the ramifications of the Jahn–Teller effect, we would expect a tigonal planar geometry of D_{3h} symmetry for the gas-phase molecules of these trihalides. However, both experiments and computations found that these gas-phase molecules have a lower, C_{2v} symmetry structure [80–83]. In the assumed D_{3h}-symmetry structure, these molecules have a partially filled e'-symmetry orbital and an E' electronic state. Using the same line of thought as for the H_3 molecule, the direct product of E' with itself reduces to $A_1' + A_2' + E'$. The four-atomic metal trihalides have 6 normal modes of vibration [(3 × 4) – 6 = 6] with symmetries $A_1' + A_2'' + 2E'$(as we discussed earlier, each doubly-degenerate vibration, E', counts as two). We can see that there is no A_2''-symmetry irreducible representation among the ones that the direct product of the ground electronic state symmetry, E', with itself reduces to. There are two matches between the irreducible representations and the normal modes of vibration: A_1 and E'. The totally symmetric A_1 vibration cannot take out the molecules from the D_{3h}-symmetry structure, so the only possibility is one of the two E' vibrations (see Figure 6.42), just as was the case with the H_3 molecule. However, while for the H_3 molecule both of these vibrations resulted in dissociation, for these metal trihalides, the angle bending vibration results in a stable structure of C_{2v} symmetry that is of lower energy

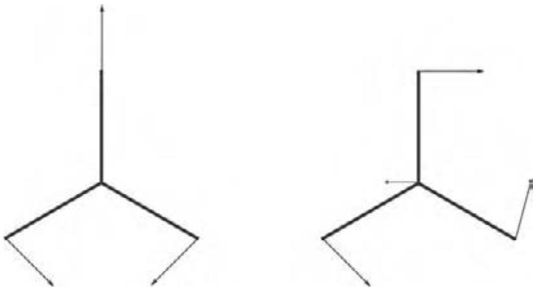

Figure 6-42. The two e' symmetry normal modes of vibration of a metal trihalide molecule.

than the higher symmetry D_{3h} structure. This is why C_{2v} symmetry is observed as the ground-state structure of these metal trihalides.

The question might arise whether it would not be more "straight-forward" for the MnF_3 molecule to distort into a structure of C_{3v} symmetry? The D_{3h} character table (Table 6-11) helps us to understand the reason. The out-of-plane vibration—that would make the molecule pyramidal—is of a_2'' symmetry. However, there is no irreducible representation with a_2'' symmetry among the irreducible representations that the direct product of E' with itself reduces to (see, above). Therefore, a C_{3v}-type of distortion is not possible—at least not in the Jahn–Teller manner.

Coming back to the C_{2v}-symmetry distortion of metal trihalides; the e'-symmetry angle bending vibration can distort the molecule in two ways. Either one of the bond angles decreases while the opposite bond lengthens, or the other way around, the bond angle increases and the opposite bond shortens (Figure 6-43). In fact, both structures are real. Figure 6-44 shows the potential energy surface (see Chapter 7) of the $AuCl_3$ molecule. This is a so-called Mexican-hat type potential energy surface. The high-energy point at the tip of the hat corresponds to an undistorted D_{3h}-symmetry structure. The surface of the brim of the hat warps producing three wells separated by three humps of equal height. The three wells correspond to the minima with a structure in which one of the bond angles opens and the opposite bond shortens (Figure 6-43 left; there are three of these structures because the same distortion might happen involving each of the three bond angles and the opposite bonds). The three humps correspond to the so-called transition-states (see Chapter 7 in more detail), and these structures have one smaller bond angle with an elongated bond opposite to it as seen in Figure 6-43 right. As Figure 6-44 shows, the Jahn–Teller

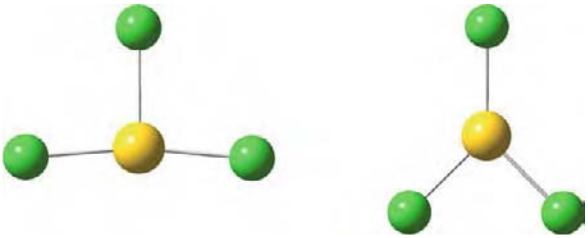

Figure 6-43. The two types of structures that might result from an e'-type vibration of a metal trihalide molecule.

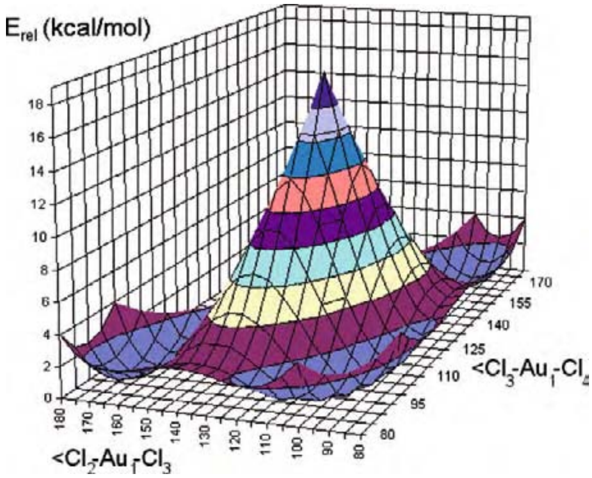

Figure 6-44. The “Mexican-hat” potential energy surface of the $AuCl_3$ molecule [84], copyright 2001, American Chemical Society.

distortion stabilizes the lower-symmetry structures compared to the high-symmetry one.

Quantum chemical calculations revealed that there are two possible E' symmetry electronic states for a D_{3h}-symmetry gold trihalide. In one of them (high-spin state) there is one electron on each of the two e' orbitals with parallel spins (see Figure 6-45); this is the one that should be the ground state according to Hund’s rule. However, symmetry lowering would not bring about any energy gain; with one orbital going up and the other down with no net change. The other E'-symmetry state (low-spin) has two electrons with opposite spins in one of the two e' orbitals and is less stable than the high-spin state. However, the distortion of this low-spin state (see Figure 6-45)

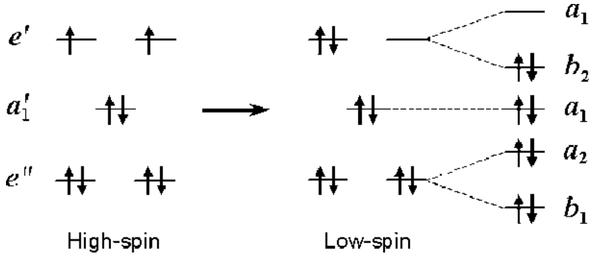

Figure 6-45. High-spin and low-spin electronic configuration of gold trihalides and the splitting of the low-spin E' state of gold trihalides.

brings about a substantial energy gain. In fact, the energy lowering is so large that the distortion of this higher energy state produces the overall lowest energy structure that will be the ground state; this is the C_{2v}-symmetry structure in Figure 6-43 left. The energy gain by the Jahn–Teller distortion of the less stable trigonal planar structure is so large that it can "pay the price" for the spin pairing and still produce an overall lower-energy structure.

At this point, it is of interest to quote Edward Teller about the discovery of the Jahn–Teller effect (Figure 6-46) [85]:

> This effect had something to do with Lev Landau. I had a German student in Göttingen, R. Renner, and he wrote a paper on degenerate electronic states in the linear carbon dioxide molecule, assuming that the excited, degenerate state of carbon dioxide is linear.

Figure 6-46. Edward Teller (courtesy of Lawrence Livermoore Nartional Laboratory) and Lev Landau (courtesy of Alexei Abrikosov, from A.A. Abrikosov: *Academician L. D. Landau: Short Biography and Review of his Scientific Work*, Nauka, Moscow, 1965, in Russian).

> In the year 1934 both Landau and I were in Niels Bohr's Institute in Copenhagen and we had many discussions. He disagreed with Renner's paper, he disliked it. He said that if the molecule is in a degenerate electronic state then its symmetry will be destroyed and the molecule will no longer be linear. Landau was wrong. I managed to convince him and he agreed with me. This was probably the only case when I won an argument with Landau.
>
> A little later I went to London, and met Jahn. I told him about my discussion with Landau, and about the problem in which I was convinced that Landau was wrong. But it bothered me that he was usually not wrong. So maybe he is always right with the exception of linear molecules. Jahn was a good group-theorist, and we wrote this paper, the content of which you know, that if a molecule has an electronic state that is degenerate, then the symmetry of the molecule will be destroyed. That is the Jahn–Teller theorem.
>
> The Jahn–Teller theorem has a footnote: this is always true with the only exception of linear molecules. So the amusing story of the Jahn–Teller effect is that I first worked with my student, Renner, on a paper that presented the only general exception to the Jahn–Teller effect. It really should be the Landau–Jahn–Teller theorem because Landau was the first one who expressed it, unfortunately using the only exception where it was not valid.

Linear molecules are the only exception to the Jahn–Teller effect. But linear molecules may also have instabilities in their degenerate electronic states and this is called the Renner–Teller effect. It was first described by Renner in a theoretical paper on the degenerate first excited electronic state of carbon dioxide [86]. It took more than twenty years to find the first experimental evidence of this effect, in the electronic absorption spectrum of the NH_2 radical [87]. The NH_2 radical has one electron on a π orbital and thus a Π electronic state

in its ground state, where it is bent; while it is linear in the excited nondegenerate state.

Another, recently found, example of the Renner–Teller effect is the chromium dichloride, $CrCl_2$, molecule [88]. Based on high-level computations and electron diffraction experiments, it was found that the gas-phase molecule is not linear as could be expected for a transition metal dihalide but rather bent. According to the computations, among the different high-spin electronic states, the Π_g twofold degenerate state is the lowest in energy. However, it is not stable and splits into two nondegenerate states, of B_2 and A_2 symmetry, respectively, of which the B_2 state is the ground state with a bond angle of about 147°.

Chromium in its dichloride has a d^4 electronic configuration and in its crystals is subject to the Jahn–Teller effect. Indeed, chromium has a tetragonally distorted octahedral coordination in its crystals [89]. $CrCl_2$ is a fascinating molecule in that it displays both the Jahn–Teller and the Renner–Teller effects.

Another structural phenomenon related to the Jahn–Teller effect is the *pseudo-Jahn–Teller effect*. This happens when two electronic states of a molecule, the ground state and an excited state are close enough in energy and thus, they can mix under nuclear displacements [90]. The pseudo-Jahn–Teller effect can appear separately from the real Jahn–Teller effect, or together with it; their magnitude can also be either very small, or substancial.

It is stressed that the physical bases for the Jahn–Teller effect and the pseudo-Jahn–Teller effect are quite different. Jahn–Teller distortion occurs due to the coupling of the electronic and vibrational motions of the molecule; i.e., the coupling of a degenerate electronic wave function with the vibrational wave function. In case of the pseudo-Jahn–Teller effect, the vibronic interaction happens between two electronic states that are close in energy and are not necessarily degenerate (although because of their similar energies we might consider them “pseudo-generate”[91]); i.e., here the vibronic coupling is between two electronic wave functions. The effect pushes the two states apart. The two states must belong to the same irreducible representation of the new point group as before and can continue to interact, which, obviously, is not the case with the Jahn–Teller effect.

In concluding this section, we mention that Bersuker points to a very general applicability of the Jahn–Teller effect, much beyond

molecules [92]. Obviously, the Jahn–Teller effect, degeneracy, and symmetry breaking are inherently related to each other. Thus, it must have been phenomena triggered by a Jahn–Teller type coupling of degenerate states to the motions of particles that led to the symmetry breaking after the Big Bang that, eventually, led to the formation of the Universe.

References

1. A. L. Mackay, *A Dictionary of Scientific Quotations*, Adam Hilder, Bristol 1991, p. 57/85.
2. I. N. Levine, *Quantum Chemistry*, Sixth Edition, Prentice Hall, Upper Saddle River, New Jersey, 2008.
3. P. Atkins, R. Friedman, *Molecular Quantum Mechanics*, Fourth Edition, Oxford University Press, New York, 2005.
4. D. V. George, *Principles of Quantum Chemistry*, Pergamon Press, New York, 1972.
5. M. W. Hanna, *Quantum Mechanics in Chemistry*, Second Edition, W. A. Benjamin, New York, Amsterdam, 1969.
6. F. A. Cotton, *Chemical Applications of Group Theory*, Third Edition, Wiley-Interscience, New York, 1990.
7. D. C. Harris, M. D. Bertolucci, *Symmetry and Spectroscopy: An Introduction to Vibrational and Electronic Spectroscopy*, Dover Publications, New York, 1989.
8. M. Orchin, H. H. Jaffe, *Symmetry Orbitals, and Spectra (S.O.S)*, Wiley-Interscience, New York, 1971.
9. Hanna, *Quantum Mechanics in Chemistry.*
10. Atkins, Friedman, *Molecular Quantum Mechanics.*
11. George, *Principles of Quantum Chemistry.*
12. Hanna, *Quantum Mechanics in Chemistry.*
13. Cotton, *Chemical Applications of Group Theory.*
14. E. P. Wigner, *Group Theory and its Application to the Quantum Mechanics of Atomic Spectra*, Academic Press, New York, 1959.
15. Harris, Bertolucci, *Symmetry and Spectroscopy.*
16. Ibid, p. 3.
17. Ibid.
18. T. H. Lowry, K. S. Richardson, *Mechanism and Theory in Organic Chemistry*; Third Edition. Harper and Row, New York (1987)
19. Maple V, Release 2, Waterloo Maple Software, University of Waterloo, Ontario, Canada.
20. C. A. Coulson, *The Shape and Structure of Molecules*, Clarendon Press, Oxford, 1973.

21. G. Lanza, Z. Varga, M. Kolonits, M. Hargittai, "On the Effect of 4f Electrons on the Structural Characteristics of Lanthanide Trihalides. Computational and Electron Diffraction Study of Dysprosium Trichloride." *J. Chem. Phys*. 2008, 128, 074301-1–14.
22. Drawn with Gaussview, Version 4.1.2, A. Frisch, R. D. Dennington II, T. D. Keith and J. Millam, Gaussview 4 Reference, Gaussian Inc., 2007.
23. Cotton, *Chemical Applications of Group Theory.*
24. Drawn with Gaussview (for reference, see, [22]).
25. Harris, Bertolucci, *Symmetry and Spectroscopy*.
26. Ibid.
27. Ibid.
28. Drawn with Gaussview (for reference, see, [22]).
29. Ibid.
30. Cotton, *Chemical Applications of Group Theory*.
31. J. L. Gay-Lussac, "Memoir on the Combination of Gaseous Substances with Each Other." *Mémoires de la Société d'Arcueil* 1809, 2, 207–234, as translated in Alembic Club Reprint No. 4, (Edinburgh, 1890).
32. Levine, *Quantum Chemistry.*
33. Atkins, Friedman, *Molecular Quantum Mechanics.*
34. George, *Principles of Quantum Chemistry.*
35. Hanna, *Quantum Mechanics in Chemistry.*
36. *Encyclopedia of Computational Chemistry*, eds. P. v. R. Schleyer, N. L. Allinger, T. Clark, J. Gasteiger, P. A. Kollman, H. F. Schaefer III, P. R. Schreiner, Wiley, Chichester, 1998.
37. I. Hargittai, M. Hargittai, *Symmetry through the Eyes of a Chemist*, Second Edition, Plenum, New York, 1995, p. 272.
38. M. Hargittai, I. Hargittai, "Aspects of Structural Chemistry in Molecular Biology", In: A. Domenicano, I. Hargittai, eds.: *Strength from Weekness: Structural Consequences of Weak Interactions in Molecules, Supermolecules, and Crystals*, Kluwer, Dordrecht, 2002, pp. 91–119.
39. M. Hargittai, I. Hargittai, "Experimental and Computed Bond Lengths: The Importance of Their Differences." *Int. J. Quant. Chem*. 1992, 44, 1057–1067.
40. I. Hargittai, M. Hargittai, "The Importance of Small Structural Differences," in *Molecular Structure and Energetics*, Vol. 2, Chapter 1, J. F. Liebman and A. Greenberg, eds., VCH Publishers, New York, 1987, pp. 1–35.
41. R. Hilgenfeld, W. Saenger, "Stetter's Complexes are no Intramolecular Inclusion Compounds." *Angew. Chem. Int. Ed. Eng.* 1982, 21, 787–788.
42. K. B. Borisenko, C. W. Bock, I. Hargittai, "Intramolecular Hydrogen Bonding and Molecular Geometry of 2-Nitrophenol from a Joint Gas-Phase Electron Diffraction and Ab Initio Molecular Orbital Investigation." *J. Phys. Chem*. 1994, 98, 1442–1448.

43. M. Hargittai, P. Schwerdtfeger, B. Réffy, R. Brown, "The Molecular Structure of Different Species of Cuprous Chloride from Gas-Phase Electron Diffraction and Quantum Chemical Calculation."*Chem. Eur. J.* 2003, 9, 327–333.
44. B. Vest, Z. Varga, M. Hargittai, A. Hermann, P. Schwerdtfeger, "The Elusive Structure of $CrCl_2$ — A Combined Computational and Gas Phase Electron Diffraction Study." *Chem. Eur. J.* 2008, 14, 5130–5143.
45. Z. Varga, G. Lanza, C. Minichino, M. Hargittai, "Quasilinear Molecule par Excellence, $SrCl_2$: Structure from High-Temperature Gas-Phase Electron Diffraction and Quantum Chemical Calculations; Computed Structures of $SrCl_2$-Argon Complexes." *Chem. Eur. J*. 2006, 12, 8345–8357.
46. R. D. Levine, "The Chemical Shape of Molecules — An Introduction to Dynamic Stereochemistry." *J. Phys. Chem*. 1990, 94, 8872–8880.
47. H. F. Schafer III., "Computers and Molecular Quantum Mechanics: 1965–2001, a personal perspective." *J. Mol. Struct. (Theochem)* 2001, 573, 129–137.
48. H. F. Schafer III, Private communication to one of the authors (IH) at the 10th Conference on the Current Trends in Computational Chemistry, Jackson, Mississippi, 2001.
49. H. Bethe, "Termaufspaltung in Kristallen (Splitting of Terms in Crystals)." *Ann. Phys*. 1929, 3, 133–208.
50. F. A. Cotton, G. Wilkinson, P. L. Gaus, *Basic Inorganic Chemistry,* Second Edition, John Wiley & Sons, New York, 1987.
51. Ibid.
52. A. Ceulemans, D. Beyens, L. G. Vanquickenborne, "Symmetry Aspects of Jahn–Teller Activity—Structure and Reactivity." *J. Am. Chem. Soc*. 1984, 106, 5824–5837.
53. H. A. Jahn, E. Teller, "Stability of Polyatomic Molecules in Degenerate Electronic States. I. Orbital Degeneracy." *Proc. Roy. Soc*. 1937, A161, 220–235.
54. T. A. Barckholtz, T. A. Miller, "Quantitative Insights about Molecules Exhibiting Jahn–Teller and Related Effects." *Int. Rev. Phys. Chem*. 1998, 17, 435–524.
55. I. B. Bersuker, *The Jahn–Teller Effect and Vibronic Interactions in Modern Chemistry,* Plenum Press, New York, 1984.
56. I. B. Bersuker and V. Z. Polinger, *Vibronic Interactions in Molecules and Crystals*, Springer-Verlag, Berlin, 1989.
57. I. B. Bersuker, *The Jahn–Teller Effect,* Cambridge University Press, Cambridge, 2006.
58. I. B. Bersuker, "Jahn–Teller Effect in Crystal-Chemistry and Spectroscopy." *Coord. Chem. Rev*. 1975, 14, 357–412.
59. I. B. Bersuker, "Modern Aspects of the Jahn–Teller Effect Theory and Applications to Molecular Problems." *Chem. Rev*. 2001, 101, 1067–1114.
60. I. B. Bersuker, "The Jahn–Teller Effect As a General Tool for Solving Molecular and Solid State Problems: Novel Findings." *J. Mol. Struct*. 2007, 838, 44–52.
61. Jahn, Teller, *Proc. Roy. Soc.* 220–235.

62. J. S. Wright, G. A. GiLabio, “Structure and Stability of Small Hydrogen Rings.” *J. Phys. Chem.* 1992, 96, 10793–10799.
63. B. E. Applegate, T. E. Miller, *J. Chem. Phys.* 2002, 17, 10654–10674.
64. Cotton et al., *Basic Inorganic Chemistry*.
65. Bersuker, *The Jahn–Teller Effect and Vibronic Interactions in Modern Chemistry.*
66. Bersuker, Polinger, *Vibronic Interactions in Molecules and Crystals*.
67. Bersuker, *The Jahn–Teller Effect.*
68. A. F. Wells, *Structural Inorganic Chemistry,* Fourth Edition, Clarendon Press, Oxford, 1975.
69. Ibid.
70. Ibid.
71. Ibid.
72. J. E. Huheey, *Inorganic Chemistry Principles of Structure and Reactivity,* Third Edition, Harper & Row Publishers, New York, 1983.
73. Bersuker, *The Jahn–Teller Effect and Vibronic Interactions in Modern Chemistry.*
74. Bersuker, Polinger, *Vibronic Interactions in Molecules and Crystals.*
75. Bersuker, *The Jahn–Teller Effect.*
76. Bersuker, Polinger, *Vibronic Interactions in Molecules and Crystals.*
77. Bersuker, *Coord. Chem. Rev.* 357–412.
78. Ibid.
79. Huheey, *Inorganic Chemistry Principles of Structure and Reactivity.*
80. M. Hargittai, B. Réffy, M. Kolonits, C. J. Marsden, J.-L. Heully, “The Structure of the Free MnF_3 Molecule – A Beautiful Example of the Jahn–Teller Effect.” *J. Am. Chem. Soc.* 1997, 119, 9042–9048.
81. B. Réffy, M. Kolonits, A. Schulz, T. M. Klapötke, M. Hargittai, “Intriguing Gold Trifluoride – Molecular Structure of Monomers and Dimers: An Electron Diffraction and Quantum Chemical Study.” *J. Am. Chem. Soc.* 2000, 122, 3127–3134.
82. M. Hargittai, A. Schulz, B. Réffy, M. Kolonits, “Molecular Structure, Bonding and Jahn–Teller Effect in Gold Chlorides: Quntum Chemical Study of $AuCl_3$, Au_2Cl_6, $AuCl_4^-$, AuCl, and Au_2Cl_2 and Electron Diffraction Study of Au_2Cl_6.” *J. Am. Chem. Soc.* 2001, 123, 1449–1458.
83. A. Schulz, M. Hargittai, “Structural Variations and Bonding in Gold Halides. A Quantum Chemical Study of Monomeric and Dimeric Gold Monohalide and Gold Trihalide Molecules, AuX, Au_2X_2, AuX_3, and Au_2X_6 (X = F, Cl, Br, I).” *Chem. Eur. J.* 2001, 7, 3657–3670.
84. Hargittai et al. *J. Am. Chem. Soc.* 2001, p. 1455.
85. I. Hargittai, M. Hargittai, “Edward Teller.” *Chem. Intell.* 1997, 3, 14–23.
86. R. Renner, “Zur Theorie der Wechselwirkung zwischen Elektronen- und Kernbewegung bei dreiatomigen, stabförmigen Molekülen.“ *Z. Phys.* 1934, 92, 172–193.
87. K. Dressler, D. A. Ramsay, “The Electronic Absorption Spectra of NH_2 and ND_2.” *Phil. Trans. Roy. Soc. London* 1959, 251A, 553–602.

88. Vest et al., *Chem. Eur. J.* 5130–5143.
89. J. W. Tracy, N. W. Gregory, E. C. Lingafelter, J. D. Dunitz, H.-C. Mez, R. E. Rundle, C. Scheringer, H. L. Yakel, M. K. Wilkinson, “The crystal structure of chromium(II) chloride.” *Acta Cryst*. 1961, 14, 927–929.
90. Bersuker, *Chem. Rev.* 1067–1114.
91. Ibid.
92. Bersuker, *J. Mol. Struct*. 44–52.

Chapter 7

Chemical Reactions

By some fortuitous concourse of atoms.
Marcus Tullius Cicero [1]

The chemical reaction is the "most chemical" event. The first application of symmetry considerations to chemical reactions can be attributed to Wigner and Witmer [2]. The Wigner–Witmer rules are concerned with the conservation of spin and orbital angular momentum in the reaction of diatomic molecules. Although symmetry is not explicitly mentioned, it is present implicitly in the principle of conservation of orbital angular momentum. It was Emmy Noether (1882–1935), a German mathematician, who established that there was a one-to-one correspondence between symmetry and the different conservation laws [3, 4].

The real breakthrough in recognizing the role that symmetry plays in determining the course of chemical reactions has occurred only recently, mainly through the activities of Woodward and Hoffmann [5, 6], Fukui [7, 8], Bader [9, 10], Pearson [11], Halevi [12, 13], and others. The main idea in their work is that symmetry phenomena may play as important a role in chemical reactions as they do in the construction of molecular orbitals or in molecular spectroscopy. It is even possible to make certain symmetry based "selection rules" for the "allowedness" and "forbiddenness" of a chemical reaction, just as is done for spectroscopic transitions.

The series of articles written by Woodward and Hoffmann in the middle of the 1960s caused a considerable stir in the organic chemistry community. For decades afterwards organic chemists were checking and trying out reactions proposed by the orbital symmetry rules. In 2003, the first paper of their series [14] was the 88th most cited paper in the *Journal of the American Chemical Society* [15].

M. Hargittai, I. Hargittai, *Symmetry through the Eyes of a Chemist,* 3rd ed.,
DOI: 10.1007/978-1-4020-5628-4_7, © Springer Science+Business Media B.V. 2009

Before describing the symmetry rules for chemical reactions, however, we would like to mention some limitations. Symmetry rules can usually be applied to comparatively simple reactions, the so-called *concerted reactions*. In a concerted reaction all relevant changes occur simultaneously; the transformation of reactants into products happens in one step with no intermediates.

At first sight it would seem logical that symmetry rules can be applied only to symmetrical molecules. However even nonsymmetric reactants can be "simplified" to related symmetrical parent molecules. As Woodward and Hoffmann put it, they can be "reduced to their highest inherent symmetry" [16]. This is, in fact, a necessary criterion if symmetry principles are to be applied.

What does this mean? For example, propylene, $H_2C{=}CHCH_3$, must be treated as its "parent molecule", ethylene. The reason is that it is the double bond of propylene which changes during the reaction, and it nearly possesses the symmetry of ethylene. Salem calls this feature "pseudosymmetry" [17].

The statement: a chemical reaction is "symmetry allowed" or "symmetry forbidden," should not be taken literally. When a reaction is symmetry allowed, it means that it has a low activation energy. This makes it possible for the given reaction to occur, though it does not mean that it always will. There are other factors which can impose a substantial activation barrier. Such factors may be steric repulsions, difficulties in approach, and unfavorable relative energies of orbitals. Similarly, "symmetry forbidden" means that the reaction, as a concerted one, would have a high activation barrier. However, various factors may make the reaction still possible; for example, it may happen as a stepwise reaction through intermediates. In this case, of course, it is no longer a concerted reaction.

Most of the symmetry rules explaining and predicting chemical reactions deal with changes in the electronic structure. However, a chemical reaction is more than just that. Breakage of bonds and formation of new ones are also accompanied by nuclear rearrangements and changes in the vibrational behavior of the molecule. (Molecular translation and rotation as a whole can be ignored.)

As has been shown previously, both the vibrational motion and the electronic structure of the molecules strongly depend on symmetry. This dependence can be fully utilized when discussing chemical reactions.

Describing the structures of both reactant and product molecules with the help of symmetry would not add anything new to our previous discussion. What is new and important is that certain symmetry rules can be applied to the transition state in between the reactants and products. This is indeed the topic of the present Chapter.

7.1. Potential Energy Surface

The potential energy surface is the cornerstone of all theoretical studies of reaction mechanisms [18]. The topography of a potential energy surface contains all possible information about a chemical reaction. However, how this potential energy surface can be depicted is another matter.

The total energy of a molecule consists of the potential and the kinetic energy of both the nuclei and the electrons. The coulombic energy of the nuclei and the electronic energy together represent the whole potential energy under whose influence the nuclei carry out their vibrations. Since the energies of the (ground and various excited) electronic states are different, each state has its own potential energy surface. We are usually interested in the lowest energy potential surface which corresponds to the ground state of the molecule. An N atomic molecule has $3N$–6 internal degrees of freedom (a linear molecule has $3N$–5). The potential energy for such a molecule can be represented by a $3N$–6-dimensional hypersurface in a $3N$–5-dimensional space. Clearly the actual representation of this surface is impossible in our limited dimensions.

There are ways, however, to plot parts of the potential energy hypersurface. For example, the energy is plotted with respect to the change of two coordinates during a reaction and molecular rearrangement in Figure 7-1a and b. Such drawings help to visualize the real potential energy surface. It is like a rough topographic map with mountains of different heights, long valleys of different depths, mountain paths and holes. Since energy increases along the vertical coordinate, the mountains correspond to energy barriers and the holes and valleys to different energy minima.

Studying reaction mechanisms means essentially finding the most economical way to go from one valley to another. Two adjacent valleys are connected by a mountain path: this is the road that the

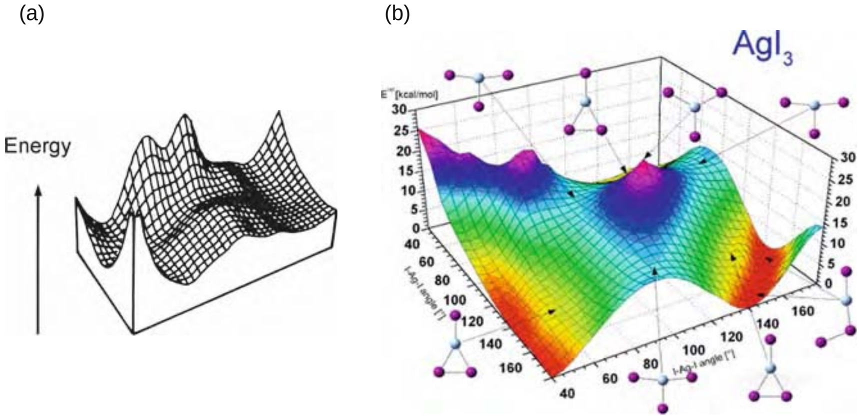

Figure 7-1. Three-dimensional potential energy surfaces: (**a**) Energy hypersurface for FSSF ⇔ SSF_2 isomerization (detail). Reproduced with permission [19] copyright (1977) American Chemical Society; (**b**) Potential energy surface of the molecular rearrangement of AgI_3, with the corresponding structures indicated on the sides [20]. Copyright (2005) American Chemical Society.

reactant molecules must follow if they want to reach the valley on the other side, which will correspond to the product(s). The top of the pass is called the *saddle point* or *col.* The name saddle point refers to the saddle on a horse. Starting from the center of the saddle, it is going up in the direction of the head as well as the tail, and it is going down in the direction of both sides. The configuration of nuclei at the saddle point is sometimes called a *transition state,* sometimes a *transition structure*, in other cases an *activated complex*, and yet in other cases, a *supermolecule.* Transition state is the most commonly used term, although it is somewhat ambiguous (see Section 7.1.1).

7.1.1. Transition State, Transition Structure

The region of the potential energy surface indicating the transition state is illustrated in Figure 7-2, while a modern sculpture reminiscent of a potential energy surface at and around the saddle point is shown in Figure 7-3.

The term *transition state* is sometimes used interchangeably with the term *transition structure,* although in a strict sense the two are not identical. Transition state is the quasi-thermodynamic state of

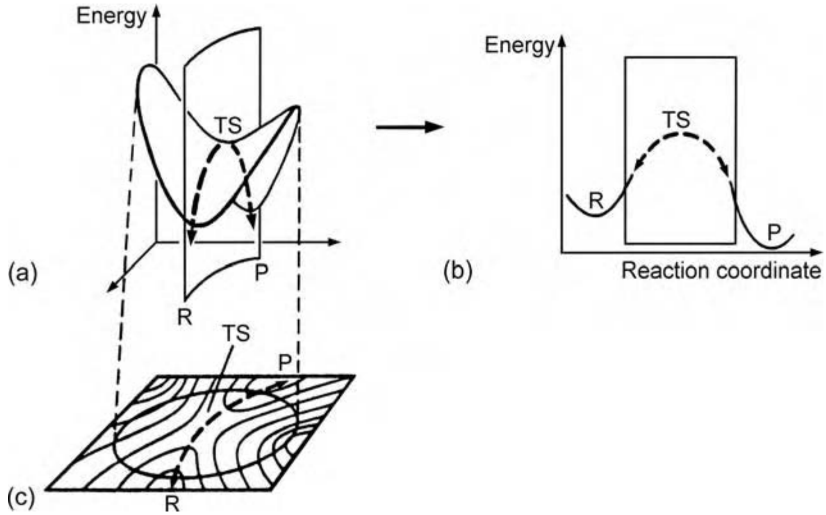

Figure 7-2. Potential energy surface by Williams in the region of the transition structure in different representations [21]: (**a**) Three-dimensional representation of the saddle-shaped potential energy surface; (**b**) Two-dimensional potential energy curve produced by a vertical cut through the surface in (**a**) along the reaction path (indicated by bold dashed line) from reactants (R) to products (P); (**c**) Energy contours produced by horizontal cuts through the potential energy sufrace in (**a**). Adapted with permission from Reference [21].

Figure 7-3. Saddle-shaped sculpture in Madrid, Spain. Photograph by the authors.

the reacting system as defined by Eyring [22]. The *transition structure*, on the other hand, is the molecular structure at the saddle point. As was shown by Houk et al. [23], when a reaction has a large activation barrier and a slowly varying entropy in the region of the potential energy maximum, the transition-state geometry and the transition structure are about the same. This is illustrated in Figure 7-4a. However, when the barrier of the reaction is low and the entropy varies rapidly in the region of the potential energy minimum, the transition-state geometry differs from the transition structure (Figure 7-4b).

As Williams stated [25]:

> The transition state is of strategic importance within the field of chemical reactivity. Owing to its location in the region of the highest energy point on the most accessible route between reactants and products it commands both the direction and the rate of chemical change. Questions of selectivity (“Which way is it to the observed product?”) and efficiency (“How easy is it to get there?”) may be answered by a knowledge of the structure and properties of the transition state.

The development of transition-state theory is due to Eyring and Polanyi [26], while the term *transition state* was first used by Evans and Polanyi [27]. Since then, it has been obvious that the properties of the region between the reactants and the products need to be

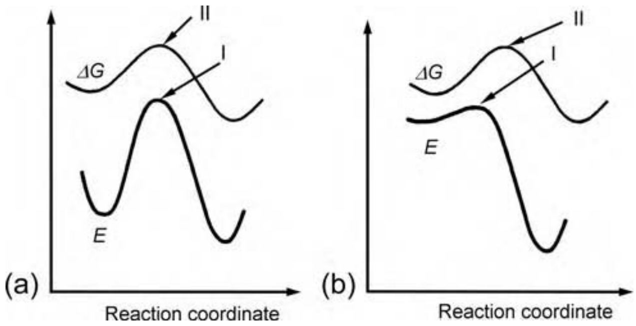

Figure 7-4. Variation of ΔG and E along a raction path, after Houk et al. [24], I, transition structure; II, transition state. (**a**) The transition state and the transition structure coincide; (**b**) The transition state and the transition structure differ. Adapted with permission.

known in order to understand reaction mechanisms. However, the lifetime of the transition state is usually less than 10^{-12} s, and, therefore, for a long time this state could only be studied by theoretical methods. Only recently have experimental techniques become available that make the study of elementary reactions possible in real time. Direct measurements of the transition state have been carried out using different sophisticated spectroscopic techniques (see, e.g., References [28–30]). An example is the laser experiments that make it possible to record snapshots of chemical reactions in the femtosecond (10^{-15} s) time scale, thus providing direct real-time observations of the transition state [31–34].

At the same time, with the ever increasing capabilities of computational techniques, it has become possible to calculate the details of transition-state geometries and energetics with great precision. Due to the increasing reliability of quantum-chemical calculations on the one hand and to the possibility of real-time experimental observation of transition-state geometries on the other, the investigation of the structure and dynamics of elementary chemical reactions has become one of the most exciting areas of modern chemical research. Nothing proves this better than the Nobel Prize for Chemistry in 1999, awarded to Ahmed Zewail "For his studies of the transition states of chemical reactions using femtosecond spectroscopy."

7.1.2. Reaction Coordinate

How does symmetry come into the picture? It happens through the movement of the nuclei along the potential energy surface. As discussed in detail in Chapter 5, all possible internuclear motions of a molecule can be resolved into sets of special motions corresponding to the normal modes of the molecule. These normal modes already have a symmetry label since they belong to one of the irreducible representations of the molecular point group. The changing nuclear positions during the course of a reaction are collectively described by the term *reaction coordinate.* In simple cases, we may assume that the chemical reaction is dominated by one of the normal modes of vibration, and thus this vibrational mode is the reaction coordinate. By selecting this coordinate, we may cut a slice through the potential energy hypersurface along this particular motion. This was done by Williams [35] in Figure 7-2 by cutting a slice of (a) in order to

produce (b). Figure 7-2b shows the reaction path along the reaction coordinate. Points R and P are minima, corresponding to the initial (reactants) and final (products) stages of the reaction, while TS is the saddle point corresponding to the transition structure and the energy barrier.

The diagram in Figure 7-2b has several important features. First of all, it represents only a slice of the potential energy hypersurface. It is the variation along one coordinate, and it is supposed that all the other possible motions of the nuclei, that is, all the other normal vibrations, are at their optimum value, so their energy is at minimum. Therefore, this reaction path can be taken as a *minimum energy path*. All other possible motions will be orthogonal to the reaction coordinate and will not contribute to it. In other words, if we would try to leave the reaction path sideways, that is, along some other vibrational mode, the energy would invariably increase.

Figure 7-2a illustrates this point. The bold line shows the reaction path. It goes through a maximum point, which is the reaction barrier. The surface, however, rises on both sides of the reaction coordinate. Thus, with respect to the energy of the other vibrational coordinates, the reaction follows a minimum energy path indeed.

7.1.3. Symmetry Rules for the Reaction Coordinate

Symmetry rules to predict reaction mechanisms through the analysis of the reacton coordinate were first applied by Bader [36] (see, also, Reference [37]) and were further developed by Pearson [38].

The energy variation along the reaction path can be characterized in the following way. The energy of all vibrational modes except the reaction coordinate is minimal all along the path, i.e.,

$$\frac{\partial E}{\partial Q_i} = 0 \quad \text{and} \quad \frac{\partial^2 E}{\partial Q_i^2} > 0 \tag{7-1}$$

where Q_i is any coordinate (3N–7 for nonlinear molecules) except Q_r, the reaction coordinate. With respect to symmetry these vibrations are unrestricted. (Of course, every normal mode must belong to one or another irreducible representation of the molecular point group.)

The energy variation of the reaction coordinate is different. At every point, except at the maximum and minimum values, it is nonzero,

$$\frac{\partial E}{\partial Q_r} \neq 0 \tag{7-2}$$

This is simply the slope of the curve on the potential energy diagram. At the minimum points (R and P in Figure 7-2a):

$$\frac{\partial E}{\partial Q_r} = 0 \quad \text{and} \quad \frac{\partial^2 E}{\partial Q_r^2} > 0 \tag{7-3}$$

At the saddle point (TS in Figure 7-2a):

$$\frac{\partial E}{\partial Q_r} = 0 \quad \text{and} \quad \frac{\partial^2 E}{\partial Q_r^2} < 0 \tag{7-4}$$

In order to predict reaction mechanisms and to estimate energy barriers, the energy can be expressed in terms of the reaction coordinate using second-order perturbation theory in such a way that the expression contains symmetry-dependent terms (see References [39] and [40] for details).

The expression of energy contains two different types of energy integrals:

$$\left\langle \Psi_0 \left| \frac{\partial E}{\partial Q_r} \right| \Psi_0 \right\rangle \quad \text{and} \quad \left\langle \Psi_0 \left| \frac{\partial E}{\partial Q_r} \right| \Psi_i \right\rangle \tag{7-5}$$

where Ψ_0 and Ψ_i are the wave functions of the ground state and an excited state, respectively. In the actual calculations, these wave functions are approximated by molecular orbitals, but their relationship remains the same.

Examine now the two energy integrals separately, bearing in mind what was said about the conditions necessary for an integral to have nonzero value (Chapter 4). The first integral contains only the ground-state wave function. It appears in the first-order perturbation energy term that expresses the effect of changing the nuclear positions on the

original electron distribution. This integral will have nonzero value only if

$$\Gamma_{\Psi_0} \cdot \Gamma_{\Psi_0} \subset \Gamma_{Q_r} \tag{7-6}$$

that is, if the direct product of the representation of Ψ_0 with itself (a function with the *same* symmetry) contains the representation of Q_r.

Concerning Ψ_0 there are two possibilities: it can be degenerate or nondegenerate. If Ψ_0 is degenerate, the molecule will be unstable (this is the case of the Jahn–Teller effect, see Section 6.6) and it will undergo a distortion that reduces the molecular symmetry and destroys the degeneracy of Ψ_0. Consider now the case when Ψ_0 is nondegenerate. We know that the direct product of two nondegenerate functions with the same symmetry always belongs to the totally symmetric irreducible representation. Therefore, Q_r must also belong to the totally symmetric irreducible representation so that the integral will have a nonzero value. We can conclude that, except at a maximum or at a minimum, *the reaction coordinate belongs to the totally symmetric irreducible representation* of the molecular point group.

The reaction coordinate is just one particular normal mode in the simplest case. It must always be, however, a symmetric mode, and this is so even if a more complicated nuclear motion is considered for the reaction coordinate. Such a motion can always be written as a sum of normal modes. Of these modes, however, only those which are totally symmetric will contribute to the reaction coordinate. The nonsymmetric modes may contribute only at the extremes of the potential energy function.

The second integral in Eq. (7-5) appears in the second-order perturbation energy term, and it expresses the mixing in of the first excited state into the ground state during the reaction:

$$\left\langle \Psi_0 \left| \frac{\partial E}{\partial Q_r} \right| \Psi_i \right\rangle . \tag{7-7}$$

This integral will be nonzero only if the direct product of the representations of the wave functions Ψ_0 and Ψ_i contains the representation to which the reaction coordinate belongs,

$$\Gamma_{\Psi_0} \cdot \Gamma_{\Psi_i} \subset \Gamma_{Q_r} \tag{7-8}$$

This expression contains important information regarding the symmetry of the excited states as well. Only those excited states can participate in the reaction whose symmetry matches the symmetry of both the ground state and the reaction coordinate. We already know that Q_r belongs to the totally symmetric irreducible representation except at maxima and minima. This implies that only those excited states can participate in the reaction whose symmetry is the same as that of the ground state. This information is instrumental in the construction of correlation diagrams, as will be seen later.

The reaction coordinate can possess any symmetry at maxima and minima provided that the condition of Eq. (7-8) is fulfilled. This also means that at the maximum point the symmetry of the excited state may differ from that of the ground state. However, any minute distortion will remove the system from the saddle point. The reaction coordinate must then become again totally symmetric. How can this happen? Obviously, this can happen by changing the point group of the system. By reducing the symmetry, nonsymmetric vibrational modes may become symmetric, and the reaction coordinate may become totally symmetric. This reasoning may even help in predicting how the symmetry will be reduced; we just have to find the point group in which the reaction coordinate becomes totally symmetric.

Two examples will illustrate how these rules work. One involves the reduction of symmetry which occurs when a linear molecule becomes bent [41]. The other example involves transforming a planar molecule into a pyramidal one.

For a linear AX_2 molecule of $D_{\infty h}$ symmetry the normal mode that reduces it to C_{2v} is the π_u bending mode (Figure 7-5a). In the C_{2v} point group, this normal mode becomes totally symmetric. (The other component of the π_u mode becomes the rotation of the molecule.)

For an AX_3 planar molecule the symmetry is D_{3h}. The puckering mode (Figure 7-5b) of A_2'' symmetry reduces it to C_{3v}. In the C_{3v} point group, the symmetry of this vibration is A_1.

Concerning the energy integral in Eq. (7-7), Bader called attention to an interesting phenomenon [42]. If the excited state Ψ_i lies very close to the ground state Ψ_0, a distortion occurs that will push the two states apart. This phenomenon is similar to the Jahn–Teller effect (but it is *not* the same) and is called the *pseudo Jahn–Teller effect* (see Chapter 6). The symmetry of the distortion is predicted by Eq. (7-7).

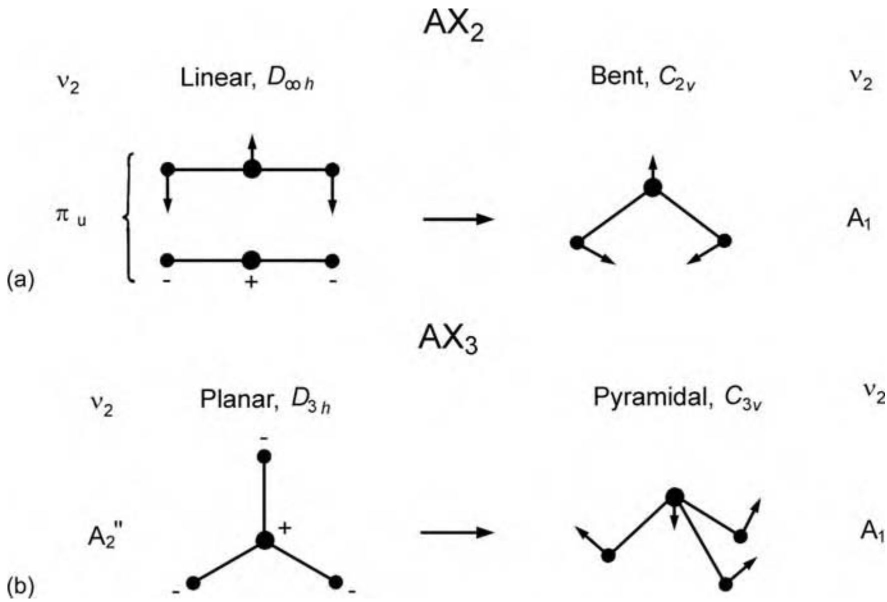

Figure 7-5. The effect of symmetry lowering on the reaction coordinate: (**a**) Bending of a linear AX_2 molecule [$\nu_2(\pi_u) \rightarrow \nu_2(A_1)$]; (**b**) Puckering of a planar AX_3 molecule [ν_2 $(A_2'') \rightarrow \nu_2(A_1)$].

7.2. Electronic Structure

7.2.1. Changes During a Chemical Reaction

A chemical reaction is a consequence of an interaction between molecules. The electronic aspects of these interactions can be discussed in much the same way as the interaction of atomic electron distributions forming molecules. The difference is that while MOs are constructed from the AOs of the constituent atoms, in describing a chemical reaction the MOs of the product(s) are constructed from the MOs of the reactants. Before a reaction takes place (i.e., while the reacting molecules are still far apart), their electron distribution is unperturbed. When they approach each other, their orbitals begin to overlap, and distortion of the original electron distribution takes place. There are two requirements for a constructive interaction between molecules: symmetry matching and energy matching. These two factors can be treated in different ways. The approaches of Fukui [43, 44], and of Woodward and Hoffmann [45, 46] differ somewhat. Since those are the two most successful methods in this field, we shall

concentrate on them. First, the basis of each method will be presented briefly, followed by a few classical examples, each of which will be treated in some detail.

7.2.2. Frontier Orbitals: HOMO and LUMO

A successful chemical reaction requires both energy and symmetry matching between the MOs of the reactants. The requirements are essentially the same as in case of constructing MOs from AOs; only orbitals of the same symmetry and comparable energy can overlap successfully. The strongest interactions occur between those orbitals which are close to each other in energy. However, the interaction between filled MOs is destabilizing since the energy of one orbital increases by about as much—actually a little more—as that of the other decreases (see Figure 7-6a). The most important interactions occur between the filled orbitals of one molecule and the vacant orbitals of the other. Moreover, since the interaction is strongest for energetically similar orbitals, the most significant interactions can be expected between the highest occupied molecular orbital (HOMO) of one molecule and the lowest unoccupied molecular orbital (LUMO) of the other (Figure 7-6b). The labels HOMO and LUMO were incorporated by Fukui into a descriptive collective name: *frontier orbitals.* The first article in this topic appeared in 1952 [47], and the idea has

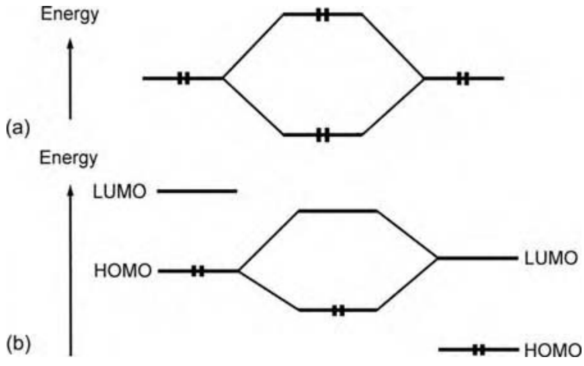

Figure 7-6. (**a**) Interaction of two filled orbitals. The interaction is destabilizing, and so the reaction will not occur; (**b**) Interaction of the highest occupied MO (HOMO) of one molecule with the lowest unoccupied MO (LUMO) of another molecule.

been extended to a host of different reactions in the succeeding years (see, e.g., References [48] and [49]).

Fukui recognized the importance of the symmetry properties of HOMOs and LUMOs perhaps for the first time in connection with the Diels-Alder reaction. According to his Nobel lecture [50], however, it was only after the appearance of the papers by Woodward and Hoffmann in 1965 that he "became fully aware that not only the density distribution but also the nodal property"—that is, symmetry—"of the particular orbitals have significance in . . . chemical reactions."

The concept of frontier orbitals simplifes the MO description of chemical reactions enormously, since only these MOs of the reactant molecules need to be considered. Several examples of this approach will be given in Section 7.3.

7.2.3. Conservation of Orbital Symmetry

The first papers by Woodward and Hoffman outlining and utilizing the idea of conservation of orbital symmetry appeared in 1965 [51–53]. Salem [54] called the discovery of orbital symmetry conservation a revolution in chemistry:

> It was a major breakthrough in the field of chemical reactions in which notions preexisting in other fields (orbital correlations by Mulliken, and nodal properties of orbitals in conjugated systems, by Coulson and Longuet-Higgins) were applied with great conceptual brilliance to a far-reaching problem. Chemical reactions were suddenly adorned with novel significance.

The idea and the principles of drawing correlation diagrams follows directly from the atomic correlation diagrams of Hund [55] and Mulliken [56]. They are very useful for predicting the "allowedness" of a given concerted reaction. In constructing correlation diagrams, both the energy and the symmetry aspects of the problem must be considered. On one side of the diagram the approximate energy levels of the reactants are drawn, while on the other side those of the product(s) are indicated. A particular geometry of approach must be assumed. Furthermore, the symmetry properties of the molecular orbitals must be considered in the framework of the point group of

the supermolecule. In contrast to the frontier orbital method, it is not necessarily the HOMOs and LUMOs that are considered. Instead, attention is focused upon those molecular orbitals which are associated with bonds that are broken or formed during the chemical reaction. We know that each acceptable molecular orbital must belong to one irreducible representation of the point group of the system. At least for nondegenerate point groups, this MO must be either symmetric or antisymmetric with respect to any symmetry element that may be present. (The character under any operation is either 1 or –1.)

Among all possible symmetry elements, those must be considered which are maintained throughout the approach and which bisect bonds that are either formed or broken during the reaction. There must always be at least one such symmetry element. The next step is to connect levels of like symmetry without violating the so-called *noncrossing rule.* According to this rule, two orbitals of the same symmetry cannot intersect [57]. Thus, the correlation diagram is completed. These diagrams yield valuable information about the transition state of the chemical reaction. The method will be illustrated with examples in Section 7.3.

7.2.4. Analysis in Maximum Symmetry

In the analysis in maximum symmetry approach two points are considered when predicting whether or not a chemical reaction can occur. One such point involves the allowedness of an electron transfer from one orbital to another. The other involves consideration of the reaction-decisive normal vibration. In both cases symmetry arguments are used. This approach, developed by Halevi, [58–60] is thorough and rigorous. It is similar in part to the Bader–Pearson method and in part to the Woodward–Hoffmann method. It incorporates several features of each of these methods. First, the transformation of *both* the molecular orbitals (electronic structure) and the displacement coordinates (vibrations) are examined in the context of the full symmetry group of the reacting system. All ways of breaking the symmetry of the system are explored, and no symmetry elements which are retained along the pathway are ignored. The correlation diagrams are called “correspondence diagrams” in this approach to distinguish them from the Woodward–Hoffmann diagrams.

Halevi's method to determine whether a chemical reaction is allowed or forbidden considers both the electronic and vibrational changes in the molecule. Of course, its high degree of rigor may render its application more complicated as compared with the methods which focus only upon changes in the electronic structure. The approaches introduced by Fukui and Woodward and Hoffmann seem to have received more widespread acceptance and utilization.

7.3. Examples

7.3.1. Cycloaddition

7.3.1.1. Ethylene Dimerization

The interaction of two ethylene molecules will be considered in two geometrical arrangements. The two molecules adopt a mutually parallel approach in one arrangement and a mutually perpendicular approach in the other. Applications of various methods will be considered briefly.

(a) Parallel Approach, HOMO-LUMO. According to the frontier orbital method only the HOMOs and the LUMOs of the two ethylene molecules need to be considered. A further simplification is introduced in the pictorial description of the interactions. Although the molecular orbitals of the reactants are used to construct the MOs of the products, the former are usually drawn schematically as atomic orbitals from which they are built. The reason is that the form of the atomic orbitals is better defined and better understood than is the form of the molecular orbitals without resorting to actual calculations.

The MOs of ethylene can be constructed according to the principles given in the preceding chapter. The HOMO of ethylene is the bonding MO, and the LUMO is the antibonding MO composed of the two p_z orbitals of carbon. These MOs are of b_{1u} and b_{2g} symmetry, respectively in the D_{2h} point group. Figure 7-7 shows them both in a simplified way along with the corresponding contour diagrams.

Consider first the frontier orbital interactions between two ethylene molecules that approach one another in parallel planes ("face to face"). Their HOMOs and LUMOs are indicated in Figure 7-8 on the left and right, respectively. Also shown is the behavior of these orbitals with respect to the symmetry plane bisecting the two

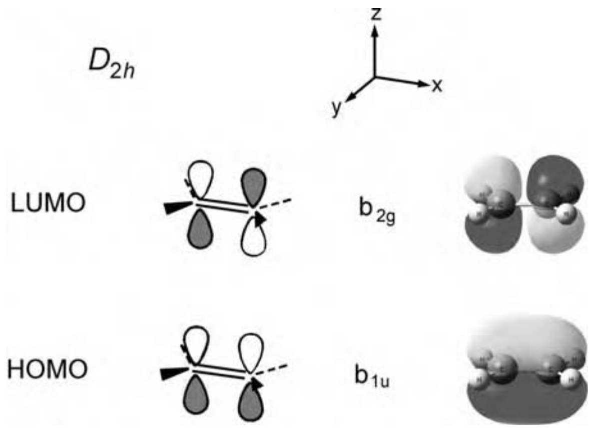

Figure 7-7. The HOMO and LUMO of ethylene.

breaking π bonds. Since the HOMOs are symmetric and the LUMOs are antisymmetric with respect to this operation, there is a symmetry mismatch between the HOMO of one molecule and the LUMO of the other. The symmetry-allowed combination is between the two filled HOMOs. Since the interaction of two filled molecular orbitals of the same energy is destabilizing, the reaction will not occur thermally.

(b) Parallel Approach, Correlation Diagram. Now consider the ethylene dimerization using the Woodward–Hoffmann approach. There is again the important condition mentioned before which must be fulfilled: for the whole reacting system at least one symmetry element

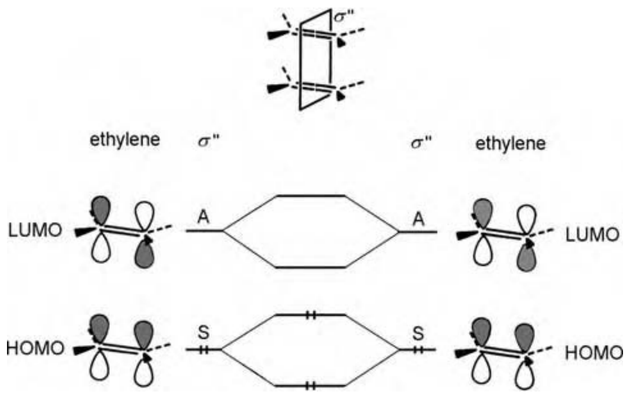

Figure 7-8. Frontier orbital interactions in the face-to-face approach of two ethylene molecules. S indicates symmetric and A indicates antisymmetric behavior with respect to the σ″ symmetry plane.

must persist throughout the entire process. Let us consider the reaction in this respect. Each separate ethylene molecule has D_{2h} symmetry. When two of these molecules approach one another with their molecular planes parallel as shown in Figure 7-9, the whole system retains this symmetry. Finally, the product cyclobutane is of D_{4h} symmetry. Since D_{2h} is a subgroup of D_{4h}, the symmetry elements of D_{2h} persist.

One of the symmetry elements in the D_{2h} point group is the symmetry plane σ' (Figure 7-9). All of the MOs considered in this reaction, that is, those associated with the broken π bonds of the two ethylene molecules and the two new σ bonds of cyclobutane lie in the plane of this symmetry element. All of them will be symmetric to reflection in this plane. There will be no change in their behavior with respect to this symmetry operation during the reaction. This brings us back to a very important point in the construction of correlation diagrams: the symmetry element chosen to follow the reaction must bisect bonds broken or made during the process. Adding extra symmetry elements, like σ' above, will not change the result. It is not wrong to include them; it is just not necessary. Considering, however, only such symmetry elements could lead to the erroneous conclusion that every reaction is symmetry allowed.

As was found to be the case when constructing MOs from AOs, the symmetry of the reacting system as a whole must be considered rather than just the symmetry of the individual molecules alone. Figure 7-10 illustrates this point with respect to one of the reflection planes. The plane transforms the MO drawn as the two p_z orbitals of the two

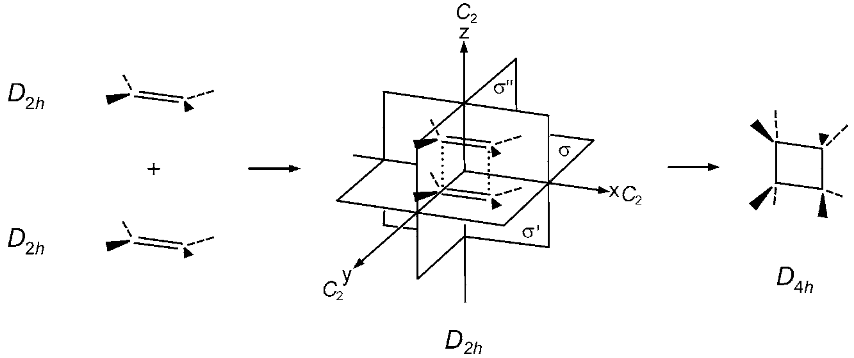

Figure 7-9. The symmetry of reactants, transition structure, and product in the face-to-face dimerization of ethylene.

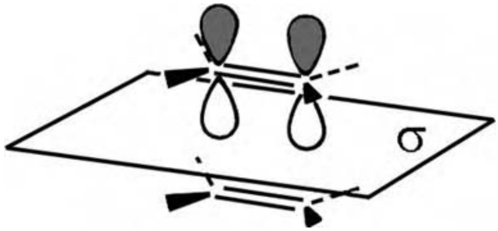

Figure 7-10. The π MO of one ethylene molecule alone does not belong to any irreducible representation of the point group of the system of two ethylene molecules.

carbon atoms of one ethylene molecule into the molecular orbital of the other ethylene molecule. Thus, each MO of the reacting system has a contribution from each p_z orbital.

The possible combinations of the π and π* orbitals of the two ethylene molecules are presented on the left side of Figure 7-11 in order of increasing energy. Consideration of these MOs shows that $\pi_1 + \pi_2$ and $\pi_1^* + \pi_2^*$ are in proper phase to form a bonding MO (that is, closing the ring). The right side of Figure 7-11 illustrates this, together with the formation of the antibonding orbitals of cyclobutane.

The construction of the correlation diagram is shown in Figure 7-12. The two crucial symmetry elements are indicated in the upper part of the figure. The molecular orbitals of the reactants and their behavior with respect to these symmetry elements are indicated in order of increasing energy at the left side of the diagram; the corresponding product MOs are shown at the right in this same figure.

Since σ and σ″ are maintained throughout the reaction, there must be a continuous correlation of orbitals of the same symmetry type. Therefore, orbitals of like symmetry correlate with one another and they can be connected. This, the crucial idea of the Woodward-Hoffmann method, is shown in the central part of the diagram.

Inspection of this correlation diagram immediately reveals that there is a problem. One of the bonding orbitals at the left correlates with an antibonding orbital on the product side. Consequently, if orbital symmetry is to be conserved, two ground state ethylene molecules cannot combine via face-to-face approach to give a ground-state cyclobutane, or vice versa. This concerted reaction is *symmetry forbidden.**

*Note that considerations of either one of the crucial symmetry elements, σ and σ″, alone would give the same result.

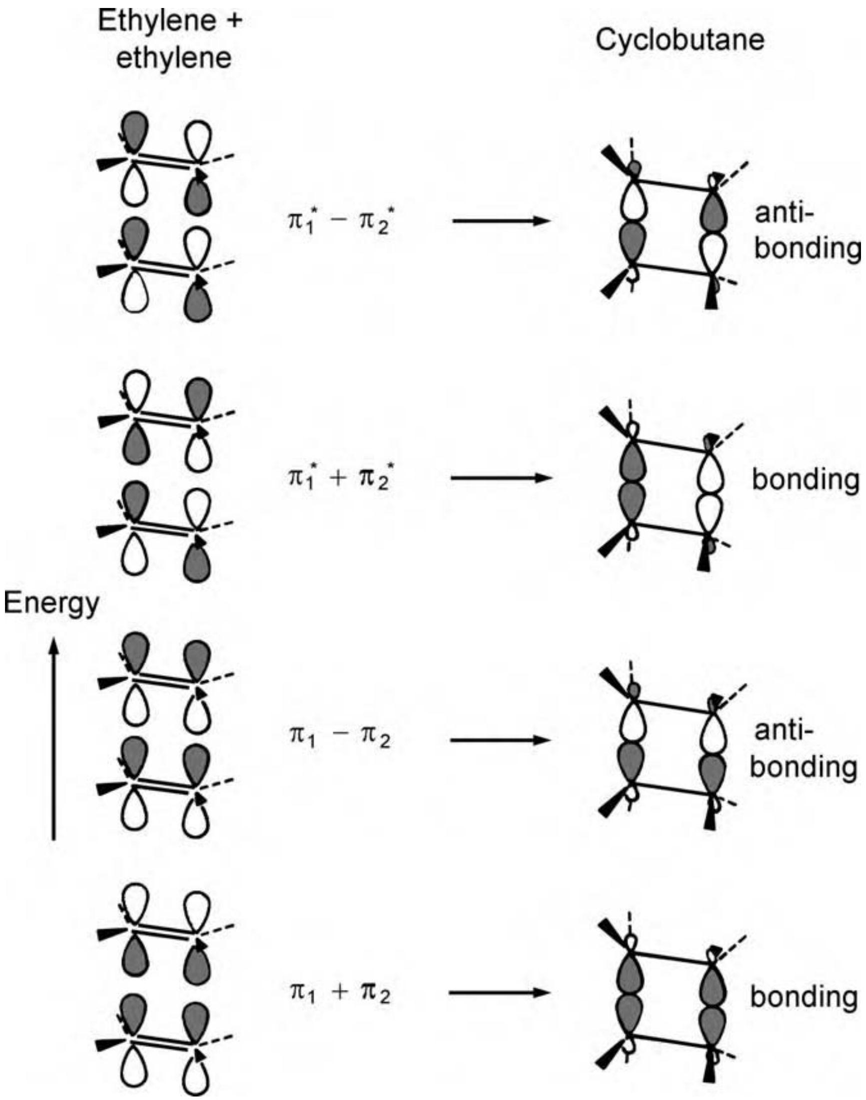

Figure 7-11. Molecular orbitals of the ethylene–ethylene system and the construction of molecular orbitals of cyclobutane. (The energy scale refers to the reactant orbitals only.)

(c) State Correlation. The correlation diagram in Figure 7-12 refers to molecular orbitals. The molecular orbitals and the corresponding electronic configurations are, however, only substitutes for the real wave functions which describe the actual electronic states. It is the electronic states that have definite energy and not the electronic

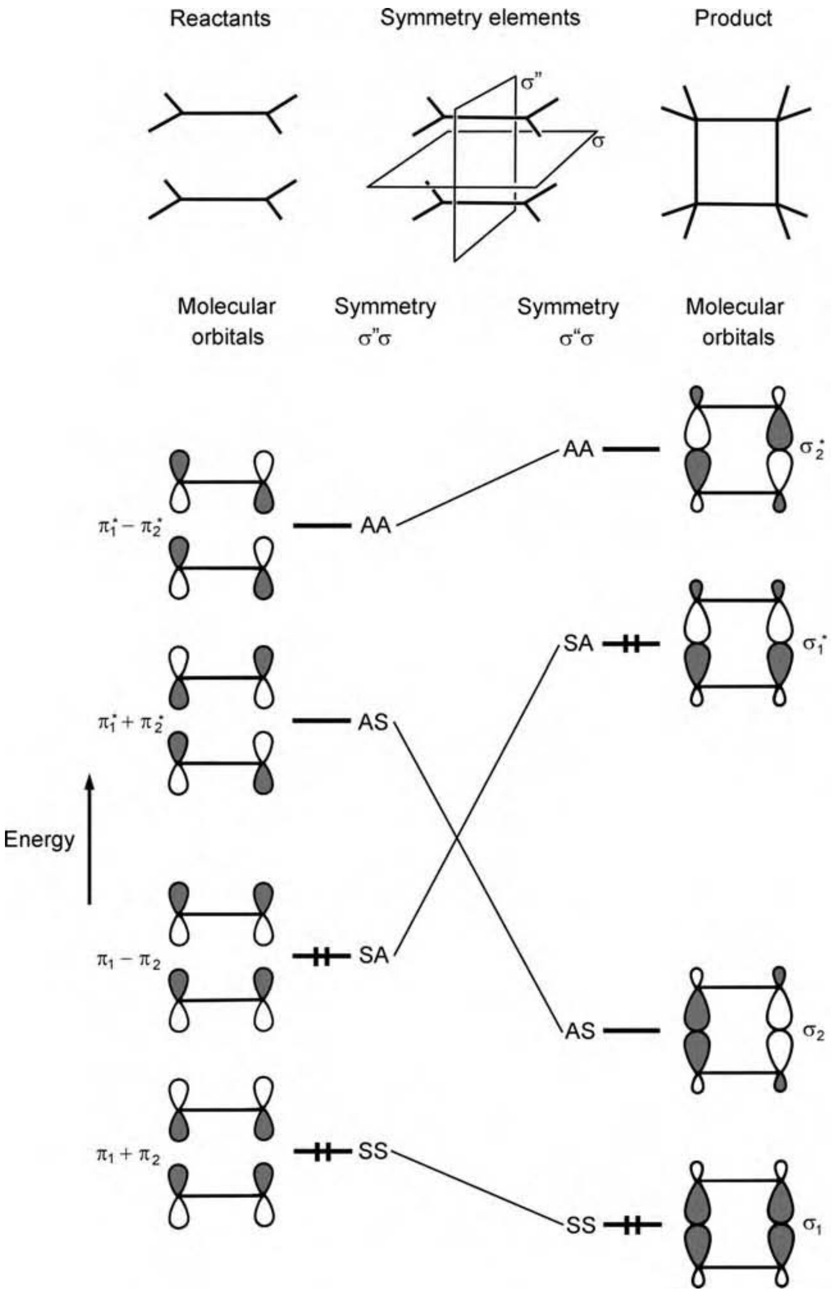

Figure 7-12. Construction of the correlation diagram for ethylene dimerization with parallel approach. Adaptation of Figure 10.19 from Reference [61] with permission.

Table 7-1. The Symmetry of Molecular Orbitals in the Face-to-Face Dimerization of Ethylene[a]

Ethylene + Ethylene					Cyclobutane				
Character under			Orbital occupation				Character under		
σ′ (*xz*)	σ (*xy*)	σ″ (*yz*)	D_{2h}			D_{2h}	σ′ (*xz*)	σ (*xy*)	σ″ (*yz*)
1	–1	–1	b_{2g}	—	—	b_{2g}	1	–1	–1
1	1	–1	b_{3u}	—	—	b_{1u}	1	–1	1
1	–1	1	b_{1u}	↑↓	↑↓	b_{3u}	1	1	–1
1	1	1	a_g	↑↓	↑↓	a_g	1	1	1

[a]The orientation of the coordinate axes is given in Figure 7-9.

configurations (cf. Chapter 6). Since electronic transitions occur physically between electronic states, the correlation of these states is of interest. It was Longuet-Higgins and Abrahamson who drew attention to the importance of state-correlation diagrams [62].

The rules for the state correlation diagrams are the same as for the orbital correlation diagrams; only states that possess the same symmetry can be connected. In order to determine the symmetries of the states, first the symmetries of the MOs must be determined. These are given for the face-to-face dimerization of ethylene in Table 7-1. The D_{2h} character table (Table 7-2) shows that the two crucial symmetry elements are the symmetry planes σ(*xy*) and σ″(*yz*). The MOs are all symmetric with respect to the third plane, σ′(*xz*) (*vide supra*). The corresponding three symmetry operations will unambiguously determine the symmetry of the MOs. Another possibility is to take the simplest subgroup of D_{2h} which already contains the two crucial symmetry operations, that is, the C_{2v} point group (cf.,

Table 7-2. The D_{2h} Character Table

D_{2h}	E	$C_2(z)$	$C_2(y)$	$C_2(x)$	i	σ(*xy*)	σ(*xz*)	σ(*yz*)		
A_g	1	1	1	1	1	1	1	1		x^2, y^2, z^2
B_{1g}	1	1	–1	–1	1	1	–1	–1	R_z	xy
B_{2g}	1	–1	1	–1	1	–1	1	–1	R_y	xz
B_{3g}	1	–1	–1	1	1	–1	–1	1	R_x	yz
A_u	1	1	1	1	–1	–1	–1	–1		
B_{1u}	1	1	–1	–1	–1	–1	1	1	z	
B_{2u}	1	–1	1	–1	–1	1	–1	1	y	
B_{3u}	1	–1	–1	1	–1	1	1	–1	x	

Reference [63]). In these two approaches only the designation of the orbitals and states is different; the outcome, i.e., the state correlation diagram, is the same.

In determining the symmetries of the states (see Chapter 6), we must remember that states with completely filled orbitals are always totally symmetric. In other cases, the symmetry of the state is determined by the direct product of the incompletely filled orbitals.

The ground-state configuration of the two-ethylene system is $a_g^2 b_{1u}^2$ (see Table 7-1). This state is totally symmetric, A_g. The excitation of an electron from the HOMO to the LUMO will give an electron configuration: $a_g^2 b_{1u} b_{3u}$. The direct product is:

$$b_{1u} \cdot b_{3u} = b_{2g}$$

This yields a state of B_{2g} symmetry. The electronic configuration of the product is $a_g^2 b_{3u}^2$, again with A_g symmetry. This electron configuration corresponds to a doubly excited state of the reactants. Finally, the state correlation diagram can be drawn (Figure 7-13).

An obvious connection between states that possess the same electronic configuration would be the one indicated by dashed lines in Figure 7-13. This does not occur, however, because states of the same symmetry cannot cross. This is, again, a realization of the noncrossing rule, which applies to electronic states as well as to orbitals. Instead of crossing, when two states are coming too close to each other they will turn away, and so the two ground states, both of A_g symmetry and also two A_g symmetry excited states will each mutually correlate.

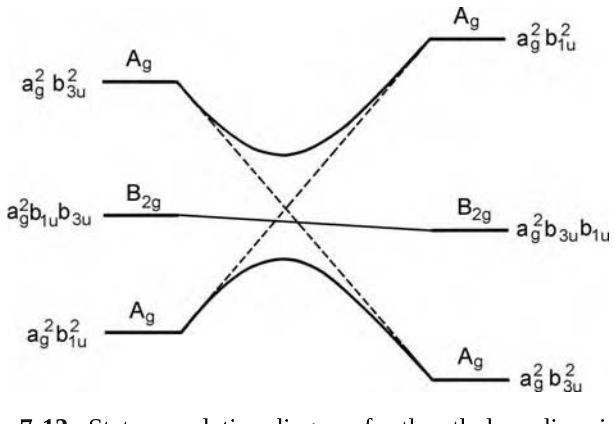

Figure 7-13. State correlation diagram for the ethylene dimerization.

The solid line connecting the two ground states in Figure 7-13 indicates that there is a substantial energy barrier to the ground-state-to-ground-state process; this reaction is said to be "thermally forbidden".

Consider now one electron in the reactant system excited photochemically to the B_{2g} state. Since this state correlates directly with the B_{2g} state of the product, this reaction does not have any energy barrier and may occur directly. It is said that the reaction is "photochemically allowed." Indeed, it is an experimental fact that olefin dimerization occurs smoothly under irradiation.

This observation can be generalized. *If a concerted reaction is thermally forbidden, it is photochemically allowed and vice versa; if it is thermally allowed then it is photochemically forbidden.*

Although the state correlation diagram is physically more meaningful than the orbital correlation diagram, usually the latter is used because of its simplicity. This is similar to the kind of approximation made when the electronic wave function is replaced by the products of one-electron wave functions in MO theory. The physical basis for the rule that only orbitals of the same symmetry can correlate is that only in this case can constructive overlap occur. This again has its analogy in the construction of molecular orbitals. The physical basis for the noncrossing rule is electron repulsion. It is important that this applies to orbitals—or states—of the same symmetry only. Orbitals of different symmetry cannot interact anyway, so their correlation lines are allowed to cross.

(d) Parallel Approach, Orbital Correspondence Analysis. It is worthwhile to see what additional information can be learned from orbital correspondence analysis [64, 65]. The correspondence diagram of the ethylene dimerization reaction is drawn after Halevi in Figure 7-14. It is essentially the same as the correlation diagram in Figure 7-12 with the following difference: Here the maximum symmetry of the system, D_{2h}, is taken into consideration, and the irreducible representation of each MO in this point group is shown. The solid lines of the diagram connect molecular orbitals of the same symmetry. This is the same as the correlation diagram derived from consideration of the crucial symmetries. In addition, we can see that the required transition toward producing a stable ground-state cyclobutane would be from an MO of b_{1u} symmetry to another MO of b_{3u} symmetry. The

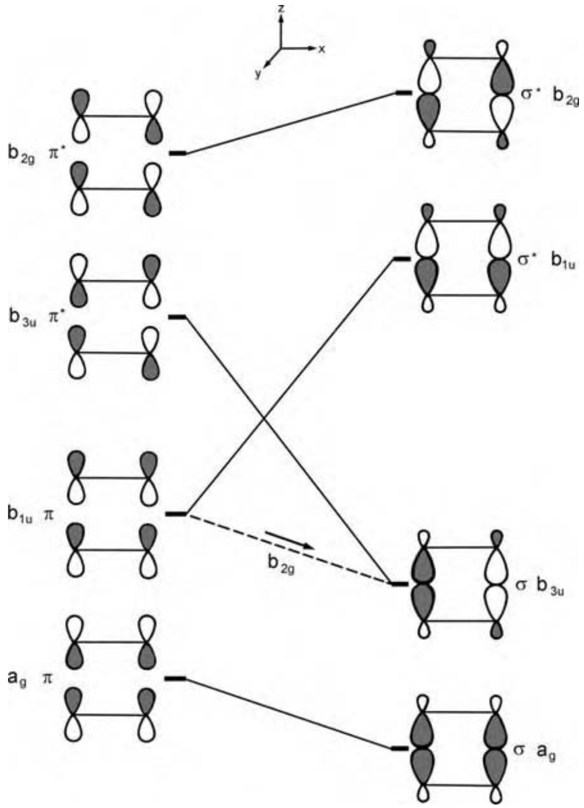

Figure 7-14. Correspondence diagram of the face-to-face dimerization of ethylene. After Reference [65] reproduced with permission.

symmetry of the necessary vibration is given by the direct product of these MOs:

$$b_{1u} \cdot b_{3u} = b_{2g}$$

The B_{2g} symmetry motion of a rectangle of D_{2h} symmetry would be an in-plane vibration that shortens one of the diagonals and lengthens the other:

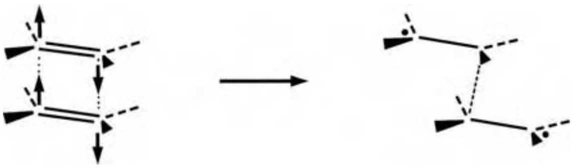

This result suggests a stepwise mechanism—and also it shows the value of the additional information yielded by the orbital correspondence approach. In the suggested stepwise mechanism the first step is the formation of a transoid tetramethylene biradical. Then, this intermediate rotates, thereby permitting closure of the cyclobutane ring in a second step. The nature of this reaction has been studied extensively. The reverse of ethylene dimerization, the pyrolysis of cyclobutane, was experimentally observed long ago [66]. Soon after, quantum chemical calculations and thermochemical considerations suggested that the pyrolysis proceeds through a 1,4-biradical intermediate [67]. As to ethylene dimerization, it is subject to continuing interest. The reactive intermediate tetramethylene radical was identified by experiment using femtosecond laser techniques. Quantum chemical calculations still do not completely agree on the nature of the reaction and of the intermediate [68], for recent literature, see, e.g., Reference [69].

(e) Orthogonal Approach. Let us consider ethylene dimerization in yet another approach. Assume that the orientation of the two molecules is orthogonal:

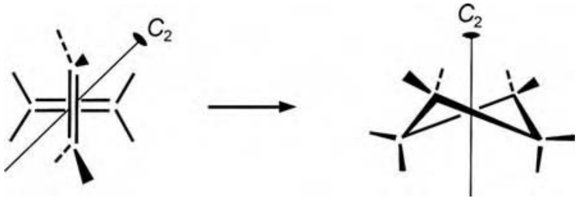

There is one symmetry element that is maintained in this arrangement, i.e., the C_2 rotation. Considering the behavior of the reactant π MOs and the product σ MOs under the C_2 operation, the correlation diagram shown in Figure 7-15 can be drawn. It shows that both bonding MOs of the reactant side correlate with a bonding MO on the product side. There is a net energy gain in the reaction, and the process is “thermally allowed”.

One of the ethylene molecules enters the above reaction *antarafacially*; this means that the two new bonds are formed on opposite sides of this molecule:

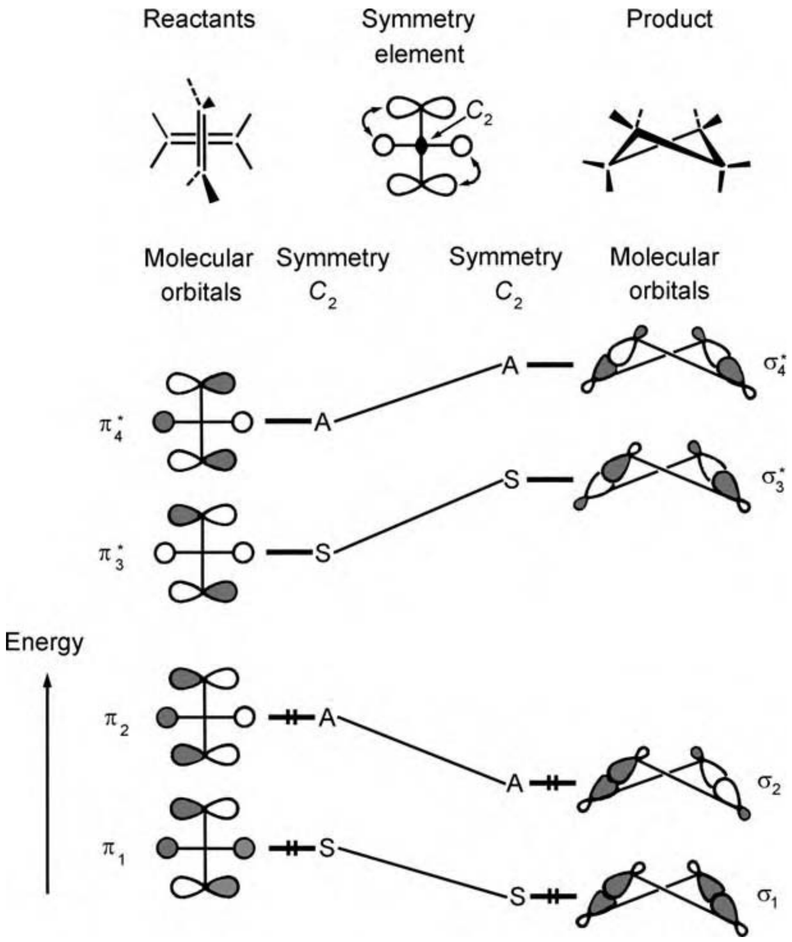

Figure 7-15. Correlation diagram for the orthogonal orientation of two ethylene molecules in the dimerization reaction. Adaptation of Figure 10.22 from reference [70] with permission.

The other ethylene molecule enters the reaction *suprafacially*; this means that the two new bonds are formed on the same side of this second molecule:

Thus, in the orthogonal approach the two molecules enter the reaction differently: one of them antarafacially and the other suprafacially.

On the other hand, in the parallel approach of two ethylenes, both molecules enter the reaction suprafacially:

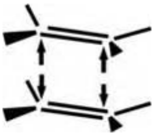

The following abbreviation is often used in the literature: ${}_{\pi}2_s + {}_{\pi}2_s$ means that both ethylene molecules are approaching in a suprafacial manner, while ${}_{\pi}2_s + {}_{\pi}2_a$ indicates that the same molecules are reacting in a process which is suprafacial for one component and antarafacial for the other. The number ${}_{\pi}2$ indicates that two π electrons are contributed by each ethylene molecule.

Just for the sake of completeness it is worthwhile mentioning that, according to the orbital correspondence analysis, this ${}_{\pi}2_s + {}_{\pi}2_a$ cycloaddition of ethylene is also thermally forbidden [71]. Quantum chemical calculations [72] reported a transition structure for this thermally allowed concerted reaction, but due to steric repulsions between some of the hydrogens, this transition structure is very high in energy. Indeed, the reaction is not observed experimentally.

7.3.1.2. Diels–Alder Reaction

(a) HOMO–LUMO Interaction. Another famous example that demonstrates the applicability of symmetry rules in determining the course of chemical reactions is the Diels–Alder reaction. It was discussed in Fukui's seminal paper [73] on the frontier orbital method. Figure 7-16 illustrates the HOMOs and LUMOs of ethylene (dienophile) and butadiene (diene). The only symmetry element common to both the diene and dienophile is the reflection plane that passes through the central 2,3-bond of the diene and the double bond of the dienophile. The symmetry behavior of the MOs with respect to this symmetry element is also shown.

There are two favorable interactions here. One is between the HOMO of ethylene and the LUMO of butadiene, and the other is between the HOMO of butadiene and the LUMO of ethylene. These two interactions occur simultaneously. There is, however, a difference in the role of these two interactions because of their different symmetry behavior. The HOMO of ethylene and the LUMO of butadiene are symmetric with respect to the symmetry element that

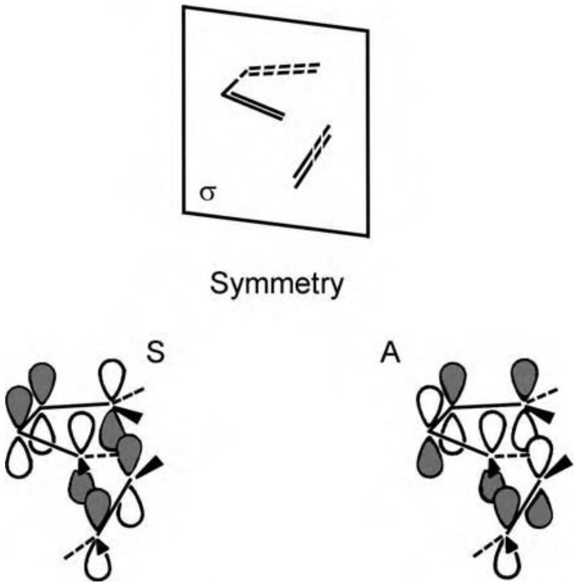

Figure 7-16. HOMO–LUMO interaction in the Diels–Alder reaction.

is maintained throughout the reaction. There is no nodal plane at this symmetry element, so the electrons can be delocalized over the whole new bond. Thus, both carbon atoms of ethylene are bound synchronously to both terminal atoms of butadiene.

The situation is different with the other HOMO–LUMO interaction. These orbitals are antisymmetric with respect to the symmetry element, and the two ends of the new linkage are separated by a nodal plane. Therefore, two separate chemical bonds will form, each connecting an ethylene carbon atom with a terminal butadiene carbon atom. From this consideration, it follows that the first symmetric interaction is the dominant one. Also, the symmetric pair (HOMO of ethylene and LUMO of butadiene) are closer in energy and thus give a stronger interaction.

(b) Orbital Correlation Diagram. The ethylene and butadiene molecules must approach each other in the manner indicated at the top of Figure 7-17 in order to participate in a concerted reaction. There is only one persisting symmetry element in this arrangement, viz. the σ plane which bisects the 2,3-bond of the diene and the double bond of the dienophile. The orbitals affected by the reaction are the π orbitals of the reactants which will be broken; two new σ bonds and one new π bond are formed in the product. The π orbitals and their

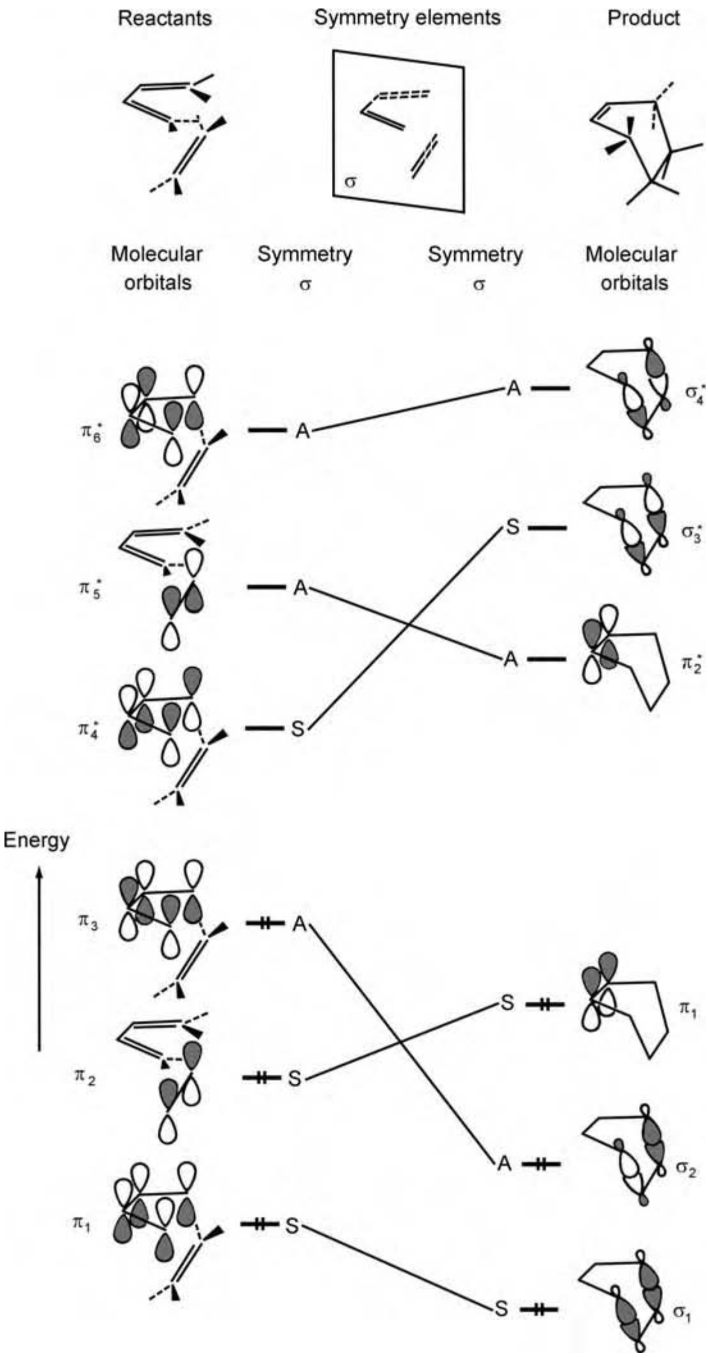

Figure 7-17. Orbital correlation diagram for the ethylene-butadiene cycloaddition. Adaptation of Figure 10.20 from reference [74] with permission.

antibonding pairs for the reactants are shown on the left-hand side of Figure 7-17. The new σ and π orbitals, both bonding and antibonding, of the product cyclohexene are on the right-hand side of this figure. These are the orbitals that are affected by the reaction. The behavior of these orbitals with respect to the vertical symmetry plane is also indicated. The correlation diagram shows that all the filled bonding orbitals of the reactants correlate with filled ground-state bonding orbitals of the product. The reaction, therefore, is symmetry allowed. The predictions that arise by application of the correlation method and by application of the HOMO–LUMO treatment are identical.

The ethylene–butadiene cycloaddition is a good example to illustrate that symmetry allowedness does not necessarily mean that the reaction occurs easily. This reaction has a comparatively high activation energy, around 120–150 kJ/mol, depending on the method of determination. A large number of quantum chemical calculations has been devoted to this reaction with conflicting results and it has been the subject of heated debates (for references, see, References [75] and [76]). The difficulty is that, apparently, the stepwise reaction has an activation energy very similar to that of the concerted reaction. The opposite reaction, the breaking of cyclohexene into butadiene and ethylene, was also studied by femtosecond-resolved mass spectrometry [77]. According to the latest results, this prototype Dields–Alder reaction follows the concerted mechanism, for which the barrier height of the transition-state is about 13 kJ/mol lower than that of the stepwise mechanism [78].

7.3.2. Intramolecular Cyclization

(a) Orbital Correlation for the Butadiene/Cyclobutene Interconversion. The electrocyclic interconversion between an open-chain conjugated polyene and a cyclic olefin is another example for the application of the symmetry rules. The simplest case is the interconversion of butadiene and cyclobutene:

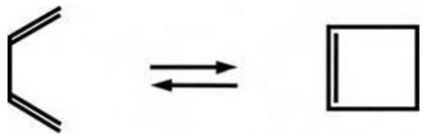

This process can occur in principle in two ways. In one the two ends of the open chain turn in the opposite direction into the transition state. This is called a *disrotatory* reaction.

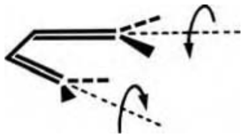

The other possibility is a *conrotatory* process in which the two ends of the open chain turn in the same direction.

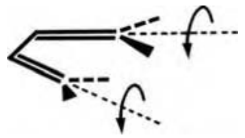

The ring opening of substituted cyclobutenes proceeds at relatively low temperatures and in conrotatory fashion [79], as illustrated by the isomerization of *cis*- and *trans*-3,4-dimethylcyclobutene [80]:

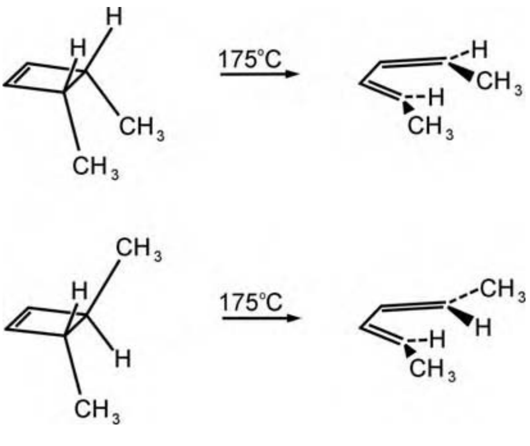

This stereospecificity is well accounted for by the correlation diagrams constructed for the unsubstituted butadiene/cyclobutene isomerization in Figs. 7-18 and 7-19. Since two double bonds in butadiene are broken and a new double bond and a single bond are formed during the cyclization, two bonding and two antibonding orbitals must be considered on both sides. The persisting symmetry element is a plane of symmetry in the disrotatory process. The correlation diagram (Figure 7-18) shows a bonding electron pair moving to an antibonding

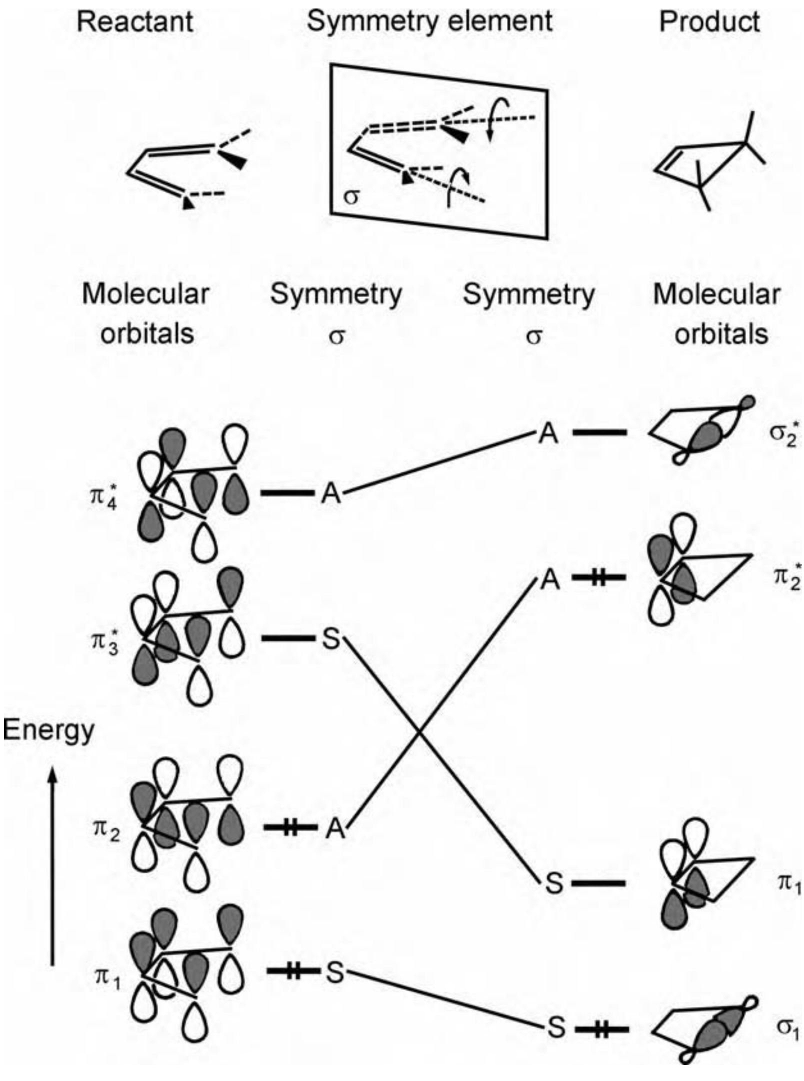

Figure 7-18. Correlation diagram for the disrotatory closure of butadiene. Adaptation of Figure 10.14 from reference [81] with permission.

level in the product, and, thus, the right-hand side corresponds to an excited-state configuration. The disrotatory ring opening is thus a thermally forbidden process.

Figure 7-19 shows the same reaction with conrotatory ring closure. Here, the symmetry element maintained throughout the reaction is the C_2 rotation axis. After connecting orbitals of like symmetry, it is

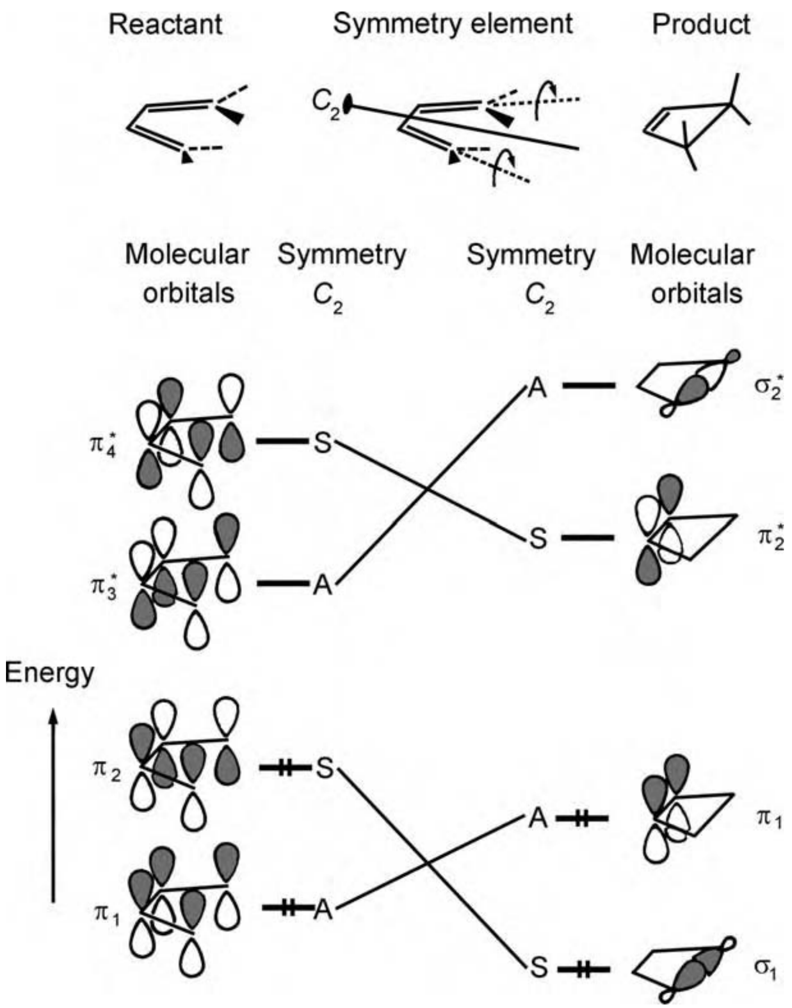

Figure 7-19. Correlation diagram for the conrotatory ring closure in the butadiene-cyclobutene isomerization. Adaptation of Figure 10.12 from reference [82] with permission.

seen that all ground-state reactant orbitals correlate with ground-state product orbitals, so the process is thermally allowed.

(b) Symmetry of the Reaction Coordinate–Cyclobutene Ring Opening. It is interesting to consider the butadiene–cyclobutene reaction from a somewhat different viewpoint, viz., to determine whether the symmetry of the reaction coordinate does indeed predict the proper reaction. Let us look at the reaction from the opposite direction, i.e.,

the cyclobutene ring opening process. From the symmetry point of view, this change of direction is irrelevant.

The symmetry group of both cyclobutene and butadiene is C_{2v} but the transition state is of C_2 symmetry in the conrotatory and C_s in the disrotatory mode. Pearson [83] suggested that this reaction might be visualized in the following way. In the cyclobutene–butadiene transition, two bonds of cyclobutene are destroyed, to wit the ring-closing σ and the opposite π bonds. Hence, four orbitals are involved in the change, the filled and empty σ and σ* orbitals and the filled and empty π and π* orbitals. These orbitals are indicated in Figure 7-20. Their symmetry is also given for the three point groups involved.

Figure 7-21 demonstrates the nuclear movements involved in the conrotatory and disrotatory ring opening. These movements define the reaction coordinate, and they belong to the A_2 and B_1 representation of the C_{2v} point group, respectively.

The two bonds of cyclobutene can be broken either by removing electrons from a bonding orbital or by putting electrons into an anti-bonding orbital. Consider the $\sigma \rightarrow \pi^*$ and the $\pi \rightarrow \sigma^*$ transitions.

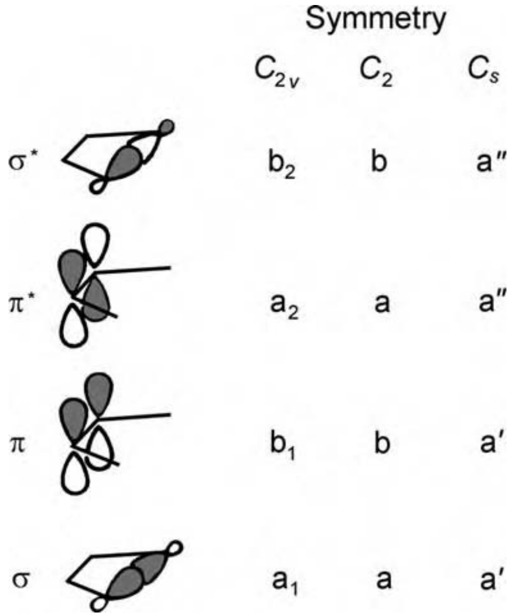

Figure 7-20. The molecular orbitals participating in the cyclobutene ring opening.

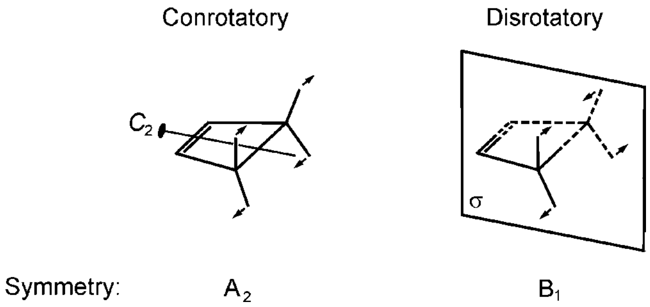

Figure 7-21. The symmetry of the reaction coordinate in the conrotatory and disrotatory ring opening of cyclobutene.

According to Pearson [84], the direct product of the two representations must contain the reaction coordinate:

$$\sigma \rightarrow \pi^*: \ a_1 \cdot a_2 = a_2$$

$$\pi \rightarrow \sigma^*: \ b_1 \cdot b_2 = a_2$$

A_2 is the irreducible representation of the conrotatory ring opening motion, so this type of ring opening seems to be possible. We can test the rules further. During a conrotatory process, the symmetry of the system decreases to C_2. The symmetry of the relevant orbitals also changes in this point group (see Figure 7-20). Both a_1 and a_2 become a, and both b_1 and b_2 become b. Therefore, these orbitals are able to mix. Also, the symmetry of the reaction coordinate becomes A. This is consistent with the rule saying that the reaction coordinate, except at maxima and minima, must belong to the totally symmetric representation of the point group.

The next step is to test whether the disrotatory ring opening is possible. The $\sigma \rightarrow \pi^*$ and $\pi \rightarrow \sigma^*$ transitions obviously cannot be used here, since they correspond to the conrotatory ring opening of A_2 symmetry. Let us consider the $\sigma \rightarrow \sigma^*$ and the $\pi \rightarrow \pi^*$ transitions:

$$\sigma \rightarrow \sigma^*: a_1 \cdot b_2 = b_2$$

$$\pi \rightarrow \pi^*: \ b_1 \cdot a_2 = b_2$$

Both direct products contain the B_2 irreducible representation. It corresponds to an in-phase asymmetric distortion of the molecule,

which cannot lead to ring opening. The symmetry of the disrotatory reaction coordinate is B_1 (Figure 7-21). Moreover, if we consider the symmetry of the orbitals in the C_s symmetry point group of the disrotatory transition, it appears that σ and σ* as well as π and π* belong to different irreducible representations. Hence, their mixing would not be possible anyway. The prediction from this method is the same as the prediction from the orbital correlation diagrams. While examination of the reaction coordinate gives more insight into what is actually happening during a chemical reaction, it is somewhat more complicated than using orbital correlation diagrams.

An ab initio calculation of the cyclobutene to butadiene ring opening [85] led to the following observation. In the conrotatory process, first the C–C carbon single bond lengthens followed by twisting of the methylene groups. The C–C bond lengthening is a symmetric stretching mode with A_1 symmetry and the methylene twist is an A_2 symmetry process which was earlier supposed to be the reaction coordinate. This apparent controversy was resolved by Pearson [86], who emphasized the special role of the totally symmetric reaction coordinate. The effect of the C–C stretch is shown in Figure 7-22. The energies of the σ and σ* orbitals increase and decrease, respectively, as a consequence of the bond lengthening. The A_1 symmetry vibrational mode does not change the molecular symmetry. The crucial σ → π* and π →σ* transitions, which are symmetry related to

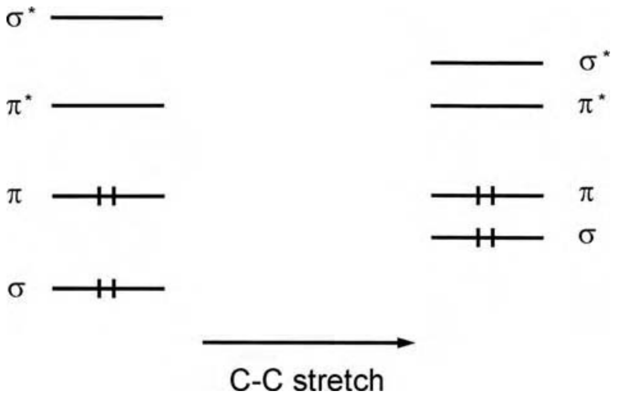

Figure 7-22. The effect of C–C stretching on the energies of the critical orbitals in the cyclobutene ring opening.

the A_2 twisting mode, occur more easily. Apparently, the large energy difference between these orbitals is the determining factor in the actual process. The transition structure for this electrocyclic reaction has been studied extensively by means of quantum-chemical calculations [87]. Their results fully support the conclusions of the above reasoning.

We have to stress again that there might be special reasons that make a disrotatory process or a stepwise mechanism favored over the conrotatory process; such as ring-strains and steric effects [88].

7.3.3. Generalized Woodward–Hoffmann Rules

The selection rules for chemical reactions derived by using symmetry arguments show a definite pattern. Woodward and Hoffmann generalized the selection rules on the basis of orbital symmetry considerations applied to a large number of systems [89]. Two important observations are summarized here; we refer to the literature for further details [90, 91].

(a) Cycloaddition. The reaction between two molecules is thermally allowed if the total number of electrons in the system is $4n + 2$ (n is an integer), and both components are either suprafacial or antarafacial. If one component is suprafacial and the other is antarafacial, the reaction will be thermally allowed if the total number of electrons is $4n$.

(b) Electrocyclic reactions. The rules are similar to those given above. A disrotatory process is thermally allowed if the total number of electrons is $4n + 2$, and a conrotatory process is allowed thermally if the number of delocalized electrons is $4n$. For a photochemical reaction, both sets of rules are reversed.

7.4. Hückel–Möbius Concept

There are a number of other methods used to predict and interpret chemical reactions without relying upon symmetry arguments. It is worthwhile to compare at least some of them with symmetry-based approaches.

The so-called "aromaticity rules" are chosen for comparison, as they provide a beautiful correspondence with the symmetry-based Woodward–Hoffmann rules. A detailed analysis [92] showed the equivalence of the generalized Woodward–Hoffmann selection rules and the aromaticity-based selection rules for pericyclic reactions. Zimmermann [93] and Dewar [94] have made especially important contributions in this field.

The word "aromaticity" usually implies that a given molecule is stable, compared to the corresponding open chain hydrocarbon. For a detailed account on aromaticity, see, e.g., Reference [95]. The aromaticity rules are based on the Hückel–Möbius concept. A cyclic polyene is called a Hückel system if its constituent *p* orbitals overlap everywhere in phase, i.e., the *p* orbitals all have the same sign above and below the nodal plane (Figure 7-23). According to Hückel's rule [96], if such a system has $4n + 2$ electrons, the molecule will be aromatic and stable. On the other hand, a Hückel ring with $4n$ electrons will be antiaromatic.

Based on simple Hückel molecular orbital calculations, Heilbronner predicted that if the Hückel ring is twisted once, as shown in Figure 7-24a, the situation is reversed [97]. Dewar [98] referred to this twisted ring as an "anti-Hückel system." It is also called a "Möbius system" [99], an appropriate name indeed. The Möbius strip is a—somewhat against common-sense—two-dimensional surface with only one side. It is formed by twisting the strip by 180° around its own axis and then attaching its two ends. There is a phase inversion at the point where the two ends meet, as seen in Figure 7-24a and b. The Möbius strip was discovered simultaneously and independently by two German mathematicians, August Ferdinand Möbius (1790–1868) and Johann Benedict Listing (1808–1882). It fascinates mathematicians and artists as well as

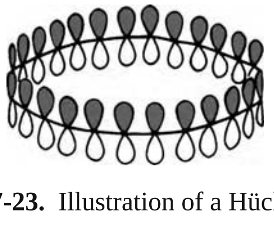

Figure 7-23. Illustration of a Hückel ring.

Figure 7-24. (**a**) Illustration of a Möbius ring; (**b**) Möbius strip. Drawing by the late Gyorgy Doczi; (**c**) Möbius strip-sculpture, Evanston, IL; (**d**) Möbius strip-sculpture, Cambridge, Massachussetts; (**e**) Möbius strip-sculpture at Fermilab in Batavia, Illinois; (**f**) Möbius strip on the facade of a Moscow scientific institute. Photographs by the authors.

chemists [100]. Figure 7-24c–f depict Möbius strips from different parts of the world.

According to Zimmermann [101] and Dewar [102], the allowedness of a concerted pericyclic reaction can be predicted in the following way: A cyclic array of orbitals belongs to the Hückel system if it has zero or an even-number phase inversions. For such a system, a transition state with $4n + 2$ electrons will be thermally allowed due to aromaticity, while the transition state with $4n$ electrons will be thermally forbidden due to antiaromaticity.

A cyclic array of orbitals is a Möbius system if it has an odd number of phase inversions. For a Möbius system, a transition state with $4n$ electrons will be aromatic and thermally allowed, while that with $4n + 2$ electrons will be antiaromatic and thermally forbidden. For a concerted photochemical reaction, the rules are exactly the opposite to those for the corresponding thermal process.

Even though the stability of Möbius systems was predicted over 40 years ago [103], for a long time no such systems were synthesized. One possible reason for this is the expected strain in the twisted structure. Based on quantum chemical calculations, different groups suggested the stability of [4n]annulenes [$(CH)_n$, with $n = 3$–5], but it was also shown that there are many possible isomers of this system that are close in energy and thus the Möbius system might easily flip back to the less strained Hückel structures [104].

The first real Möbius systems ([16]annulenes) were only synthesized a few years ago [105]. In these systems the authors achieved enough rigidity for the molecules so that they would not flip back to a Hückel system. It was also determined that these Möbius-twisted annulenes are more aromatic in their character than the Hückel-systems [106].

The rules based on the Hückel–Möbius concept have their counterpart among the Woodward–Hoffmann selection rules. There was a marked difference between the suprafacial and antarafacial arrangements in the application of the Woodward–Hoffmann treatment of cycloadditions. The disrotatory and conrotatory processes in electrocyclic reactions presented similar differences. The suprafacial arrangement in both of the reacting molecules in the cycloaddition as well as the disrotatory ring closure in Figure 7-25 correspond to

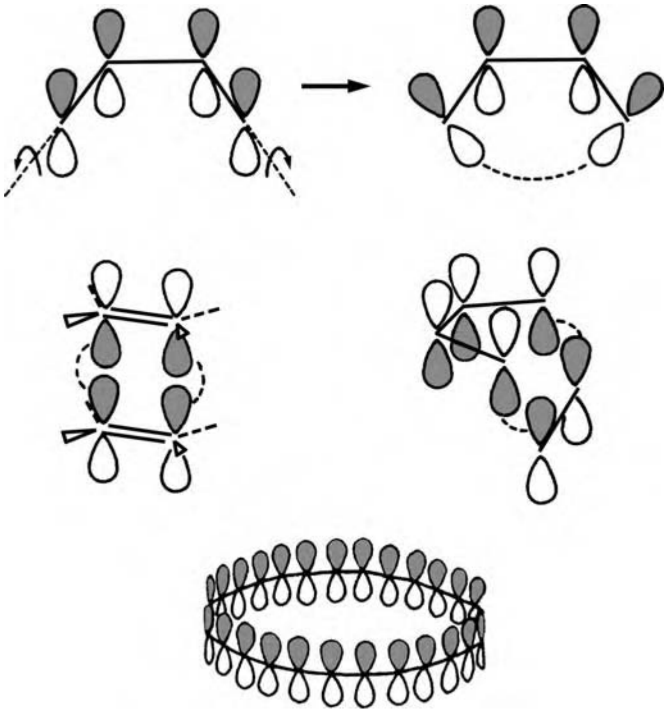

Figure 7-25. Comparison of the disrotatory ring closure and the ${}_{\pi}2_s + {}_{\pi}2_s$ reaction with the Hückel ring.

the Hückel system. On the other hand, the suprafacial–antarafacial arrangement as well as the conrotatory cyclization have a phase inversion (Figure 7-26), and they can be regarded as Möbius systems. All the selection rules mentioned above are summarized in Table 7-3; their mutual correspondence is evident.

Both the Woodward–Hoffmann approach and the Hückel–Möbius concept are useful for predicting the course of concerted reactions. They both have their limitations as well. The application of the Hückel–Möbius concept is probably preferable for systems with low symmetry. On the other hand, this concept can only be applied when there is a cyclic array of orbitals. The conservation of orbital symmetry approach does not have this limitation.

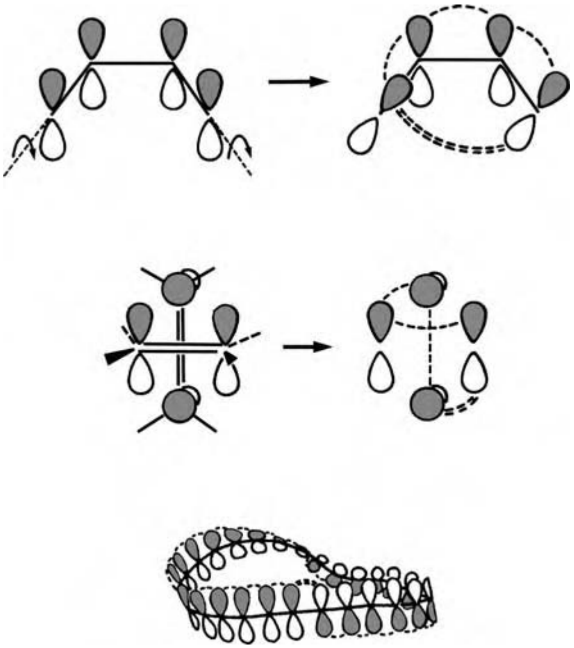

Figure 7-26. Comparison of the conrotatory ring closure and the ${}_{\pi}2_s + {}_{\pi}2_a$ reaction with the Möbius ring.

Table 7-3. Selection Rules for Chemical Reactions from Different Approaches

Approach[a]	Reaction	Thermally Allowed	Thermally Forbidden
1	s + s	$4n + 2$	$4n$
	a + a	$4n + 2$	$4n$
	s + a	$4n$	$4n + 2$
2	Disrotatory	$4n + 2$	$4n$
	Conrotatory	$4n$	$4n + 2$
3	Hückel system: sign inversion even or 0	$4n + 2$	$4n$
	Möbius system: sign inversion odd	$4n$	$4n + 2$

[a] 1: Woodward–Hoffmann cycloaddition; 2: Woodward–Hoffmann electrocyclic reaction; 3: Hückel–Möbius concept.

7.5. Isolobal Analogy

So far, our discussion of reactions has been restricted to organic molecules. However, all the main ideas are applicable to inorganic systems as well. Thus, for example, the formation of inorganic donor–acceptor complexes may be conveniently described by the HOMO–LUMO concept. A case in point is the formation of the aluminum trichloride–ammonia complex (cf. Figure 3-15). This complex can be considered to result from interaction between the LUMO of the acceptor ($AlCl_3$) and the HOMO of the donor (NH_3).

The potential of a unified treatment of organic and inorganic systems has been expressed eloquently in Roald Hoffmann's Nobel lecture [107] entitled "Building Bridges between Inorganic and Organic Chemistry."

The main idea is to examine the similarities between the structures of relatively complicated inorganic complexes and relatively simple and well-understood organic molecules. Then the structure and possible reactions of the former can be understood and even predicted by the considerations working so well for the latter. Two important points were stressed by Hoffmann:

1. "It is the resemblance of the frontier orbitals of inorganic and organic moieties that will provide the bridge that we seek between the subfields of our science."
2. Many aspects of the electronic structure of the molecules discussed and compared are heavily simplified, but "the time now, here, is for building conceptual frameworks, and so similarity and unity take temporary precedence over difference and diversity."

One of the fastest growing areas of inorganic chemistry is transition metal organometallic chemistry. In a general way, the structure of transition metal organometallic complexes can be thought of as containing a transition metal–ligand fragment, such as $M(CO)_5$, $M(PF_3)_5$, M(allyl) and MCp (Cp = cyclopentadienyl), or in general, ML_n. All these fragments may be derived from an octahedral arrangement:

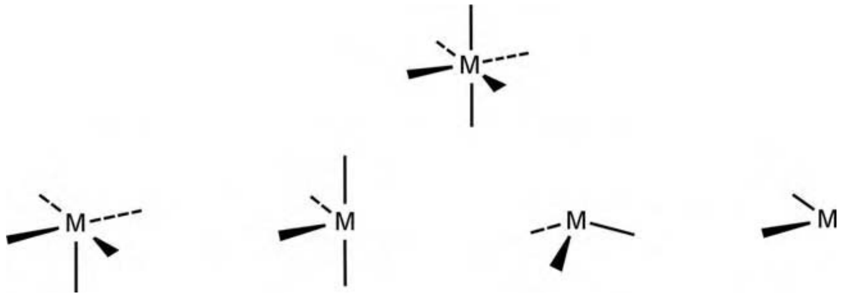

In describing the bonding in these fragments, first the six octahedral hybrid orbitals on the metal atom are constructed. Hybridization is not discussed here, but symmetry considerations are used in constructing hybrid orbitals just as in constructing molecular orbitals [108]. In an octahedral complex, the six hybrid orbitals point towards the ligands, and together they can be used as a basis for a representation of the point group. The O_h character table and the representation of the six hybrid orbitals are given in Table 7-4. The representation reduces to

$$\Gamma_{O_h} = A_{1g} + E_g + T_{1u}$$

Inspection of the O_h character table shows that the only possible combination from the available $(n–1)d$, ns, and np orbitals of the metal is:

s	p_x, p_y, p_z	$d_{x^2-y^2}, d_{z^2}$
a_{1g}	t_{1u}	e_g

These six orbitals will participate in the hybrid, and the remaining t_{2g} symmetry orbitals (d_{xz}, d_{yz}, and d_{xy}) of the metal will be nonbonding.

Six ligands approach the six hybrid orbitals of the metal in forming an octahedral complex. These ligands are supposed to be donors, or, in other words, Lewis bases with even numbers of electrons. Six bonding σ orbitals and six antibonding σ* orbitals are formed, with the ligand electron pairs occupying the bonding orbitals as seen in Figure 7-27. As a consequence of the strong interaction, all six hybrid orbitals of the metal are removed from the frontier orbital region, and only the unchanged metal t_{2g} orbitals remain there.

We can also deduce the changes that will occur in the five-, four-, and three–ligand fragments as compared to the ideal six-ligand case

Table 7-4. The O_h Character Table and the Representation of the Hybrid Orbitals of the Transition Metal in an ML_6 Complex

O_h	E	$8C_3$	$6C_2$	$6C_4$	$3C_2$ $(=C_4^2)$	i	$6S_4$	$8S_6$	$3\sigma_h$	$6\sigma_d$		
A_{1g}	1	1	1	1	1	1	1	1	1	1		$x^2+y^2+z^2$
A_{2g}	1	1	–1	–1	1	1	–1	1	1	–1		
E_g	2	–1	0	0	2	2	0	–1	2	0		$(2z^2-x^2-y^2, x^2-y^2)$
T_{1g}	3	0	–1	1	–1	3	1	0	–1	–1	(R_x, R_y, R_z)	
T_{2g}	3	0	1	–1	–1	3	–1	0	–1	1		(xz, yz, xy)
A_{1u}	1	1	1	1	1	–1	–1	–1	–1	–1		
A_{2u}	1	1	–1	–1	1	–1	1	–1	–1	1		
E_u	2	–1	0	0	2	–2	0	1	–2	0		
T_{1u}	3	0	–1	1	–1	–3	–1	0	1	1	(x, y, z)	
T_{2u}	3	0	1	–1	–1	–3	1	0	1	–1		
Γ_h	6	0	0	2	2	0	0	0	4	2		

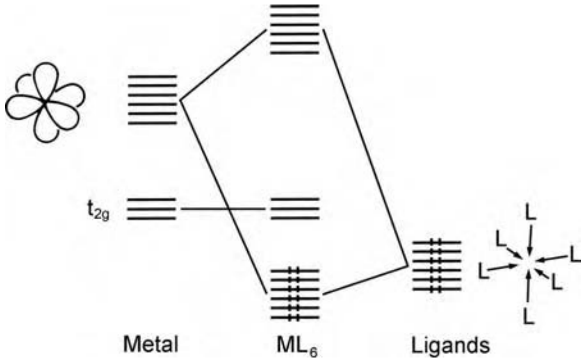

Figure 7-27. Molecular orbital construction in an ideal octahedral complex formation. Reproduced by permission [109], copyright (1982) The Nobel Foundation.

with the help of Figure 7-27. The situation is illustrated in Figure 7-28. With five ligands, only five of the six metal hybrid orbitals will interact; the sixth orbital, the one pointing to where no ligand is, will be unchanged. Consequently, this orbital will remain in the frontier orbital region, together with the t_{2g} orbitals. With four ligands, two of the six hybrid orbitals remain unchanged and with three ligands, three. Always, those metal hybrid orbitals, which point towards the missing ligands in the octahedral site, remain unchanged.

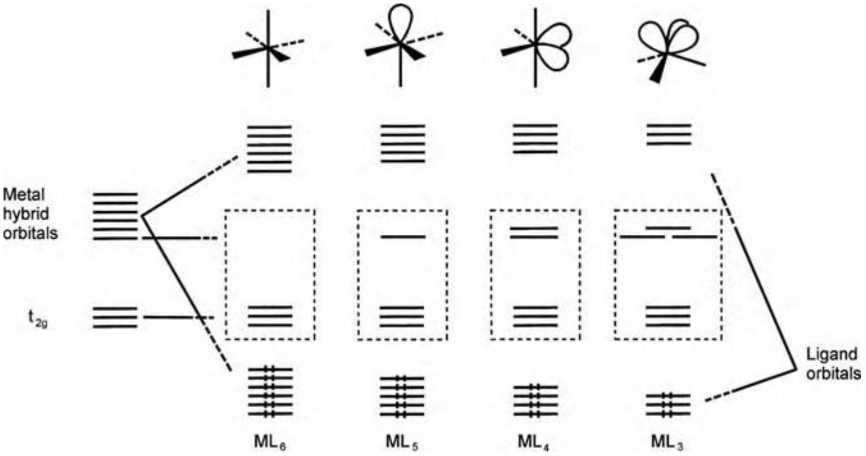

Figure 7-28. Molecular orbitals in different ML_n transition metal-ligand fragments. Adapted with permission [110], copyright (1982) The Nobel Foundation.

Now we shall seek analogies between transition metal complexes and simple, well-studied organic molecules or fragments. In principle, any hydrocarbon can be constructed from methyl groups (CH_3), methylenes (CH_2), methynes (CH), and quaternary carbon atoms. They can be imagined as being derived from the methane molecule itself which has a tetrahedral structure:

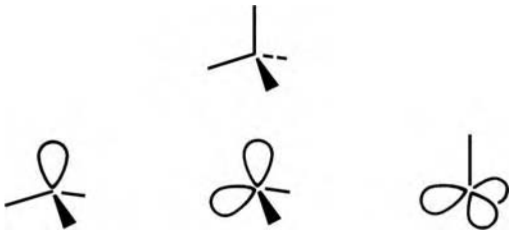

The essence of the "isolobal analogy" concept is to establish similarities between these simple organic fragments and the transition metal ligand fragments, and then to build up the organometallic compounds. As defined by Hoffmann, "two fragments are called *isolobal*, if the number, symmetry properties, approximate energy and shape of the frontier orbitals and the number of electrons in them are similar—not identical, but similar" [111]. However the molecules involved are not and need not be either isoelectronic or isostructural.

The first analogy considered here is a d^7-metal-ligand fragment, for example, $Mn(CO)_5$ and the methyl radical, CH_3:

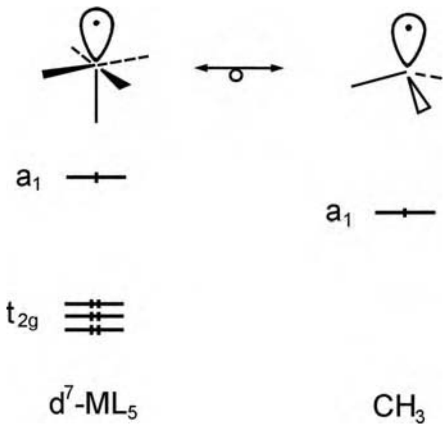

Though the two fragments belong to different point groups, C_{4v} and C_{3v}, respectively, the orbitals that contain unpaired electron belong

to the totally symmetric representation in both cases. Since the three occupied t_{2g} orbitals of the ML_5 fragment are comparatively low lying, the frontier orbital pictures of the two fragments should be similar. If this is so, then they are expected to show some similarity in their chemical behavior, notably in reactions. Indeed, both of them dimerize, and even the organic and inorganic fragments can codimerize, giving $(CO)_5MnCH_3$:

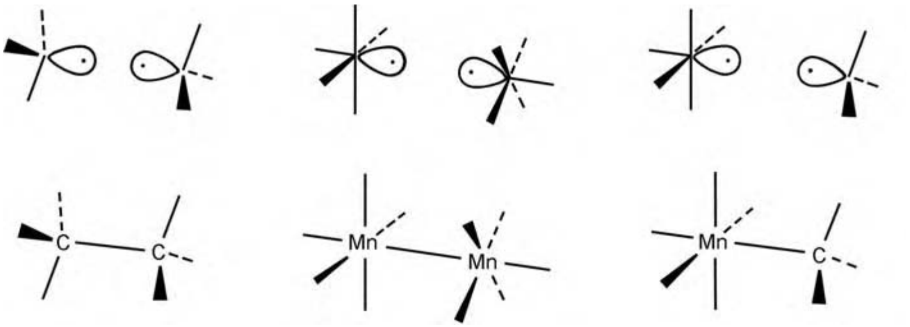

Following this analogy the four-ligand d^8-ML_4 fragments (e.g., $Fe(CO)_4$) are expected to be comparable with the methylene radical, CH_2:

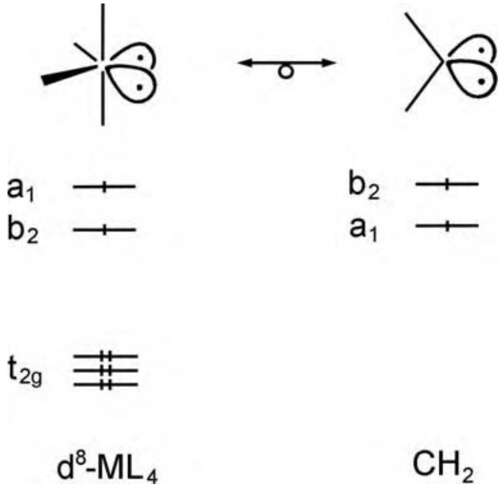

Both fragments belong to the C_{2v} point group, and the representation of the two hybrid orbitals with the unpaired electrons is:

C_{2v}	E	C_2	σ	σ'
Γ	2	0	0	2

This reduces to $a_1 + b_2$. Although the energy ordering differs in the two fragments, this fact is not important, since both will participate in bonding when they interact with another ligand, and their original ordering will thereby change anyway.

Consider the possible dimerization process: two methylene radicals give ethylene, which is a known reaction. Similarly the mixed product, $(CO)_4FeCH_2$, or at least its derivatives, can be prepared. The $Fe_2(CO)_8$ dimer, however, is unstable; and has only been observed in a matrix; it was prepared by the photolysis of $Fe_2(CO)_9$ at low temperature [112, 113]. Spectroscopic studies [114] as well as computations [115] suggest that there are two isomers of this species, one with two CO bridges and another with an Fe–Fe bond. The latter, with D_{2h} symmetry, would be the isolobal analogue of ethylene. However, it is not clear yet what the symmetry of this species is. All this illustrates that the isolobal analogy suggests only the possible consequences of the similarity in the electronic structure of two fragments. It says nothing, however, about the thermodynamic and kinetic stability of any of the possible reaction products.

Although $Fe_2(CO)_8$ is unstable, it can be stabilized by complexation. The molecule in Figure 7-29a consists of two $Fe_2(CO)_8$ units connected through a tin atom [116]. Using the inorganic/organic analogy, this molecule can be compared to spiropentane (Figure 7-29b).

An example of a d^9-ML_3 fragment is $Co(CO)_3$. This is isolobal to a methyne radical, CH:

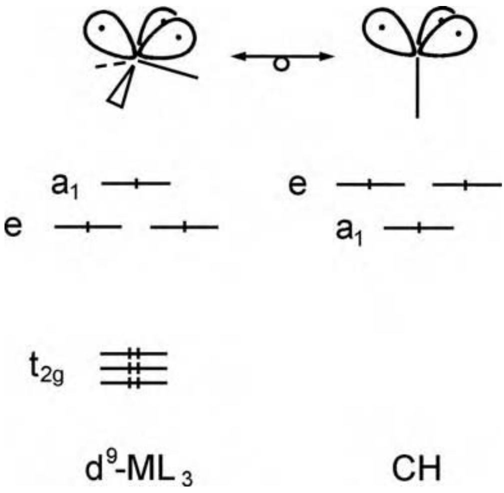

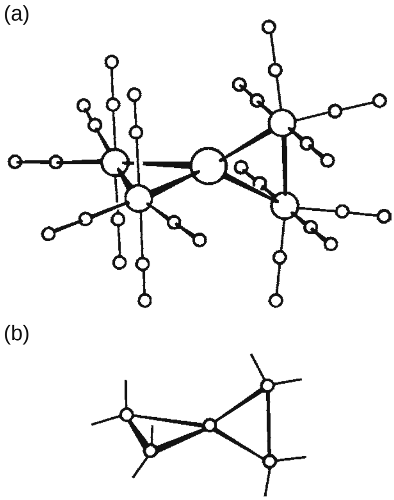

Figure 7-29. (**a**) The molecular geometry of $Sn[Fe_2(CO)_8]_2$. Reproduced by permission [117], copyright (1982) The Nobel Foundation; (**b**) The organic analog: spiropentane.

Both have C_{3v} symmetry. The representation of the three hybrid orbitals with an unpaired electron is:

C_{4v}	E	$2C_2$	$3\sigma_v$
Γ	3	0	1

It reduces to $a_1 + e$. Again, the ordering is different, but the similarity between their electronic structure is obvious. A series of molecules and their similarities are illustrated in Figure 7-30. The first molecule is tetrahedrane and the last one is a cluster with metal-metal bonds which can be considered as being the inorganic analog of tetrahedrane.

Only a few examples have been given to illustrate the isolobal analogy. Hoffmann and his co-workers have extended this concept to other metal–ligand fragment compositions with various *d* orbital participations. Some of these analogies are summarized in Table 7-5. Hoffmann's Nobel lecture [119] contained several of them, and many more can be found in the references given therein and in later works. Just to mention one example: recent computational studies, based on the isolobal analogy, suggest that by substituting CH groups by their isolobal large-metal fragments (such as $Os(PH_3)_3$), the activation

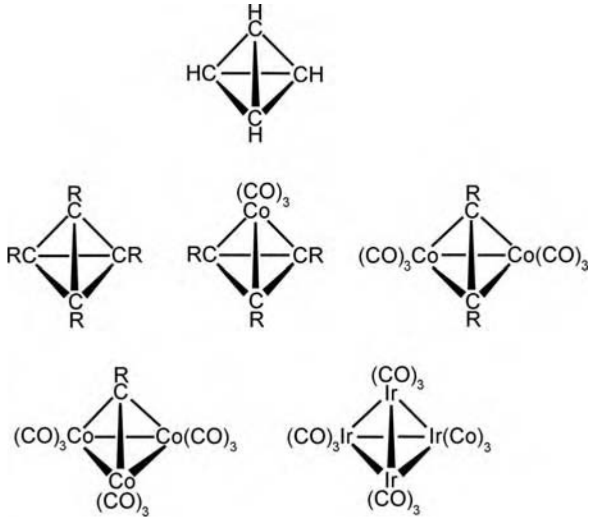

Figure 7-30. Molecular geometries from tetrahedrane to its inorganic analog. Adapted with permission [118], copyright (1982) The Nobel Foundation.

Table 7-5. Isolobal Analogies

Organic	Transition metal coordination number				
fragment	9	8	7	6	5
CH_3	d^1–ML_8	d^3–ML_7	d^5–ML_6	d^7–ML_5	d^9–ML_4
CH_2	d^2–ML_7	d^4–ML_6	d^6–ML_5	d^8–ML_4	d^{10}–ML_3
CH	d^3–ML_6	d^5–ML_5	d^7–ML_4	d^9–ML_3	

barrier of a reaction may be reduced and thus potentially important new molecules could be prepared [120].

References

1. A. L. Mackay, *A Dictionary of Scientific Quotations*, Adam Hilger, Bristol, 1991, p. 57/85.
2. E. Wigner, E. E. Witmer, "Über die Struktur der zweiatomigen Molekelspektren nach der Quantenmechanik." *Z. Phys.* 1928, 51, 859–886.
3. A. Dick, *Emmy Noether: 1882–1935*, Birkhauser, Boston, 1989.
4. I. Hargittai, M. Hargittai, *In Our Own Image: Personal Symmetry in Discovery*, Kluwer-Plenum, 2000, pp. 200–201.
5. R. B. Woodward, R. Hoffmann, *The Conservation of Orbital Symmetry*, Verlag Chemie, Weinheim, 1970.

6. R. B. Woodward, R. Hoffmann, "The Conservation of Orbital Symmetry." *Angew. Chem. Int. Ed. Engl*. 1969, 8, 781–853.
7. K. Fukui, *Theory of Orientation and Stereoselection,* Springer-Verlag, Berlin, 1975; *Top. Curr. Chem*. 1970, 15, 1.
8. K. Fukui, in *Molecular Orbitals in Chemistry, Physics and Biology,* P. O. Löwdin and B. Pullmann, eds., Academic Press, New York, 1964.
9. R. F. W. Bader, "Vibrationally Induced Perturbations in Molecular Electron Distributions." *Can. J. Chem*. 1962, 40, 1164–1175.
10. R. F. W. Bader, P. L. A. Popelier, T. A. Keith, "Theoretical Definition of a Functional Group and the Molecular Orbital Paradigm." *Angew. Chem. Int. Ed. Engl*. 1994, 33, 620–631.
11. R. G. Pearson, *Symmetry Rules for Chemical Reactions, Orbital Topology and Elementary Processes,* Wiley-Interscience, New York, 1976; R. G. Pearson, "Symmetry Rules for Chemical Reactions." In I. Hargittai, ed., *Symmetry: Unifying Human Understanding,* Pergamon Press, Oxford, 1986, pp. 229–236.
12. E. A. Halevi, *Orbital Symmetry and Reaction Mechanisms: The OCAMS View*, Springer-Verlag, Berlin, 1992.
13. E. A. Halevi, "Orbital Correspondence Analysis in Maximum Symmetry." *Helv. Chim. Acta* 1975, 58, 2136–2151.
14. R. R. Woodward, R. Hoffmann, "Stereochemistry of Electrocyclic Reactions." *J. Am. Chem. Soc*. 1965, 87, 395–397.
15. S. Wilkinson, "Woodward and Hoffmann's 1965 Paper Set Rules for Outcome of Many Organic Reactions." *Chem. Eng. News* 2003, 81(4), 59.
16. Woodward, Hoffmann, *The Conservation of Orbital Symmetry.*
17. L. Salem, *Electrons in Chemical Reactions: First Principles*, Wiley-Interscience, New York, 1982.
18. Ibid.
19. B. Solouki, H. Bock, "Photoelectron Spectra and Molecular Properties. 59. Ionization Energies of Disulfur Dihalides and Isomerization Surfaces XSSX<=> SSX_2." *Inorg. Chem*. 1977, 16(3), 665–669.
20. M. C. Müller-Rösing, A. Schulz, M. Hargittai, "Structure and Bonding in Silver Halides. A Quantum Chemical Study of the Monomers: Ag_2X, AgX, AgX_2, and AgX_3 (X = F, Cl, Br, I)." *J. Am. Chem. Soc.* 2005, 127, 8133–8145.
21. I. H. Williams, "Interplay of Theory and Experiment in the Determination of Transition-State Structure." *Chem. Soc. Rev.* 1993, 22(4), 277–283.
22. H. Eyring, M. Polanyi, "Simple Gas Reactions." *Z. Phys. Chem. B*, 1931, 12, 279–311; H. Eyring, "Activated Complex in Chemical Reactions." *J. Chem. Phys*. 1935, 3, 107–115; H. Eyring, "The Activated Complex and the Absolute Rate of Chemical Reactions." *Chem. Rev*. 1935, 17, 65–77.
23. K. N. Houk, Y. Li, J. D. Evanseck, "Transition Structures of Hydrocarbon Pericyclic-Reactions." *Angew. Chem. Int. Ed. Engl*. 1992, 31, 682–708.
24. Ibid.

25. Williams, *Chem. Soc. Rev*. 277–283.
26. Eyring, Polanyi, *Z. Phys. Chem. B*, 279–311.
27. M. G. Evans, M. Polanyi, “Some Applications of the Transition State Method to the Calculation of Reaction Velocities, Especially in Solution.” *Trans. Faraday Soc*. 1935, 31, 875–894.
28. *Structure and Dynamics of Reactive Transition States, Faraday Discuss. Chem. Soc*. 1991, 91, 1–496.
29. E. R. Lovejoy, S. K. Kim, and C. B. Moore, “Observation of Transition-State Vibrational Thresholds in the Rate of Dissociation of Ketene.” *Science*, 1992, 256, 1541–1544.
30. A. H. Zewail, “Laser Femtochemistry.” *Science*, 1988, 242, 1645–1653.
31. Ibid.
32. A. H. Zewail, *Femtochemistry*, World Scientific, Singapore, 1994.
33. M. Kimple, W. Castleman, Jr. (eds.) *Femtochemistry VII: Fundamental Ultrafast Processes in Chemistry, Physics, and Biology*, Elsevier, Amsterdam, 2006.
34. M. M. Martin, J. T. Hynes (eds.), *Femtochemistry and Femtobiology: Ultrafast Events in Molecular Science*, Elsevier, Amsterdam, 2004.
35. Williams, *Chem. Soc. Rev*. 277–283.
36. Bader, *Can. J. Chem*. 1164–1175.
37. Bader et al., *Angew. Chem. Int. Ed. Engl*. 620–631.
38. Pearson, *Symmetry Rules for Chemical Reactions, Orbital Topology and Elementary Processes.*
39. Ibid.
40. Bader, *Can. J. Chem*. 1164–1175.
41. Pearson, *Symmetry Rules for Chemical Reactions, Orbital Topology and Elementary Processes.*
42. Bader, *Can. J. Chem*. 1164–1175.
43. Fukui, in *Molecular Orbitals in Chemistry, Physics and Biology.*
44. Fukui, *Theory of Orientation and Stereoselection*.
45. Woodward, Hoffmann, *The Conservation of Orbital Symmetry.*
46. Woodward, Hoffmann, *Angew. Chem. Int. Ed. Engl*. 781–853.
47. K. Fukui, T. Yonezawa, and H. Shingu, “A Molecular Orbital Theory of Reactivity in Aromatic Hydrocarbons.” *J. Chem. Phys*. 1952, 20, 722–725.
48. Fukui, in *Molecular Orbitals in Chemistry, Physics and Biology.*
49. Fukui, *Theory of Orientation and Stereoselection.*
50. K. Fukui, “Role of Frontier Orbitals in Chemical Reactions.” *Science*, 1982, 218, 747–754.
51. Woodward, Hoffmann, *J. Am. Chem. Soc*. 395–397.
52. R. Hoffmann, R. B. Woodward, “Selection Rules for Concerted Cycloaddition Reactions.” *J. Am. Chem. Soc*. 1965, 87, 2046–2048.
53. R. B. Woodward, R. Hoffmann, “Selection Rules for Sigmatropic Reactions” *J. Am. Chem. Soc*. 1965, 87, 2511–2513.

54. Salem, *Electrons in Chemical Reactions: First Principles.*
55. F. Hund, “Interpretation of the Spectra of molecules.” *Z. Phys*. 1927, 40, 742–764; “Interpretation of the spectra of molecules. II.” 1927, 42, 93–120; “Molecular Spectra.” 1928, 51, 759–796.
56. R. S. Mulliken, “The assignment of quantum numbers for electrons in molecules. I.” *Phys. Rev*. 1928, 32, 186–222.
57. J. von Neumann and E. Wigner, “Über das Verhalten von Eigenwerten bei adiabatischen Prozessen.” *Phys. Z.* 1929, 30, 467–470; E. Teller, “Crossing of Potential Surfaces.” *J. Phys. Chem.* 1937, 41, 109–116.
58. Halevi, *Orbital Symmetry and Reaction Mechanisms: The OCAMS View.*
59. Halevi, *Helv. Chim. Acta* 2136–2151.
60. J. Katriel, E. A. Halevi, “Orbital Correspondence Analysis in Maximum Symmetry—Formulation and Conceptual Framework.” *Theor. Chim. Acta* 1975, 40, 1–15.
61. T. H. Lowry, K. S. Richardson, *Mechanism and Theory in Organic Chemistry,* Third Edition, Harper & Row, New York, 1987.
62. H. C. Longuet-Higgins, E. W. Abrahamson, “The Electronic Mechanism of Electrocyclic Reactions.” *J. Am. Chem. Soc.* 1965, 87, 2045–2046.
63. F. A. Cotton, *Chemical Applications of Group Theory,* Second Edition, Wiley-Interscience, New York, 1971.
64. Halevi, *Orbital Symmetry and Reaction Mechanisms: The OCAMS View.*
65. Halevi, *Helv. Chim. Acta* 2136–2151.
66. R. W. Carr, Jr., W. D. Walters, “The Thermal Decomposition of Cyclobutane.” *J. Phys. Chem*., 1963, 67, 1370–1372.
67. R. Hoffmann, S. Swaminathan, B. G. Odell, and R. Gleiter, “A Potential Surface for a Nonconcerted Reaction. Tetramethylene.” *J. Am. Chem. Soc.* 1970, 92, 7091–7097; G. A. Segal, “Organic Transition States. III. An ab Initio Study of the Pyrolysis of Cyclobutane via the Tetramethylene Diradical.” *J. Am. Chem. Soc.* 1974, 96, 7892–7898; H. E. O’Neal and S. W. Benson, “The Biradical Mechanism in Small Ring Compound Reactions. ” *J. Phys. Chem.* 1968, 72, 1866–1887.
68. S. Pedersen, J. L. Herek, A. H. Zewail, “The Validity of the “Diradical” Hypothesis: Direct Femtosecond Studies of the Transition-State Structures.” *Science*, 1994, 266, 1359–1364; J. C. Polanyi, A. H. Zewail, “Direct Observation of the Transition State.” *Acc. Chem. Res*. 1995, 28, 119–132.
69. Y. Dou, Y. Lei, A. Li, Z. Wen, B. R. Torralva, G. V. Lo, R. E. Allen, “Detailed Dynamics of the Photodissociation of Cyclobutane.” *J. Phys. Chem. A*, 2007, 111, 1133–1137.
70. Lowry, Richardson, *Mechanism and Theory in Organic Chemistry*.
71. Halevi, *Helv. Chim. Acta* 2136–2151.
72. F. Bernardi, M. Olivucci, J. J. W. McDuall, M. A. Robb, “Diabatic Surfaces for Two-Bond Addition Reactions. Role of Resonance Interaction.” *J. Am. Chem. Soc*. 1987, 109, 544–553.
73. Fukui, Yonezawa, Shingu, *J. Chem. Phys*. 722–725.
74. Lowry, Richardson, *Mechanism and Theory in Organic Chemistry.*

75. Houk et al., *Angew. Chem. Int. Ed. Engl*. 682–708.
76. S. Sakai, "Theoretical Analysis of Concerted and Stepwise Mechanisms of Diels–Alder Reaction Between Butadiene and Ethylene." *J. Phys. Chem. A*, 2000, 104, 922–927.
77. E. W.-G. Diau, S. De Feyter, A. H. Zewail, "Femtosecond Dynamics of Retro Diels–Alder Reactions: the Concept of Concertedness." *Chem. Phys. Lett*. 1999, 304, 134–144.
78. Sakai, *J. Phys. Chem. A* 922–927.
79. Woodward, Hoffmann, *The Conservation of Orbital Symmetry*.
80. R. E. K. Winter, "The Preparation and Isomerization of *cis*- and *trans*-3, 4-Dimethylcyclobutene." *Tetrahedron Lett*. 1965, 6, 1207–1212.
81. Lowry, Richardson, *Mechanism and Theory in Organic Chemistry*.
82. Ibid.
83. Pearson, *Symmetry Rules for Chemical Reactions, Orbital Topology and Elementary Processes*.
84. Ibid.
85. K. Hsu, R. J. Buenker, S. D. Peyerimhoff, "Theoretical Determination of the Reaction Path in the Prototype Electrocyclic Transformation between Cyclobutene bnd *cis*-Butadiene. Thermochemical Process." *J. Am. Chem. Soc*. 1971, 93, 2117–2127.
86. Pearson, *Symmetry Rules for Chemical Reactions, Orbital Topology and Elementary Processes*.
87. Houk et al., *Angew. Chem. Int. Ed. Engl*. 682–708.
88. C. S. Lopez, O. N. Faza, A. R. de Lera, "Electrocyclic Ring Opening of cis-Bicyclo[*m*.*n*.0]alkenes: The Anti-Woodward–Hoffmann Quest." *Chem. Eur. J*. 2007, 13, 5009–5017.
89. Woodward, Hoffmann, *The Conservation of Orbital Symmetry.*
90. Ibid.
91. Lowry, Richardson, *Mechanism and Theory in Organic Chemistry*.
92. A. C. Day, "Aromaticity and the Generalized Woodward-Hoffmann Rules for Pericyclic Reactions." *J. Am. Chem. Soc.* 1975, 97, 2431–2438.
93. H. E. Zimmermann, "On Molecular Orbital Correlation Diagrams, the Occurrence of Möbius Systems in Cyclization Reactions, and Factors Controlling Ground- and Excited-State Reactions. I." *J. Am. Chem. Soc*. 1966, 88, 1564–1565; "Molecular Orbital Correlation Diagrams, Mobius Systems, and Factors Controlling Ground- and Excited-State Reactions. II." *J. Am. Chem. Soc*. 1966, 88, 1566–1567; "Möbius-Hückel Concept in Organic Chemistry. Application of Organic Molecules and Reactions." *Acc. Chem. Res*. 1971, 4, 272–280.
94. M. J. S. Dewar, "A Molecular Orbital Theory of Organic Chemistry–VIII: Aromaticity and Electrocyclic Reactions." *Tetrahedron Suppl*. 1966, 8, 75–92; "Aromaticity and Pericyclic Reactions." *Angew. Chem. Int. Ed. Engl*. 1971, 10, 761–776; *The Molecular Orbital Theory of Organic Chemistry,* McGraw-Hill, New York, 1969.

95. V. I. Minkin, M. N. Glukhovtsev, B. Ya. Simkin, *Aromaticity and Antiaromaticity: Electronic and Structural Aspects*, John-Wiley and Sons, New York, 1994.
96. E. Hückel, “Quantentheoretische Beiträge zum Benzolproblem I. Die Elektronenkonfiguration des Benzols und verwandter Verbindungen.” *Z. Phys*. 1931, 70, 204–286; “Quantentheoretische Beiträge zum Problem der aromatischen und ungesättigten Verbindungen. III.” 1932, 76, 628–648; “Die freien Radikale der organischen Chemie: Quantentheoretische Beiträge zum Problem der aromatischen und ungesättigten Verbindungen. IV.” 1933, 83, 632–668.
97. E. Heilbronner, “Hückel Molecular Orbitals of Möbius-Type Conformations of Annulenes.” *Tetrahedron Lett*. 1964, 5, 1923–1928.
98. Dewar, *Tetrahedron Suppl*. 75–92; *Angew. Chem. Int. Ed. Engl*. 761; *The Molecular Orbital Theory of Organic Chemistry.*
99. Zimmermann, *J. Am. Chem. Soc*. 1564–1565; *J. Am. Chem. Soc*. 1566–1567; *Acc. Chem. Res*. 272–280.
100. C. A. Pickover, *The Mobius Strip: Dr. August Möbius’s Marvelous Band in Mathematics, Games, Literature, Art, Technology, and Cosmology,* Thunder’s Mouth Press, 2006.
101. Zimmermann, *J. Am. Chem. Soc*. 1564–1565; *J. Am. Chem. Soc*. 1566–1567; *Acc. Chem. Res*. 272–280.
102. Dewar, *Tetrahedron Suppl*. 75–92; *Angew. Chem. Int. Ed. Engl*. 761–776; *The Molecular Orbital Theory of Organic Chemistry.*
103. E. Heilbronner, *Tetrahedron Lett*. 1964, 1923.
104. S. Martin-Santamaria, B. Lavan, H. S. Rzepa, “Hückel and Möbius Aromaticity and Trimerous Transition State Behaviour in the Pericyclic Reactions of [10], [14], [16] and [18]Annulenes.” *J. Chem. Soc. Perkin Trans. 2*, 2000, 1415–1417; C. Castro, C. M. Isborn, W. L. Karney, M. Mauksch, P. von R. Schleyer, “Aromaticity with a Twist: Möbius [4*n*]Annulenes.” *Org. Lett*. 2002, 4, 3431–3434.
105. D. Ajami, O. Oeckler, A. Simon, R. Herges, “Synthesis of a Möbius Aromatic Hydrocarbon.” *Nature*, 2003, 426, 819–821.
106. D. Ajami, K. Hess, F. Köhler, C. Näther, O. Oeckler, A. Simon, C. Yamamoto, Y. Okamoto, R. Herges, “Synthesis and Properties of the First Möbius Annulenes.” *Chem. Eur. J*. 2006, 12, 5434–5445.
107. R. Hoffmann, “Building Bridges between Inorganic and Organic Chemistry (Nobel Lecture).” *Angew. Chem. Int. Ed. Engl*. 1982, 21, 711–724.
108. Cotton, *Chemical Applications of Group Theory.*
109. Hoffmann, *Angew. Chem. Int. Ed. Engl*. 711–724.
110. Ibid.
111. Ibid.
112. M. Poliakoff, J. J. Turner, “Infrared Spectrum and Photochemistry of Di-Iron Enneacarbonyl in Matrices at 20 K: Evidence for the Formation of $Fe_2(CO)_8$.” *J. Chem. Soc. A*, 1971, 2403–2410.

113. S. Fedrigo, T. L. Haslett, M. Moskovits, "Direct Synthesis of Metal Cluster Complexes by Deposition of Mass-Selected Clusters with Ligand: Iron with CO." *J. Am. Chem. Soc.* 1996, 118, 5083–5085.
114. S. C. Fletcher, M. Poliakoff, J. J. Turner, "Structure and Reactions of Octacarbonyldiiron: An IR Spectroscopic Study Using Carbon-13 Monoxide, Photolysis with Plane-Polarized Light, and Matrix Isolation." *Inorg. Chem.* 1986, 25, 3597–3604.
115. L. Bertini, M. Bruschi, L. De Gioia, P. Fantucci, "Structure and Energetics of $Fe_2(CO)_8$ Singlet and Triplet Electronic States" *J. Phys. Chem. A* 2007, 111, 12152–12162.
116. J. D. Cotton, S. A. R. Knox, I. Paul, and F. G. A. Stone, "Chemistry of the Metal Carbonyls. Part XXXIX. Organotin(carbonyl)-iron Complexes." *J. Chem. Soc. A* 1967, 264–269.
117. Hoffmann, *Angew. Chem. Int. Ed. Engl*. 711–724.
118. Ibid.
119. Ibid.
120. E. M. Brzostowska, R. Hoffmann, C. A. Parish, "Tuning the Bergman Cyclization by Introduction of Metal Fragments at Various Positions of the Enediyne. Metalla-Bergman Cyclizations." *J. Am. Chem. Soc.* 2007, 129, 4401–4409.

Chapter 8

Space-Group Symmetries

The beauty of life is,... geometrical beauty...
J. Desmond Bernal [1]

8.1. Expanding to Infinity

Up to this point, structures of mostly finite objects have been discussed. Thus, point groups were applicable to their symmetries. A simplified classification of various symmetries was presented in Chapter 2 (cf., Figure 2-31 and Table 2-2). Point-group symmetries are characterized by the lack of periodicity in any direction. However, repetition is a fundamental feature in our world, both in nature and in what we create. "Whatever can be done once can always be repeated," this is how Louise B. Young begins the description of shapes and structures of nature in the book, *The Mystery of Matter* [2]. Periodicity may be introduced by translational symmetry. If periodicity is present, space groups are applicable for the symmetry description. There is a slight inconsistency here in the terminology. Even a three-dimensional object may have point-group symmetry. On the other hand, the so-called dimensionality of the space group is not determined by the dimensionality of the object. Rather, it is determined by its periodicity. The following groups are space-group symmetries where the superscript refers to the dimensionality of the object, and the subscript to the periodicity.

$$
\begin{array}{lll}
G_1^1 & & \\
G_1^2 & G_2^2 & \\
G_1^3 & G_2^3 & G_3^3
\end{array}
$$

M. Hargittai, I. Hargittai, *Symmetry through the Eyes of a Chemist,* 3rd ed.,
DOI: 10.1007/978-1-4020-5628-4_8, © Springer Science+Business Media B.V. 2009

Objects or patterns which are periodic in one, two, and three directions will have one-, two-, and three-dimensional space groups, respectively. The dimensionality of the object/pattern is merely a necessary but not a satisfactory condition for the "dimensionality" of their space groups. We shall first describe a planar pattern after Budden [3] in order to get the flavor of space-group symmetry. Also, some new symmetry elements will be introduced. Later in this chapter, the simplest one-dimensional and two-dimensional space groups will be presented. The next Chapter will be devoted to the three-dimensional space groups which characterize crystal structures.

A symmetric pattern expanding to infinity always contains a basic unit, a motif, which is then repeated infinitely throughout the pattern. Figure 8-1a presents a planar decoration. The pattern shown is only part of the whole as the latter expands, in principle, to infinity! The pattern is obviously highly symmetrical. Figure 8-1b shows the system of mutually perpendicular symmetry planes by solid lines.

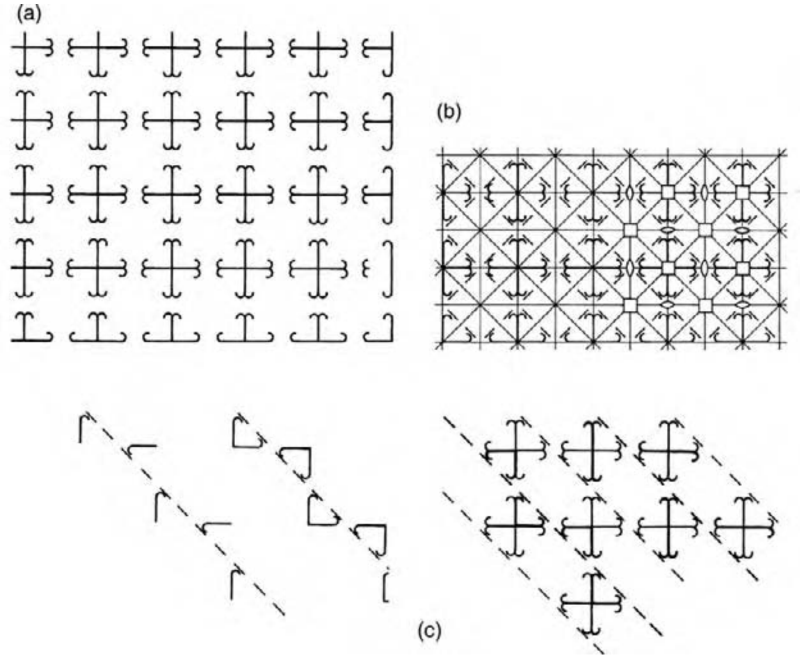

Figure 8-1. Planar decoration with two-dimensional space group after Budden [4]. (**a**) The decoration; (**b**) Symmetry elements of the pattern; (**c**) Some of the glide reflection planes and their effects in the pattern.

Some of the fourfold and twofold rotation axes are also indicated in this figure. A new symmetry element in our discussion is the glide reflection (called also, glide mirror), which is shown by a dashed line. Some of these glide reflections are indicated separately in Figure 8-1c. A glide-mirror plane is a combination of translation and reflection. It is a symmetry element that can be present in space groups only. The glide-reflection plane involves an infinite sequence of consecutive translations and reflections. Whereas in a simple canon, there is only repetition of the tune at certain intervals in time, as shown in Figure 8-2a; Figure 8-2b shows a different canon in which repetition is combined with reflection. Two further patterns with glide-reflection symmetry are given in Figure 8-3. They are also thought to extend to infinity, at least in our imagination.

Simple *translation* is the most obvious symmetry element of the space groups. It brings the pattern into congruence with itself over and over again. The shortest displacement through which this translation brings the pattern into coincidence with itself is the elementary translation or elementary period. Sometimes it is also called the identity period. The presence of translation is seen well in the pattern in Figure 8-1. The symmetry analysis of the whole pattern was called by Budden the analytical approach. The reverse procedure is the
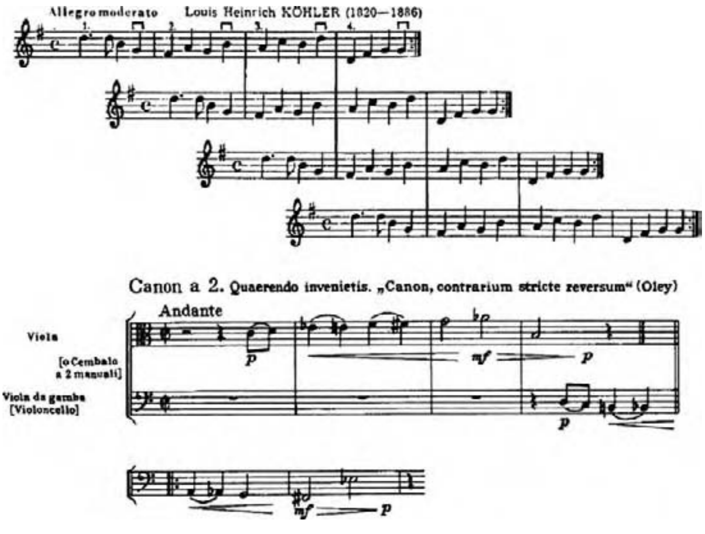
Figure 8-2. *Top*: Canon illustrating simple repetition; *Bottom*: repetition combined with glide reflection.

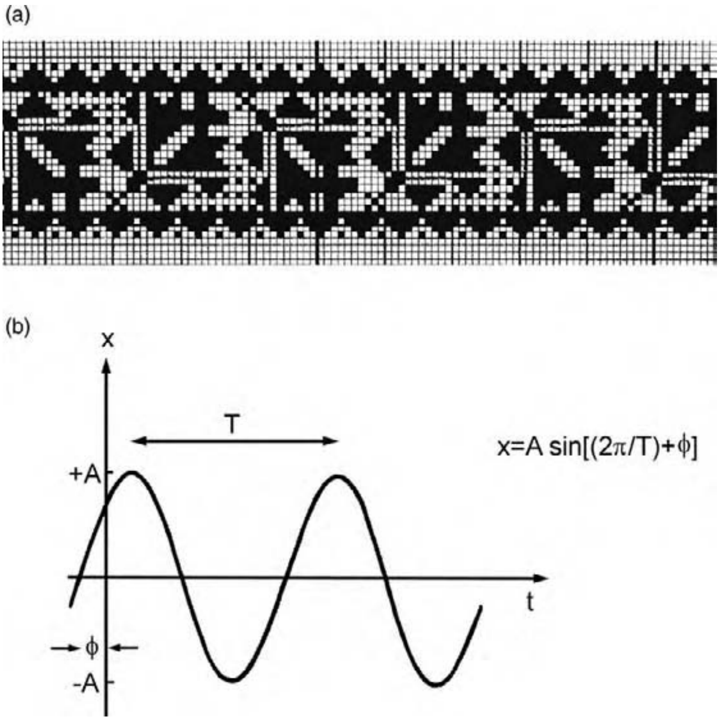

Figure 8-3. Illustrations for glide mirrors. (**a**) Pillow-edge from Buzsák, Hungary (used with permission from Györgyi Lengyel); (**b**) Function describing simple harmonic motion (reflection occurs following translation along the *t* axis by half a period, *T*/2).

synthetic approach in which the infinite and often complicated pattern is built up from the basic motif. Thus, the pattern of Figure 8-1a may be built up from a single crochet. There are several ways to proceed. For example, the crochet may be subjected to simple translation, then reflection, and then transverse reftection. The horizontal array obtained this way is a one-dimensional pattern. It can be extended to a two-dimensional pattern by simple translation or by glide reflection. Eventually the complete two-dimensional pattern of Figure 8-1 can be reconstructed. In this synthetic approach, instead of the single crochet, any other motif combined from it could be selected for the start. If the crosslike motif were chosen, which contains eight of these crochets, then only translations in two directions would be needed to build up the final pattern. To learn the most about the structure and symmetries

of a pattern, it is advantageous to select the smallest possible motif for the start.

The one-dimensional space groups are the simplest of the space groups. They have periodicity only in one direction. They may refer to one-dimensional, two-dimensional, or three-dimensional objects, cf., G_1^1, G_1^2, and G_1^3, of Table 2-2, respectively. The "infinite" carbon chains of the carbide molecules

. . . =C=C=C=C=C= . . .

. . . –C≡C–C≡C–C≡ . . .

represent one-dimensional patterns. The elementary translation or identity period is the length of the carbon–carbon double bond in the uniformly bonded chain while it is the sum of the lengths of the two different bonds in the chain consisting of alternating bonds. As the chain of molecules extends along the axis of the carbon–carbon bonds, this axis can be called the translation axis. The carbon-carbon axis is a singular axis, and it is not polar as the two directions along the chain are equivalent. Earlier we have seen the binary array ... A B A B A B ... in a crystal. The unequal spacings between the atom A and the two adjacent atoms B produced a polar axis (cf., Section 2.6 on polarity).

8.2. One-Sided Bands

Figure 8-4 presents two band decorations; one of them has a polar axis while the other has a nonpolar axis. An important feature of these patterns is that they have a polar singular plane, which is the plane of the drawing. This plane is left unchanged during the translation. Such two-dimensional patterns with periodicity in one direction are called one-sided bands [5].

There are altogether seven symmetry classes of one-sided bands. They are illustrated in Figure 8-5 for a suitable motif, a black triangle. A brief characterization of the seven classes is given here, following their notation:

1. (*a*). The only symmetry element is the translation axis. The translation period is the distance between two identical points of the consecutive black triangles.

Figure 8-4. Polar (**a**) And nonpolar; (**b**) Decorations of Byzantine mosaics from Ravenna, Italy, with one-dimensional space-group symmetry (photographs by the authors).

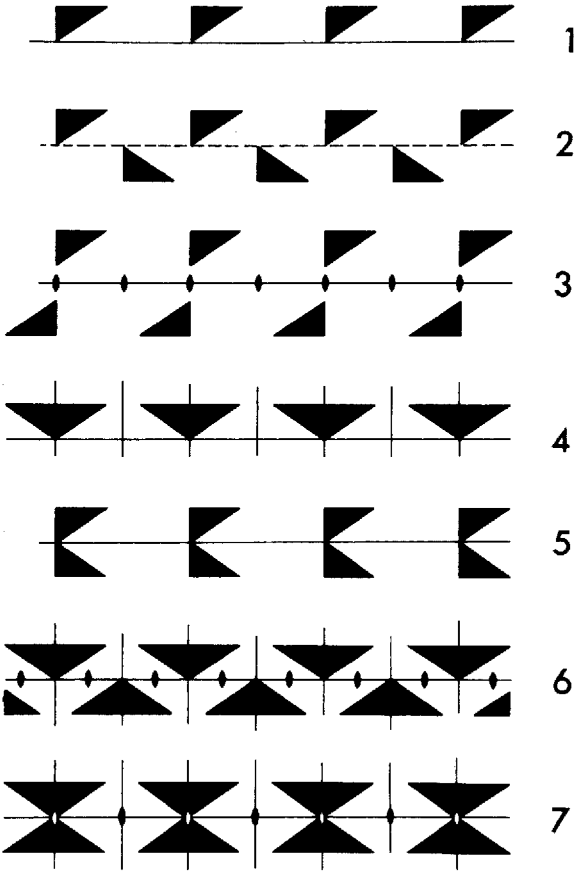

Figure 8-5. The seven symmetry classes of one-sided bands.

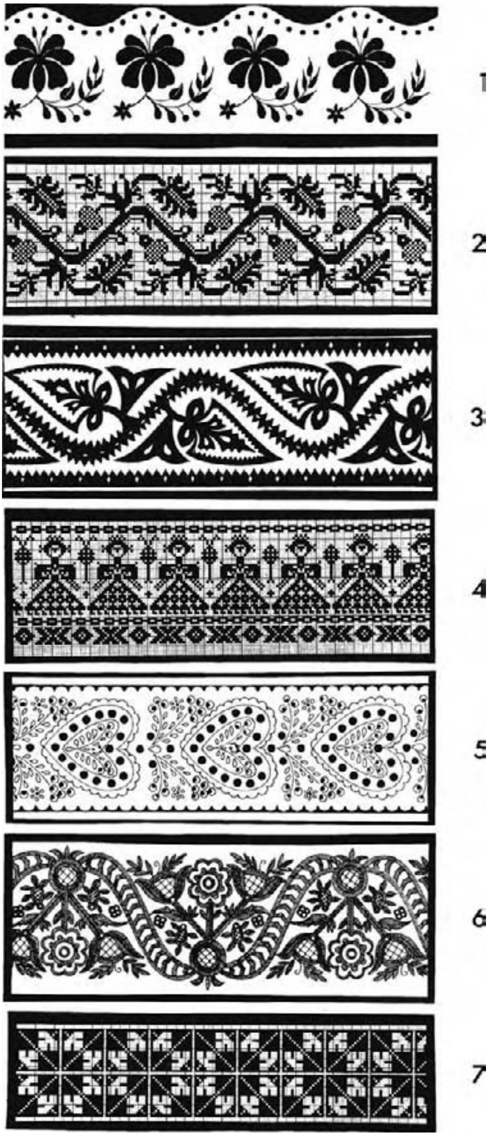

Figure 8-6. Illustration of the seven symmetry classes of one-sided bands by Hungarian needlework [8]. The numbering corresponds to that of Figure 8-5. (**1**) Edge decoration of table cover from Kalocsa, Southern Hungary; (**2**) Pillow-end decoration from Tolna county, Southwest Hungary; (**3**) Decoration patched onto a long embroidered felt coat of Hungarian shepherds in Bihar county, Eastern Hungary; (**4**) Embroidered edge-decoration of bed-sheet from the 18th century. Note the deviations from the described symmetry in the lower stripes of the pattern; (**5**) Decoration of shirt-front from Karád, Southwest Hungary; (**6**) Pillow decoration pattern from Torocko (Rimetea), Transylvania, Romania; (**7**) Grape-leaf pattern from the territory east of the river Tisza.

2. $(a)\cdot\tilde{a}$. Here the symmetry element is a glide-reflection plane ($\tilde{a}$). The black triangle comes into coincidence with itself after translation through half of the translation period ($a/2$) and reflection in the plane perpendicular to the plane of the drawing.
3. (a):2. There is translation and twofold rotation axis in this class. The twofold rotation axis is perpendicular to the plane of the one-sided band.
4. $(a):m$. The translation is achieved by transverse symmetry planes in this pattern.
5. $(a)\cdot m$. Here the translation axis is combined with a longitudinal symmetry plane.
6. $(a)\cdot\tilde{a}:m$. Combination of glide-reflection plane with transverse symmetry planes characterizes this class. These elements generate new ones such as twofold rotation. Consequently, there are alternative descriptions of this symmetry class. One of them is by combining twofold rotation with glide reflection—the corresponding notation is $(a):2\cdot\tilde{a}$. Another is by combining twofold rotation with transverse reflection for which the notation is $(a):2:m$.
7. $(a)\cdot m:m$. This pattern has the highest symmetry achieved by a combination of transverse and longitudinal symmetry planes. In this description the twofold axes perpendicular to the plane of the drawing are generated by the other symmetry elements. An alternative description is $(a):2\cdot m$.

The seven one-dimensional symmetry classes for the one-sided bands are illustrated by patterns of Hungarian needlework in Figure 8-6 [6]. This kind of needlework is a real “one-sided band.” Figure 8-7 presents a scheme to facilitate establishing the symmetry class of one-sided bands [7].

8.3. Two-Sided Bands

If the singular plane of a band is not polar, the band is two-sided. The one-sided bands are a special case of the two-sided bands. Figure 8-8a shows a one-sided band generated by translation of a leaf motif. Figure 8-8b depicts a two-sided band characterized by a glide-reflection plane. There is a translation by half of the translation period and then a reflection in the plane of the drawing. The leaf patterns are paralleled by patterns of the triangle in Figure 8-8. A new symmetry

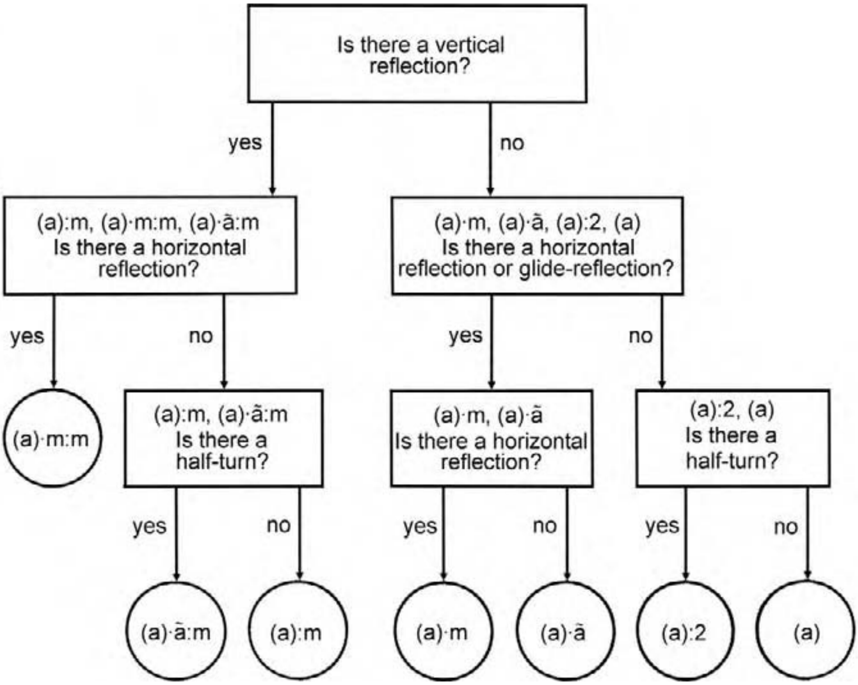

Figure 8-7. Scheme for establishing the symmetry of a one-sided band after Crowe [9].

element is illustrated in Figure 8-8c, the twofold (or second-order) *screw axis*, 2_1. The corresponding transformation is a translation by half the translation period and a 180° rotation around the translation axis. Bands have altogether 31 symmetry classes, including the seven one-sided bands. Table 8-1 gives two different notations for the seven one-sided band classes and for the two two-sided ones shown in Figure 8-8b and c as illustrations.

The so-called coordinate, or international, notation refers to the mutual orientation of the coordinate axes and symmetry elements [11]. The notation always starts with the letter *p*, referring to the translation group. Axis *a* is directed along the band, axis *b* lies in the plane of the drawing, and axis *c* is perpendicular to this plane. The first, second, and third positions of the symbol after the letter *p* indicate the mutual orientation of the symmetry elements with respect to the coordinate axes. If no rotation axis or normal of a symmetry plane coincides with a coordinate axis, the number 1 is placed in the corresponding position in the symbol. The coincidence of a rotation axis,

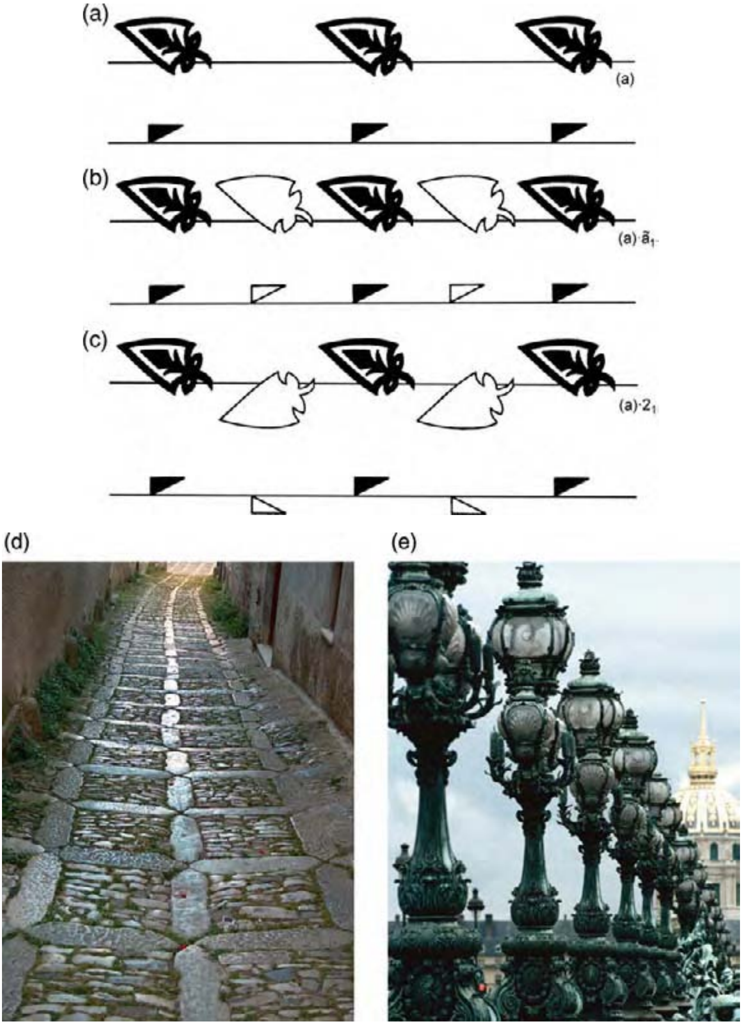

Figure 8-8. One-sided and two-sided bands using a one-sided leaf motif and a one-sided black triangle motif. (**a**) One-sided bands generated by simple translation. The plane of the drawing is a polar singular plane; (**b**) Two-sided bands generated from the same motifs as before, by introducing a glide-reflection plane. The singular plane in the plane of the drawing is no longer polar. The glide-reflection plane coinciding with the plane of the drawing is labeled $\tilde{a}_{11}$ [10]. Note that the two sides of the leaves are of different color (*black* and *white*); (**c**) Two-sided bands generated from the same motifs as before, by introducing a screw axis of the second order, 2_1. Used with permission from Nauka Publishers, Moscow; (**d**) Pavement in Erice, Italy as an example of a one-sided band; (**e**) Lamps on the Alexander III Bridge in Paris (photographs by the authors).

Table 8-1. Examples of Notations of Band Symmetries

Noncoordinate notation	Coordinate (international) notation
(a)	$p1$
$(a)\cdot\tilde{a}$	$p1a1$
(a):2	$p112$
$(a):m$	$pm11$
$(a)\cdot m$	$p1m1$
$(a)\cdot 2:m \equiv (a):2\cdot\tilde{a} \equiv (a):\tilde{a}\cdot m$	$pma2$
$(a)\cdot m:m \equiv (a):2\cdot m$	$pmm2$
$(a)\cdot 2_1$	$p2_111$
$(a)\cdot \tilde{a}_{11}$	$p11a$

2 or 2_1, or the normal of a symmetry plane, m or $\tilde{a}$, with one of the coordinate axes is indicated by placing the symbol of this element in the corresponding position in the notation.

8.4. Rods, Spirals, and Similarity Symmetry

The "infinite" carbide molecule is, of course, of finite width. It is indeed a three-dimensional construction with periodicity in one direction only. Thus, it has one-dimensional space-group symmetry (G_1^3). It is like an infinitely long rod. For a rod, the axis is a singular axis, and it has no singular plane. All kinds of symmetry axes may coincide with the axis of the rod, such as a translation axis, a simple rotation axis, or a screw-rotation axis. Of course, these symmetry elements, except the simple rotation axis, may characterize the rod only if it expands to infinity. As regards symmetry, a tube, a screw, or various rays are as much rods as are the stems of plants, vectors, or spiral stairways. A conspicuous example is the nanotubes and nanorods that are finding broadening applications in current science and technology due to their ability of providing novel mechanical, electrical, and thermal properties, and other uses, such as hydrogen storage [12]. A computer drawing and an analogy in artistic expression are shown in Figure 8-9. The symmetries of the structural diversity in the nanoworld have been discussed extensively [13]. Many of our examples throughout this book would also qualify for belonging to the nanoworld.

We have stressed above the necessity of considering our objects extending to infinity at least in one direction in order to qualify

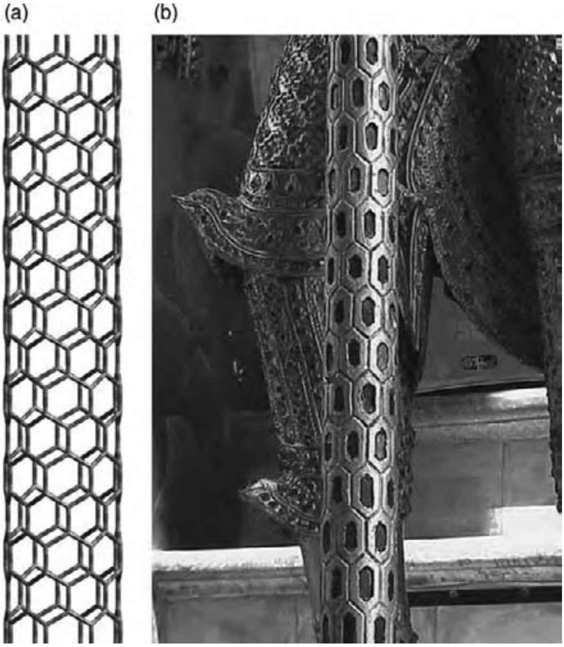

Figure 8-9. Nanotubes; (**a**) Computer graphic by Zoltán Varga, Budapest; (**b**) Decoration in the Royal Palace in Bangkok, Thailand (photograph by the authors).

for applying space-group symmetry description to them. However, real objects are, of course, not infinite. For symmetry considerations, it may be convenient to look only at some portions of the whole, where the ends are not yet in sight, and extend them in thought to infinity. A portion of an iron chain and a chain of beryllium dichloride in the crystal are shown in Figure 8-10. Translation from unit to unit is accompanied by a 90° rotation around the translation axis. A portion of a spiral stairway displaying screw-axis symmetry is shown in Figure 8-11a. The imaginary impossible stairway of Figure 8-11b indeed seems to go on forever.

A screw axis brings the infinite rod into coincidence with itself after a translation through a distance t accompanied by a rotation through an angle α. The screw axis is of the order $n = 360^\circ/\alpha$. It is a special case when n is an integer. The iron chain and the beryllium dichloride chain have a fourfold (or fourth-order) screw axis, 4_2. Their overall symmetry is $(a){\cdot}m{\cdot}4_2{:}m$. For the screw axis of the second order, the direction of the rotation is immaterial. Other screw axes may be either

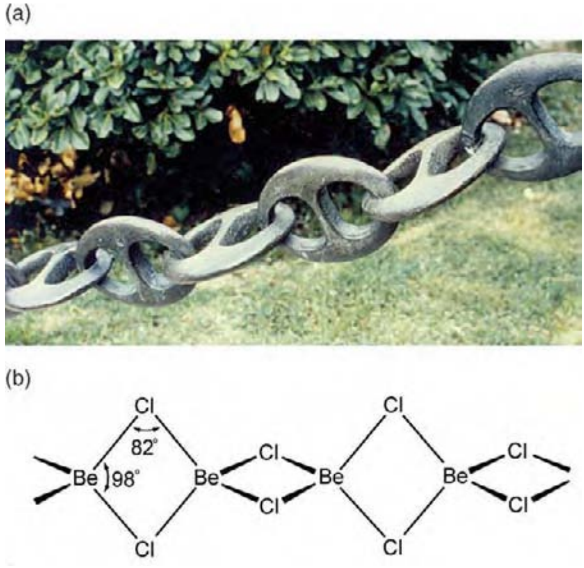

Figure 8-10. Rods with 4_2 screw-axis. (**a**) Iron-chain in the vicinity of the Royal Palace in Madrid (photograph by the authors); (**b**) Beryllium dichloride chain in the crystal.

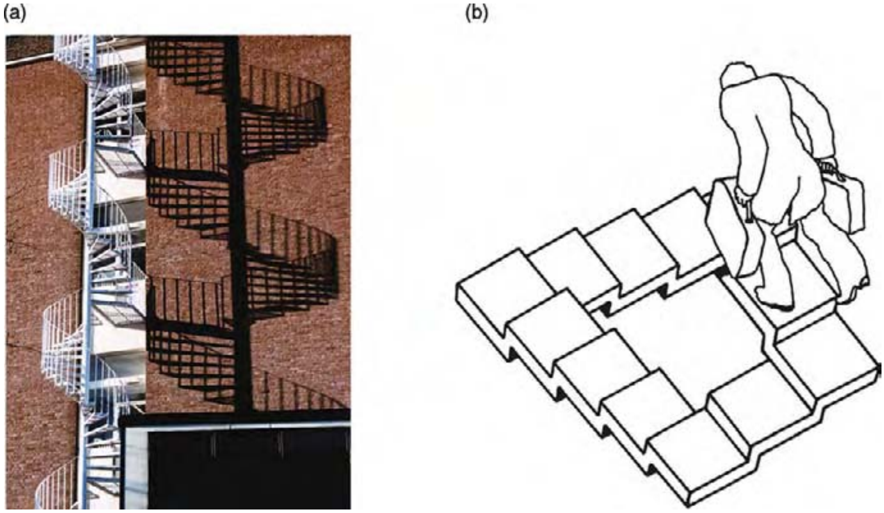

Figure 8-11. (**a**) Spiral staircase (and its shadow) in Cambridge, England, displaying screw-axis symmetry (photograph by the authors); (**b**) “Impossible stairway” (drawn after a movie poster advertising *Glück im Hinterhaus*).

left-handed or right-handed. The pair of left-handed and right-handed helices of Figure 2-39 is an example.

The scattered leaf arrangement around the stems of many plants is a beautiful occurrence of screw-axis symmetry in nature. The stem of *Plantago media* shown in Figure 8-12a certainly does not extend to infinity. It has been suggested, however, that for plants the plant/seed/plant/seed ... infinite sequence, at least in time, provides enough justification to apply space groups in their symmetry description. Let us consider now the relative positions of the leaves around the stem of *Plantago media*. Starting from leaf "0," leaf "8" will be in eclipsed orientation to it. In order to reach leaf "8" from leaf "0,"

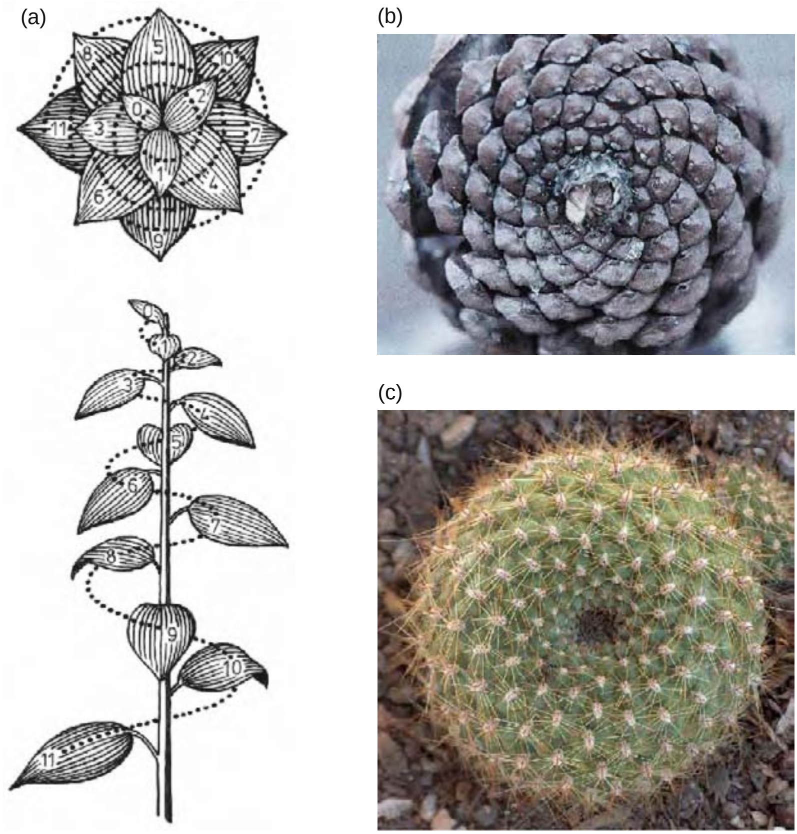

Figure 8-12. (**a**) The scattered leaf arrangement (phyllotaxis) of *Plantago media* (drawing by Ferenc Lantos, Pécs). Fibonacci numbers of spirals in the patterns of; (**b**) Scales of a pinecone; and (**c**) A cactus in Hawaii (**b** and **c**, photographs by the authors).

the stem has to be circled three times. The ratio of the two numbers, viz., 3/8, tells us that a new leaf occurs at each three/eighths part of the circumference of the stem. The ratio 3/8 is characteristic in phyllotaxis, as are 1/2, 1/3, 2/5, and even 5/13. Very little is known about the origin of phyllotaxis. What has been noted a long time ago is that the numbers occurring in these characteristic ratios, viz.,

$$1, 1, 2, 3, 5, 8, 13, \ldots$$

are members of the so-called Fibonacci series, in which each consecutive number is the sum of the previous two. Fibonacci numbers can be observed also in the numbers of the spirals of the scales of pine cones as viewed from below, displaying 13 left-bound and 8 right-bound spirals of scales as in Figure 8-12b. Left-bound and right-bound spirals in strictly Fibonacci numbers are found in other plants as well. The plate of seeds of the sunflower appears as if a compressed scattered arrangement around the stem. Another example is the spirals of cactus thorns in Figure 8-12c. It is a striking observation that the continuation of the ratios of the characteristic leaf arrangements eventually leads to a famous irrational number, 0.381966..., expressing the *golden mean*!

An important application of one-dimensional space groups is for polymeric molecules in chemistry. Figure 8-13 illustrates the structure and symmetry elements of an extended polyethylene molecule. The translation, or identity period, is shown, which is the distance between two carbon atoms separated by a third one. However, any portion with this length may be selected as the identity period along the polymeric chain. The translational symmetry of polyethylene is characterized by this identity period.

The discovery of stereoregular organic polymers dates back to the mid-1950s. First, Karl Ziegler used his catalysts to produce such polymers under mild conditions, but they were not highly ordered structurally. This problem was solved by Giulio Natta, who—in the words of the Swedish presenter of their Nobel Prizes—broke the monopoly of nature over making stereoregular polymers [14]. The structural aspects had great importance for practical applications that skyrocketed following Ziegler and Natta's works. There is a schematic representation of the configuration of isotactic, syndiotactic, and atactic vinyl polymers in Figure 8-14, which was shown in Natta's Nobel

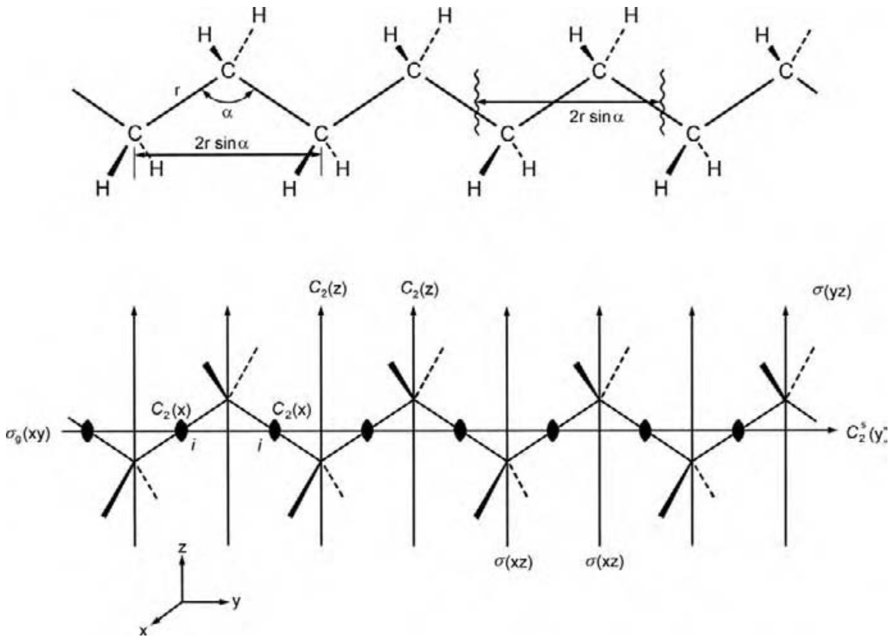

Figure 8-13. *Top*: The structure and translation period of the polyethylene chain molecule; *Bottom*: Symmetry elements of the polyethylene chain molecule.

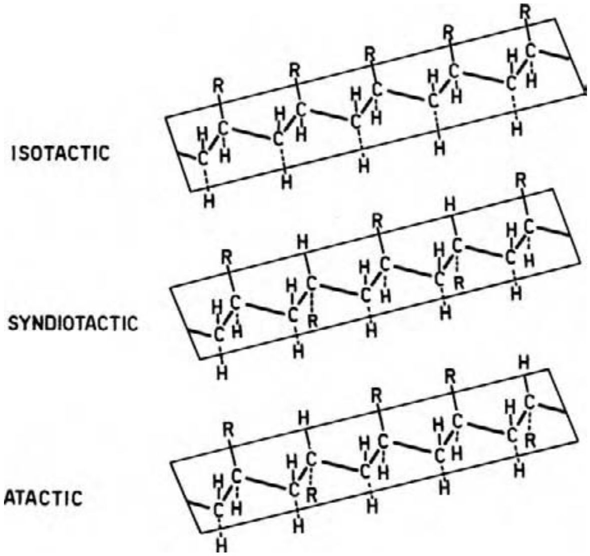

Figure 8-14. Schematic representation of the structures of isotactic (*top*); syndiotactic (*middle*); and atactic (*bottom*) vinyl polymers [15].

lecture and has been quoted in many other publications ever since. The labels to characterize the configurations were carefully chosen, using Greek words. *Isos* is the same and *tasso* means to put in order, hence “isotactic”; *syn dyo* means every two and combined with reference to order yields “syndiotactic”; finally “atactic” means lacking order. The isotactic structure can be imagined as achieved by repetition through simple translation, whereas the syndiotactic structure by repetition through glide reflection. Usually, these polymers take a helical structure whose determination was greatly aided by the fact that, by then, there was a lot of information available about the structure of the alpha-helix of proteins as well as about the double helix of nucleic acids.

Biological macromolecules are often distinguished by their helical structures to which one-dimensional space-group symmetries are applicable. Figure 8-15a shows Linus Pauling’s sketch of a polypeptide chain, which he drew while he was looking for the structure of alpha-keratin. When he decided to fold the paper, he arrived at the alpha-helix. The solution may have come in a sudden moment,

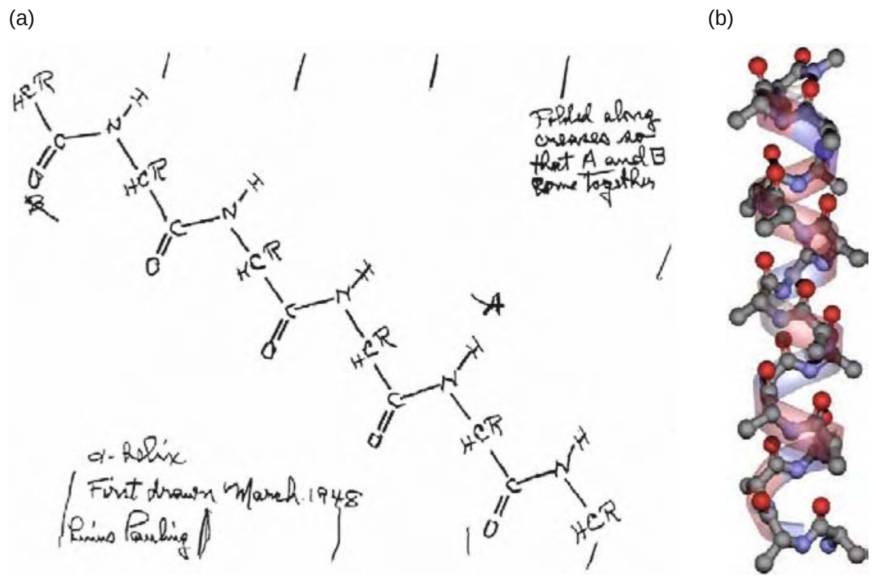

Figure 8-15. (**a**) Linus Pauling’s sketch of the polypeptide chain in 1948. The alpha-helix came together eventually when he folded the paper along the creases [16]; (**b**) Computer-drawing of the alpha-helix (courtesy of Ilya Yanov, Jackson, Mississippi).

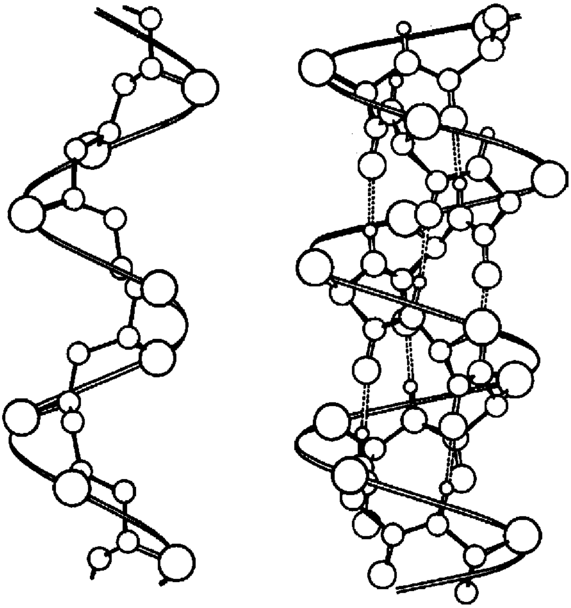

Figure 8-16. Helical segments; *Left*: isotactic poly-4-methylpentene having 3.5 monomeric units per pitch; *Right*: alpha-helix having 3.7 amino acid residues per pitch [17].

but Pauling had been working on the problem on and off for almost two decades. Figure 8-15b also depicts an alpha-helix structure as a computer drawing. A segment of one of Natta's polymers and that of alpha-helix are given in Figure 8-16. The structure of alpha-helix is accomplished by intramolecular hydrogen bonds.

When James Watson and Francis Crick reported their suggestion for the structure of deoxyribonucleic acid (DNA) [18], it had important novel features. One was that it had two helical chains, each coiling around the same axis, but having opposite direction. The two helices complement each other, which is a simple consequence of the twofold symmetry of the double helix with the axis of twofold rotation being perpendicular to the axis of the molecule. The other novel feature was the manner in which the two chains are held together by the purine and pyrimidine bases. They wrote: [the bases] "are joined in pairs, as a single base from one chain being hydrogen-bonded to a single base from the other chain, so that the two lie side by side with identical *z*-coordinates. One of the pair must be purine and the other a pyrimidine for bonding to occur" [19]. A little later they mention that

". . .if the sequence of bases on one chain is given, then the sequence on the other chain is automatically determined" [20]. Thus, symmetry and complementarity appear most beautifully in this model. The paper culminates in a final remark that sounds like a symmetry description of a simple rule to generate a pattern: "It has not escaped our notice that the specific pairing we have postulated immediately suggests a possible copying mechanism for the genetic material" [21].

A diagrammatic sketch of the double helix by Odile Crick illustrates this article, whose harmony and proportions have remained unsurpassed. It is also interesting that when Crick decided to erect a metallic sculpture above the entrance to his Cambride home, he chose a single helix rather than a double helix (Figure 8-17). The reason may have been that the realization of the helical structure of biological macromolecules was a most important milestone. It was also Crick and his two colleagues who worked out the theory of diffraction of the polypeptide (single) helix [22], which was then applicable to the description of diffraction by any helical structure. In their study, Crick and his associates assumed a structure that was based on Pauling's alpha-helix.

Figure 8-17. Francis Crick's Golden Helix structure above the entrance to the Cricks' former home in Cambridge, UK. (Photograph by the authors).

We have mentioned above the long quest by Pauling for the structure of alpha keratin. Symmetry considerations helped him greatly in finding the solution. At one point he remembered a mathematical theorem that referred to a general operation that converts an asymmetric object into another asymmetric object. The asymmetric object might be an amino acid and the operation was a rotation–translation—that is, a rotation around an axis combined with a translation along the axis—and repetition of this operation produces a helix. This put Pauling onto the right course [23]. Artistic representations of the double helix are shown in Figure 8-18. The double helix is held together by the hydrogen bonds of the base pairs in between the two helices. This is depicted in one of the artistic expressions of the double helix (Figure 8-18c).

It has been a question of contention whether, and to what extent, Erwin Chargaff's findings about the 1:1 ratios of purine and pyrimidine bases in the DNA molecules of diverse organisms helped Watson and Crick's discovery [24]. For our discussion it is instructive to note the importance and relevance of Chargaff's observation. What he did was nothing less than the discovery of a pattern where there seemed to be none. Looking at the raw data and their scatter on the purine and pyrimidine contents of DNA from various organisms, it is understandable that Chargaff felt "a great reluctance to accept such

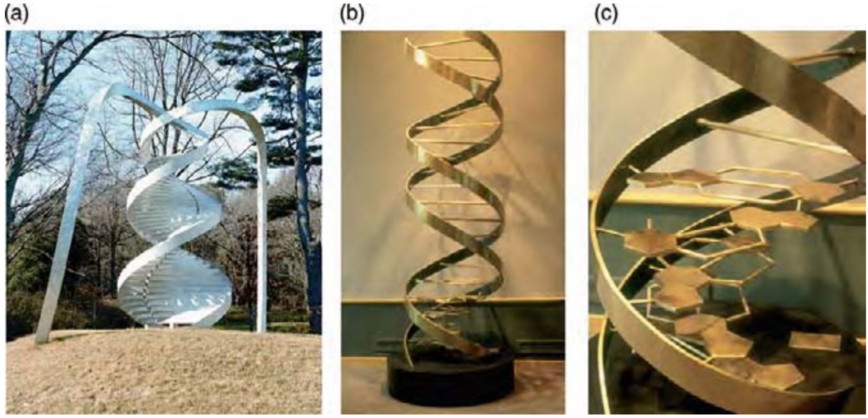

Figure 8-18. Artistic representations of the double helix; (**a**) *Spirals Time—Time Spirals* by Charles A. Jencks; (**b** and **c**) Sculpture of the double helix in the lobby of the Watson School; both sculptures are at Cold Spring Harbor Laboratory, Cold Spring Harbor, New York (photographs by the authors).

regularities" [25]. However, at the end, he did, and communicated the 1:1 ratios.

The structure and assembly of the tobacco mosaic virus (TMV) is an interesting example of helical symmetry. It has a simple rod shape with a regular helical array of protein molecules and there is a single-stranded ribonucleic acid molecule embedded in this protein coat. The model of TMV is shown in Figure 8-19 in two representations. Aaron Klug called attention to an important difference between ordinary polymers and biological macromolecules: "The key to biological specificity is a set of weak interactions. A polymer chemist could start building the model in the middle or at any other point." However, for building a model for a biological macromolecule, it is "important to find the special sequence for initiating nucleation" [26].

Whereas *helical symmetry* is characterized by a constant amount of translation accompanied by a constant amount of rotation, in *spiral symmetry* the amounts of translation and rotation *change* gradually and regularly. D'Arcy Thompson capitalized this word in his description, "...a Spiral is a curve which, starting from a point of origin,

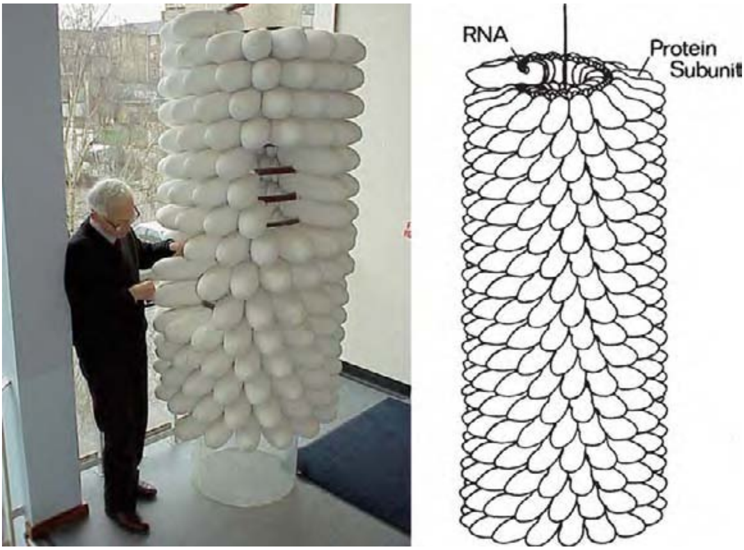

Figure 8-19. Models of the tobacco mosaic virus (TMV) structure; *Left*: Aaron Klug with the model at the Laboratory of Molecular Biology, Cambridge, UK (photograph by the authors); *Right*: graphical representation of the model (courtesy of Aaron Klug, Cambridge, UK).

continually diminishes in curvature as it recedes from that point; or, in other words, whose radius of curvature continually increases. . .” [27]. An important difference between helices and rods is that while helices can only form around rods, spirals may form along a rod or in a plane and the scattered leaf arrangement and the sunflower seed-plate may serve as their respective examples. An artistic double spiral is seen in Figure 8-20 as detail of a sculpture from the garden of a research institute where structures of biological macromolecules are investigated.

Interesting chemical examples of spirals occur in systems with chemical oscillations. Oscillating reactions are often called Belousov–Zhabotinsky reactions. Boris Belousov communicated his first observation in an obscure Russian medical publication [28] in the 1950s and it was followed by Anatol Zhabotinsky’s first systematic studies [29] in the 1960s. Although the chemical community was slow in catching up and many viewed the first reports on oscillating reactions with scepticism, research on nonlinear chemical phenomena has greatly expanded by now along with research of nonlinear phenomena in

Figure 8-20. Artistic double spiral. Detail of a sculpture in the garden of the Weizmann Institute, Rehovot, Israel (*The Inner Light* by Gidon Graetz; photograph by the authors).

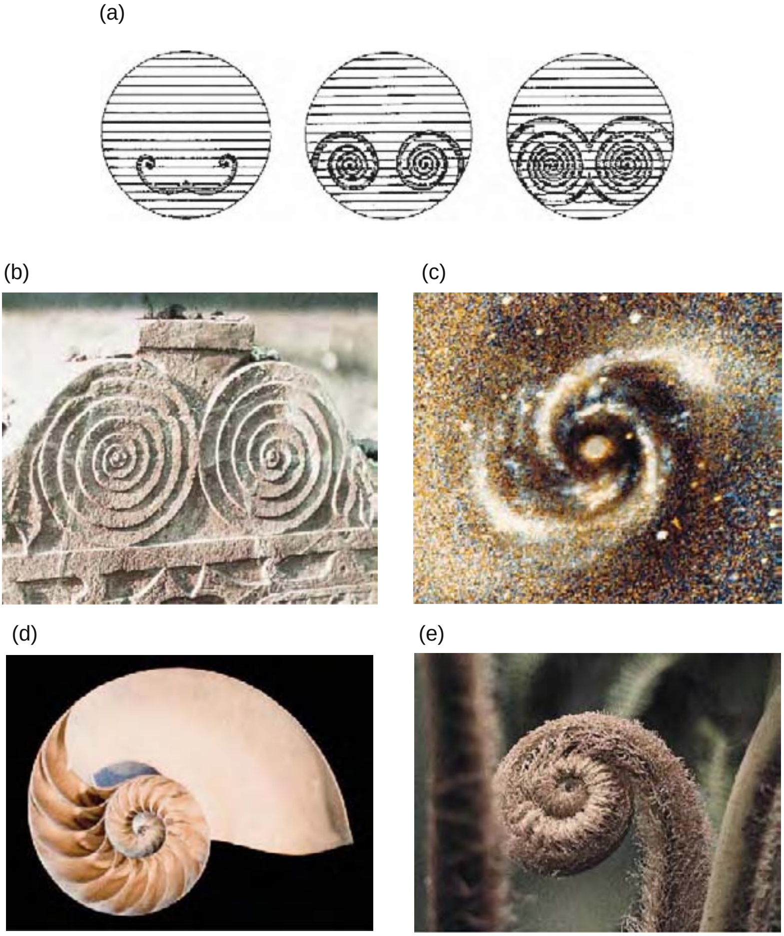

Figure 8-21. (**a**) Spiral ring pattern in a reacting Belousov-Zhabotinsky system [30]; (**b**) Tombstone in the Jewish cemetery, Prague (photograph by the authors); (**c**) Galaxy, courtesy of Bruce Elmegreen, Yorktown Heights, New York [31]; (**d**) Nautilus (photograph by and courtesy of Lloyd Kahn, Bolinas, California); (**e**) Fern from the Big Island, Hawaii (photograph by the authors).

other fields. Figure 8-21 illustrates the spiral structure in a Belousov–Zhabotinsky reaction. The two spirals shown make a heterochiral pair, paralleled by one on a tombstone in Figure 8-21. Spirals abound in nature. Some examples are shown also in Figure 8-21.

A gradual and regular change in size may appear by itself, that is, without being part of a spiral. A regular change in size characterizes, for example, homologous series, such as the alkanes, C_nH_{2n+2},

$$\ldots C_4H_{10}, C_5H_{12}, C_6H_{14}, C_7H_{16}, \ldots$$

with the increment of a methylene group, CH_2. Examples from outside chemistry are shown in Figure 8-22, where, again, it is up to our imagination to extend the series to infinity. All the spirals above and the phenomenon of phyllotaxis as well as the homologous series, the series of railway wheels, and the family of mountain goats can be considered as examples of *similarity symmetry* [32]. The mathematical concept of similarity holds one of the keys to understanding the processes of growth in the natural world [33]. Similarity symmetry is a good example of the convenient extension of the symmetry concept. In addition to the definitions offered in the Introduction, here, we suggest another one: *A pattern is symmetrical if there is a simple rule*

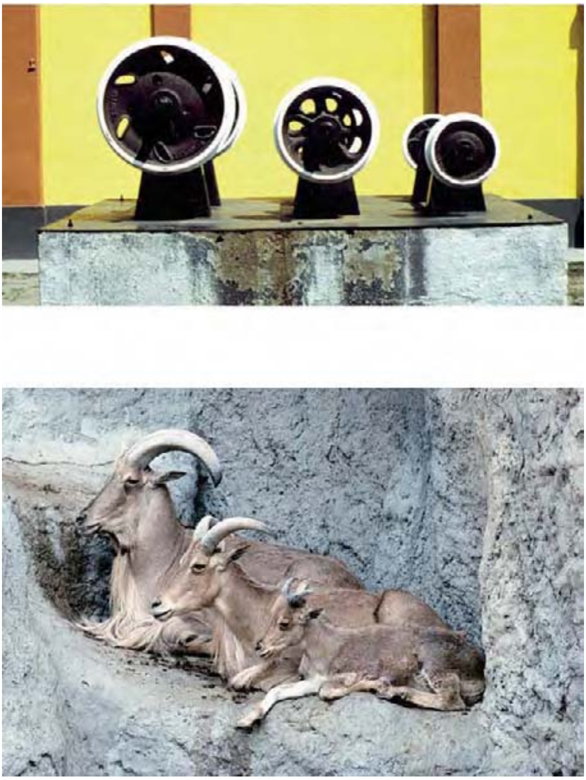

Figure 8-22. Examples of similarity symmetry (photographs by the authors). *Top*: railway wheels, Foundry Museum, Budapest; *Bottom*: mountain goats, Budapest Zoo.

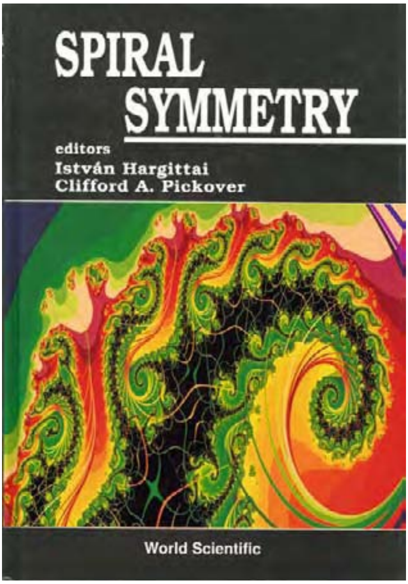

Figure 8-23. Fractals decorating a book cover [34]. (Computer graphics by and courtesy of Clifford A. Pickover, Yorktown Heights, New York).

to generate it. According to this inclusive definition, for example, Mandelbrot's fractals fall naturally into the realm of symmetry. An example is shown in Figure 8-23.

8.5. Two-Dimensional Space Groups

There are altogether 17 symmetry classes of one-sided planar networks. Figure 8-24 illustrates them in a way analogous to the seven symmetry classes of the one-sided bands (Figs. 8-5 and 8-6). The most important symmetry elements and the coordinate notations of the symmetry classes are also given. The first letter (*p* or *c*) in this notation refers to translation. The next three positions carry information on the presence of various symmetry elements, where *m* denotes a symmetry plane, *g* a glide-reflection plane, and 2, 3, 4, or 6 denotes a rotation axis. The number 1, or a blank, indicates the absence of a symmetry element. The representations of the symmetry classes in Figs. 8-5 and 8-24 were inspired by the illustrations inside the covers of Buerger's *Elementary Crystallography* [35]. Along with the purely geometrical configurations, Figure 8-24 presents 17 Hungarian

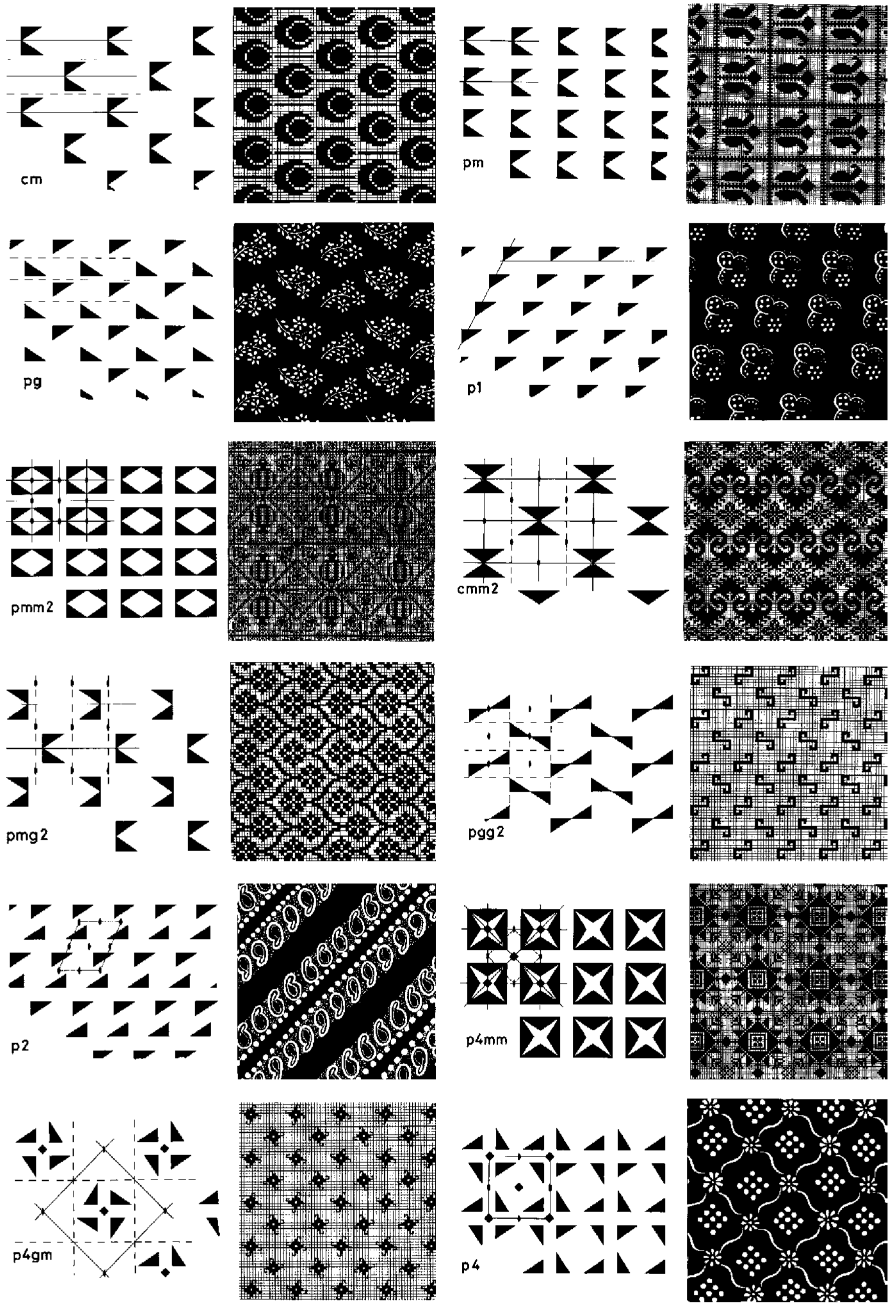

Figure 8-24. (Continued on next page)

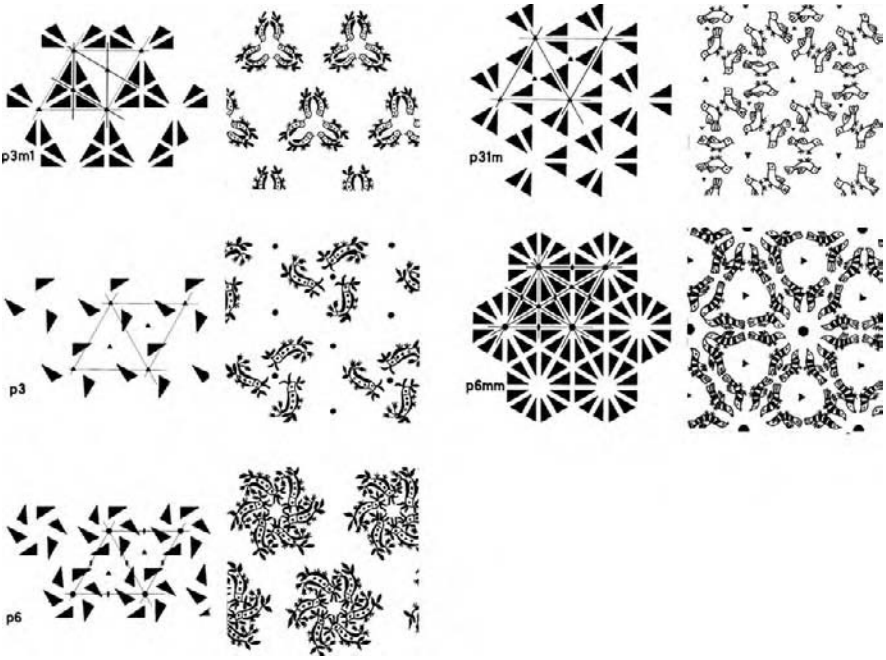

Figure 8-24. The 17 symmetry classes of one-sided planar networks with the most important symmetry elements and the notations of the classes indicated. Along with the geometrical configurations, Hungarian needlework patterns are presented for illustration. A brief description of the origin of these patterns is given here [36]:

*p*1 and *p*4 Patterns of indigo dyed decorations on textiles for clothing. Sellye, Baranya county, 1899.

*p*2 Indigo dyed decoration with palmette motif for curtains. Currently very popular pattern.

*p*3, *p*6, *p*6*mm*, *p*3*m*1, and *p*31*m* Decorations with characteristic bird motifs from peasant vests. Northern Hungary.

pm Decoration with tulip motif for table-cloth. Cross-stitched needlework. From the turn of the last century.

*pmm*2 Bed-sheet border decoration with pomegranate motif. Northwest Hungary, 19th century.

*p*4*mm* Pillow-slip decoration with stars. Cross-stitched needlework. Transylvania, 19th century.

cm Pillow-slip decoration with peacock tail motif. Cross-stitched needlework. Much used throughout Hungary around the turn of the last century.

*cmm*2 Bed-sheet border decoration with cockscomb motif. Cross-stitched needlework. Somogy county, 19th century.

pg From a pattern-book of indigo dyed decoration. Pápa, Veszprém county, 1856.

*pgg*2 Children's bag decoration. Transylvania, turn of the last century.

*pmg*2 Pillow-slip decoration with scrolling stem motif. Much used throughout Hungary around the turn of the last century.

*p*4*gm* Blouse-arm embroidery. Bács-Kiskun county, 19th century.

needlework patterns. A scheme for establishing the symmetry class of one-sided two-dimensional space groups is given in Figure 8-25.

The lattice of the planar networks with two-dimensional space groups is defined by two noncollinear translations. Such a lattice is shown in Figure 8-26a. Given a particular lattice, the question is, which pair of translations should be selected to describe it? An infinite number of choices exists for each translation because a line joining any two lattice points is a translation of the lattice. Figure 8-26b shows a plane lattice and some of the possible choices for translation pairs to describe it. A primitive cell is defined by choices of translation pairs such as $t_1$and t_2 or t_3 and t_4. Only one lattice point is associated with each primitive cell. This is understood if each lattice point in Figure 8-26 is considered to belong to four adjacent cells, or only one fourth of each point to belong to any one cell. As each cell contains four corners, all this adds up to one whole point. Alternatively, by displacing any one primitive cell, each primitive cell will contain only one lattice point. On the other hand, a multiple cell contains one or more lattice points in addition to the one shared at the corners. The translation pair t_5 and t_6, for instance, defìnes a double cell. A cell is called a unit cell if the entire lattice can be derived from it by translations. Thus, a unit cell may be either primitive or multiple. The unit cell is chosen usually to represent best the symmetry of the lattice. The translations selected as the edges of the plane unit cell are a and b, and for a space lattice, a, b, and c. The latter are called the crystallographic axes. The angles between the edges of the three-dimensional unit cell are α, β, and γ, but only γ is needed for the plane lattice.

Figure 8-27 shows three planar networks based on the same plane lattice. Two and only two lines intersect in each point of all three networks. Accordingly, the parallelograms of all three networks have the same area. All of them are unit cells, in fact, primitive cells. Each of these parallelograms is determined by two sides a and b, and the angle γ between them. These are called the cell parameters.

The general plane lattice (a) shown in Figure 8-28 is called a parallelogram lattice. The other four plane lattices of Figure 8-28 are special cases of the general lattice. The rectangular lattice (b) has a primitive cell with unequal sides. The so-called diamond lattice (c) has a unit cell with equal sides. A special case of the diamond lattice is when the angle between the equal sides of the unit cell is 120 degrees, and this lattice (d) is then called rhombic, or triangular since the short

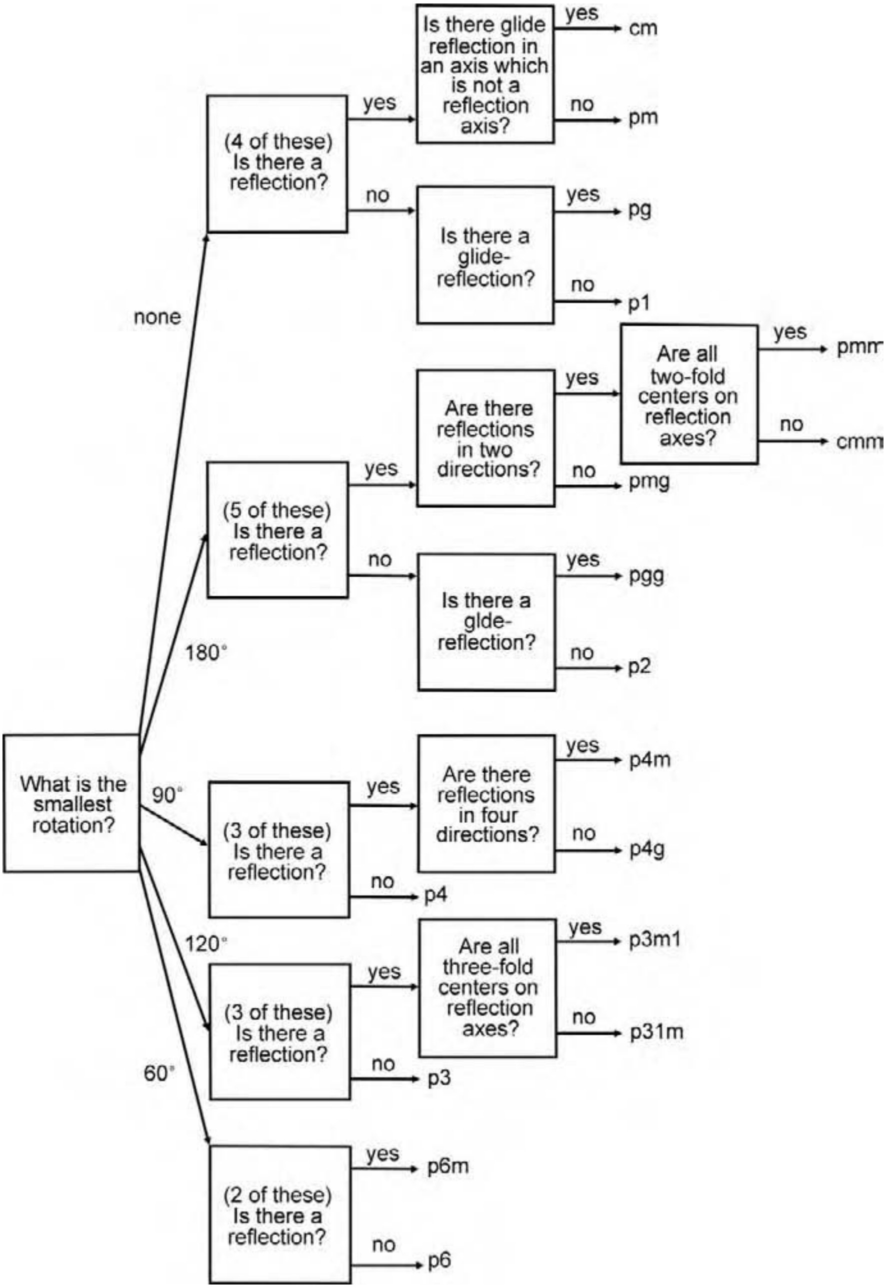

Figure 8-25. Scheme for establishing the symmetry of planar networks after Crowe [37].

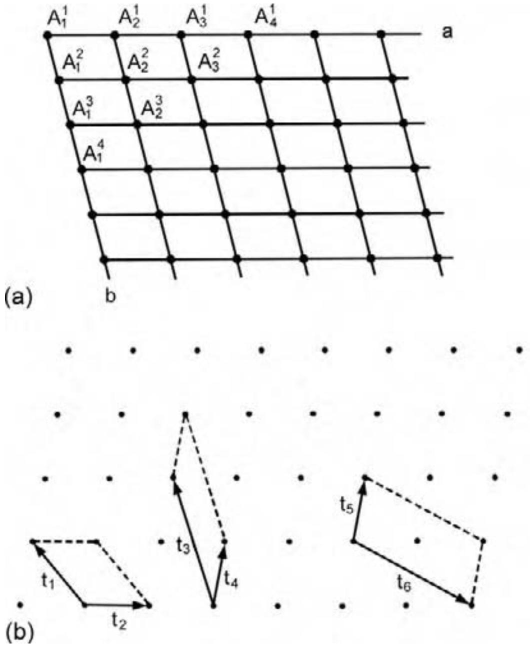

Figure 8-26. (**a**) Plane lattice defined by two non-collinear translations; (**b**) Illustration of primitive and unit cells on a plane lattice (after Azaroff, [38] used with permission from McGraw-Hill and L. V. Azaroff).

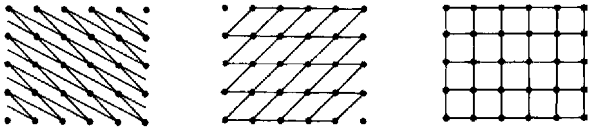

Figure 8-27. Different networks based on the same plane lattice.

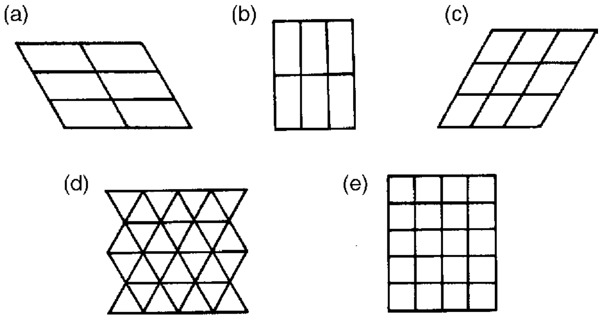

Figure 8-28. The five unique plane lattices (**a**–**e**, see text).

Table 8-2. Symmetries of the Five Unique Plane Lattices

Lattice	Space group	
	Noncoordinate notation	Coordinate (international) notation
a) Parallelogram lattice	(*b/a*):2	*p*2
b) Rectangular lattice	(*b:a*):2·*m*	*pmm*2
c) Diamond lattice	(*a/a*):2·*m*	*cmm*2
d) Hexagonal or triangular lattice	(*a/a*):6·*m*	*p*6*mm*
e) Square lattice	(*a:a*):4·*m*	*p*4*mm*

cell diagonal divides the unit cell into two equilateral triangles. This lattice may also be considered as having hexagonal symmetry. Finally there is the square lattice (e).

The five unique plane lattices were described above under the assumption that the lattice points themselves have the highest possible symmetry. In this case these five unique lattices will have the symmetries listed in Table 8-2.

When the point-group symmetries are combined with the plane lattices, 17 two-dimensional space groups can be produced. In such treatment, severe limitations are imposed on the possible point groups that may be combined with lattices to produce space groups. Some symmetry elements, such as the fivefold rotation axis, are not compatible with translational symmetry and from this, forbidden symmetries follow in classical crystallography. This and the lifting of such limitations in modern crystallography will be examined in Chapter 9.

8.5.1. Simple Networks

The simplest two-dimensional space group is represented in four variations in Figure 8-29. This space group does not impose any restrictions on the parameters a, b, and γ. The equal motifs repeated by the translations may occur in the following four different versions (strating from the upper left and clockwise): they may be completely separated from one another; they may consist of disconnected parts; they may intersect each other and; finally, they may fill the entire plane without gaps and overlaps. Of course, such variations are possible for any of the more complicated two-dimensional space groups as well.

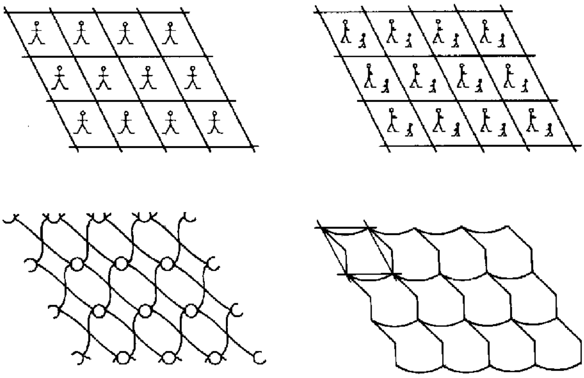

Figure 8-29. The simplest two-dimensional space group in four variations.

Especially intriguing are those variations which cover the whole available surface without gaps. Of the regular polygons, this is possible only with the equilateral triangle, the square, and the regular hexagon. For the latter, characteristic examples are shown in Figure 8-30 including some in which the hexagons have only approximately regular shapes.

Planar motifs of irregular shape can be used in infinite numbers to construct planar patterns covering the entire available surface. M. C. Escher is famous—among others— for his periodic drawings which fill the plane without gaps and overlaps [39]. Their symmetry aspects have been discussed in detail by crystallographer Caroline MacGillavry. She worked closely with the artist to create a set of periodic drawings for instructions in crystallography. The patterns in Figure 8-31 are from her book [40]. One of them has *p*1 symmetry. The unit cell is the combination of a fish and a boat. The repetition of the flies, butterflies, falcons, and bats in the Escher drawing, also in Figure 8-31, is accomplished by mirror planes. The two-dimensional space group is *pmm* and the mirror planes are indicated separately as the borders of the primitive cell.

Canadian crystallographer François Brisse has designed a series of two-dimensional space-group drawings related to Canada and dedicated to the XIIth Congress of the International Union of Crystallography (IUCr), Ottawa, 1981 [44]. One of them is shown in Figure 8-32. The symbol of the XIIth IUCr Congress was a unit of four stylized maple leaves related by fourfold rotation, and this is the unit cell of the drawing. The maple leaf, Canada’s symbol, is shown

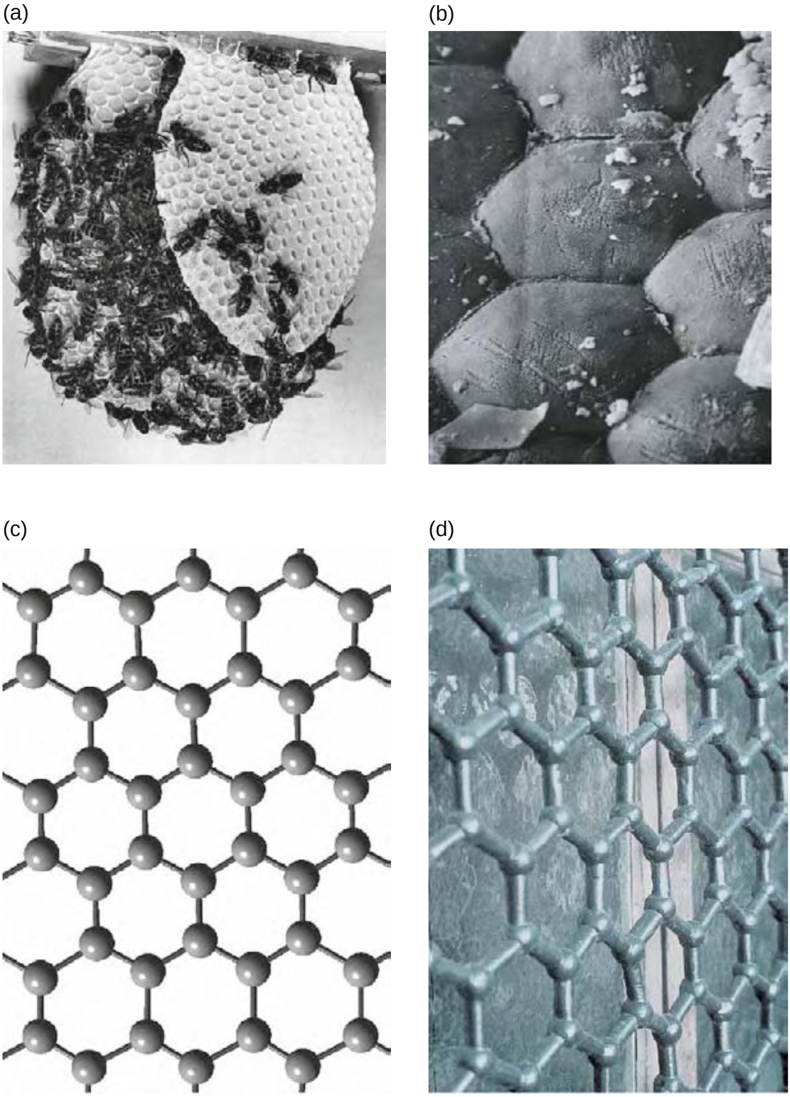

Figure 8-30. Networks of regular hexagons covering the surface without gaps or overlaps. (**a**) Honeycomb. Photograph by and courtesy of Pál Zoltán Örösi, Budapest; (**b**) Moth compound eye (magnified x 2000). Photograph by and courtesy of J. Morral, Storrs, Connecticut; (**c**) Computer-generated graphene-sheet model; (**d**) Graphite-sheet-like window fence at Topkapi Sarayi in Istanbul (photograph by the authors).

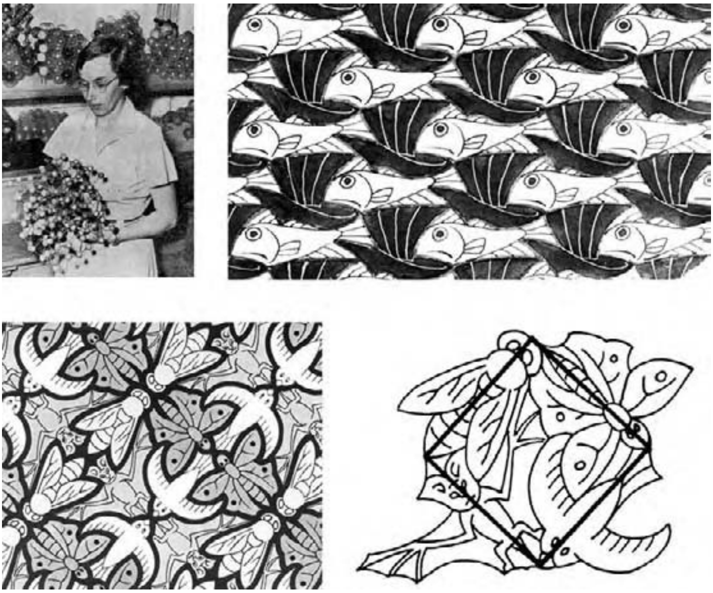

Figure 8-31. *Top*: Caroline H. McGillavry [41] and one of M. C. Escher's periodic drawings, of fish and boats with space group *p*1 [42] (reproduced with permission from the International Union of Crystallography). The unit cell consists of one fish and one boat; *Bottom*: Another of Escher's periodic drawings, of flies, butterflies, falcons and bats [43] (reproduced with permission from the International Union of Crystallography). The primitive cell is framed by the square whose sides are parts of the mirror planes in the periodic drawing.

in a more natural appearance on a stamp. Disregarding the coloring, the two-dimensional space group of the pattern is *p*4*gm*, the same as that of the Portugese tile decoration in Figure 8-32.

Khudu Mamedov was another crystallographer who created periodic drawings. His purpose was to immortalize ancient patterns found in his native Azerbaijan. He and his pupils published a remarkable little book *Decorations Remember* [46]. The space group of the drawing *Unity* of Figure 8-33 is *p*l, with the basic motif consisting of an old man and a young warrior. The repetition of the uniform shapes truly satisfies the requirement of it being a two-dimensional space group. A closer look, however, reveals distinct individuality of facial expressions, especially for the old men. This diversity of the individuals in the uniformity of the space goup is refreshing. Mamedov's former associates recently published a renewed version [47] of the

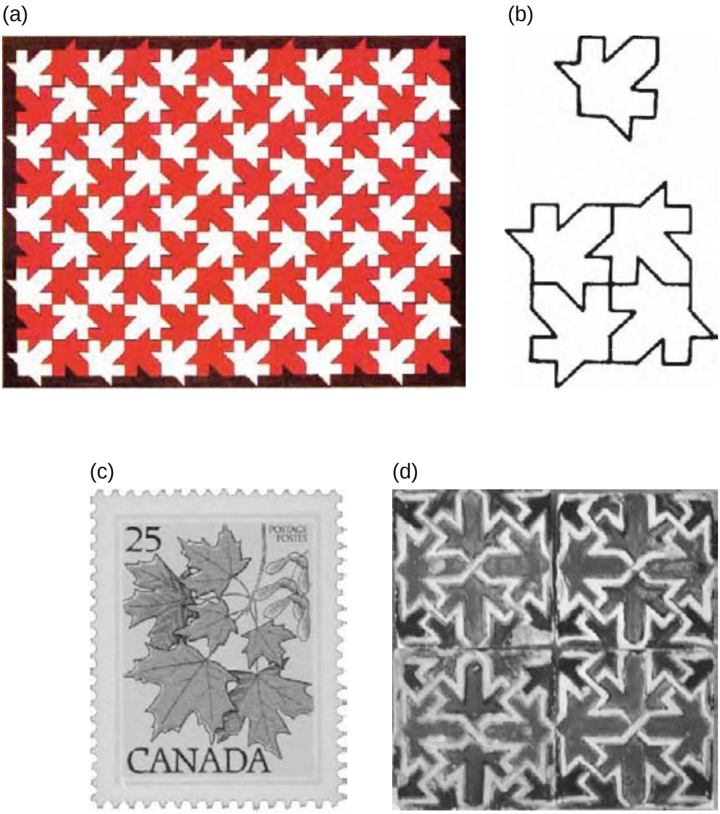

Figure 8-32. (**a**) Periodic drawing by François Brisse [45] (reproduced with permission); (**b**) The basic motif is a stylized maple leaf and the unit cell displays fourfold rotation; it was the symbol of the XIIth Congress of the International Union of Crystallography, Ottawa, 1981; (**c**) Canadian stamp with the maple leaf; and (**d**) A Portugese tile decoration (photograph by the authors). The patterns in the tile and in Brisse's drawing are related by a quarter of a circle rotation.

old book. The volume is luxuriously produced and many new patterns have been added. However, this time computer graphics replaced the original hand-drawings and the diversity of individuality is gone in the new version of *Unity* [48].

The mathematician George Pólya prepared a set of drawings for the 17 two-dimensional space groups with patterns that completely fill the surface without gaps or overlaps (Figure 8-34) [50]. A comprehensive and in-depth treatise of tilings and patterns has been published by Grünbaum and Shephard [51].

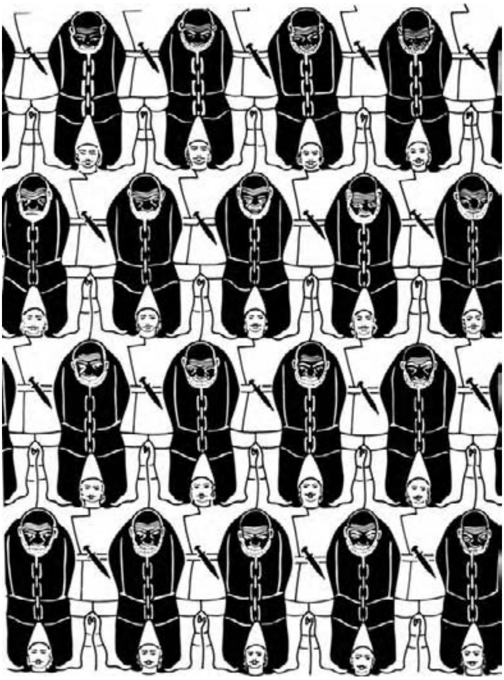

Figure 8-33. Khudu Mamedov's periodic drawing *Unity* [49].

8.5.2. Side-Effects of Decorations

Shubnikov and Koptsik analyzed the influence of the various space groups of bands and networks on people's perception of movement [53]. A one-sided band decoration without a polar axis induces no feeling of movement (see, e.g., Figure 8-4b). On the other hand, bands with polar axes (an example is shown in Figure 8-4a) convey the impression as if inducing left-bound or right-bound motion. A further pattern of band decoration with no symmetry plane is shown in Figure 8-35. A symmetry plane conveys the impression of preventing motion perpendicular to it. They are supposed to induce calmness and thus may be recommended for decorating the walls of halls for serious meetings. On the other hand, the walls of dancing halls should probably be decorated with patterns of rotational symmetry only. Two wall decorations, both from the Alhambra so rich in such patterns, are shown in Figure 8-36. The pattern of the Escher-like airline advertisement in Figure 8-37 conveys a strong feeling of motion, both left-bound and right-bound. There are no symmetry planes "preventing"

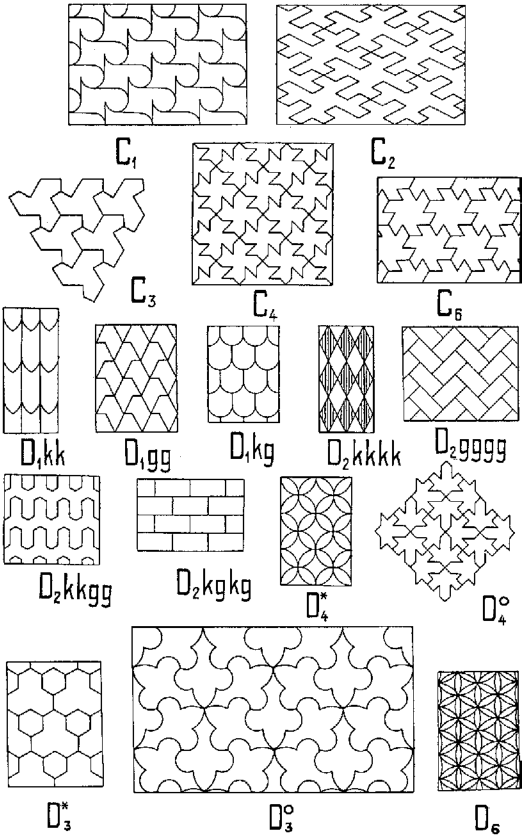

Figure 8-34. The 17 two-dimensional plane groups by George Pólya [52].

Figure 8-35. Ancient band decoration in the Tarxien Temple in Malta, from 3600–2500 BCE, with no symmetry planes induces the feeling of motion (photograph by the authors).

Figure 8-36. Wall decorations with symmetry planes (*left*) and without (*right*) in the Alhambra, Granada, Spain (photographs by the authors).

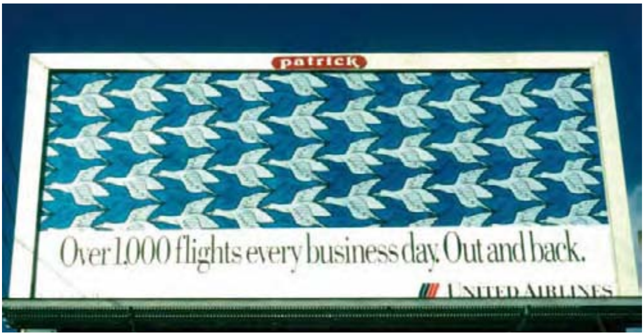

Figure 8-37. Airline advertisement near O’Hare Airport, Chicago (photograph by the authors).

left-bond or right-bound motion. The effects are enhanced by the different coloring of the birds flying in opposite directions. Up and down motion is perceived as if being hindered; there seem to be horizontal symmetry planes (although they are approximate only, due to the birds’ tails of the same color tilting in one direction, that is, nonsymmetrically).

8.5.3. Moirés

The so-called Moiré patterns are created by superimposing infinite planar patterns. The resulting pattern is a new two-dimensional network. The simplest cases are illustrated in Figure 8-38. Consider first two identical systems of lines on transparent paper being superimposed. The starting and resulting systems have a period of λ and d,

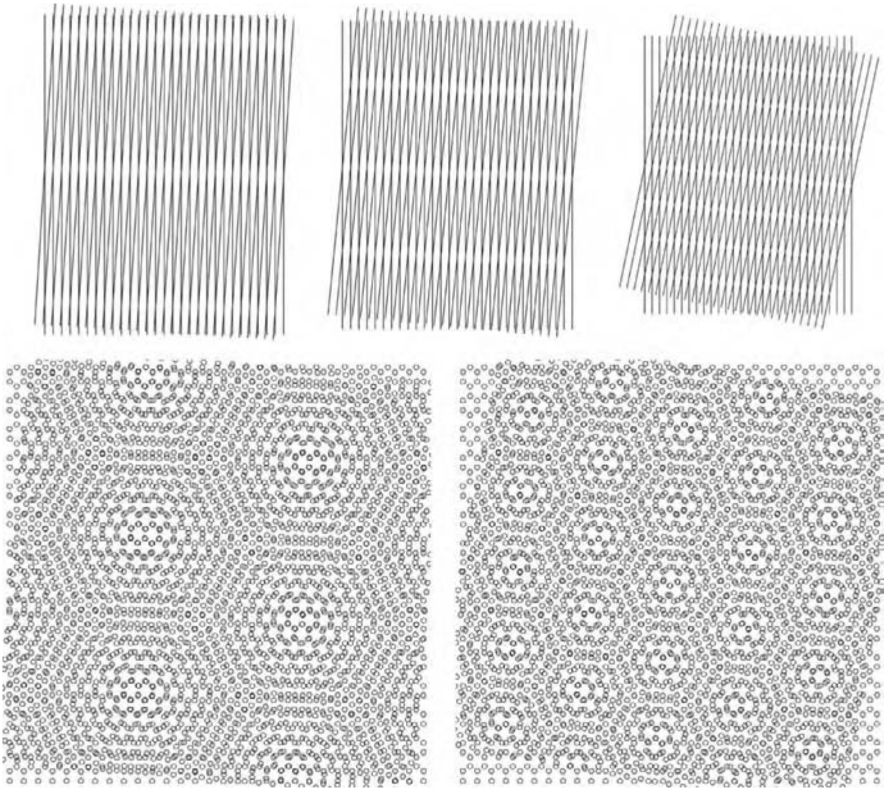

Figure 8-38. Moiré patterns from the superposition of two patterns at increasing angles. *Top*: two line systems; *Bottom*: two circle systems [54].

respectively and they are superimposed at an angle Θ. These parameters have the following relationship:

$$\lambda = 2d \sin(\Theta/2).$$

This expression is well known as the Bragg law in X-ray diffraction of crystals, where λ is the wave length of the X-rays, d is the distance between atomic layers in the crystal, and $\Theta/2$ is the angle at which the X-rays hit the atomic layer. The patterns produced in Figure 8-38 have twofold rotation axes perpendicular to their plane. Thus the superposition at angle Θ will produce the same result as at angles $180 + \Theta$. Figure 8-38 (bottom) shows the interference of two identical infinite systems of small circles at two different angles.

Moirés patterns occur in the most diverse natural phenomena and often occure in artistic creations as well [55]. They can be treated by fairly simple mathematics [56].

References

1. J. D. Bernal, *The Origin of Life*. Weidenfeld and Nicolson, London, 1967.
2. L. B. Young, *The Mystery of Matter*. Oxford University Press, New York, 1965.
3. F. J. Budden, *The Fascination of Groups*. University Press, Cambridge, 1972.
4. Ibid.
5. A. V. Shubnikov, V. A. Koptsik, *Symmetry in Science and Art*, Plenum Press, New York and London, 1974. Russian original: *Simmetriya v nauke i iskusstve*, Nauka, Moscow, 1972.
6. I. Hargittai, G. Lengyel, "The Seven One-Dimensional Space-Group Symmetries Illustrated by Hungarian Folk Needlework."*J. Chem. Educ*. 1984, 61, 1033–1034.
7. I. Hargittai, "Real turned ideal through symmetry." In *Symmetrie in Geistes- und Naturwissenschaft*, R. Wille, ed., Springer-Verlag, Berlin, 1988, pp. 131–161; D. W. Crowe, in *The Geometric Vein. The Coxeter Fertschrift*, C. Davis, B. Grünbaum, F. A. Sherk, eds., Springer-Verlag, New York, 1982.
8. Hargittai, Lengyel, *J. Chem. Educ*. 1033–1034.
9. Hargittai, *Symmetrie in Geistes- und Naturwissenschaf*; Crowe, *The Geometric Vein. The Coxeter Fertschrift*.
10. Shubnikov, Koptsik, *Symmetry in Science and Art.*
11. Ibid.
12. See, e.g., Q. Liu, W. Liu, Z.-M. Cui, W.-G. Song, L.-J. Wan, "Synthesis and Characterization of 3D Double Branched K Junction Carbon Nanotubes and Nanorods." *Carbon* 2007, 45, 268–273; X. Ye, X. Gu, X. G. Gong, T. K. M. Shing, Z.-F. Liu, "A Nanocontainer for the Storage of Hydrogen." *Carbon* 2007, 45, 315–320.
13. See, e.g., V. Ya. Shevchenko, Ed., *Nanoparticles, Nanostructures and Nanocomposites*. ECRS, Saint-Petersburg, 2006.
14. A. Fredga, "Chemistry 1963." In *Nobel Lectures Including Presentation Speeches and Laureates' Biographies: Chemistry 1963–1970*. World Scientific, Singapore, 1999, pp. 3–5, p. 4.
15. P. Corradini, "The Role of the Discovery and Investigation of Stereoregular Polymers in Macromolecular Chemistry." In S. Carra, F. Parisi, I. Pasquon, P. Pino, eds., *Giulio Natta: Present significance of his scientific contribution*. Editrice di Chimica, Milan, 182, pp. 126–146, p.136.
16. L. Pauling, "The Discovery of the Alpha Helix." *Chem. Intell.* 1996, 2(1), 32–38 (posthumous publication).
17. Corradini, *Giulio Natta*, p. 134.

18. J. D. Watson, F. H. C. Crick, “Molecular Structure of Nucleic Acids: A Structure for Deoxyribose Nucleic Acid.” *Nature* 1953, 171, 737–738.
19. Ibid., p. 737.
20. Ibid.
21. Ibid., p. 738.
22. W. Cochran, F. H. C. Crick, V. Vand, “The Structure of Synthetic Polypeptides. I. Transform of Atoms on a Helix.” *Acta Cryst*. 1952, 5, 581–586.
23. Pauling, *Chem. Intell.* 32–38.
24. See, e.g., the relevant discussions in I. Hargittai, *The DNA Doctor: Candid Conversations with James D. Watson.* World Scientific, Singapore, 2007.
25. E. Chargaff, *Heraclitean Fire: Sketches from a Life before Nature*. The Rockefeller University Press, New York, 1978, p. 106.
26. I. Hargittai, *Candid Science II: Conversations with Famous Biomedical Scientists*. Ed. M. Hargittai. Imperial College Press, London, 2002, “Aaron Klug,” pp. 306–329, p. 312.
27. D’Arcy Thompson, *On Growth and Form.* Cambridge University Press, Cambridge, 1917.
28. B. P. Belousov, in *Sbornik Referatov po Radiatsionnoi Medicine*, pp. 145-7, Medgiz, Moscow, 1958. “The tragic story of Belousov’s life and his unsuccessful struggles to publish his discovery has been told.” In S. E. Shnol, *Geroi, zlodei, konformosti rossiiskoi nauki* (in Russian, *Heroes, villains, and conformists of Russian science*). Second, augmented edition. Kron-Press, Moscow, 2001, pp. 278–307.
29. A. M. Zhabotinsky, “Periodic Kinetics of Oxidation of Malonic Acid in Solution (Study of the Belousov Reaction Kinetics).” *Biofizika* 1964, 9, 306–311; A. N. Zaikin, A. M. Zhabotinsky, “Concentration Wave Propagation in Two-dimensional Liquid-phase Self-oscillating System.” *Nature* 1970, 225, 535–537. See, also, a conversation with Anatol M. Zhabotinsky, I. Hargittai, *Candid Science III: More Converstions with Famous Chemists*. (ed. M. Hargittai.) Imperial College Press, London, 2003, pp. 432–447.
30. E. Körös, “Oscillations, Waves, and Spirals in Chemical Systems.” In *Spiral Symmetry*, I. Hargittai and C. A. Pickover, eds., World Scientific, Singapore, 1992, pp. 221–249, p. 241.
31. See, B. G. Elmegreen, “Spiral Galaxies.” In *Spiral Symmetry*, I. Hargittai and C. A. Pickover, eds., World Scientific, Singapore, 1992, pp. 95–106.
32. A. V. Shubnikov, “Symmetry of Similarity.” *Soviet Phys. Crystallogr*. 1961, 5, 469–476; reprinted in *Crystal Symmetries*, I. Hargittai and B. K. Vainshtein, eds., Pergamon Press, 1988, pp. 365–371.
33. I. Hargittai, C. A. Pickover, “Preface.” In I. Hargittai, C. A. Pickover, eds., *Spiral Symmetry*. World Scientific, Singapore, 1992, pp. v–xi, p. x.
34. Hargittai, Pickover, *Spiral Symmetry*.
35. M. J. Buerger, *Elementary Crystallography, An Introduction to the Fundamental Geometrical Features of Crystals* (Fourth printing), Wiley, New York, London, Sydney, 1967.

36. I. Hargittai and G. Lengyel, “The Seventeen Two-Dimensional Space-Group Symmetries in Hungarian Needlework.” *J. Chem. Educ*. 1985, 62, 35–36.
37. Crowe, *Geometric Vein.*
38. L.V. Azaroff, *Introduction to Solids*, McGraw-Hill, New York, Toronto, London, 1960.
39. D. Schattschneider, *Visions of Symmetry. Notebooks, Periodic Drawings, and Related Work of M. C. Esher*, W. H. Freeman and Co., New York, 1990.
40. C. H. MacGillavry, *Symmetry Aspects of M. C. Escher’s Periodic Drawings*, Bohn, Scheltema and Holkema, Utrecht, 1976.
41. From an article in *Algemeen Handelsblat*, 1952 (courtesy of Henk Schenk, Amsterdam).
42. MacGillavry, *Symmetry Aspects of M. C. Escher’s Periodic Drawings*,
43. Ibid.
44. F. Brisse, “La symétrie bidimensionelle et le Canada.” *Can. Mineral.* 1981, 19, 217–224.
45. Brisse, *Can. Mineral.* 217–224.
46. Kh. S. Mamedov, I. R. Amiraslanov, G. N. Nadzhafov, A. A. Muzhaliev, *Decorations Remember* (in Azerbaijani), Azerneshr, Baku, 1981.
47. I. Amiraslan, H. Necefoglu, *Azerbajani Tessellations*, Published by Hacali Necefoglu, Kars, Turkey, 2006.
48. See, also, I. Hargittai, “Crystal Structures and Culture: In Memoriam Khudu Mamedov (1927–1988).” *Struct. Chem.* 2007, 18, 535–536.
49. Mamedov et al., *Decorations Remember*, Hargittai, *Struct. Chem*. 535–536.
50. G. Pólya, “Über die Analogie der Kristallsymmetrie in der Ebene.” *Z. Krist*. 1924, 60, 278–282.
51. B. Grünbaum, G. C. Shephard, *Tilings and Patterns*, W. H. Freeman, New York, 1987.
52. Pólya, *Z. Kristallogr*. 278–282.
53. Shubnikov, Koptsik, *Symmetry in Science and Art.*
54. See, H. Giger, “Moirés.” In *Symmetry: Unifying Human Understanding*. Ed. I. Hargittai. Pergamon Press, Oxford, 1986, pp. 329–361; W. Witschi, “Moirés.” In *Symmetry, Unifying Human Understanding*, I. Hargittai, ed., Pergamon Press, New York and Oxford, 1986, pp. 363–378.
55. Ibid.
56. Giger, *Symmetry, Unifying Human Understanding*, pp. 329–361.

Chapter 9

Crystals

...all the works of the crystallographers
...demonstrate that there is only variety
everywhere where they suppose uniformity...
Georges Leclerc [Comte de] Buffon [1]

... But I must speak again about crystals, shapes, colors. There are crystals as huge as the colonnade of a cathedral, soft as mould, prickly as thorns; pure, azure, green, like nothing else in the world, fiery black; mathematically exact, complete, like constructions by crazy, capricious scientists, or reminiscent of the liver, the heart ... There are crystal grottos, monstrous bubbles of mineral mass, there is fermentation, fusion, growth of minerals, architecture and engineering art ... Even in human life there is a hidden force towards crystallization. Egypt crystallizes in pyramids and obelisks, Greece in columns; the middle ages in vials; London in grinny cubes ... Like secret mathematical flashes of lightning the countless laws of construction penetrate the matter. To equal nature it is necessary to be mathematically and geometrically exact. Number and phantasy, law and abundance—these are the living, creative strengths of nature; not to sit under a green tree but to create crystals and to form ideas, that is what it means to be at one with nature!

M. Hargittai, I. Hargittai, *Symmetry through the Eyes of a Chemist,* 3rd ed.,
DOI: 10.1007/978-1-4020-5628-4_9, © Springer Science+Business Media B.V. 2009

These are the words of Karel Čapek the Czech writer after his visit to the mineral collection of the British Museum [2]. He added a drawing (Figure 9-1) to his words to express his humility in front of these miracles of nature. Figure 9-2 displays crystal images from the mineral collection of Eötvös University, Budapest.

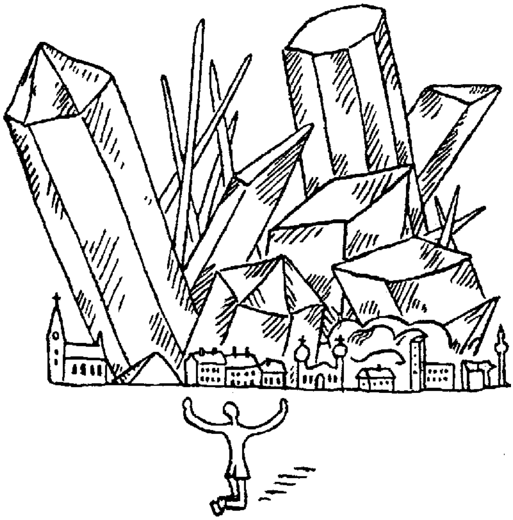

Figure 9-1. Karel Čapek's drawing after his visit to the mineral collection of the British Museum (reproduced with permission) [3].

The word crystal comes from the Greek *krystallos*, meaning clear ice. The name originated from the mistaken belief that the beautiful transparent quartz stones found in the Alps were formed from water at extremely low temperatures. By the 18th century, the name crystal was applied to other solids that were also bounded by many flat faces and had generally beautiful symmetrical shapes. Crystals have also been considered to be mystical. A sad angel looks hopelessly at the huge polyhedron in Albrecht Dürer's *Melancholia,* which is a truncated rhombohedron (Figure 9-3). There has been some discussion as to whether Dürer meant a particular mineral by it and, if so, which one. It was concluded that this polyhedron "is simply an exercise in accurate draughtsmanship and that the art historians have made rather heavy weather of its explanation ... The integral proportions show that no particular mineral was intended" [4]. The polyhedron was even given a name, melancholyhedron and has been claimed to be formed

(a) (b) (c)

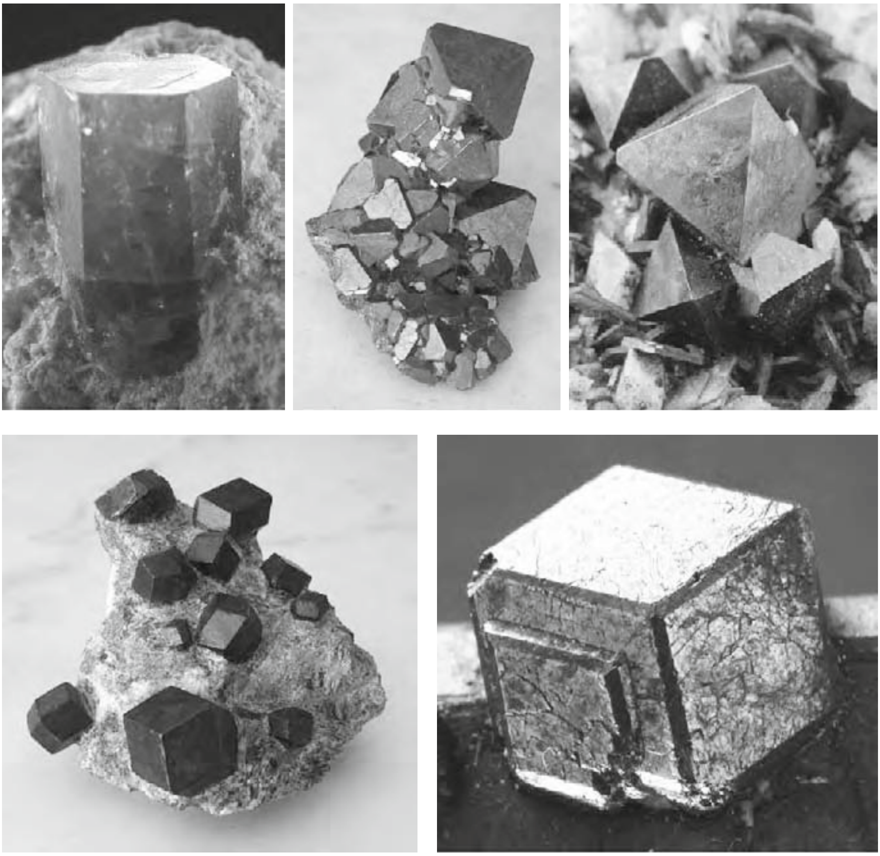

(d) (e)

Figure 9-2. Crystals (**a–c, e**) Photographs by and courtesy of the associates of the Mineral Collection of Eötvös University, Budapest; (**d**) Photograph by the authors from the collection of Aldo Domenicano and Anna Rita Campanelli, Rome.

by twelve arsenic atoms around a nickel atom in the solid-state structure of nickel arsenide [5].

Space-group symmetries have played an outstanding role in Escher's graphic art. So what he wrote about crystals is also of interest [7]:

> Long before there were men on this globe, all the crystals grew within the earth's crust. Then came a day when, for the very first time, a human being perceived one of these glittering fragments

Figure 9-3. The polyhedral arsenic skeleton in the NiAs crystal, resembling the polyhedron in Dürer's *Melancholia* [6].

> of regularity; or maybe he struck against it with his stone ax; it broke away and fell at his feet; then he picked it up and gazed at it lying there in his open hand. And he marveled.
>
> There is something breathtaking about the basic laws of crystals. They are in no sense a discovery of the human mind; they just "are"—they exist quite independently of us. The most that man can do is to become aware, in a moment of clarity, that they are there, and take cognizance of them.

The symmetry of the shapes of the crystals is their most easily recognizable feature. The Russian crystallographer E. S. Fedorov

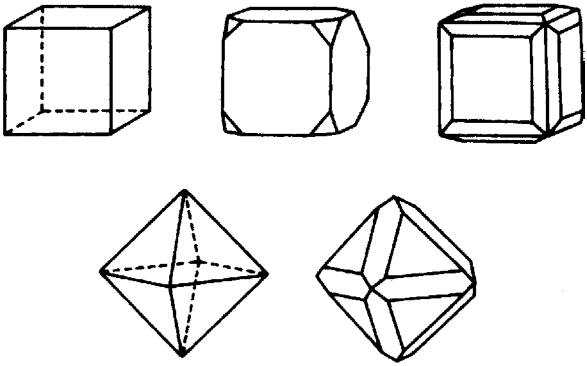

Figure 9-4. Different shapes of sodium chloride crystals as a consequence of the influence of impurities.

remarked that "the crystals glitter with their symmetry." Obviously, this outer symmetry is a consequence of the inner structure. However, with the same inner structure, crystals may grow into different forms. Besides, under natural conditions, crystals seldom grow into their well-known regular forms. Under different conditions, in the presence of different impurities, for example, different forms may grow. Figure 9-4 shows the influence of impurities upon the form of sodium chloride crystals.

9.1. Basic Laws

It has been recognized already in the earliest stages in the history of crystallography [8] that the most important characteristic of the outer symmetry of the crystals is not really the form itself but rather two phenomena expressed by two rules. One is the constancy of the angles made by the crystal faces. The other is the law of rational intercepts or the law of rational indices.

As early as 1669 the Danish crystallographer Steno made a detailed study of ideal and distorted quartz crystals (Figure 9-5). He traced their outlines on paper and found that the corresponding angles of different sections were always the same regardless of the actual sizes and shapes of the sections. Thus, all quartz crystals, however much distorted from the ideal, could result from the same fundamental mode of growth and, accordingly, corresponded to the same inner structure.

Instruments were developed to measure the angles made by the crystal faces. In 1780 the contact goniometer, Figure 9-6a, was already in usage. Later, for more precise measurement of the interfacial angles, the reflecting goniometer was introduced (Figure 9-6b).

Another interesting phenomenon observed early in crystals is their cleavage. It is characteristic that they break along well-defined planes.

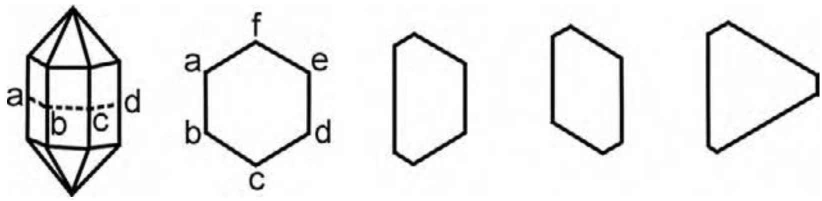

Figure 9-5. Sections of ideal and distorted quartz crystals.

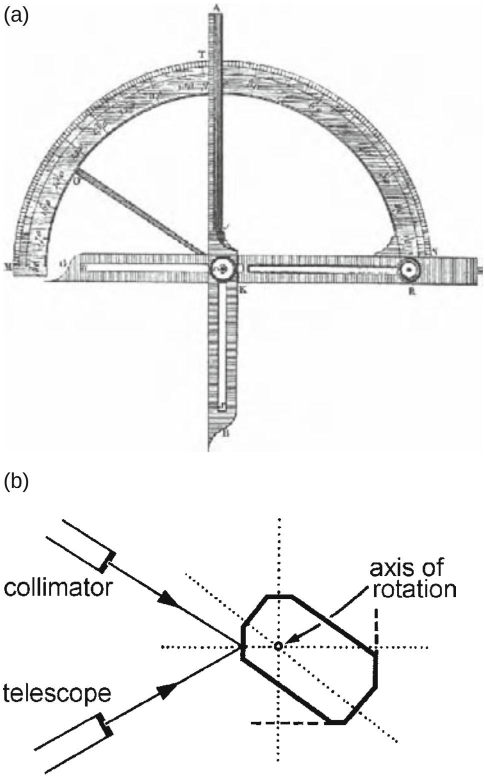

Figure 9-6. Goniometers; (**a**) Contact goniometer from Haüy [9]; (**b**) Scheme of reflecting goniometer.

Haüy noticed that the cleavage rhombs from any calcite crystal always had the same interfacial angles. Thus, he suggested that all calcite crystals could be built of these fundamental cleavage rhombs. This is illustrated in Figure 9-7 which is from Haüy's *Traité de Cristallographie* [10]. From the units shown in Figure 9-7, it is possible to build straight edges corresponding to the faces of a cube, as well as inclined edges corresponding to the faces of an octahedron. Edges inclined at other edges may also be built. Let the dimensions of the cleavage unit be a and b (Figure 9-8); then $\tan \Theta_1 = b/a$ and $\tan \Theta_2 = b/2a$, and generally $\tan\Theta = mb/na$, where m and n are rational integers. By extension into the third dimension, we may have a reference face making intercepts a, b, c on three axes. The intercepts made by any other face must be in proportion of rational multiples of these intercepts. This is called the law of rational intercepts.

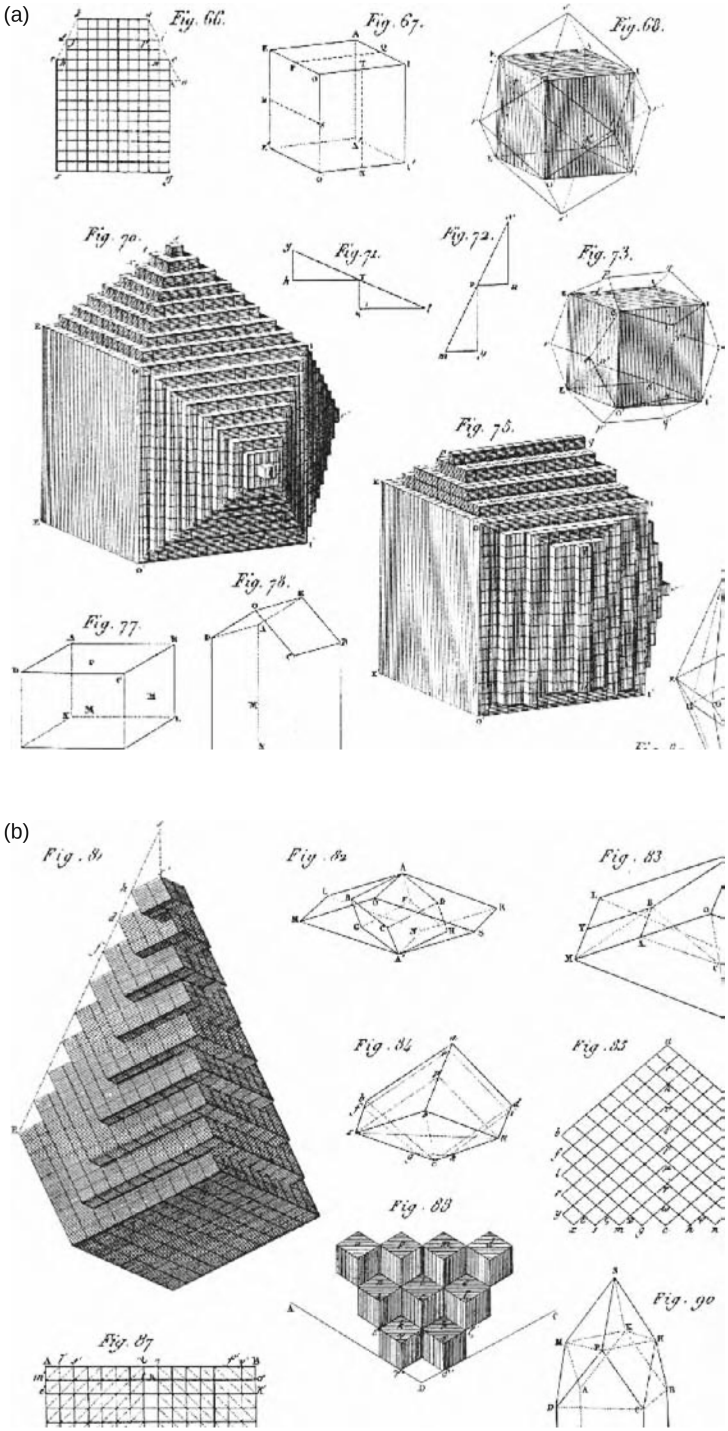

Figure 9-7. Cleavage rhombs and the stacking of cleavage rhombs from Haüy [11].

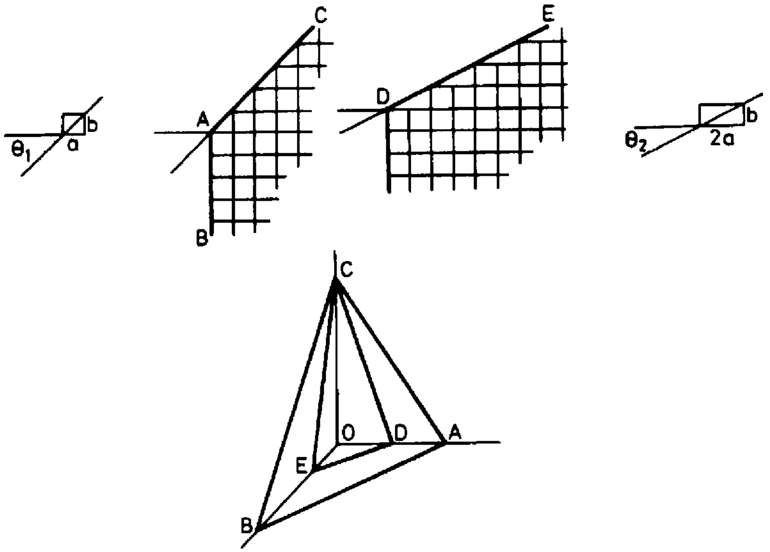

Figure 9-8. Inclined edges from cleavage units and illustration for the law of rational intercepts.

Usually the crystal faces are described by the reciprocals of the multiples of the standard intercepts, hence the name "the law of rational indices." In Figure 9-8 three lines are adopted as axes which may also be directions of the crystal edges. A reference face *ABC* makes intercepts *a*, *b*, *c* on these axes. Another face of the crystal, e.g., *DEC*, can be defined by intercepts *a*/*h*, *b*/*k*, *c*/*l*. Here *h*, *k*, *l* are simple rational numbers or zero. They are called Miller indices. The intercept is infinite if a face is parallel to an axis, and *h* or *k* or *l* will be zero. For orthogonal axes the indices of the faces of a cube are (100), (010), and (001). The indices of the face *DEC* in Figure 9-8 are (231).

The simple cleavage model of Haüy indeed revealed a lot about the structure of crystals. However, it was not generally applicable since cleavages do not always lead to cleavage forms that can necessarily fill space by repetition, and, as is known, there are only a limited number of space-filling polyhedra.

The characterization of the regularities in the outer form of the crystals has led to the recognition of three-dimensional periodicity in their inner structure. This was long before the possibility of determining the atomic arrangements in crystals by diffraction techniques had materialized.

It was 200 years before Dalton and 300 years before X-ray crystallography that Kepler discussed the atomic arrangement in crystals. In his *Strena seu de nive sexangula* he presented arrangements of close-packed spheres [12]. These are reproduced in Figure 9-9. Incidentally, close packing of spheres was invoked and illustrated in Dalton's works (Figure 9-10) in relation to gas absorption [13]. A close-packed arrangement of cannon balls expressing close packing is shown in Figure 9-11. The fundamental importance of Kepler's idea is that he correlated, for the first time, the external forms of solids with their inner structure. Kepler's search for harmonious proportions is the bridge between his epoch-making discoveries in heavenly mechanics and his less widely known but similarly seminal ideas in what is called today crystallography. As Schneer has remarked [14], the renaissance era has provided a stimulating background for the beginnings of the science of crystals.

It is to be noted that even after the discovery of Haüy's model, attention was focused on the packing in crystals. The aim was to find those arrangements in space that are consistent with the properties of the crystals.

The symmetry of the form of the crystal is a consequence of its structure. The same high symmetry of the form, however, may be easily achieved for a piece of glass by artificial mechanical intervention. By acquiring the same outer form, as is typical for a piece of diamond, the piece of glass will not acquire all the other properties

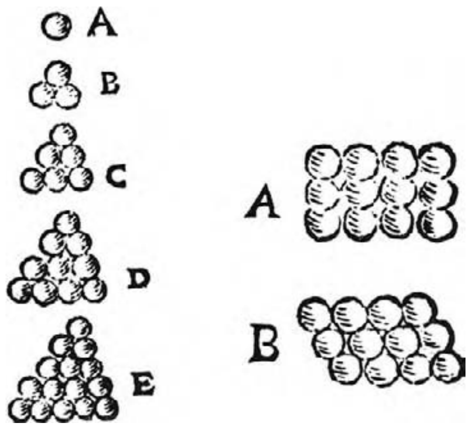

Figure 9-9. Closely packed spheres by Kepler [15].

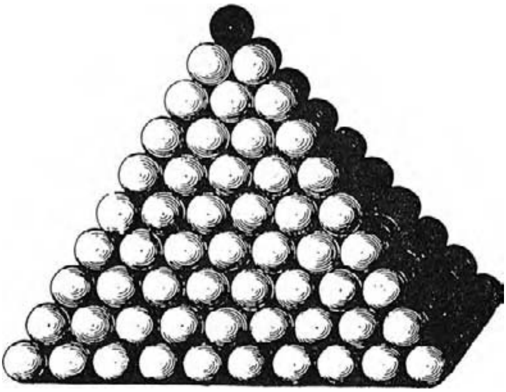

Figure 9-10. Closely packed spheres by Dalton [16].

that the diamond possesses. The difference in value has long ago been recognized. In the India of the sixth century portrayed by *Kama Sutra* of Vatsayana, one of the arts which a courtesan had to learn was mineralogy. If she were paid in precious stones, she had to be able to distinguish real crystals from paste [17].

It is primarily the structure, and, accordingly, the outer and inner symmetry properties of the crystal, that determines its many outstanding physical properties. The mechanical, electrical, magnetic, and optical properties of crystals are all in close conjunction with their symmetry properties [18].

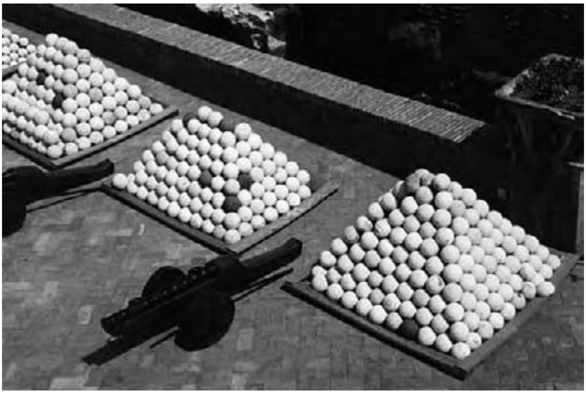

Figure 9-11. Arrangements of close packing: Cannon balls in the Castel Sant' Angelo in Rome (photograph by the authors).

In an actual crystal the atoms are in permanent motion. However, this motion is much more restricted than that in liquids, let alone gases. As the nuclei of the atoms are much smaller and heavier than the electron clouds, their motion can be well described by small vibrations about the equilibrium positions. In our discussion of crystal symmetry, as an approximation, the structures will be regarded as rigid. However, in modern crystal molecular structure determination atomic motion must be considered [19]. Both the techniques of structure determination and the interpretation of the results must include the consequences of the motion of atoms in the crystal.

9.2. The 32 Crystal Groups

Although the word crystal in its every-day usage is almost synonymous with symmetry, in classical crystallography there are severe restrictions on crystal symmetry. While there are no restrictions in principle for the number of symmetry classes of molecules, this is not so for the crystals. All crystals, as regards their form, belong to one or another of only 32 symmetry classes. They are also called the 32 *crystal point groups*. Figures 9-12 and 9-13 show them by examples of actual minerals and by stereographic projections with symmetry elements, respectively.

Stereographic projection starts by representing the crystal through a set of lines perpendicular to its faces. The introduction of this method of representation followed soon after the invention of the reflecting goniometer. Let us place the crystal in the center of a sphere and extend its face normals to meet the surface of the sphere as seen in Figure 9-14a. A set of points will occur on the surface of the sphere representing the faces of the crystal. Join now all the points in the northern hemisphere to the South Pole, and mark the points on the equatorial plane where these connecting lines intersect this plane. This will create a representation of the faces on the upper half of the crystal within a single circle as seen in Figure 9-14b. Performing a similar operation for the points of the equator (Figure 14-c) and for the points in the southern hemisphere (Figure 14-d), we arrive at the representation of the whole crystal within the circle (Figure 14-e). The points from the northern hemisphere are marked by dots, and those

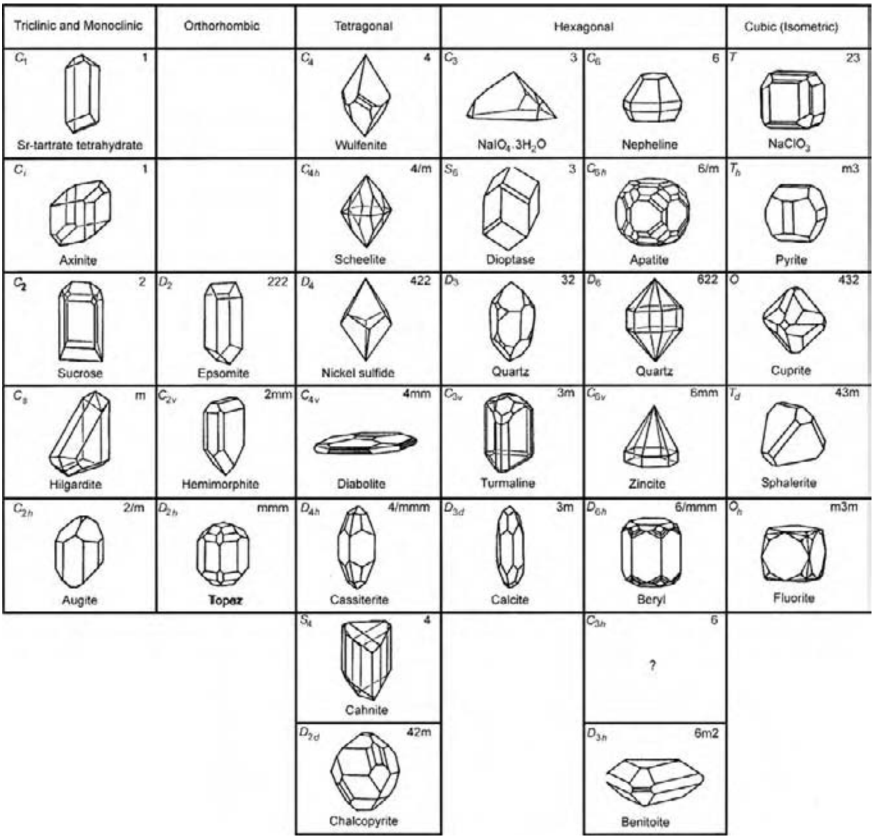

Figure 9-12. Representation of the 32 crystal point groups by actual minerals (after Buerger; Dana; and Zorky) [20].

from the southern hemisphere by small circles. Some examples for simple polyhedra are shown in Figure 9-15.

9.3. Restrictions

The restrictions we discuss in this Section are valid for classical crystallography, but are no longer so in a broader domain of science about crystals, called often generalized crystallography. Our discussion will consider the broadening meaning of crystallography with emphasis on the discovery of the so-called quasicrystals. However, it is instructive to examine the origins of the restrictions in classical crystallography. To have 32 symmetry classes for the external forms of crystals is a

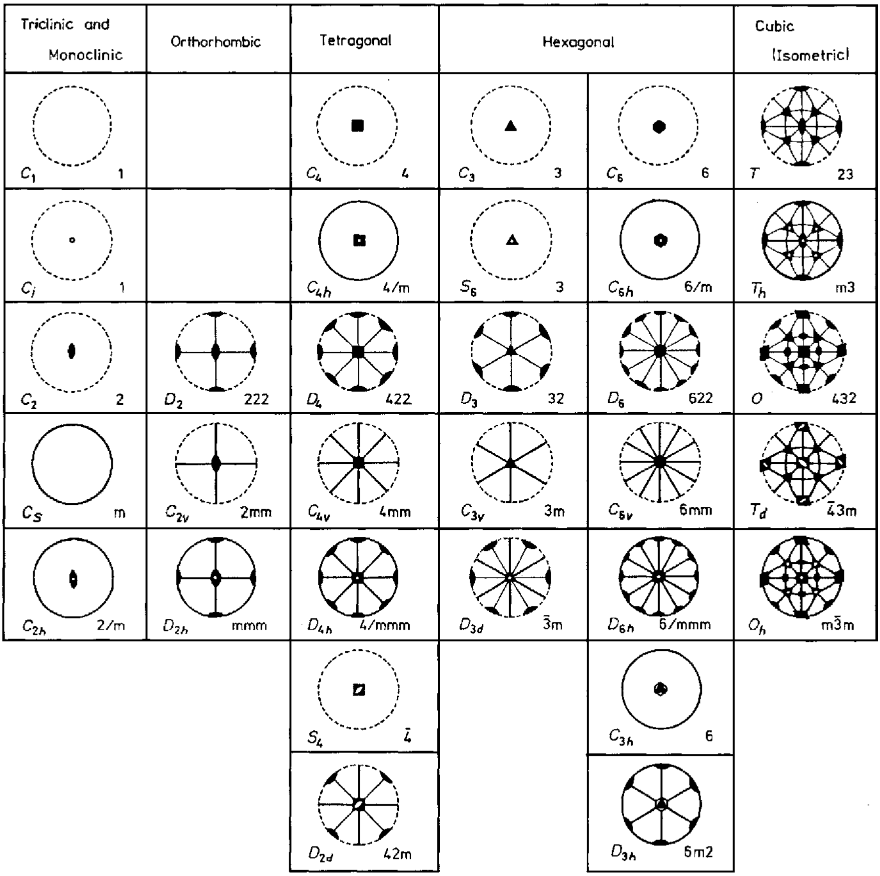

Figure 9-13. Representation of the 32 crystal point groups by stereographic projections.

definite restriction, and it is the consequence of periodicity in the inner structure. The translation periodicity limits the symmetry elements that may be present in a crystal. The most striking limitation is the absence of fivefold rotation. Consider, for example, planar networks of regular polygons (Figure 9-16). Those with threefold, fourfold, and sixfold symmetry cover the available surface without any gaps, while those with fivefold, sevenfold, and eightfold symmetry leave gaps on the surface. Figure 9-17 presents a planar network of octagons. It is evident that the regular octagons cannot cover the surface without gaps, and there are smaller squares among the octagons.

Let us examine now the possible types of symmetry axes in space groups [22]. Figure 9-18 shows a lattice row with a period *t*. An *n*-fold

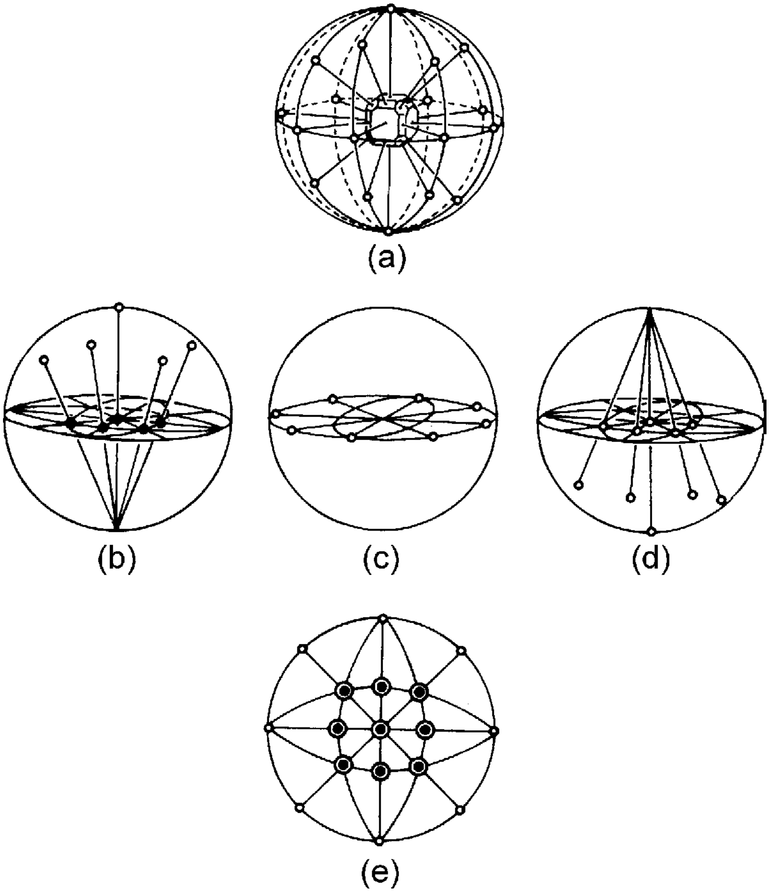

Figure 9-14. The preparation of stereographic representation.

rotation axis, C_n, is placed in each lattice point. Since n rotations, each by an angle φ, must lead to superposition, it does not matter in which direction the rotations are performed. Two rotations by φ about two axes but in opposite directions are shown in Figure 9-18. The two new lattice points produced this way are labeled p and q. These two new points are equidistant from the original row, and hence the line joining them is parallel to the original lattice row. The length of the parallel line joining p and q must be equal to some integer multiple m of the period t. Were it not, then the line joining the two new lattice points p and q would not be a translation of the lattice and the resulting array would not be periodic.

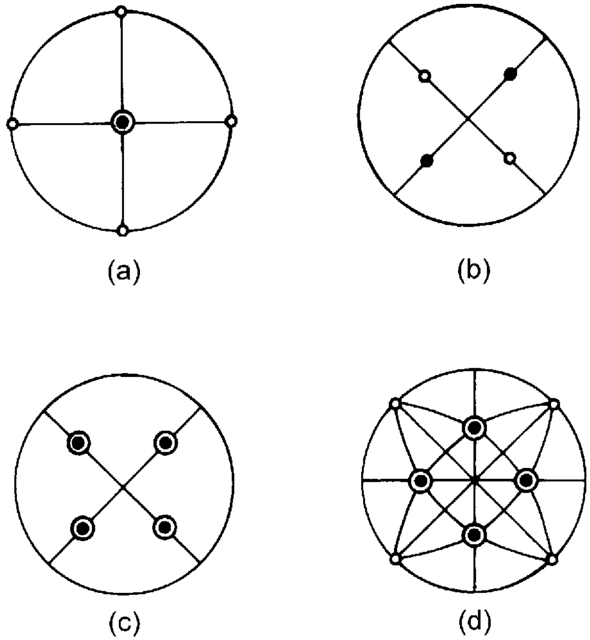

Figure 9-15. Representation of simple highly symmetrical shapes: (**a**) Cube; (**b**) Tetrahedron; (**c**) Octahedron; (**d**) Rhombic dodecahedron.

Using Figure 9-18, it is possible to determine the possible values that the rotation angle φ can have in the lattice,

$$mt = t + 2t\cos\varphi \qquad m = 0, \pm 1, \pm 2, \pm 3, \ldots$$

where $+m$ or $-m$ is taken depending on the direction of the rotation:

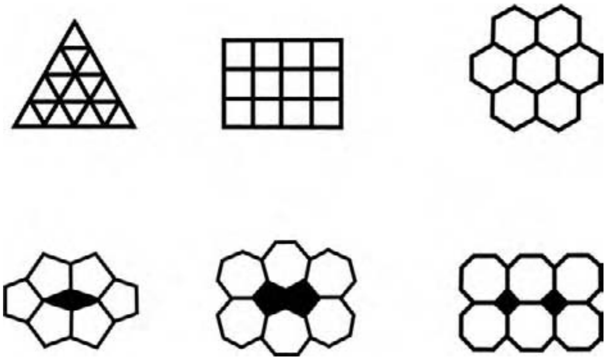

Figure 9-16. Planar networks of regular polygons with up to eight-fold symmetry.

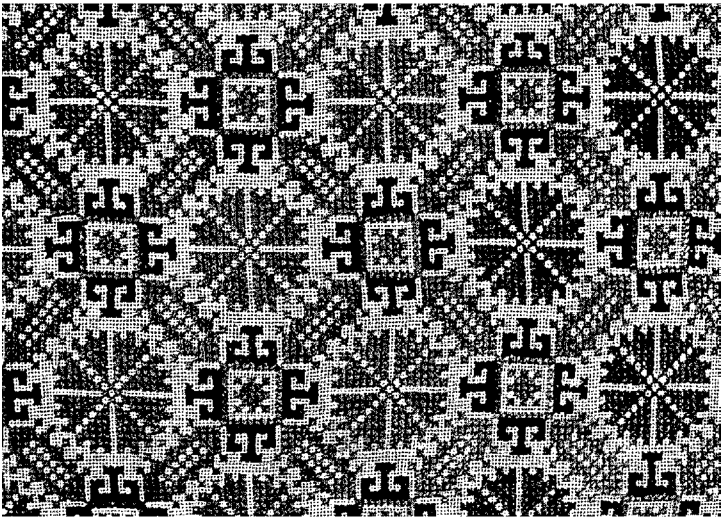

Figure 9-17. Octagonal planar network: Hungarian needlework [21].

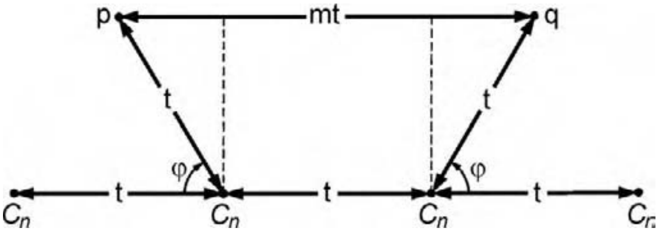

Figure 9-18. Illustration to the determination of the possible throws that rotation axes can have in space groups. After Azaroff [23]; Copyright (1960) McGraw-Hill, Inc.; used with permission.

$$\cos \varphi = \frac{m-1}{2}$$

Only the solutions corresponding to the range

$$-1 \leq \cos \varphi \leq 1$$

need be considered, and these are shown in Table 9-1. Five solutions are possible, and, accordingly, only five kinds of rotation axes are compatible with a lattice. Thus, not only fivefold symmetry is not allowed in crystal structures in classical crystallography, but all periods larger than six are impossible. Naturally, this applies to the planar networks as well.

Table 9-1. Allowed Rotation Axes *n* in a Lattice

Possible values of $m - 1$	$\cos \varphi$	$\varphi(^\circ)$	n
–2	-1	180	2
–1	$-\frac{1}{2}$	120	3
0	0	90	4
+1	$+\frac{1}{2}$	60	6
+2	+1	360 or 0	1

The permissible periods of mirror-rotation axes have the same limitations as those of the proper rotation axes.

Let us examine now the limitations on the screw axes. In a lattice the screw axes must be parallel to a translation direction. After n rotations by an angle φ and n translations by the distance T, that is, after n translations along the screw axis, the total amount of translation distance in the direction of this axis must be equal to some multiple of the lattice translation mt,

$$nT = mt$$

where n and m are integers. Rearranging this equation,

$$T = \frac{mt}{n},$$

where m, of course, may be 0, 1, 2, 3, etc., but n may only be 1, 2, 3, 4, or 6. It is then possible to determine the permissible values of the pitch of the screw axes in lattices. They are summarized in Table 9-2, taking also into consideration that $(3/2)t = t + (1/2)t$, $(5/4)t = t + (1/4)t$, etc. There are only eleven screw axes that are allowed in a lattice, n_m, according to Table 9-2. The subscript in the notation is the m of the expression $T = (mt)/n$. The proper rotation axes may be considered to be special cases of the screw axes, with $m = 0$ and $m = n$. The 11 screw axes are shown in perspective in Figure 9-19. It is seen there that some pairs are identical except for the direction of the screw motion. Such screw axes are enantiomorphous. The enantiomorphous screw axis pairs are the following:

3_1 and 3_2

4_1 and 4_3

6_1 and 6_5

6_2 and 6_4.

Table 9-2. Possible Values of the Pitch T of an n-Fold Screw Axis

A. Possible values of T								
$n = 1$	$0t$,	$1t$,	$2t, \ldots$					
$n = 2$	$0t$,	$(1/2)t$,	$(2/2)t$,	$(3/2)t, \ldots$				
$n = 3$	$0t$,	$(1/3)t$,	$(2/3)t$,	$(3/3)t$,	$(4/3)t, \ldots$			
$n = 4$	$0t$,	$(1/4)t$,	$(2/4)t$,	$(3/4)t$,	$(4/4)t$,	$(5/4)t, \ldots$		
$n = 6$	$0t$,	$(1/6)t$,	$(2/6)t$,	$(3/6)t$,	$(4/6)t$,	$(5/6)t$,	$(6/6)t$,	$(7/6)t, \ldots$
B. Possible values of T (redundancies eliminated)								
$n = 1$								
$n = 2$		$(1/2)t$,						
$n = 3$		$(1/3)t$,	$(2/3)t$					
$n = 4$		$(1/4)t$,	$(2/4)t$,	$(3/4)t$				
$n = 6$		$(1/6)t$,	$(2/6)t$,	$(3/6)t$,	$(4/6)t$,	$(5/6)t$		
C. Notation of screw axes in a lattice								
$n = 2$		2_1						
$n = 3$		3_1	3_2					
$n = 4$		4_1	4_2	4_3				
$n = 6$		6_1	6_2	6_3	6_4	6_5		

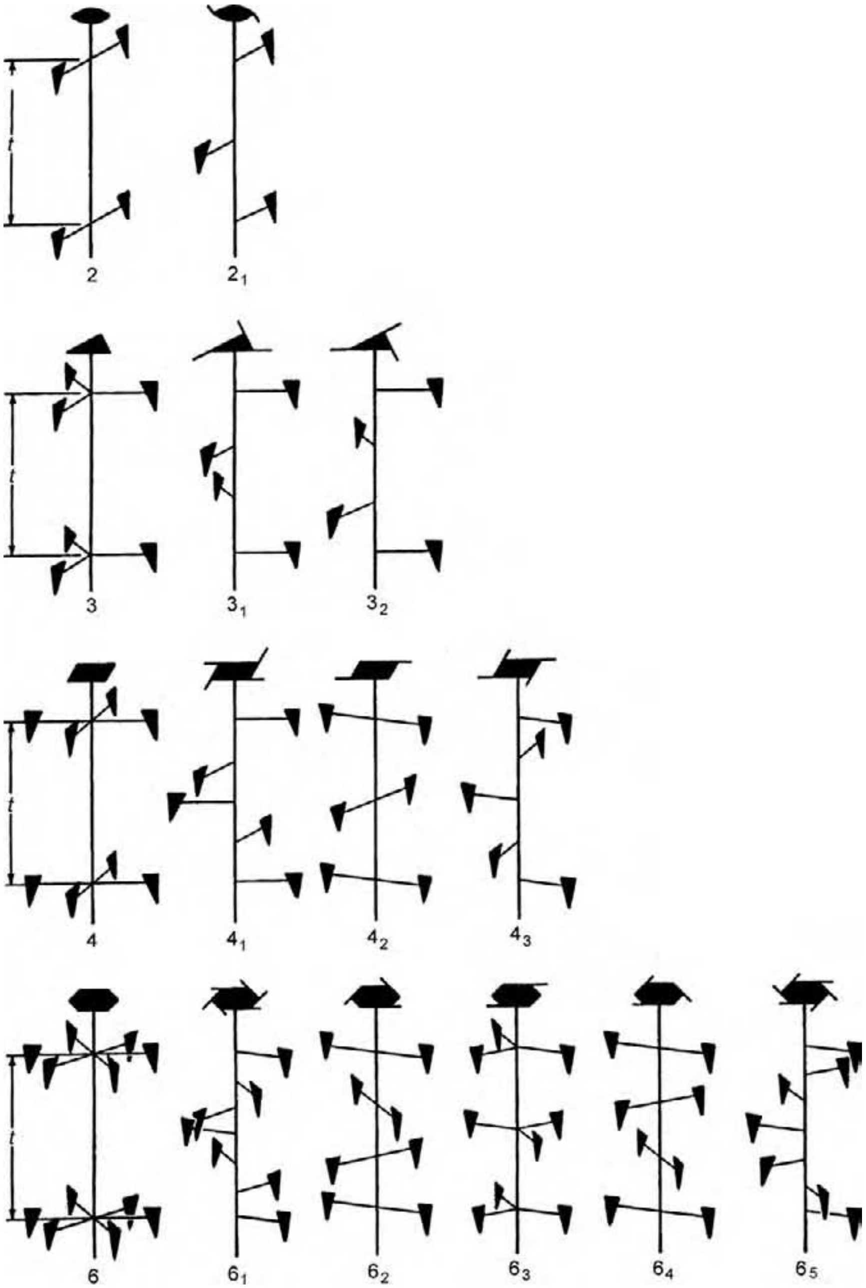

Figure 9-19. The eleven screw axes. The simple twofold, threefold, fourfold and sixfold axes are also shown for completeness. After Azaroff [24]; copyright (1960) McGraw-Hill, Inc.; used with permission.

Table 9-3. Possible Glide Planes

Glide type	Symbol	Translation component
Axial	a	$a/2$
Axial	b	$b/2$
Axial	c	$c/2$
Diagonal	n	$a/2 + b/2$; $b/2 + c/2$; or $c/2 + a/2$
Diamond[a]	d	$a/4 + b/4$; $b/4 + c/4$; or $c/4 + a/4$

[a]Translation component is one-half of the true translation along the face diagonal of a centered plane lattice.

Finally, the only remaining symmetry element is considered, the glide-reflection plane. It causes glide reflection as a result of reflection *and* translation. The translation component T of a glide plane is one-half of the normal translation of the lattice in the direction of the glide. A glide along the a axis is $T = (1/2)a$ and this is called an a glide. Similarly, a diagonal glide can have $T = (1/2)a + (1/2)c$. The different possible glides are summarized in Table 9-3.

The fact that the crystal has a lattice framework imposes strict limitations on the symmetry of its outer form. On the other hand, the question arises as to whether it is possible to derive any information about the crystal lattice from the knowledge of the symmetry of its outer form.

The 32 crystal point groups can be classified by symmetry criteria. They are usually grouped according to the highest ranking rotation axis that they contain. The resulting groups are called crystal systems. There are altogether seven of them and they are listed in Table 9-4. The crystal point groups have to be combined with all possible space lattices in order to produce the space groups.

9.4. The 230 Space Groups

There are 14 infinite lattices, called Bravais lattices, in three-dimensional space. They are shown in Figure 9-20. These lattices are the analogs of the five infinite lattices in two-dimensional space (Figure 8-28). The Bravais lattices are presented as systems of points at vertices of parallelepipeds. The corresponding parallelepipeds are capable of filling space without gaps or overlap. The representation of the lattices by systems of points is especially useful as it makes it possible to join the lattice points in any desired way conforming

Table 9-4. Characterization of Crystal Systems

System	Minimal symmetry (diagnostic symmetry elements)	Relations between edges and angles of unit cell	Lattice type	Numbering in Figure 20
Triclinic	1 (or $\bar{1}$)	$a \neq b \neq c$ $\alpha \neq \beta \neq \gamma \neq 90^\circ$	*P*	1
Monoclinic	2 (or $\bar{2}$)	$a \neq b \neq c$ $\alpha = \gamma = 90^\circ \neq \beta$	*P* *C* (or *A*)	2 3
Orthorhombic	222 (or $\overline{222}$)	$a \neq b \neq c$ $\alpha = \beta = \gamma = 90^\circ$	*P* *C*(or *B* or *A*) *I* *F*	4 5 6 7
Trigonal (rhombohedral)	3 ($\bar{3}$)	$a = b = c$ $\alpha = \beta = \gamma \neq 90^\circ$	*R*	8
Hexagonal	6 ($\bar{6}$)	$a = b \neq c$ $\alpha = \beta = 90^\circ,\ \gamma = 120^\circ$	*P*	9
Tetragonal	4 (or $\bar{4}$)	$a = b \neq c$ $\alpha = \beta = \gamma = 90^\circ$	*P* *I*	10 11
Cubic	Four 3 (or $\bar{3}$)	$a = b = c$ $\alpha = \beta = \gamma = 90^\circ$	*P* *I* *F*	12 13 14

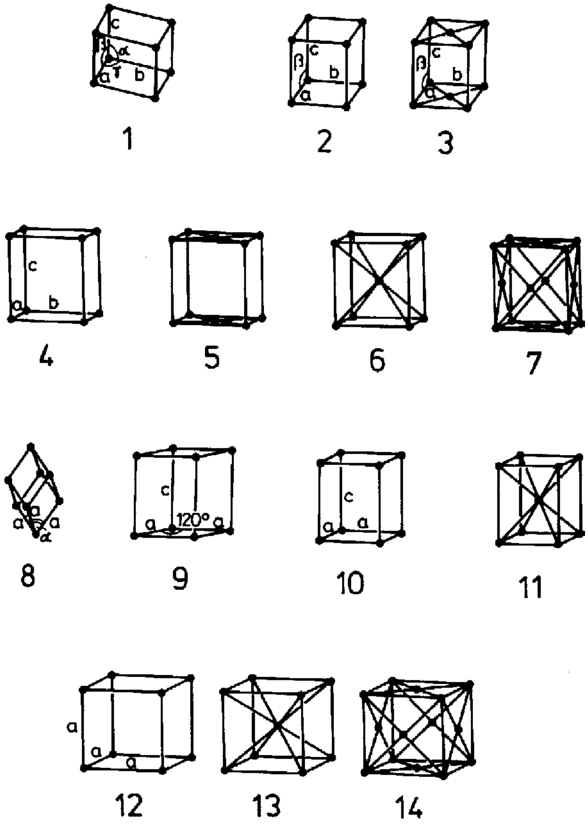

Figure 9-20. The 14 Bravais lattices.

with the symmetry requirements. In this way, not only the original parallelepipedal forms but any other possible figures may be used as building units for the space lattice.

The 14 Bravais lattices are enumerated in Table 9-4 as the following types: primitive (*P*, *R*), side-centered (*C*), face-centered (*F*), and body-centered (*I*). The numbering of the Bravais lattices in Table 9-4 corresponds to that in Figure 9-20. The lattice parameters are also enumerated in the table. In addition, the distribution of lattice types among the crystal systems is shown.

The actual infinite lattices are obtained by parallel translations of the Bravais lattices as unit cells. Some Bravais cells are also primitive cells, others are not. For example, the body-centered cube is a unit cell but not a primitive cell. The primitive cell in this case is an oblique parallelepiped constructed by using as edges the three directed

segments connecting the body center with three nonadjacent vertices of the cube.

The three-dimensional space groups are produced by combining the 32 crystallographic point groups with the Bravais lattices. Since the symmetry elements in a space lattice can have translation components, indeed not only the 32 groups but also the analogous groups, which have screw axes and glide planes, have to be considered. There are altogether 230 three-dimensional space groups! Their complete description can be found in Volume A of the *International Tables for Crystallography* [25]. Only a few examples are discussed here.

There are only two combinations possible for the triclinic system. They are named $P1$ and $P\bar{1}$. For the monoclinic system three point groups are to be considered and two lattice types. Combining P and I lattices, on one hand, and point group 2 and symmetry 2_1 on the other hand, the four possible combinations are $P2$, $P2_1$, $I2$, and $I2_1$. The latter two, however, are equivalent; only their origins differ.

The description of the symmetry elements of the space groups is similar to that of the point groups [26]. The main difference is that the order by which the symmetry elements of the space groups are listed may be of great importance, except for the triclinic system. The order of the symmetry elements expresses their relative orientation in space with respect to the three crystallographic axes. For the monoclinic system, the unique axis may be the *c* or the *b* axis. For the $P2$ space group, the complete symbol may be $P112$ or $P121$. The ordering of symbols for the orthorhombic system is especially important. The symmetry elements are usually listed in the order *abc*. The space groups which belong to the crystal class 2*mm* are properly presented as *Pmm*2, *c* being the unique axis.

In the tetragonal system, the *c* axis is the fourfold axis. The sequence for listing the symmetry elements is *c*, *a*, [110], since the two crystallographic axes orthogonal to *c* are equivalent. For example, the three-dimensional space group notation $P\bar{4}m2$ has the following meaning: the unique axis in a primitive tetragonal lattice is a $\bar{4}$ axis, the two *a* $\bar{4}$ axes are parallel to *m*, and the [110] direction has twofold symmetry. A similar sequence is used for listing the symmetry elements of the hexagonal system, for which the *c* axis again is the unique axis and the other two are equivalent. *P* denotes the primitive hexagonal lattice while *R* denotes the centered hexagonal lattice in which the primitive rhombohedral cell is chosen as the unit cell.

All three crystallographic axes are equivalent in the cubic system. The order of listing the symmetry elements is *a*, [111], [110]. When the number 3 appears in the second position, it merely serves to distinguish the cubic system from the hexagonal one.

It may be of interest to add some new symmetry to a group or to decrease its symmetry and examine the consequences. If the addition produces a new group, it is called a supergroup of the original group. If eliminating symmetry leads to a new group, it is usually a subgroup of the original one. For example, the point group 1 is obviously a subgroup of all the other 31 groups as it has the lowest possible symmetry. On the other hand, the highest symmetry cubic group can have no supergroups.

It is important to distinguish between the symmetry of the lattice and the symmetry of the actual building elements of the crystal—the atoms, ions, or molecules. In the illustration of Figure 9-21 the lattice positions are occupied by spheres which have the highest possible symmetry, while there is no discernible symmetry of the lattice. However, the building elements have usually lower symmetries, especially in molecular crystals. There is a common misconception about the difference between the crystal and its lattice. A crystal is an array of units (atoms, ions, or molecules) in which a structural motif is repeated in three dimensions. A lattice is an array of points, and every point has the same environment of points in the same orientation. Each crystal has an associated lattice, whose origin and basis vectors can be chosen in various ways. Accordingly, for example, it

Figure 9-21. Artistic expression of atomic arrangement in an extended structure. Sculpture *Cosmonergy* by Kawan-Mo Chung in downtown Seoul (photograph by the authors).

would be improper to speak about "interpenetrating lattices," while it is correct to talk about interpenetrating arrays of atoms [27].

The system of the 230 three-dimensional space groups was established a long time ago, well before X-ray diffraction could have been applied to the determination of crystal structure. These 230 three-dimensional space groups were derived in their entirety by Fedorov, Schoenflies, and Barlow working independently at the end of the 19th century, and it will always be considered a great scientific feat. The amateur Barlow considered oriented motifs; his method was hanging pairs of gloves on a rack to make space group models. It was a truly empirical approach. "He bought gloves by the gross, so the story goes, mystifying the sales lady by answering 'I don't care' to her first question, 'What size sir?' " [28].

An interesting statistical test was performed concerning the total number of three-dimensional space groups some time in the mid-1960s [29]. It was a uniquely appropriate point in the history of crystallography for such a test: Already a large number of crystal structures had been determined, but examples of all the space groups had not yet been found among the actual crystals. The total number of three-dimensional space groups had long before been firmly established. Thus, the test was considered as much to be a check of the applied statistical method as to be a source of crystallographic information. Although there are 230 space groups, not all of them are in practice distinguishable. So 11 enantiomorphous groups were excluded from the count as were two more groups for other reasons. Thus, the number of space groups to be considered was 217. The 3782 crystal structures that were reviewed showed a wide variation in the frequency of occurrence of the different space groups. One group occurred 355 times, while 33 groups occurred only once each. It was also interesting that only 178 groups out of the total of 217 occurred. Based on the available data of the distribution of the space groups among the determined structures, the findings were extrapolated to an indefinitely large sample. The statistical test led to an extrapolated value of 216. The estimated accuracy of the procedure was 2%. Thus, the estimate agreed with the accepted value of the total number of the practically distinguishable space groups of 217.

The statistical analysis has also been applied separately to the data on inorganic and organic crystals. In both cases the extrapolated estimate for the total number of three-dimensional space groups was smaller than when all data had been considered together. The total

numbers estimated for the inorganic and organic structures were 209 and 185, respectively. Thus the conclusion could be made that the inorganic and organic crystals belong to space groups with different population distributions. Statistical analysis of population distributions among the three-dimensional space groups, according to various criteria, has remained an important research tool [30].

In the following section, we will look in some more detail at the symmetry systems of two fundamentally important crystals, rock salt and diamond, following the descriptions by Shubnikov and Koptsik [31]. The descriptions will be far from complete; they will aim at giving some flavor for the characterization of these two highly symmetrical structures.

9.4.1. Rock Salt and Diamond

The unit cell of the rock salt structure and the projection of this structure along the edges of the unit cell onto a horizontal plane are shown in Figure 9-22a and b. The equivalent ions are related by translations $a = b = c$ along the edges of the cube, or $(a + b)/2$, $(a + c)/2$, $(b + c)/2$ along the face diagonals. All this corresponds to the face-centered cubic group (F). The structure coincides with itself not only after these translations, but also after the operations of the point group $m\bar{3}m$ (or in other notation $\tilde{6}/4$). The point-group symmetry elements are shown also in Figure 9-22c. The symmetry elements of this group intersect at the centers of all ions and thus they become symmetry elements for the whole unit cell and, accordingly, for the whole crystal.

Among the projected symmetry elements in Figure 9-22c, there are some which are derived from the generating elements. This is the case, for example, for vertical glide-reflection planes with elementary translations $a/2$ and $b/2$ (represented by broken lines), translations (dot-dash lines), vertical screw axes 2_1 and 4_2, and symmetry centers (small hollow circles, some of which lie above the plane by 1/4 of the elementary translation).

Two very simple descriptions of the rock salt crystal structure are also given. According to one, the sodium and chloride ions occupy positions with point-group symmetry $m\bar{3}m$ forming a checkered pattern in the $Fm\bar{3}m$ space group. According to the other description, the structure consists of two cubic sublattices in parallel orientation, one of sodium ions and the other of chloride ions.

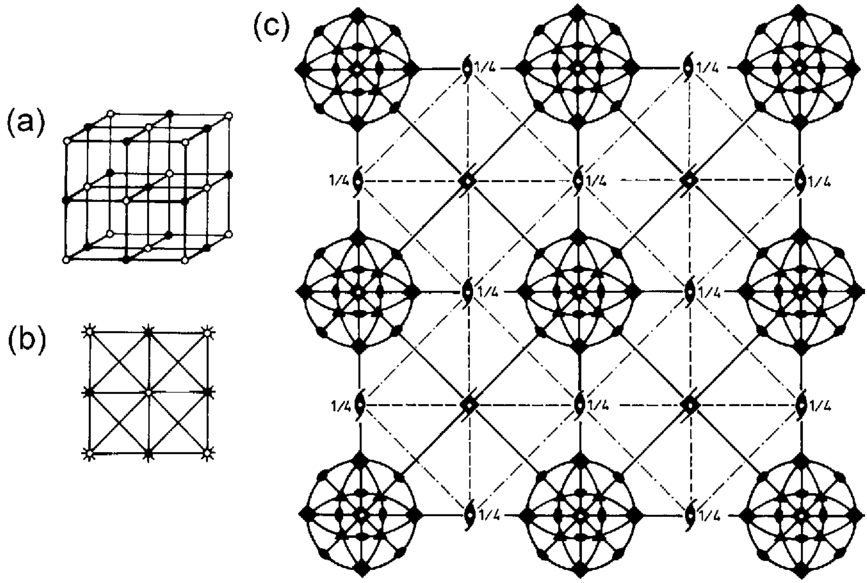

Figure 9-22. The crystal structure of the rock salt after Shubnikov and Koptsik [32]. (**a**) A unit cell; (**b**) Projection of the structure along the edges of the unit cell onto a horizontal plane; (**c**) Projection of some symmetry elements of the $Fm\bar{3}m$ space group onto the same plane. The vertical screw axes 2_1 and 4_2 are marked by their respective symbols. Used with permission.

Figure 9-23 illustrates the diamond structure. It can be regarded as a set of two face-centered cubic sublattices displaced relative to each other by 1/4 of the body diagonal of the cube. Each of the two sublattices has the $F\bar{4}3m$ space group, and in addition there are some operations transforming one to the other. The complete diamond structure has the space group $Fd\bar{3}m$, where "d" stands for a "diamond" plane.

Among the projected symmetry elements in Figure 9-23c, there are again some which are produced by the generating elements. Special for the diamond structure are the symmetry elements which connect the two subgroups $F\bar{4}3m$. They include vertical left-handed and right-handed screw axes, 4_1 and 4_3, respectively, symmetry centers (small hollow circles, 1/8 and 3/8 of the elementary translation c above the plane), vertical "diamond" glide-reflection planes d represented by dot-dash lines with arrows, and similar systems of connecting elements in the horizontal directions.

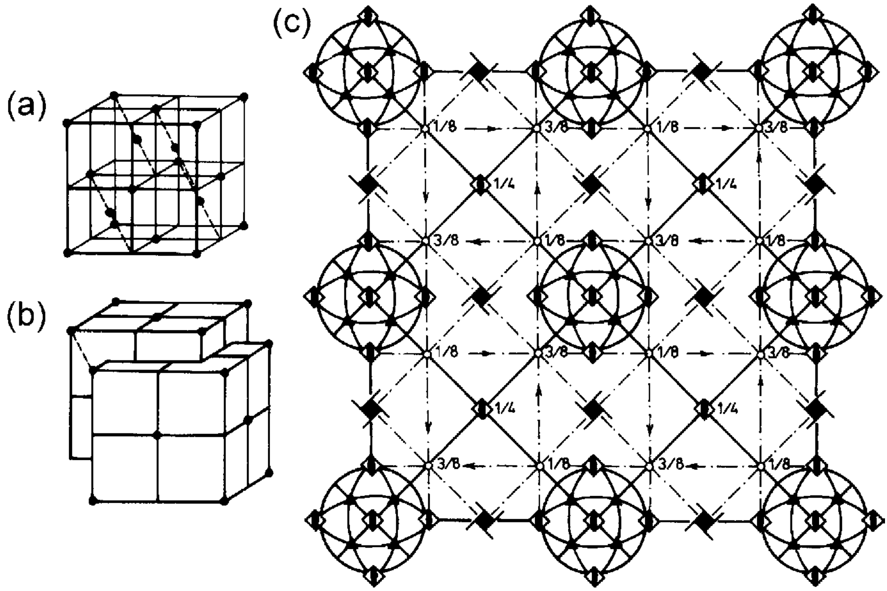

Figure 9-23. The diamond structure after Shubnikov and Koptsik [33]. (**a**) A unit cell; the edges of the cube are the *a*, *b*, and *c* axes; (**b**) Two face-centered cubic sublattices displaced along the body diagonal of the cube; (**c**) Projection of some symmetry elements of the $Fd\bar{3}m$ space group onto a horizontal plane. The vertical screw axes 4_1 and 4_3 are marked by appropriate symbols. Used with permission.

The subgroup $F\bar{4}3m$ is common both to the rock salt space group $Fm\bar{3}m$ and to the diamond space group $Fd\bar{3}m$. The space group $Fd\bar{3}m$ is obtained from $Fm\bar{3}m$ by replacing the symmetry planes *m* by glide-reflection planes *d* with the latter displaced 1/8 along the cube edges.

9.5. Dense Packing

Dalton [34] envisaged the structural difference between water and ice in packing properties. Figure 9-24 reproduces a drawing from his 1808 book *A New System of Chemical Philosophy*. According to Dalton, the "atoms" of ice arrange themselves in a hexagonal scheme, while the "atoms" of water do not. In any case it is remarkable that the principal difference between the water and ice structures is expressed in packing density. Figure 9-25 originates from a different age and shows the atomic and molecular arrangements in the crystals of 2Zn-insulin from the work of Dorothy Hodgkin and her associates [35]. The

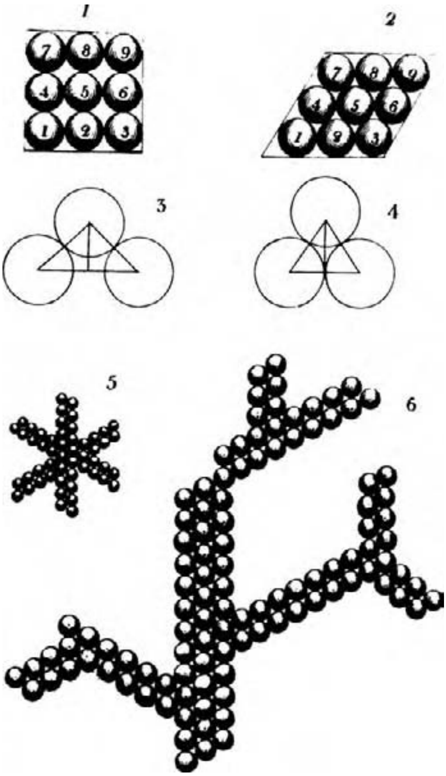

Figure 9-24. Dalton's models for water (1 and 3) and ice (2 and 4–6) [36].

molecular structure of insulin is extremely complicated but the molecular packing, especially the arrangement of the insulin hexamers, reminds us of Dalton's hexagonal ice.

The symmetry of the crystal structure is a direct consequence of dense packing. The densest packing is when each building element makes the maximum number of contacts in the structure. First, the packing of equal spheres in atomic and ionic systems will be discussed. Then molecular packing will be considered. Only characteristic features and examples will be dealt with here, following Kitaigorodskii [38].*

*A. I. Kitaigorodskii's name appears in two versions in this book and even more in the literature. The rules of transliterations from the original Russian suggest Kitaigorodskii, but his name was transliterated on many of his publications as Kitaigorodsky.

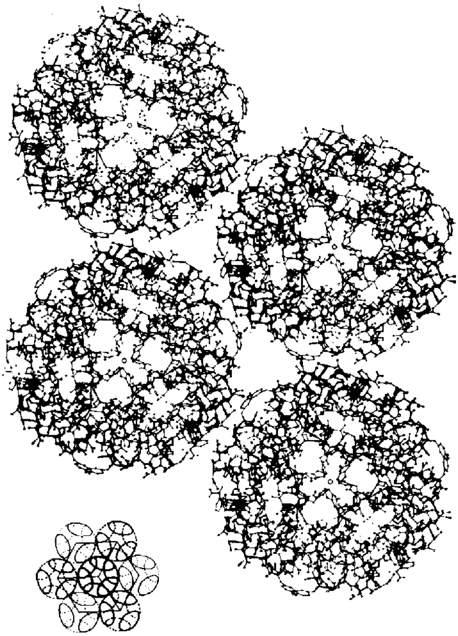

Figure 9-25. Atomic arrangement in the 2Zn-insulin crystal. The smaller projection drawing shows the molecular packing in the insulin hexameters. Courtesy of Dorothy Hodgkin [37].

9.5.1. Sphere Packing

The most efficient packing results in the greatest possible density. The density is the fraction of the total space occupied by the packing units. Only those modes of packing are considered here in which each sphere is in contact with at least six neighbors. The densities of some packings are given in Table 9-5. There are stable arrangements with

Table 9-5. Densities of Sphere Packing[a]

Coordination number	Name of packing	Density
6	Simple cubic	0.5236
8	Simple hexagonal	0.6046
8	Body-centered cubic	0.6802
10	Body-centered tetragonal	0.6981
12	Closest packing	0.7405

[a] After A. F. Wells, *Structural Inorganic Chemistry*, 5th Edition, Clarendon Press, Oxford, 1984.

smaller numbers of neighbors, meaning lower coordination numbers, when directed bonds are present. In our discussion, however, the existence of chemical bonds is not a prerequisite at all.

For three-dimensional six-coordination, the most symmetrical packing is when the spheres are at the points of a simple cubic lattice (Figure 9-26a). Each sphere is in contact with six others situated at the vertices of an octahedron. In order to increase clarity, the atoms are shown separated in the figure. The packing is more realistically represented when the spheres touch each other. Already Kepler (Figure 9-9), and later Dalton (Figures 9-10, 9-24), employed such representations.

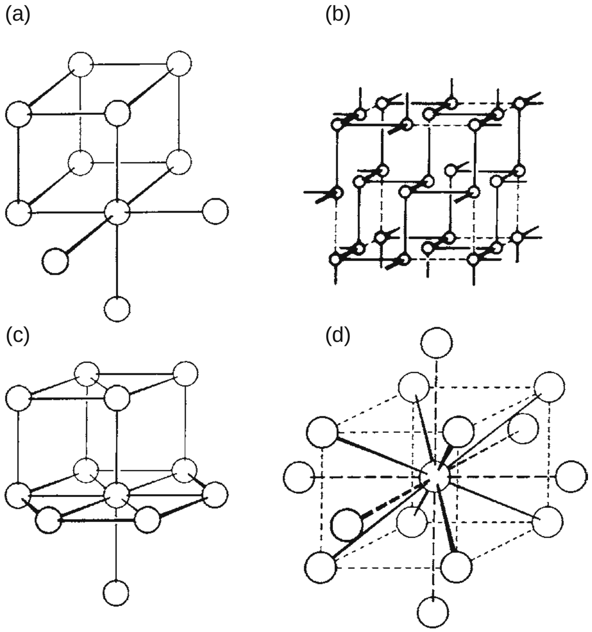

Figure 9-26. Examples of sphere packing after Wells [39]. Reproduced with permission. (**a**) Simple cubic; (**b**) The somewhat distorted cubic packing of arsenic; (**c**) Simple hexagonal; (**d**) Body-centered cubic.

The structure of crystalline arsenic provides an example of somewhat distorted simple cubic packing. It is illustrated in Figure 9-26b. The atoms are in the positions of the cubic structure. Each has three nearest and three more distant neighbors. The layers formed by the nearest bonded atoms may also be derived from a plane of hexagons. These layers buckle as the bond angle decreases from 120°.

The simple hexagonal sphere packing is shown in Figure 9-26c. The coordination number is eight. It is not very important for crystal structures. Figure 9-26d shows the body-centered packing with 8-coordination. For the central atom the six next nearest neighbors are at the centers of neighboring unit cells. In terms of polyhedral domains, a truncated octahedron is adopted here. The central atom, in fact, has a coordination number of 14.

It may often be convenient to describe the crystal structure in terms of the domains of the atoms [40]. The domain is the polyhedron enclosed by planes drawn midway between the atom and each neighbor, these planes being perpendicular to the lines connecting the atoms. The number of faces of the polyhedral domain is the coordination number of the atom and the whole structure is a space-filling arrangement of such polyhedra.

The closest packing of equal circles on a plane surface has already been considered. The closest packing of spheres on a plane surface poses a similar problem. Again, the densest arrangement is when a sphere is in contact with six others. Layers of spheres may then be superimposed in various ways. The closest packing is when each sphere touches three others in each adjacent layer, the total number of contacts then being 12. Closest packing is thus based on closest packed layers. Figure 9-27 illustrates this. The spheres in one layer are

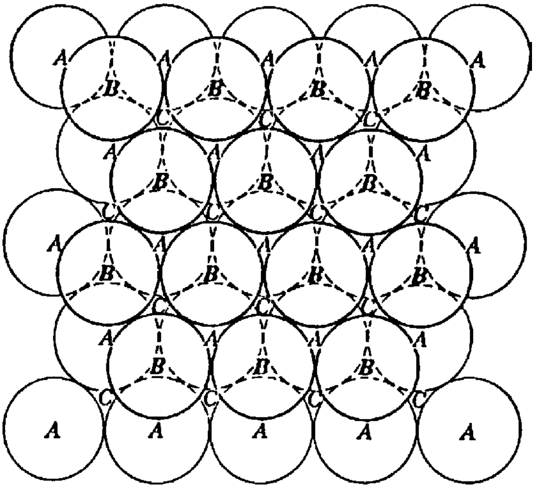

Figure 9-27. Closest packing of ABC layers after Wells [41]. Reproduced with permission.

labeled *A*, and a similar layer can be placed above the first so that the centers of the spheres in the upper layer are vertically above the positions *B* (or *C*). The third layer can be placed in two ways. The centers of the spheres may lie above either the *C* or the *A* positions. The two simplest sequences of layers are then *ABABAB* ... and *ABCABC* ... They will have the same density (0.7405).

The packing based on the sequence *ABABAB*... is called hexagonal closest packing and is illustrated by Figure 9-28a. Each sphere has 12 neighbors situated at the vertices of a coordination polyhedron. The packing based on the sequence *ABCABC*... is called cubic closest packing. It is illustrated in Figure 9-28b, and is characterized by cubic symmetry.

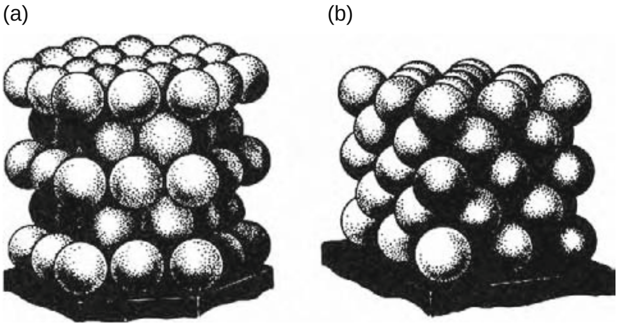

Figure 9-28. Close packing of spheres after Shubnikov and Koptsik [42]. (**a**) Hexagonal closest packing; (**b**) Cubic closest packing. Used with permission.

The closest packing of equal spheres is achieved in an arrangement in which each sphere touches three others in each adjacent layer. The total number of neighbors is then 12. Although the packing in any layer is evidently the densest possible packing, this is not necessarily true of the space-filling arrangements resulting from stacking such layers. Thus, consider the addition of a fourth sphere to the most closely packed triangular arrangement [43]. The maximum number of contacts is three in the emerging tetrahedral group. The space-filling arrangement would require each tetrahedron to have faces common with four other tetrahedra. However, regular tetrahedra are not suitable to fill space without gaps or overlaps because the angle of the tetrahedron, $70^{\circ}32'$, is not an exact submultiple of 360°.

Alternatively, continue placing spheres around a central one, all spheres having the same radius. The maximum number that can be

placed in contact with the first sphere is 12. However, there is a little more room around the central sphere than just for 12, but not enough for a 13th sphere. Because of the extra room there is an infinite number of ways of arranging the 12 spheres [44].

The question of densest packing of spheres has been an intriguing problem in mathematics for centuries; it has been labeled “one of the oldest math problems in the world” [45].

9.5.2. Icosahedral Packing

The most symmetrical arrangement is to place the 12 spheres at the vertices of a regular icosahedron, which is the only regular polyhedron with 12 vertices. Thus, the icosahedral packing is the most symmetrical. However, it is not the densest packing. Also, it is not a crystallographic packing in terms of classical crystallography. When icosahedra are packed together they will not form a plane, but will gradually curve up and will eventually form a closed system as is illustrated in Figure 9-29 [46].

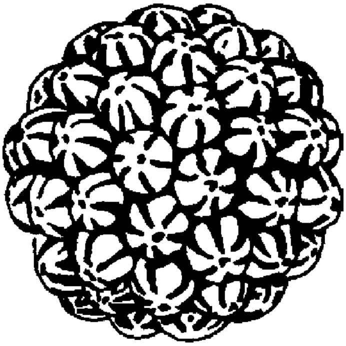

Figure 9-29. Icosahedral polyoma virus drawn after Adolph et al. [47].

Buckminster Fuller recognized early the importance of icosahedral construction and its great stability in geodesic shapes as well as in viruses. He may have not had the rigorous scientific bases about nucleic acids and about the viruses, but had a fertile imagination and connected seemingly distant pieces of information about structures. This is what he wrote [48]:

> This simple formula governing the rate at which balls are agglomerated around other balls or shells

> in closest packing is an elegant manifest of the reliably incisive transactions, formings, and transformings of Universe. I made that discovery in the late 1930s and published it in 1944. The molecular biologists have confirmed and developed my formula by virtue of which we can predict the number of nodes in the external protein shells of all the viruses, within which shells are housed the DNA-RNA-programmed design controls of all the biological species and of all the individuals within those species. Although the polio virus is quite different from the common cold virus, and both are different from other viruses, all of them employ frequency to the second power times ten plus two in producing those most powerful structural enclosures of all the biological regeneration of life. It is the structural power of these geodesic-sphere shells that makes so lethal those viruses unfriendly to man. They are almost indestructible.

Indeed, the discoverers of virus structures, Donald Caspar and Aaron Klug stated that

> the solution we have found ... was, in fact, inspired by the geometrical principles applied by Buckminster Fuller in the construction of geodesic domes ... The resemblance of the design of geodesic domes ... to icosahedral viruses had attracted our attention at the time of the poliovirus work ... Fuller has pioneered in the development of a physically orientated geometry based on the principles of efficient design [49].

The length of an edge of a regular icosahedron is some 5% greater than the distance from the center to vertex. Thus, the sphere of the outer shell of 12 makes contact only with the central sphere. Conversely, if each sphere of an icosahedral group of 12, all touching the central sphere, is in contact with its 5 neighbors, then the central sphere must have a radius of some 10% smaller than the radius of the outer spheres. The relative size considerations are important in the

structures of free molecules as well if the central atom or group of atoms is surrounded by 12 ligands [50].

An interesting case, and a step forward from the isolated molecule towards more extended systems is when an icosahedron of 12 spheres about a central sphere is surrounded by a second icosahedral shell exactly twice the size of the first [51]. This shell will contain 42 spheres and will lie over the first so that spheres will be in contact along the fivefold axes. Further layers can be added in the same fashion. The third layer is shown in Figure 9-30, and this is what is known as the Mackay icosahedron. It is an example of icosahedral packing of equal spheres. The layers of spheres succeed each other in cubic close packing sequence on each triangular face. Each sphere which is not on an edge or vertex touches only six neighbors, three above and three below. Each such sphere is separated by a distance of 5% of its radius from its neighbors in the plane of the face of the icosahedron. The whole assembly can be distorted to cubic close packing in the form of a cuboctahedron. This distortion may be envisaged as a reversible process by the kind of transformation discussed earlier. The Mackay icosahedron has “made tremendous impact on particle, cluster, intermetallics, and quasicrystal researchers. . .” [52].

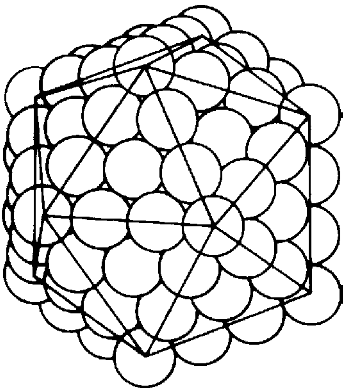

Figure 9-30. Icosahedral packing of spheres showing the third shell [53]. This is popularly called “the Mackay icosahedron.”

Herbert Hauptman, a mathematician turned crystallographer and chemistry Nobel laureate for 1985, has devoted a lot of attention to close packing of spheres in the icosahedron. Figure 9-31 shows one of his beautiful stained-glass models.

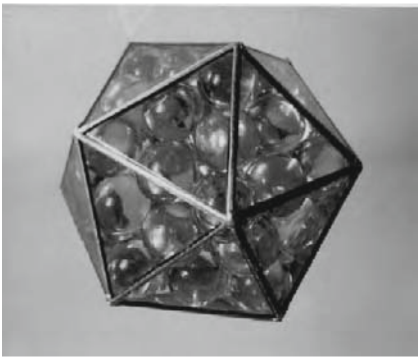

Figure 9-31. Herbert Hauptman (photograph by the authors) and one of his stained-glass models—an icosahedron—with densely packed spheres (photograph courtesy of Herbert Hauptman, Buffalo, New York).

While the most symmetrical arrangement of 12 neighbors, viz., the icosahedral coordination, does not lead to the densest possible packing, others do. The cuboctahedron and its "twinned" version, alone or in combination, lead to infinite sphere packing with the same high density (0.7405). Both coordination polyhedra are shown in Figure 9-32. The "twinned" polyhedron is obtained by reflecting one half of a cuboctahedron cut parallel to a triangular face across the plane of section.

9.5.3. Connected Polyhedra

There are, of course, more complex forms of closest packing than those considered so far. Besides, the species to be packed need not be identical. Thus, close packing of atoms of two kinds could be considered. Close-packed structures with atoms in the interstices are also important. The interstice arrays may have very different

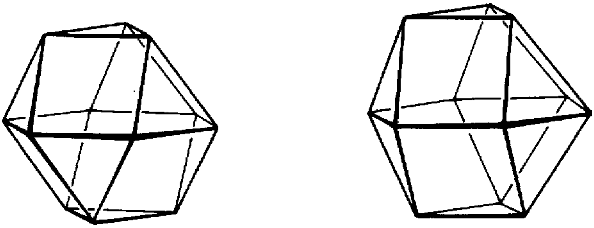

Figure 9-32. Cuboctahedron and "twinned" cuboctahedron.

arrangements in various structures. A shorthand notation of some configurations has been worked out [54] to facilitate the description of more complicated systems, which is illustrated in Figure 9-33. Suppose, for example, that in a compound with composition AX_2, each atom A is bonded to four X atoms and that all four X atoms are equivalent. Each X atom must then be bonded to two A atoms. The lines of the squares in Figure 9-33 do not represent chemical bonds; rather, these squares stand for polyhedral arrangements. Among the AX_n polyhedral groups the most common are the AX_4 tetrahedra and AX_6 octahedra. They may appear in various orientations in the crystal structures. Similar structural features have already been discussed for the polyhedral molecular geometries. Whereas in molecules only two, or at most a few, polyhedra were joined, here we deal with their infinite networks.

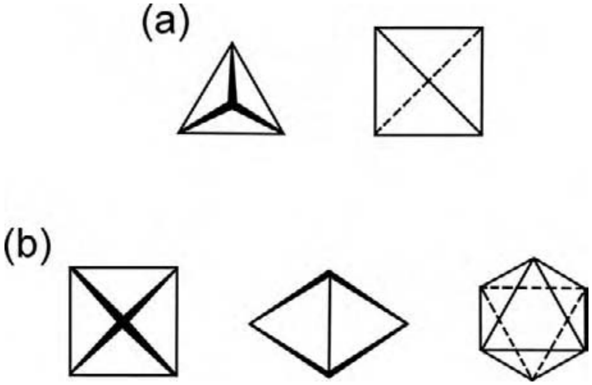

Figure 9-33. Shorthand notation for some common structural units after Wells [55]; (**a**) Notations for tetrahedron; (**b**) Notations for octahedron.

Many crystal structures may be built from the two most important coordination polyhedra, the tetrahedron and octahedron. They may share vertices, edges, or faces. The ways how the polyhedra are connected introduce certain geometrical limitations with important consequences as to the variations of the interatomic distances and bond angles. Examples are shown in Figure 9-34 and Figures 9-36–9-39 for a variety of ways to connect tetrahedral and octahedral units. Tetrahedra share two vertices or/and three vertices in Figure 9-34. For one of these, decorations analogous to its projection is shown in Figure 9-35. Octahedra share adjacent vertices and

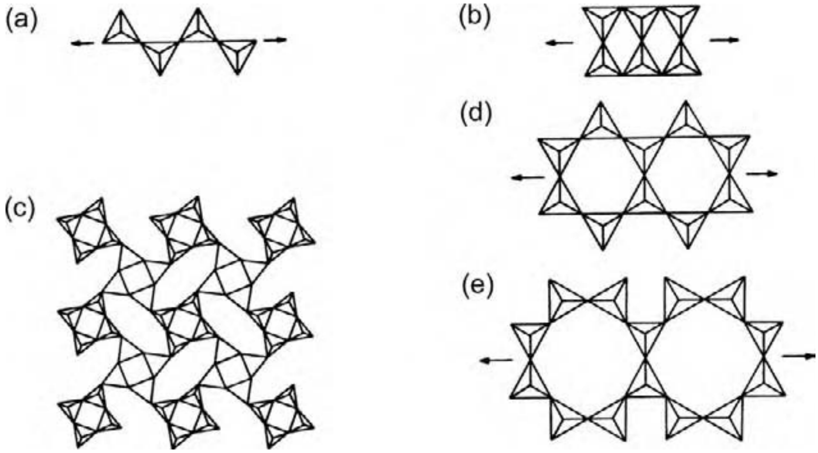

Figure 9-34. Connected tetrahedra [56]. (**a**) All tetrahedra share two vertices; (**b**) and (**c**) All tetrahedra share three vertices; (**d**) and (**e**) Some tetrahedra share two, others share three vertices.

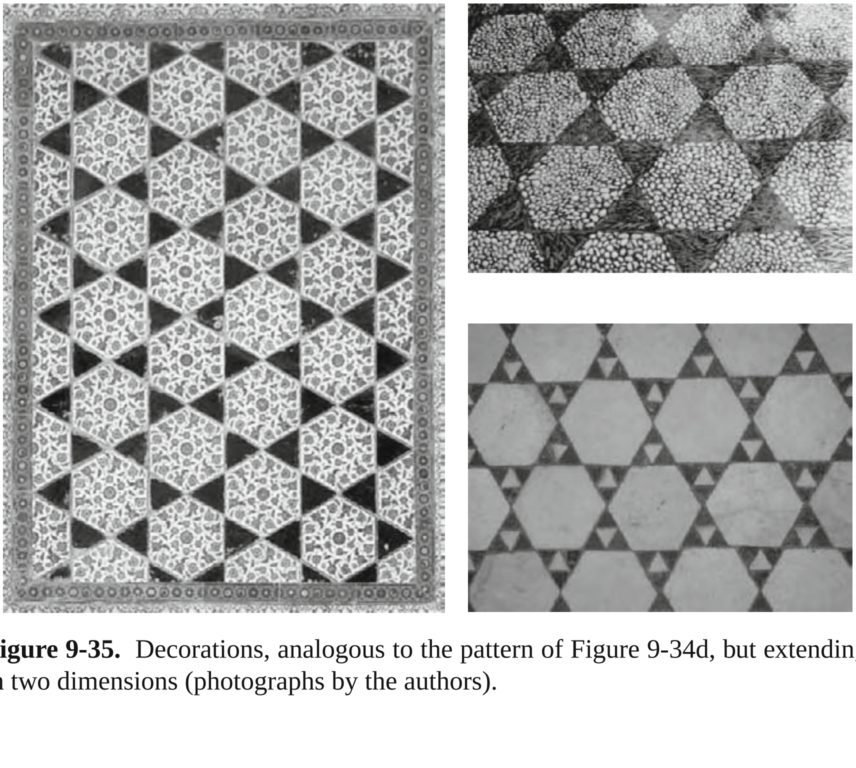

Figure 9-35. Decorations, analogous to the pattern of Figure 9-34d, but extending in two dimensions (photographs by the authors).

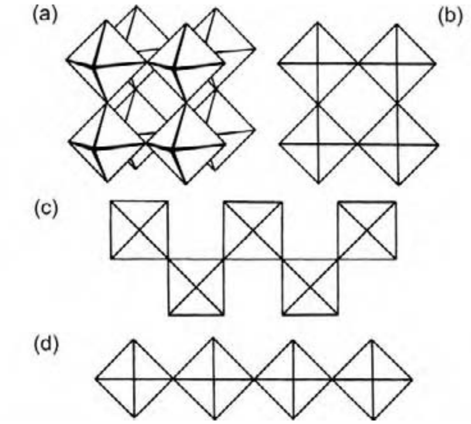

Figure 9-36. Connected octahedra: (**a**) and (**b**) Two representations of four octahedra sharing adjacent vertices and forming a tetramer; (**c**) Infinite chain of octahedra connected at adjacent vertices; (**d**) Infinite chain of octahedra connected at nonadjacent vertices.

form a tetramer in two representations in Figure 9-36a and b. Two more examples show infinite chains of octahedra sharing adjacent (Figure 9-36c) and nonadjacent (Figure 9-36d) vertices. Octahedra sharing two, four, or six edges are presented in Figure 9-37. An example of octahedra sharing faces and edges is seen in Figure 9-38. Finally, a composite structure from tetrahedra and octahedra is shown in Figure 9-39.

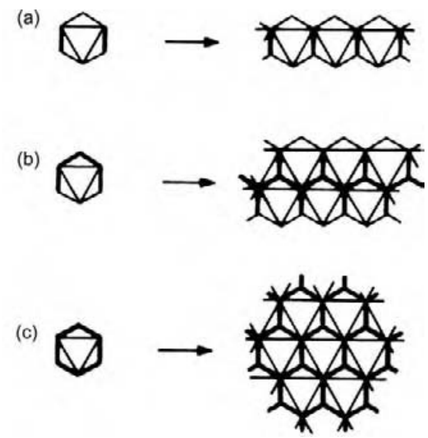

Figure 9-37. Octahedra sharing edges: (**a**) Two edges; (**b**) Four edges; (**c**) Six edges.

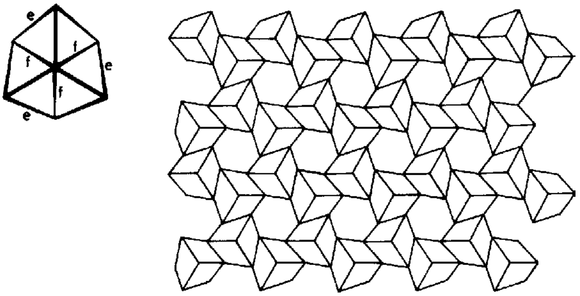

Figure 9-38. Joined octahedra: sharing faces and edges in the Nb_3S_4 crystal [57].

The tetrahedra and octahedra are important building blocks of crystal structures. The great variety of structures combining these building blocks, on one hand, and the conspicuous absence of some of the simplest structures, on the other hand, together suggest that the immediate environment of the atoms is not the only factor which determines these structures. Indeed, the relative sizes of the participating atoms and ions are of great importance.

9.5.4. Atomic Sizes

The interatomic distances are primarily determined by the position of the minimum in the potential energy function describing the interactions between the atoms in the crystal. The question is then, what are the sizes of the atoms and ions? The extension of electron density for an atom or an ion is not rigorously defined; no exact size can be

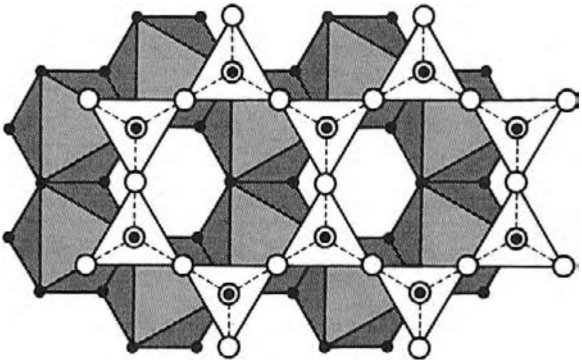

Figure 9-39. A composite structure (kaolin) built from joined tetrahedra and octahedra (reproduced with permission) [58].

assigned to it. Atoms and ions change relatively little when forming a strong chemical bond, and even less for weak bonds. For the present discussion of crystal structures, the atomic and ionic radii should, when added appropriately, yield the interatomic and interionic distances characterizing these structures.

Covalent and metallic bondings suppose a strong overlap of the outermost atomic orbitals and so the atomic radii will be approximately the radii of the outermost orbitals. The atomic radii are empirically obtained from interatomic distances [59]. For example, the length of the bond C–C is 154 pm in diamond, Si–Si is 234 pm in disilane, and so on. The consistency of this approach is shown by the agreement between the Si–C bond lengths determined experimentally and calculated from the corresponding atomic radii. The interatomic distances appreciably depend on the coordination. With decreasing coordination number, the bonds usually get shorter. For coordinations 8, 6, and 4, the bonds get shorter by about 2, 4, and 12%, respectively, as compared with the coordination number of 12.

The covalent bond is directional and multiple covalent bonds are considerably shorter than the corresponding single ones. For carbon as well as for nitrogen, oxygen, or sulfur, the decrease on going from a single bond to a double and a triple bond amounts to about 10 and 20%, respectively.

Establishing the system of ionic radii is even a less unambiguous undertaking than that for atomic radii. The starting point is a system of analogous crystal structures. Such is, for example, the structure of sodium chloride and the analogous series of other alkali halide face-centered crystals. In any case the ionic radii represent relative sizes, and if the alkali and halogen ions are chosen for starting point, then the ionic radii of all ions represent the relative sizes of the outer electron shells of the ions as compared with those of the alkali and halogen ions.

Consider now the sodium chloride crystal structure shown in Figure 9-40. It is built from sodium ions and chloride ions, and it is kept together by electrostatic forces. The chloride ions are much larger than the sodium ions. As equal numbers of cations and anions build up this structure, the maximum number of neighbors will be the number of the larger chloride ions that can be accommodated around the smaller sodium ion. The opposite would not work: although more sodium ions could surround a chloride ion, the same coordination

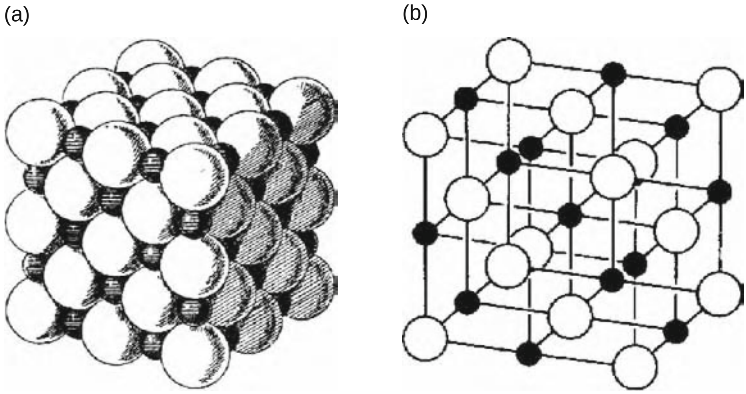

Figure 9-40. The sodium chloride crystal structure in two representations. The space-filling model is from W. Barlow [60].

could not be achieved around the sodium ions. Thus, the coordination number will obviously depend on the relative sizes of the ions. In the simple ionic structures, however, only such coordination numbers may be accomplished that make a highly symmetrical arrangement possible. The relative sizes of the sodium and chloride ions allow six chloride ions to surround each sodium ion in six vertices of an octahedron. Figure 9-41 shows the arrangement of ions in cube-face layers of alkali halide crystals with the sodium chloride structure. As

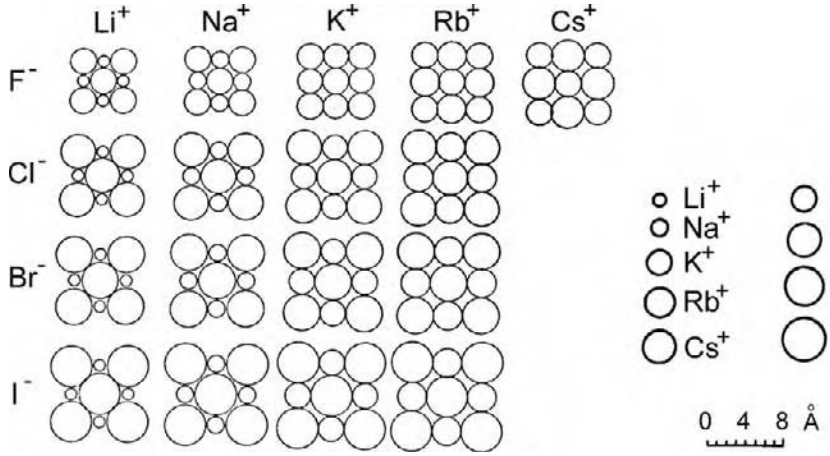

Figure 9-41. The arrangement of ions in cube-face layers of alkali halide crystals with the sodium chloride structure. Adaptation from Pauling [61]. Copyright (1960) Cornell University. Used by permission of the publisher, Cornell University Press.

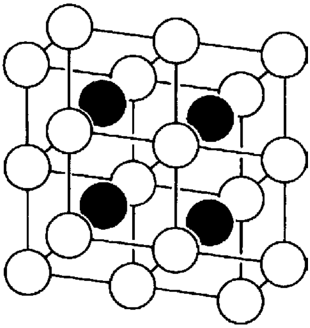

Figure 9-42. Cesium chloride crystal structure.

the relative size of the metal ion increases with respect to the size of the halogen anion, greater coordination may be possible. Thus, for example, the cesium ion may be surrounded by eight chloride ions in eight vertices of a cube in the cesium chloride crystal as shown in Figure 9-42.

9.6. Molecular Crystals

A molecular crystal is built from molecules and is easily distinguished from an ionic/atomic crystal on a purely geometrical basis. At least one of the intramolecular distances of an atom in the molecule is significantly smaller than its distances to the adjacent molecules. Every molecule in the molecular crystal may be assigned a certain well-defined space in the crystal. In terms of interactions, there are the much stronger intramolecular interactions and the much weaker intermolecular interactions. Of course, even among the intramolecular interactions, there is a range of interactions of various energies. Bond stretching, for instance, requires a proportionately higher energy than angular deformation, and the weakest are those interactions that determine the conformational behavior of the molecule [62]. On the other hand, there are differences among the intermolecular interactions as well. For example, intermolecular hydrogen bond energies may be equal to or even greater than the conformational energy differences. Thus, there may be some overlap in the energy ranges of the intramolecular and intermolecular interactions.

The majority of molecular crystals are organic compounds. There is usually little electronic interaction between the molecules in these

crystals, although even small interactions may have appreciable structural consequences. The physical properties of the molecular crystals are primarily determined by the packing of the molecules.

9.6.1. Geometrical Model

As structural information for large numbers of molecular crystals has become available, general observations and conclusions have appeared. An interesting observation was that there are characteristic shortest distances between the molecules in molecular crystals. The intermolecular distances of a given type of interaction are fairly constant. From this observation a geometrical model has been developed for describing the molecular crystals [63]. First, the shortest intermolecular distances were found, and then the so-called "intermolecular atomic radii" were postulated. Using these quantities, spatial models of the molecules were built. Fitting together these models, the densest packing could be found empirically. An example of a packing arrangement is shown in Figure 9-43. The molecules are packed together in such a way as to minimize the empty space among them. The concave part of one molecule accommodates the convex part of the other molecule. The example is the packing of 1,3,5-triphenylbenzene molecules in their crystal structure. The arrangement of the areas designated to the molecules is analogous to a characteristic decoration pattern, an example of which is also shown in Figure 9-43. The analogy is not quite superficial. The decoration is from the metal-net dress of a Chinese warrior. The dress was made of small units to maintain flexibility, the small units were identical for economy, and they covered the whole surface without gaps to ensure maximum protection.

The importance of symmetry in structure does not mean that the highest symmetry is the most advantageous. This can be illustrated beautifully in molecular crystals. Lucretius proclaimed two millennia ago in his *De rerum natura* [65]:

> Things whose fabrics show opposites that match,
> one concave where the other is convex, and vice
> versa, will form the closest union.

Lucretius could have meant this as a fundamental principle of the best packing arrangements for molecules in crystals had he known

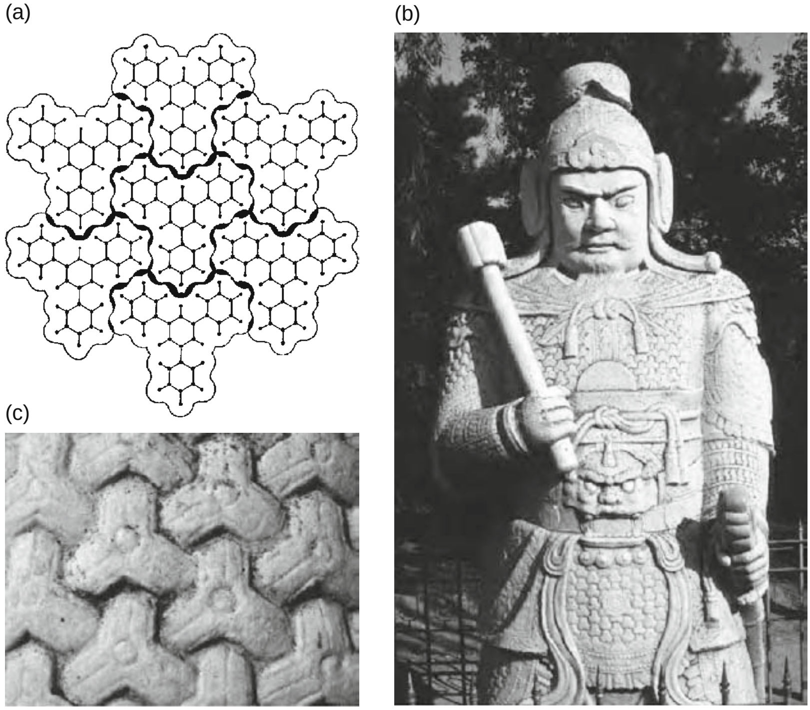

Figure 9-43. (**a**) Dove-tail dense packing of 1,3,5-triphenylbenzene molecules [64]; (**b**) Chinese decoration on a sculpture in the sculpture garden of the Ming tombs, near Beijing; and (**c**) Detail of the armor (photographs by on the authors).

about molecules of arbitrary shape. At the dawn of the 20th century, Lord Kelvin (William Thomson) returned to Lucretius's observation.

Lord Kelvin's geometry [66] was mostly forgotten, but we find it instructive in understanding the development of crystal chemistry and the teachings of symmetry in crystallography [67]. As Lord Kelvin was building up the arrangement of molecular shapes, he examined two basic variations (Figure 9-44). In one, the molecules are all oriented in the same way, while, in the other, the rows of molecules are alternately oriented in two different ways. Lord Kelvin considered the puzzle of the boundary of each molecule as a purely geometrical problem. He used nearly rectilinear shapes for partitioning the plane but he did not let the molecules touch each other. Apart from this, he created a modern representation of molecular packing in the plane,

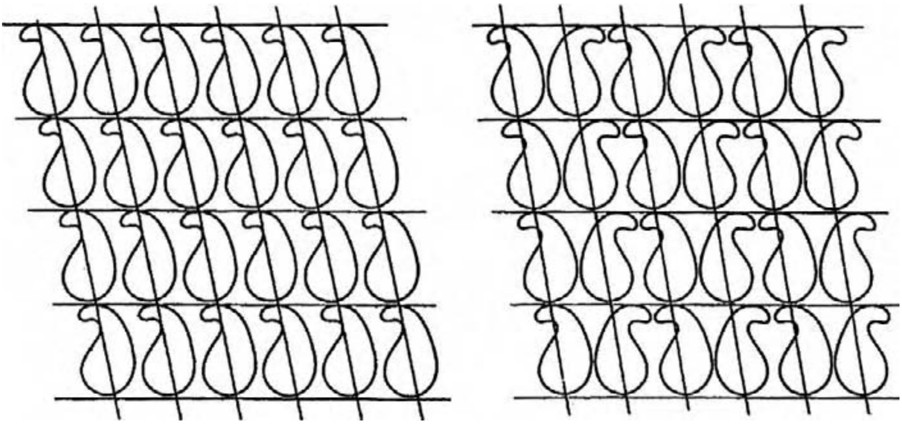

Figure 9-44. Arrangements of molecular shapes by Lord Kelvin (1904) [68].

including the recognition of the most important complementariness in packing.

Lord Kelvin then came to extending the division of continuous two-dimensional space into the third dimension. However, he restricted his examinations to polyhedra and found one of the five space-filling parallelohedra, which were discovered by E. S. Fedorov as capable of filling the space in parallel orientation without gaps or overlaps. The Fedorov polyhedra are the cube, the hexagonal prism, the rhombic dodecahedron, an elongated rhombic dodecahedron with eight rhombic and four hexagonal faces, and the truncated octahedron.

The complementary character of molecular packing is well expressed by the term of *dove-tail packing* [69]. The arrangement of the molecules in Figure 9-45a can be called *head-to-tail*. On the other hand, the molecules of a similar compound are arranged *head-to-head* as seen in Figure 9-45b. The head-to-head arrangement is less advantageous for packing. This is well seen in the arrangement of the molecules in the crystal displayed in the lower part of Figure 9-45b. Many of Escher's periodic drawings with interlocking motifs are also excellent illustrations for the dove-tail packing principle. Figure 9-46 reproduces one of them. Note how the toes of the black dogs are the teeth of the white dogs and vice versa in this drawing.

An important contribution appeared in 1940 by the structural chemist Linus Pauling and the physicist turned biologist Max Delbrück. They titled their note in *Science*, "The Nature of the

(a)

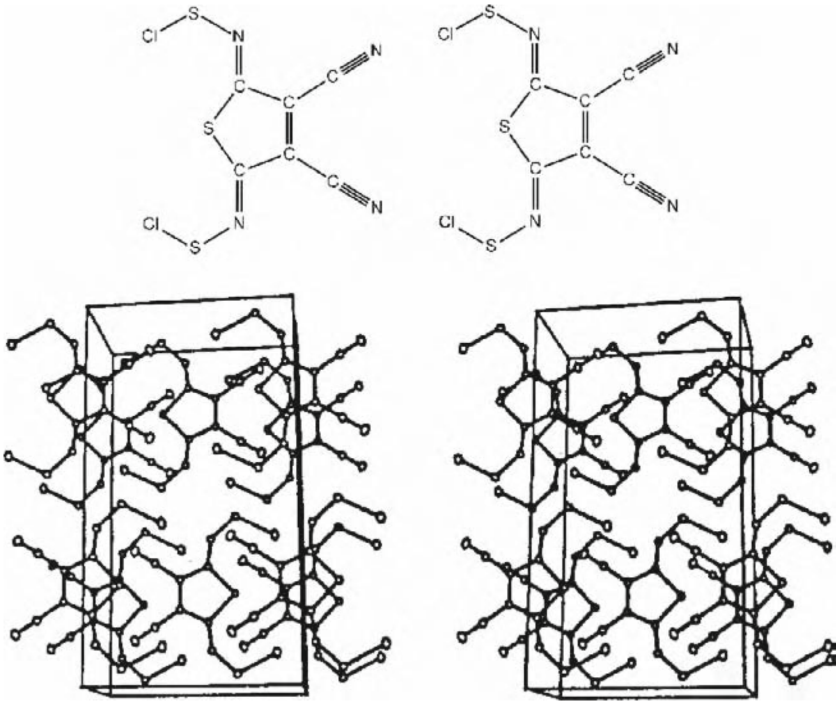

(b)

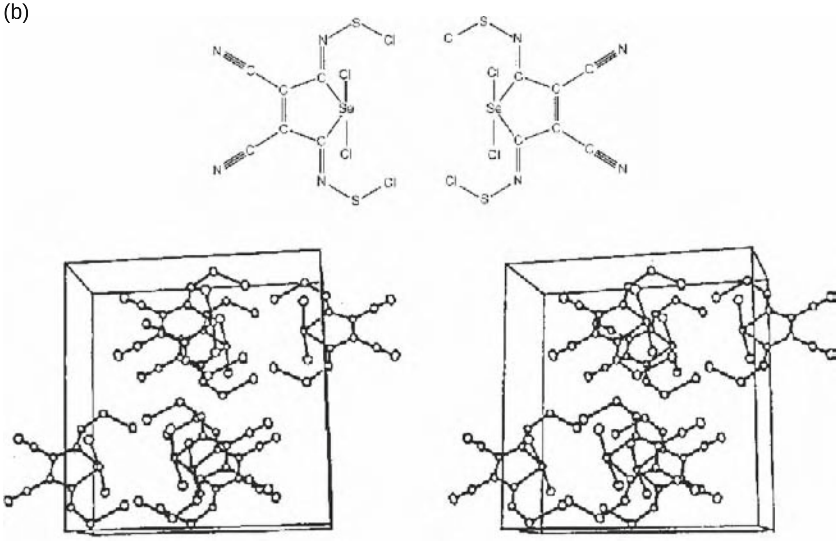

Figure 9-45. (**a**) Head-to-tail [70]; and (**b**) Head-to-head [71] arrangement of molecules and the crystal structure [70].

Figure 9-46. Escher's periodic drawing of dogs from MacGillavry's book [72]. Reproduced with permission from the International Union of Crystallography.

Intermolecular Forces Operative in Biological Processes" [73]. The note was prepared in response to a series of papers by the physicist Pascual Jordan, who had suggested that a quantum mechanical stabilizing interaction operates preferentially between identical or nearly identical molecules or parts of molecules. The suggestion came up in connection with the process of biological molecular synthesis, leading to replicas of molecules present in the cell. Pauling and Delbrück suggested precedence for interaction between complementary parts, instead of the importance of interaction between identical parts. They argued that the intermolecular interactions of van der Waals attraction and repulsion, electrostatic interaction, hydrogen bond formation, and so forth give stability to a system of two molecules with complementary structures in juxtaposition, rather than two molecules with identical structures. Accordingly, they argued that complementariness should be given primary consideration in discussing intermolecular interactions. They summarize their general argument as follows [74]:

> Attractive forces between molecules vary inversely with a power of the distance, and maximum stability of a complex is achieved by bringing the molecules as close together as possible, in such a way that positively charged groups are brought

> near to negatively charged groups, electric dipoles are brought into suitable mutual orientation, etc. The minimum distances of approach of atoms are determined by their repulsive potentials, which may be expressed in terms of van der Waals radii; in order to achieve maximum stability, the two molecules must have complementary surfaces, like die and coin, and also complementary distribution of active groups.
>
> The case might occur in which the two complementary structures happened to be identical; however, in this case also the stability of the complex of two molecules would be due to their complementariness rather than their identity.

Complementariness remained on Pauling's mind, and in 1948, he discussed molecular replication [75]:

> The detailed mechanism by means of which a gene or a virus molecule produces replicas of itself is not yet known. In general the use of a gene or a virus as a template would lead to the formation of a molecule not with identical structure but with complementary structure... If the structure that serves as a template (the gene or virus molecule) consists of, say, two parts, which are themselves complementary in structure, then each of these parts can serve as the mold for the production of a replica of the other part, and the complex of two complementary parts thus can serve as the mold for the production of duplicates itself.

At the time Pauling was working on the structure of proteins culminating eventually in his discovery of the alpha-helix. Yet this declaration sounds as if he were anticipating the mechanism of DNA replication via the double helix. It came, however, only in 1953, and it was not Pauling, but Watson and Crick, who discovered it.

Kitaigorodskii started his studies of molecular packing in the 1940s under severe conditions at war time. His first paper [76] was very brief but much to the point with the following title: "The Close-Packing of

Molecules in Crystals of Organic Compounds.” He introduced “the concept of shape of the molecule, what in turn makes it possible to raise ... the question concerning the packing of the molecules within the crystal” [77]. In this paper, Kitaigorodskii proposed a three-axial ellipsoid for the shapes of molecules, which was soon replaced by arbitrary shapes that facilitated making observations of general validity.

Because of the interlocking character, the packing in organic molecular crystals is usually characterized by large coordination numbers, i.e., by a relatively large number of adjacent or touching molecules. Experience shows that the most often occurring coordination number in organic structures is 12, so it is the same as for the densest packing of equal spheres. Coordinations 10 or 14 occur also but less often.

Kitaigorodskii was a true pioneer in the field of molecular crystals. First of all, he assigned real sizes and volumes to the molecules by accounting for the hydrogen atoms, however poorly their positions could be determined at the time. The whole molecule was considered in examining their packing, rather than the heavy-atom skeleton only. Figuratively speaking, and using Kitaigorodskii’s own expression, he “dressed the molecules in a fur-coat of van der Waals spheres” [78]. This was in complete agreement with the molecular models introduced from the early 1930s by Stuart and Briegleb to represent the space-filling nature of molecular structures [79].

The geometrical model allowed Kitaigorodskii to make predictions of the structure of organic crystals in numerous cases, knowing only the cell parameters and, obviously, the size of the molecule itself [80]. In the age of fully automated, computerized diffractometers, this may not seem to be so important, but it indeed is for our understanding the packing principles in molecular crystals.

The packing as established by the geometrical model is what is expected to be the ideal arrangement. Usually it does not differ much from the real packing as determined by X-ray diffraction measurements. When there are differences between the ideal and experimentally determined packings, it is of interest to examine the reasons of their occurrence. The geometrical model has some simplifying features. One of them is that it considers uniformly the intermolecular atom–atom distances. Another is that it considers interactions only between adjacent atoms.

The development of experimental techniques and the appearance of more sophisticated models have pushed the frontiers of molecular crystal chemistry much beyond the original geometrical model. Some of the limitations of this model will be mentioned later. However, its simplicity and the facility of visualization ensure this model a lasting place in the history of molecular crystallography. It has also exceptional didactic value.

The so-called coefficient of molecular packing (k) has proved useful in characterizing molecular packing. It is expressed in the following way:

$$k = \frac{\text{molecular volume}}{\text{crystal volume/molecule}}$$

The molecular volume is calculated from the molecular geometry and the atomic radii. The quantity crystal volume/molecule is determined from the X-ray diffraction experiment. For most crystals k is between 0.65 and 0.77. This is remarkably close to the coefficient of the dense packing of equal spheres (the density of closest packing of equal spheres being 0.7405). If the form of the molecule does not allow the coefficient of molecular packing to be greater than 0.6, then the substance is predicted to transform into a glassy state with decreasing temperature. It has also been observed that morphotropic changes associated with loss of symmetry led to an increase in the packing density. Comparison of analogous molecular crystals shows that sometimes the decrease in crystal symmetry is accompanied by an increase in the density of packing.

Another interesting comparison involves benzene, naphthalene, and anthracene. When their coefficient of packing is greater than 0.68, they are in the solid state. There is a drop in this coefficient to 0.58 when they go into liquid phase. Then, with increasing temperature, their k is decreasing gradually down to the point where they start to boil. The fused-ring aromatic hydrocarbons have served subsequently as targets of a systematic analysis of packing energies and other packing characteristics [81].

Geometrical considerations have gained additional importance due to their role in molecular recognition which implies “the (molecular) storage and (supramolecular) retrieval of molecular structural information” [82]. The formation of supramolecular structures necessitates commensurable and compatible geometries of the

partners. The molecular structure of the inclusion complex para-*tert*-butylcalix[4]arene and anisole [83] is shown in Figure 9-47. The representation is a combination of a line drawing of the calixarane molecule and a space-filling model of anisole.

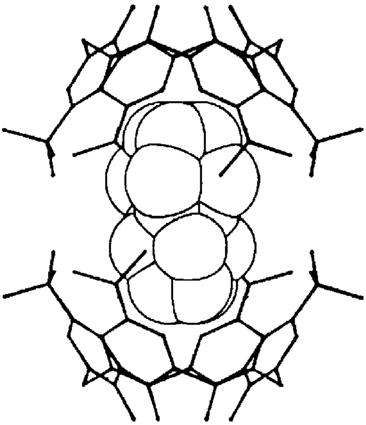

Figure 9-47. Two para-*tert*-butylcalix[4]arene molecules envelope an anisole molecule after Andreetti et al. [84].

The supramolecular formations and the molecular packing in the crystals show close resemblance, and the nature of the interactions involved is very much the same. There is great emphasis on weak interactions in both. According to Lehn, "beyond molecular chemistry based on the covalent bond lies supramolecular chemistry based on molecular interactions—the associations of two or more chemical entities and the intermolecular bond" [85]. Dunitz expressed eloquently the relevance of supramolecular structures to molecular crystals and molecular packing [86]:

> ... a crystal is, in a sense, the supramolecule *par excellence*—a lump of matter, of macroscopic dimensions, millions of molecules long, held together in a periodic arrangement by just the same kind of non-bonded interactions as those that are responsible for molecular recognition and complexation at all levels. Indeed, crystallization itself is an impressive display of supramolecular self-assembly, involving specific molecular recognition at an amazing level of precision.

9.6.2. Densest Molecular Packing

Kitaigorodskii examined the relationship between densest packing and crystal symmetry by means of the geometrical model [87]. He determined that real structures will always be among those that have the densest packing. First of all, he established the symmetry of those two-dimensional layers that allow a coordination number of six in the plane at an arbitrary tilt angle of the molecules with respect to the axes of the layer unit cell. In the general case for molecules with *arbitrary* form, there are only two kinds of such layers. One has inversion centers and is associated with a non-orthogonal lattice. The other has a rectangular net, from which the associated lattice is formed by translations, plus a second-order screw axis parallel to a translation. The next task was to select the space groups for which such layers are possible. This is an approach of great interest since the result will answer the question as to why there is a high occurrence of a few space groups among the crystals while many of the 230 groups hardly ever occur.

We present here some of the highlights of Kitaigorodskii's considerations [88]. First, the problem of dense packing is examined for the plane groups of symmetry. The distinction between dense-packed, densest-packed, and maximum density was introduced for the plane layer of molecules. The plane was called dense-packed when coordination of six was achieved for the molecules. The term densest-packed meant six-coordination with any orientation of the molecules with respect to the unit cell axes. The term maximum density was used for the packing if six-coordination was possible at any orientation of the molecules with respect to the unit cell axes while the molecules retained their symmetry.

For the plane group *p*1 it is possible to achieve densest packing with any molecular form if the translation periods t_1 and t_2 and the angle between them are chosen appropriately as illustrated in Figure 9-48. The same is true for the plane group *p*2, shown also in Figure 9-48. On the other hand, the plane groups *pm* and *pmm* are not suitable for densest packing. As is seen in Figure 9-49, the molecules are oriented in such a way that their convex parts face the convex parts of other molecules. This arrangement, of course, counteracts dense packing. The plane groups *pg* and *pgg* may be suitable for six-coordination as an example shows it in Figure 9-50a. This layer is not of maximum density and in a different orientation of the molecules

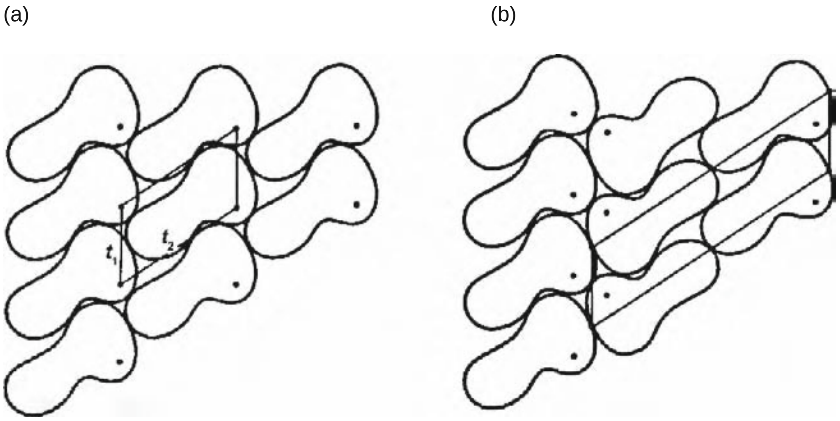

Figure 9-48. Densest packing with space groups (**a**) *p*1; and (**b**) *p*2 after Kitaigorodsky [89].

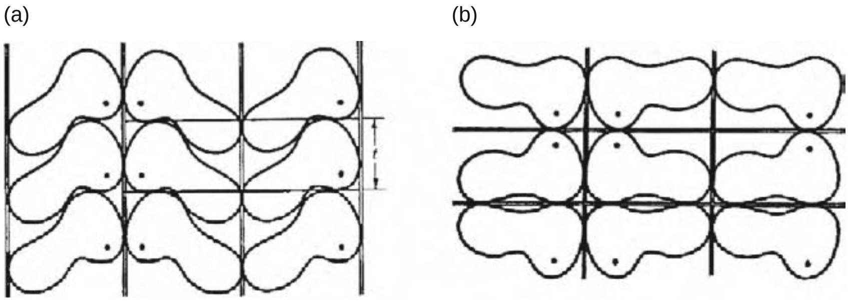

Figure 9-49. The symmetry planes in the space groups (**a**) *pm*; and (**b**) *pmm* prevent dense packing; after Kitaigorodsky [90].

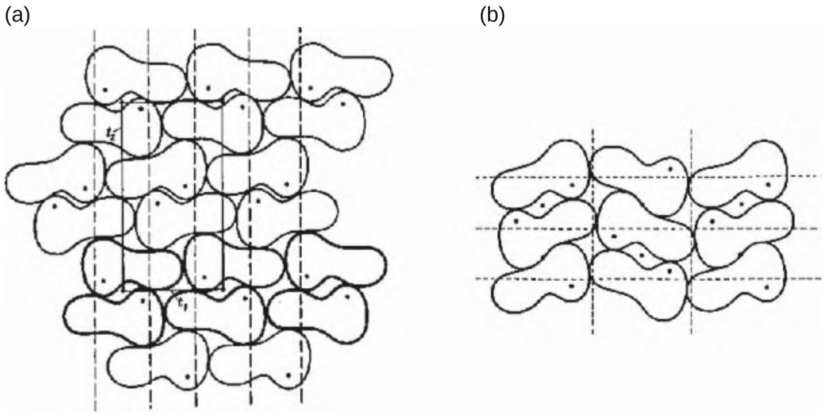

Figure 9-50. Two forms of packing with *pgg* space groups after Kitaigorodsky [91]. (**a**) Densest packing of molecules with arbitrary shape; (**b**) Another orientation of the molecules which reduces the coordination number to four.

only four-coordination is achieved as seen in Figure 9-50b. For the plane groups *cm*, *cmm*, and *pmg*, six-coordination cannot be achieved for a molecule with arbitrary shape. For higher symmetry groups, for example, tetragonal *p*4 or hexagonal *p*6, the axes of the unit cell are equivalent, and the packing of the molecules is not possible without overlaps. This is illustrated for group *p*4 in Figure 9-51.

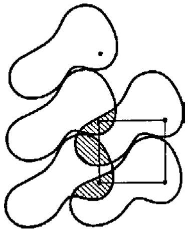

Figure 9-51. Molecules of arbitrary shape cannot be packed in space group *p*4 without overlaps after Kitaigorodsky [92].

If the molecule, however, retains a symmetry plane, then it may be packed with six-coordination in at least one of the plane groups, *pm*, *pmg*, or *cm*. The form shown in Figure 9-52 is suitable for such packing in *pmg* and *cm*, though not in *pm*. Thus, depending on the molecular shape, various plane groups may be applicable in different cases.

The criteria for the suitability as well as incompatibility of plane groups for achieving molecular six-coordination have been considered. The next step is to apply the geometrical model to the examination of the suitability of three-dimensional space groups for densest

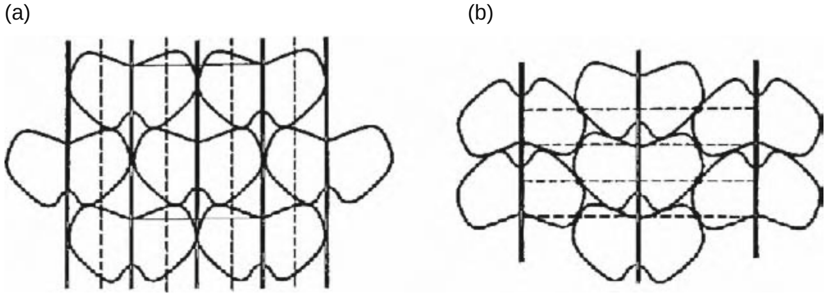

Figure 9-52. Molecules with a symmetry plane achieve 6-coordination in the space groups (**a**) *cm*; and (**b**) *pmg* after Kitaigorodsky [93].

packing. The task in this case is to select those space groups in which layers can be packed allowing the greatest possible coordination number. Mirror planes, for instance, would not be applicable for repeating the layers.

Low-symmetry crystal classes are typical for organic compounds. Densest packing of the layers may be achieved either by translation at an arbitrary angle formed with the layer plane, or by inversion, glide plane, or by screw-axis rotation. In rare cases closest packing may also be achieved by twofold rotation.

Kitaigorodskii [94] analyzed all 230 three-dimensional space groups from the point of view of densest packing. Only the following space groups were found to be available for the densest packing of molecules of arbitrary form:

$$P\bar{1},\ P2_1,\ P2_1/c,\ Pca,\ Pna,\ P2_12_12_1$$

For molecules with symmetry centers, there are even fewer suitable three-dimensional space groups, namely:

$$P\bar{1},\ P2_1/c,\ C2/c,\ Pbca$$

In these cases all mutual orientations of the molecules are possible without losing the six-coordination.

The space group $P2_1/c$ occupies a strikingly special position among the organic crystals. This space group has the unique feature that it allows the formation of layers of densest packing in all three coordinate planes of the unit cell.

The space groups $P2_1$ and $P2_12_12_1$ are also among those providing densest packing. However, their possibilities are more limited than those of the space group $P2_1/c$, and these space groups occur only for molecules that take either left-handed or right-handed forms. According to statistical examinations performed some time ago, these three groups are the first three in frequency of occurrence.

An interesting and fundamental question is the conservation of molecular symmetry in the crystal structure. Densest packing may often be well facilitated by partial or complete loss of molecular symmetry in the crystal structure. There are, however, space groups in which some molecular symmetry may “survive” densest packing when building the crystal. Preserving higher symmetry though usually

costs too great a sacrifice of packing density. On the other hand, there may be certain energy advantage of some well-defined symmetrical arrangements. The alternative to the geometrical model for discussing and establishing molecular packing in organic crystals has been the calculations of energy, based on carefully constructed potential energy functions [95].

9.6.3. Energy Calculations and Structure Predictions

It is important to be able to determine *a priori* the arrangement of molecules in crystals. The correctness of such predictions is a test for our understanding of how crystals are built. A further benefit is the possibility of calculating even those structures whose determination is not amenable to experimental analysis. But even as part of an experimental study, it is instructive to build good models, which can then be refined. The main advantages of the geometrical model have been seen above. Its main limitations are the following: It cannot account for the structural variations in a series of analogous compounds. It is restricted in correlating structural features with various other physical properties. Finally, it is unable to make detailed predictions for unknown structures. Calculations seeking the spatial arrangement of molecules in the crystal corresponding to the minimum of free energy have become a much used tool. If the system is considered completely rigid, the molecular packing may be determined by minimizing the potential energy of intermolecular interactions.

Considering the molecules to be rigid, i.e., ignoring the vibrational contribution, the energy of the crystal structure is expressed as a function of geometrical parameters including the cell parameters, the coordinates of the centers of gravity of the symmetrically independent molecules, and parameters characterizing the orientation of these molecules. In particular cases the number of independent parameters can be reduced. On the other hand, considerations for the non-rigidity of the molecules necessitate additional parameters. Minimizing the crystal structure energy leads to structural parameters corresponding to optimal molecular packing. Then it is of great interest to compare these findings with those from experiment.

To determine the deepest minimum on the multidimensional energy surface as a function of many structural parameters is a formidable mathematical task. Usually, simplifications and assumptions are

introduced concerning, for example, the space-group symmetry. Accordingly, the conclusions from these theoretical calculations cannot be considered to be entirely a priori.

The considerations on the intermolecular interactions can be conveniently reduced to considerations of atom–atom nonbonded interactions. Although these interactions can be treated by nonempirical quantum mechanical calculations, empirical and semi-empirical approaches have also proved useful in dealing with them. In the description of the atom–atom nonbonded interactions it is supposed that the van der Waals forces originate from a variety of sources.

In addition to the intermolecular interactions, the intramolecular interactions may also be taken into account in a similar way. This rather limited approach may nevertheless be useful for calculating molecular conformation and even molecular symmetry. Deviations from the ideal conformations and symmetries may also be estimated this way, provided they are due to steric effects.

By summation over the interaction energies of the molecular pairs, the total potential energy of the molecular crystal may be obtained in an atom–atom potential approximation. The result is expected to be approximately the same as the heat of sublimation extrapolated to 0 K provided that no changes take place in the molecular conformation and vibrational interactions during evaporation.

In many of the molecular packing studies, the crystal classes are taken from the experimental X-ray diffraction determinations. The optimal packing is then determined for the assumed crystal class. In other cases, the crystal classes have also been established in the optimization calculations.

Ideally, it should be possible to predict molecular packing, and thus the crystal structure, from the knowledge of the composition of a compound and the symmetry and geometry of its molecule. It has proved, however, a rather elusive task. Two decades ago, the editor of *Nature* expressed the frustration over the difficulty in predicting crystal structures in the following words: “One of the continuing scandals in the physical sciences is that it remains impossible to predict the structure of even the simplest crystalline solids from a knowledge of their chemical composition” [96]. There has been considerable progress in this respect, however, mainly due to the utilization of the wealth of information from data banks, and in particular, from the Cambridge Crystallographic Data Centre.

It has also proved fruitful to use energy calculations with computer graphic analysis. Plausible crystal-building scenarios have been described which, while not being necessarily unique solutions, seem to point in the right direction in conquering this important frontier of structural science. An example is the construction of organometallic crystals, illustrated here with $Ru_3(CO)_{12}$ in Figure 9-53. It is a simultaneous process in reality, but is broken down into three steps in the model. First, a row of molecules is constructed in a head-to-tail arrangement. The second step involves adding rows to form a layer utilizing interlocking interactions. Finally, whole layers are added to form a crystal [97]. By now, these studies have acquired rather historical importance because there is an increasing number of computational efforts to predict molecular packing from the composition of substances. These efforts concentrate on selected classes of related

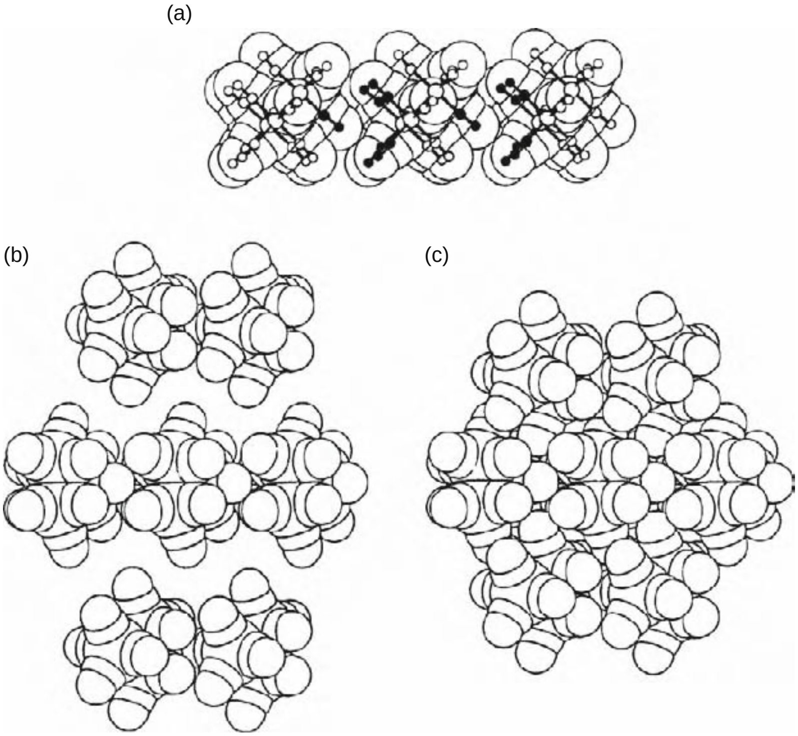

Figure 9-53. Building a crystal of $Ru_3(CO)_{12}$ according to Braga and Grepioni [98]; (**a**) Row of molecules; (**b**) Forming a layer; (**c**) Extending in three dimensions. Copyright (1991) American Chemical Society.

compounds rather than aim at finding a general approach. Maddox's two-decade-old lamentation seems to maintain its general validity.

A concerted use of geometry and energy considerations, as demonstrated by the crystal-building of $Ru_3(CO)_{12}$, seems very promising. Extending such studies point in the direction of a "Kitaigorodskian dream," as they "provide the starting point for the formulation of a generalized force field for intermolecular interactions in organic crystals" [99].

There seems to be a remarkable consistency between Buckminster Fuller's evaluation of chemistry ("chemists consider volumes as material domains and not merely as abstractions," see Chapter 1—Introduction) and Kitaigorodskii's geometrical model of crystal structures. In one of his last statements Kitaigorodskii (Figure 9-54) said (when asked about his most important achievements in science): "I've shown that the molecule is a body.† One can take it, one can hit with it; it has mass, volume, form, hardness. I followed the ideas of Democritos..." [100].

Figure 9-54. A. I. Kitaigorodskii (1914–1985) among his students in the late 1960s in Moscow. István Orosz's rendition of "Complementary Kitaigorodsky" [101].

†Another version is also attributed to Kitaigorodskii, "The molecule also has a body; when it's hit, it feels hurt all over." This implied the possibility of structural changes in the molecule upon entering the crystal structure, a symbolic departure from Kitaigorodskii's earlier views about the constancy of molecular geometry regardless whether in the gas phase or in the crystal.

9.6.4. Hypersymmetry

There are some crystal structures in which further symmetries are present in addition to those prescribed by their three-dimensional space groups. The phenomenon is called hypersymmetry [102]. Thus, it refers to symmetry features not included in the system of the 230 three-dimensional space groups. For example, phenol molecules, connected by hydrogen bonds, form spirals with threefold screw axes as indicated in Figure 9-55. This screw axis does not extend, however, to the whole crystal, and it does not occur in the three-dimensional space group characterizing the phenol crystal.

A typical characteristic of hypersymmetry operations is that they exercise their influence in well-defined discrete domains. These domains do not overlap—they do not even touch each other. The usual hypersymmetry elements lead to point-group properties. This means that no infinite molecular chains could be selected, for example, to which these hypersymmetry operations would apply. They affect, instead, pairs of molecules or very small groups of molecules. Thus, they can really be considered as local point-group operations. These hypersymmetry elements, accordingly, divide the whole crystalline system into numerous small groups of molecules, or transform the crystal space into a layered structure.

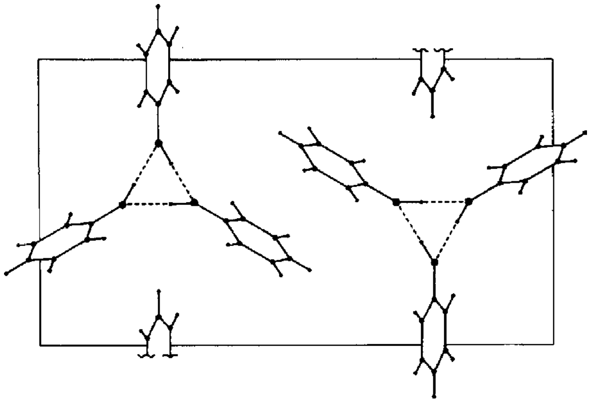

Figure 9-55. The molecules in the phenol crystal are connected by hydrogen bonds and are forming spirals with a threefold screw axis. This symmetry element is not part of the three-dimensional space group of the phenol crystal. After Zorky and Koptsik [103].

A prerequisite for hypersymmetry is that there should be chemically identical (having the same structural formula), but symmetrically independent, molecules in the crystal structure—symmetrically independent, that is, in the sense of the three-dimensional space group to which the crystal belongs. The question then arises as to whether these symmetrically independent but chemically identical molecules will have the same structure or not. Only if they do have the same structure, conformation as well as bond configuration, can we talk about the validity of the hypersymmetry operations. Here, preferably, quantitative criteria should be introduced, which is the more difficult since, for example, with increasing accuracy, structures that could be considered identical before, may no longer be considered so later when more accurate data become available.

On the other hand, since even a slightly different environment will have some influence on the molecular structure, the hypersymmetry operations will not be absolute. In this, the hypersymmetry operations are somewhat different from the usual symmetry operations. The ultimate goal is to find such a generalized formulation of the space-group system that would allow the simultaneous consideration of the usual symmetry as well as the hypersymmetry. When such a generalized formulation of space groups encompassing usual and hypersymmetry operations becomes available, the task of discovering crystals with hypersymmetry will be greatly facilitated.

A special case of hypersymmetry is when the otherwise symmetrically independent molecules in the crystal are related by hypersymmetry operations making them enantiomorphous pairs.

Hypersymmetry is a rather widely observed, and sometimes ignored, phenomenon which is not restricted to any special class of compounds. It may be supposed, however, that certain types of molecules are more apt to have this kind of additional symmetry in their crystal structures than others.

There are hypersymmetry phenomena in some crystal structures that are characterized by extra symmetry operations applicable to infinite chains of molecules. This kind of hypersymmetry has proved to be more easily detectable and has been reported often in the literature [104].

Hypersymmetry may be interpreted on the basis of the symmetry of the potential energy functions describing the conditions of the formation of the molecular crystal. The molecules around a certain

starting molecule will be related by the symmetry of the potential energy function itself or the symmetry of certain combinations of the potential energy functions. The occurrence of some screw axes of rotation by hypersymmetry elements has been successfully interpreted this way. In some instances energy calculations as well as geometrical reasoning have shown the physical importance of hypersymmetry. This may appear, e.g., as stronger chemical bonding among molecules. Hypersymmetry may often be described as involving layered structure of a molecular crystal. This, again, may have advantages for geometrical and energy considerations. Thus, the phenomenon of hypersymmetry is another good example of how symmetry properties and other properties are related to each other.

9.6.5. Crystal Field Effects

Elucidating the effects of intermolecular interactions may greatly facilitate our understanding of the structure and energetics of crystals. The geometrical changes of molecular structures cover a wide range in energy. Molecular shape, symmetry, and conformation change more easily upon the molecule becoming part of a crystal than do bond angles and especially bond lengths.

Kitaigorodskii suggested four approaches to investigating the effects of the crystalline field on molecular structure [105]: (1) comparison of gaseous (i.e., free) and crystalline molecules; (2) comparison of symmetrically (i.e., crystallographically) independent molecules in the crystal; (3) analysis of the structure of molecules whose symmetry in the crystal is lower than their free molecular symmetry; and (4) comparison of the molecular structure in different polymorphic modifications.

It is also possible that the molecule has higher symmetry in the crystal than as a free unit in the gas. Thus, e.g., biphenyl has a higher molecular symmetry—a coplanar structure—in the crystal than in the vapor, where the two benzene rings are rotated by about 45° relative to each other as shown below (**9-1**).

9-1

9.6.5.1. Structure Differences in Free and Crystalline Molecules

The points 1 and 3 above both refer to the comparison of the structures of free and crystalline molecules as does the last example in the previous section. Such comparisons provide, perhaps, the most straightforward information, since the structure of the free molecule is determined exclusively by intramolecular interactions. Any difference that is reliably detected will carry information as to the effects of the crystal field on the molecular structure. However, before discussing more subtle structural differences in molecular crystals as compared with free molecules, it is appropriate to point out some more striking differences between ionic crystals and the corresponding vapor-phase molecules.

Although molecules cannot be identified as the building blocks of ionic crystals, the free molecules of *some* compounds may be considered as if they were taken out of the crystal. A nice example is sodium chloride whose main vapor components are monomeric and dimeric molecules. They are indicated in the crystal structure in Figure 9-56, as is a tetrameric species. Mass spectrometric studies of cluster formation determined a great relative abundance of a species with 27 atoms in the cluster. The corresponding $3\times3\times3$ cube may, again, be considered as a small crystal [106].

Another series of simple molecules whose structure may easily be traced back to the crystal structure is shown in Figure 9-57. It is evident, for example, that various MX_2 and MX_3 molecules may take different shapes and symmetries from the same kind of

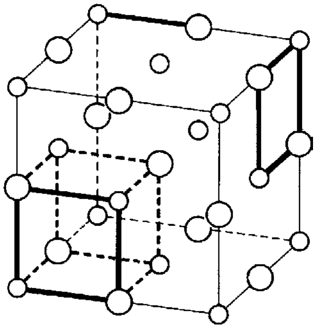

Figure 9-56. Part of sodium chloride crystal structure with NaCl, $(NaCl)_2$, and $(NaCl)_4$ units indicated. The species of 3x3x3 ions itself has a high relative abundance in cluster formation.

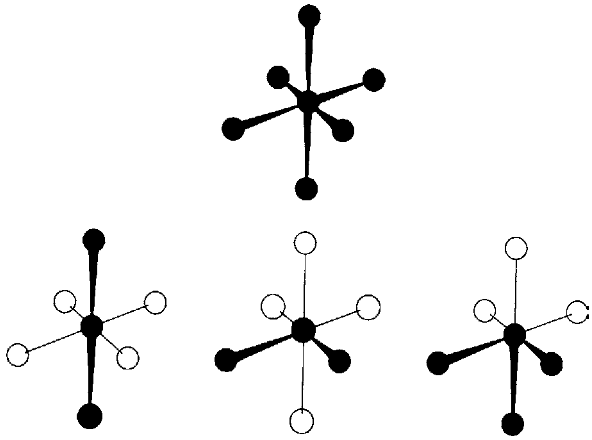

Figure 9-57. Different shapes of MX_2 and MX_3 molecules derived from the crystal structure in which the central atom has an octahedral environment.

crystal structure. The crystal structure is represented by the octahedral arrangement of six “ligands” around the “central atom.”

There seems to be even less structural similarity for many other metal halides as the crystalline systems are compared with the molecules in the vapor phase. Aluminum trichloride, e.g., crystallizes in a hexagonal layer structure. Upon melting, and then, upon evaporation at relatively low temperatures, dimeric molecules are formed. At higher temperatures they dissociate into monomers (Figure 9-58) [107]. The coordination number decreases from 6 to 4 and then to 3 in this process. However, at closer scrutiny, even the dimeric aluminum trichloride molecules can be derived from the crystal structure. Figure 9-59 shows another representation of crystalline aluminum trichloride which facilitates the identification of the dimeric units. A further example is chromium dichloride illustrated in Figure 9-60. The small oligomers in its vapor have structures [108] that are closely related to the solid structure [109]. Correlation between the molecular composition of the vapor and their source crystal has been established for some metal halides [110].

Gas/solid differences of different nature may occur in substances forming molecular crystals. In some cases, e.g., the vapor contains more rotational isomers than the crystal. Thus, for example, the vapor of ethane–1,2–dithiol, $HS–CH_2–CH_2–SH$, consists of *anti* and *gauche*

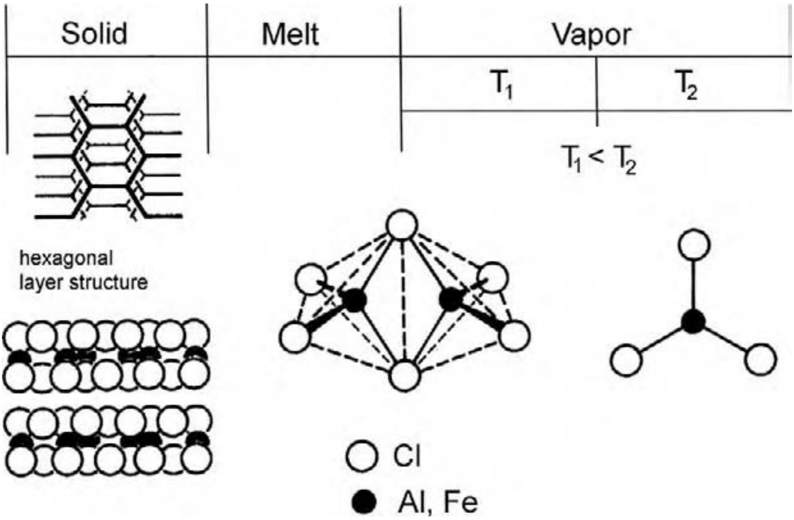

Figure 9-58. Structural changes upon evaporation of aluminium trichloride.

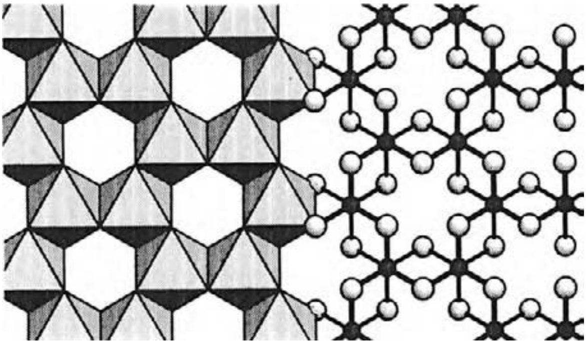

Figure 9-59. The crystal structure of aluminium trichloride after Müller [111]. The dimeric unit with four-member ring is discernible. Copyright 1993 John Wiley & Sons. Used by permission.

forms with respect to rotation about the central bond while only the *anti* form was found in the crystal [113].

The comparison of the structures of free and crystalline molecules has been based predominantly on the application of various experimental techniques, but theoretical calculations play an ever increasing role. Thus, it is important to comment upon the inherent differences in the physical meaning of the structural information originating from such different sources [114]. The consequences of intramolecular vibrations on the geometry of free molecules have already been

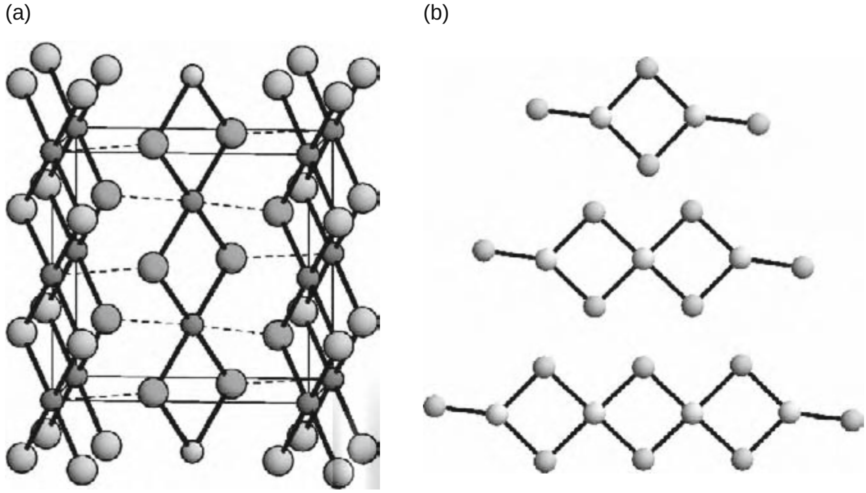

Figure 9-60. Four-membered rings are present both in (**a**) The crystal; and (**b**) The vapor-phase molecules of chromium dichloride [112].

mentioned. The effects of molecular vibrations and librational motion in the crystal are not less important. To minimize their effects, it is desirable to examine the crystal molecular structure at the lowest possible temperatures. Also, the corrections for thermal motion are of great importance. Especially when employing older data in comparisons and discussing subtle effects, these problems have to be considered. There is another source for differences in structural information, which are only apparent differences and originate from the difference in the physical meaning of the physical phenomena utilized in the experimental techniques. When all sources of apparent differences have been eliminated, and the molecular structure still differs in the gas and the crystal, the intermolecular interactions in the crystal may indeed be responsible for these differences [115].

The comparisons of gas/crystal structures may stimulate more accurate structure determinations by experiment as well as calculations of ever increasing sophistication. The gas/crystal structural changes depend on the relative strengths of the intramolecular and intermolecular interactions. More pronounced changes are expected, for example, in relatively weak coordination linkages under the influence of the crystal field than in stronger bonds. Thus, the N–B bond of donor-acceptor complexes is considerably longer in the gas than in the crystal. The difference is about 5 pm for $(CH_3)_3N–BCl_3$ (**9-2**) [116]

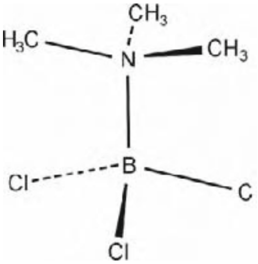

9-2

and it may be supposed that the intermolecular forces somewhat compress the molecule along the coordination bond in the crystal. An extreme case of an 84 pm difference was reported for HCN–BF_3 [117]. Another example is the silatrane structures where the relatively weak N–Si dative bond is much longer in the gas than in the crystal. This difference is 28 pm for 1-fluorosilatrane [118], represented here (**9-3**) by the heavy-atom skeleton.

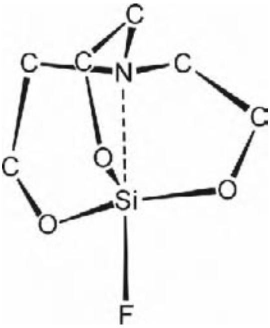

9-3

Gas/crystal comparisons are as of yet mainly confined to registering structural differences. The interpretation of these results is at a qualitative initial stage. Further investigation of such differences will enhance our understanding of the intermolecular interactions in crystals.

9.6.5.2. Conformational Polymorphism

The investigation of different rotational isomers of the same compound in different crystal forms (*polymorphs*) is another efficient tool in elucidating intermolecular interactions. The phenomenon is called conformational polymorphism. The energy differences between

the polymorphs of organic crystals are similar to the free energy differences of rotational isomers of many free molecules, viz., a few kilocalories per mole. When the molecules adopt different conformations in the different polymorphs, the change in rotational isomerism is attributed to the influence of the crystal field since the difference in the intermolecular forces is the single variable in the polymorphic systems.

Polymorphism is ubiquitous [119], and most compounds can exist in more than one crystalline form. Conformational polymorphism of various organic compounds has been studied with a variety of techniques in addition to X-ray crystallography. Among the molecules investigated were N-(p-chlorobenzylidine)-p-chloroaniline, [**9-4**, X = Cl (**I**)]

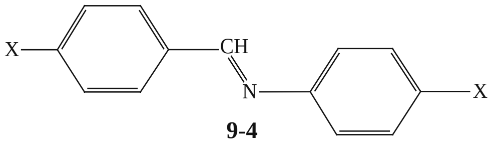

9-4

which exists in at least two forms, and p-methyl-N-(p-methylbenzylidene)aniline, [**9-4**, X = CH_3 (**II**)], which exists in at least three forms. For **I,** a high-energy planar conformation was shown to occur with a triclinic lattice. A lower-energy form with normal exocyclic angles was found in the orthorhombic form. It was an intriguing question as to why molecule **I** would not always pack with its lowest-energy conformation.

The X-ray diffraction work has been augmented by lattice energy calculations employing different potential functions. The results did not depend on the choice of the potential function, and they showed that the crystal packing and the (intra)molecular structure together adopt an optimal compromise. The minimized lattice energies were analyzed in terms of partial atomic contributions to the total energy. Even for the trimorphic molecule (**II**) the relative energy contributions of various groups were similar in all polymorphs. However, this could only be achieved in some lattices by adopting a conformation, different from the most favorable, with respect to the structure of the isolated molecule. The investigation of conformational polymorphism proved to be a promising tool for understanding the nature of the crystal forces influencing molecular conformation, and even molecular structure, in a broader sense.

Possible variations in bond angles and bond lengths have been ignored in the considerations described above. The energy requirements for changing bond angles and bond lengths are certainly higher than those for conformational changes, and, accordingly, higher than what may be available in polymorphic transitions. However, some relaxation of the bond configuration may take place, especially if considering that the (intra)molecular structure is also adopted as a compromise between the bond configurations and the rotational forms.

Bond configuration relaxation during internal rotation is another phenomenon whose understanding might throw some light on the correlations among the various intramolecular and intermolecular interactions. In this case, quantum chemical calculations may be the technique of choice. An early study, for example, targeted a series of 1,2-dihaloethanes [120]. The bond angle C–C–X was observed to change as much as 4° during internal rotation according to these calculations. If there is then a mixture of, say, *anti* and *gauche* forms, as is often the case, and the relaxation of the bond configuration is ignored, this may lead to considerable errors in the determination of the *gauche* angle of rotation.

9.7. Beyond the Perfect System

The 230 space groups exhaustively characterize all the symmetries possible for infinite lattice structures. So "exhaustively" that some time ago some crystallographers and other scientists started viewing this perfect system as a little too perfect and a little too rigid. These views pointed toward the further development of our ideas on structures and symmetries.

There is an inherent deficiency in crystal symmetry in that crystals are not really infinite. Alan Mackay argued that the crystal formation is not the insertion of components into a three-dimensional framework of symmetry elements; on the contrary, the symmetry elements are the consequence [121]. The crystal arises from the local interactions between individual atoms. He furthermore said that a regular structure should mean a structure generated by simple rules, but the list of rules considered to be simple and "permissible" should be extended. These rules would not necessarily form groups. Furthermore, Mackay found the formalism of the *International Tables for X-Ray Crystallography*

to be too restrictive and quoted Bell, the historian of mathematics, on the rigidity of the Euclidean geometry formalism: “The cowboys have a way of trussing up a steer or a pugnacious bronco which fixes the brute so that it can neither move nor think. This is the hog-tie and it is what Euclid did to geometry” [122].

Mackay had a long list covering a whole range of transitions from classical crystallographic concepts to what is termed the modern science of structure at the atomic level. This list is reproduced in Table 9-6. There is resonance of several of Mackay’s ideas with other directions in modern chemistry, where the non-classical, the

Table 9-6. Mackay’s List of Transition from the Classical Concepts of Crystallography to the Modern Concepts of a Science of Structure[a]

Classical concepts	Modern concepts
Absolute identity of components	Substitution and nonstoichiometry
Absolute identity of the environment of each unit	Quasi-identity and quasiequivalence
Operations of infinite range	Local elements of symmetry of finite range
“Euclidean” space elements (plane sheets, straight lines)	Curved space elements. Membranes, micelles, helices. Higher structures by curvature of lower structures
Unique dominant minimum in free energy configuration space	One of many quasi-equivalent states; metastability recording arbitrary information (pathway); progressive segregation and specialization of information structure
Infinite number of units. Crystals	Finite numbers of units. Clusters; “crystalloids”
Assembly by incremental growth (one unit at a time)	Assembly by intervention of other components (“crystalase” enzyme). Information-controlled assembly. Hierarchic assembly
Single level of organization (with large span of level)	Hierarchy of levels of organization. Small span of each level
Repetition according to symmetry operations	Repetition according to program. Cellular automata
Crystallographic symmetry operations	General symmetry operations (equal “program statements”)
Assembly by a single pathway in configuration space	Assembly by branched lines in configuration space. Bifurcations guided by “information”, i.e., low-energy events of the hierarchy below

[a] A. L. Mackay, “De Niva Quinquangula: On the pentagonal snowflake.” *Kritallografiya* (*Sov. Phys. Crystallogr.*) 1981, 26, 910–919 (517–522).

non-stoichiometrical, the non-stable, the non-regular, the non-usual, the non-expected are gaining importance. For crystallography it seems to be a long way yet to perform all the suggested transitions but the breakthroughs so far have been fascinating and promising. Impressive progress has been reported in the studies of liquids, amorphous materials, metallic alloys as regards the description of their structural regularities.

Liquid structures, for example, cannot be characterized by any of the 230 three-dimensional space groups and yet it is unacceptable to consider them as possessing no symmetry whatsoever. Bernal noted presciently that the major structural distinction between liquids and crystalline solids is the absence of long-range order in the former [123]. A generalized description should also characterize liquid structures and colloids, as well as the structures of amorphous substances. It should also account for the greater variations in their physical properties as compared with those of the crystalline solids. Bernal's ideas have greatly encouraged further studies in this field which is usually called generalized crystallography. Referring to Bernal's geometrical theory of liquids, Belov noted in Bernal's obituary: "... his last enthusiasm was for the laws of lawlessness" [124].

The paradoxical incompleteness and inadequacy of perfect symmetry, compared with less-than-perfect symmetry, are well expressed in a short poem entitled "Gift to a Jade" by the English poet Anna Wickham [125]:

For love he offered me his perfect world.
This world was so constricted and so small
It had no loveliness at all,
And I flung back the little silly ball.
At that cold moralist I hotly hurled
His perfect, pure, symmetrical, small world.

The structures intermediate between the perfect order of crystals and the complete disorder of gases are not merely rare exceptions. On the contrary, they are often found in substances which are very common in our environment or are widely used in various technologies. They include plastics, textiles, and rubber, among others. Glass is an especially fascinating material whose amorphous atomic network was discussed by Zachariasen a long time ago, but his teachings are still considered to be valid [126]. Figure 9-61 shows Zachariasen's

two-dimensional representations of crystalline and amorphous structures of compounds of the same composition, A_2O_3. Guinier discussed the intermediate structures between the extreme types of perfect order and disorder, and he declared a quarter of a century ago that “The distinction into two well separated classes is an oversimplification of the complex reality” [127]. He envisaged a continuous passage from the exact scheme of neighboring atoms in a crystal to the very flexible arrangement in an amorphous body. The term paracrystal was coined for domains with approximate long-distance order in the range of a few tens to a few hundreds of atomic diameters. Today we call the discipline dealing with such structures nanoscience. Figure 9-62 provides a schematic representation of a paracrystal lattice with one atom per unit cell. The blackened areas indicate the regions where an atom is likely to be found around the atom fixed at the origin. At greater distances the neighboring sites first overlap, then merge, and thus eventually the long-range order vanishes completely. Guinier’s teachings have further enriched recent studies of complex intermetallic structures [128].

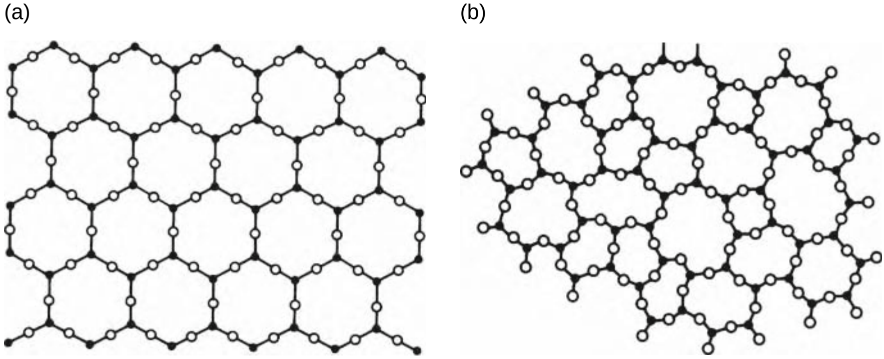

Figure 9-61. Zachariasen’s [129] representation of the atomic arrangement in the crystal (**a**) and glass (**b**) of A_2O_3.

One of the most fascinating examples of non-periodic regular arrangements was described by Mackay in a paper titled—in obvious reference to Kepler’s treatise about the six-cornered snowflake—D*e nive quinquangula* (on the pentagonal snowflake) [131]. A regular but “non-crystalline” structure is built from regular pentagons in a plane. It starts with a regular pentagon of given size (zeroth-order pentagon). Six of these pentagons are combined to make a larger one (first-order

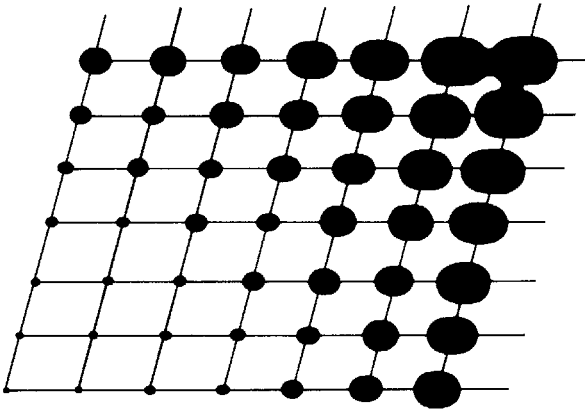

Figure 9-62. Paracrystal lattice with one atom per unit cell adapted from Guinier [130]. Used with permission.

pentagon). As is seen in Figure 9-63, the resulting triangular gaps are covered by pieces from cutting up a seventh zeroth-order pentagon. This indeed yields five triangles plus yet another regular pentagon of the order –1. This construction is then repeated on an ever increasing scale as indicated in Figure 9-63. The hierarchic packing of pentagons builds up like a pentagonal snowflake. Attempts of pentagonal tiling of the plane were already quoted in the Introduction, and will be referred to again in the next Section.

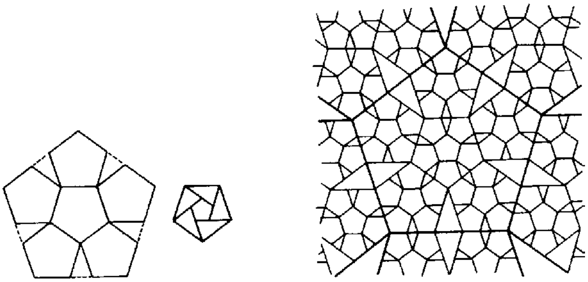

Figure 9-63. Tiling with regular pentagons after Mackay [132].

Mackay called attention to yet another limitation of the 230 space-group system. It covers only those helices that are compatible with the three-dimensional lattices. All other helices that are finite in one or two dimensions are excluded. Some important virus structures with icosahedral symmetry are among them. Also, there are very small

particles of gold that do not have the usual face-centered cubic lattice of gold. They are actually icosahedral shells. The most stable configurations contain 55 or 147 atoms of gold. But icosahedral symmetry is not treated in the *International Tables* and crystals are only defined for infinite repetition.

Crystals are really advantageous for the determination of the structure of molecules. A crystal provides an amplification which multiplies the scattering of the X-rays from a single molecule by the number of molecules in the array, perhaps by 10^{15}. It also minimizes the damage to individual molecules by the viewing radiation. The spots are emphasized in the diffraction pattern and the background is neglected. The damaged molecules transfer their scattering contribution to the background as do those which are not repeated with regular lattice periodicity. However, defects and irregularities may be important and may well be lost in present-day sophisticated structural analyses.

It is perhaps worth pointing out that every crystal is in fact defective, even if its only defect is that it has surfaces. However, if a crystal is only a ten-unit-cell cube, about half of the unit cells lie in the surface and thus have environments very different from those of the other half. The physical observation is that very small aggregates need not be crystalline, although they may nevertheless be perfectly structured. Mackay's proposal is to apply the name *crystalloid* to them. He offered the following definitions [133]:

Crystal: The unit cell, consisting of one or more atoms, or other identical components, is repeated a large number of times by three noncoplanar translations. Corresponding atoms in each unit cell have almost identical surroundings. The fraction of atoms near the surface is small and the effects of the surface can be neglected.

Crystallite: a small crystal where the only defect is the existence of the external surface. The lattice may be deemed to be distorted but it is not dislocated. Crystallites may further be associated into a mosaic block.

Crystalloid: a configuration of atoms, or other identical components, finite in one or more dimensions, in a true free energy minimum, where the units are not related to each other by three lattice operations.

The above ideas have been further developed mainly by translating them into more quantitative descriptions and by applying them to

various structural problems. They can also be compared with similarly new definitions mentioned in the next Section. These new attempts of taxonomy by no means belittle the great importance of the 230 three-dimensional space groups and their wide applicability. What is really expected is that they will eventually help in the systematization and characterization of the less easily handled systems with varying degrees of regularity in their structures.

The appearance of *quasicrystals* on the scene of materials has given a great thrust to these developments.

9.8. Quasicrystals

The term "quasicrystal" was coined by Dov Levine and Paul Steinhardt, who studied the structure of metallic glasses by theoretical means and modeling [134]. Using this term, they wanted to express the connection between crystals on the one hand and *quasiperiodic* long-range translational order, on the other. Here, long-range translational order means that the position of a unit cell far away in the lattice is determined by the position of a given unit cell. In a crystal structure there is only one unit cell, whereas in a quasiperiodic structure there is more than just one. The repetition of the unit cell is regular in the crystal whereas it is not regular, nor is it random, in the quasiperiodic structure. In the two-dimensional space this is accomplished, for instance, by a Penrose tiling [135], which was originally created more as recreational mathematics than an extraordinarily important scientific tool that it has eventually become. A Penrose tiling is shown in the Introduction where some attempts of pentagonal tiling over the centuries are also mentioned. There is a detailed and systematic discussion of pentagonal tilings in Grünbaum and Shephard's book [136].

The discovery of the Penrose tilings was a breakthrough in that pentagonal symmetry occurred in a pattern otherwise described by space group symmetry. Curiously, the Penrose tiling was first communicated not by its inventor but by Martin Gardner in the January 1977 issue of *Scientific American* [137]. Mathematical physicist Roger Penrose himself published subsequently a paper in a university periodical which was then reprinted in a mathematical magazine. The title

of the communication was rather telling, *Pentaplexity*, with a more somber subtitle, *A Class of Non-Periodic Tilings of the Plane* [138].

Alan Mackay made the connection with crystallography [139]. He designed a pattern of circles based on a quasi-lattice to model a possible atomic structure. An optical transformation then created a simulated diffraction pattern exhibiting local tenfold symmetry (see, in the Introduction). In this way, Mackay virtually predicted the existence of what was later to be known as quasicrystals, and issued a warning that such structures may be encountered but may stay unrecognized if unexpected![‡]

The unique moment of discovery came in April 1982 when Dan Shechtman was doing some electron diffraction experiments on alloys, produced by very rapid cooling of molten metals. In the experiments with molten aluminum with added magnesium, cooled rapidly, he observed an electron diffraction pattern with tenfold symmetry (see, the pattern in the Introduction). It was as great a surprise as it could have been imagined for any well-trained crystallographer. Shechtman's surprise was recorded with three question marks in his lab notebook, "10-fold???" [140].

Fortunately, Mackay's fear that quasicrystals may be encountered but may stay unrecognized did not materialize. Although Shechtman was not familiar with the Penrose tiling and its potential implications for three-dimensional structures, he had what Louis Pasteur called, a *prepared mind* for new things [141]. He did not let himself discouraged by the seemingly well-founded disbelief of many though did not attempt to publish his observations until he and his colleagues found a model that could be considered a possible origin of the experimental observation. Ilan Blech constructed a three-dimensional model of icosahedra filling space almost at random, and added restrictions to the model stipulating that the adjacent icosahedra touch each other at edges, or, in a later version, at vertices. The model simulated a diffraction pattern, which was consistent with Shechtman's observations.

The first report about Shechtman's seminal experiment did not appear until two and a half years after the experiment. The delay

[‡]Alan L. Mackay gave two remarkable lectures on fivefold symmetry at the Hungarian Academy of Sciences, Budapest, in September, 1982, where he issued this warning.

was caused by Shechtman's cautiousness and by some journal editors' skepticism. The paper was titled modestly *Metallic Phase with Long-Range Orientational Order and No Translational Symmetry* [142]. It starts with the following sentence: "We report herein the existence of a metallic solid which diffracts electrons like a single crystal but has point group symmetry $m\bar{3}\bar{5}$ (icosahedral) which is inconsistent with lattice translations." The three-page report was followed by an avalanche of papers, conferences, schools, special journal issues, and monographs.

Independent of Mackay's predictions and Shechtman's experiments, there was another line of research by Steinhardt and Levine, leading to a model encompassing all the features of shechtmanite (the original quasiperiodic alloy was eventually named so) and other materials that are symmetric and icosahedral, but nonperiodic [143]. It was a perfect timing that as soon as they built up their model and produced its simulated diffraction pattern, they could see its proof from a real experiment.

Steinhardt, like Mackay before (see, Section 9.7), felt the need for redefinition of materials categories [144]. His suggestions now included the newly discovered quasicrystals. Steinhardt has succinctly characterized the crystals, glassy materials, and quasicrystals as follows:

> *Crystal*: highly ordered, with its atoms arranged in clusters which repeat periodically, at equal intervals, throughout the solid.
> *Glassy material*: highly disordered, with atoms arranged in a dense but random array.
> *Quasicrystal*: highly ordered atomic structure, yet the clusters repeat in an extraordinarily complex nonperiodic pattern.

The appearance of quasicrystals caused a minirevolution in crystallography. The lack of periodicity was a major obstacle in applying the traditional terms and approaches to this domain of materials. This was an interesting development also from the point of view of Mackay's suggestions for generalized crystallography. He truly anticipated the breakdown of the perfect traditional system, which he felt a little too perfect and, certainly, too rigid.

It has been suggested to treat quasicrystals as three-dimensional sections of materials that are periodic in more than three dimensions. On the other hand, a new and more general formulation of crystallography has also been proposed by David Mermin, which would stay within the realm of three-dimensionality and would not have the concept of periodicity in the focus of its foundation [145]. He compared abandoning the traditional classification scheme of crystallography, based on periodicity, to abandoning the Ptolemaic view in astronomy and likened changing it to a new foundation to astronomy's adopting the Copernican view. This is why he gave the title "Copernican Crystallography" to his communication. The suggestion was to build the new foundation on the three-dimensional concept of point-group operations that would have the concept of indistinguishable densities in its focus, rather than identical densities, to correspond to the character of quasisymmetries, describing, among others, the quasicrystals. Incidentally, the first challenge to the periodicity paradigm of crystallography was the observation of incommensurately modulated structures [146]. At that time, however, the new observations were brought into line with classical crystallography. The change in the periodicity paradigm has been discussed [147] in the light of Thomas Kuhn's *The Structure of Scientific Revolutions* [148]. Sadly, the giant of 20th century structural chemistry, Linus Pauling never accepted the notion of quasicrystals; instead, he maintained that the phenomena interpreted as quasicrystals could be explained in terms of known crystal formations within the realms of classical crystallography [149].

Figure 9-64 shows some beautiful representatives of quasicrystals and Figure 9-65 depicts another quasicrystal and a modern sculpture that could be taken as an artistic expression of a quasicrystal although the artist was not aware of the existence of such materials. The artistic appearance of quasicrystals, however, predates their scientific entry by centuries [150]. The discovery of such cultural monuments has generated lively discussions even in the general press [151].

Concluding, we quote again Mackay [155], who stated that

> Amorphous materials may be shapeless, but they are not without order. Order, like beauty, is in the eyes of the beholder. If you look only with X-ray diffraction eyes, then all you see is translational

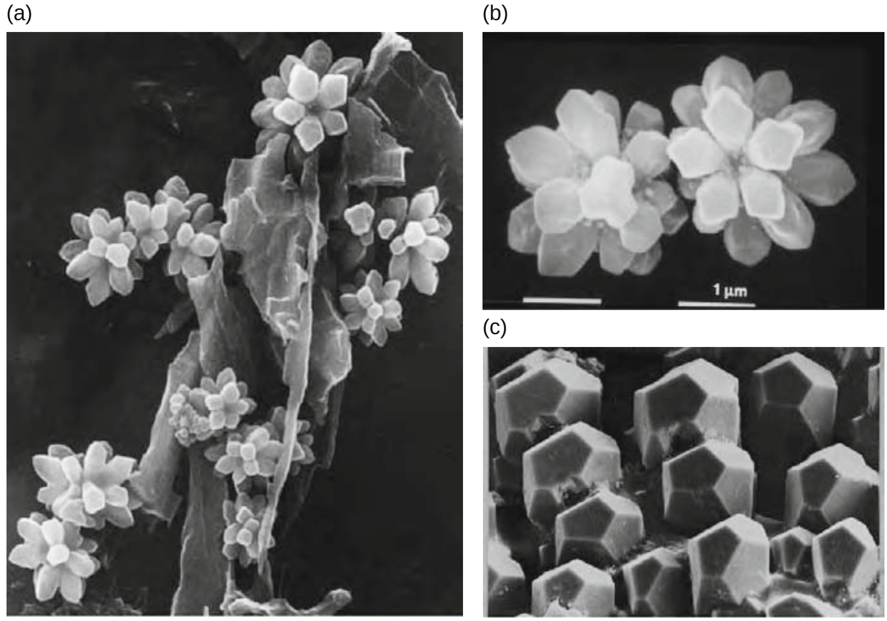

Figure 9-64. Quasicrystals: (**a–b**) Flower-like icosahedral quasicrystal in a quenched Al/Mn sample (from Csanády et al.) [152]; (**c**) Pentagonal dodecahedron in quasicrystalline Al/Cu/Ru obtained by slow cooling from melt (courtesy of H.-U. Nissen, Zurich) [153].

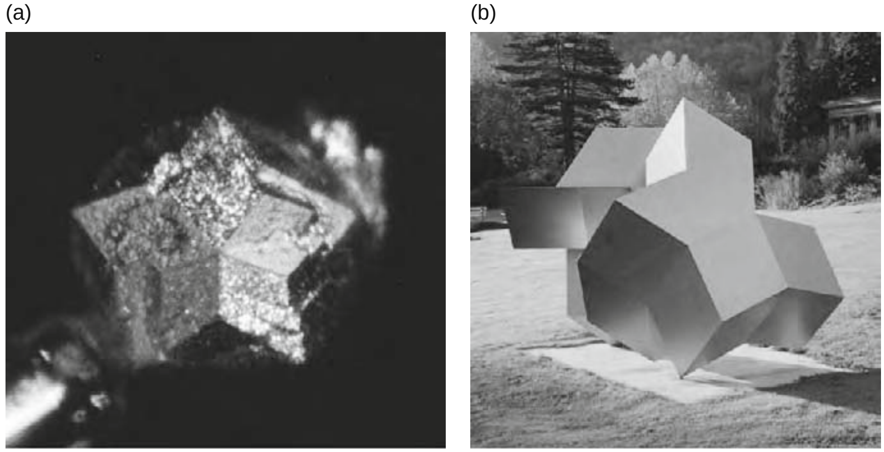

Figure 9-65. (**a**) Triacontrahedral quasicrystal Al/Li/Cu (courtesy of F. Dénoyer, Orsay) [154]; (**b**) Sculpture resembling a quasicrystal, by Peter Hächler, Switzerland. Photograph by the authors.

> order, to wit crystals. ... there is a wider range of structures, between those of crystals and those of gases, ... Other structures need not be failed crystals but are *sui generis*.

As crystallography is becoming more general, transforming itself into the science of structures, so may we anticipate a broadening application of the symmetry concept in the description and understanding of all possible structures [156].

9.9. Returning to Shapes

Concluding our discussion of crystal symmetries, let us return now to those exquisite shapes that we think of when the word *crystal* is mentioned. The words of the 19th century English writer John Ruskin [157] and drawings of C. Bunn [158] (Figure 9-66) are cited here.

> And remember, the poor little crystals have to live their lives, and mind their own affairs, in the midst of all this, as best they may. They are wonderfully like humane creatures—forget all that is going on if they don't see it, however dreadful; and never think what is to happen tomorrow. They are spiteful or loving, and indolent or painstaking, with no thought whatever of the lava or the flood which may break over them any day; and evaporate them into air-bubbles, or wash them into a solution of salts. And you may look at them, once understanding the surrounding conditions of their fate, with an endless interest. You will see crowds of unfortunate little crystals, who have been forced to constitute themselves in a hurry, their dissolving element being fiercely scorched away; you will see them doing their best, bright and numberless, but tiny. Then you will find indulged crystals, who have had centuries to form themselves in, and have changed their mind and ways continually; and have been tired, and taken heart again; and have been sick, and got well again; and thought they would

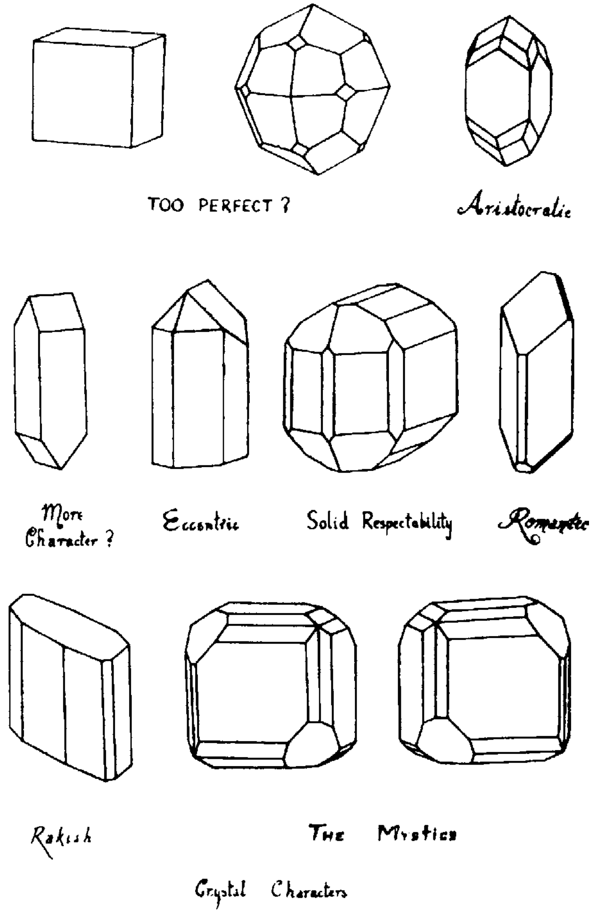

Figure 9-66. *Crystal characters* from C. Bunn's book [159]. Reproduced with permission.

try a different diet, and then thought better of it; and made but a poor use of their advantages, after all.

And sometimes you may see hypocritical crystals taking the shape of others, though they are nothing like in their minds; and vampire crystals eating out the hearts of others; and hermitcrab crystals living on the shells of others; and parasite crystals living on the means of others; and courtier crystals glittering in the attendance upon others; and all these, besides the two great companies of war and peace, who ally themselves, resolutely to

> attack, or resolutely to defend. And for the close, you see the broad shadow and deadly force of inevitable fate, above all this: you see the multitudes of crystals whose time has come; not a set time, as with us, but yet a time, sooner or later, when they all must give up their crystal ghost—when the strength by which they grew, and the breath given them to breathe, pass away from them; and they fail, and are consumed, and vanish away; and another generation is brought to life, framed out of their ashes.

References

1. G. Leclerc (Comte de) Buffon, *Historie Naturelle des Minéraux, III*. Paris, 1783–1788, p. 433; as quoted in A. L. Mackay, *A Dictionary of Scientific Quotations*. Adam Hilger, Bristol, 1991, p. 43.
2. K. Čapek, *Anglické Listy*, Československý Spisovatel, Praha, 1970. The English version cited in our text was kindly provided by Alan L. Mackay, London.
3. Ibid.
4. A. L. Mackay, "Duerer's technique." *Nature* 1983, 301, 652. A careful analysis of the drawing is available: E. Schröder, *Dürer. Kunst und Geometrie*, Akademie Verlag, Berlin, 1980.
5. S. Alvarez, "Polyhedra in (inorganic) chemistry." *Dalton Trans*. 2005, 2209-2233.
6. Ibid.
7. B. Ernst, *The Magic Mirror of M. C. Escher*, Ballantine Books, New York, 1976.
8. There is a beautiful book on the history of crystallography, *Historical Atlas of Crystallography*, J. Lima-de-Faria, ed., Kluwer, Dordrecht, 1990.
9. R. J. Haüy, *Traité de Cristallographie*, 1822. Reprinted by Culture et Civilisation, Bruxelles, 1968.
10. Ibid.
11. Ibid.
12. J. Kepler, *Strena seu de nive sexangula*, Francofurti ad Moenum: Godefridum Tampach, 1611. English translation, *The Six-Cornered Snowflake*, Clarendon Press, Oxford, 1966.
13. J. Dalton, *Memoirs and Proceedings of the Manchester Literary and Philosophical Society*, Manchester, 1805, vol. 6, p. 271; Alembic Club Reprints, Edinburgh, 1961, no. 2, p. 15.

14. C. J. Schneer, “The Renaissance Background to Crystallography.” *Am. Sci*. 1983, 71, 254–263; C. Schneer, “Kepler’s New Year’s Gift of a Snowflake.” *Isis* 1960, 51, 531–545.
15. Kepler, *The Six-Cornered Snowflake*.
16. Dalton, *Memoirs and Proceedings of the Manchester Literary and Philosophical Society*, p. 15.
17. A. L. Mackay, “Generalised Crystallography.” *Izvj. Jugosl. Cent. Kristallogr*. 1975, 10, 15−36. See, also, A. L. Mackay, “Generalised Crystallography.” *J. Mol. Struct*. (*Theochem*) 1995, 336, 293–303; A. L. Mackay, “Generalized Crystallography.” *Struct. Chem.* 2002, 13, 215–220.
18. See, e.g., L. A. Shuvalov, A. A. Urosovskaya, I. S. Zheludev, A. V. Zaleskii, S. A. Semiletov, B. N. Grechushnikov, I. G. Chistyakov, S. A. Pikin, *Sovremennaya Kristallografiya*, Vol. 4, *Fizicheskie Svoistva Kristallov*, Nauka, Moscow, 1981.
19. See, e.g., K. N. Trueblood, “Diffraction Studies of Molecular Motion in Crystals” and also, C. M. Gramaccioli, “Lattice-dynamical Interpretation of Crystallographic Thermal Parameters,” both in *Accurate Molecular Structures. Their Determination and Importance*, A. Domenicano, I. Hargittai, eds., Oxford University Press, Oxford, 1992, pp. 199–219 and pp. 220–236, respectively.
20. M. J. Buerger, *Elementary Crystallography, An Introduction to the Fundamental Geometrical Features of Crystals* (Fourth Printing), Wiley, New York, London, Sydney, 1967; E. S. Dana, *A Textbook of Mineralogy,* Fourth Edition, revised and enlarged by W. E. Ford, Wiley, New York, London, Sydney, 1932; P. M. Zorky, *Arkhitektura Kristallov*, Nauka, Moscow, 1968.
21. Gy. Lengyel, *Kézimunkák*, Kossuth, Budapest, 1978.
22. See, e.g., L. V. Azaroff, *Introduction to Solids*, McGraw-Hill, New York, Toronto, London, 1960.
23. Ibid.
24. Ibid.
25. *International Tables for Crystallography,* Volume A: *Space-group symmetry*. Ed. Th. Hahn. Corrected reprint of the fifth edition. Springer, 2005.
26. A. V. Shubnikov, V. A. Koptsik, *Symmetry in Science and Art*, Plenum Press, New York and London, 1974. Russian original: *Simmetriya v nauke i iskusstve*, Nauka, Moscow, 1972.
27. C. P. Brock and E. C. Lingafelter, “Common Misconceptions about Crystal Lattices and Crystal Symmetry.” *J. Chem. Educ.* 1980, 57, 552–554.
28. M. Senechal, “Brief History of Geometrical Crystallography.” In *Historical Atlas of Crystallography*, J. Lima-de-Faria, ed. International Union of Crystallography and Kluwer Academic publishers, Dordrecht, Holland, 1990, pp. 43–59, p. 48.
29. A. L. Mackay, “The Statistics of the distribution of crystalline substances among the space groups.”*Acta Crystallogr.* 1967, 22, 329–330.
30. See, e.g., A. I. Kitaigorodsky, *Molecular Crystals and Molecules,* Academic Press, New York, 1973. Russian original: A. I. Kitaigorodskii, *Molekulyarnie*

Kristalli, Nauka, Moscow, 1971; A. D. Mighell, V. L. Himes, J. R. Rodgers, "Space-group Frequencies for Organic Compounds." *Acta Crystallogr. A* 1983, 39, 737–740; J. Donohue, "Revised Space-group Frequencies for Organic Compounds." *Acta Crystallogr. A* 1985, 41, 203–204; R. Srinivasan, "On the Space-group Frequency in Organic Structures." *Acta Crystallogr. A* 1991, 47, 452; C. P. Brock, J. D. Dunitz, "Space-group frequencies." *Acta Crystallogr. A* 1991, 47, 854; A. J. C. Wilson, "Kitajgorodskij and Space-group Popularity." *ACH—Models in Chemistry* 1993, 130, 183–196; C. P. Brock and J. D. Dunitz, "Towards a Grammar of Crystal Packing." *Chem. Mater.* 1994, 6, 1118–1127.

31. Shubnikov, Koptsik, *Symmetry in Science and Art*. Russian original: *Simmetriya v nauke i isskustve.*
32. Ibid.
33. Ibid.
34. J. Dalton, *A New System of Chemical Philosophy,* p. 128, plate III, Manchester 1808.
35. D. Hodgkin, "Moments of Discovery." *Kristallografiya* (*Sov. Phys. Crystallogr.*) 1981, 26, 1029–1045.
36. Dalton, *A New System of Chemical Philosophy,* p. 128.
37. Hodgkin, *Kristallografiya* (*Sov. Phys. Crystallogr.*) 1029–1045.
38. Kitaigorodsky, *Molecular Crystals*; A. F. Wells, *Structural Inorganic Chemistry,* Fifth Edition, Clarendon Press, Oxford, 1984.
39. Wells, *Structural Inorganic Chemistry*.
40. Ibid.
41. Ibid.
42. Shubnikov, Koptsik, *Symmetry in Science and Art*.
43. Ibid.
44. Ibid.
45. G. G. Szpiro, *Kepler's Conjecture: How Some of the Greatest Minds in History Helped Solve One of the Oldest Math Problems in the World*. Wiley, Hoboken, New Jersey, 2003.
46. K. W. Adolph, D. L. D. Caspar, C. J. Hollingshed, E. E. Lattman, W. C. Phillips, W. T. Murakami, "Polyoma Virion and Capsid Crystal Structures." *Science* 1979, 203, 1117–1120.
47. Ibid.
48. R. B. Fuller, *Synergetics: Explorations in the Geometry of Thinking*, Macmillan, New York, 1975; p. 37.
49. D. L. D. Caspar, A. Klug, "Physical Principles in the Construction of Regular Viruses." *Cold Spring Harbor Symposia on Quantitative Biology* 1962**,** 27, 1–24.
50. R. E. Benfield, B. F. G. Johnson, "The Structures and Fluxional Behaviour of the Binary Carbonyls—A New Approach. 2. Cluster Carbonyls $M_m(CO)_n$ (n = 12,13,14,15, or 16)." *J. Chem. Soc. Dalton Trans*. 1980, 1743–1767.
51. A. L. Mackay, "A dense non-crystallographic packing of equal spheres." *Acta Crystallogr.* 1962, 15, 916−918.

52. K. H. Kuo, “Mackay, Anti-Mackay, Double-Mackay, Pseudo-Mackay, and Related Icosahedral Shell Clusters.” *Struct. Chem.* 2002, 13, 221–230.
53. Mackay, *Acta Crystallogr*. 916−918.
54. Wells, *Structural Inorganic Chemistry*.
55. Ibid.
56. See, e.g., B. C. Chakoumakos, R. J. Hill, G. V. Gibbs, “A Molecular-Orbital Study of Rings in Silicates and Siloxanes.” *Am. Mineral*. 1981, 66, 1237–1249.
57. Wells, *Structural Inorganic Chemistry.*
58. Ibid.
59. L. Pauling, *The Nature of the Chemical Bond*, Third Edition, Cornell University Press, Ithaca, NY, 1960.
60. W. Barlow, “Geometrische Untersuchung über eine mechanische Ursuche der Homogenitaet der Struktur und der Symmetrie.” *Z. Krist.* 1898, 29, 433–588.
61. Pauling, *The Nature of the Chemical Bond*.
62. J. Bernstein, “Effects of Crystal Environment on Molecular Structure.” In *Accurate Molecular Structures. Their Determination and Importance*, A. Domenicano and I. Hargittai, eds., Oxford University Press, Oxford, 1992, pp. 469–497; I. Hargittai, J. B. Levy, “Accessible Geometrical Changes.” *Struct. Chem.* 1999, 10, 387–389; V. Horváth, I. Hargittai, “Geometrical Changes and Their Energies in the Formation of Donor–Acceptor Complexes.” *Struct. Chem.* 2004, 15, 233–236.
63. Kitaigorodsky, *Molecular Crystals.*
64. Ibid.
65. Lucretius, *The Nature of Things* (*De rerum natura*). First edition, translated by F. O. Copley. W. W. Norton & Co., New York, 1977. This passage is quoted from Book VI, lines 1084–1086, p. 72.
66. Lord Kelvin, *Baltimore Lectures on Molecular Dynamics and the Wave Theory of Light*, Appendix H. C. J. Clay & Sons, London, 1904, pp. 618–619.
67. I. Hargittai, “Symmetry in Crystallography.” *Acta Crystallogr*. 1998, A54, 697–706; M. Hargittai, “Symmetry, crystallography, and art.” *Appl. Phys. A* 2007, 89, 889–898.
68. Lord Kelvin, *Baltimore Lectures on Molecular Dynamics and the Wave Theory of Light*, pp. 618–619.
69. A. I. Kitaigorodsky, in *Advances in Structure Research by Diffraction Methods*, R. Brill, R. Mason, eds., Vol. 3, p. 173, Pergamon Press, Oxford, etc., Friedr. Vieweg and Sohn, Braunschweig, 1970.
70. F. Wudl, E. T. Zellers, “2,5-Di-N-Chlorothioimino-3,4-Dicyanothiophene – A Novel Monomer of Unusual Molecular and Solid-State Structure” *J. Am. Chem. Soc*. 1980, 102, 4283–4284.
71. F. Wudl, E. T. Zellers, “1,1-Dichloro-2,5-Bis(N-Chlorothioimino)-3, 4-Dicyanoselenophene” *J. Am. Chem. Soc*. 1980, 102, 5430–5431.
72. C. H. MacGillavry, *Symmetry Aspects of M. C. Escher’s Periodic Drawings*, Bohn, Scheltema and Holkema, Utrecht, 1976.

73. L. Pauling, M. Delbrück, "The Nature of the Intermolecular Forces Operative in Biological Processes." *Science* 1940, 92, 77–79.
74. Ibid., p. 78.
75. Linus Pauling's Sir Jesse Boot Foundation Lecture titled "Molecular Architecture and the Process of Life" in Nottingham, England, 1948, is quoted by J. D. Dunitz, "Linus Carl Pauling, February 28, 1901-August 19, 1994." In *Biographical Memoirs*, vol. 71, National Academy Press, Washington, DC, 1997, p. 236.
76. A. I. Kitaigorodskii, "The Close-Packing of Molecules in Crystals of Organic Compounds." *J. Phys. (USSR)* 1945, 9, 351–352.
77. Ibid. *J. Phys. (USSR)* was an English-language periodical at one time in the Soviet Union.
78. P. M. Zorky, "The Development of Organic Crystal Chemistry at the Moscow State University." *ACH—Models in Chemistry* 1993, 130, 173–181.
79. H. A. Stuart, "Über neue Molekülmodelle." *Z. Phys. Chem.* (B) 1934, 27, 350–358; G. Briegleb, *Fortschr. chem. Forsch.* 1950, 1, 642.
80. Kitaigorodsky, *Molecular Crystals*; Kitaigorodsky, *Advances in Structure Research*.
81. A. Gavezzotti, G. R. Desiraju, "A Systematic Analysis of Packing Energies and other Packing Parameters for Fused-Ring Aromatic Hydrocarbons." *Acta Crystallogr. B* 1988, 44, 427–434.
82. J.-M. Lehn, "Supramolecular Chemistry." *Science* 1993, 260, 1762–1763.
83. G. D. Andreetti, A. Pochini, R. Ungaro, "Molecular Inclusion in Functionalized Macrocycles. 6. The Crystal and Molecular-Structures of the Calix[4]arene from Para-(1,1,3,3-Tetramethylbutyl)Phenol and Its 1-1 Complex with Toluene." *J. Chem. Soc. Perkin Trans II* 1983, 1773–1779; G. D. Andreetti, F. Ugazzoli, in *Calixarenes: A Versatile Class of Macrocyclic Compounds*, J. Vicens and V. Böhmer, eds. Kluwer, Dordrecht, 1991.
84. Andreetti, Ugazzoli, in *Calixarenes: A Versatile Class of Macrocyclic Compounds*.
85. J.-M. Lehn, "Supramolecular Chemistry—Receptors, Catalysts, and Carriers." *Science* 1985, 227, 849–856.
86. J. D. Dunitz, in *Host-Guest Molecular Interactions: From Chemistry to Biology*, D. J. Chadwick and K. Widdows, eds., John Wiley & Sons, Chichester, 1991, p. 92.
87. Kitaigorodsky, *Molecular Crystals*; Kitaigorodsky, *Advances in Structure Research*.
88. Kitaigorodsky, *Molecular Crystals*.
89. Ibid.
90. Ibid.
91. Ibid.
92. Ibid.
93. Ibid.
94. Ibid.
95. See, e.g., K. Mirsky, "Early Days in the Atom−Atom Potential Approach to Intermolecular Interactions." *ACH—Models in Chemistry* 1993, 130,

197–204; A. Gavezzotti and G. Filippini, "The Crystal Packing of Chlorine- and Sulfur-Containing Compounds." *ACH—Models in Chemistry* 1993, 130, 205–220, and references therein.

96. J. Maddox, "Crystals from 1st Principles." *Nature* 1988, 335, 201.
97. D. Braga and F. Grepioni, "Molecular Self-Recognition and Crystal Building in Transition-Metal Carbonyl Clusters—The Cases of $Ru_3(CO)_{12}$ and $Fe_3(CO)_{12}$." *Organometallics* 1991, 10, 1254–1259.
98. Ibid.
99. Mirsky, *ACH—Models in Chemistry,* 197–204; Gavezzotti, Filippini, *ACH—Models in Chemistry*, 205–220.
100. Zorky, *ACH—Models in Chemistry*, 173–181.
101. I. Hargittai, M. Hargittai, *In Our Own Image*: Personal Symmetry in Discovery. Plenum/Kluwer, New York, 2000, p. 112.
102. See, e.g., P. M. Zorky, E. E. Dashevskaya, "Hypersymmetry in Polysystem (Particularly in Multisystem) Molecular Crystals." *ACH—Models in Chemistry* 1993, 130, 247–259; P. M. Zorky, O. N. Zorkaya, "Specific Intermolecular Interactions in Organic Crystals: Conjugated Hydrogen Bonds and Contacts of Benzene Rings." In M. Hargittai, I. Hargittai, eds., *Advances in Molecular Structure Research*, Vol. 3, 1997, pp. 147–188.
103. P. M. Zorky, V. A. Koptsik, in *Sovremennie Problemi Fizicheskoi Khimii*, Ya. I. Gerasimov, P. A. Akishin, eds., Izd. Moskov. Univ., Moscow, 1979.
104. See, e.g., the special thematical issue devoted to the memory of P. M. Zorky in *Structural Chemistry* 2007.
105. Kitaigorodsky, in *Advances in Structure Research by Diffraction Methods*.
106. T. P. Martin, "Alkali-Halide Clusters and Micro-Crystals." *Phys. Rev*. 1983, 95, 167–199.
107. M. Hargittai, "Molecular Structure of Metal Halides." *Chem. Rev*. 2000, 100, 2233–2301.
108. B. Vest, Z. Varga, M. Hargittai, A. Hermann, P. Schwerdtfeger, "The Elusive Structure of $CrCl_2$ – A Combined Computational and Gas-Phase Electron Diffraction Study." *Chem. Eur. J*. 2008, 14, 5130–5143.
109. A. Hermann, B. Vest, P. Schwerdtfeger, "Density Functional Study of a-$CrCl_2$: Structural, Electronic, and Magnetic Properties." *Phys. Rev. B* 2006, 74.
110. Hargittai, *Chem. Rev*. 2233–2301.
111. U. Müller, *Inorganic Structural Chemistry*, Wiley, Chichester and New York, 1993.
112. Vest et al., *Chem. Eur. J.* 5130–5143.
113. Gas-phase study: G. Schultz, I. Hargittai, "Electron diffraction investigation of ethane-1,2-dithiol." *Acta Chim. Hung*. 1973, 75, 381–388; solid-state study: M. Hayashi, Y. Shiro, T. Oshima, and H. Murata, "The Vibrational Assignment, Rotational Isomerism and Force Constants of 1,2-Ethanedithiol." *Bull. Chem. Soc. Japan* 1965, 38, 1734–1740.
114. A. Domenicano, I. Hargittai, eds., *Accurate Molecular Structures. Their Determination and Importance*. Oxford University Press, Oxford, 1992.
115. I. Hargittai, M. Hargittai, "The importance of small structural differences" in *Molecular Structure and Energetics*, Vol. 2, Chapter 1, J. F. Liebman,

A. Greenberg, eds., VCH Publishers, Deerfield Beach, FL, 1986, pp. 1–35; M. Hargittai, I. Hargittai, “Gas-solid molecular structure differences.” *Phys. Chem. Miner*. 1987, 14, 413–425.
116. M. Hargittai, I. Hargittai, “Electron diffraction investigation of the molecular structures of two trimethylamine–boron halide adducts in the vapour phase.” *J. Mol. Struct*. 1977, 39, 79–89.
117. W. A. Burns, K. R. Leopold, “Unusually Large Gas-Solid Structure Differences—A Crystallographic Study of HCN–BF_3.” *J. Am. Chem. Soc*. 1993, 115, 11622–11623.
118. G. Forgács, M. Kolonits, I. Hargittai, “The gas-phase molecular structure of 1-fluorosilatrane from electron diffraction.” *Struct. Chem.* 1990, 1, 245–250.
119. J. Bernstein, *Polymorphism in Molecular Crystals*. Clarendon Press, Oxford, UK, 2002.
120. P. Scharfenberg, I. Hargittai,“ On the structural differences of conformers (A study on 1,2-disubstituted ethanes and ethenes).” *J. Mol. Struct*. 1984, 112, 65–70.
121. A. L. Mackay, “Crystal Symmetry.” *Phys. Bull*. 1976, 495–497; A. L. Mackay, “De Niva Quinquangula: On the pentagonal snowflake.” *Kritallografiya* (*Sov. Phys. Crystallogr*.) 1981, 26, 910–919 (517–522).
122. Ibid.
123. J. D. Bernal, “The Importance of Symmetry in the Solids and Liquids.” *Acta Phys. Acad. Sci. Hung*. 1958, 8, 269–276.
124. N. V. Belov, *Kristallografiya* 1972, 17, 208.
125. A. Wickham, *Selected Poems*, Chatto and Windus, London, 1971.
126. W. H. Zachariasen, “Atomic Arrangement in Glass.” *J. Am. Chem. Soc*. 1932, 54, 3841–3851; A. R. Cooper, “Zachariasen,WH – The Melody Lingers on.” *J. Non-Crystalline Solids* 1982; 49, 1–17.
127. A. Guinier, “Intermediary States between Order and Disporder.” In *Diffraction Studies on Non-Crystalline Substances*, I. Hargittai, W. J. Orville Thomas, eds., Elsevier, Amsterdam, 1981, pp. 411–438, p. 413.
128. M. Laridjani, P. Donnadieu, F. Dénoyer, “Experimental Overview of Complex Intermetallic Structures.” *Struct. Chem.* 2002, 13, 385–396.
129. Zachariasen, *J. Am. Chem. Soc*., 3841–3851.
130. Guinier, in *Diffraction Studies on Non-Crystalline Substances*, pp. 411–438, p. 417.
131. Mackay, *Kristallografiya*, 910–919.
132. Ibid.
133. Ibid.
134. D. Levine, P. J. Steinhardt, “Quasicrystals: A New Class of Ordered Structures.” *Phys. Rev. Lett.* 1984, 53, 2477−2480; For an overview, see, M. La Brecque, *Mosaic* 1987/88, 18, 1.
135. R. Penrose, “Pentaplexity.” *Eureka* 1978, 39, 16–22; R. Penrose, “Pentaplexity: A Class of Nonperiodic Tilings of the Plane.” *Math Intell*. 1979/80, 2, 32–37.
136. B. Grünbaum, G. C. Shephard, *Tilings and Patterns*, W. H. Freeman, New York, 1987.

137. M. Gardner, "Extraordinary Nonperiodic Tiling that Enriches the Theory of Tiles." *Sci. Amer*. 1977, 236, 110–121.
138. Penrose, *Eureka* 16–22; *Math. Intell*. 32–37.
139. A. L. Mackay, "Crystallography and the Penrose pattern." *Physica* 1982, 114A, 609–613.
140. Hargittai, Hargittai, *In Our Own Image*, p. 159.
141. "Dans les champ de l'observation, l'hasard ne favorise que les esprits préparés." (In the field of observation, chance only favors those minds which have been prepared). *Encyclopaedia Britannica* 1911, 11th edition, volume 20, quoted here after A. L. Mackay, *A Dictionary of Scientific Quotations*, Adam Hilger, Bristol, 1991.
142. D. Shechtman, I. Blech, D. Gratias, J. W. Cahn, "Metallic Phase with Long Range Orientational Order and No Translational Symmetry." *Phys. Rev. Lett*. 1984, 53, 1951−1953.
143. Levine, Steinhardt, *Phys. Rev. Lett*. 2477–2480.
144. P. J. Steinhardt, "Quasi-Crystals—A New Form of Matter." *Endeavour*, New Ser. 1990, 14(3), 112–116.
145. N. D. Mermin, "Copernican Crystallography" *Phys. Rev. Lett*. 1992, 68, 1172–1175.
146. P. M. de Wolff, W. van Aalst, "The Four-dimensional Space Group of γ-Na_2Co_3." *Acta Crystallogr. A* 1972, 28, S111; A. Janner, T. Janssen, "Superspace Groups." *Physica A* 1979, 99, 47–76.
147. J. W. Cahn, "Epilogue." In C. Janot, R. Mosseri, eds., *Proceedings of the 5th International Conference on "Quasicrystals," Avignon, 22–26 May 1995*. World Scientific, Singapore, 1995, pp. 806–810.
148. T. S. Kuhn, *The Structure of Scientific Revolutions*. Second, enlarged edition. The University of Chicago Press, 1970.
149. L. Pauling, "Apparent icosahedral symmetry is due to directed multiple twinning of cubic crystals." *Nature* 1985, 317, 512–514; L. Pauling, "Interpretation of So-called Icosahedral and Decagonal Quasicrystals of Alloys Showing Apparent Icosahedral Symmetry Elements as Twins of an 820-Atom Cubic Crystal." In I. Hargittai, ed., *Symmetry 2: Unifying Human Understanding*. Pergamon Press, Oxford, 1989, pp. 337–339.
150. P. J. Lu, P. J. Steinhardt, "Decagonal and Quasi-Crystalline Tilings in Medieval Islamic Architecture." *Science* 2007, 315, 1106−1110; E. Makovicky, F. Rull Pérez, P. Fenoll Hach-Alí, "Decagonal patterns in the Islamic ornamental art of Spain and Morocco." *Boletín de la Solidad Española de Mineralogía* 1998, 21, 107–127; I. Hargittai, "Pentagonal Decoration in Granada." *Math. Intell*. 1993, 15(2), 46–47.
151. See, e.g., J. N. Wilford, "In Medieval Architecture, Signs of Advanced Math." *The New York Times* 2007, February 27, p. F2. The findings and their reports generated some discussion of priority. On a similar controversy concerning the original discovery of quasicrystals, see, I. Hargittai, M. Hargittai, *In Our Own Image*, pp. 169–174.

152. A. Csanády, K. Papp, M. Dobosy, M. Bauer, “Direct Observation of the Phase Transformation of quasicrystals to Al_6Mn Crystals.” *Symmetry* 1990, 1, 75–79.
153. I. Hargittai, ed., *Fivefold Symmetry*. World Scientific, Singapore, 1992, p. xiv.
154. F. Dénoyer, “X-Ray Diffraction Study of Slowly Solidified Icosahedral Alloys.” In I. Hargittai, ed., *Quasicrystals, Networks, and Molecules of Fivefold Symmetry*, VCH, New York, 1990, pp. 69–82.
155. A. L. Mackay, “Quasi-Crystals and Amorphous Materials.” *J. Non-Cryst. Solids* 1987, 97&98, 55−62.
156. I. Hargittai, “Quo Vadis Crystallography?” *Z. Kristallogr*. 2002, 217, 314–315.
157. John Ruskin’s words are quoted here after L. V. Azaroff, *Introduction to Solids*. McGraw-Hill, 1960.
158. C. Bunn, *Crystals: Their Role in Nature and Science*. Academic Press, New York, 1964.
159. Ibid.

Epilogue

At the end of our journey with symmetry in chemistry, we may ask the question whether there is any specific chemical symmetry. Because of its unifying nature, the answer should be that there is only one symmetry concept. Yet there are different emphases in different fields. In chemistry, we are seeking more the presence of symmetry whereas in physics, the stress on symmetry breaking appears more manifested. Crystals, for example, are often used in physics to demonstrate symmetry breaking. This is understandable if we imagine ourselves to shrink to the atomic size. In this case our wandering inside the crystal gives us the impression of broken symmetry. For a chemist though the regularity of a crystal projects perfect symmetry. Thus, we have to take the scale into account when judging the presence or absence of symmetry.

Another consideration is the extent that determines the effect on whose basis we judge a property. Even the most extended monocrystal is finite hence cannot be considered infinite to satisfy the requirement of space-group symmetry. For an X-ray diffraction pattern though, whose existence testifies to its symmetry, the crystal needs to be merely *large enough* to produce such a pattern. Thus the infinity criteria can be fulfilled even within finite domains.

There is then the interesting question whether symmetry can be quantified or not? There have been elaborate and bona fide attempts for such quantification and quantitative comparisons. Their success is limited though because such questions can only be answered for specific features but usually not in a general sense.

Returning to the question whether chemical and physical symmetries may be different, there is, again, a difference in current research. In the physics of fundamental particles, the quest is still going on for

uncovering the most fundamental level of the organization of matter and finding the most universal level of symmetry. In chemistry, the quest is more for the enhanced utilization of the already familiar symmetries in areas of chemistry where they heretofore have not yet found application. A shining example of success was the introduction of symmetry considerations in predicting the feasibility of chemical reactions. Current studies are aiming at explaining and predicting structural differences between gaseous and crystalline structures and predicting and explaining different preferences of different substances for crystallization. Further successes may occur in areas that we might not even be thinking of yet as the next ones in the utilization of the symmetry concept. Symmetry has been a most fruitful concept in chemistry in understanding our science and making it more powerful. It has also enhanced our pleasures in doing chemistry and connecting it with other human endeavors.

In conclusion, we would like to stress that while symmetry is very important in chemistry, it is only an ingredient. There is no chemistry without the substances and their reactions and the separation of the products, and so on. We have to bear this in mind even when we are indulging in the symmetry aspects of our science.

Other Titles by the Authors

M. Hargittai, I. Hargittai, *Visual Symmetry*. World Scientific, Singapore, 2008.

I. Hargittai, *The DNA Doctor: Candid Conversations with James D. Watson*. World Scientific, Singapore, 2007.

I. Hargittai, *The Martians of Science: Five Physicists Who Changed the Twentieth Century*. Oxford University Press, New York, 2006 (soft cover, 2008).

I. Hargittai, *Our Lives: Encounters of a Scientist*. Akadémiai Kiadó, Budapest, 2004. German translation: *Wege zur Wissenschaft*, Lj-Verlag, Merzhausen, Germany, 2006.

M. Hargittai, I. Hargittai, *Képes szimmetria* (in Hungarian, *Pictorial Symmetry*), Galenus, Budapest, 2004.

I. Hargittai, *The Road to Stockholm: Nobel Prizes, Science, and Scientists*. Oxford University Press, Oxford, 2002 (soft cover, 2003). Japanese translation: Morikita, Tokyo, 2007; Chinese translation, Shanghai Scientific, 2007.

I. Hargittai, T. C. Laurent, eds., *Symmetry 2000* (in two volumes). Portland Press, London, 2002.

I. Hargittai, M. Hargittai, B. Hargittai, *Candid Science I – VI: Conversations with Famous Scientists*. Imperial College Press, London, 2000–2006.

I. Hargittai, M. Hargittai, *In Our Own Image: Personal Symmetry in Discovery*. Kluwer/Plenum, New York, 2000.

M. Hargittai, I. Hargittai, *Upptäck symmetri!* (In Swedish, *Discover Symmetry!*). Natur och Kultur, Stockholm, 1998. In Hungarian, *Fedezzük fel a szimmetriát*, Tankönyvkiadó, Budapest, 1989.

M. Hargittai, I. Hargittai, eds., *Advances in Molecular Structure Research*, Vols. 1–6. JAI Press, 1995–2000.

I. Hargittai, M. Hargittai, *Symmetry: A Unifying Concept*. Shelter, Bolinas, California, 1994. Abridged version in German: *Symmetrie: Eine neue Art, die Welt zu sehen*, Rowohlt Taschenbuch Verlag, Reinbek, 1998.

R. J. Gillespie, I. Hargittai, *The VSEPR Model of Molecular Geometry*. Allyn & Bacon, Boston, 1991. Russian translation: MIR, Moscow, 1992; Italian translation: Zanichelli, Bologna, 1994.

A. Domenicano, I. Hargittai, eds., *Accurate Molecular Structures*. Oxford University Press, Oxford, 1992. Russian translation: MIR, Moscow, 1997.

I. Hargittai, ed., *Fivefold Symmetry*. World Scientific, Singapore, 1992.

I. Hargittai, C. A. Pickover, eds., *Spiral Symmetry*. World Scientific, Singapore, 1992.

I. Hargittai, ed., *Quasicrystals, Networks, and Molecules of Fivefold Symmetry*. VCH, New York, 1990.

I. Hargittai, ed., *Symmetry 2: Unifying Human Understanding*. Pergamon Press, Oxford, 1989.

I. Hargittai, M. Hargittai, eds., *Stereochemical Applications of Gas-Phase Electron Diffraction* (in two volumes). VCH Publishers, New York, 1988.

I. Hargittai, B. K. Vainshtein, eds., *Crystal Symmetries, Shubnikov Centennial Papers*. Pergamon Press, Oxford, 1988.

I. Hargittai, ed., *Symmetry: Unifying Human Understanding*. Pergamon Press, Oxford, 1986.

M. Hargittai, I. Hargittai, *The Molecular Geometries of Coordination Compounds in the Vapor Phase*, Elsevier, Amsterdam, 1977. Russian translation, Mir, Moscow, 1976.

Index

A
Abelian groups, 171
Acetanilide crystal, 57–60
Acetic acid, 99
Acetylene (HC≡CH), 133
Adamantane ($C_{10}H_{16}$), 131–133
$Al_2Cl_7^-$ ion, 133–134
Al_2Cl_6 molecule, 133–134
Alkali sulfates, 138–139
Alkanes, 393
Alpha-helix, 387, 388, 389, 462
Aluminosilicates, 89
Aluminum trichloride, 117–118, 133–134, 356, 478–479
  ammonia complex, 117, 118, 356
  crystal structure, 478–479
Amino acids, 61, 69
Ammonia (NH_3) molecule
  atomic orbitals by symmetry properties, 274
  MO construction in, 268–269, 271–277
  symmetry operations, 171–172
Amorphous materials, 485, 492
Animals, 28, 43, 69, 70
Anisole, 465
Antarafacial approach, 338, 339
π Antibonding orbitals, 254–256, 264, 265, 268, 276, 280, 281, 283, 284, 287, 328, 331, 343, 344, 357
Anti-Hückel system, 351
Antiidentity operation, 197
Antimirror symmetry, 197–202
Antiprisms, 89–90, 130
Antisymmetry, 66, 67, 197–203
  elements, 197, 198
  operations, 197, 199
A_2O_3, 486
Arachno boranes, 124–126
Archimedean (semiregular) polyhedra, 88
Aristotle, 169
Aromaticity, 351, 353
Arsenic, 415, 416, 443
Asparagin, 74
Asymmetry, 34, 66–70, 107
Atomic orbitals (AOs), 249–250, 252–258, 260–261, 267–268, 291
$AuCl_3$ molecule, 303–304
Aulonia hexagona, 6
Average structures, 154, 300
Avogadro’s law, 5

B
Bach, J. S., 63
Bader-R. F. W., 313
Bader-Pearson method, 327
Balloon groups, 142
Band symmetries
  one-sided, 375–380
  two-sided, 378–381
Barlow, W., 437, 455
Bartók, B., 1, 32, 33
Basic laws of crystals, 416
Basis for representation, 222
Beauty and harmony, 17, 19–20
Bell, E. T., 484
Belousov, B. P., 392, 393
Belousov–Zhabotinsky reactions, 392–393
Belov, N. V., 79, 485
Bentley, W. A., 44, 48, 50
Benzene (C_6H_6), 116–118, 276–286
Bernal, J. D., 46, 371, 485
Berry, R. S., 156, 158
Berry pseudorotation, 158
Bersuker, I. B., 294, 295, 300, 301, 307–308
Berthelot, M., 2
Beryllium dichloride crystal, 382–383
Bethe, H., 290
Bickart, P., 16

Bicone, 40–41
Bijvoet, J. M., 62
Bilateral symmetry, 25–33
Biological macromolecules, 288, 387, 389, 391, 392
Biot, J. P., 61
Biphenyl, 476
Bipyramids, 40–41, 148
Blech, I., 490
Bochvar, D. A., 6
Bond length variation, 483
Bonding orbital, 254, 255, 264, 268, 276, 280, 331, 343, 347, 348, 357
Boranes, 120, 123, 124, 125, 159
Born–Oppenheimer approximation, 252, 295
Braga, D., 472
Bragg law, 409
Bravais lattices, 432–435
Brisse, F., 402, 405
Broken symmetries, 14–15
Brown, I. D., 149
Buckminsterfullerene, 4–6, 8–10, 89, 122–123
Bullvalene, 155, 157
Buerger, M., 395, 424
Bunn, C., 494, 495
Butadiene, 340–349

C

Calcium carbonate, 31
Čapek, K., 414
Carbides, 375, 381
Carbon dioxide (CO_2), 231, 233–236, 306
Carboranes, 123, 125
Carrol, L., 71
Cartesian displacement vectors, 185, 208, 213, 214, 221, 222, 235
Caspar, D. L. D., 447
Causes and effects, 68
Cesium chloride, crystal structure, 456
Character tables
- C_6, 280
- C_{2h}, 191, 195, 206, 207, 230
- C_{2v}, 209, 221, 263
- C_{3v}, 193, 194, 209, 271, 273
- C_{4v}, 259
- $D_{\infty h}$, 234
- D_{2h}, 334
- D_{3h}, 296
- D_{6h}, 278
- O_h, 358

Chargaff, E., 390
Chemical reactions, 313–370
Chiral drugs, 73
Chiral separation, 74
Chirality
- achiral, 68, 69, 74–76
- chiral forms, 64–65
- heterochiral, 61, 66, 74, 75, 76, 393
- homochiral, 61, 62, 65, 66, 75, 76, 78
- definition, 63–65
- importance, 69–74
- *La coupe du roi*, 74–77

Chiral pairs, 61–63, 69
Chromium dichloride, $CrCl_2$, 307, 478, 480
- Renner-Teller effect in, 307

Clifford, W. K., 239, 307
Close packing, 421, 422, 444, 445, 448, 449, 462
Closo boranes, 123–125
Closo carboranes, 123, 125
$Co_4(CO)_{12}$ structure, 159
$[Co_6(CO)_{14}]^{4-}$ structure, 160
Color symmetry, 200
Combined symmetries, 37–53
- rotation axis with intersecting symmetry planes, 37–39

Complementariness, 459, 461–462
Concerted reaction, 314, 326, 331, 336, 340–341, 343, 354
Conformational polymorphism, 481–482
Conformers, 100
Conical symmetry, 29
Conjugacy class, 174
Conjugates, 174
Connected polyhedra, in crystal dense packing, 449–453
Conrotatory process, 344, 348–350, 353
Conservation laws, 14, 313
Constitutional isomers, 99–100
Contergan, 72
Copernican crystallography, 492
Copernicus, 86
Correlation diagrams, 323, 326, 327, 330, 334, 344, 349
Correspondence diagrams, 327, 336, 337
Cotton, F. A., 135
Coulson, C. A., 19, 250, 326
Covalent radii, 137
Coxeter, H. S. M., 15–16, 79, 81, 119
Crick, F., 3, 4, 388–390, 462
Crick, O., 389
Crowe, D. W., 10, 379, 399
Crystal
- characters, 495
- definition of, 488, 491
- morphology, 2
- point groups, 423–425
- *See also* crystal symmetries

Crystal field effects, 476–483
Crystal field theory, 291–292
Crystallites, definition of, 488
Crystallographic groups, symmetry notations of, 104–105
Crystallography, 2, 10–11, 62, 81, 119, 401–402, 421, 424, 446, 461, 464, 482, 485, 490–492
  transition from classical to modern concepts of, 484
Crystalloid, definition of, 488
Crystal symmetries
  atomic arrangement in, 421–423
  axes in space groups, 425–426
  basic laws, 417–423
  Bravais lattices, 432–435
  characterization of, 432–433
  cleavage, 417–420
  crystal point groups, 423–425
  dense packing, 440–456
    atomic sizes, 453–456
    connected polyhedra, 414, 449–453
    icosahedral packing, 446–449
    molecular packing, 466–470
    sphere packing, 442–446
  infinite lattices, 432–434
  limitations on screw axes, 429–431, 435
  of minerals, 423–425
  molecular crystals
    crystal field effects, 476–483
    densest molecular packing, 466–470
    energy calculations, 470–473
    geometrical model, 457–465
    hypersymmetry, 474–476
    structure predictions, 470–473
  planar networks, 425, 427–428
  quasicrystals, 424, 489–494
  restrictions, 424–432
  space groups, 432–440
  stereographic projections, 423–426
  See also crystal
Cubane $(CH)_8$, 126–127, 129–130
Cube (hexahedron), 76, 79–80, 83
Cuboctahedron, 87–88, 90, 159, 448, 449
Curie, P., 67, 68, 69
Curie, M., 68, 69
Curl, R. F., 6, 7
Curtin, D. Y., 57, 59, 60
Cycloaddition reactions, 328–340, 350, 353
Cyclobutane, 330–335, 338
Cyclopentane $(CH_2)_5$, 153
Cylindrical symmetry, 29–32, 40–41

D
Dalton, J., 421, 422, 440, 443
da Vinci, Leonardo, 7, 8, 82
Decorations, side-effects of, 406–408
Degas, E., 101, 102
Degeneracy, 192, 243–244, 258, 260–261
Deisenhofer, J., 108, 109
Delbrück, M., 459, 461
Democritos, 473
Dendrimers, 44
Dense packing in crystals, 440–456
  connected polyhedra, 449–453
  icosahedral packing, 446–449
  molecular packing, 466–470
  sphere packing, 442–446
Densest molecular packing, 466–470
Deoxyribonucleic acid (DNA)
  C_2 symmetry in, 107–108
  double helix, 71
  molecular structure of, 3, 388
Descartes, 48
Dewar, M. J. S., 351, 353
Diadamantane, 132–133
Diamond structure, 438–440
Diastereomers, 99
Diatomic molecule
  rotation of, 218–220
  translational degrees of freedom of, 219–220
Dibenzene chromium, $(C_6H_6)_2Cr$, shape and symmetry, 134–135
1,2-Dibromo-1,2-dichloro-ethane molecule, 53
1,7-Dicarba-*closo*-dodecaborane (m-$C_2B_{10}H_{12}$), 159, 160
1,2-Dicarba-*closo*-dodecaborane (o-$C_2B_{10}H_{12}$), 159, 160
1,12-Dicarba-*closo*-dodecaborane (p-$C_2B_{10}H_{12}$), 159, 160
1,2-Dichloroethylene, 102–104
Diels–Alder reaction, 326, 340–343
1,2-Dihaloethanes, 483
Diimide (HNNH), 184, 204, 207, 229–233
Dimensionality, 56, 57, 58, 195, 371, 372, 492
Dimethyl sulfate, 146
Dimolybdenum tetraacetate, 136
Dirac, P. A., 14
Direct product, 209, 241, 262, 263, 302, 348
Disrotatory reaction, 344–345
Dissymmetry, 66–70
Dodecahedrane $(CH)_{20}$, 127–129
Dodecahedron, 76–77, 79–80, 82–85, 122
Donor-acceptor complexes, 356, 480
Double-headed eagles, 33

Double helix, 3, 71, 107, 387–390
Dove-tail packing, 458, 459
Dunitz, J. D., 465
Dürer, A., 10, 16, 414, 416
Dynamic properties, 212–213

E
Eclipsed conformation, 101, 134
Egyptian sculptures, 27
Eiffel Tower, 41
Einstein, A., 14
Electrocyclic reactions, 350
Electron diffraction, 11–12, 146, 158, 307, 490
Electronic structure
  changes during chemical reaction, 324–325
  conservation of orbital symmetry, 326–327
  frontier orbitals, 325–326
  maximum symmetry analysis, 327–328
  wave function description of, 241–249
Electronic wave function
  fundamental property, 240
  of hydrogen atom, 241–249
  many-electron atoms, 249–251
  one-electron atom, 241–249
  symmetry properties of, 240–241, 246
Emerson, R. W., 217
Enantiomers, 71, 73, 100
Enantiomorphs, 61, 68–69
Energy calculations, for molecular crystals, 470–473
Environmental symmetry, influence of, 290–294
Equilibrium structure, 154–155
Erni, H., 65, 66
Escher, M. C., 119, 402, 404, 406, 415, 459, 461
Ethambutol, 74
Ethane, 103, 104, 133, 362
Ethylene cycloaddition, 343
Ethylene dimerization, 328–340
  correlation diagram, 332–333, 335
  correspondence diagram, 337
  frontier orbital method, 328–329
  HOMO and LUMO of, 328–329
  MOs of ethylene–ethylene system, 332, 335
  orthogonal approach, 338–340
  parallel approach, 328–332, 336–338
  state correlation, 332–336
  symmetry of reactants, transition structure and product in, 330
  Woodward–Hoffmann approach, 329
Euclid, 484
Euler, 78, 80

F
Faraday, M., 19
Fedorov, E. S., 15, 46, 416, 437, 459
Fejes Tóth, L., 81
Ferrocene, 134–135
Fibonacci series, 384–385
Fischer, E., 62
Flowers, 28–29, 34–35, 37–39, 43, 47
Folk music, 31–33
Free and crystalline molecules, structure differences in, 477–481
Frontier orbitals, 325–326
Fukui, K., 3, 313, 324, 325, 326, 328, 340
Fuller, R. B., 4, 5, 6, 9, 446, 447, 473
Fullerenes, 5–6, 8, 122–123

G
Gal'pern, E. G., 6, 7
Gardner, M., 65, 489
Gas/solid structural differences, 478
Gaudi, A., 200, 201
Gay-Lussac, J. L., 287
Generalized crystallography, 424, 485, 491
Generalized Woodward-Hoffmann rules, 350
Genuine modes, 220
Geodesic Dome, 6, 447
Geometrical isomers, 100
Geometrical model, of molecular crystals, 457–465
  arrangements of molecular shapes, 458–459
  dove-tail packing, 459–460
  head-to-head arrangement, 459–460
  head-to-tail arrangement, 459–460
Geometrical symmetry, 37
Gillespie, R. J., 151
Glassy materials, definition of, 491
Glide mirror, *see* Glide reflections
Glide reflections, 372–374, 378
Goniometers, 417–418
Graphite, 6, 9, 122, 403
Great dodecahedron, 85
Great icosahedron, 85
Great stellated dodecahedron, 85
Grepioni, F., 472
Gross, D. J., 12
Groth, P., 59
Group orbitals, 258
Groups, 169–197, 204–215
  classes of, 174
  elements, 170–172
  irreducible representation of, 189
  multiplication tables for, 172, 173
  order of class and subgroup, 175

reducible representation of, 189
representation of, 183–189
similarity transformations in, 174–175
subgroups, 174
Group theory,120, 169–197, 204–215
Grünbaum, B., 405, 489
Guinier, A., 486, 487

H

Haeckel, E., 39, 80, 81
Häckel, E., 6
Haldane, J. B. S., 70, 71
Halevi, F. A., 313, 327, 328, 336
Halevi's method, 328
Hamiltonian operator, 240
Handedness, 3, 65, 70–72
Hauptman, H., 448, 449
Haüy, 418, 419, 420, 421
Helical symmetry, 391
Helices, translational symmetry of, 3
Helium (He), MO construction in, 265
Helix structure, 389
Heptaprismane ($C_{14}H_{14}$), 130
Heraldic symmetry, 33
See also bilateral symmetry
Hermann-Mauguin symmetry notations, 104
Heterochiral, 61
chairs, 66
pairs of hands, 61
segment, 74–75
Heteronuclear diatomic molecules, 256
Hexaprismane ($C_{12}H_{12}$), 127, 130
Highest occupied molecular orbital (HOMO), 325–327
of ethylene, 328–329
$H_3N \cdot AlCl_3$ donor–acceptor complex, 117–118
Hodgkin, D., 440, 442
Hoffmann, R., 3, 4, 313, 314, 324, 326, 327, 328, 329, 331, 350, 351, 353, 354, 355, 356, 360, 363
HOMO, 325–329, 335, 340, 341, 343, 356
Homochiral, 61
chairs, 66
pairs of hands, 61–62
segment, 75
Homomers, 100
Homonuclear diatomic molecules, 256–257, 263–266
Houk, K. N., 318
Hubcaps, 34–35
Hückel–Möbius concept, 350–355
Hückel ring, 351, 354
Hückel system, 351, 353
Huffman, D., 9, 10
Human body
bilateral symmetry of, 27
symmetry of, 25–27, 30
Human face, symmetry plane of, 30
Humphreys, W. J., 48, 50
Hund, F., 251, 304, 326
Hund's rule, 304
Hydrogen atom, 241–249
Hydrogen (H_2) molecule, 263–264
Hydrogen-like orbitals, *see* Atomic orbitals (AOs)
Hypersymmetry, in molecular crystals, 474–476
Hypostrophene, 156, 157

I

Iceane hydrocarbon molecule, 131
Ice crystal, 131
Icosahedral packing, 446–449
Icosahedral quasicrystal, 493
Icosahedral structures, 9
Icosahedron, 77, 79, 80, 83–85, 106, 125, 159
Icosidodecahedron, 87–88
Identity operation, 197
Infinite lattices of crystal, 432–434
Insulin, 440, 441, 442
Intermolecular atomic radii, 457
Internal coordinates, 213, 214, 224, 225, 229, 230, 236
International notations, *see* Symmetry
Intramolecular
cyclization, 343–450
orbital correlation for, 343–346
symmetry of reaction coordinate, 346–350
motion consequences, 153–161
nonbonded interactions, 136–138
geometrical consequences of, 138
1,3 separations, 136–137
van-der-Waals interactions, 137
Inversion operation, 205, 246, 249
Inversion symmetry, 53–55
Iodine atom, total wave function of, 248
Iodine heptafluoride (IF_7), 158
$Ir_4(CO)_{12}$, 160
Iron dendrites formation, 31–32
Irreducible representation, 189–191
properties, 191–197
symbols for, 194
Isolobal analogy, 356–364
Isomers, 98–100
conformers, 100
constitutional, 99

diastereomers, 99–100
enantiomers, 100
geometrical, 100
hierarchy of, 100
homomers, 100
rotational, 99–100
structural, 99–100

J

Jahn–Teller active vibrations, 296
Jahn–Teller distortion, 295–297, 300–305, 307
Jahn–Teller effect, 294–308, 323
Jahn–Teller phase transition, 301
Jahn–Teller stabilization energy, 300
Jones, D. E. H., 5–6

K

Kaolin, 453
Kekulé, 19
Kelvin, Lord/Thomson, W. H., 60, 458, 459
Kepler, J., 10, 28, 42, 47, 80, 82, 161, 421, 443, 486
Keplerates, 81
Kitaigordskii/Kitaigorodsky, A. I., 441, 467, 468, 473
Klug, A., 391, 447
Knowles, W. S., 74
Koestler, A., 1, 2, 80
Kohn, W., 287, 288
Kolbe, H., 97
Koptsik, V. A., 75, 406, 438, 439, 440, 445, 474
Kotel'nikova, A., 135
Krätschmer, W., 9, 10
Kroto, H. W., 6, 7
Kuhn, T., 492

L

Landau, L. D., 305, 306
Law of rational indices, 417, 420
Law of rational intercepts, 417, 418, 420
Laws of nature, and symmetry, 12–14
Leaves, bilateral symmetry in, 28–29
Le Bel, J. A., 97
Lee, T. D., 14, 15
Left-and-right symmetry, 14
Left-handed helices, 65
Lehn, J.-M., 465
Levine, D., 489, 491
Levine, R. D., 289
Lewis, G. N., 71, 151, 152, 357
Lewis' theory, 151–152
Ligand field theory, 214, 290
Limiting groups, 104–105
Limonene, 74
Linear combination of atomic orbitals (LCAO), 252
Lipscomb, W. N., 159
Lipscomb model, of rearrangement in polyhedral boranes, 159
L-nucleotides, 71
Logos with rotational symmetry, 35–36
Long-range pentagonal symmetry, 10
Longuet-Higgins, H. C., 326, 334
Lowest unoccupied molecular orbitals (LUMO), 325–329
Lu, G.-D., 47
Lucretius, 2, 457, 458
Lunar Module, 30

M

MacGillavry, C., 402, 461
Mackay, A. L., 10, 11, 31, 70, 448, 483, 484, 486, 487, 488, 490, 491, 492
Mackay icosahedron, 448
Mamedov, K., 404, 406
Manganese trifluoride molecule, MnF_3, Jahn–Teller distortion of, 302–303
Mann, T., 25, 26, 44, 46
Many-electron atoms
order of orbital energies in, 250–251
wave function, 249–251
Marginal stability, 42
Matisse, H., 30, 153, 154, 155
Matrices
character of, 190
column matrices, 177
dimension, 176
mathematical tool for symmetry operations, 176–183
square matrix, 176
unit matrix, 176
vectors and, 177–178
Maximum symmetry analysis, 327–328
Mazurs, E. G., 17
Mendeleev, D. I., 17, 18, 30
Mendeleev's periodic system, 18
Mermin, D., 492
Metal halide molecules, 155
Metal–carbonyl clusters, 160–161
Metal–metal multiple bonds, 135
Methane, 133
consequences of substitution on symmetry of, 115–118
molecular shape, 120–121, 143–145
2-Methyl-1,4-butandiol, 75, 77

p-Methyl-N-(p-methylbenzylidine) aniline, 482
Mexican-hat type potential energy surface, 303–304
Meyer, V., 97
Michelangelo, 253
Miller indices, 420
Minimum energy path, 320
Mirror operation for movements, 213
Mirror-rotation symmetry axis, 55
Mirror symmetry, 175, 197–198
Mislow, K., 16, 78
Moiré patterns, 408–410
Molecular crystals
  arrangements of molecular shapes, 458–459
  crystal field effects, 476–483
  densest molecular packing, 466–470
  energy calculations, 470–473
  geometrical model, 457–465
  hypersymmetry, 474–476
  structure predictions, 470–473
Molecular orbitals (MOs), 252–261
  antibonding orbital, 254–255
  from atomic orbitals, 253–257
  bonding orbital, 254–255
  construction of
    ammonia, 268–269, 271–277
    benzene, 276–286
    helium molecule, 265
    homonuclear diatomics, 263–266
    hydrogen molecule, 263–264
    polyatomic molecules, 266–286
    water molecule, 266–270
  energy changes during formation of, 256–257
  rule for construction of, 253–254
  symmetry of, 258
Molecular packing, 466–470
Molecular point groups
  establishing, 105–107
  symmetries, 104
Molecular polarity, 57–60
Molecular recognition, 289, 464, 465
Molecular shapes
  electronegative ligands and, 146–148
  with lone pair, 145–147, 149
  with multiple bonds, 145–146
  from points-on-the-sphere model, 141
  relative availability of space in valence shell and, 147–148
  VSEPR model, 143–151
Molecular vibrations
  of carbon dioxide, 231, 233–236
  in diimide, 229–233
  normal modes, 217–225
  selection rules, 227–229
  symmetry coordinate, 225–227
Molecules, 252–287
  consequences of substitution on symmetry of, 115–118
  electronic states, 261–263
  homonuclear diatomics, 263–266
    helium, 265
    hydrogen, 263–264
  many-electron atom, 249–251
  molecular orbitals, 252–261, 264, 286–287
  one-electron wave function, 241–249
  polyatomic molecules, 266–286
    ammonia, 268–269, 271–277
    benzene, 276–286
    water, 266–268
Movements, mirror operation for, 213
Möbius ring, 352, 355
Möbius systems, 351, 353–354
Muetterties, E., 119, 123, 125, 126
Mulliken, R. S., 193, 195, 326
Mulliken symbols, 193, 195
Multiplicity, 55
Music, 31–33

N

Nakaya, U., 48, 49, 50, 51, 52, 53
Nanoscience and nanotechnology, 4, 122
Nanotubes and nanorods, 381–382
Naproxen, 74
Natta, G., 385, 388
Needham, J., 47
Newman, J., 169
Noether, E., 313
Nonbonded distances, regularities in, 136–139
Noncrossing rule, 327, 335, 336
Noncrystallographic symmetry, 10
Non-enantiomorphous symmetry, 63
Norgestrel, 74
Normal coordinate analysis, 214, 226
Normal modes
  bending mode, 224
  deformation modes, 224
  of molecular vibrations, 217–225
  number, 218–220
  stretching modes, 224
  symmertry, 220–224
  types, 224–225
n-Prismanes ($C_{2n}H_{2n}$), 130
Noyori, R., 74
Nyholm, R. S., 151

O

$OClF_3$, molecular configuration of, 140
Octahedral AX_6 molecules, consequences of substitution, 115–117, 150
Octahedron, 76, 79–81, 83
  notations, 450, 452–453
One-dimensional space-groups, 376, 381, 385, 387
  scheme for establishing symmetry class of, 398–399
One-electron atom
  wave functions, 241–249
  radial wave function, 241–242, 244–245
  symmetry properties, 246
One-electron orbitals, shapes of, 246–247
One-sided bands, symmetry classes, 375–378
One-sided planar networks, symmetry classes of, 397
ONF_3 molecular geometry, 136
OPF_3 molecular configuration, 140, 149
Optical activity, 61–63, 92
Orbital correlation diagrams for
  butadiene–cyclobutene interconversion, 343–346
  Diels–Alder reaction, 340–343
  ethylene–butadiene cycloaddition, 342–343
  intramolecular cyclization, 343–346
Orbitals, 242
  effect of inversion on, 246, 248–249
  sequence of energies in, 250–251, 266
  symmetry conservation, 3, 326–327
d orbitals
  energies in octahedral and cubic environment, 292–293
  splittings in different ligand environments, 292–294
  symmetry in octahedral and cubic environment, 291–292
Orgel, L. E., 71, 72
Osawa, E., 6, 7
Oscillating reactions, 392

P

Pacioli, L., 7, 8, 82
Paddlanes, 135–136
Paracrystal lattice, 486–487
Parity violation, 70
Pasteur, L., 61, 62, 64, 67, 68, 70, 71, 490
Pasteur's models, 61, 64
Paul, I. C., 59, 60
Pauli exclusion principle, 151, 251
Pauling, L., 17, 137, 387, 388, 389, 390, 455, 459, 461, 462, 492
p-chloroacetanilide crystal, 57, 59
Pearson, R. G., 313, 320, 327, 347, 348, 349
Penicillamine, 74
Penrose, R., 10, 11, 489, 490
Penrose tilings, 11, 489
Pentagonal dodecahedron, 79, 80, 82, 84, 493
Pentagonal prism, 40–41
Pentagonal symmetry, 10, 79, 489
Pentaprismane ($C_{10}H_{10}$), 127, 130, 156
Periodic tables, 17–19
Permutational isomerism, 156–157
PF_3Cl_2, 149
PF_2Cl_3, 149
PF_5-type molecules, 158
Phosphine, 147
Photosynthetic reaction center, 107–109
Piezoelectricity, 60
Pinecone scales, 384
Planetary model, 80, 82
Plantago media, 384–385
Plato, 76
Platonic solids, 76–81, 88, 126, 128
  See also regular convex polyhedra
Point group
  dimensionality and periodicity in symmetry, 56–58
  establishing, 105–107
  symmetry, 55–56, 104–105
Point groups, 105–115
  C_{2h}, 105, 191, 195, 230
  C_{nh}, 105, 107
  C_{nv}, 105, 107
  C_s, 105, 109, 178, 179, 349
  C_1, 105, 189
  C_2, 105, 108, 170, 173, 184
  C_3, 105, 108, 173, 193, 272, 273
  C_4, 105, 108, 115
  C_5, 105, 108, 115
  C_6, 108, 115
  C_{2v}, 105, 111, 193–194, 209, 221
  C_{3v}, 105, 111, 209, 268, 271, 273
  C_{4v}, 105, 111, 258–260, 360
  $C_{\infty v}$, 105, 111
  D_{2d}, 105, 112
  D_{3d}, 105, 112
  D_{4d}, 125, 112
  $D_{\infty h}$, 105, 114, 231, 263, 264, 265
  D_{2h}, 105, 113, 328, 330
  D_{3h}, 105, 113
  D_{4h}, 105, 113
  D_{5h}, 105, 113
  D_{6h}, 105, 113, 277–278
  D_{nd}, 106–107
  D_{nh}, 106
  D_2, 105, 111, 328, 330

D_3, 105, 111
D_4, 105, 111
D_5, 105, 111
I_h, 115
O_h, 115, 261, 291
S_4, 105, 110
S_6, 105, 110
T, 105
T_d, 105, 125
T_h, 105
Points-on-the-sphere model, 141
Polanyi, M., 17, 318
Polar axis, 57
Polarity and symmetry, 57, 59–60
Polar line, 57
Polycyclic hydrocarbons, 125–132
Polyethylene chain molecule, 385–386
Polyhedral boranes, 159
Polyhedral molecular geometries, 119–161
boron hydride cages, 123–125
intramolecular motion consequences, 153–161
non-bonded distances regularities, 136–139
polycyclic hydrocarbons, 125–132
structures with central atom, 133–136
VSEPR model, 139–153
analogies, 142–143
historical perpectives, 151–153
molecular shapes, 143–151
Polyhedrane molecules, 119, 128
Polyhedra, 76–90
Polymorphism, 481–483
Polypeptide chain, helical structures, 387–388
P_4O_6, 132
$(PO)_4O_6$ molecule structure, 132
Pople, J., 287, 288
Potassium tetrafluoroaluminate ($KAlF_4$), 133–134
Potential energy surface, 315–324
reaction coordinate, 319–320
saddle point, 316, 318
transition state and transition structure, 316–319
Powell, H. M., 151
Pólya, G., 405, 407
Prelog, V., 2, 65, 66, 69, 70
Primitive organisms, pentagonal symmetry of, 79–80
Principal quantum numbers, 241–242
Prismane molecules, 119, 130
Prismatic cyclopentadienyl, 134
Prisms, 89–90, 125, 130
symmetry, 40–41
Projection formulae, 101
Projection operator, 211–212
Propoxyphene, 74
Pseudo-Jahn–Teller effect, 294, 307, 323
Pseudorotation, 153, 154, 158, 159
Pseudosymmetry, 314
Pyroelectricity, 60

Q
Quantum chemical calculations, 151, 154, 258, 287–290, 304, 319, 338, 340, 343, 350, 353, 483
Quantum numbers, 241–242, 250
Quartz crystals, 63, 68, 417
Quasicrystals, 4, 9, 11, 424, 489–494
Quasi-regular polyhedra, 89

R
Radial symmetry, 29, 31
Radiolarians, 80, 81
Rational indices, law of, 417, 420
Rational intercepts, law of, 417–418, 420
Reaction coordinate, 319–320
symmetry rules for, 320–324
Reducible representation, 189–191
Regular convex polyhedra, 76–80, 83–85, 89–90
characteristic symmetry elements, 77, 79–80
Regular dodecahedron, 79, 84, 119
Regular icosahedron, 79, 123
Regular pentagonal dodecahedron, 80, 82
Regular polygons, 77, 78, 84, 90
Regular star polyhedra, 85
Regular tetrahedron, 117, 121, 133
Renner, R., 294, 305, 306, 307
Renner–Teller effect, 294, 306–307
Representation
character of, 191–197
of groups, 183–189
irreducible, 189–191
reducible, 189–191
reduction, 206–208
shortcut to determine, 204–205
Reston, J., 54
Reverse coupe du roi, 76
$Rh_4(CO)_{12}$, 159
Rhombicosidodecahedron, 87
Rhombicuboctahedron, 87
Rock salt crystal structure, 438–440
Rotational isomerism, 100–104
projectional representation, 102, 104
Rotational isomers, 99–100
Rotational symmetry, 33–36
elemental angle, 34

in flowers, 34
in hubcaps, 34–35
logos with, 35–36
in machinery rotating parts, 34–35
in Norwegian tulip, 37–38
order of, 33–34
in sculptures of interweaving fish and dolphins, 36
in Taiwanese stamp with two fish, 33–34
in *Vinca minor*, 37–38
in yin yang contour, 33–34
Rotation axis with intersecting symmetry planes, 37–39
$Ru_3(CO)_{12}$, 472–473
Ruskin, J., 494

S

Saddle-shaped sculpture, 317
Salem, L., 314, 326
Scattered leaf arrangements , 384, 392
Schoenflies notation, 104–105
Schrödinger, E., 240, 241, 252
Schrödinger equation, 240–241, 252
Scoresby, W., 48, 49
Screw-axis symmetry, 382–384
Screws, 64–65
Scriven, M., 16
Selection rules, in molecular vibrations, 227–229
Semiregular (Archimedean) polyhedra, 87–90
Shared electron pair, 151–152
Sharpless, K. B., 74
Shechtman, D., 11, 12, 490–491
Shephard, G. C., 405, 489
Shubnikov, A. V., 10, 15, 67, 68, 75, 198, 199, 406, 438, 439, 440, 445
$SiBr_2$, bending potential energy functions, 156
Sidgwick, N. V., 151
Similarity transformation, 174
Simulated diffraction pattern, 11
Single bond, rotational isomerism relative to, 103–104
Singular point symmetry, 55–57
Small stellated dodecahedron, 85
Smalley, R. E., 6, 7
$Sn[Fe_2(CO)_8]_2$, molecular geometry of, 363
Snow crystals, 40, 42, 43, 46, 47, 48, 49, 53
Snowflakes
classification, 50–53
formation, 44, 49–50
hexagonal symmetry, 42, 47–50
malformed crystals, 50
morphology of, 40, 42–44
photomicrographs, 48, 50
symmetries, 39–53, 55
Snub cube, 87, 90
Snub dodecahedron, 87
SO_2Cl_2, 171, 182
Sodalite unit, 89
Sodium chloride, 416–417, 454–455, 477
Space-groups symmetries, 56
band symmetries, 375–381
in crystal symmetries, 432–440
dimensionality, 372
expanding to infinity, 371–375
glide-reflection, 373–374, 380
identity period in, 373, 385
one-sided bands, 375–380
planar decoration with, 372–373
rods, 381–395
similarity symmetry, 381–395
spirals, 381–395
translation presence in, 373, 378–379, 385
two-dimensional, 395–410
two-sided bands, 378–381
Sphere, 85–86
Sphere packing, 442–446
Spin quantum number, 250
Spiral staircase, 71
screw-axis symmetry in, 382–383
Spiral symmetry, 391–393
Square matrix, 176
Square prismatic $[Re_2Cl_8]^{2-}$ ion structure, 134–135
$SrBr_2$, bending potential energy functions, 155–156
Staggered conformation, 101, 104
Stalactites and stalagmites, 31
Standing wave theory, 43–44
Starfish, 38–40
Steno, 417
Steinhardt, P., 489, 491
Structural isomerism and isomers, 99–100
Sulfones, 138
Sulfur dichloride, 146
Sulfur difluoride, 145–146
Sulfur hexafluoride (SF_6), consequences of substitution, 115–116
Sulphuric acid, 138
Symmetry
bands symmetry, 375–381
bilateral, 25–33
broken, 14–15
center, 53–55
chemical, 2–3, 14, 16
chirality, 60–76
classes of one-sided

bands, 375–380
planar networks, 395–401
combined, 37–53
concept of, 1–3, 16
consequences of substitution on, 115–119
coordinate in molecular vibrations, 225–227
definitions, 15–16
and degeneracy of energy levels, 243–244, 260–261
element and consequences, 37
environmental, 290–294
forbidden chemical reactions, 314, 331
and group theory, 169–170
and harmony, 18
of human body, 25–27
importance of, 14, 19
inversion, 53–55
and Jahn–Teller effect, 294–308
laws of nature and, 12–14
left-and-right, 14
notations, 104–105
of crystallographic groups, 105
of limiting groups, 104–105
planes, rotation axis with in, 37–39
polarity, 57–60
polyhedra, 76–90
rods, 381–395
rotational, 33–36
rotation axis, 37–39
rules
for chemical reactions, 313–315, 320, 340, 343
for reaction coordinate, 320–324
similarity symmetry, 381–395
singular point, 55–58
snowflakes, 39–53, 55
species, 189
spirals symmetry, 381–395
translational, 55–57
Symmetry-adapted linear combinations (SALCs), 258, 266–267, 271–274, 277, 279–281, 283, 285–287
Synergy, importance for chemistry, 5

T
‘t Hooft, G., 14
Teller, E., 294–297, 299, 300–302, 305–308, 322, 323
Tetraarsene (As_4), 120–121
Tetragonal bipyramidal systems, 148
Tetrahedral AX_4 molecule, consequences of substitution, 115–116
Tetrahedral sulphur configurations, 138
Tetrahedrane $(CH)_4$, 126–127, 129, 363, 364
Tetrahedron notations, 450–451, 453
Tetralithiotetrahedrane $(CLi)_4$, 134
Tetra-*tert*-butyltetrahedrane, 126–127
Thalidomide, 72–73
Thompson, D. W., 6, 97, 391
Thompson, W. H./Lord Kelvin, 60, 458, 459, 499
Three-dimensional space-groups, 375, 437, 469, 474–475, 485
unit cell, 433, 438, 439, 444
Tobacco mosaic virus (TMV), 391
Transition-state geometries, of chemical reactions, 316–319
Translational antisymmetry, 200–201
Translational symmetry, 55–57
Trees, conical and radial symmetries of, 29
Triacontrahedral quasicrystal, 493
Triamantane molecule structure, 132–133
1,3,5-Triphenylbenzene molecules, packing in crystal structure, 457–458
Triprismane $(CH)_6$, 127, 130
Tronev, V. G., 135
Truncated cube, 87–88
Truncated cuboctahedrane $(CH)_{48}$, 129
Truncated cuboctahedron, 87
Truncated dodecahedrane $(CH)_{60}$, 129
Truncated dodecahedron, 87–88
Truncated icosahedral geometry, 6, 9
Truncated icosahedrane $(CH)_{60}$, 129
Truncated icosahedron, 7–8, 88–89
Truncated icosidodecahedrane $(CH)_{120}$, 129
Truncated icosidodecahedron, 87
Truncated octahedron, 87–89
Truncated tetrahedron, 87–88
T symmetry, 114
Twinned cuboctahedron, 449
Two-dimensional space-groups, 375, 395–410
lattice point, 398–399
Moirés, 408–410
planar decorations with, 372–373
plane lattices, 398, 400–402
primitive cell, 398
scheme for establishing symmetry class of, 398–399
side-effects of decorations, 406–408
simple networks, 401–406
symmetry classes, 395–401
unit cell, 398, 402, 405

U
Unit matrix, 176

V
Valence Shell Electron Pair Repulsion (VSEPR) model, 139–153
analogies, 142–143
historical perceptives, 151–153
molecular shapes, 143–151
quantum-mechanical foundations for, 151
three-dimensional consequences of, 142–143
van der Waals radii, 137
van 't Hoff, J. H., 97
Vatsayana, 422
Vectors
and matrix, 177–178
reflection by horizontal mirror plane, 179
representation in three-dimensional space, 177
rotation by an angle α in *xy* plane, 180
Vibrational transitions, 228
Vinca minor, rotational symmetry in, 37–38
Vinyl polymers, 385–387

W
Wald, G., 62
Walnut clusters, 143
Water and ice, structural difference between, 440–441
Water (H_2O) molecule
cartesian displacement vectors, 222
MO construction in, 266–270
molecular shapes, 143–145
normal modes of vibration for, 220
symmetry coordinates of, 225–227
Watson, J. D., 3, 4, 388, 390, 462
Wave function, *see* Electronic wave function
Weinberg, S., 13
Wells, A. F., 442, 443, 444, 450
Weyl, H., 16, 33, 79
Whyte, L. L., 42, 63
Wickham, A., 485
Wigner, E. P., 12, 13, 14, 17, 240, 313
Wigner's theorem, 240
Wigner–Witmer rules, 313
Witmer, E. E., 313
Williams, I. H., 317
Woodward, R. B., 313, 314, 324, 326, 327, 328, 329, 331, 350, 351, 353, 354, 355
Woodward–Hoffmann diagrams, 327
Woodward–Hoffmann rules, 350–351, 353–354
$W_6S_8(Pet_3)_6$ crystal structure, 81, 83

Y
Yang, C. N., 14, 15, 47, 197
Young, L. B., 371

Z
Zachariasen, W. H., 485, 486
Zhabotinsky, A. M., 392, 393
Zeolites structure, 89
Ziegler, K., 385
Zimmerman, H. E., 351, 353
Zirconium borohydride $[Zr(BH_4)_4]$, 121
$ZnCl_2$, bending potential energy functions, 155–156